WOODHEAD PUBLISHING IN MATERIALS

Durability of concrete and cement composites

Edited by C. L. Page and M. M. Page

CRC

WP

Durability of concrete and cement composites

Related titles:

Corrosion of reinforcement in concrete – Mechanisms, monitoring inhibitors and rehabilitation techniques (EFC 38)
(ISBN 978-1-84569-210-0)
Corrosion of metal within reinforced concrete is one of the most important problems facing the construction industry. Key research on this topic is summarised in this latest volume of 24 chapters from the prestigious European Federation of Corrosion. The book begins by reviewing findings from various experiments designed to test the corrosion rate of metals induced by a range of factors. Later chapters discuss techniques for monitoring and testing for corrosion. Important methods of prevention, including inhibitors and protective coatings are evaluated. The book concludes with the discussion of electrochemical methods for protection and rehabilitation procedures for susceptible structures.

The electrochemistry and characteristics of embeddable reference electrodes for concrete (EFC 43)
(ISBN 978-1-84569-234-6)
Using reference electrodes to monitor the electrochemical potential of steel reinforcement in concrete is a well-established technique for assessing the severity of corrosion and for controlling cathodic protection systems. This report gives a state-of-the-art overview of the electrochemical and physical characteristics and performance of embeddable reference electrodes for concrete, and the method used for installing them.

Local probe techniques for corrosion research (EFC 45)
(ISBN 978-1-84569-236-0)
The effective investigation of corrosion requires the use of methods that can probe material surfaces at the atomic or molecular level and can be used *in situ*. This important collection reviews the range of techniques available and how they can be used to analyse different types of corrosion.

Details of these and other Woodhead Publishing materials books, as well as materials books from Maney Publishing, can be obtained by:

- visiting our web site at www.woodheadpublishing.com
- contacting Customer Services (e-mail: sales@woodhead-publishing.com; fax: +44 (0) 1223 893694; tel.: +44 (0) 1223 891358 ext. 130; address: Woodhead Publishing Limited, Abington Hall, Abington, Cambridge CB21 6AH, England)

Maney currently publishes 16 peer-reviewed materials science and engineering journals. For further information visit www.maney.co.uk/journals.

Durability of concrete and cement composites

Edited by
C. L. Page and M. M. Page

Woodhead Publishing and Maney Publishing
on behalf of
The Institute of Materials, Minerals & Mining

CRC Press
Boca Raton Boston New York Washington, DC

WOODHEAD PUBLISHING LIMITED
Cambridge England

Woodhead Publishing Limited and Maney Publishing Limited on behalf of
The Institute of Materials, Minerals & Mining

Published by Woodhead Publishing Limited, Abington Hall, Abington,
Cambridge CB21 6AH, England
www.woodheadpublishing.com

Published in North America by CRC Press LLC, 6000 Broken Sound Parkway, NW,
Suite 300, Boca Raton, FL 33487, USA

First published 2007, Woodhead Publishing Limited and CRC Press LLC

British Library Cataloguing in Publication Data
A catalogue record for this book is available from the British Library.

Library of Congress Cataloging in Publication Data
A catalog record for this book is available from the Library of Congress.

Woodhead Publishing Limited ISBN 978-1-85573-940-6 (book)
Woodhead Publishing Limited ISBN 978-1-84569-339-8 (e-book)
CRC Press ISBN 978-0-8493-9129-3
CRC Press order number WP9129

The publishers' policy is to use permanent paper from mills that operate a sustainable forestry policy, and which has been manufactured from pulp which is processed using acid-free and elementary chlorine-free practices. Furthermore, the publishers ensure that the text paper and cover board used have met acceptable environmental accreditation standards.

Project managed by Macfarlane Production Services, Dunstable, Bedfordshire, England (macfarl@aol.com)
Typeset by Godiva Publishing Services Limited, Coventry, West Midlands, England
Printed by TJ International Limited, Padstow, Cornwall, England

Contents

Contributor contact details

(* = main contact)

Editors
Professor C. L. Page
University of Birmingham
Department of Civil Engineering
Birmingham B15 2TT
UK
E-mail: c.l.page.1@bham.ac.uk

Dr M. M. Page
University of Birmingham
Department of Civil Engineering
Birmingham B15 2TT
UK
E-mail: m.page@bham.ac.uk

Chapter 1
Professor C. L. Page and
Dr M. M. Page
(as above)

Chapter 2
Professor S. Diamond
Purdue University
West Lafayette
Indiana
USA
E-mail: diamond@ecn.purdue.edu

Chapter 3
Dr J. J. Brooks
Formerly University of Leeds
School of Civil Engineering
Leeds LS2 9JT
UK
E-mail: jj.brooks@ntlworld.com

Chapter 4
Professor J. Bensted*
University College London
Materials Chemistry Centre
Gordon Street
London WC1H 0AJ
UK
E-mail: bensted.j@btinternet.com

Dr A. R. Brough
Formerly University of Leeds
School of Civil Engineering
Leeds LS2 9JT
UK
E-mail: brough@waitrose.com

Dr M. M. Page
(as above)

Chapter 5
Professor C. L. Page
(as above)

Chapter 6
Prof. Dr-Ing. U. Nürnberger* and Dr. Ing. G. Sawade
Materials Testing Institute
University of Stuttgart
Pfaffenwaldring 4
D-70569 Stuttgart
Germany
E-mail: ulf.nuernberger@po.uni-stuttgart.de
gottfried.sawade@po.uni-stuttgart.de

Prof. Dr-Ing. B. Isecke
Federal Institute for Materials Research and Testing
Unter den Eichen 87
D-12205 Berlin
Germany
E-mail: bernd.isecke@bam.de

Chapter 7
Professor M. D. A. Thomas*
Department of Civil Engineering
University of New Brunswick
H-124, Head Hall
17 Dineen Drive
P.O. Box 4400
Fredericton N.B.
E3B 5A3
Canada
E-mail: mdat@unb.ca

Dr K. J. Folliard
The University of Texas at Austin
Department of Civil Engineering
1 University Station C2100
Austin
Texas 78712
USA
E-mail: folliard@mail.utexas.edu

Chapter 8
M. Richardson
School of Architecture, Landscape and Civil Engineering
University College Dublin
Belfield
Dublin 4
Ireland
E-mail: mark.richardson@ucd.ie

Chapter 9
Dr P. Purnell
School of Engineering
University of Warwick
Coventry CV4 7AL
UK
E-mail: pp@eng.warwick.ac.uk

Chapter 10
Dr N. R. Short
School of Engineering & Applied Science
Aston University
Birmingham B4 7ET
UK
E-mail: n.r.short@aston.ac.uk

1
Introduction

C L PAGE and M M PAGE, University of Birmingham, UK

The purpose of this book is to bring together a series of reviews on topics of current relevance to the durability of concrete and cement-based composites. One might reasonably ask why such a book is now believed to be needed as concrete and related materials have been used with outstanding success in major construction projects for well over two thousand years. Indeed numerous ancient concrete structures, such as the Pantheon in Rome, and masonry structures with mortar joints, such as the Pont du Gard Aqueduct near Nîmes in southern France (see Fig. 1.1), have survived to the present day in excellent states of preservation. These and other examples of Roman construction works incorporating hydraulic cements made from lime and volcanic earth (or similar vitrified alumino-silicates, known collectively as pozzolanas, after Pozzuoli near Naples where a natural source of such material exists) have shown remarkable durability even where they have been exposed to damp, aggressive environments. An impressive illustration was provided by Davey (1974) whose photograph of part of a Roman breakwater that had been exposed to the sea near Naples for two millennia (reproduced in Fig. 1.2), demonstrates that the mortar joints had endured far more successfully than the now heavily eroded stone blocks which they had been connecting.

Whilst the Romans had probably discovered the art of producing durable pozzolanic hydraulic cements by the end of the third century BC, the compositional features and properties of these materials appear to have remained largely unexplored until about 250 years ago when John Smeaton (see Fig. 1.3), the first Englishman to describe himself as a civil engineer, carried out systematic investigations into the behaviour of mortars incorporating limes and pozzolanas from various sources. This work, performed with the practical objective of selecting an appropriately durable blend of pozzolanic cement for use in the construction of the Eddystone Lighthouse (1756–59), produced important findings that were eventually published (Smeaton, 1791) and this paved the way for a number of advances in the development of hydraulic cement binders over the next half century or so. The most significant of these advances was the invention of ‘Portland cement’, produced by heating together mixtures

1.1 The Pont du Gard, part of a 50 km aqueduct constructed by the Romans in the first century AD near Nîmes in southern France, with mortar joints containing pozzolanic cement.

of calcareous (lime-based) and argillaceous (clay-based) substances at suitably high temperatures. A synthetic cement of this name was patented in 1824, exactly a century after Smeaton's birth, by another former inhabitant of Leeds, Joseph Aspdin, whose contribution (like Smeaton's) is commemorated by a blue plaque on one of the city's buildings (see Fig. 1.4).

Fitting testimony to the durability of Aspdin's product is provided in Fig. 1.5, which shows a mortar statuette depicting 'The Prophet Samuel in Infancy', thought to have been made *circa* 1850 by James Aspdin, Joseph's elder son. The statuette was brought to light in 1974, standing in the Yorkshire garden of a great-great niece of Joseph Aspdin. It had apparently been exposed to the vagaries of the weather for well over a century and was found covered with moss and lichen. Further details of the statuette's provenance are given in a note by Barfoot (1975), which supplements a longer article by the same author, relating the story of Joseph Aspdin and his two sons, James and William, both of whom also played a part in the early development of the cement industry (Barfoot, 1974).

Aspdin's original 1824 version of 'Portland cement' is now thought to have been fired at temperatures too low to have induced effective vitrification of the

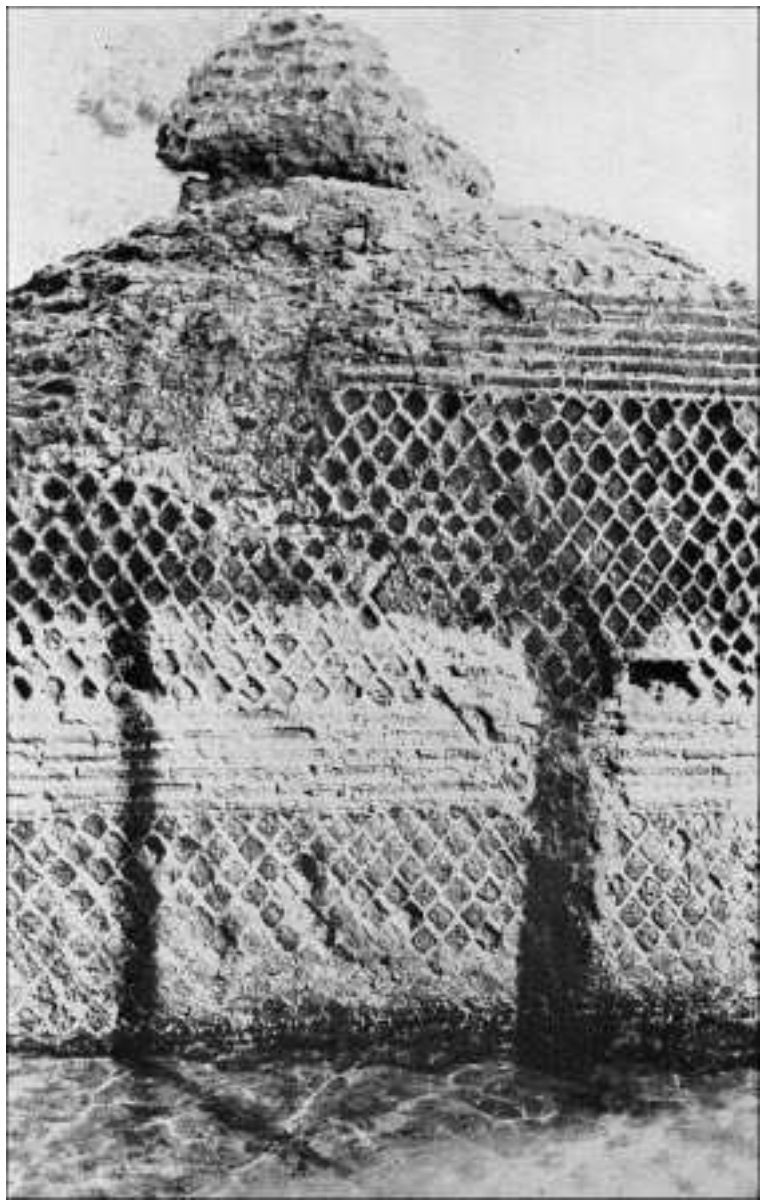

1.2 A Roman breakwater constructed from 'opus reticulatum', with mortar joints containing a pozzolanic cement. (Reproduced with permission of The Structural Engineer from the 1974 paper by Davey, to which reference has been made. The photograph also appeared in a book by the same author: Davey, N (1961), *A History of Building Materials*, Phoenix House, London.)

1.3 A blue plaque on a building in Leeds commemorating John Smeaton (1724–1792).

1.4 A blue plaque on a building in Leeds commemorating Joseph Aspdin (1778–1855).

1.5 'The Prophet Samuel in Infancy', a mortar statuette believed to have been made by James Aspdin, *circa* 1850.

constituents and the development of mass-produced cements of consistent quality therefore required several further technological advances to be made (Blezzard, 1998). By the latter part of the 19th century, however, reliable Portland cements with mineralogical features that were more similar to those of present-day varieties of the material were becoming widely available and this led to massive expansion in the use of concrete for many of the major infrastructure developments of the Victorian era in Britain. Once again, it is

1.6 The Glenfinnan Viaduct, a 21-arch concrete railway viaduct constructed in 1897 in the West Highlands of Scotland.

apparent from the number of structures of this period that have survived to the present day that the durability of Portland cement concrete can be remarkably good, as exemplified by the excellent condition of the Glenfinnan Viaduct, built in Scotland in 1897 by Robert McAlpine as part of the Fort William to Mallaig extension of the West Highland Railway (see Fig. 1.6).

In comparison with the example shown in Fig. 1.6, it must be admitted that some of our more modern structures have aged rather less gracefully and, on the basis of contemporary press reports (see Fig. 1.7), one might reasonably conclude that the construction industry, in recent times, had not entirely mastered the art of creating durable and sustainable products from cement-based materials. As a generalisation, however, this is somewhat harsh because the vast majority of such products of the 20th century have not actually shown signs of premature degradation in spite of the fact that, at no previous time in history, has the industry been forced to adapt so rapidly to the pressures of change arising from a great variety of causes. What was until quite recently an activity relying on the availability of suitable local materials and labour, employing well-established craft-based practices, has been radically transformed in many

1.7 Some late-20th century press cuttings concerning the performance of concrete.

parts of the world over a period of just a few decades. Not only has this led to significant changes in compositional features and properties of many of the constituents of the family of materials we call concrete and cement composites, it has also revolutionised the range of fabrication methods applied to them and thereby greatly extended their range of applications. World production of cement is continuing to grow at a significant rate and had already amounted to some 1.9 billion tonnes p.a. by 2003, representing an average annual usage of concrete of nearly 1 m^3 per person. Little wonder then that when something does go wrong, it can go wrong on a scale large enough to produce headlines of the sort illustrated in Fig. 1.7.

Since the pressures that have driven innovation throughout the last century are now increasingly acute, there is every reason to think that the 21st century will present even greater challenges for those involved in the applications of concrete and cement composites. The need to create sustainable construction products that are expected to fulfil their intended functions, remaining in

serviceable condition for very long periods with only minimal maintenance before being recycled efficiently, will lead to many changes in current practices. This will inevitably raise questions regarding the durability issues concerned because, in the absence of adequate prior experience of relevant long-term performance, it becomes increasingly difficult to continue to justify the prescriptive 'deemed-to-satisfy' approach towards specifying durability that has been a feature of traditional codes and standards.

The holy grail of much of the durability-related research conducted over the past twenty years or so, has therefore been to provide the underpinning theory needed to allow the development of quantitative models of degradation phenomena that may lead in turn to new methods of durability design for structures and components exposed to stated environmental actions for specified intended service lives. To become generally acceptable, these new design methods must be firmly supported by scientific principles that will allow materials selection to be made on the basis of performance testing, rather than by prescription, and the performance tests concerned need to satisfy appropriate criteria of convenience, reliability, and precision. The approach clearly has much to offer as a means of enabling fair comparisons to be made between competitor materials and thus of promoting technical innovation of a kind that is becoming increasingly urgent.

While considerable progress has been made in the above-mentioned areas, with international organisations such as RILEM playing an influential role, it must be noted that the way forward has been far from easy for a variety of reasons which will become apparent in several of the chapters of this book. One of the major difficulties has undoubtedly been the continuing uncertainty over key microstructural features of cement-based materials that affect the development and continuity of the pores of different size ranges within them. These features in turn influence the evolution of the resistance of the materials to the processes of mass transport that are involved in degradation phenomena of different kinds. This has been an area of intensive debate amongst researchers ever since the classic investigations carried out at the laboratories of the Portland Cement Association were published more than half a century ago (Powers and Brownyard, 1948). Equally, and in spite of the important development during the early 1970s of a viable method for extracting samples of the liquid phase associated with hardened cements and related materials (Longuet *et al.*, 1973), it has proved to be difficult to resolve fully the compositional features of the aqueous solution phase residing within sub-surface pores of different forms of concrete subjected to various conditions of exposure. This has also presented a considerable barrier to understanding of many of the most important degradation phenomena that affect these materials.

The following chapter of this book therefore presents a state-of-the-art review of the pore structure and pore solution chemistry of cement-based materials, setting the scene for subsequent chapters that deal with major specific forms of

degradation to which concrete and cement composites are potentially vulnerable. It should be made quite clear, however, that we do not attempt to suggest that the book can provide a comprehensive treatment of this vast subject area. There are some omissions of which we are aware, and no doubt others of which we are not, but we hope that the work as a whole will prove helpful to those who require a reasonably detailed treatment of some of the many facets of the durability of the world's most widely used man-made materials.

Finally, we would like to acknowledge the fact that a book of this kind could not have been produced without the sustained efforts of many busy individuals who were cajoled into writing chapters when more immediately pressing demands were being made on their time. We are grateful to all of them for their contributions to the work and to the publishers for their patience in dealing with the delays that inevitably seem to crop up with undertakings such as this.

1.1 References

Barfoot, R J (1974), 'Joseph, James and William – The Aspdin Jigsaw', *Concrete*, 8(8), 18–26.

Barfoot, R J (1975), 'Found – Aspdin's missing statuette!', *Concrete*, 9(5), 22.

Blezzard, R G (1998), 'The history of calcareous cements', *Lea's Chemistry of Cement and Concrete*, Hewlett P C (ed.), Arnold, London, 1–23.

Davey, N (1974), 'Roman concrete and mortar', *The Structural Engineer*, 52(6), 193–195.

Longuet P, Burglen L, Zelwer A (1973), 'La phase liquide du ciment hydraté', *Revue des Matériaux de Construction*, 676, 35–41.

Powers T C, Brownyard T L (1948), 'Studies of the physical properties of hardened cement paste', Bulletin 22, Research Laboratories of the Portland Cement Association, Chicago.

Smeaton J (1791), *A narrative of the building and a description of the construction of the Edystone Lighthouse with stone*, H. Hughs, London.

2

Physical and chemical characteristics of cement composites

S DIAMOND, Purdue University, USA

2.1 Introduction

The aim of this chapter is to provide information on aspects of the internal characteristics of concrete that relate to concrete durability. Pertinent chemical and physical characteristics, particularly those involving pore solutions and pore structures, are discussed in some detail, as these most closely affect most durability concerns.

Concrete is an unusual engineering material. Unlike most engineering materials it is held together by a *porous* binder, specifically a complex of solids and pores called 'hydrated cement paste'. The binder is the continuous phase in the composite; thus the fact that it is porous is critical with respect to movement of water and chemical substances into or out of the concrete. This is a feature extremely relevant to the durability of the concrete in service.

A further characteristic that sets concrete apart from most other engineering materials is that the porous binder is intrinsically *hydrous* – that is, except for any residual unhydrated cement, it is made up of compounds that are all hydrated solids. These compounds (calcium silicate hydrate or C-S-H, calcium hydroxide, ettringite, monosulfate, and others) develop spontaneously within the structure as the result of chemical reactions between water and ground Portland cement. They are deposited within the particular internal chemical environment of the specific concrete, and in service they are in at least temporary equilibrium with that internal environment. It is sometimes not fully appreciated that these hydrated compounds are subject to reorganization if the local internal chemical environment is modified – by leaching, by intrusion of dissolved salts, or by other processes. This is the unfortunate origin of many durability problems.

Yet another distinction sets concrete apart from most other engineering materials. Not only is the hydrous binder porous, but at least some of the pores contain a highly concentrated solution of alkali hydroxide. Under some unusual exposure conditions, the pores within a given concrete structure may be fully saturated with this solution. Generally they are not; the larger pores may commonly be empty, especially those near concrete surfaces that have been exposed

to evaporation, or within concretes that have been mixed at low enough water: cement (w:c) ratios that they are subject to self-desiccation. On the other hand, even prolonged exposure to dry conditions in service does not fully empty the finest pores.

The actual concentrations of dissolved substances in the solution retained in the pores of concretes may be significantly affected by leaching, by partial drying, or by intrusion of ions and other dissolved substances from the outside of the concrete.

The details of the solid pore structures bordering and defining the pores of the binder in a given concrete play a significant role in most concrete durability problems. Since the aggregates used in most concretes have few interconnected pores, the paste pore structures almost always govern the rates at which water or ion movements can occur.

In this connection it is often suggested that permeability to water is the single most important pore structure-related characteristic controlling the potential durability of a given concrete. Strictly speaking, permeability refers to rate of mass transfer of a fluid (usually water) as a function of applied hydraulic head. This actually may be less important in the context of concrete durability than other related parameters, such as the rates of ion transfer, or rates of internal water vapor transfer in unsaturated concretes.

Because of these various concerns, the present writer proposes to use a more general term '*permeation capacity*' instead of 'permeability' in discussing the durability-related transport characteristics of concretes. It is noted that a dictionary definition of the verb 'to permeate' is 'to penetrate through the pores, interstices, etc.', without any particular permeating substance or mechanism being specified. It is well known that the permeability of concrete is a strong function of its water:cement (w:c) ratio, and within concrete of a particular w:c ratio, of the degree of cement hydration.

Figure 2.1, the classical relationship derived from Powers *et al.*,[1] illustrates the extremely non-linear effect of the w:c ratio on the permeability, in this case as measured in thin specimens of almost fully hydrated (93% hydrated) cement pastes. A similar trend in the effect of w:c ratio on permeability is usually expected with concretes.

It is well understood that permeability of young concretes is initially high and decreases with degree of hydration. The degree of hydration experienced in most field concretes is limited, especially in those of low w:c ratios; practically speaking, concretes almost never actually approach the degree of hydration of the paste specimens measured by Powers *et al.*[1]

Other characteristics of concrete that measure its permeation capacity, such as ion diffusion coefficients or electrical conductivity values, generally reflect tendencies similar to those of permeability with respect to variations in w:c and degree of hydration. However, some of these measurements may be influenced by factors that do not necessarily affect permeability measurements. For

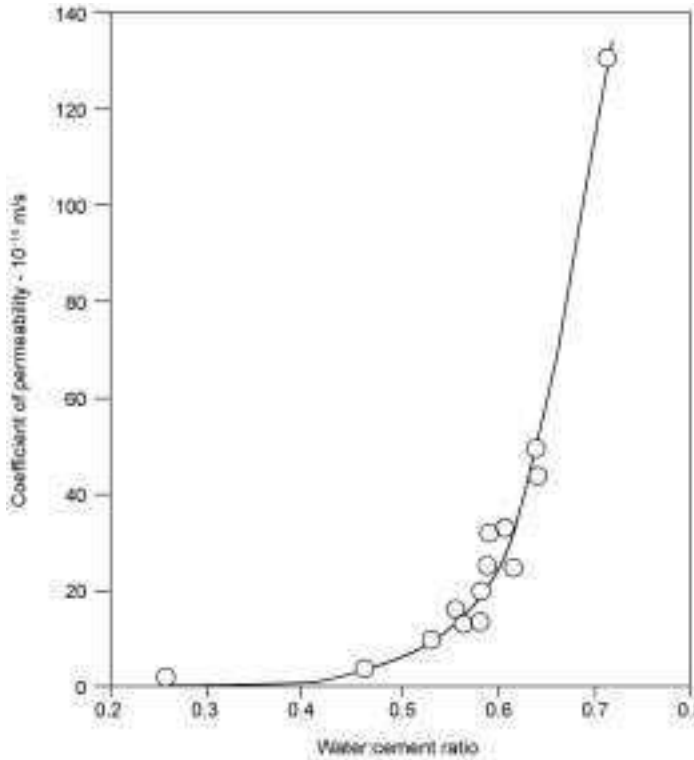

2.1 Measured permeabilities of almost fully hydrated (93% hydrated) cement pastes as a function of w:c ratio. After Powers *et al.*[1]

example, the chemistry of the particular cement used exerts a major influence on the concentration of ions in the pore solution of the concrete, and therefore on its electrical conductivity.

The incorporation of silica fume, fly ash, or other supplementary cementitious components in concretes exerts a very strong influence in reducing permeation capacity, although not necessarily to the same extent in different types of measurements. Similarly, the conditions under which hydration takes place, especially whether or not the concrete was steam cured, may exert important effects.

Once placed in a structure, concrete is exposed to in-service conditions that may alter both pore solution composition and pore structures. Entry of chemical substances, leaching, repeated wetting and drying, freezing events, carbonation, etc., all may induce significant internal changes in pore fluid composition and in pore structure. Some of these alterations may induce specific durability problems.

Often durability problems such as alkali silica reaction (ASR), steel corrosion, delayed ettringite formation (DEF), etc., result in expansion-induced

cracking. Cracking may also result from shrinkage rather than from expansion. However induced, cracks inevitably increase the effective permeation capacity compared to that of similar intact concrete. Attempts to predict potential service life of concrete structures often founder on how to account for the effects of future crack development on the expected permeation capacity.

The present chapter is designed to provide an overview of internal chemical and physical characteristics of cement paste binders in concretes, especially focused on pore solutions and pore structures. Some discussion of permeation capacity-related measurements that depend on interconnections between pores and in certain cases on the effects of pore solutions is also provided.

In this chapter the writer has deliberately chosen to confine himself to findings based on experimental evidence, and has omitted mention of a parallel literature in which the microstructures and processes considered here are *modeled*, rather than *investigated*.

2.2 Variations among concretes, and 'archetypical concrete'

Modern concretes are extremely varied in their characteristics relevant to the concerns of this chapter. To begin with, concretes designed for different applications are currently produced at widely different w:c ratios. The writer has extensive personal experience in the examination of concretes that were placed at w:c ratios of 0.8, 0.9, or even higher. At the other extreme, modern high performance concretes are successfully produced at effective water:cementitious material ratios as low as 0.25. Enormous variations in internal concrete properties result from this wide variation in w:c ratio.

The chemistry of the Portland cement used in the concrete is another relevant factor; cements vary considerably in chemical characteristics that affect the developing pore solution chemistry and to a lesser degree, the paste structure. The specific content of the minor alkali-bearing components (mostly potassium sulfates or potassium calcium sulfates) in the specific cement strongly influence concrete pore solution chemistry. Cement alkali contents, usually expressed as equivalent % Na_2O (= %Na_2O + 0.659% K_2O), may vary from a few tenths of a percent to well over 1%.

Other important variations in Portland cement chemistry often escape notice in considerations of permeation capacity. A peculiarity of cement chemistry is that very small differences in analytical CaO contents mark major differences in the relative proportions of the calcium silicate components C_3S and β-C_2S. The relative proportions of the two calcium silicates exert significant influence on paste microstructure, not least in terms of the relative amount of calcium hydroxide that is generated. Similarly, the proportions of the aluminum-bearing phases C_3A and ferrite (nominally 'C_4AF') in the cement influence the rate and extent of ettringite production.

In most countries the addition of small but sometimes potentially significant proportions of non-Portland cement components (such as ground limestone or fly ash) is permitted in Portland cement specifications. Furthermore, provision is also usually made for cements that contain larger proportions of non-Portland cement components. These additions certainly impact on the internal characteristics of the binders produced, as does incorporation of such materials as silica fume, fly ash, slag, metakaolin, and similar substances by concrete producers.

Chemical admixtures induce additional sources of variation. While most chemical admixtures are designed to carry out a particular function in concrete, their direct or indirect effects on pore solution chemistry and on microstructure may sometimes be considerable.

The growing importance of precast steam cured concrete elements introduces still further variations. Steam curing, even at moderate temperatures, strongly affects the development of both pore solutions and microstructure.

The relatively new category of self-compacting concretes (SCCs) is also growing in popularity. The combination of viscosity modifiers, dispersants, and mineral fillers encountered in such concretes has significant effects on pore solutions and on paste structures, many of which are just beginning to be understood.

The enormous numbers of different effects that these many variations can induce, individually and in combination, renders discussion of all of them in this chapter quite impractical, even if the information were available. However, in many cases, the effects can be viewed as inducing departures from a typical pattern that would be observed for 'ordinary' concretes. Accordingly, in the present chapter the writer will generally confine himself to concretes of the ordinary or typical pattern, with only occasional mention of some of the effects induced by some of the many possible variations. For brevity, such concretes will be referred to as '*archetypical concretes*', an 'archetype' being defined in dictionaries as 'the original pattern or model after which a thing is made'.

Archetypical concretes are here taken to mean conventional, properly consolidated field- or laboratory-mixed Portland cement concretes of w:c ratios of the order of 0.4 to 0.6, produced from 'ordinary' Portland cement with conventional aggregates, hydrated without steam curing, and incorporating either no other supplementary components or else only minimal contents of supplementary components and/or modest dosages of conventional chemical admixtures.

2.3 The genesis and chemistry of pore solutions in archetypical concretes

2.3.1 Introduction

The chemistry of the pore solution resident in the pores of a given concrete may strongly influence its potential durability. The potential for development of

ASR, steel corrosion, sulfate attack, 'sea water attack' and concrete spalling, among others, all directly reflect the influence of pore solution chemistry and of changes that may take place within it. Unfortunately, concrete pore solutions and their potential changes under different field exposure conditions are not particularly well understood by many who are concerned with concrete durability.

In this section the writer hopes to provide a realistic treatment of the origin and evolution of pore solutions in concretes, and of some of the changes that may be induced in them by exposures to different external environments.

2.3.2 Genesis and early development of pore solutions

When concrete is mixed, chemical reactions occur immediately after the mix water is added. The water used is typically specified as 'potable' water; these reactions quickly result in a drastic change in its chemical character. Within a very few minutes this 'potable water' becomes a high ionic strength solution of greatly altered chemical properties. The chemistry of this solution depends very much on the chemistry of the particular cement used.

Before setting takes place, this concentrated 'mix solution' constitutes the continuous phase in which aggregate and cement particles are suspended. On setting, the mix solution is seamlessly carried over to become the 'pore solution' contained within the concrete pores.

The composition of this mix solution/pore solution evolves over time, with major changes occurring especially during the first day. This evolution can be readily followed in the laboratory. It is possible to separate mix solution for chemical analysis from freshly-mixed cement paste (or concrete) by gas pressure-assisted filtration. Repeated sampling can be carried out at intervals until the approach of setting renders it impractical. After setting and some strength gain, pore solutions can again be expressed for analysis, for example by the pore solution expression equipment described by Barneyback and Diamond.[2]

Table 2.1 provides an illustrative set of the results of analyses of such a series of mix/pore solutions developed in a Portland cement paste that might be found in an archetypical concrete. The paste was prepared from a relatively low alkali Portland cement (0.45% $Na_2O_{equiv.}$), and was mixed at a w:c ratio of 0.5. The data were taken from the thesis of Penko.[3]

The ionic species listed in Table 2.1 are universally found in significant concentrations in the mix/pore solutions developed during the early hydration of Portland cements. These are K^+, Na^+, Ca^{2+}, SO_4^{2-}, and OH^-. Aluminum, iron, and silicate ions are present only in concentrations that are orders of magnitude lower than those of the five listed.

The high concentrations of alkali metal ions and of sulfate ions seen in Table 2.1 are derived from the alkali sulfate 'impurities' carried by the cement. Even with the comparatively low alkali content of the particular cement, the early

Table 2.1 Changes in pore solution concentrations measured during the first day of hydration for a w:c 0.50 Portland cement paste

	Ion concentration in milli-equivalents/liter				
Time, hrs	K^+	Na^+	Ca^{2+}	SO_4^{2-}	OH^-
1	0.27	0.03	0.07	0.17	0.15
2	0.27	0.03	0.072	0.17	0.15
3	0.27	0.03	0.06	0.17	0.16
4	0.27	0.03	0.06	0.18	0.15
6	0.28	0.04	0.06	0.20	0.14
12	0.30	0.04	0.06	0.15	0.24
15	0.31	0.04	0.006	0.09	0.29
18	0.31	0.04	0.006	0.05	0.32
24	0.34	0.05	0.005	0.00	0.39

sulfate ion concentration found in solution vastly exceeds that of a saturated solution of gypsum. More importantly, it also exceeds that of ettringite; and ettringite will precipitate rapidly as aluminate ions become available following the dormant period.

For the paste of Table 2.1, the dormant period ended at a little less than three hours after mixing. Initial set occurred at ca. 3.5 hours, and final set at slightly over 5 hours. The peak temperature indicative of the maximum rate of hydration was measured at 8.5 hours. It is seen that almost equal concentrations of hydroxide and sulfate ions were present throughout the early stage of hydration. Nevertheless, the presence of the hydroxide ions from the time of earliest analysis makes it evident that earliest reaction was not confined to dissolution of alkali sulfates, but included reaction with C_3S as well. With respect to the alkali metal cations, it is seen that the K^+ concentration vastly exceeds the Na^+ concentration at all stages. This is a feature common in modern cements, but not universally so.

It is seen in Table 2.1 that little change takes place in concentrations of any of the ions during at least the first six hours, despite the fact that within this period the dormant period ended and both initial set and final set occurred. This is a common pattern; neither the onset of active hydration after the dormant period nor the occurrence of setting produces significant changes in mix/pore solution ion concentrations.

Some years ago it was established that rapid ettringite formation after the end of the dormant period quickly removes sulfate from the pore solution, but that the sulfate lost from solution is continually replaced by progressive dissolution of the gypsum.[4] Thus the dissolved sulfate ion concentration is maintained at least approximately constant as long as some solid gypsum persists, apparently in response to an equilibrium involving the simultaneous presence of syngenite, gypsum and ettringite. The dissolution of the last of the solid gypsum marks a

turning point; subsequent ettringite precipitation progressively reduces the sulfate concentration of the pore solution – in properly formulated Portland cements – to very low levels by the end of the first day. For the specific paste of Table 2.1, the turning point marked by the depletion of the solid gypsum apparently occurred some time shortly after 6 hours.

A crucial feature of the post-turning point changes in pore solution composition is that, as the sulfate concentration is depleted, electrical neutrality is maintained by parallel increases in the OH^- ion concentration, rather than by reductions in the alkali cation concentrations. Thus the pH goes up sharply as the sulfate is depleted from solution. As the pH goes up, the already relatively modest calcium ion concentration (modest in absolute terms, not in degree of supersaturation) is reduced to a very low value. The result of these changes is that the pre-existing mix/pore solution is progressively transformed into a concentrated solution of potassium and sodium hydroxide. This transformation has highly significant consequences with respect to possible development of ASR and with respect to the maintenance of steel passivation in concrete, among other effects.

It appears that this enhancement of pH, while universal in properly formulated Portland cements, is not inevitable. It has been shown[3] that if sufficient excess gypsum is added to the cement, the exhaustion of the available aluminate can end the precipitation of ettringite before the solid gypsum is fully depleted. Under these circumstances the usual pH transformation can be postponed or perhaps prevented indefinitely. Conversely, in the absence of gypsum, as, for example, in laboratory experiments when ground clinker is hydrated without any inter-ground gypsum, the decline of sulfate ion concentration and the concomitant pH increase begin almost immediately after mixing, and are quickly completed.

2.3.3 Long-term status of pore solutions in mortars and concretes, and effects of exposures to different environments

In *sealed* laboratory cement pastes (or in concretes protected against either leaching or drying effects), the exhaustion of sulfate from the pore solution does not yet mark the maximum level of alkali hydroxide concentration. Instead, as hydration proceeds, the limited content of solvent water is progressively depleted, and the concentration of alkali hydroxide in the remaining volume of pore solution progressively increases.

The eventual concentration of the hydroxide ions found in the pore solution in sealed pastes and mortars of a given w:c ratio is closely related to the alkali content of the cement used. Some years ago the writer[5] collected and published a set of analyses from various literature sources for solutions expressed from w:c 0.50 pastes or mortars. All of these were hydrated at room temperature for the traditional 28-day period, and the chemical compositions of all of the cements

used were reported in the original publications. The reported OH^- ion concentrations were plotted against the alkali contents of the cements used, and a quite good linear relationship was found, especially considering the disparity of the data sources. It was found that the 28-day OH^- ion concentration (expressed in mol/l) was in each case about 0.7 times the % Na_2O equivalent of the cement. Thus in archetypical concretes, particularly high alkali cements can be expected to produce alkali hydroxide concentrations approaching or even exceeding 1 mol/l, i.e. pH values of the order of 14.

It was calculated that globally, about 80% of the alkali present in the various cements was found in the pore solutions of sealed specimens at 28 days.[5] Presumably some portion of alkali remained fixed in clinker minerals that had not yet hydrated, and some of the alkali hydroxide that had been in solution had been adsorbed by the solid components of the cement paste, primarily by C-S-H.

Much more detailed treatments of these phenomena have since been presented by several authors. The development of alkali concentrations in pore solutions of hydrating cements has been modeled by Brouwers and van Eijk[6] in terms of calculated rates of release of alkalis from cements and calculated binding coefficients of the ions into hydration products. Rothstein *et al.*[7] have treated the development of pore solutions in terms of saturation indexes, that is, the degree of undersaturation or supersaturation with respect to the solids calculated to be present at each stage based on hydration equilibrium equations derived originally by Taylor.[8]

Concentrated alkali hydroxide pore solutions have high electrical conductivities. As will be discussed later, electrical methods of assessing permeance in cement paste are influenced by these pore solution conductivity values. Snyder *et al.*[9] proposed a method of calculating the electrical conductivity of pore solutions from the specific potassium and sodium hydroxide concentrations. This is useful, since sufficient pore solution can generally be expressed from sealed samples for chemical analysis, but not necessarily sufficient for the measurement of electrical conductivity.

As mentioned previously, many modern concretes contain various added solid components besides the Portland cement used. The effects are generally to reduce the alkali hydroxide concentrations produced, but not always.

Most low-calcium fly ashes tend to reduce the pore solution alkali hydroxide concentrations[10,11]; however, the reverse effect is often found for very high calcium fly ashes[12,13] or fly ashes that carry significant contents of available alkali.[13] A summary of these effects was provided by Shehata *et al.*[13]

The influence of silica fume on alkali hydroxide concentration of pore solutions also appears to be complicated. Many years ago the present writer[14] found that incorporation of a silica fume resulted in slightly increased sodium hydroxide concentrations at very early ages, but that after some hours, further reaction reduced alkali hydroxide concentrations to much lower levels. Similar reduced alkali hydroxide levels have been observed by many authors, for

example Kawamura *et al.*[15] However the effect may not necessarily be permanent. Both Duchesne and Bérubé[16] and Shehata and Thomas[17] found that after some weeks of sealed storage the alkali hydroxide concentrations started to increase again, and the secondary increases observed were substantial. This secondary increase in alkali hydroxide concentration may have unexpected consequences with respect to long-term durability. The effect was not found when both silica fume and fly ash were simultaneously incorporated.[17]

Incorporation of slag reduces the alkali hydroxide content significantly,[17] an especially important effect since the proportion of slag usually added is substantial. Incorporation of ground limestone probably has little effect except that due to dilution of the cement.

Somewhat surprisingly, the incorporation of certain alkali-metal bearing admixtures such as sodium-neutralized naphthalene sulfonate may add significantly to the alkali hydroxide content of the pore solution.[18]

The alkali hydroxide concentrations and the changes in them referred to above reflect *sealed* storage exposures, i.e. environments where neither water nor dissolved substances are interchanged with the external environment. In real-world exposures, concrete pore solutions can undergo significant changes in water content, in contents of dissolved components, or in both.

Concretes may be exposed to leaching, either by virtue of being underwater or through long-continued rainfall. The pores in such concretes will become water solution-saturated if not previously so saturated, and prolonged wet exposures can induce significant loss of the alkali hydroxide leached from the pore solution. A similar leaching effect is often noticed in casual handling of small specimens exposed to laboratory fog-room conditions; an unpleasant 'soapy' feel is induced by contact of the skin with the leached alkali hydroxide.

Unexpectedly, it has been found that prolonged partial drying to moderately low RH values, especially when accompanied by some carbonation, 'fixes' much of the pore solution alkali hydroxide in the hydrated cement, significantly reducing the effective concentration found in expressed pore solutions.[19,20] Once fixed by such exposure, it is extremely difficult for subsequent re-saturation to redissolve the alkali hydroxide and bring the pore solution concentration back to its original value. This phenomenon may at least partly explain the highly beneficial effects of drying in mitigating the effects of ongoing ASR.

Some field concretes are exposed to salt (NaCl), either by deliberate applications of de-icing salts or by contact with sea water or salt spray. Some of the sodium chloride in such salt solutions may penetrate into pore solutions of the outer layers of the concrete, and appear as additional sodium hydroxide in them.[21,22] Conversion of the sodium chloride to sodium hydroxide is usually a consequence of the binding of the chloride ions as Friedel's salt. While the increased hydroxide ion concentration is favorable toward maintaining steel passivation, any significant entry of unbound chloride ions has the opposite effect. Pitting corrosion, as described for example in Ref. 23 may readily result.

Less widely appreciated, but equally important, is the influence of dissolved chloride in augmenting the harmful effects of ASR.[22,24,25]

2.4 Pore structures in hardened concrete

2.4.1 Introduction

In the previous section it was rather cavalierly remarked that at setting, 'the mix solution is seamlessly carried over to become the pore solution' of the hardened cement paste in concrete. The development and characteristics of the pores into which the pore solution is 'carried over' is an important and complicated feature of the internal structure of concrete binders. A completely realistic understanding of the developing pore structures in concretes is not available, despite many years of active research and literally thousands of research publications.

The usual division of pores in the binder of Portland concrete given in textbooks and even in most current research papers is overly simplistic. Pores are generally considered to be either *capillary pores* or *gel pores* after the classic proposal by Powers and Brownyard.[26] As will be seen subsequently, such a division seems to be far from an adequate classification. A more detailed and a perhaps more realistic picture of various types of pores to be found in archetypical concretes is presented in this section, along with some limited insight into how these pore structures evolve with time.

In this treatment the pore structure of aggregates in concrete is generally ignored, as it usually is. However, most aggregates have some pores, some aggregates have substantial contents of pores, and lightweight aggregates in particular have very extensive pore structures. Thus in at least some cases aggregate pores may play a significant role in fluid or ion transport, and in such cases these effects need to be considered.

It is also necessary to consider the possible contribution to permeation capacity of *air void*s, especially in heavily air-entrained concretes. Air voids occupy an ambiguous status in the literature; sometimes they are recognized as pores in the context of pastes in concretes; sometimes they are considered, but only as an afterthought; in many treatments of pore structures in concrete their existence is ignored entirely. Air voids are *always* present in archetypical concretes (and also in laboratory-mixed cement pastes), whether or not they have been deliberately air entrained. The only exception might be for concretes or cement pastes purposely mixed under vacuum.

2.4.2 The genesis of 'capillary pores' in concretes

The usual pattern of cement hydration involves rapid reactions of cement components exposed on the fractured surfaces of the individual ground clinker grains. It is commonly accepted that these fast reactions generate surface

hydration products (presumably mostly ettringite or ettringite-like), and that these products serve to temporarily isolate the underlying cement grains from effective contact with the mix solution, inducing the so-called dormant period of restricted hydration. Some hours later the barrier to further hydration is broached, and rapid autocatalytic hydration follows. Other explanations of the dormant period are sometimes advanced.

In any event, a few hours after rapid hydration recommences, sufficient hydration product is generated to induce setting, marking a conversion from fresh concrete (a dense suspension) to newly-hardened concrete (a porous viscoelastic solid). Except for air voids, the pores in the newly-hardened concrete are generally full or nearly full of solution, except in the case of low w:c concretes that undergo self-desiccation.

Some insight into the spatial arrangement of cement grains in fresh concrete can be derived from Fig. 2.2, kindly supplied by K.O. Kjellsen.[27] Figure 2.2 is a backscatter-mode SEM produced from a thin area of freshly-mixed w:c 0.40 fly ash-bearing mortar which was quick-frozen in liquid nitrogen shortly after being mixed. The quick-frozen specimen was sublimed to remove the frozen water, and then impregnated with epoxy resin to fill the space left by the water. The epoxy resin-stabilized preparation was then carefully polished and carbon coated for examination in backscatter SEM.

The smooth gray areas in Fig. 2.2 are sand grains. The spaces between them contain bright white unhydrated cement grains, some fly ash particles of varying gray levels, and black epoxy resin occupying the spaces originally filled with water. To the extent that the pre-existing grain assemblage was not perturbed, the black areas constitute the immediate 'ancestors' of most of the larger pores that will be present in the hardened mortar once it has set. As will be discussed later, the word 'most' is used deliberately. Unknown to Powers and Brownyard,[26] a substantial proportion of the larger pores in many concretes arise from space originally *within* certain cement grains, rather than from the originally water-filled space between them.

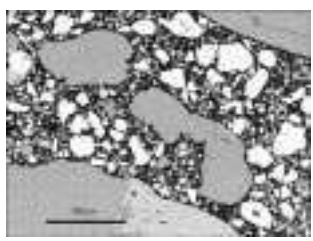

2.2 Backscatter SEM image of a freshly-mixed mortar, prepared by quick-freezing in liquid nitrogen, subliming off the frozen water, and impregnating with epoxy resin. The gray areas are sand, the white areas are cement grains, and the black areas are epoxy-filled spaces that were occupied by water in the fresh mortar. Figure kindly supplied by K. O. Kjellsen.[27]

Cement is usually ground to particle sizes ranging from ca. 80 μm down to ca. 1 or 2 μm. The particle sizes of the white cement grains seen in Fig. 2.2 are consistent with this expected range. The thickness of the black spaces separating them – which might be considered in the Powers-Brownyard[26] treatment as 'capillary pores to be' – range downward from ca. 20–30 μm.

Within concrete, once setting fixes the cement particles in place, the newly created and highly interconnected pores are also fixed in place. Subsequent hydration and deposition of cement hydration products progressively reduce the sizes and change the connections between the larger pores. These processes turn out to be complex geometrically as well as chemically and, contrary to the traditional assumption, they do not result in straightforward subdivision of the pore spaces.

2.4.3 Hydration modes and their consequences for pore structures

SEM examinations reveal that two distinct patterns of cement hydration may occur simultaneously in different cement grains near each other in the same concrete, leading to different consequences with respect to pore structure.

It is well established that the larger cement grains tend to hydrate inward from their outer boundaries, forming relatively dense 'inner products' of hydration.[8] These inner products were so designated because they are produced *within* the space marked by the original boundaries of the individual cement grains; the nomenclature was originally suggested by Taplin.[28] The inner products are primarily C-S-H. They can be readily recognized in backscatter SEM examination, and appear initially as thin gray layers around cores of white residual cement grains. As hydration proceeds, these thin layers become thicker and progress inward, sometimes irregularly in response to the varying internal arrangements of the different cement components within a particular cement grain. The residual unhydrated cement cores simultaneously shrink. In some cement grains the cores may eventually disappear entirely, except that often small bright 'shards' of C_4AF within them tend to resist hydration and may be preserved indefinitely. Within the same concrete, other residual cement cores may persist indefinitely, especially where local areas exist of high concentration of cement grains.

An example of a backscatter SEM showing these features is provided as Fig. 2.3. Figure 2.3 was taken in a relatively porous local area within a w:c 0.30 Portland cement paste hydrated for more than three months under sealed conditions. Examples of an inner product hydration shell, a residual unhydrated cement core, and a fully hydrated cement grain are indicated by arrows. It should be understood that the 'fully hydrated cement grain' is known to be fully hydrated only on the plane of observation; it may have had a residual core above or below the plane. In Fig. 2.3 about a dozen examples can be seen of residual

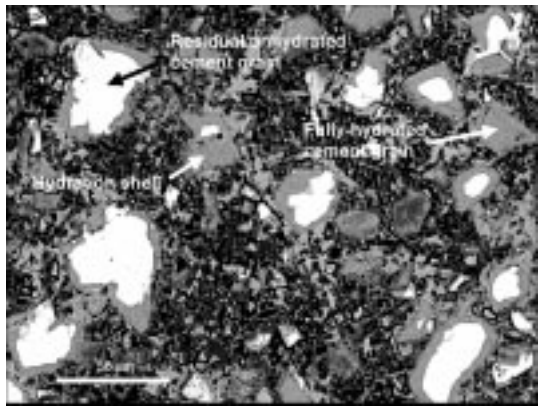

2.3 Backscatter SEM image of an area in a w:c 0.30 cement paste, illustrating inner product hydration of large cement grains and the porous groundmass surrounding them.

cores and their surrounding gray inner product hydration shells, and a number of apparently fully hydrated cement grains without cores can be seen.

How do these features impact on considerations of pore structure?

The original Portland cement grains are usually mostly non-porous clinker grains composed primarily of calcium silicates and aluminates. Hydration within the original cement grain boundaries – i.e. local conversion of the cement components to hydrated C-S-H within the grains – necessarily requires penetration of water into them. It also requires the development of internal space so as to accommodate the C-S-H product, which is much less dense than the cement components from which it is generated. Such space must have been produced by dissolution and removal of some portion of the cement substance within the zone that becomes the inner product shell.

Cement components so dissolved and removed from within this hydrated zone are precipitated as hydration products elsewhere, mostly (but probably not entirely) in the adjacent water-filled space. These deposits constitute the so-called 'outer products' of hydration;[8,28] they form a groundmass of smaller particles surrounding the larger cement grains and occupying the formerly water-filled space between them. These outer products can be seen in Fig. 2.3 as small particles of varying shades of gray. They contain mostly C-S-H, but also usually a significant content of calcium hydroxide, and some ettringite and monosulfate.

In Fig. 2.3 it can be seen that the groundmass areas are far from being entirely filled with deposited solids; many individual black epoxy-filled pores a few μm in size can be distinguished. The generally dark tone of much of the groundmass area reflects the presence in it of innumerable unresolved sub-μm-sized pore spaces.

The extent to which the groundmass space is filled with outer product deposits depends very much on the w:c ratio, which controls how much space

there is to fill, and on the progress of hydration. In low w:c concretes the expectation is that such deposits will eventually *almost* fill the space. The converse is true for high w:c concretes, in which the wider groundmass areas surrounding the large cement grains are expected to always retain significant pore space in large sizes.

Figure 2.3 was taken at a relatively low magnification, so as to show an area large enough to illustrate the various features present. One detail that cannot be seen in Fig. 2.3 is that the perimeters of the inner product grains and some of the particles within the groundmass have spiny protuberances. These spines were the 'Type I C-S-H' particles recorded in secondary electron images of fracture surfaces in the early days of SEM investigations. They can be seen in backscatter SEM, but require higher than normal resolution to resolve them.

Figure 2.4 was taken using a field emission backscatter SEM operated at low voltage[29] and, as such, is a higher-than-normal resolution image. The specimen was a w:c 0.40 paste hydrated for 28 days. In Fig. 2.4, 'A' marks the unhydrated core, 'B' the inner hydration product, 'C' the groundmass incorporating the outer hydration products and residual unoccupied space, and 'D' a monosulfate deposit within the groundmass. It is seen here that at high resolution the inner product is not as uniform as it appears, for example, in Fig. 2.3. The 'spiny' morphology is not well resolved around the inner product boundary, but it is clearly evident within the groundmass. Significant pore space is retained in the groundmass; within the small area depicted, there is one ca. 5 μm pore (containing a spiny C-S-H deposit within it), four or five less distinct pores of ca. 0.5 μm sizes, and innumerable ill-resolved smaller spaces.

The resolution of Fig. 2.4 is sufficient to hint at the existence of finely divided internal porosity within the inner product, but not to resolve the pores. The results of TEM examinations reported by Richardson[30] indicate that such

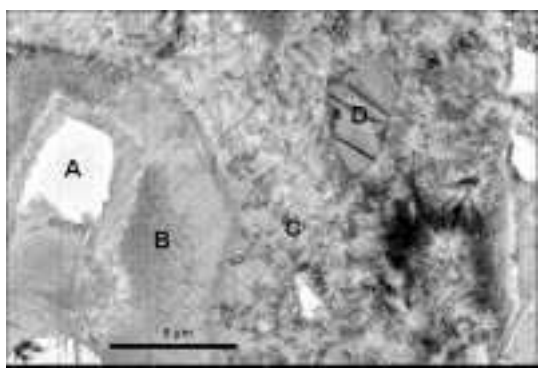

2.4 FE-SEM backscatter image of an hcp specimen showing an area around a single hydrating cement grain. 'A' is the residual unhydrated core, 'B' the inner product, 'C' the surrounding groundmass, and 'D' a deposit of monosulfate within the groundmass.

inner products typically contain extremely fine pores of diameters of the order of 10 nm. Such pores are far too small to resolve in backscatter SEM examination.

Thus at least two pore families of different origin exist: pores varying in size downward from multi-μm levels within the groundmass, and extremely fine (ca. 10 nm) pores within the inner product. The former is necessarily involved in water and ion movement through the paste; the latter almost certainly is not.

A further set of complications now needs to be considered. In contrast to the 'inner product' hydration pattern illustrated and described above, an entirely different local hydration pattern takes place for many smaller cement grains. The dividing line seems to be typically around 15 μm or so. With these smaller cement grains, a thin shell of hydration product is quickly deposited around the grains, but the shell does not get progressively thicker. Rather, the core within it proceeds to hollow out by progressive dissolution. The result is the production of partly or completely emptied out 'hollow shell grains', the so-called 'Hadley grains'.[31,32] These hollow shells enclose a class of pores in cement paste not known to Powers and Brownyard.[26]

The internal structure of these hollow grains can best be illustrated in high magnification secondary electron images of fracture surfaces, such as that of Fig. 2.5, which was taken many years ago by D.W. Hadley.[31] The particular hollow cement grain shell, about 10 μm in length, was adventitiously fractured in preparing the fracture surface specimen, thus permitting observation of the separation that has opened up between the shell and the core of unhydrated cement. The spiny feature of the outer C-S-H shell has been mentioned previously.

Figure 2.6, taken at relatively low magnification in backscatter SEM, illustrates the common occurrence of such hollow shells in archetypical concretes.

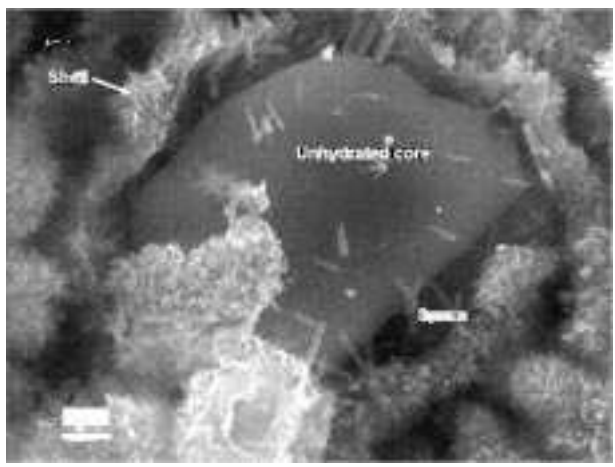

2.5 Secondary electron SEM image of an early-stage hollow shell grain. The shell was fractured adventitiously in preparing the fracture surface specimen. From Hadley.[32]

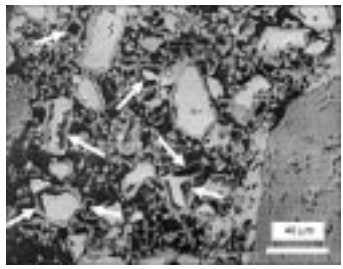

2.6 Backscatter SEM image from a porous area in a 3-day old w:c 0.45 concrete showing the local prevalence of hollow shell grains.

The specimen was a w:c 0.45 laboratory-mixed concrete hydrated for three days; the area imaged was relatively porous. White arrows point to some of the grains that are in the process of hollowing out, and to other, mostly finer grains, that are completely hollowed out.

These empty spaces within hollow shells constitute a class of pores of substantial sizes, ranging upward to ca. 15 μm. While the shells surrounding them may impede fluid and ion transport across these spaces, the shells must be presumed to be 'leaky' since they permit the transfer of dissolved cement components into the surrounding space during the hollowing out process.

The two modes of hydration, i.e. 'inner product' and 'hollow shell', are not necessarily entirely mutually incompatible. Indeed, Scrivener[33] considered that within large grains hydrating in the inner product mode, a solution-filled annulus of appreciable thickness separates the advancing layer of inner hydrated product from the retreating solid core. The present writer has not seen evidence for this concept in his own examinations.

Hollow shell pores are not confined to cement pastes or archetypical concretes. As indicated by Kjellsen and Helsing Atlassi[34] multi-μm-sized hollow shells are prominent in silica fume-bearing high performance concretes, often constituting the only pore space visible in an otherwise extremely dense microstructure.

A further peculiarity with respect to hollow shell pores is that some of them may be considered as only temporary pores. Deposition of secondary C-S-H may take place within some of them even at relatively young ages. Furthermore, as available and accessible open spaces, they are inevitably subject to subsequent deposition of later hydration products. Secondary deposits of C-S-H may eventually fill some of them up and, as shown by Kjellsen and Helsing Atlassi,[34] some hollow-shells may be eventually filled with CH deposits.

Figure 2.6 was taken in a relatively porous local area to facilitate presentation of the morphological features of the pore spaces. Cement pastes in archetypical concretes often contain such porous open areas, but also may contain relatively dense areas as well. An example is shown as Fig. 2.7, taken in a 28-day-old w:c 0.45 laboratory-mixed concrete. The groundmass is still definitely porous and

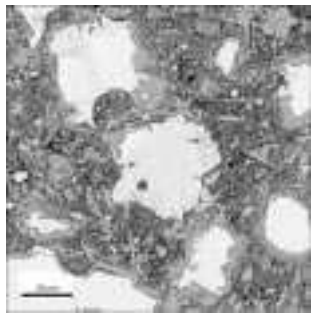

2.7 Backscatter SEM image showing a relatively dense groundmass area in a 28-day old w:c 0.45 concrete. Fine hollow shell grains and other pores are still visible.

hollow shell grains can still be picked out, but the general infilling of hydration products has reduced the sizes of the pores and the pore content significantly. This process continues as long as hydration proceeds; concretes permitted to hydrate indefinitely by continued availability of water may show very dense groundmass structures with still further reduced porosity, at least in some areas. The key clause in the preceding sentence was 'in some areas'. In many concretes, such dense areas of very limited porosity may border adjacent areas which display relatively large open pores and hollow shell grains. This irregular 'patchy' structure will be discussed in a subsequent section.

2.5 The question of gel pores

Pore structures surveyed so far include (1) air voids, typically tens or hundreds of μm in size; (2) hollow shell pores, usually roughly 3 to 15 μm in size, sometimes smaller; (3) groundmass spaces ('capillary pores') ranging from multi-μm sizes to sizes well below the resolution of backscatter SEM, and (4) extremely fine, ca. 10 nm-sized pores within inner hydration products. In this section a discussion is provided of presumably even finer '*gel pores*' that have long been considered to be present in hardened cement pastes.

The existence of gel pores in cement pastes was postulated by Powers and Brownyard[26] primarily on the basis of water vapor adsorption isotherms measured after drying thin paste specimens over hydrated magnesium perchlorate ('P-drying'); in each case they calculated BET surface areas from the adsorption isotherms. These experiments were carried out for cement pastes of different w:c ratios and of various degrees of hydration. Their results led Powers and Brownyard to infer that the product of hydration was a characteristic 'cement gel' of high surface area. The volume of water absorbed by this cement gel at high RH values was always found to be at least equivalent to four surface monolayers of condensed water. The spaces into which this 4-monolayer thickness of water was adsorbed were considered to constitute a set of characteristic

'gel pores' inherent in all normally cured (not steam cured) cement hydration products.

Water adsorbed in excess of four monolayers was believed to occupy empty space outside the boundary of the cement gel, and was termed 'capillary water'; the space occupied was termed 'capillary pore space'. Powers and Brownyard went on to provide the classic gel pore/capillary pore model that has been almost universally employed ever since. These authors estimated gel pores to be ca. 1 nm in size, based on hydraulic radius considerations; they considered that such pores occupy ca. 28% of the volume of the cement gel. Gel pore sizes have been re-assigned variously by succeeding authors.

Some years later Feldman and Sereda[35,36] carried out extensive water vapor sorption studies in compacts of dry cement which had been hydrated after being pressed together. Rather than drying their specimens first, they initially established desorption isotherms from the wet state, drying to various end points before beginning adsorption measurement. Various drying and wetting scanning loops were measured, and simultaneously these authors measured a number of physical and dimensional changes taking place in the hydrated compacts.

Their results led them to the conclusion that the ultimate structure of the C-S-H hydration products formed in cement hydration contained deformed nanometer-scale layer structures with interlayer spaces initially occupied by water. The interlayer spaces were thought to be only one or at most a few water monolayers thick. Water vapor could desorb from these deformed layer structures readily, but the structures were said to collapse when dried below 11% RH, i.e. as had been done as a preliminary step in the studies of Powers and Brownyard.[26] The collapsed layer structures were considered to be difficult or impossible to reopen in subsequent adsorption cycles, and Feldman and Sereda considered that water vapor surface areas measured by water vapor adsorption measurements after drying were incorrect.

These concepts would seem to negate those of Powers and Brownyard,[26] and indeed in their various publications Feldman and Sereda systematically declined to use the term 'gel pores'; the collapsible interlayer spaces were not really considered by them to be 'pores' at all.

Nevertheless, subsequent authors somehow have succeeded in fusing the two concepts. The cartoon originally published by Feldman and Sereda[36] to illustrate their concepts has been republished ad infinitum, but usually with the Powers and Brownyard model and its associated calculation of gel porosity also invoked in the same treatment.

It should also be remarked that these gel pores or collapsible interlayer structures, both thought to be 1 nm or less in size, are an order of magnitude smaller than the ca. 10 nm pores reported within inner hydration product by Richardson.[30] Whatever the ultimate resolution, it seems that neither gel pores, nor alternatively, deformed nanometer-scale layer structures, are likely to be significantly involved in fluid transmission in concrete.

2.6 Assessments of pore size distributions

It is evident from the current literature that mercury intrusion porosimetry (MIP) continues to be by far the most widely used method to evaluate the size distributions of pores in cement pastes and concretes.

It is most unfortunate that the MIP procedure, which is a simple, straightforward, highly reproducible experimental method, gives size distributions for hydrated cement materials that are badly flawed. Indeed, they are so badly flawed that the results obtained do not in any real sense reflect the actual sizes of the pores present.

Results of comparative examinations of the same cement pastes by MIP and by backscatter SEM image analysis[37] were published some years ago. For 28-day old w:c 0.40 pastes, substantial contents of pores were found in sizes between ca.10 μm and the lower measurement limit of 0.8 μm, corresponding to the pores seen directly in visual SEM examinations of the same specimens. MIP tallied the same pores, but in sizes almost entirely smaller than ca. 200 nm. Air voids, deliberately entrained in some of the pastes, were also tallied below 200 nm in the MIP results.

The problem with MIP, as indicated again in a more recent paper,[38] is that it is necessary for mercury intruding from the outside of a specimen to successively penetrate dozens (or hundreds) of restricted interstices on its inward path in order to reach the larger pores in the bulk of the interior of the specimen.

Figure 2.8 illustrates the concept of such restricted interstices along a flow path. The figure was originally published some years ago by Hearn *et al.*[39] to illustrate the effect of such interstices on water vapor transport, but it can just as well be applied to mercury intrusion penetration, with the understanding that MIP specimens are dried and the condensed water in the interstices has been evaporated. General penetration of mercury through a series of successive 'choke points', such as those shown in Fig. 2.8, will not occur until the necessary pressure is reached that corresponds to their size range. Once this 'threshold pressure' is reached, interior pores of all sizes (including air voids, as shown in Ref. 37) can be reached by mercury, and are filled indiscriminately as they are encountered by the incoming mercury front. In the MIP tally, they appear as sizes slightly smaller than the threshold diameter.

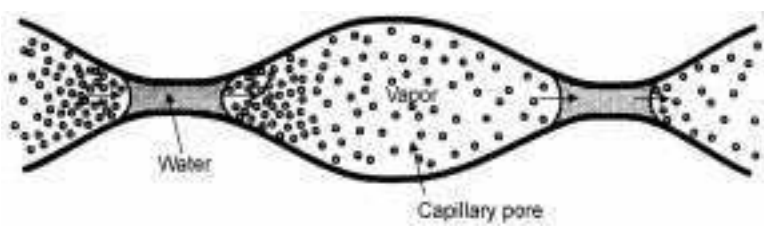

2.8 Cartoon illustrating the concept of restricted interstices or 'choke points' along a flow path for water vapor diffusive flow, from Hearn *et al.*[39]

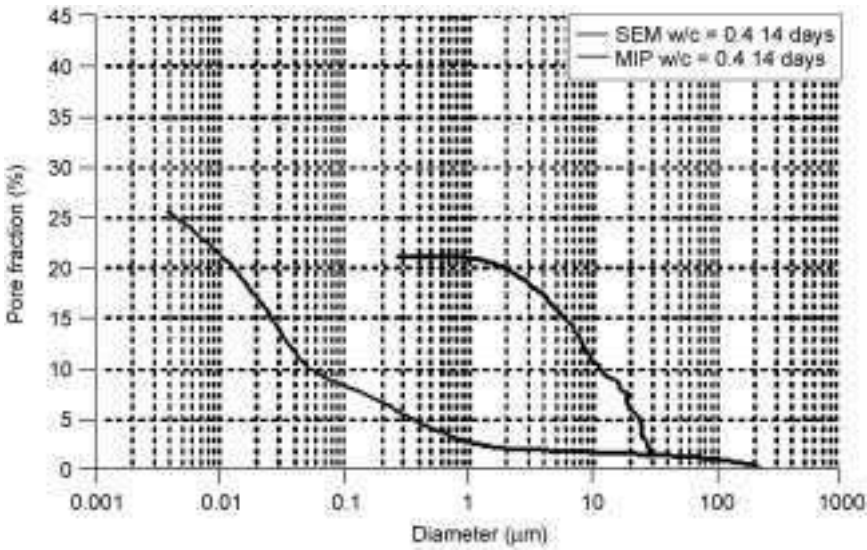

2.9 Comparison of pore size distribution obtained by backscatter SEM image analysis with MIP pore size distribution obtained on the same paste, from Ye.[40] The specimen was a w:c 0.40 paste hydrated for 14 days.

Some years passed before the experiments described in Ref. 37 were independently repeated.

Recently, Ye[40] conducted similar comparisons of MIP and image analysis pore size distributions at the Technical University of Delft. His findings fully confirmed the earlier results of Diamond and Leeman.[37] An example of Ye's results comparing pore size distributions measured by the two techniques for a 14-day old w:c 0.40 paste is given as Fig. 2.9.

These results confirm and emphasize that continued reliance on MIP for measurement of pore size distribution in cement pastes and concretes is not justified, as the sizes obtained by MIP are not even approximately correct.

MIP results do, however, provide two useful parameters. The value of the threshold diameter found in a given concrete provides a measure of the degree of restriction of access by mercury to the interior of the specimen. Assuming that the same restrictions also influence the movement of water and ions, the threshold diameter can provide a useful comparative measure of permeation capacity. Furthermore, the total pore space intruded by mercury at maximum pressure provides a useful comparative, albeit incomplete, indication of the total porosity of the specimen.

2.7 Spatial distribution of pores in concretes: the ITZ

Pores, especially the larger pores visible in backscatter SEM, are not distributed entirely uniformly within cement paste in concrete. One commonly discussed

aspect of this non-uniformity relates to the interfacial transition zone or ITZ; i.e. the local region of cement paste surrounding (and in contact with) sand and coarse aggregate grains.

Cement paste in concrete has been looked on by many authors as consisting of two distinct entities: 'bulk' cement paste removed from the local influence of sand or aggregates, and 'ITZ cement paste' close enough to the nearest aggregate to be affected by its presence. 'Close enough' has been frequently redefined, but it is generally taken as within 35 μm of the nearest aggregate. While various differences between the two 'cement pastes' can be detected by image analysis – especially in the contents of residual unhydrated cement – the important difference usually is considered to be the pore content, specifically the content of pores large enough to be tallied in backscatter SEM.

Scrivener[41] reported spatially-related backscatter SEM image analysis porosity data derived from Crumbie,[42] for a w:c 0.40 concrete evaluated at several ages. The *average* detectable pore content found in 'bulk' paste in the mature concrete was ca. 10%. Average pore contents reported for successive ITZ 'slices' taken progressively inward from the bulk paste to the aggregate interface itself were progressively larger as the aggregate was approached, and jumped remarkably for the innermost 5 μm-wide slice. This innermost slice adjacent to the aggregate was indicated as retaining as much as ca. 26% of SEM-detectable pores at 1 year.

Diamond and Huang,[43] studying a set of w:c 0.50 concretes, found slightly smaller average values for the 'bulk' paste porosity, and recorded much more modest increases as the aggregate surfaces were approached. Since the width of their slices was 10 μm as compared to the 5 μm slices in the data reported by Scrivener[41] no direct comparison for the innermost 5 μm slice was possible. However, extensive visual examinations of the areas immediately adjacent to the aggregates reported by Diamond and Huang[43] for their specimens showed only a limited content of detectable pores, and were not at all commensurate with the very high values reported by Scrivener.[41] Indeed, it was found that a significant portion of the areas immediately bordering aggregates were entirely blocked by $Ca(OH)_2$ layers deposited directly on the aggregate surface, and commonly extending 5 μm or more into the surrounding paste.

Elsharief *et al.*[44] recently reported average pore contents for a w:c 0.40 mortar (not a concrete) to be about 8% at maturity (180 days); the average pore content found for the innermost segments adjacent to the aggregates was ca.15% at maturity, higher than those reported by Diamond and Huang,[43] but very much lower than those reported by Scrivener.[41]

Diamond and Huang[43] called specific attention to the fact that whatever the average values, compilation of averages masked large variations in porosity among adjacent sampling units. Some adjacent segments at a given distance from the aggregate were highly porous; others were almost lacking in detectable pores. The general inhomogeneity of the interfacial zone ITZ has also been stressed by Scrivener[41] and others.

The possible effects of the existence of a more porous ITZ on various properties of concrete have been explored by a number of authors. A representative result was that of Delagrave *et al.*,[45] who found that the numerous ITZs in the mortar they studied had no measurable effect on the kinetics of leaching of calcium hydroxide. Many studies aimed at elucidating the effects of ITZs on permeation capacity-related properties similarly showed little or no effect. Summarizing some of them, Scrivener[41] concluded that, while the higher porosity in the ITZ might be expected to increase permeability, the presence of impermeable aggregate particles, around which the ITZs form, combined with the lower local w:c induced in the 'bulk' paste will work in the opposite sense; thus the increased porosity of the ITZ is of minor importance compared to other factors.

2.8 Spatial distribution of pores in concretes: local porous patches

The present writer has recently attempted to call attention to a feature observed in the microstructure of many concretes that appears to have been generally overlooked,[46–48] although it had been mentioned previously.[43] Some of the cement paste in many archetypical concretes consists of distinct patches or local areas that are visibly highly porous and contain few if any large cement grains; these are intermingled with other areas locally rich in large cement grains and exhibiting only limited pore space. An example is provided as Fig. 2.10, taken from a 28-day old laboratory mixed w:c 0.45 concrete.

Such areas (or 'patches') of sharply differing local porosity were found by the writer[46] in laboratory mortars prepared so as to duplicate those studied by Winslow *et al.*,[49] but not examined microscopically by them. MIP results from these mortars had previously been interpreted as indicating percolation of ITZs for mortars of high sand content. The present writer[46] suggested that in fact percolation of porous patches, rather than of ITZs, might explain the earlier MIP results.

The sizes of the individual porous patches vary, but are often of the order of 200 μm across; a roughly spherical patch of such dimensions in concrete would incorporate a paste volume of ca. $4 \times 10^6\ \mu m^3$.

In many cases the boundaries between adjacent dense and porous patches are seen to be surprisingly sharp. Figure 2.11 shows such a boundary, in a mortar specimen hydrated in limewater for about 7 years. The mortar depicted was actually one of those originally prepared by Winslow *et al.*;[49] part of it was sampled at 28 days for examination in MIP, and the remainder was stored in limewater. In 2003 the mortar was again sampled and examined in SEM.[46] It is seen that, while long-term hydration products have infilled the dense area to the right leaving few visible pores, the porous patch to the left has remained very noticeably porous despite the long underwater storage.

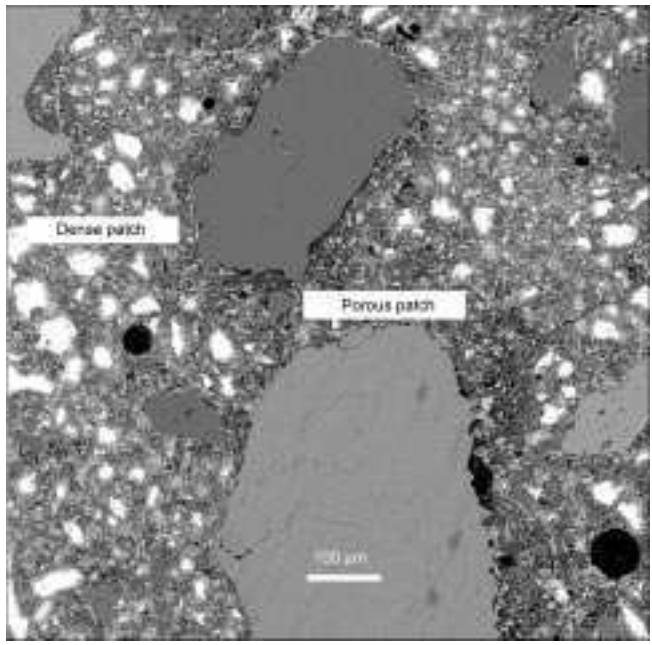

2.10 Example of porous and dense patches in a 28-day-old w:c 0.45 concrete.

While no quantitative study has been made, in the writer's experience the proportion of the porous patches is clearly higher for concretes with higher w:c ratios. For concretes of w:c ratios around 0.4, i.e. at the lower end of the archetypical concrete w:c ratio range, porous patches are relatively few in number and tend to be generally isolated from each other. In contrast, in many very high w:c ratio concretes examined by the writer, porous areas tend to predominate and appear to 'percolate'; local areas of dense paste, similar in appearance to the dense area in the right side of Fig. 2.11, are also found, but appear to be isolated from each other.

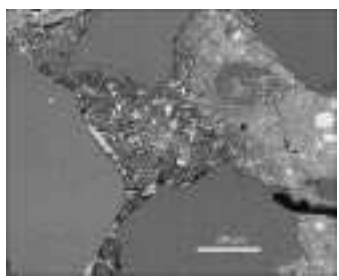

2.11 Sharp boundary between porous and dense areas in a w:c 0.45 mortar hydrated in limewater for approximately 7 years. Note the essentially complete filling of the pores in the dense paste to the right of the boundary.

Especially in lower w:c ratio concretes, many of the porous patches border on sand grains, as in the example shown in Fig. 2.10; however some apparently do not. Porous patches that border on sand grains extend far beyond even the widest estimate of the extension of conventional ITZs. It should be noted that sizes of such porous patches are of the same general order of magnitude as the spacings between many sand grains in concretes.

It should be mentioned that recently Wong and Buenfeld[50] questioned the existence of dense and porous patches, attributing their appearance in back-scatter SEM to an artifact associated with incomplete penetration of the epoxy resin used in backscatter SEM. The present writer[51] and Diamond and Thaulow[52] have demonstrated that this suggestion was incorrect. While the existence of complementary porous and dense patches have been observed by the present writer primarily in backscatter SEM, they are also readily observable in secondary electron SEM examination of polished surfaces, and in fluorescent optical microscopy of thin sections.

Furthermore, several years ago, Landis[53] prepared a conventionally mixed w:c 0.6 mortar using a fine concrete sand (maximum size of about 0.4 mm). A portion of the mortar was cast as a 4 mm diameter cylinder and moist cured for about 30 days, and then air-dried for a like period. A small chip was broken off and exposed to a synchrotron beam line at the National Synchrotron Light Source at Brookhaven National Laboratory, so as to generate data for computed tomography imaging. The results were kindly provided to the present writer in the form of a series of approximately 500 successive resolved images, each 1.2 μm apart. The in-plane resolution was also 1.2 μm per pixel.

Figure 2.12 shows one of these slices. The larger, mostly uniform gray features are sand grains. The individual smaller white particles are clearly residual unhydrated cement cores, surrounded by groundmass. It is seen that the lower left corner of the mortar chip (marked 'A') constitutes a dense patch

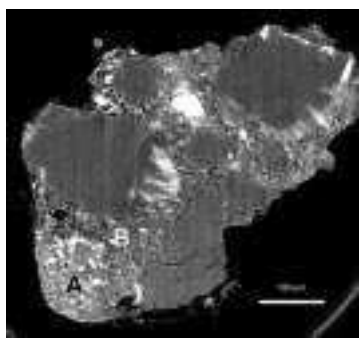

2.12 Computed tomographic image of a plane from a three-dimensional image of an air dried w:c 0.45 mortar, provided by Landis.[53] The lower left corner area ('A') constitutes a dense patch, with a porous patch ('B') separating it from the sand grain above it.

containing closely-spaced unhydrated cement grain cores. Above and slightly to the right of this patch, and sharply delineated from it, is a region of more visibly porous paste containing almost no unhydrated cement. This delineation of a dense patch – porous patch structure in Landis's mortar specimen is of particular interest since the examination involved no specimen preparation, and thus no specimen preparation artifacts are possible.

So far as the writer knows, perhaps the first clear published recognition of the existence and potential importance of such local patches in field concrete was provided by Idorn,[54] on the basis of observations made in fluorescent thin section examinations of a deteriorating marine concrete. The concrete appeared to have an overall w:c ratio of ca. 0.45, but Idorn observed distinct porous and dense patches of wildly different apparent local w:c ratios, as indicated by local intensity of the fluorescence. He estimated that the porous patches exhibited local w:c ratios tending toward 1.0; in contrast, the dense patches appeared to exhibit local w:c ratios of only about 0.20.

Idorn[54] considered that the patchy structure derived from porous and dense 'micropatches' that had previously existed in the fresh concrete. Close examination of backscatter SEM images of the freshly mixed mortars prepared by Kjellsen,[27] one of which was shown as Fig. 2.2, appears to support this idea. Examination of Fig. 2.2 suggests the grouping of large cement grains into local areas, leaving what appear to be other areas of higher local water content that are almost devoid of such cement grains.

Such considerations imply the possibility that the local patches may simply be due to inadequate mixing. However, in a trial to specifically investigate this hypothesis, it was found[48] that long-continued mixing of fresh concrete in an efficient pan mixer apparently did not succeed in eliminating the local patches. Furthermore, a recent trial[55] indicated that, surprisingly, complete dispersion of fresh concrete induced by an extremely heavy dose of superplasticizer did not eliminate them either.

The possible implications of these findings with respect to concrete permeation capacity and durability concerns remain to be established. Idorn[54] specifically attributed the deterioration of the marine concrete he examined to the easy entry of external ions through the porous patches. The degree to which local porous patches exist and might connect in the three dimensional structure of ordinary concretes is certainly worth exploring.

2.9 Measurement of permeation capacity-related parameters in archetypical concretes

2.9.1 Introduction

The general notion of permeation capacity and its importance with respect to concrete durability has been introduced previously. In this section, some of the

several measurements employed to quantify different aspects of permeation capacity in concretes are briefly discussed.

These various techniques quantify the ability of a given concrete to transmit liquid water, water vapor, electrical current, or ions primarily through the pores within the concrete binder. Obviously this ability depends on the sizes of the pores, and on the degree to which the larger pores are effectively interconnected. A high degree of interconnectedness between the large pores is often referred to in the literature as 'percolation'; its gradual elimination by progressive hydration constitutes 'depercolation'. It is often suggested that in depercolation the larger pores are effectively isolated so that the only remaining connections between them are through 'gel pores'. The present writer considers this most unlikely, in the light of his prior discussion of the concept of gel pores. The idea of progressively narrower 'restricted interstices', as diagrammed in Fig. 2.8, seems much more reasonable.

2.9.2 Permeation capacity as measured by water permeability

The classical measure of permeation capacity in concrete is *permeability*, i.e. the measure of the rate of mass transfer of water under a given pressure head, once steady-state flow has been established. The concept is straightforward, but experimental measurement is difficult for most concretes. The disparity of values found in replicate measurements is often appreciable, and the general scatter of the results is unfortunately very high.[39] The usual range in values for reasonably mature archetypical concretes is of the order of 10^{-12}–10^{-14} m/s; lower values are obtained for concretes with supplementary cementing components.

Permeability values generally decrease with increasing hydration, as would be expected; they are also reported to show reductions with time during a particular test,[39] which is somewhat disconcerting.

2.9.3 Permeation capacity as measured by DC electrical conductivity

Several different measures of permeation capacity involve the ability of concrete specimens to transmit direct current.

Of these methods, the so-called 'chloride permeability' measurement is by far the most widely used, and is generally familiar to concrete researchers and technologists in North America and elsewhere. Standardized as ASTM Method C1202-97,[56] the measurement quantifies the total passage of current (in coulombs) during a six-hour period across a 50 mm-thick slice of saturated concrete in contact with NaCl and NaOH electrode solutions; the voltage is maintained throughout the test at 60 volts DC. The range of values for archetypical concretes (as measured at the 28 days specified in the standard) is between ca. 6000 coulombs and ca. 1500 coulombs, depending mostly on w:c

ratio. Like water permeability, the measured coulomb values are smaller for concretes of lower w:c ratios, and smaller yet for concretes incorporating supplementary cementing components. Concretes tested periodically as hydration proceeds show progressive reductions in the coulomb values measured.

The method is rapid and fairly reproducible, but the high voltage used produces heating effects in the more permeable concretes that lead to complications. The procedure was originally developed to provide a means to rank the effectiveness of different treatments designed to prolong the service life of bridge deck concretes against steel corrosion; it was not specifically designed to measure either electrical conductivity or chloride diffusivity per se.

More fundamental electrical measurements of permeation capacity in concretes have been developed over the last 25 years. Early work by Whittington *et al.*[57] provided a basis for understanding the principles of electrical conduction in concrete. It was shown that electrical conductivity was almost entirely dependent on the conductivity of the cement paste binder and, as expected, was found to be higher for higher w:c ratio concretes; conductivity decreased with time as the binder became more impermeable with continued hydration.

Christensen *et al.*[58] later summarized the principles involved in the conduction of current through the cement paste binder phase. 'Bulk' paste conductivity was generally found to be several orders of magnitude smaller than the conductivity of the alkali hydroxide pore solution within it. The governing relationships were expressed as the joint product of three factors: the conductivity of the pore solution; the effective volume fraction of current-carrying 'capillary pores' in the paste; and a 'β factor', which constitutes an inverse measure of the tortuosity of these current-carrying channels. While the conductivity of the expressed pore solution may increase slightly as hydration proceeds, this is outweighed by the reduction in the effective volume of pores through which ions carrying the current can pass, and especially by the increase in the tortuosity of the flow path (reducing 'β'). The net result is that electrical conductivity progressively reduces with hydration, paralleling the reduction shown in other methods of measuring permeation capacity.

DC conductivity thus can serve as a convenient index of permeation capacity of a concrete, especially if its pore solution conductivity can be established or estimated.

These ideas have been recently applied by Nokken and Hooton[59] to formulate a procedure for the routine measurement of permeation capacity by measuring DC conductivity, with the goal of providing a basis for concrete durability specifications. Their procedure used the widely available ASTM C1202-97 apparatus and specimen configuration, but details of the measurement differed significantly from those of the ASTM procedure. To avoid heating effects, the voltage was reduced to 15 volts and the measurement time to 15 minutes; and 0.3M NaOH was used to provide electrical contact at both concrete faces. Bulk

electrical conductivity values measured this way for archetypical concretes ranged from roughly 800 mS/cm for permeable concretes to ca.100 mS/cm for impermeable ones. Values for silica fume and fly ash-bearing concretes were lower.

Concrete pore solutions were expressed and analyzed by Nokken and Hooton,[59] and solution conductivities were calculated for them by the method of Snyder *et al.*[9] It was found that, while the pore solution conductivities were several orders higher than the bulk conductivities, normalizing the latter values (i.e. them dividing by the solution conductivity) provided only slightly better correlation with water permeability and other measures of permeation capacity than did the raw bulk conductivity values.

2.9.4 Permeation capacity measurements derived from AC complex impedance spectra

Much of the focus of research on electrical property measurements of concretes (or more commonly, cement pastes) has involved the development and interpretation of AC complex impedance spectroscopy ('ASIC') procedures. These developments were summarized by Christensen *et al.*[58] Such methods provide much more sophisticated assessments of electrical conductivity for cement pastes, and shed light on various related factors such as dielectric behavior and properties linked to ion diffusivities. Recent treatments of the subject and its relationship to pore parameters in concrete have been provided by McCarter *et al.*[60] and by Beaudoin and Marchand.[61]

2.9.5 Permeation capacity as measured by water vapor transport

Measurements of water vapor transport through concrete has been mentioned briefly in the introduction of the concept of permeation capacity, and the peculiarity inherent in the transport of water vapor through partly dry specimens was illustrated in Fig. 2.8.

An ASTM standard test method for water vapor transmission of materials (ASTM E96-00)[62] specifies a method to measure the rate of water vapor transmission across a unit thickness of material as driven by vapor pressure differences maintained between the two surfaces of the material. The method is not specifically designed for concrete, and does not consider the degree of saturation of the specimen itself; this is obviously a controlling factor with partly dry concrete. A somewhat similar but more flexible ISO specification[63] was designed for building materials in general. It provides for water vapor transport measurements under several different boundary conditions, and it further specifies that the specimen be conditioned to 50%RH.

Using a variant of one of the ISO methods, Nilsson[64] has measured long-term water vapor diffusion coefficients for very mature concretes, but only between boundary conditions of 65% RH and 100% RH. Moisture diffusion coefficients showed the expected dependency on w:c ratio. As expected, moisture diffusion coefficients were found to be substantially lower for concretes with silica fume, and were especially low for concretes containing both silica fume and fly ash.

Somewhat similar studies were carried out by Jooss and Reinhardt,[65] but in this case the study was focused on effects of increasing temperatures. Higher temperatures were found to increase diffusion coefficients substantially. In their analyses, Jooss and Reinhardt[65] formally recognized the separate contributions to the observed diffusion coefficients by diffusion through the unfilled pores and by liquid transport through the filled 'choke points' such as was illustrated in Fig. 2.8, but were unable to break down the overall flow into the separate components. This is a fundamental problem that apparently remains to be solved.

2.9.6 Permeation capacities as measured by ion diffusivities

Another important (albeit extremely complex) aspect of permeation capacity in concrete involves measurement of ion diffusivities. Diffusion coefficients of specific ions, principally Cl^- ions, have been studied for many years, primarily in connection with estimating the time that a given concrete cover will protect reinforcing steel against chloride-induced corrosion (as discussed in further detail in Chapter 5). Typical values quoted for Cl^- ion apparent diffusion coefficients in archetypical concretes are of the order of ca. 2×10^{-12} to ca. 10×10^{-12} m^2/s.[23] As might be expected, diffusion coefficients are lower for lower w:c ratio concretes, and again, still lower values are typically found for concretes with substantial contents of fly ash, silica fume, or slag.

As pointed out by Delagrave *et al.*,[66] the specific ion diffusion coefficient values obtained depend very much on the particular method of measurement and calculation procedure used. However, each of the methods surveyed by these authors is sensitive to differences in concrete microstructure, and it was suggested that any of them could serve as a measure of permeation capacity in the sense used in this chapter.

It was pointed out by these authors, however, that ions do not diffuse independently; interactions occur between different types of ions diffusing simultaneously, as well as with the microstructure. As might be expected, interactions with the microstructure are more severe at low w:c ratios, and when components such as silica fume are present.

Much current effort is underway to mathematically describe ion migration as part of the more general processes of ionic transport. A general method for doing so for all ions, based on migration test results, was recently provided by Samson *et al.*[67]

2.10 Future trends

As mentioned in the introduction, in the present chapter the writer has deliberately confined himself to findings based on experimental evidence, rather than on modeling. The bases of at least some of the current models seem to him overly unrealistic in terms of their representations of the features found in concrete.

However, he sees as a future trend a progressive development of more realistic models, based on keener appreciations of actual microstructures in concrete, and of how the microstructural features actually control the transport processes involved in permeating water, ions, etc. through them. Anticipated further increases in computer power and speed would presumably be helpful in facilitating such developments.

Another future trend that may be realized is the ability to visualize the actual, three-dimensional structure of cement paste – including pores – in concretes, by computed tomographic methods at a resolution fine enough to be definitive. As was indicated earlier, computed tomography renderings can currently be produced at voxel sizes close to 1 μm, and at dynamic ranges adequate to distinguish cement grains and at least the coarser pores. Potential improvements in resolution (and dynamic range) for computed tomography could provide three dimensional information with much the same level of detail as is provided by current backscatter SEM. Meanwhile, improvements in SEM instrumentation should certainly provide the facility for more detailed two-dimensional study of pores and other microstructural features.

In particular, it is hoped that some combination of computed tomography, higher resolution SEM capability, and realistic modeling will clarify details that govern permeation in actual concretes.

2.11 Sources of further information and advice

A useful but somewhat dated review covering permeability and many of the permeation capacity-related processes considered here was provided by Hearn *et al.*[39]

In general, however, references relating to the structures and properties discussed in this chapter are unfortunately widely dispersed in the journal and conference proceedings literature. Much of the journal literature is becoming available via on-line access, but unfortunately that is not generally true of conference proceedings, which are often difficult to obtain.

The relevant technical journals include *Cement and Concrete Research*, *Cement and Concrete Composites*, *Materials and Structures*, and others less commonly cited.

The use of backscatter SEM to characterize the microstructures of concretes was featured in a recently published special issue of the journal *Cement and Concrete Composites.*[68]

2.12 Acknowledgments

The writer is deeply indebted to K.O. Kjellsen, Eric Landis, and Guang Ye for permitting the inclusion of certain of their unpublished results, and to many colleagues who so kindly and patiently responded to requests for specific information in certain special areas.

2.13 References

1. Powers, T.C., Copeland, L.E., Hayes, J.C. and Mann, H.M., 'Permeability of Portland cement paste', *J Amer Concr Inst* 1954 **51**(11) 285–298.
2. Barneyback, R.S., Jr. and Diamond, S., 'Expression and analysis of pore fluids from hardened cement paste and mortars', *Cem Concr Res* 1981 **11**(2) 279–285.
3. Penko, M., 'Some early hydration processes in cement paste as monitored by liquid phase composition measurements', Ph.D. thesis, Purdue University, 1983.
4. Ong, S., 'Studies on effects of steam curing and alkali hydroxide additions on pore solution chemistry, microstructure, and alkali silica reaction', Ph.D. Thesis, Purdue University, 1993.
5. Diamond, S., 'ASR – Another look at mechanisms', Proc 8th Intl Conf Alkali Aggregate Reaction, Kyoto 1989 83–94.
6. Brouwers, H.J.H and van Eijk, R.J., 'Alkali concentrations of pore solutions in hydrating OPC', *Cem Concr Res* 2003 **33**(2) 191–196.
7. Rothstein, D., Thomas, J.J., Christensen, B.J. and Jennings, H.M., 'Solubility behavior of Ca-, S-,Al-, and Si- bearing solid phases in Portland cement pore solutions as a function of hydration time', *Cem Concr Res* 2002 **32**(10) 1663–1671.
8. Taylor, H.F.W., *Cement Chemistry*, 2nd edn, London, Thomas Telford, 1997.
9. Snyder, K.A., Feng, X, Keen, B.D., and Mason, T.O., 'Estimating the electrical conductivity of cement paste pore solutions from OH^-, K^+, and Na^+ concentrations', *Cem Concr Res* 2003 **33**(6) 793–798.
10. Diamond, S., 'The effects of two Danish fly ashes on alkali contents of pore solutions of cement-fly ash paste', *Cem Concr Res*, 1981 **11**(3) 383–394.
11. Duchesne, J. and Bérubé, M.-A., 'The effectiveness of supplementary cementing materials in suppressing expansion due to ASR: Another look at the reaction mechanisms, part 2: Pore solution chemistry', *Cem Concr Res*, 1994 **24**(2) 221–230.
12. Diamond, S. and Lopez-Flores, F., 'Comparative studies of the effects of lignitic and bituminous fly ashes in hydrated cement systems', *Effects of Fly Ash Incorporation in Cement and Concrete*, Proc MRS Symposium, Pittsburgh, Materials Research Society, 1981 112–123.
13. Shehata, M.H., Thomas, M.D.A. and Bleszynski, R.F., 'The effect of fly ash composition on the chemistry of pore solution', *Cem Concr Res* 1999 **29**(12) 1915–1920.
14. Diamond, S., 'Effect of microsilica (silica fume) on the pore solution chemistry of cement paste', *J Amer Ceram Soc* 1983 **66**(5) 82–84.
15. Kawamura, M., Takemoto, K. and Hasaba, S., 'Effectiveness of various silica fumes in preventing alkali-silica expansion', 1987 *Amer Concr Inst Special Publication* SP-100, 1992, 1810–1819.
16. Duchesne, J. and Bérubé, M.-A., 'Long-term effectiveness of supplementary cementing materials against alkali silica reaction', *Cem Conc Res* 2001 **31**(7) 1057–1063.

17. Shehata, M.H. and Thomas, M.D.A., 'Use of ternary blends containing silica fume and fly ash to suppress expansion due to alkali-silica reaction in concrete', *Cem Concr Res* 2002 **32**(3) 341–349.
18. Matsukawa, K. and Diamond, S. 'Quantitative study of naphthalene sulfonate effects on cement paste pore solution chemistry', in 'Advances in Cement Materials', *Ceramic Transactions* 1991 **16**, 41–55.
19. Constantiner, D. and Diamond, S., 'Fixation of alkalis in cement pore solutions', in *Mechanisms of Degradation of Cement Based Systems*, London, E & FN Spon 1997 67–74.
20. Rivard, P., Bérubé, M.-A., Ballivy, G., and Ollivier, J.P., 'Effect of drying–rewetting on the alkali concentration of the concrete pore solution', *Cem Concr Res* 2003 **33**(6) 927–929.
21. Page, C.L. and Vennesland, G., 'Pore solution composition and composition and chloride binding capacity of silica fume cement pastes', *Mater Struct* 1979 **16** (919) 19–25.
22. Nixon, P.J., Canham, I., Page C.L.and Bollinghouse, R., 'Sodium chloride and alkali aggregate reaction', Proc. 7th Intl Conf. Alkali Aggregate Reactions, Ottawa 1987 110–118.
23. Bentur, A., Diamond, S. and Berke, N.S., *Steel Corrosion in Concrete*, London, E and FN Spon, 1997.
24. Chatterji, S., Thaulow, N., Jensen, A.D. and Christiansen, P., 'Mechanism of accelerating effect of NaCl and $Ca(OH)_2$ on alkali silica reaction', Proc 7th Intl Conf Alkali Aggregate Reactions, Ottawa 1987.
25. Kawamura, M., and Kimatsu, S., 'Behavior of various ions in pore solutions in NaCl-bearing mortars with a reactive aggregate at early ages', *Cem Concr Res* 1997 **27**(1) 29–36.
26. Powers, T.C. and Brownyard, T.L., 'Studies of the physical properties of hardened cement paste', Bulletin 22, Research Laboratories of the Portland Cement Association, Chicago, 1948.
27. Kjellsen, K.O., personal communication Feb. 2005.
28. Taplin, J.H., 'A method for following the hydration reaction in Portland cement paste', *Australian J Appl Sci* 1959 **10** 329–345.
29. Diamond, S. and Kjellsen, K.O., 'Resolution of fine fibrous C-S-H in backscatter SEM examination', *Cem Concr Composites* 2006 **28** 130–132.
30. Richardson, I.G., 'The nature of C-S-H in hardened cements', *Cem Concr Res* 1999 **29**(8) 1131–1147.
31. Hadley, D. W., 'The nature of the paste-aggregate interface', Ph.D. Thesis, Purdue University, 1972.
32. Hadley, D.W., Dolch, W.L., and Diamond, S., 'On the occurrence of hollow-shell hydration grains in hydrated cement paste', *Cem Concr Res* 2000 **30**(1) 1–6.
33. Scrivener, K.L., 'Backscattered electron imaging of cementitious microstructures: understanding and quantification', *Cem Concr Composites* 2004 **26**(8) 935–945.
34. Kjellsen, K.O. and Helsing Atlassi, E., 'Pore structure of cement-silica fume systems: presence of hollow-shell pores', *Cem Concr Res* 1999 **29**(1) 133–142**.**
35. Feldman, R.F. and Sereda, P., 'A model for hydrated Portland cement paste as deduced from sorption – length change and mechanical properties', *Mater Struct* 1968 **1**(6) 509–520.
36. Feldman, R.F. and Sereda, P., 'A new model of hydrated cement and its practical implications', *Engineering Journal, Canada* 1970 **53** 53–59.
37. Diamond, S and Leeman, M.E., 'Pore size distributions in hardened cement pastes

by SEM image analysis', MRS Symposium Proc. V. 137, *Microstructure of Cement Based Systems*, Pittsburgh, PA, Materials Research Society, 1989 217–226.
38. Diamond, S., 'Mercury porosimetry: An inappropriate method for the measurement of pore size distributions in cement-based materials', *Cem Concr Res* 2000 **30**(10) 1517–1525.
39. Hearn, N., Hooton, R. D. and Mills, R.H., 'Pore structure and permeability', in *ASTM STP 169C, Significance of tests and properties of concrete and concrete making materials*, Philadelphia, ASTM Intl., 1994 240–262.
40. Ye, G., 'The microstructure and permeability of cementitious materials', Ph.D. Thesis, Technical University of Delft, 2003.
41. Scrivener, K.L., 'Characterization of the ITZ and its quantification by test methods', in *Engineering and Transport Properties of the Interfacial Transition Zone in Cementitious Composites*. Report 20, Paris, RILEM Publications SARL, 1999 3–15.
42. Crumbie, A.K., 'Characterization of the microstructure of concrete', Ph.D. Thesis, Univ. of London, 1994.
43. Diamond, S. and Huang, J., 'The Interfacial Transition Zone: Reality or Myth?', in Proc. 2nd Intl. Conf. on the Interfacial Zone in Cementitious Composite, Haifa (1998), London, E. and F. Spon, 1998 3–39.
44. Elsharief, A., Cohen, M.D., and Olek, J., 'Influence of aggregate size, water cement ratio and age on the microstructure of the interfacial transition zone', *Cem Concr Res* 2003 **33**(11) 1837–1849.
45. Delagrave, A., Marchand, J., and Pigeon, M., 'Influence of the interfacial transition zone on the resistance of mortar to calcium leaching', in *Engineering and Transport Properties of the Interfacial Zone in Cementitious Composites, Report 20, Paris, RILEM Publications S.A.R.L., 1999 103–113.*
46. Diamond, S., 'Percolation due to overlapping ITZs in laboratory mortars? A microstructural evaluation', *Cem Concr Res* 2003 **33**(7) 949–955.
47. Diamond, S., 'The patchy structure of cement paste in conventional concretes', in *Concrete Science and Engineering: A Tribute to Arnon Bentur*, RILEM PRO 36, Paris, RILEM Publications S.A.R.L., 2004 85–94.
48. Diamond, S., 'The patch microstructure in concrete: the effect of mixing time', *Cem Concr Res* 2005 **35**(5) 1014–1016.
49. Winslow, D.N., Cohen, M.D., Bentz, D.P., Snyder, K.A. and Garboczi, E.J., 'Percolation and pore structures in mortars and concrete', *Cem Concr Res* 1994 **24**(1) 25–37.
50. Wong, H.S. and Buenfeld, N.R., 'Patch microstructure in cement-based materials: Fact or artefact', *Cem Concr Res* 2006 Corrected Proof available on-line 6 March 2006.
51. Diamond, S., 'A discussion of paper ''Patch microstructure in cement based materials: Fact or artefact'' by H.S. Wong and N.R. Buenfeld', *Cem Concr Res* 2006 Corrected Proof available on-line 6 March 2006.
52. Diamond, S. and Thaulow, N., 'The patch microstructure in concrete: evidence that it exists and is not a backscatter SEM artifact', C*em Concr Composites* 2006 **28**(7) 606–612.
53. Landis, E., personal communication, June 2005.
54. Idorn, G.M., 'Marine concrete technology', *J Coastal Res* 1991 **7**(4) 1043–1056.
55. Diamond, S., 'The patch microstructure in concrete: the effect of superplasticizer', 2006 *Cem Concr Res* **36** (4) 776–779.
56. ASTM Method C 1202-97, 'Standard test method for electrical indication of a concrete's ability to resist chloride ion penetration', Philadelphia, ASTM

International, 1995.
57. Whittington, H.W., McCarter, J. and Forde, M.C., 'The conduction of electricity through concrete', *Mag Concr Res* 1981 **33**(114) 48–60.
58. Christensen, B.J., Coverdale, R.T., Olsen, R.A., Ford, S.J., Garboczi, E.J., Jennings, H.M., and Mason, T.O., 'Impedance spectroscopy of hydrating cement-based materials: measurements, interpretations, and application', *J Amer Ceram Soc* 1994 **77**(11) 2789–2804.
59. Nokken, M. and Hooton, D.R., 'Development of early age impermeability in high-performance concretes', Proc. PCI-FHWA Intl. Symp. On High Performance Concretes, Orlando, FL, 2003.
60. McCarter, W.J., Starrs, G. and Chrisp, T.M., 'Electrical monitoring methods in cement science', in *Structure and Performance of Cements*, 2nd edn, London, E and F Spon Press, 2002, 442–456.
61. Beaudoin, J.J. and Marchand, J., 'Pore structure', Chapter 14 in *Handbook of Analytical Techniques in Concrete Science and Technology*, New York, Noyes Publications 2001 528–628.
62. ASTM Method E 96-00, 'Standard test method for water vapor transmission of materials', Philadelphia, ASTM International, 2000.
63. ISO International Standard 12572-2001E, 'Hygrothermal performance of building materials and products – determination of water vapor transmission properties', Geneva, ISO, 2001.
64. Nilsson, L.-O, 'Long-term moisture transport in high performance concrete', *Mater Struct* 2002 **33** 641–649.
65. Jooss, M and Reinhardt, H.W., 'Permeability and diffusivity of concrete as a function of temperature', *Cem Concr Res* 2002 **32**(9) 1497–1504.
66. Delagrave, A., Marchand, J. and Samson, E., 'Prediction of diffusion coefficients in cement-based materials on the basis of migration experiments', *Cem Concr Res* 1996 **26**(12) 1831–1842.
67. Samson, E., Marchand, J. and Snyder, A., 'Calculation of ionic diffusion coefficients on the basis of migration test results', *Mater Struct* 2003 **36**(257) 156–165.
68. Special Issue: Scanning Electron Microscopy of Cements and Concretes', *Cem Concr Composites* 2004 **26**(8) 917–1013.

3

Dimensional stability and cracking processes in concrete

J J BROOKS, formerly University of Leeds, UK

3.1 Introduction

To calculate the long-term deformation and deflection of structural concrete members for their design life, the relations between stress, strain, time and temperature are required. In common with other engineering materials, concrete deforms almost elastically when a load is first applied, but under sustained load, the deformation increases with time at a gradually reducing rate under normal environmental conditions. Timber behaves in a similar manner, whereas steel only creeps under very high stress at normal temperature or under low stress at very high temperature. With all engineering materials, dimensional instability can occur at high loads in the form of a time-dependent failure or creep rupture, but this can be avoided with concrete if stresses are kept below approximately 60% of the short-term strength. Elasticity and creep are considered in Sections 3.2.1 and 3.2.4, respectively.

In addition to deformation caused by the applied stress, time-dependent volume changes due to shrinkage (or swelling) and temperature variation of concrete are of considerable importance because they can contribute significantly to elasticity and creep of concrete members in assessing the total time-dependent deformation. There are different types of shrinkage, the most common being drying shrinkage, the rate of which gradually reduces with time. Like creep, drying shrinkage is associated with the movement of gel water within and from the hardened cement paste. Shrinkage and temperature movement are discussed in Sections 3.2.3 and 3.2.5, respectively.

In other practical cases, movements are often partly or wholly restrained thereby inducing tensile stress, the level of which needs to be minimised to avoid cracking. Concrete is of course very weak in tension so that cracks must be avoided or controlled as they can impair durability as well as structural integrity, besides being aesthetically undesirable. The subject of non-structural or intrinsic cracking processes, as opposed to structural cracking associated with external loading, is dealt with in Section 3.3. First, the different types of cracks are described (3.3.1) then plastic shrinkage cracking (3.3.2), followed by early-

age thermal cracking (3.3.3), types of restraint (3.3.4 and 3.3.5) and drying shrinkage cracking (3.3.6). Theoretical aspects of cracking are summarised under fracture mechanics in Section 3.3.7, which precedes Future trends and suggested further information (3.4), and finally References (3.5).

3.2 Dimensional stability

Short- and long-term deformations of concrete are influenced by many factors and the following sections consider the main ones related to four types of deformations: elastic strain, creep, shrinkage and thermal movement. The deformations are treated independently of each other, which may not be fundamentally correct but that approach has been used historically and is the basis on which prediction methods in Codes of Practice have been developed.

3.2.1 Elasticity

The definition of *pure elasticity* is that strains appear and disappear on application and removal of stress. The elastic properties of engineering materials fall into four categories, as illustrated in Fig. 3.1, which show two categories of pure elasticity: (a) linear and elastic and (b) non-linear and elastic. In both cases, the ascending curve coincides with the descending curve. The other two categories are: (c) linear and non-elastic and (d) non-linear and non-elastic, where the ascending and descending curves are separate so that after removal of load there is a permanent strain or deformation. The area enclosed by the two curves is termed *hysteresis*, which represents the energy absorbed by the material due to the damage caused by loading. In the case of concrete, the hysteresis is due mainly to microcracking at the aggregate-cement paste interface and irreversible creep, its magnitude depending on the age of the concrete and especially the rate of loading. An increase in age or maturity reduces the hysteresis, while very rapid loading reduces the curvature of the stress-strain behaviour and hysteresis considerably.

The slope of the stress-strain curve gives the *modulus of elasticity*, known generally as *Young's modulus*. Whereas for steel the slope is constant, for concrete it can be seen that the modulus varies according to the level of stress (as well as rate of loading and age) and whether the load is increasing or decreasing. The various types of modulus used to describe the elastic behaviour of concrete are fully detailed elsewhere (Neville, 1995; Neville and Brooks, 2002). When the load is applied for the first time to a particular level, the *secant modulus* yields the strain response and the starting point for creep, if the load is subsequently sustained. In a creep test, the strain on application of load is termed the *elastic strain at loading* and the time of application of load should always be stated.

Repeating the cycles of loading and unloading reduces the hysteresis so that the ascending and descending stress-strain curves eventually coincide and

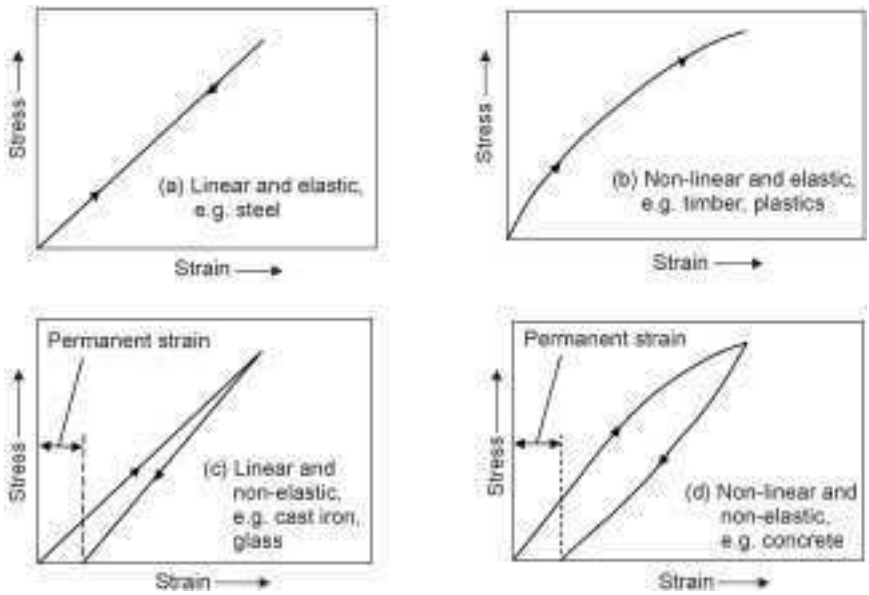

3.1 Categories of elasticity for engineering materials (Neville and Brooks, 2002. From *Concrete Technology*, Fig. 12.1, published by Pearson Education Ltd).

become approximately linear. This procedure is the basis of standard methods of test for the determination of the *static modulus of elasticity* such as ASTM C469-94 and BS 1881: Part 121:1983. The modulus of elasticity generally follows the pattern of strength, although not always. For example, wet concrete tends to have a greater modulus than dry concrete, while strength varies in the opposite sense. The type of aggregate can also be different in its effect on modulus and strength. However, for design purposes, most Codes of Practice give empirical relationships between modulus and strength. Generally, with normal weight concrete of density, $\rho = 2320\,\text{kg/m}^3$, the static modulus, E_c (GPa), can be related to the cube compressive strength, f_{cu} (MPa), by the expression:

$$E_c = 9.1 f_{cu}^{0.33} \tag{3.1}$$

When the density is between 1400 and 2320 kg/m^3, the expression for static modulus is:

$$E_c = 1.7\rho^2 f_{cu}^{0.33} \times 10^{-6} \tag{3.2}$$

Alternative expressions are given by BS 8110: Part 2: 1985.

ACI 318-95 (1996) gives the following expression for the static modulus of normal weight concrete:

$$E_c = 4.7 f_{cyl}^{0.5} \tag{3.3}$$

where f_{cyl} = cylinder compressive strength (MPa).

When the density is between 1500 and 2400 kg/m^3, the modulus is given by:

$$E_c = 43\rho^{1.5} f_{cyl}{}^{0.5} \times 10^{-6} \qquad 3.4$$

The influence of aggregate on modulus of elasticity of concrete has already been mentioned, the two-fold effect arising from the stiffness (modulus) of the aggregate and its volumetric proportion in concrete. The stiffer the aggregate, the greater the modulus of concrete and, for aggregate having a greater modulus than hardened cement paste, the greater the volume of aggregate the greater the modulus of concrete. The modulus of elasticity of lightweight aggregate concrete is usually between 40 and 80% of the modulus of normal weight concrete of the same strength, the mix proportions having little influence.

The relationships between modulus of elasticity and compressive strength (equations 3.1–3.4) are not appreciably different when either chemical or mineral admixtures are used to make concrete (Brooks, 1999).

3.2.2 Poisson's ratio

The design and analysis of some types of structure require the knowledge of volume changes in concrete members subjected to external load. In this case, Poisson's ratio is required, viz. the ratio of lateral strain to the axial strain resulting from an axial load. Figure 3.2 shows the trends of lateral, axial and volumetric strains as the level of stress is increased up to failure. At low levels of stress, there is a lateral extension and an axial contraction so that Poisson's ratio

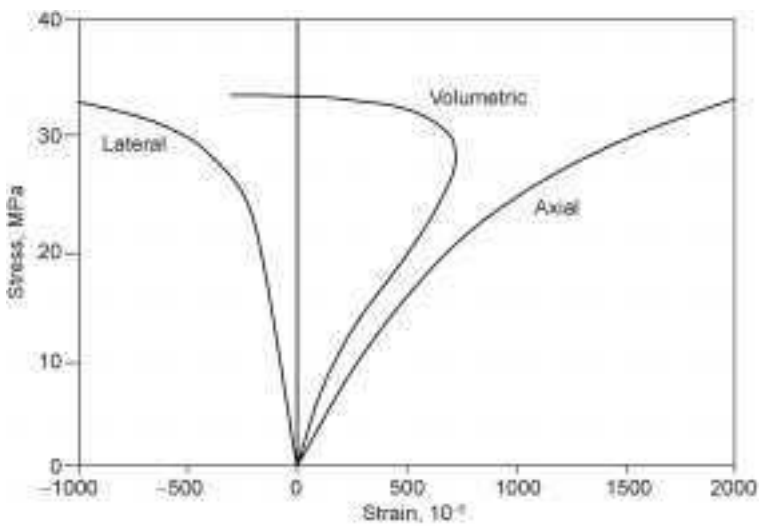

3.2 Axial, lateral and volumetric strains in concrete cylinder under an increasing axial compressive stress (Neville, 1995. From *Properties of Concrete*, Fig. 9.6, published by Pearson Education Ltd).

is approximately constant and negative, but this sign is ignored in concrete technology. As the stress approaches failure, the Poisson's ratio increases rapidly due to vertical cracking and the volumetric strain changes from a contraction to an extension.

In general, for practical levels of stress, Poisson's ratio lies in the range of 0.15 to 0.20 when determined from strain measurements in a static modulus of elasticity test. An alternative method is to determine Poisson's ratio by dynamic means using ultrasonic and resonant frequency tests (Neville, 1995; Neville and Brooks, 2002). In the latter case, the *dynamic Poisson's ratio* is greater than that from a static test, typically ranging from 0.2 to 0.24.

With both the static and dynamic methods, the measured Poisson's ratios are elastic values. Under a sustained load, the term *creep Poisson's ratio* strictly applies, but for stresses less than approximately 0.5 of the short-term strength, creep Poisson's ratio can be assumed to be similar to the elastic value (Neville, 1995).

3.2.3 Shrinkage and swelling

Shrinkage of concrete is caused by loss of water by evaporation or by hydration of cement, and also by carbonation. The resulting reduction in volume as a fraction of the original volume, i.e. volumetric strain, is equal to three times the linear strain, so in practice shrinkage is simply measured as a linear strain. The units are mm per mm, usually expressed as microstrain (10^{-6}).

When freshly laid and before setting, concrete can undergo *plastic shrinkage* due to the loss of water from the surface or by suction by dry concrete below, a situation that can lead to plastic cracking (see Section 3.3.2). Plastic shrinkage is greater the larger the cement content of the mix and it can be minimised by complete prevention of evaporation immediately after casting.

Even when no moisture movement to or from the set concrete is possible *autogenous shrinkage* occurs, which is caused by loss of water used by the hydrating cement. Except in large volume pours (mass concrete), autogenous shrinkage is not distinguished from shrinkage of hardened concrete due to loss of water to a dry surrounding environment. In normal strength concrete, autogenous shrinkage is small (50 to 100 $\times$ 10^{-6}), but can be large in high performance concrete, i.e. high durability and high strength concrete. Such concrete usually contains a high cementitious materials content consisting of cement and a mineral admixture, such as silica fume or fly ash. In addition, the mix has a low water/cementitious materials ratio so that a superplasticising chemical admixture is required to make the mix workable. Such composition yields a finer pore structure than normal strength concrete, which causes high early autogenous shrinkage when measured from initial set but, when measured from the age of 28 days, it is small.

If concrete is stored continuously in water during hydration, the concrete expands due to absorption of water by the cement paste, a process known as

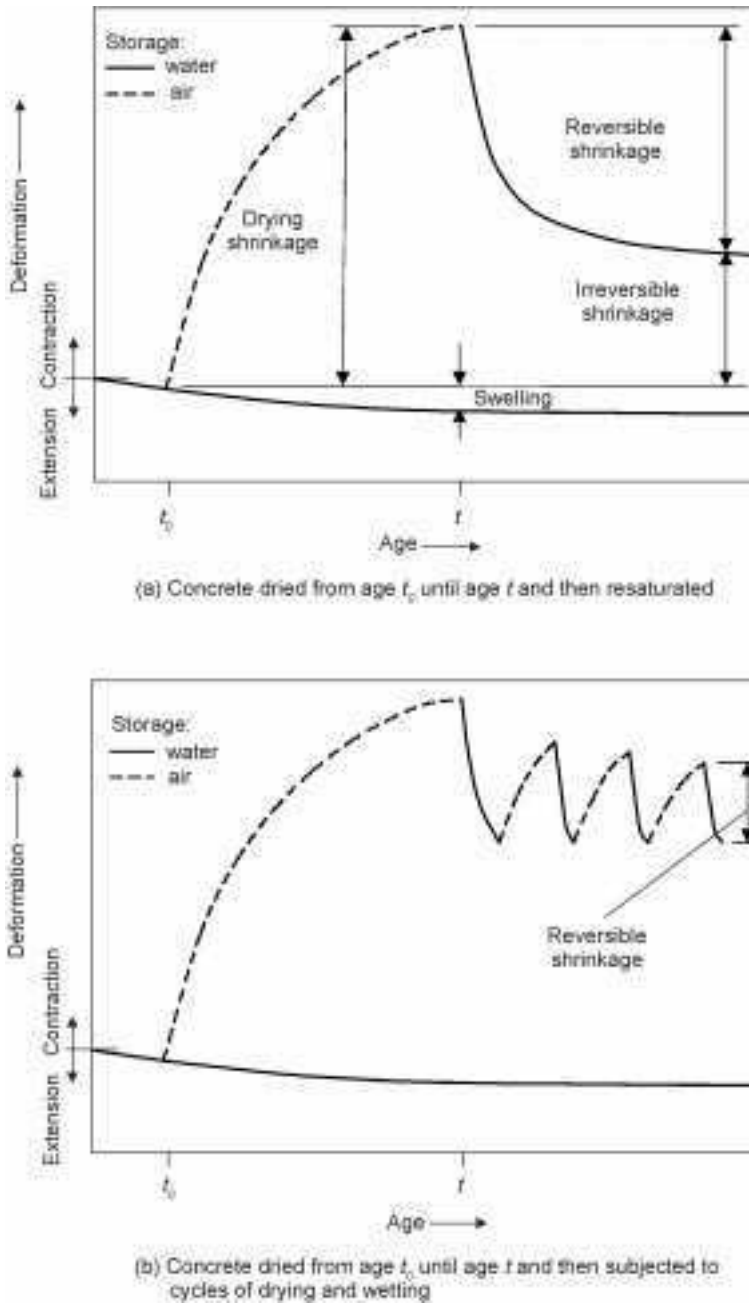

3.3 Reversible and irreversible drying shrinkage of concrete initially stored in water until exposure to drying, compared with swelling of concrete continuously stored in water (Neville and Brooks, 2002).

swelling. In concrete made with normal weight aggregate, swelling is 5–10% of shrinkage of hardened concrete. On the other hand, swelling of lightweight aggregate concrete can be much greater, viz. 25–80% of shrinkage after 30 years (Brooks, 2005).

The loss of water from hardened concrete stored in dry air causes *drying shrinkage*. To some extent the process is reversible, i.e. re-absorption of water will cause expansion of the concrete, but not back to its original volume (see Fig. 3.3(a)). In normal concretes, reversible shrinkage is between 40 and 70% of the drying shrinkage depending upon the age of the concrete when first drying occurs. If the concrete is cured so that it is fully hydrated at the time of exposure, more of the drying shrinkage is reversible but, if drying is accompanied by hydration and carbonation, the porosity of the cement paste will decrease, thus preventing some ingress of water (Neville and Brooks, 2002).

Another type of shrinkage that occurs in concrete is *carbonation shrinkage*, which normally accompanies drying shrinkage, although it is different in nature. Carbonation, which is known to be a potential cause of corrosion of steel in reinforced concrete, describes the reaction of calcium hydroxide with the carbon dioxide of the atmosphere in the presence of moisture. The carbon dioxide first dissolves in moisture and then reacts with calcium hydroxide to form calcium carbonate, the process resulting in a volume contraction known as carbonation shrinkage. The rate of carbonation depends upon the permeability of the concrete, the moisture content and the relative humidity of the environment, the severest conditions for high carbonation shrinkage being 55% relative humidity and high water/cement ratio (Neville, 1995). The effect of carbonation shrinkage in concrete is normally small as it is restricted to the outer layers, but can cause warping of thin panels. A practical benefit is in the manufacture of porous concrete blocks where curing in an atmosphere of carbon dioxide results in the calcium carbonate products being deposited in the pores. This restricts moisture movement (reversible shrinkage) and enhances strength.

The pattern of concrete subjected to cycles of drying and wetting, simulating daily weather changes in practice, is illustrated in Fig. 3.3(b). The magnitude of the cyclic change depends upon the duration of periods, the ambient humidity and the composition of the concrete, but it is important to note that drying is slower than wetting. Consequently, shrinkage resulting from a prolonged dry weather can be reversed by a short period of rain. Generally, shrinkage of lightweight aggregate concrete is more reversible than that of normal weight concrete.

Three mechanisms are thought to be responsible for reversible drying shrinkage: capillary tension, disjoining pressure and changes in surface energy (Mindess and Young, 1981). Removal of water from larger capillaries of the cement paste to the drier outside air causes little shrinkage, but this disturbs the internal equilibrium so that water is transferred from smaller capillaries to larger ones. When capillaries empty, a meniscus forms and a surface tension is

developed. This induces a balancing compressive stress in the calcium silicate hydrate (C-S-H) and results in a volume contraction or shrinkage. Stresses are higher in smaller capillaries and when the humidity is low due to the increasing curvature of menisci, but at very low humidity capillary stresses do not exist because the menisci are no longer stable.

With the disjoining pressure theory, the adsorption of water on the C-S-H particles affects the Van der Waals surface forces of attraction between adjacent particles in areas of hindered adsorption. The adsorbed water creates a disjoining pressure, which increases with the thickness of the adsorbed water. When the disjoining pressure exceeds the Van der Waals forces the particles are forced apart and swelling occurs. Conversely, as the pressure decreases due to a reduction in relative humidity, the particles are drawn together and drying shrinkage occurs.

The change in surface energy is thought to be responsible for drying shrinkage occurring at very low humidity (below 40%) when capillary stress and disjoining pressure are no longer present. Solid particles are subjected to a pressure due to surface energy and the pressure is decreased by water adsorbed on the surface. Loss of water will allow the surface energy pressure to increase, resulting in further shrinkage.

A significant part of the initial drying shrinkage is irreversible and this is explained by the changes that take place in the C-S-H. When adsorbed water is removed on first drying, additional physical and chemical bonds are formed as the particles become more closely packed. Moreover, additional bonds can occur due to hydration and carbonation (see later). Consequently, the porosity and connectivity of the pore system of the C-S-H change with drying, which reduces ingress of water on re-wetting.

Drying shrinkage of concrete is affected by several factors, the main ones as recognised by Codes of Practice being: water/cement ratio, aggregate, relative humidity, size of member and time. Figure 3.4 demonstrates that, for a constant volume of aggregate, drying shrinkage increases as the water/cement ratio increases and, for a constant water/cement ratio, drying shrinkage increases as the volume of the aggregate decreases. The influence of the aggregate is to restrain the shrinkage of the cement paste. Aggregates of low stiffness (low modulus of elasticity) provide less restraint and result in more drying shrinkage than non-shrinking good quality aggregates. Thus, lightweight aggregate concrete has a higher drying shrinkage than normal weight aggregate concrete as shown in Fig. 3.5. The size of aggregate hardly affects shrinkage but, at a constant water/cement ratio, larger aggregate allows the use of a leaner mix (more aggregate by volume) to achieve the same workability, which results in less shrinkage. Most aggregates are dimensionally stable; however, there are exceptions and the use of aggregates having high drying shrinkage should be avoided.

As already mentioned, the relative humidity of the air surrounding the concrete is a main factor and the lower the humidity the greater the loss of water

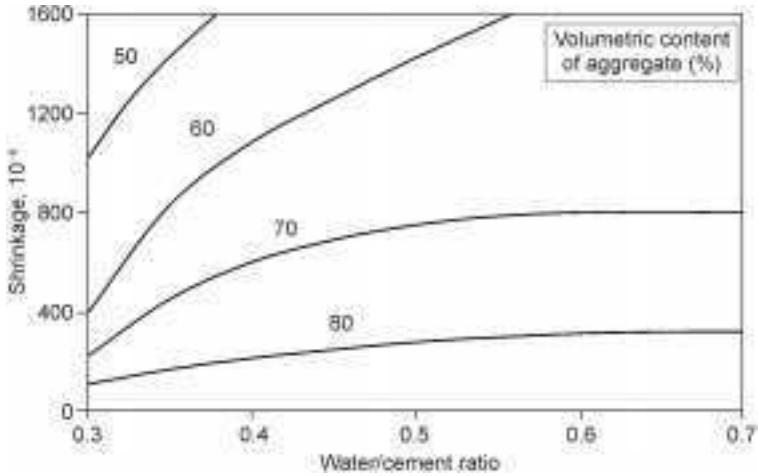

3.4 Influence of water/cement ratio and aggregate content on drying shrinkage (Odman, 1968. From 'Effects of variations in volume, surface area exposed to drying, and composition of concrete on shrinkage', Figs. 3 and 4, published in the Proceedings of Int. Colloquium on the Shrinkage of Hydraulic Concretes, RILEM/CEMBUREAU, Madrid. Courtesy RILEM).

and drying shrinkage. Similarly, an important factor is the size of member. Drying shrinkage of a large member is less than that of a small member because it is more difficult for water to escape from the former, which has a longer drying path The effect of size is expressed as the volume/surface area ratio

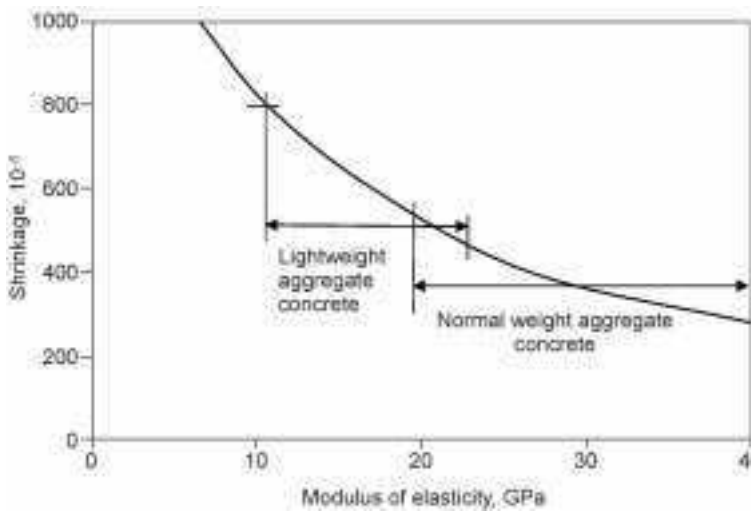

3.5 Effect of modulus of elasticity of aggregate on drying shrinkage (Mindess and Young, 1981. From *Concrete*, Fig. 18.16, reprinted by permission of Pearson Education, Inc., Upper Saddle River, NJ).

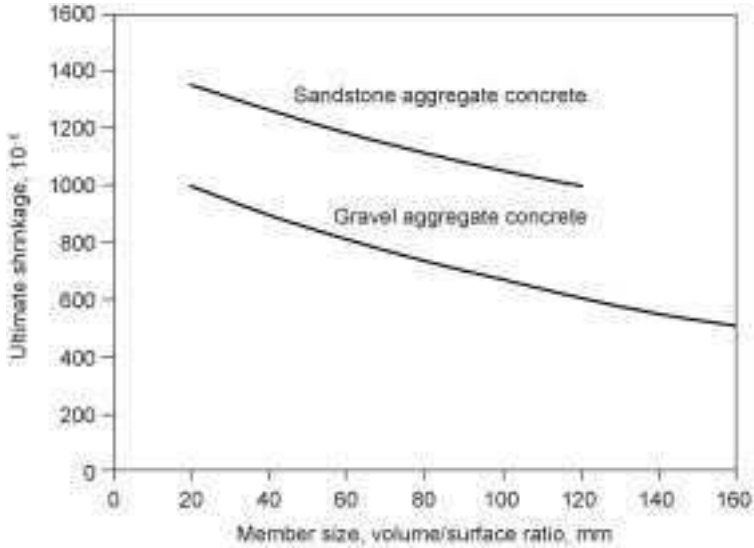

3.6 Relation between ultimate drying shrinkage and size of member (Hanson and Mattock, 1966. Adapted from 'The Influence of Size and Shape of Member on the Shrinkage and Creep of Concrete', Figs. 4 and 5, *ACI Journal Proceedings*, Vol. 63, pp. 267–290.).

(V/S) or effective thickness ($= 2V/S$), the surface area being that exposed to drying (see Fig. 3.6). There is a secondary influence of shape of member on drying shrinkage that is normally neglected.

Drying shrinkage occurs over a long period of time with a high initial rate after exposure to drying, which then gradually decreases to a very low rate after several years. It is believed that shrinkage does not have an ultimate value, although for design purposes, a final value after a time of 50 years is often assumed. Typically, a shrinkage-time characteristic would be 20% of 20-year shrinkage occurring in two weeks, 60% occurring in three months and 75% occurring in one year (Neville and Brooks, 2002).

Accelerators, retarders and other chemical admixtures that affect the rate of strength development of concrete will also affect the rate of drying shrinkage; however, the long-term shrinkage is not affected to a great extent. With water-reducing admixtures (plasticisers and superplasticisers) there is a general increase in drying shrinkage of 20% due to the presence of the admixture itself, e.g. as in the case of flowing concrete (Brooks, 1999) but, when used as a water reducer, shrinkage is affected by the change in mix proportions as well as the admixture. Nowadays, shrinkage-reducing chemical admixtures are available, which appear to reduce shrinkage by suppressing hydration of cement. Any reduction in strength can be offset by decreasing the water/cement ratio, thus reducing shrinkage even more.

When the mix proportions are unchanged, the use of certain mineral admixtures (fly ash, blast-furnace slag) as partial replacement of cement do not affect long-term drying shrinkage appreciably (Brooks, 1999). On the other hand, for a constant water/cementitious materials ratio, increasing the level of cement replacement by silica fume and metakaolin reduces both autogenous and drying shrinkage of high performance concrete. For example, drying shrinkage is reduced by approximately 25% for a 10% replacement of cement (Brooks and Megat Johari, 2001).

Drying shrinkage causes loss of prestress in prestressed concrete, increases deflections of asymmetrically reinforced concrete and, together with differential temperature, contributes to the warping of thin slabs. As discussed in Section 3.3.6, restraint of shrinkage often leads to cracking.

Several methods are available for estimating drying shrinkage and swelling for design purposes and these are considered together with creep in Section 3.2.4.

3.2.4 Creep

Creep is defined as the gradual increase in strain with time for a constant applied stress after accounting for other time-dependent deformations not associated with stress, namely, shrinkage or swelling and thermal strain. Hence, creep is reckoned from the elastic strain at loading, which depends upon the rate of application of stress (see Section 3.2) so that the time taken to apply the load should be quoted. Also, since the secant modulus of elasticity increases with time, the elastic strain decreases so that creep should be taken as the strain in excess of the elastic strain at the time in question. However, the change in elastic strain is usually small and creep is reckoned from the elastic strain on first application of load.

Like other engineering materials, concrete can suffer a time-dependent failure, which is known as *creep rupture* or static fatigue. Figure 3.7 represents the general strain-time history of such a material. Initially, there is a high rate of primary creep and then a steady rate of secondary creep before failure occurs after the tertiary creep stage, as characterised by the rapid development of strain. In the case of concrete, the stress needs to exceed approximately 0.6 to 0.8 of the short-term strength for creep rupture to occur in either compression or tension. Concrete is often described as a brittle material since it readily cracks under small strains, but in the case of creep rupture it can develop large strains prior to failure, providing an advantage of early warning in the case of sudden and catastrophic failure.

Figure 3.8 illustrates the pattern of stress and strain for varying rate of loading and level of sustained stress leading to creep rupture; actual experimental results for compression were obtained by Rusch (1960) and for tension by Domone (1974). Very high rate of loading produces a near linear stress-strain curve with

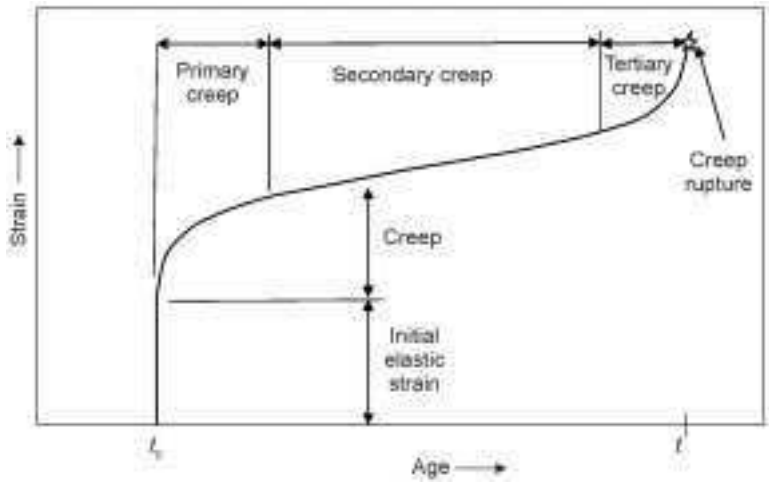

3.7 General strain-time characteristic of a material loaded at age t_0 and failing by creep rupture at age t (Neville and Brooks, 2002. From *Concrete Technology*, Fig. 11.7, published by Pearson Education Ltd).

a higher strength than in the usual standard test (Fig. 3.8(a)), but decreasing the rate of loading or increasing the test duration produces non-linear curves due to creep and microcracking with a lower strength (creep rupture). The creep rupture envelope tends to a constant limit of between 0.6 and 0.8 of the usual short-term strength, depending on the type of concrete and mode of loading.

With sustained stresses below approximately 0.6 of short-term strength, creep rupture is avoided and time-dependent strain due to primary and some secondary creep takes place for several years. Depending on the type of mix and other factors, creep of dry-stored concrete can be between two and nine times the elastic strain at loading, with around 70% occurring after one year under load (Brooks, 2005).

As stated earlier, the definition of creep is the increase in strain for a constant sustained stress and is determined from concrete specimens after deducting any drying shrinkage (measured on a separate specimen) and the *initial elastic strain*. Figure 3.9(a) shows the components of strain involved. In the case of sealed concrete, which represents mass or large-volume concrete where little or no moisture is lost, only *basic creep* occurs, but when the concrete is allowed to dry additional *drying creep* occurs even though drying shrinkage has been deducted from the measured strain; the sum of basic and drying creep is sometimes called *total creep*. Creep is a partly reversible phenomenon. When the load is removed, there is an immediate, almost full, *elastic recovery* of the initial elastic strain, followed by a gradual decrease of strain called the *creep recovery* (Fig. 3.9(b)). The recovery quickly reaches a maximum and is only small, e.g. 1–25% of the 30-year creep (Brooks, 2005). Consequently, creep is mostly irreversible in nature.

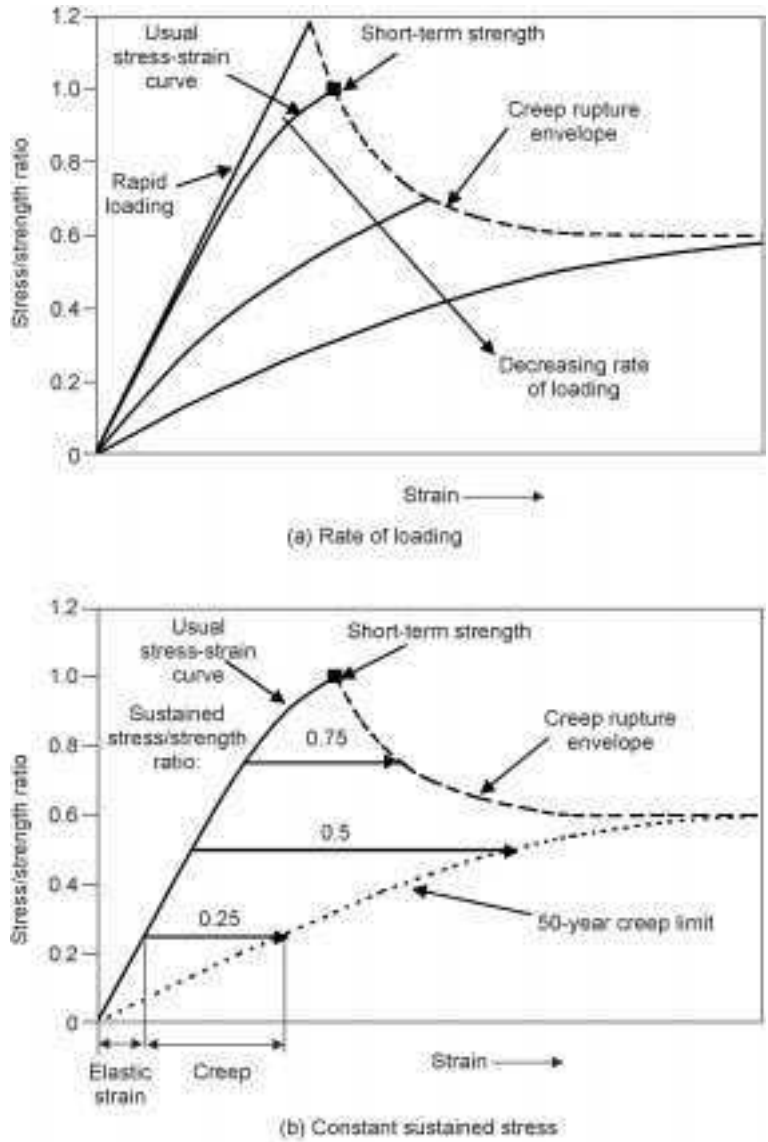

3.8 Influence of rate of loading and level of sustained stress on stress-strain curves leading to time-dependent creep rupture of concrete (Rusch, 1960. Adapted from 'Researches Toward a General Flexural Theory for Structural Concrete', Fig. 14, *ACI Journal Proceedings*, Vol 75, No 1, pp. 1–28).

Like shrinkage, creep can be expressed in units of microstrain (10^{-6}), but because of the dependency on stress, *specific creep* (C_s) is often used with units of 10^{-6} per MPa. Other terms are *creep coefficient* (ϕ), sometimes called the creep factor, and *creep compliance* (Φ). The creep coefficient is defined as the

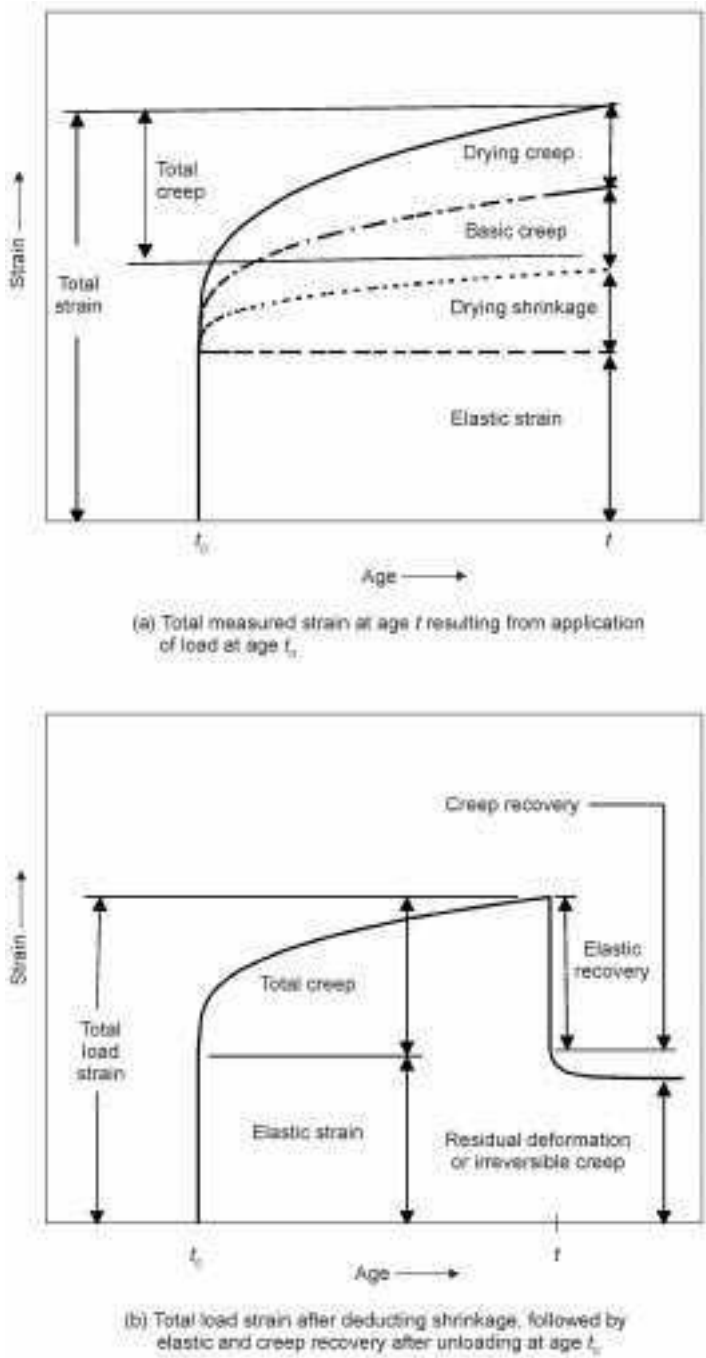

3.9 Components of time-dependent strain resulting from (a) application of load to drying concrete and (b) removal of load.

ratio of creep to the elastic strain on loading and for a unit stress:

$$\phi = \frac{C_s}{\dfrac{1}{E \times 10^3}} = C_s E \times 10^3 \qquad 3.5$$

where E = modulus of elasticity at the age of loading (GPa).

The creep compliance is the total load strain per unit of stress (10^{-6} per MPa) i.e. the sum of the elastic strain per unit of stress and specific creep so that:

$$\Phi = \frac{1}{E \times 10^3} + C_s = \frac{1}{E \times 10^3}(1 + \phi) \qquad 3.6$$

The effects of creep can be realised from another viewpoint. When a concrete specimen is loaded and then prevented from deforming, then creep will manifest itself as a gradual decrease or *relaxation* of stress with time, as illustrated in Fig. 3.10. Relaxation is of interest in connection with loss of prestress in prestressed and post-tensioned concrete and cracking processes (see Section 3.3).

Apparatus for the determination of creep of any type of concrete is recommended in ASTM C512 (1987) and for prefabricated aerated or lightweight concrete by BS EN 1355 (1997). Alternative methods are described in Neville *et al.* (1983) and Newman and Choo (2003).

There have been many theories proposed to explain the creep of hardened cement paste and concrete, which are too numerous to include within the scope of this chapter. Most agree that creep at normal stresses is caused by the internal movement of water adsorbed or held within the C-S-H, since concrete from which all the evaporable water has been removed exhibits little or no creep unless high temperatures are involved. Movement of water to the outside environment is required for drying creep to occur. Although basic creep is associated with sealed or mass concrete, it is thought that internal movement of water occurs because all the pores do not remain full of water. The dependency of basic creep on strength is indirect evidence that empty or part-empty pores are a main factor. Creep also occurs at high temperatures when non-evaporable water is removed and this is thought to be due to movement of interlayer or zeolitic water, viscous flow or sliding between gel particles (Illston *et al.*, 1979; Mindess and Young, 1981; Neville *et al.*, 1983; Bazant, 1988; Brooks, 2001).

The source of creep of concrete is the hydrated cement paste and not normal weight aggregate of good quality. Some light aggregates may exhibit creep. However, like shrinkage, the role of aggregate is an important factor in creep due to the restraining influence on the cement paste through its stiffness or modulus of elasticity and volume concentration. The relationship between modulus of elasticity of aggregate and relative creep of concrete is shown in Fig. 3.11.

For a constant water/cement ratio, the volume of cement paste or total aggregate in concrete has a significant effect on creep (Neville and Brooks, 2002). However, in practice, concretes with similar workability normally have

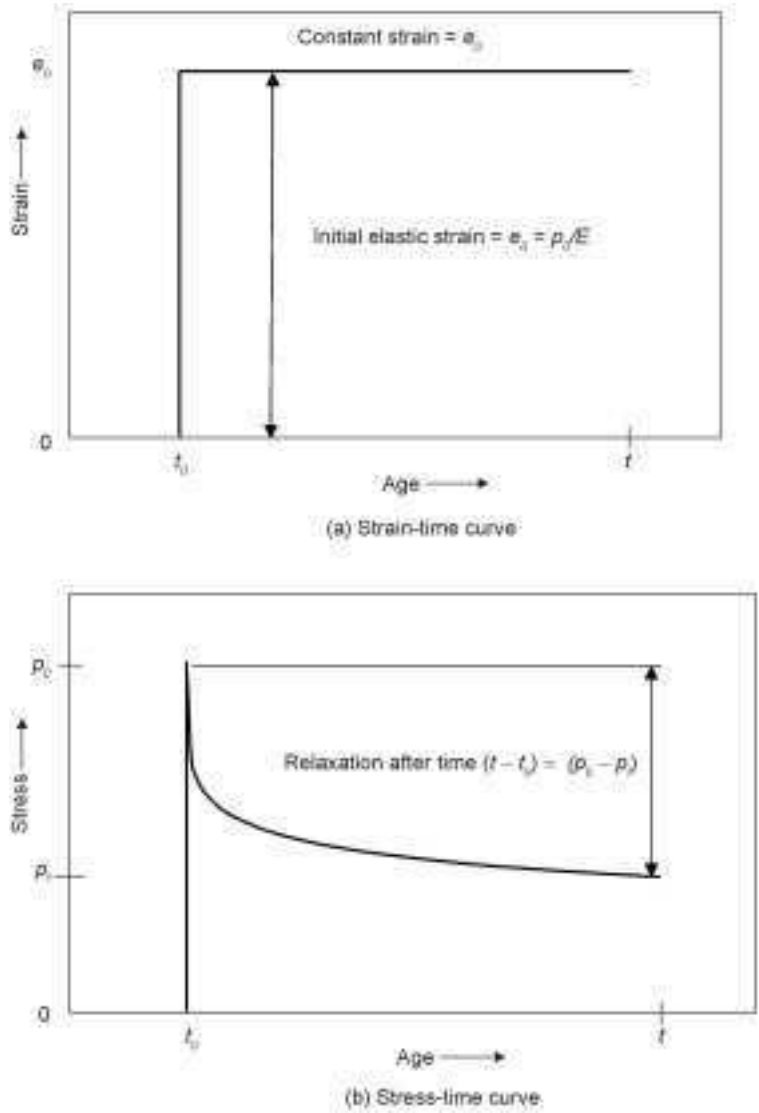

3.10 Definition of relaxation of concrete after time $t - t_0$ subjected initially to stress p_0 and elastic strain e_0 at age t_0, and then maintained constant at e_0; E = modulus of elasticity.

similar cement paste contents and so the differences in creep are not large. For example, in normal weight concretes having aggregate/cement ratios of 9, 6 and 4.5, and corresponding water/cement ratios of 0.75, 0.55 and 0.40, the cement paste contents are 24, 27 and 29%, respectively. On the other hand, when the cement paste content is constant, an increase in water/cement ratio increases creep as shown in Fig. 3.12.

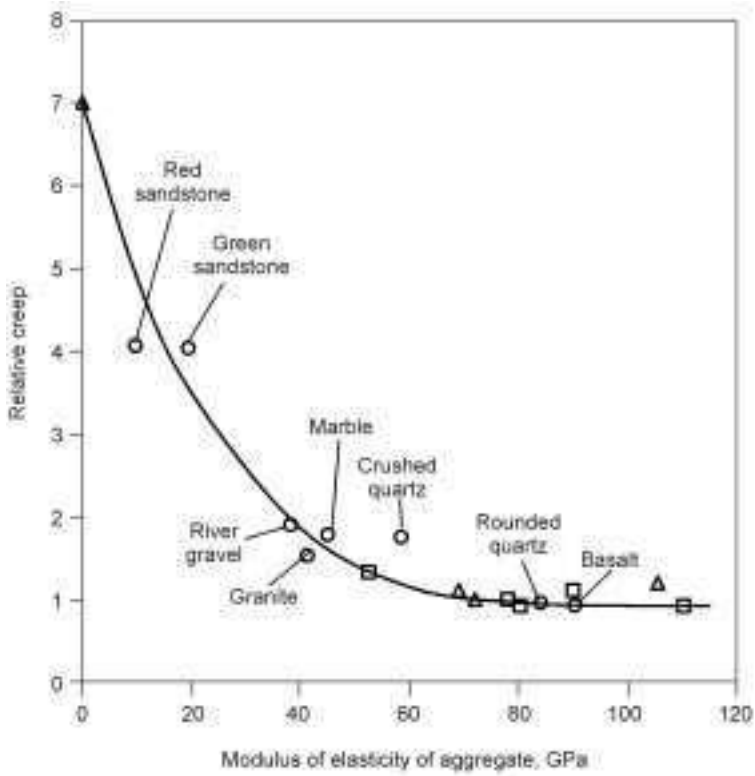

3.11 Effect of modulus of elasticity of aggregate on relative creep of concrete (= 1 for an aggregate modulus = 60 GPa) (based on Kordina, 1960. From 'Experiments on the influence of the mineralogical character of aggregate on creep of concrete', Figs. 3.11, published in RILEM Bulletin 6. Courtesy RILEM).

Since creep is related to the water/cement ratio it can be expected to be related to strength. Indeed, it has been found that over a wide range of mixes made with similar materials, creep is approximately inversely proportional to the strength of the concrete at the age of application of load. Moreover, for stresses less than approximately 0.6 of the short-term strength, creep is proportional to the applied stress, so that combining the dual influences leads to the stress/strength ratio rule, namely, that creep is approximately proportional to the stress/strength ratio (Neville *et al.*, 1983). Consequently, since the strength increases with age, creep can be expected to decrease as the age at loading increases (Fig. 3.13).

Experimental work on saturated concrete specimens exposed to the atmosphere at different relative humidities shows that the drier the atmosphere the higher the creep. Figure 3.14 demonstrates that trend, the 100% curve approximating to that of basic creep so that the additional creep for 75 and 50%

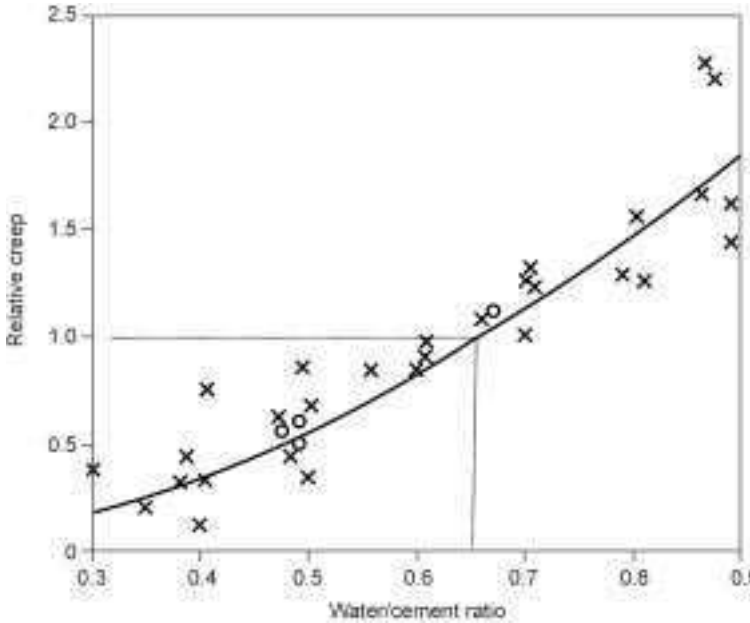

3.12 Effect of water/cement ratio on relative creep (= 1 for a water/cement ratio = 0.65) for a constant cement paste content (Wagner, 1958. From 'Das Kriechen unbewehrten Betons', *Deutscher Ausschuss für Stahlbeton*, 131).

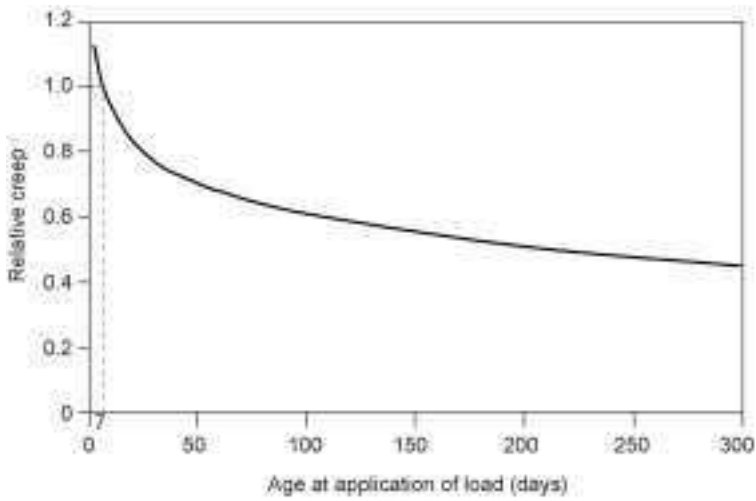

3.13 Influence of age at application of load on relative creep (= 1 for age = 7 days) (L'Hermite, 1959. From 'What do we know about the plastic deformation of concrete?', Figs 3 and 13, published in RILEM Bulletin 1. Courtesy RILEM).

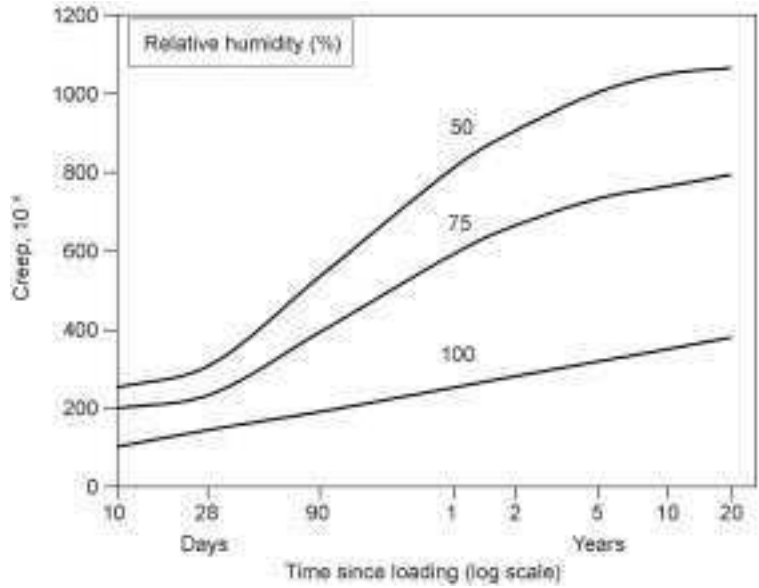

3.14 Creep of concrete cured in fog for 28 days, then loaded and stored at different relative humidity (Troxell *et al.*, 1958. From 'Long-time creep and shrinkage tests of plain and reinforced concrete', *Proc. ASTM*, 58, 1101–1120).

relative humidities is drying creep. If the concrete is allowed to dry out prior to application of load then creep is much less. However, it is ill-advised to allow concrete to dry out prematurely in order to reduce creep because of the risk of inadequate curing and cracking due to restrained or differential drying shrinkage (see Section 3.3.6).

Creep of concrete is affected by size of member in a similar manner to drying shrinkage (see Fig. 3.6). Expressing size as the volume/exposed surface area ratio (V/S) or effective thickness ($= 2V/S$), which represents the average drying path length, total creep decreases as the volume/surface ratio or size increases (Fig. 3.15). Of course, it is the drying creep component that is influenced since basic creep is unaffected by size. This can be seen when the size of the member is large (mass concrete) when no moisture transfer to the environment takes place and basic creep occurs. It is also apparent from Fig. 3.15 that the influence of shape of concrete member is a secondary factor in creep and can be neglected.

The influence of temperature on creep is complex and not fully understood, as it depends upon the time when the temperature of the concrete rises relative to the time of application of load (Neville *et al.*, 1983). Figure 3.16 demonstrates different experimental results for concrete stored at elevated temperature in water (basic creep). Compared with normal-temperature creep, heating just prior to loading accelerates creep, and heating just after loading produces an additional component termed *transitional thermal creep*. In the case of drying

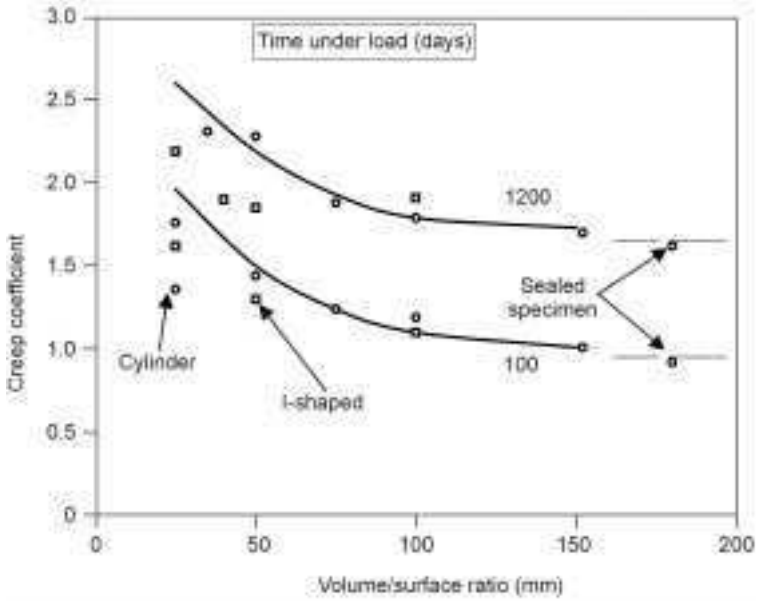

3.15 Effect of volume/surface ratio on creep coefficient of concrete (Hanson and Mattock, 1966).

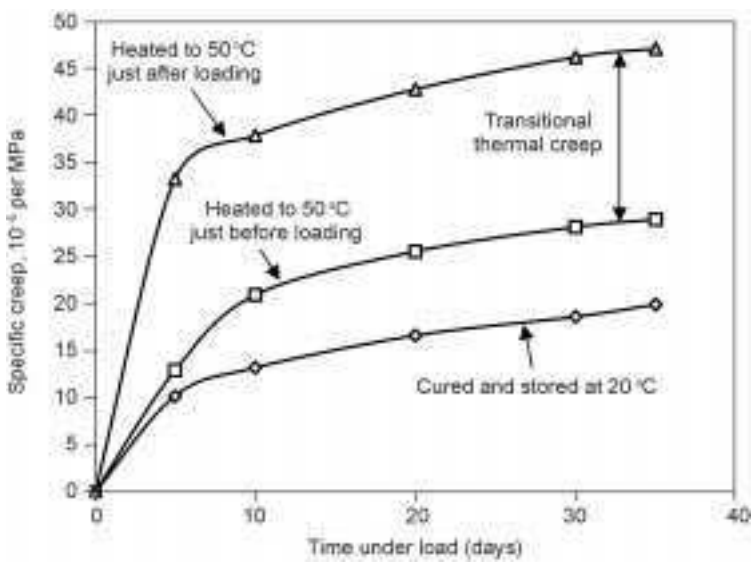

3.16 Influence of temperature on basic creep of concrete (Brooks, 2001. From 'A theory for drying creep of concrete', *Magazine of Concrete Research*, 53, 1, 51–61).

concrete (total creep), elevated temperature causes increases in creep in a similar manner, but when the evaporable water has been removed (between approximately 80 and 120 ºC) there is a decrease in creep before increasing again (Neville *et al.*, 1983). At very high temperatures, such as in fire, very high creep occurs, termed *transient thermal strain* (Khoury *et al.*, 1985).

The type of cement will affect creep if the strength changes at the time of application of load. When the stress/strength ratio at the age of loading is the same, most Portland cements lead to approximately the same creep, but the strength development under load is a factor, e.g. creep will be lower for a greater strength development (Neville and Brooks, 2002).

The latter influence is apparent when certain mineral admixtures, such as fly ash and ground granulated blast-furnace slag, are used as partial replacements for Portland cement. The resulting slower pozzolanic reaction often leads to a later strength development than in the case of Portland cement. Figure 3.17 shows the general trends for fly ash, blast-furnace slag, silica fume and metakaolin, which are mainly based on the analysis of results of previously published data (Brooks, 2000). That analysis accounted for any changes in aggregate content and water/cementitious materials ratio on creep by considering the relative stress/strength ratio so that the effect of just the mineral admixture could be assessed. Although there is a large variation, it can be seen that fly ash and slag can lead to significant reductions in creep. In the case of the finer mineral admixtures: silica fume and metakaolin, there are larger reductions in creep for replacement levels of up to 15%, but then for silica fume creep increases as the replacement level increases.

Generally, the addition of chemical admixtures, plasticisers and superplasticisers, to make flowing concrete causes a 20% reduction in creep at a constant stress/strength ratio, although the effects do vary widely (Brooks, 2000). When the same admixtures are used as workability aids or water reducers, creep will be less due to the lower water content. As well as reducing shrinkage (see Section 3.3), the use of a shrinkage-reducing admixture appears to reduce drying creep, although experimental verification is limited.

For design purposes, estimation of elastic deformation, creep and drying shrinkage are considered together in Codes of Practice. From only a knowledge of strength, mix composition and physical conditions, BS 8110: Part 2 (1985) gives creep and shrinkage after 6 months and 30 years, depending upon the relative humidity and size of member. ACI 209 (1992) and CEB-FIP (1999) methods express creep and shrinkage as functions of time and allow for all the main influencing factors that have been discussed earlier. Alternative models are available by Bazant and Baweja (1995) and Gardner and Lockman (2001). Creep and drying shrinkage estimates by all methods are not particularly accurate ($\pm$30% at best) mainly because they fail to account for the type of aggregate (Brooks, 2005). For more accurate estimates and for high performance concretes containing several admixtures, short-term tests are recommended. The

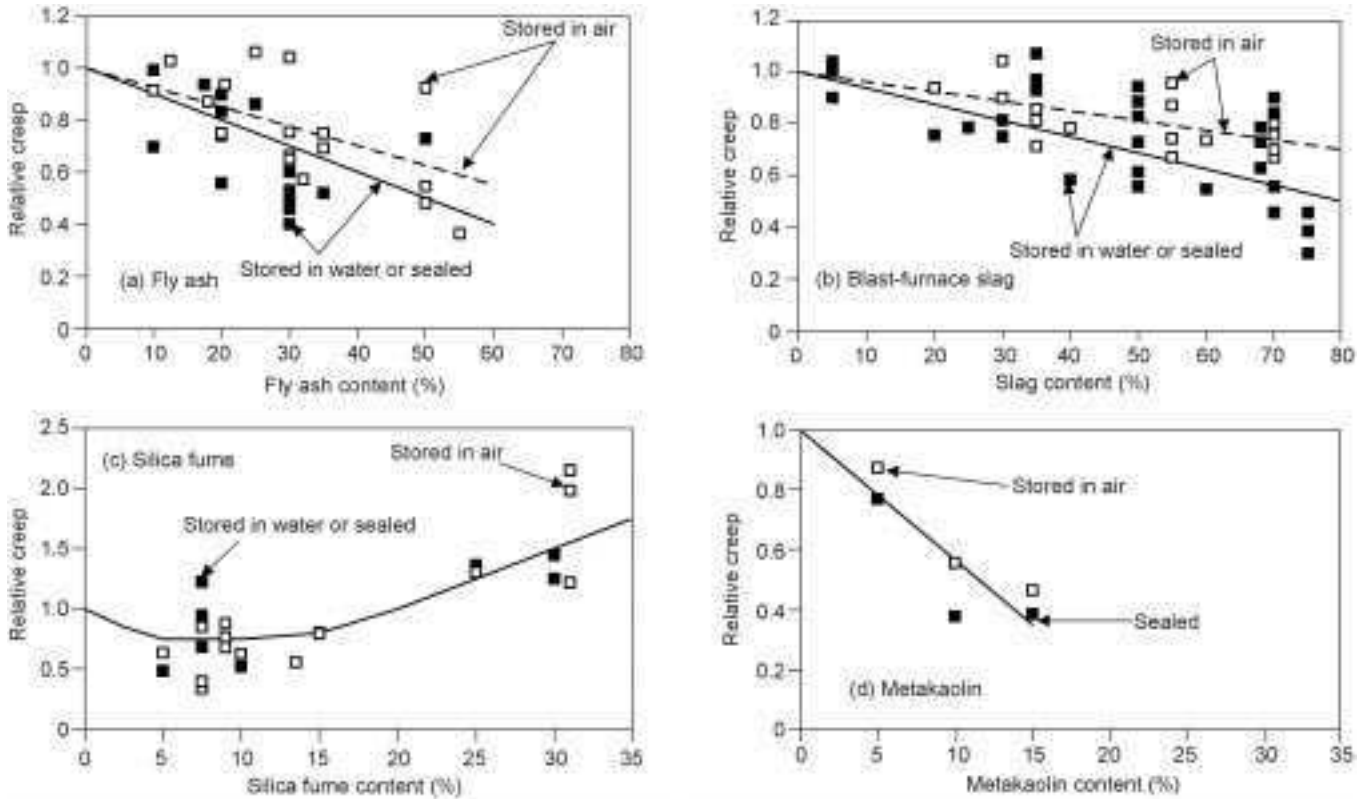

3.17 General trends of creep as affected by mineral admixtures; relative creep is that at a constant stress/strength ratio of the admixture concrete relative to the admixture-free concrete.

test duration should be of at least 28 days using small laboratory specimens made from the actual concrete mix and then measured creep and shrinkage-time data extrapolated to obtain long-term values, which are then adjusted according to the required member size and the average relative humidity of the storage conditions (Brooks and Al-Quarra, 1999). All methods of prediction give an estimate of the creep function (equation 3.6) and drying shrinkage, the total strain, $\xi(t, t_o)$, at age t when determined from age t_o being given by:

$$\xi(t, t_o) = \sigma(t_o)\left\{\frac{1}{E(t_o)}[1 + \theta(t, t_o)]\right\} + S(t, t_o) + \alpha_c \Delta T(t, t_o) \qquad 3.7$$

where $\sigma(t_o) =$ stress applied at age t_o, $E(t_o) =$ modulus of elasticity at t_o, $\phi(t_o) =$ creep coefficient, $S(t, t_o) =$ drying shrinkage or swelling, $\alpha_c =$ coefficient of thermal expansion and $\Delta T =$ change in temperature (see Section 3.2.5).

It should be noted that equation 3.7 applies for a constant stress and, if the stress or strain varies with time, calculation of the resulting strain or stress can be made by the age adjusted effective modulus or other methods (Neville *et al.*, 1983).

The importance of creep in structural concrete lies mainly in the fact that, in the long term, it can be several times the elastic deformation when first loaded. Consequently, the designer has to assess creep in order to comply with the serviceability requirement of deflection in particular. There are other effects of creep, most of which are detrimental, such as loss of prestress in prestressed concrete and differential movements in tall buildings, but creep can be beneficial when relieving stress induced by restraint of deformations.

3.2.5 Thermal movement

As shown in the last term of equation 3.7, thermal strain is the product of the coefficient of thermal expansion and temperature change, which is usually within the range of -22 to 65ºC. Since cement paste and aggregate have dissimilar thermal coefficients, the coefficient for concrete depends upon its composition and also the moisture condition at the time of temperature change. The role of aggregate is similar to that in shrinkage and creep, namely, the aggregate restrains the thermal movement of the cement paste since the latter has a higher thermal coefficient. The coefficient of thermal expansion for concrete is related to thermal coefficients of cement paste and aggregate as follows (Hobbs, 1971):

$$\alpha_c = \alpha_p - \frac{2g(\alpha_p - \alpha_g)}{1 + \dfrac{k_p}{k_g} + g\left[1 - \dfrac{k_p}{k_g}\right]} \qquad 3.8$$

where $g =$ volumetric content of aggregate, $k_p/k_g =$ stiffness ratio of cement paste to aggregate $\approx$ elastic modulus ratio $= E_p/E_g$.

The range of values of coefficient of thermal expansion for air-cured concrete is 7.4 to 13.1 $\times$ 10^{-6} per ºC and, for water-cured concrete, 6.1 to 12.2 $\times$ 10^{-6} per ºC, a typical average being taken as 10 $\times$ 10^{-6} per ºC.

3.3 Cracking processes

The design of reinforced concrete structures is based on the assumption that concrete does not withstand tension stresses induced by bending, and steel reinforcement is provided to resist these stresses. The concrete in the tension zone will crack and measures are taken to provide sufficient reinforcement to ensure that if cracks do occur they are acceptable both functionally and visually. This type of cracking, along with any cracking due to external loading, is called *structural cracking*.

Concrete is also liable to crack due to internal tensile stresses induced by some form of restraint to free movement. The heterogeneous composite nature of concrete induces differential stresses and strains due to differing properties of the ingredients, as well as when there are moisture and thermal gradients present. Since concrete is weak in tension, induced tensile stress can often lead to cracking but the problem is compounded by creep. Such cracks are known as *intrinsic cracks* or *non-structural cracks*. The types of cracks are wide-ranging and their diagnosis is often difficult so that the decisions as to what remedial action to take and when to apply it are correspondingly difficult.

The causes and remedies of common types of intrinsic cracks occurring in concrete construction are discussed in this chapter together with the study of stress and strain in the vicinity of cracks, viz. fracture mechanics. Techniques for the repair of cracks and materials used are specialised subjects; this topic is dealt with in detail elsewhere: Concrete Society Technical Report No. 22, 1992 and ACI 224R, 1996.

3.3.1 Types of cracks

Figure 3.18 lists the main types of crack that can occur in concrete both before hardening and after hardening. Included in the types that occur before hardening are *plastic shrinkage cracks* and *plastic settlement cracks*, which are highlighted because they will be discussed in detail later. As Fig. 3.18 shows, three categories of intrinsic cracks can occur after hardening: physical, chemical and thermal, as well as structural cracks. *Drying shrinkage cracks* and *early-age thermal contraction cracks*, which are also highlighted, will be discussed later. Table 3.1 lists the locations, causes, remedies and times of occurrence of intrinsic cracks, while examples are shown in a hypothetical structure in Fig. 3.19.

It is convenient to consider the various types of intrinsic cracks as a group so as to aid diagnosis. One basis for classification is the time of occurrence, for example plastic shrinkage cracks occur during the first few hours of placing,

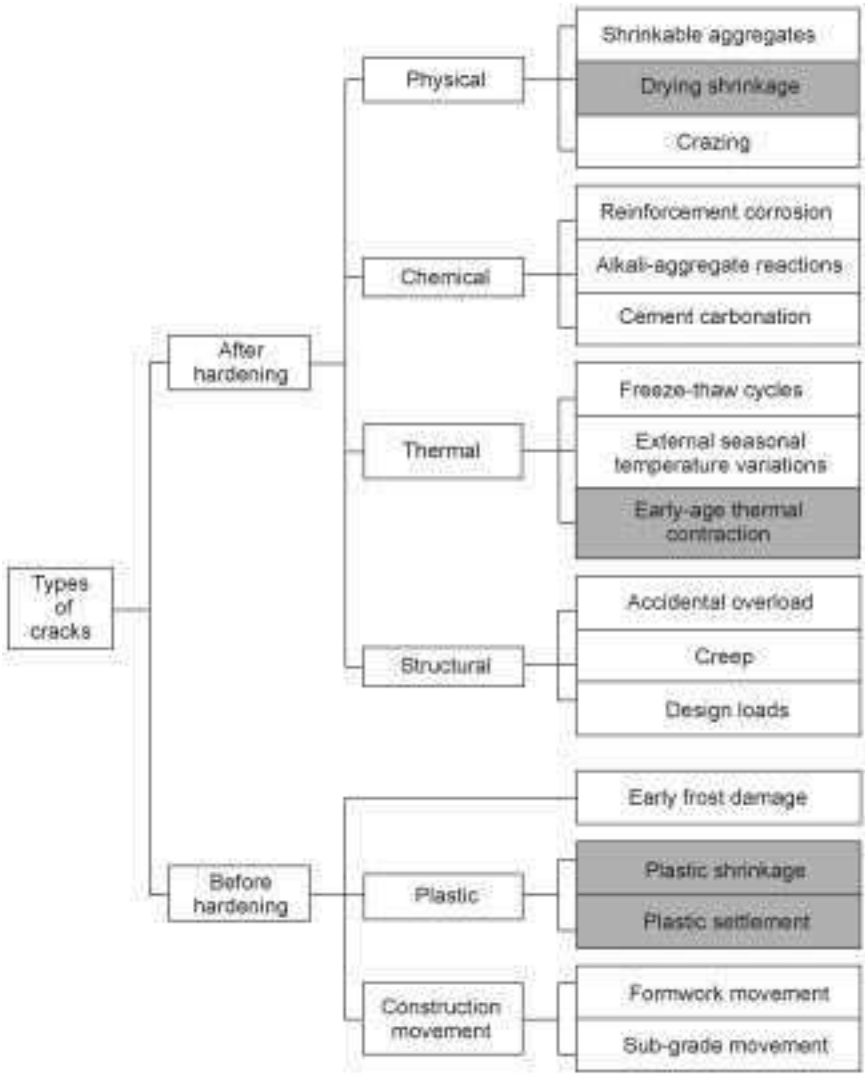

3.18 Types of crack (Concrete Society, 1992. Adapted from 'Non-structural cracks in concrete', Technical Report No. 22, Third Edition, Slough, UK, The Concrete Society).

early-age thermal cracks occur between one day and three weeks, and drying shrinkage cracks occur after several weeks.

Some cracks are not necessarily dependent on time, for example crazing, while other types are related to particular conditions that may be looked upon as malpractice in the light of current knowledge, namely cracking due to alkali-silica reaction or excessive use of calcium chloride leading to corrosion of steel reinforcement.

Table 3.1 Classification of intrinsic cracks (Concrete Society, 1992)

Type of cracking	Subdivision	Most common location	Primary cause (excluding restraint)	Secondary cause or factor	Remedy*	Time of appearance
Plastic settlement	Over reinforcement	Deep sections	Excess bleeding	Rapid early drying	Reduce bleeding/air entrainment or revibrate	Ten min. to three hours
	Arching	Top of columns				
	Change of depth	Trough and waffle slabs				
Plastic shrinkage	Diagonal	Roads and slabs	Rapid early drying	Low rate of bleeding	Improve early curing	30 min. to six hours
	Random	Reinforced slabs				
	Over reinforcement	Reinforced slabs	Ditto plus steel near surface			
Early thermal contraction	External restraint	Thick walls	Excess heat generation	Rapid cooling	Reduce heat and/or insulate	One day to two or three weeks
	Internal restraint	Thick slabs	Excess temp. gradients			

Long-term drying shrinkage		Thin slabs and walls	Inefficient joints	Excess shrinkage; inefficient curing	Reduce water content; improve curing	Several weeks or months
Crazing	Against formwork	'Fair faced' concrete	Impermeable formwork	Rich mixes; poor curing	Improve curing and finishing	One to seven days, or even later
	Floated concrete	Slabs	Over-trowelling			
Corrosion of steel reinforcement	Natural	Columns and beams	Lack of cover	Poor quality concrete	Eliminate causes listed	More than two years
	Calcium chloride	Precast concrete	Excess calcium chloride			
Alkali-silica reaction		Damp locations	Reactive aggregate plus high alkali cement		Eliminate causes listed	More than two years

* Assuming basic redesign is impossible. In all cases reduce restraint.

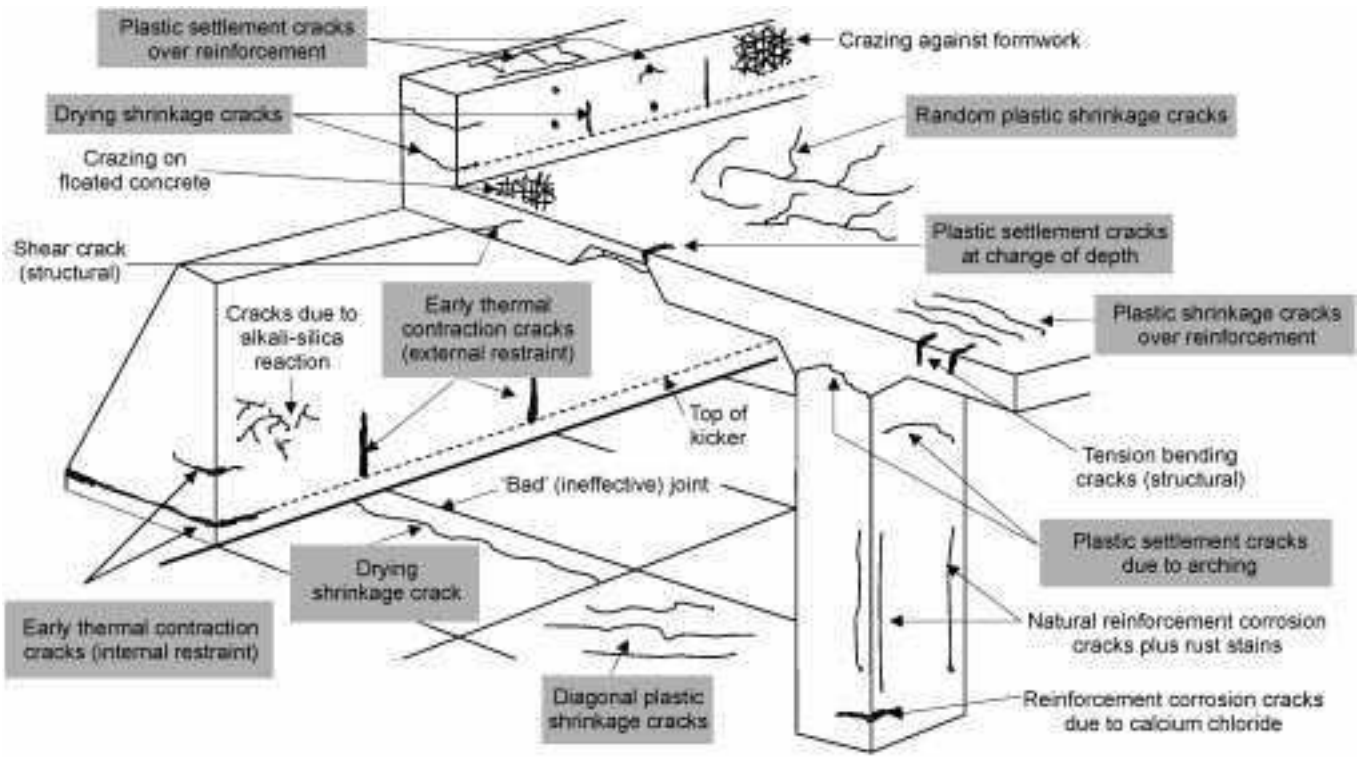

3.19 Examples of intrinsic cracks in a schematic concrete structure (Concrete Society, 1992. Adapted from 'Non-structural cracks in concrete', Technical Report No. 22, Third Edition, Slough, UK, The Concrete Society).

3.3.2 Plastic cracking

The two types, plastic settlement and plastic shrinkage cracks, both occur between one and eight hours after placing of the concrete due to the process of bleeding, namely the action of water rising to the surface shortly after compaction.

Bleeding is caused by the water being forced upwards when heavier solid particles settle downwards. Bleed water is only seen at the surface when the rate of evaporation is less than the rate of bleeding and should be distinguished from laitance, which is a mixture of water, cement and very fine particles. A wet mix will bleed more than a dry one, so excessive water contents should be avoided.

Plastic settlement cracking

This type of cracking occurs when there is a large amount of bleeding and settlement, and there is some form of restraint or obstruction to free settlement As illustrated in Fig. 3.19, cracks occur mainly at a change in section, in narrow columns and walls due to arching, and in trough or waffle slabs; other locations are formwork tie bolts and fixed reinforcement near the top of the concrete where voids can form underneath the reinforcement. Plastic settlement cracks can be prevented by reducing the bleeding using air entrainment or by incorporating fibre reinforcement. If possible, a reduction of restraint and re-vibration of the concrete are also other ways to avoid or eliminate plastic settlement cracks.

Plastic shrinkage cracking

Plastic shrinkage is caused by the loss of water by evaporation from the surface of newly laid concrete or by suction of dry concrete underneath. At the surface, plastic shrinkage occurs when the rate of evaporation exceeds the rate of bleeding. Contraction induces tensile stress in the surface layers because they are restrained by the non-shrinking inner concrete. Since concrete has a low tensile strength or low strain capacity in its plastic state, cracking can readily occur.

Plastic shrinkage cracks are most common in slabs, occurring randomly, diagonally and over reinforcement (see Fig. 3.19). Prevention of plastic shrinkage cracking is achieved by covering the surface of the concrete as early as possible and protecting it from the effects of drying winds. Spraying of resin-based curing compounds (unless in emulsion form) cannot be done effectively until the free water has evaporated. It is therefore difficult to ensure that the compound is applied before plastic shrinkage cracks have begun to form. Covering with polythene sheet is the most effective solution. On concrete roads and other surfaces, where the finished texture is vital, the covering must be suspended clear of the surface. The risk of cracking is also reduced by the use of

fibre reinforcement, which significantly increases the tensile strain capacity of concrete in its plastic state. In some cases, cracks can be eliminated by re-vibration of the concrete or by power floating and trowelling of flat surfaces.

3.3.3 Early-age thermal cracking

In large elements of concrete, the rate of heat development due to hydration of cement in the first one to three days after casting is likely to exceed the rate of heat loss to the atmosphere, causing the temperature in the concrete to rise. Thermal expansion thus occurs, which is followed by thermal contraction later as the concrete cools. Typical early age temperature histories are shown in Fig. 3.20, where the influences of both an increase in cement content and in section size of the element are seen to increase the peak temperature.

Internal stress will be set up in the concrete due to restraints of thermal movement as it is virtually impossible to construct large concrete mass without restraints. They take the forms of *internal restraint* due to the different rates of heating and cooling between the core and surface of the concrete section, and *external restraint* caused by casting on, or adjacent to, previously hardened concrete. The presence of steel reinforcement also provides restraint, but this can be beneficial rather than detrimental. Reinforcement that is uniformly distributed and situated near the surface of the concrete can be utilised to control the width and number of cracks.

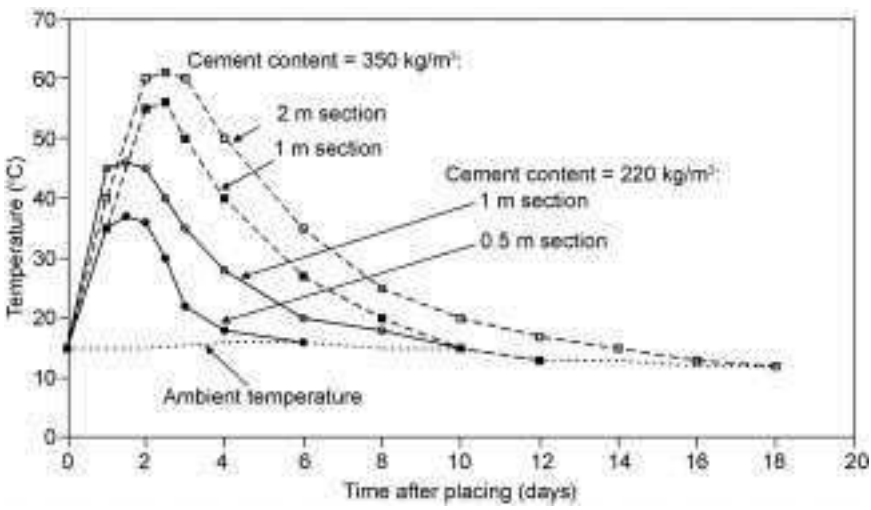

3.20 Effect of cement content and section size on the early age temperature history of concrete (Concrete Society, 1992. Adapted from 'Non-structural cracks in concrete', Technical Report No. 22, Third Edition, Slough, UK, The Concrete Society).

3.3.4 Internal restraint

Figure 3.21 illustrates the stress induced when concrete is subjected to early-age temperature history. After placing a large mass of concrete, the temperature rise due to the heat of hydration generated causes the interior of the concrete to become hotter than the surface layers, where heat is lost to the atmosphere unless the mass is completely insulated. The consequent differential expansion results in the interior section being restrained by the outer section generating compressive stresses in the interior and tensile stresses in the surface section. These stresses are relieved to a significant extent by creep, as illustrated in Fig. 3.22, since at this stage creep is large because the concrete is young and of low maturity. At peak temperature, the interior section will be in relieved compression, while the surface could crack if the relieved tensile stress exceeds the tensile strength of the young concrete (Fig. 3.22).

As the concrete starts to cool, the inner section now tends to contract more than the outer section so the effect of this internal restraint is to reduce the compression in the inner section and reduce the tension or close any cracks in the outer section. Creep will again relieve the stresses but to a lesser extent than during the heating cycle because the concrete is now more mature. Eventually, as the temperature of the concrete approaches the ambient temperature, the stress in the inner section could change from compression to tension, with a risk of cracking, while the outer section will be in compression.

In the foregoing situation, it is apparent that creep could be a cause of potential cracking because of too much early relief of compressive stress during the heating cycle compared with tensile stress relief during the cooling cycle.

Internal restraint may be quantified in terms of the restraint factor, R, which is defined as:

$$R = \frac{\epsilon_f - \epsilon_a}{\epsilon_f} \tag{3.9}$$

where ϵ_f = free thermal strain and ϵ_a = actual strain. Thus for no restraint, $R = 0$ as the actual strain is equal to the free strain, and full restraint is when the actual strain is zero, i.e. $R = 1$.

Generally, cracking due to internal restraint in a large concrete mass will occur if:

$$\sigma_t = \alpha \cdot \Delta T \cdot R \cdot E_e \geq f_{cr} \tag{3.10}$$

where σ_t = tensile stress, α = coefficient of thermal expansion, ΔT = temperature differential across the section, f_{cr} = tensile creep rupture strength and E_e = effective or reduced modulus due to creep, viz.

$$E_e = \frac{\sigma_t}{e_o + C} = \frac{E\sigma_t}{\sigma_t + EC} = \frac{E}{1 + EC_s} \tag{3.11}$$

where e_o = elastic strain at loading, C = creep, E = modulus of elasticity and C_s = specific creep.

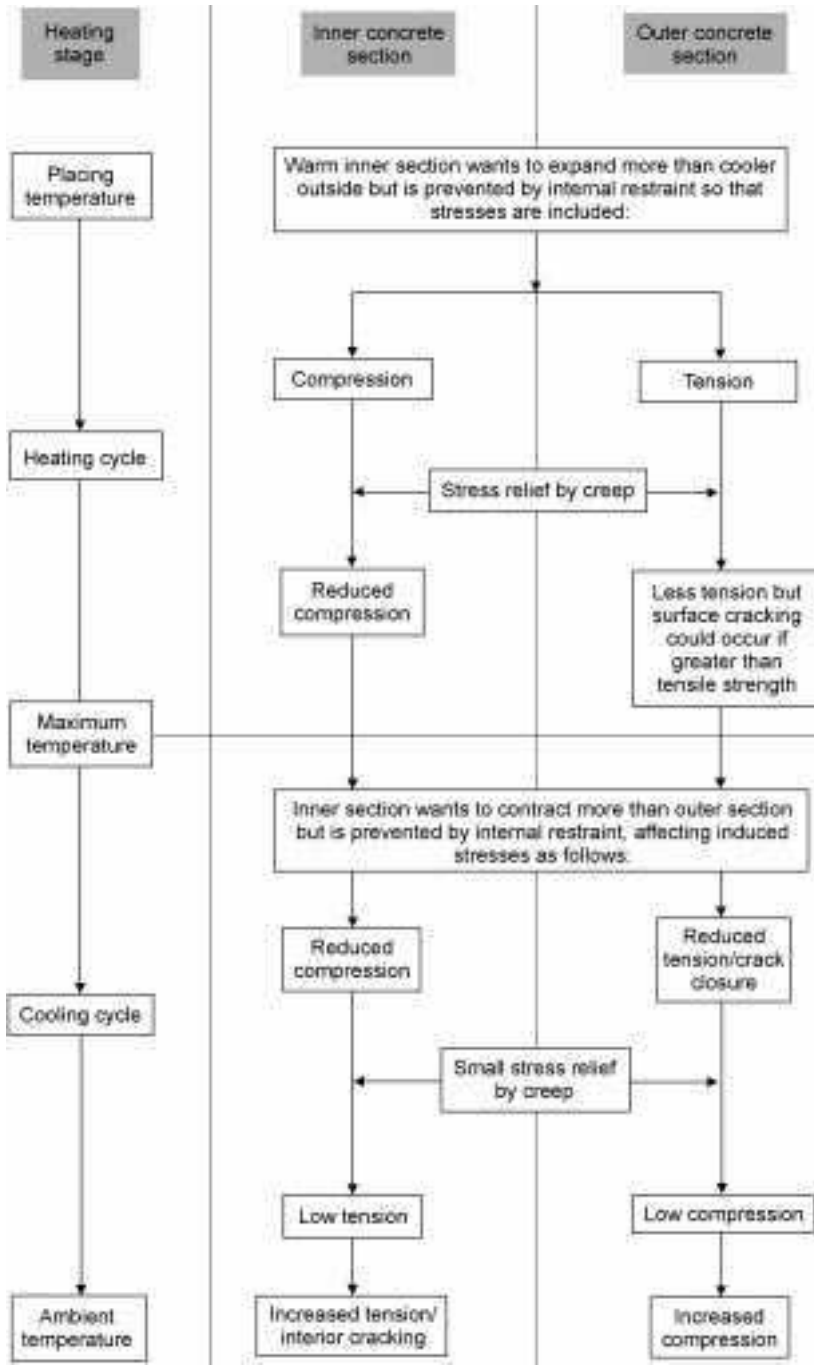

3.21 Representation of the development of induced stresses in a large concrete section subjected to early-age temperature history due to heat of hydration.

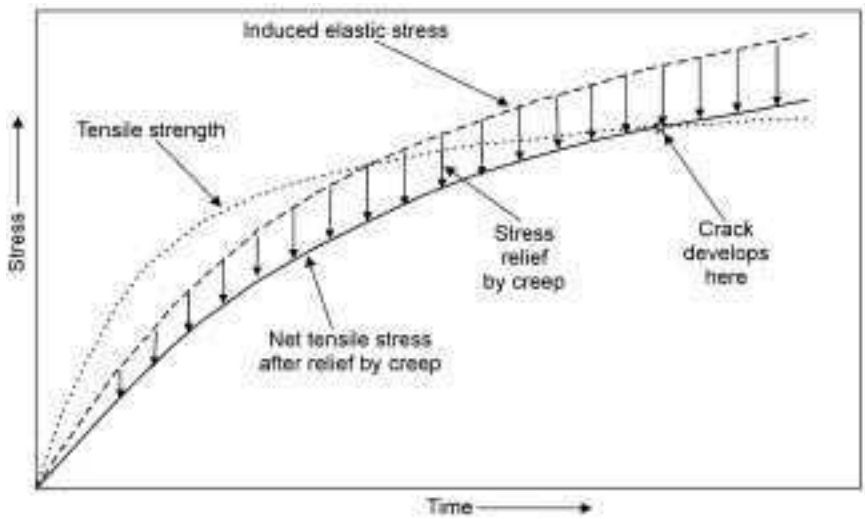

3.22 Schematic pattern of crack development when tensile stress induced by restrained movement is relieved by creep (Neville and Brooks, 2002. From *Concrete Technology*, Fig. 13.13, published by Pearson Education Ltd).

It is important to note that the tensile creep rupture strength, f_{cr}, which determines the condition for cracking in the cases of early age thermal cracking and restrained drying shrinkage cracking, is less than the value determined in the laboratory under short-term loading and typically it is taken as 60% of the short-term strength (see Section 3.2.4).

3.3.5 External restraint

It may be possible to avoid external restraint by the provision of movement joints, but in most structures it is necessary to cast subsequent pours against hardened concrete in order to satisfy the requirements of continuity in the structural design. The risk of thermal cracking is particularly great in cantilevered retaining walls for reservoirs, basements, bridge abutments, etc. When a vertical section of a wall is being cast, the restraint provided by the base of the wall and by adjoining sections is considerable. Cracks are likely to occur unless precautions are taken. The spacing of joints and the sequence and timing of concrete pours must be carefully planned.

If the whole concrete mass is insulated so as to eliminate internal restraint, there will be no cracking provided also there is no external restraint. When the latter is not possible, the risk of cracking can be minimised in several ways by considering the conditions for cracking to occur, namely:

$$\sigma_t = \alpha \cdot (T_p - T_a) \cdot R \cdot E_e \geq f_{cr} \qquad 3.12$$

where $(T_p - T_a)$ = the difference between peak and ambient temperatures.

Thus, the induced tensile stress will be minimised by reducing the terms of equations 3.10 and 3.12 namely:

- The coefficient of thermal expansion can be reduced by selecting the concrete mix ingredients carefully. For example, lightweight aggregate has a lower thermal coefficient as well as a lower effective modulus (more creep). Other types of aggregate (notably limestone) have low coefficients of thermal expansion (BS 8110: Part 2, 1985).
- The difference between peak and ambient temperature $(T_p - T_a)$ is reduced by cooling the mix ingredients. For example, when the ambient temperature is around 20 ºC, cooling the mixing ingredients to approximately 7 ºC will reduce the peak temperature, T_p, by a corresponding amount. Compared with cooling the cement and aggregate, it is often more convenient and effective to cool the mixing water with the addition of ice, which uses the heat from the other ingredients to provide the latent heat of fusion.
- The peak temperature can also be minimised by choosing a low-heat type of cement, such as blended cement with fly ash (pulverised fuel ash) or ground granulated blastfurnace slag, which will reduce the rate of temperature rise as well as the peak temperature.
- The restraint factor, R, can be reduced by insulating formwork for thick sections ($\geq$ 500 mm) and by having longer formwork striking times. Timber formwork provides better insulation than steel or glass reinforced plastic.

3.3.6 Drying shrinkage cracking

Long-term drying shrinkage cracks are formed when drying shrinkage is restrained and typical locations are thin slabs and walls, as illustrated in Fig. 3.19. The main causes of shrinkage cracking are inefficient or insufficient joints, inadequate reinforcement, poor curing and too high a water content in the original concrete mix. Remedies are to address those causes at the design stage and to consider the use of a shrinkage reducing admixture as well as the factors affecting drying shrinkage discussed in Section 3.2.3.

As in the case of early-age thermal cracking, the form of restraint can either be internal or external. An example of external restraint is that of an unreinforced concrete built-in slab drying from the surface as shown in Fig. 3.23. If, after being relieved by creep, the induced tensile stress exceeds the strength, the result would be a single crack through the slab. For cracking to occur, the tensile stress is given by:

$$\sigma_t = S \cdot R \cdot E_e \geq f_{cr} \qquad 3.13$$

where $S =$ drying shrinkage.

Since the slab is fully restrained, $R = 1$ and therefore:

$$\sigma_t = S \cdot E_e \geq f_{cr} \qquad 3.14$$

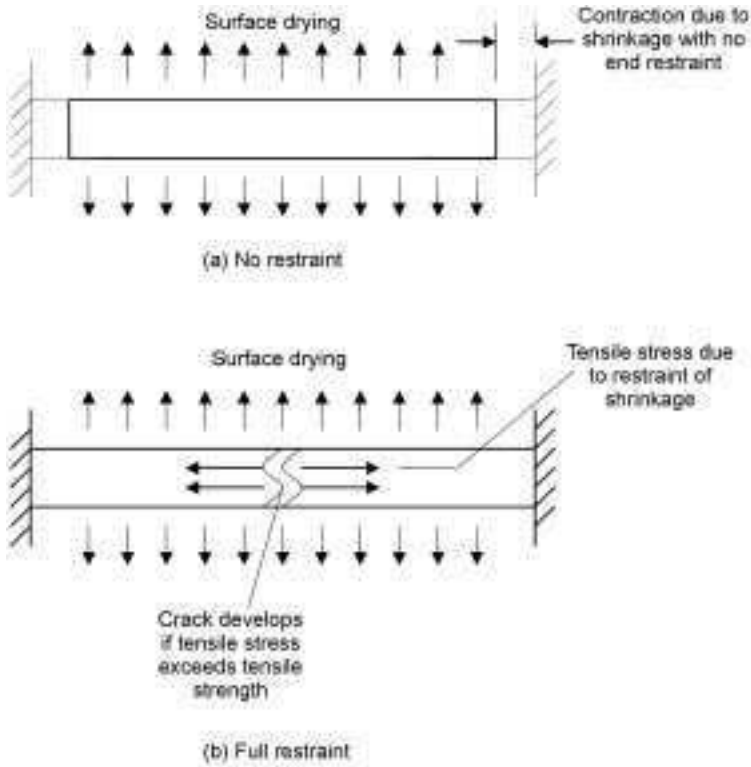

3.23 Example of full restraint of drying shrinkage in a concrete slab.

Of course, in practice, steel reinforcement would be provided for structural reasons. Reinforcement does not prevent cracking but instead of a single crack, much smaller cracks are produced that are distributed over the surface of the slab according to the amount and spacing of the reinforcement (Beeby, 1979; Carino and Clifton, 1995).

In concrete members having thicker sections, drying from the surface results in a moisture gradient since the inner layers have a greater moisture content than the surface layers. This moisture gradient causes internal restraint and can also lead to surface cracking. In fact, drying shrinkage is not a 'true' shrinkage in the sense that it is simply proportional to the loss of water but is the combination of 'true' shrinkage and strain induced by the moisture gradient. 'True' shrinkage cannot really be measured although researchers have attempted to determine it using very thin cement paste sections. Figure 3.24 demonstrates what would happen in the case of a long member drying from the surface whose end is sealed. 'True' shrinkage would result in the end developing a parabolic shape (Fig. 3.24(b)) but, because of the moisture gradient, the contracting surface layers are restrained by the inner layers so that tension develops in the surface

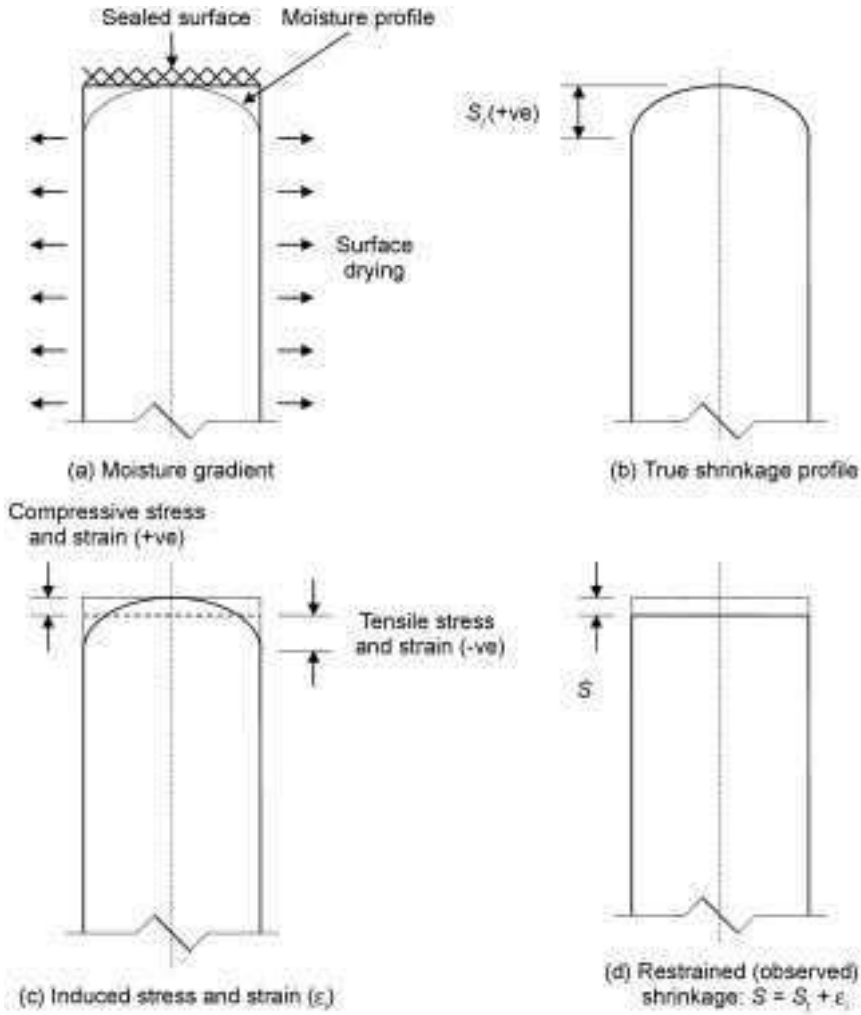

3.24 Example of partial restraint of drying shrinkage of concrete by a moisture gradient.

and this is balanced by compression in the interior (Fig. 3.24(c)). The net result is a restrained (observed) shrinkage (Fig. 3.24(d)) and the induced tensile stress at the surface is responsible for potential drying shrinkage cracks. The condition for cracking is:

$$\sigma_t = S_t \cdot R \cdot E_e \geq f_{cr} \qquad 3.15$$

where $S_t =$ true shrinkage, $R = (S_t - S)/S_t$ and $S =$ actual or restrained shrinkage.

3.3.7 Fracture mechanics

Linear elastic fracture mechanics is concerned with predicting conditions that give rise to rapid crack propagation in brittle materials that are considered to be elastic, homogeneous and isotropic at the onset of fracture; it involves the study of stress and displacement at the microscopic level in the region of a crack tip (Mindess and Young, 1981). The field developed from the pioneering work of Griffith (1920) who proposed criteria for the fracture of brittle solids that explained the discrepancy between their low observed bulk strengths and their much higher theoretical strengths (estimated for perfect crystals to be ~ $E/10$) by postulating the existence of microscopic flaws, which serve as stress concentrators. As illustrated in Figure 3.25, for an elliptical crack with dimensions as indicated, the maximum tensile stress near the crack tip is intensified by a factor that depends on the crack length and end radius according to the relationship:

$$\frac{\sigma_m}{\sigma} = 2\left(\frac{c}{r}\right)^{0.5} \qquad 3.16$$

Hence the local tensile stresses at the tips of very sharp cracks can reach values (~$E/10$) high enough to break the bonds between atoms at relatively low nominal stresses; crack propagation is then liable to become progressive because as the

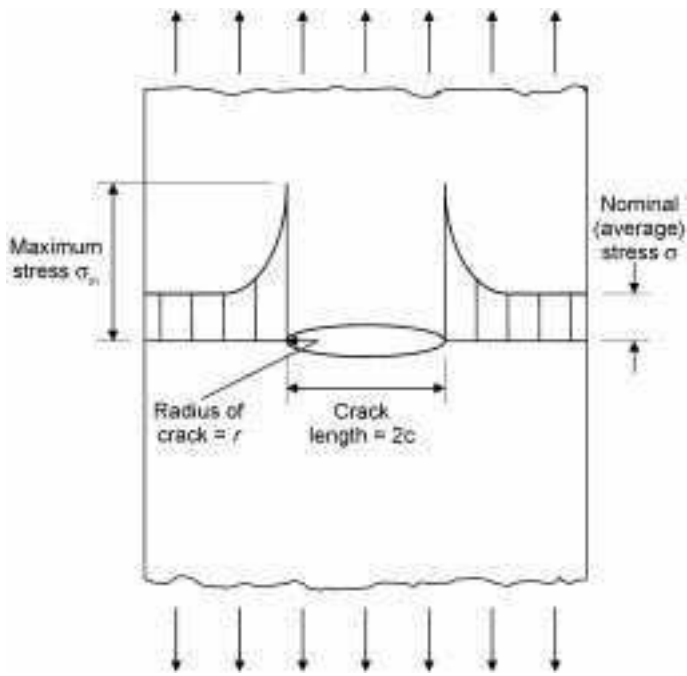

3.25 Stress concentration at the tip of a crack in a brittle material subjected to a tensile stress (Neville and Brooks, 2002. From *Concrete Technology*, Fig. 6.1, published by Pearson Education Ltd).

crack length increases the maximum stress at the tip increases (equation 3.16) while the theoretical stress required to induce energetically favoured crack growth in a brittle material, σ_f, decreases in accordance with the following expression (Illston *et al.*, 1979):

$$\sigma_f = \left(\frac{2 \cdot \gamma \cdot E}{\pi \cdot c}\right)^{0.5} \qquad 3.17$$

where $\gamma =$ surface energy required to cause fracture and $E =$ modulus of elasticity.

Similar reasoning has been used to explain the failure of concrete (Kaplan, 1961), which is generally regarded as being brittle with failure occurring at low strains due to linking of existing and newly-formed microcracks.

Strictly speaking, however, concrete exhibits some plasticity (non-linear stress-strain behaviour) prior to failure. It is also evidently heterogeneous as the properties of its constituents are not all identical and it develops a relatively large fracture zone due to microcracking which causes progressive softening of the material prior to complete failure. Various ways of incorporating the above effects into models of the fracture of concrete specimens of different sizes and shapes under different states of applied stress have been proposed and the application of non-linear fracture mechanics is believed to provide a more representative means of describing the fracture behaviour and ultimate capacity of concrete structures. Further consideration of this field is beyond the scope of the present chapter and readers who require more a detailed treatment are referred to specialist works such as the following (ACI SP-118, 1989; ACI Committee 446, 1991; Karihaloo, 1995; Shah *et al.*, 1995).

3.4 Conclusions

The knowledge of movements and cracking processes presented in this chapter has been developed from theories, research and technical field data published over many years for conventional types of concrete, namely low-strength mixes using natural aggregates. Although the principles are not expected to change, in the future design methods given in Codes of Practice will be continuously amended to account for the use of more sophisticated concreting materials, such as high performance concrete, which refers to both high durability (low permeability) and/or high strength concrete. In some cases, the high strength is required to design smaller concrete elements or low deflections through a corresponding high modulus of elasticity, low creep and low shrinkage. Such concrete tends to be more brittle and prone to cracking so that ductility needs to added, say, in the form of fibre reinforcement. High performance is achieved by the combined use of chemical and mineral admixtures: high range water-reducers (superplasticisers) and fine cement replacement materials to replace part of cement, e.g. silica fume.

On the other hand, admixtures designed to reduce shrinkage, creep and the risk of cracking are likely to be used more frequently in conjunction with, say, superplasticisers to offset any reduction in strength. Little is known about the long-term behaviour of concretes made with cocktails of different admixtures and the possible interactions between supplementary cementing materials (or mineral admixtures) and multi-functional chemical admixtures need to be assessed. Advanced methodologies may have to be developed for evaluating the early age cracking characteristics of some of the newer formulations being considered for use in high strength applications and repair situations (Bentur and Kovler, 2003). The increased usage of recycled concrete and other waste materials to replace or augment natural aggregates in concrete has also to be considered in the context of prediction models and design documents.

It should be emphasised that it has been only possible to present brief details of movements and cracking processes experienced by concrete in this chapter, there being a huge amount of research and technical literature available. From the references given in Section 3.5, further background information is recommended as follows:

- Movements in plain and reinforced concrete: Illston *et al.*, 1979; Mindess and Young, 1981; Neville *et al.*, 1983; Bazant, 1988; Gilbert, 1988; Neville, 1995; Neville and Brooks, 2002.
- Non-structural cracking: Harrison, 1981; Concrete Society, 1992; ACI 224R-90, 1996.
- Fracture mechanics: Mindess and Young, 1981; ACI SP-118, 1989; ACI Committee 446, 1991; Karihaloo B I, 1995; Shah *et al.*, 1995.

3.5 References

ACI SP-118 (1989), *Fracture Mechanics: Application to Concrete*, Editors: Li V C and Bazant Z P, Detroit, USA, American Concrete Institute.

ACI Committee 209 (1992), *Prediction of creep, shrinkage and temperature effects in concrete structures*. Detroit, American Concrete Institute.

ACI 224R-90 (1996), *Control of Cracking in Concrete Structures*, ACI Manual of Concrete Practice, Part 3, Detroit, USA, American Concrete Institute.

ACI 224.1R-93 (1996), *Causes, Evaluation and Repair of Cracks in Concrete Structures*, ACI Manual of Concrete Practice, Part 3, Detroit, USA, American Concrete Institute.

ACI 318-95 (1996), *Building Code Requirements for Structural Concrete* and ACI 318R-95 (1996), *Commentary*, ACI Manual of Concrete Practice, Part 3, Detroit, USA, American Concrete Institute.

ACI Committee 446 (1991), *Fracture Mechanics of Concrete: Concepts, Models and Determination of Material Properties,* ACI Report 446.IR-91. Farmington Mills, Mich., American Concrete Institute.

ASTM C469 (1994), *Test for Static Modulus of Elasticity of Concrete in Compression*, Philadelphia, American Society for Testing and Materials.

ASTM C512 (1987), *Test Method for Creep of Concrete in Compression*, Philadelphia,

American Society for Testing and Materials.
Bazant Z P (Editor) (1988), *Mathematical Modeling of Creep and Shrinkage of Concrete*, John Wiley and Sons, Chichester, UK.
Bazant Z P and Baweja S (1995), 'Creep and shrinkage prediction for analysis and design of concrete structures – Model B3', *Materials and Structures*, 28, 357–365, 415–430, 488–495.
Beeby A W (1979), 'The prediction of crack widths in hardened concrete', *The Structural Engineer*, 57A, 1, 9–17.
Bentur A and Kovler K (2003), 'Evaluation of early age cracking characteristics in cementitious systems', *Materials and Structures*, 36, 183–190.
British Standard DDENV 1992-1-1 (1992), *Eurocode 2:Design of concrete structures – Part1 general rules and rules for buildings,* Milton Keynes, British Standards Institution.
Brooks J J (1999), 'How admixtures affect shrinkage and creep', *Concrete International*, 21, 4, 35–38.
Brooks J J (2000), 'Elasticity, Creep and Shrinkage of Concretes Containing Special Admixtures', Adam Neville symposium: 'Creep and Shrinkage-Structural Design Effects', Edited by Al-Manaseer A, *ACI Special Publication, SP 194*, 283–360.
Brooks J J (2001), 'A theory for drying creep of concrete', *Magazine of Concrete Research*, 53, 01, 51–61.
Brooks J J (2005), '30-year creep and shrinkage of concrete', *Magazine of Concrete Research*, 57, 9, 545–546.
Brooks J J and Al-Quarra H (1999), 'Assessment of creep and shrinkage for the Flintshire Bridge', *The Structural Engineer*, 77, 5, 21–26.
Brooks J J and Megat Johari M A (2001), 'Long-term deformations of high-strength concrete containing silica fume and metakaolin', *Proceedings of 5th CANMET/ACI International Conference on Recent Advances in Concrete Technology*, ACI SP-200, Singapore, 97–112.
BS 1881: Part 121 (1983), Method for determination of static modulus of elasticity in compression, Milton Keynes, British Standards Institution.
BS 8110: Part 2 (1985), Structural use of concrete: Code of Practice for special circumstances, Milton Keynes, British Standards Institution.
BS EN 1355 (1997), *Determination of creep strains under compression of autoclaved aerated concrete or lightweight aggregate concrete with open structure*, Milton Keynes, British Standards Institution.
Carino N J and Clifton R C (1995), *Prediction of cracking in reinforced concrete structures*, NISTIR 5634, Gaithersburg, Maryland, USA, Building and Fire Research Laboratory, National Institute of Standards and Technology, US Department of Commerce.
Comite Euro-International du Beton (CEB) (1999) *Structural concrete-textbook on behaviour, design and performance. Updated knowledge of the CEB/FIP model Code 90*, Lausanne, FIP bulletin 2, Federation International du Beton, 37–52.
Concrete Society (1992), *Non-structural cracks in concrete*, Technical Report No. 22, Third Edition, Slough, UK, The Concrete Society.
Domone P L (1974), 'Uniaxial tensile creep and failure of concrete', *Magazine of Concrete Research*, 26, 88, 144–152.
Gardner N J and Lockman M. J (2001), 'Design provisions for drying shrinkage and creep of normal strength concrete', *ACI Materials Journal*, 98, 2, 159–167.
Gilbert R I (1988), *Time effects in concrete structures*, Developments in Civil Engineering, 23, New York, Elsevier.

Griffith A A (1920), 'The phenomenon of rupture and flow in solids', *Phil Trans Royal Soc*, A221, 163–198.

Hanson T C and Mattock A H (1966), 'The influence of size and shape of member on the shrinkage and creep of concrete', *ACI Journal*, 63, 267–290.

Harrison T A (1981), *Early-age thermal crack control in concrete*, CIRIA Report 91, London, Construction Industry Research and Information Association.

Hobbs D W (1971), 'The dependence of the bulk modulus, Young's modulus, creep, shrinkage and thermal expansion of concrete upon aggregate volume concentration', *Materials and Structures*, 4, 20, 107–114.

Illston J M, Dinwoodie J M and Smith A A (1979), *Concrete, Timber and Metals – The Nature and Behaviour of Structural Materials*, New York, Van Nostrand Reinhold.

Kaplan M F (1961), 'Crack propagation and fracture of concrete', *Proceedings ACI Journal*, 58, 5, 591–610.

Karihaloo B I (1995), *Fracture Mechanics and Structural Concrete*, London, Longman and New York, Wiley.

Khoury G A, Grainger B N and Sullivan P J E (1985), 'Transient thermal strain of concrete: literature review, conditions within specimen and behaviour of individual constituents', *Magazine of Concrete Research*, 37, 133, 131–144.

Kordina K (1960), 'Experiments on the influence of the mineralogical character of aggregate on the creep of concrete', *RILEM Bulletin*, 6, 7–22.

L'Hermite R L (1959), 'What do we know about the plastic deformation of concrete?', *RILEM Bulletin*, 1, 22–25.

Mindess S and Young J F (1981), *Concrete*, New Jersey, USA, Prentice-Hall.

Neville A M (1995), *Properties of Concrete*, Fourth Edition, Harlow, UK, Longman.

Neville A M and Brooks J J (2002), *Concrete Technology*, Revised Edition-2001 Standards Update, Harlow, UK, Pearson Prentice Hall.

Neville A M, Dilger W H and Brooks J J (1983), *Creep of Plain and Structural Concrete*, London and New York, Construction Press.

Newman J and Choo B S (2003), Editors, *Advanced Concrete Technology-Concrete Properties*, Oxford, UK, Butterworth-Heinemann.

Odman S T A (1968), 'Effects of variations in volume, surface area exposed to drying, and composition of concrete on shrinkage', *Proceedings of Int. Colloquium on the Shrinkage of Hydraulic Concretes*, *RILEM/CEMBUREAU*, Madrid, 1.

Rusch H (1960), 'Researches towards a general flexural theory for structural concrete', *ACI Journal*, 57, 1, 1–28.

Shah S P, Swartz S and Ouyang S (1995), *Fracture Mechanics of Concrete*, New York, Wiley.

Troxell G E, Raphael J M and Davis R E (1958), 'Long-time creep and shrinkage tests of plain and reinforced concrete', *Proc. ASTM*, 58, 1101–1120.

Wagner O (1958), 'Das Kriechen unbewehrten Betons', *Deutscher Ausschuss fur Stahlbeton*. 131.

4

Chemical degradation of concrete

J BENSTED, University College London, UK,
A R BROUGH, formerly University of Leeds, UK and
M M PAGE, University of Birmingham, UK

4.1 Introduction

Chemical attack on concrete is a rather complicated subject since the chemistry of concrete itself is complex and the material is used in a very wide variety of environments. Of the types of degradation that are associated primarily with chemical changes occurring within the hydrated cement matrix, sulfate attack in its various guises is probably the most widespread threat to concrete durability, but acid attack can also take place in concrete sewers, silos, dairies, etc. and bacteria can mediate sulfate and acid attack in various environments. This chapter presents a brief overview of these important forms of degradation.

Acid attack on Portland cement concrete is not unexpected, since all of the phases in cement paste are basic, and many of them (for example, calcium hydroxide) are readily dissolved by acids. Typically, acid attack leads to loss of binder and strength in concrete and eventually to loss of section. Unlike acid attack, sulfate attack commonly involves expansive reactions which fracture the concrete leading to ongoing degradation, loss of strength and function. Several different processes may be involved and the literature on this subject has grown remarkably in recent years, prompting one reviewer to describe the current situation as more than a little confused (Neville, 2004). Notwithstanding the confusion, the topic is of evident interest and, while recognising that overlaps exist and that other classifications might be preferred by some workers in this diverse field, we shall attempt to provide a simplified account here of the following three categories:

- sulfate attack involving expansive ettringite formation along with other reactions, in which the sulfate is introduced principally from the external environment
- thaumasite sulfate attack (TSA), a combined attack requiring both sulfate and carbonate sources
- delayed ettringite formation (DEF), sulfate attack arising from vigorous heat curing, in which the source of sulfate is internal to the concrete.

Apart from TSA, the usual mechanisms of sulfate attack have generally been thought to involve changes in the chemistry of the hydrated aluminate phases in the concrete (accompanied by other processes that are dependent on the nature of the cations introduced with the sulfate anions). TSA is the exception in attacking the calcium silicate hydrate (C-S-H). Thus many instances of sulfate attack might be mitigated in principle by the use of a siliceous cement (based on alite and belite) in which aluminate phases are not present. Such a cement, however, would be very expensive to manufacture since the aluminates and ferrites act as fluxes in the kiln, significantly lowering the cement burning temperature and time. Aluminates are also naturally present in most large scale silicate sources. Sulfate Resisting Portland Cements (SRPC) (BS 4027, 1996) with low aluminate levels are obtainable (for a small price premium) and resist sulfate attack on the hydrated aluminate phases, although they remain vulnerable to TSA and may be subject to attack by salts such as magnesium sulfate which can interact deleteriously not only with aluminates but also with other hydration products such as CH and C-S-H. Since the sulfate exposure conditions in different countries differ, selection of SRPC is a trade-off between performance and cost, and specifications remain as national standards, having not yet been incorporated into the common European cement standard (BS EN 197-1, 2000).

For a general introduction to cement chemistry the reader is referred to standard textbooks on concrete (Neville, 1995; Mindess *et al.*, 2002) or cement (Bensted and Barnes, 2002; Bye, 1999; Hewlett, 1998; Taylor, 1997; Lea, 1970). Only the barest outline is given here. Cement clinker coming out of the kiln consists of:

- calcium silicates
  - alite (impure C_3S)
  - belite (impure C_2S)
- calcium aluminates
  - impure C_3A
  - various ferrite phases approximated by C_4AF but with a wide range of compositions and with extensive substitution.

All of these phases react with water at varying rates to form a range of hydrated silicates and aluminates along with calcium hydroxide. The C_3A, when present at appreciably high levels, tends to cause flash set (i.e., rapid heat evolution and initial stiffening but suppression of subsequent hardening) unless low levels of sulfate are added to the cement to modify its hydration so avoiding this potential problem. Traditionally gypsum was added, which often partially dehydrated during grinding, and its role in set regulation of Portland cement-based systems has been considered elsewhere (Bensted, 2002a); now iron (II) sulfate is commonly used instead to reduce Cr(VI) in order to comply with EU directive 2003/53/EC (British Cement Association, 2005).

Table 4.1 describes the shorthand system often used to represent the oxides in cement chemistry and lists the various phases discussed in this chapter. For the purposes of discussion of sulfate attack, and assuming gypsum to be the sulfate source, we can simplify the hydration of the aluminate phase as follows at early ages when ettringite, $C_6As_3H_{32}$, is formed:

$$C_3A + 26H + 3CsH_2 = C_6As_3H_{32} \quad 4.1$$

To some extent the aluminium in ettringite is partially substituted by iron and the impure form is referred to as AFt, the 'A' and 'F' denoting the presence of aluminium and iron and the 't' indicating 'trisulfate'.

At later stages of cement hydration, the gypsum runs out, and additional aluminate reacts with the ettringite to form C_4AsH_{12} or AFm phases in which 'm' denotes 'monosulfate' (reaction 4.2). In addition to sulfate-bearing AFm, hydroxy (and carbonate) AFm phases such as $C_4(A,F)H_{13}$, hydrocalumite, may also be formed depending on the available anions. These can enter into solid solutions with the sulfate AFm phases.

Table 4.1 Cement chemical nomenclature system (CCNS)

In cement science a shorthand system uses capital letters to represent the nominal constituent oxides of cement minerals:

A – Al_2O_3 C – CaO F – Fe_2O_3 H – H_2O M – MgO S – SiO_2 T – TiO_2

If the same initial letter is used for different oxides, then the other oxide either has a bar across the top to avoid confusion or (increasingly now) a small case letter is used instead:

c – CO_2 f – FeO s – SO_3

C-S-H is hyphenated to represent a variable (nonstoichiometric) entity without a precise chemical composition.

Examples given in the text are set out below:

CCNS	Oxide content	Chemical composition
Portland cements		
C_3S	$3CaO.SiO_2$	Ca_3SiO_5
C_2S	$2CaO.SiO_2$	Ca_2SiO_4
C_3A	$3CaO.Al_2O_3$	$Ca_3Al_2O_6$
C_4AF	$4CaO.Al_2O_3.Fe_2O_3$	Ca_2AlFeO_5
$C_3S_2H_3$	$3CaO.2SiO_2.3H_2O$	$Ca_3Si_2O_73H_2O$
CsH_2	$CaO.SO_3.2H_2O$	$CaSO_42H_2O$
CH	$CaO.H_2O$	$Ca(OH)_2$
$C_6As_3H_{32}$	$6CaO.Al_2O_3.3SO_3.32H_2O$	$[Ca_3Al(OH)_6.12H_2O]_2.(SO_4)_3.2H_2O$
C_4AsH_{12}	$4CaO.Al_2O_3.SO_3.12H_2O$	$[Ca_2Al(OH)_6.2H_2O]_2.SO_4.2H_2O$
C_4AH_{13}	$4CaO.Al_2O_3.13H_2O$	$Ca_2Al(OH)_7.3H_2O$

$$2C_3A + C_6As_3H_{32} + 4H = 3C_4AsH_{12} \quad 4.2$$

The hydration of the calcium silicates can be represented approximately by reaction 4.3 below. The calcium silicate hydrate (C-S-H) that forms is actually non-stoichiometric and of variable composition depending on the conditions under which it is formed; we represent it here as $C_3S_2H_3$ but the true CaO/SiO_2 ratio is usually closer to 1.7 (Taylor 1997):

$$2C_3S + 6H = C_3S_2H_3 + 3CH \quad 4.3$$

C_2S reacts similarly to C_3S but less calcium hydroxide is formed. Many types of cement now also contain blended pozzolanic or latently hydraulic compounds such as fly ash, ground granulated blast furnace slag, microsilica or metakaolin, which hydrate alongside the cement phases to give a modified chemistry and microstructure. Most provide additional silica, reducing the amounts of free calcium hydroxide formed, and some also provide additional reactive alumina. In some cases (provided they have had sufficient curing to react) such blending agents can confer additional chemical durability, and this is discussed below for the different forms of chemical attack on concrete.

4.2 External sulfate attack involving expansive ettringite formation

4.2.1 Basic phenomena

The expansive ettringite form of sulfate attack in concrete exposed to aggressive ground is probably the most familiar type that occurs in the field (Bensted, 1981a,b) and was at one time regarded as the only serious phenomenon involved. Indeed sulfate attack was given a formal definition by the American Society of Testing and Materials (ASTM) in the 1970s as follows: 'Sulfate attack can be defined as a chemical or physical reaction, or both, between sulfates usually in soil or ground water and concrete or mortar, primarily with calcium aluminate hydrates in the cement paste matrix, often causing deterioration' (Bensted, 1981a). Although thaumasite sulfate attack has come into increased prominence recently (see Section 4.3) and involves the silicate as well as the aluminate phases, this does not render the above definition inappropriate insofar as what is now regarded as the conventional form of sulfate attack is concerned.

Sulfate attack has attracted increasing interest over the years as its complexities have become more apparent. There have been a number of recent review articles (Skalny and Marchand, 2001; Santhanam *et al.*, 2001; Bensted, 2002b; Neville, 2004) and even books on the subject (Marchand and Skalny, 1999; Skalny *et al.*, 2002). Ettringite formation features prominently in many situations but there are several other processes, such as the conversion of portlandite to gypsum and reversible hydration/dehydration reactions of sulfate

salts, such as the Na_2SO_4 (thenardite) ↔ $Na_2SO_4.10H_2O$ (mirabilite) system, that have also been implicated. In this context it may be noted that there has been disagreement over the terminology used to classify these various phenomena and some authors consider processes such as the thenardite/mirabilite transformation to be purely physical phenomena, as distinct from chemical forms of attack. It is generally agreed that sulfate attack needs the presence of moisture and it is believed to involve 'through-solution' mechanisms, with transport of sulfate ions through the surface of the concrete or mortar. Normally such transmission is of extraneous sulfate ions, but internal sulfates within the structure can also contribute if the amounts contained in the concrete mix materials are not controlled within acceptable limits (Skalny *et al.*, 2002). An example of the sort of degradation that may be produced is illustrated in Fig. 4.1.

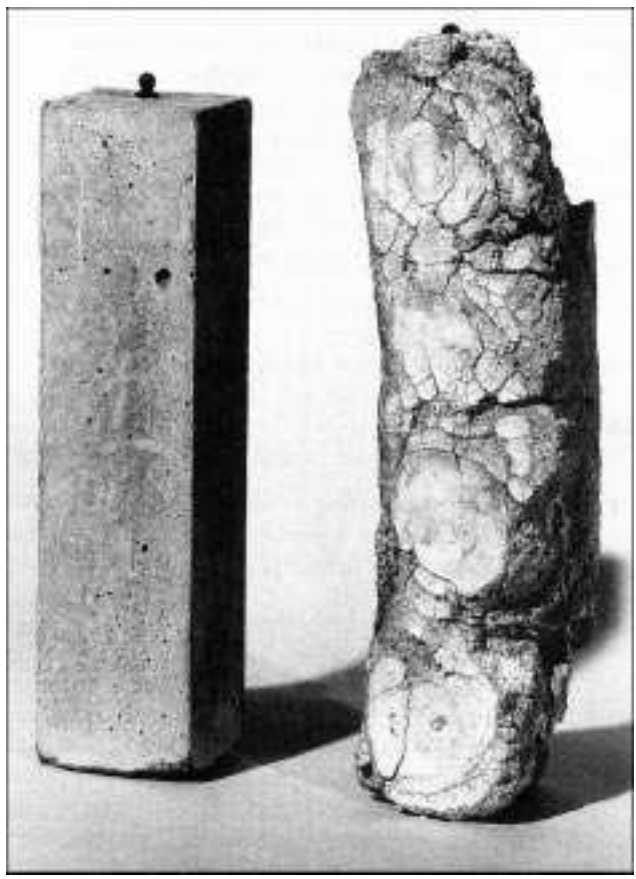

4.1 Conventional sulfate attack associated with expansive ettringite formation in a concrete prism (RHS) and non-degraded control prism (LHS). Photograph reproduced from CEB Design Guide, *Durable Concrete Structures*, London, Thomas Telford, 1989.

In its initial stages, sulfate attack may result in a general hardening of the cement matrix. This usually arises from the pores and voids present becoming filled, through the ingress of SO_4^{2-} ions, by crystals of gypsum and/or ettringite, which tend to increase the overall density of the concrete or mortar. These crystals, which are formed in the pores and voids, may cause expansion directly by anisotropic growth or indirectly by increasing the pore water pressure, giving rise to internal stresses that might ultimately, in specific instances, destroy the concrete or mortar. For instance, in transforming one mole of calcium hydroxide CH to gypsum CsH_2, the volume of solids is more than doubled (from 33.2 cm^3 to 74.3 cm^3) and the transformation of calcium aluminate hydrate and gypsum to ettringite also involves more than doubling of the volume of solids (Bensted, 1981a; Lea, 1970; Eglinton, 1998).

4.2.2 Exposure conditions

Groundwaters and soils containing sulfate salts may be liable to cause expansive sulfate attack. Sulfuric acid can also occur naturally in groundwaters and soils as a consequence of oxidative weathering of sulfide minerals such as pyrite and marcasite, both of which have the chemical formula FeS_2. Oxidation to ferrous sulfate and sulfuric acid may arise in the presence of oxygen and moisture:

$$2FeS_2 + 7O_2 + 2H_2O \rightarrow 2FeSO_4 + 2H_2SO_4 \qquad 4.4$$

The reaction commonly stops here unless certain aerobic bacteria are present to produce further oxidation cycles (see Section 4.7). In undisturbed soils, the position of the water table is of great importance for determining access of air and therefore the extent to which oxidation can take place. If the pyrite is always below the water level, no oxidation occurs, whilst in areas of fluctuating water levels that permit replenishment of oxygen to the soil, the reaction proceeds readily. If there is sufficient calcium carbonate or other basic minerals in the soil, the sulfuric acid is neutralised as gypsum is formed. If not, as in some instances where sulfuric acid production is marked, the acid may persist in the groundwater (Eglinton, 1998).

Disturbance of natural ground conditions by excavation or drainage is a common cause of pyrite oxidation by providing access for air. Rapid oxidation has been reported when compressed air has been employed to keep back water during underground work, as in tunnel construction (Lea, 1970). This can result in large increases of acidity and in the sulfate content of groundwater. The oxidation of pyrite can be followed by other reactions that cause expansion, such as production of gypsum from any calcite present, which gives a solid volume increase of 103%, and the reaction of gypsum with the monosulfate-hydrocalumite solid solution in hardened concrete to re-form ettringite. The free sulfuric acid can also attack clay minerals like illite to form jarosite $KFe_3(SO_4)_2(OH)_6$, a hydrated potassium iron (III) sulfate that produces a volume 115% greater than that of pyrite. Ground

heave can be caused adjacent to buried concrete structures by production of gypsum and other hydrated sulfates (Hawkins and Pinches, 1997; Cripps and Edwards, 1997). All these reactions can give rise to expansive forces within the concrete, which lower the long-term durability (Bensted, 1981a,b; Eglinton, 1998).

Ettringite is sometimes associated with thaumasite in aggressive ground when the temperatures are low (normally below *ca.* 15ºC) and either or both may be associated with expansion of the concrete if it arises (see Section 4.3). However, the mere presence of ettringite in a hardened concrete is not *per se* proof that it has produced expansion of the concrete. For instance, the ettringite which forms during the early stages of hydration of Portland cement does not cause expansion as it is not rigidly packed. Often, this ettringite is only partially converted to monosulfate-hydrocalumite solid solution (AFm) during the subsequent stages of cement hydration (Bensted, 2002c). Thus observation of ettringite, particularly by techniques such as SEM/EDXA spot analysis that sample only minute volumes within the specimens of concrete examined, clearly does not provide conclusive evidence of sulfate attack, as has been noted elsewhere (Bensted, 2002b; Neville, 2004).

Only a minority of the sulfate from the original gypsum ground in with the Portland cement clinker during manufacture ends up as ettringite, and most of its formation happens during the first day of hydration at normal ambient temperatures (Bensted, 1983). A substantial part of the sulfate derived from the gypsum actually ends up in the calcium silicate hydrate (C-S-H phase) either sorbed or in solid solution. Expansion of concrete takes place when the hardened monosulfate-hydrocalumite solid solution reacts with gypsum (either from external sources or still present in unhydrated parts of the cement along with unhydrated clinker minerals) to produce ettringite.

4.2.3 Preventative measures

For concrete in contact with aggressive ground, it is obviously desirable that cement with a good record of sulfate resistance is used, e.g. a suitable extended cement containing ground granulated blastfurnace slag (ggbs) or pulverised fuel ash (pfa) which has been adequately cured prior to exposure. The concrete should be of low penetrability, having an appropriately low water/cement ratio, achieved through the use of admixtures where necessary, to minimise the rate of ingress of extraneous sulfates from the environment into the material. Detailed guidance applicable to UK exposure conditions has been given in BRE Special Digest 1, which has already undergone significant revisions since it was first introduced in 2001 and is currently in its 3rd edition (Building Research Establishment, 2005), as discussed in Section 4.5.

One of the many difficulties in formulating simple guidance rules stems from the fact that the conditions to which concrete is exposed prior to coming in

contact with sulfate-bearing groundwater can have a marked influence on the severity of sulfate attack. Thus even mild atmospheric carbonation can play a significant role in modifying the surface pore structure of the material, thereby reducing its penetrability. Current guidance recognises this effect in providing protection to precast products which are exposed to non-acidic sulfate-bearing environments (Building Research Establishment, 2005).

As already mentioned, a recent review has highlighted several other features that contribute to the confused state of knowledge of sulfate attack (Neville, 2004). Amongst these is the influence of the cation, with sodium, calcium and magnesium sulfates all having different effects. Sulfate-resisting Portland cement (ASTM Type V cement), which was developed to minimise reaction with hydration products of the C_3A (aluminate) phase does not offer special protection against attack upon C-S-H or CH and the combined presence of Mg^{2+} and SO_4^{2-} ions can result in the conversion of these hydrates to magnesium hydroxide (brucite), silica gel and gypsum. The concomitant lowering of the pore solution pH, due to the low solubility product of brucite (for which a saturated solution has an equilibrium pH of ~10.5), destabilises the C-S-H and accounts for the fact that magnesium sulfate is more aggressive than sodium sulfate or calcium sulfate. If the pH is maintained at an artificially high level, however, as in some laboratory tests involving magnesium sulfate, unrealistic results may be obtained because brucite can sometimes form an insoluble protective layer upon concrete unless it becomes mechanically damaged.

Altogether the state of current knowledge of external sulfate attack under field conditions remains inadequate and although the problem is generally avoidable by following prescriptive guidance of the kind given in BRE Digest 1 (Building Research Establishment, 2005) it is difficult to devise appropriate laboratory tests for assessing the resistance of different types of concrete subject to different exposures; this problem with performance tests is discussed in further detail in chapter 9 of the book by Skalny *et al.* (2002). Various attempts to devise mathematical models that might serve as aids in predicting performance have been made by researchers in this field and a recent review of the work appears in chapter 7 of the book by Skalny *et al.* (2002) – see also Section 4.6.4 of the present chapter. Unsurprisingly, however, it is fair to say that progress to date has been rather limited.

4.3 Thaumasite form of sulfate attack

4.3.1 Background

Although thaumasite had been known as a rare calcium carbonate-silicate-sulfate hydrate of the composition $CaCO_3.CaSiO_3.CaSO_4.15H_2O$ since 1878, it was not until the 1960s that it first became more generally known as a deterioration product of cement and concrete. The first major report that clearly

documented thaumasite as a concrete deterioration product was published in the Highway Research Record in the United States (Erlin and Stark, 1965). This article mentioned occurrences in two sewer pipes, in a grout and in a pavement core base. For example, in the sewer pipes, the deteriorated areas contained brucite, calcite, gypsum and thaumasite. The presence of thaumasite, frequently in association with ettringite, appeared to represent situations involving attack by sulfate solutions over a number of years. No technical investigation on how the thaumasite had been formed had been undertaken at the time.

The first known occurrence of thaumasite sulfate attack in Europe occurred in the UK in February 1969 in a mortar containing a Portland masonry cement inside some new houses being constructed at Stoke-on-Trent during wintertime. The masonry cement, which contained a limestone filler and an air-entraining admixture, had been applied to the internal walls of these houses as a rendering and been covered with gypsum plaster as a finish. Where the mix had been improperly dispersed and applied under cold damp conditions, blistering arose within six to eight weeks with the cold damp conditions remaining prevalent. The blisters were sometimes up to 3 cm in diameter and contained both ettringite and thaumasite that had clearly arisen as a result of sulfate attack. The thaumasite was in a very poor crystalline form and the limestone filler had entered into some chemical reaction (Bensted, 1977a, 2000).

Some of the thaumasite crystals formed here appeared to produce over-growths on some of the ettringite crystals. However, there was no evidence for any extensive degree of solid solution between these two minerals. The lack of expansive reaction at the plaster-cement interface with the properly dispersed mix under ordinary conditions was attributed to low porosity, limiting the ingress of sulfate ions, which requires continuous moisture-filled pores to be available. The expansive effects were not observed when the masonry cement containing limestone filler had been properly rendered and coated with plaster under conditions that had not been cold and damp (Bensted, 1977a).

An extensive search of the technical literature at the time revealed no experimental work explaining how thaumasite can form. As a result, a detailed study was undertaken to synthesise thaumasite. More than 200 small-scale experiments were carried out for up to four years at 1–4ºC in air with excess water present. Thaumasite was found to form generally under these conditions, when there were carbonate (including atmospheric CO_2 in some of the experiments), silicate and sulfate ions with sufficient calcium ions and excess water available (Varma and Bensted, 1973; Bensted and Varma, 1973a). Under these cold, damp conditions, samples of Portland cement (including Sulfate Resisting Portland cement) and Portland masonry cement formed some thaumasite. No thaumasite was formed in any experiments undertaken at ambient temperature (*ca.* 20ºC). During the early 1970s, examples of thaumasite in deteriorated building materials were reported in the technical literature (Leifeld *et al.*, 1970; Fleurence *et al.*, 1972).

What is serious about thaumasite sulfate attack is that the main binding constituent of hardened cement, C-S-H, becomes converted into thaumasite, which is a non-binding powdery material having no inherent compressive strength. The key question that had been raised was: why was thaumasite formation facilitated at low temperatures? The answer to this question became apparent from a wide range of instrumental investigations involving X-ray crystallography (Lafaille and Protas, 1970; Edge and Taylor, 1969, 1971), infrared spectroscopy (Bensted and Varma, 1973a; Moenke, 1964; Bensted, 1977b, 1994) and laser Raman spectroscopy (Varma and Bensted, 1973; Bensted, 1988, 1999), which demonstrated that the thaumasite structure contains silicon surrounded by six hydroxyl groups and not the more usual number of four. Six-co-ordination of silicon by hydroxyl (OH groups) or directly by oxygen is very rare (Bensted and Varma, 1973b) and normally needs high pressure or low temperature to facilitate such a molecular arrangement. An important characteristic of thaumasite is that, once formed, it is stable up to *ca.* 110ºC, when it decomposes sharply to a disordered structure known as thaumasite glass (Bensted and Varma, 1973a); it is actually more stable to temperature changes associated with gentle heating than is ettringite, which starts to decompose below 100ºC.

With the benefit of hindsight it is apparent that, in the past, thaumasite was often confused with carbonated ettringite because of discrepancies in data reported in the older technical literature for DTA, optical microscopy and infrared spectroscopy. X-ray diffraction is normally the best technique to employ for characterising thaumasite, because the main crystal lattice d-spacings for thaumasite and ettringite are sufficiently far apart to enable independent identification of both these minerals to be clearly made (Bensted, 1977b). Since then, instrumental techniques have improved and such identification is now easier. Not surprisingly, thaumasite has now been identified in many countries as a deterioration product (Macphee and Diamond, 2003).

De Ceukelaire, at the University of Ghent, Belgium, made the important discovery that the expansive capability of thaumasite formed from ettringite via the woodfordite route (Bensted, 2003a) – as explained below in Section 4.3.2 – is much less than the volumetric expansion of ettringite. He found that thaumasite only occupies about 45% of the volume of ettringite from which it has been derived (De Ceukelaire, 1989, 1990).

4.3.2 Main mechanisms of thaumasite sulfate attack

Thaumasite can be formed below 15ºC (ideally at 0–5ºC) by two sets of reactions that are very slow to get going. These reactions are known as the *direct route* and the *woodfordite route* (Bensted, 2003a). Note: Woodfordite is the mineral name for the partial solid solution that can arise between ettringite and thaumasite.

In the *direct route*, there is a general reaction of sulfate with carbonate, silicate (from the main cementitious binder C-S-H) and excess water in the presence of calcium ions. The reaction is very slow and normally takes several months to obtain a significant yield. Both the alite and belite phases provide the binder, C-S-H, by normal hydration, which can then react with the other ingredients to form the non-binder, thaumasite. This reaction may be represented in a very simplified way as follows:

$$\underset{\text{C-S-H}}{C_3S_2H_3} + \underset{\text{gypsum}}{2CsH_2} + \underset{\text{calcite}}{2Cc} + \underset{\text{water}}{24H} \rightarrow \underset{\text{thaumasite}}{2[Cc.CS.Cs.H_{15}]} + \underset{\text{portlandite}}{CH} \qquad 4.5$$

The portlandite formed would be expected to carbonate, reacting with atmospheric CO_2 dissolved in the water to form more calcite and water, which in turn could serve as reactants for producing more thaumasite:

$$CH + c \rightarrow Cc + H \qquad 4.6$$

In the *woodfordite route*, the aluminate C_3A and ferrite phase C_4AF also participate. The name woodfordite refers to the partial solid solution whose end members are ettringite and woodfordite (Ramdohr and Strunz, 1967). A simplified representation of the *woodfordite route* is as follows:

$$\underset{\text{ettringite}}{C_3A.3Cs.H_{32}} + C_3S_2H_3 + \underset{\text{carbon dioxide}}{Cc + c} + xH \rightarrow \underset{\text{thaumasite}}{2[Cc.CS.Cs.H_{15}]} + CsH_2 + \underset{\text{alumina gel}}{AH_x} + 3CH \qquad 4.7$$

The *woodfordite route* is also slow, but somewhat quicker than the *direct route*. This situation arises because there is already an octahedral arrangement for Al (and Fe) in ettringite, into which Si from the C-S-H can displace Al (and Fe) initially by solid solution to form woodfordite and then to 'overwhelm' the Al (and Fe) by exsolving of the latter. The portlandite formed readily carbonates to give calcite Cc, which can serve as a reactant for producing more thaumasite.

Sulfate Resisting Portland cements, although discouraging ordinary sulfate attack, associated with expansive ettringite formation, are no better than Ordinary Portland cements when subjected to thaumasite sulfate attack because the main cement binder, C-S-H, is a reactant for producing the non-binder, thaumasite. As an illustration of this and a demonstration of the influence of temperature on thaumasite formation, the effects of exposing hydrated specimens of high w/c made from 50% SRPC/50% limestone powder to $MgSO_4$ solution (18000 mg/l with respect to SO_4) for 100 days at 5ºC and 20ºC are shown in Fig. 4.2 (Francis, 1999). Magnesium sulfate attack reinforces thaumasite sulfate attack and makes the overall deterioration worse. Both the direct and the woodfordite routes are involved, with thaumasite and brucite (MH) being formed as products (Bensted, 2003a).

Thaumasite is not just a form of sulfate attack, but of carbonate attack, too. Some interesting studies have been made of the role of carbon dioxide in the

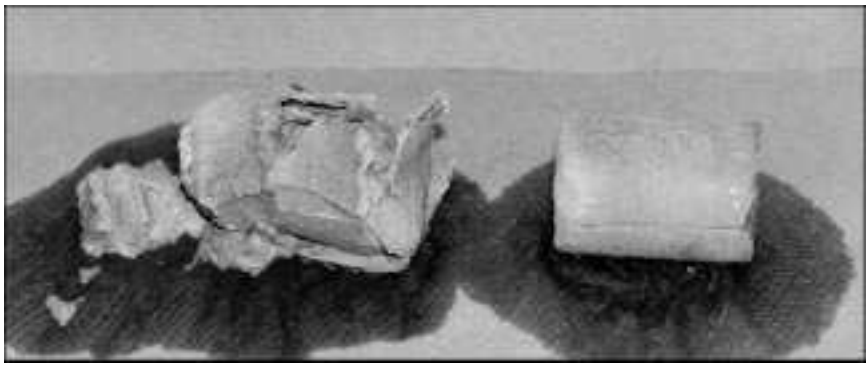

4.2 Thaumasite sulfate attack in SRPC/powdered limestone paste specimen exposed to $MgSO_4$ solution for 100 days at 5ºC (LHS) and absence of attack on similar specimen exposed at 20ºC (RHS).

formation of thaumasite (Collett *et al.*, 2004). The authors have stated that relatively high pH values, generally > 10.5, are needed for thaumasite formation and these conditions are maintained by the continual dissolution of portlandite from the cement hydration products in the presence of aggressive CO_2 and bicarbonate ions dissolved in groundwater, suggesting a requirement for portlandite to be present as a reactant. This, however, overlooks the fact that other cement hydrates, such as C-S-H, also buffer the pore solution at pH values > 10.5 so thaumasite can be expected to form without portlandite *per se* being present as an initial reactant. The influence of stereochemistry seems to play a crucial role in governing the reaction kinetics as it would appear that thaumasite is not produced until a stable transition state intermediate can form, having six OH^- groups around a highly polarising Si^{4+} cation with nearby carbonate groups to assist in charge delocalisation away from the silicon cation, in order to give a stable thaumasite structure.

4.3.3 Possibility of thaumasite formation under pressure at ambient and higher temperatures

Thaumasite is normally formed at temperatures below *ca.* 15ºC and preferably at 0–5ºC, which seems to be the optimal temperature range because the solubility of silicate, though very small (in ppm levels), is relatively greater within this temperature range. A through-solution mechanism is more likely to arise under such conditions and its existence would explain the general slowness of the thaumasite-forming reaction, especially in the first few weeks and months. However, there is circumstantial evidence that, in some instances, thaumasite might actually be produced when the temperatures are above *ca.* 15ºC (Bensted, 2001).

The possibility of thaumasite appearing at more elevated temperatures had not been definitively proven (Luke, 1998; Bensted, 2001), but could (theoretically at

least) arise at higher temperatures under pressure, when an arrangement of $[Si(OH)_6]^{2-}$ groups might be sufficiently stable to promote formation of thaumasite. Such a situation would be most likely to be facilitated if crystallisation pressures were sufficiently high to enhance the stability of a transition state intermediate of six OH^- ions surrounding the highly polarising Si^{4+} cations for sufficient time to allow thaumasite to emerge as a deterioration product.

Surveys of thaumasite sulfate attack (Diamond, 2003; Sims and Huntley, 2004) suggested that thaumasite sulfate attack might occur at temperatures above 15ºC but there was no definitive evidence given by them. The first conclusive evidence for thaumasite forming above 15ºC revealed that small quantities of thaumasite had been produced after 720 days at 20ºC by the direct route. This was contrasted with the analagous situation at 5ºC when extensive formation of thaumasite had been observed (Malolepsy and Mróz, 2006).This was in accord with an earlier prediction (Bensted, 2001).

4.3.4 Means of alleviating formation of thaumasite

Notwithstanding the uncertainties regarding aspects of the mechanism of formation of thaumasite, several measures have been suggested to minimise the risks of TSA (Bensted, 1998), namely:

- Lower water/cement ratio as far as is practically possible coincident with good concrete (or mortar) workability with a suitable superplasticiser in the mix, so as to minimise internal transport of ions in the pore solution of the hardened material.
- Reduce permeability of the concrete (or mortar) with ground granulated blastfurnace slag (ggbs) or fly ash (pfa) additions, or else by utilising blended cements like Portland-slag cement (e.g., CEM II/A-S) or Portland-fly ash cement (e.g., CEM IIB-V), as given in the European standard for common cements BS EN 197-1 (2000).
- Seek to reduce the C_3S (alite) and C_3A (aluminate) levels as far as is practical or feasible.
- Amend codes of practice for producing concrete (or mortar) liable to be exposed in sulfated environments where temperatures of 15ºC or less are likely to be encountered on a regular basis each year. This fourth recommendation has been subsequently enacted, following the publication of the 'Thaumasite Expert Group Report' in 1999.

4.3.5 The 'Thaumasite Expert Group Report' and its ramifications

Because of extensive thaumasite sulfate attack found in Gloucestershire, UK during the late 1990s, particularly on bridges on the M5 motorway, a

'Thaumasite Expert Group (DETR)' was set up by the UK government to examine the situation. The Group reported its findings in 1999 (Department of Environment Transport and the Regions, 1999), and this was followed by some annual reviews. The Report covered risks, diagnosis, remedial works and guidance on new construction. Reassurance was offered that the number of structures in the UK potentially at risk of thaumasite sulfate attack (TSA) was relatively small.

Importantly, TSA was distinguished from mere thaumasite formation (TF). Small occurrences of thaumasite are widespread and do not pose any structural risk in the overwhelming majority of instances. Nevertheless, there are occasions when concrete may be apparently affected by TF upon initial inspection but the affected zones may increase in volume over the ensuing months, in which case the onset of TSA is suspected. In such instances, tests and remedial action may need to be undertaken.

The Thaumasite Expert Group (DETR) Report gave guidance for both below-ground and above-ground construction and relied considerably upon technical investigations carried out at the Building Research Establishment in the UK (Crammond, 2003).

The primary risk factors identified were:

- Presence of a sulfate source including sulfide that might oxidise to sulfate.
- Presence of mobile water (groundwater in the instance of buried concrete).
- Presence of carbonate (generally found in the aggregate).
- Low temperatures, generally below 15ºC.

For new below-ground construction, the report recommended revision of key guidance documents for buried concrete and revisions to British Standards on concrete and aggregates. It also examined the issue of acceptable carbonate levels as either aggregate or cement filler permitted within a buried concrete. Three ranges of aggregates were defined in terms of sources that could generate TSA in Portland cement concretes exposed to moderate levels of sulfate. The Ranges, designated A, B and C, refer to those with sufficient carbonate to generate TSA, low carbonate and very low carbonate respectively.

The Report dealt with the use of Portland limestone cement that can contain 6–35% by weight of limestone filler, recommending that these cements should not be used in conditions where the sulfate concentration of the groundwater (as SO_4) was above 0.4 g/l. Also addressed was the fact that the European cement standard BS EN 197-1 (2000) permits up to 5% limestone filler to be incorporated in all 'common' cements (as defined). At the time the Report was issued, the addition of 5% limestone filler had been found to make sulfate resistance marginally worse at cold temperatures, when compared with the behaviour of plain Portland cements. The Thaumasite Expert Group reported that there was insufficient evidence to suggest that this would significantly affect the performance of concretes or mortars in the field.

For above-ground construction, TSA had been identified in the UK in lime-gypsum plasters, sulfate-bearing brickwork, ground-floor slabs and concretes contaminated with sulfates and sulfides. All of these types of deterioration can be caused by failure to carry out recommended good practice, either by using unsuitable materials for given service conditions, by poor workmanship on site, or by failure to keep the structures dry. The Group decided that there were already sufficient recommendations in place to combat TSA in above-ground construction. In particular, common sulfate-bearing bricks should not be utilised in exposed conditions, even if they are subsequently rendered, because of poor water-tightness through poor detailing or defective rendering.

TSA may develop as long as the pore solution at the reaction front is kept cold and is maintained at a pH of above 10.5. However, sometimes the deterioration, once started, can continue even if the pH drops below 10.5. This appears to be due to the situation that can arise when thaumasite becomes unstable at around pH 7 and degrades to give secondary calcite ('popcorn calcite') of irregularly shaped spheres as the ultimate deterioration product of TSA (Crammond, 2003).

Work carried out at the University of Sheffield showed that thaumasite can readily form at low temperatures, not just with Portland limestone cements, but also with limestone filler (up to 5% by weight) in Portland cements (Hartshorn *et al.*, 1999). These results suggested that Portland limestone cements should not be utilised where there is a high risk of TSA taking place, although they have been employed successfully over many years in France, for example, where their use is particularly recommended for internal walls of buildings. In such an application, however, the temperatures are unlikely to fall below *ca.* 15ºC over lengthy periods and TSA is therefore unlikely to be a problem with normal sound workmanship.

The three-year review of the Thaumasite Expert Group Report (Nixon and Longworth, 2003) noted that new guidance documents (Building Research Establishment, 2001; British Cement Association, 2001; BS 8500-1 and -2, 2002) have increased awareness of TSA and how to achieve preventative measures and drew attention to various points including the following:

- Two new field cases of TSA had arisen (in the UK) in buried concrete containing siliceous aggregates. These justify concerns expressed in the Report that concretes whose aggregates contain little or no carbonate can be affected by TSA if an external source of carbonate ions is available, e.g. from groundwater where dissolved bicarbonate is continually available.
- Cements with a substantial proportion of ground granulated blast furnace slag (ggbs) had so far been shown to offer good resistance to TSA.

In the 2005 revision of BRE Special Digest 1, it is recognised that carbonate required for TSA can be supplied externally, principally from bicarbonates in groundwaters (see equations 8–10, Section 4.6.2), and so the concrete quality is

not relaxed for carbonate-free aggregates, as in the earlier version of this guidance.

In some comments on the aforementioned three-year review, the question of pfa in relation to ggbs for minimising TSA occurrences has been mentioned (BS 8500-2, 2002). Ggbs exhibits delayed hydraulicity, being protected by surface films from significant reaction at the beginning of hydration, whilst pfa is not intrinsically hydraulic and needs a source of OH^- ions to instigate pozzolanic reactivity in the presence of Ca^{2+} ions. Pfa may not always be effective in combating TSA if the pozzolanic reaction has not already proceeded to a significant extent to form additional C-S-H as at *ca.* 5ºC. In such an event the pfa would essentially act as a filler, for example if the OH^- ions are depleted by reaction with CO_2 to form soluble hydrogen carbonate ions: $OH^- + CO_2 \rightarrow HCO_3^-$ rather than initiating more C-S-H formation. A Portland-based cement with a high proportion of unreacted pfa would be likely to be vulnerable to TSA in such circumstances, since the permeability would not be satisfactorily reduced. However, formation of thaumasite is slow and, when (as in most cases) the pozzolanic reaction is well under way by the time thaumasite is likely to be produced, then the pfa may perform a similar function to ggbs as an extended cement component. More reactive pozzolans such as microsilica and metakaolin do not appear to be affected as pfa can at times be. Initiation of extended hydration by slags and pozzolans (like pfa) needs to be more fully investigated in the context of potential for TSA and its minimisation. It should then be possible to achieve optimal TSA resistance in practice under given field conditions (Bensted, 2003b).

An interesting study (Sims and Huntley, 2004) has shown that TF or TSA can occur even when the primary risk factors (Department of Environment, Transport and the Regions, 1999) are not all obviously present. A source of external or internal sulfate was always present in these cases, but water was not always abundant or mobile. There was not always a direct internal source of carbonate and temperatures were not always low.

Results from an extensive programme of laboratory tests on concrete cubes of water/binder ratio 0.45, made with three different cements and moist cured for 28 days before being exposed to various sulfate solutions at 5ºC, have also been published recently (Zhou *et al.*, 2006). Some of the main conclusions of this work are summarised below:

- For cubes stored at pH 12 in solutions of calcium sulfate (1.4 g SO_4/l) + magnesium sulfate (1.6 g SO_4/l) – corresponding to Design Sulfate Class DS-3 (Building Research Establishment, 2005) – TSA was observed within 5 months and significant damage within 12 months.
- The attack was found to be severe for cubes made with Portland limestone cement containing 20% by weight of limestone filler, but also evident in cubes from OPC (with 5% by weight of limestone filler), and SRPC with neither added limestone filler nor containing limestone aggregate. It was

therefore suggested that both SRPC and PC containing 5% by weight of limestone filler should be used cautiously in buried concrete liable to come into contact with sulfate-containing groundwater.

- The presence of acid did not promote formation of thaumasite. Although thaumasite was observed in lesser amounts in cubes immersed in sulfuric acid solution at 5ºC, the nature of the corrosive attack was different from TSA. It was suggested, however, that initial attack of concrete by acid could result in its being highly vulnerable to TSA, should this be followed by alkaline high sulfate conditions.
- Both C-S-H gel and calcium hydroxide were consumed during formation of thaumasite, which was often accompanied by formation of gypsum and, when magnesium was present, by magnesium hydroxide (brucite).
- It is likely that the TSA observed in the buried concrete associated with the M5 motorway in the west of England was due to the increased sulfate content from oxidation of pyrite (iron disulfide FeS_2) rather than due to low pH associated with the production of sulfuric acid.

In conclusion it appears that, while the state-of-the-art is still not yet clearly defined in all important respects, a great deal of new knowledge has been gained through recent research on thaumasite formation and thaumasite sulfate attack. When fully digested, this should help to minimise future occurrences of this relatively uncommon but insidious form of sulfate attack.

4.4 Internal sulfate attack and delayed ettringite formation

4.4.1 Background

During the hydration of Portland cement at temperatures around ambient, ettringite is formed at early ages, a consequence of the use of gypsum as a set regulator (Bensted, 2002a). Since the cement paste is still plastic, it is able to accommodate the volume changes associated with the conversion of precursor phases to ettringite and significant expansion is not observed unless excessive levels of sulfate are present in the mix materials. Most national and international standards therefore put restrictive limits on the sulfate contents of cements (and on C_3A contents), as well as on the soluble sulfate contents derived from aggregates, etc., in order that the formation of ettringite is virtually completed at about the time of setting and does not generate stresses that could cause what is sometimes referred to as ‘internal sulfate attack’ in concrete subjected to curing at normal ambient temperatures (Skalny *et al.*, 2002).

However, if Portland cement with a sulfate content within the normal accepted limits is cured at elevated temperatures, ettringite is destabilised and does not form at early age. Instead ‘delayed ettringite formation’ (DEF) takes place on subsequent cooling of the concrete concerned and, in some circum-

stances, this may cause significant expansion, which represents a particular form of 'internal sulfate attack'. German guidance suggests that expansion from DEF can be avoided if concrete is not heated above 60ºC (*Deutsche Ausschuß für Stahlbeton*, 1989).

QXRD results for ettringite formation in a mortar cured at 20ºC and 100ºC (Yang *et al.*, 1999) are shown Fig. 4.3(a), with corresponding expansion data in Fig. 4.3(b). Similar results were found by Scrivener and Lewis (1996). Whereas at 20ºC, substantial ettringite is produced within one day with no expansion, upon heat curing, ettringite formation is delayed until about 25 days and is followed by expansion over the period 25 days to 400 days. Cement hydrated at either room temperature or elevated temperatures contains similar amounts of ettringite after sufficiently long storage times. Thus, the presence of ettringite in concrete which has undergone expansion is not a sufficient indicator to diagnose DEF damage. During the heat curing regime, the components of ettringite must be stored, and it is suggested that excess sulfate sorbs onto C-S-H gel while

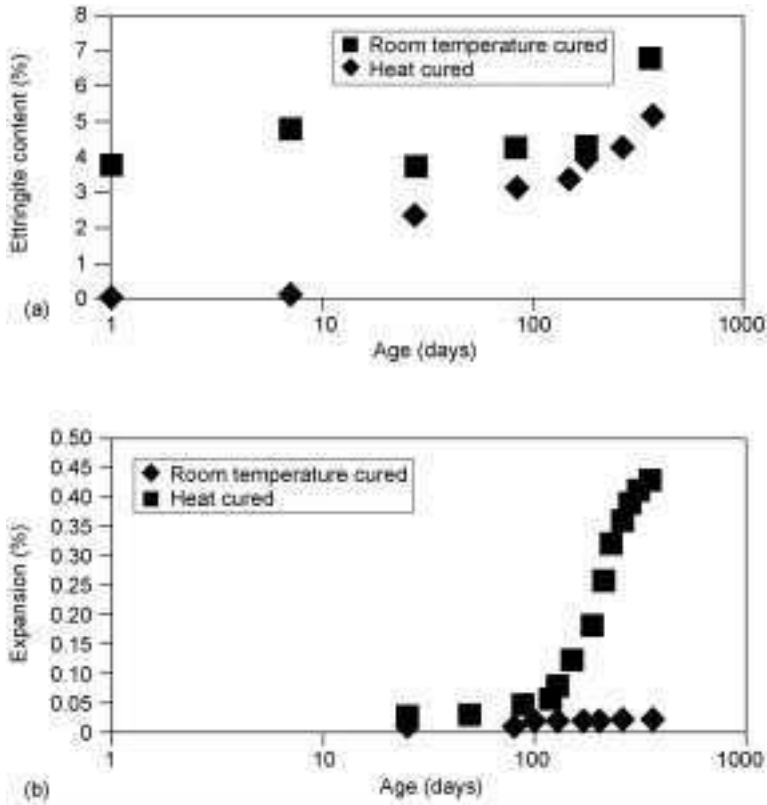

4.3 (a) Ettringite contents of cement pastes in mortars cured at 20ºC and 100ºC (data taken from Yang *et al.*, 1999). (b) Corresponding expansion data for mortars cured at 20ºC and 100ºC (data taken from Yang *et al.*, 1999).

aluminate either forms AFm type phases or is sorbed on the C-S-H gel. Note that much of the Al analysed in regions of C-S-H gel can be shown by NMR to be incorporated into the silicate chains.

The state of the art was reviewed comprehensively by Taylor *et al.* (2001) and Famy *et al.* (2002a) and there are significant sections as well as two case studies concerning DEF in the recent book by Skalny *et al.* (2002). There is some confusion in the terminology used by different authors, with the terms 'delayed ettringite formation', 'secondary ettringite formation' and 'ettringite reformation' all used. Skalny *et al.* (2002) have suggested that it would be more consistent to refer to DEF as 'Heat induced internal sulfate attack' but here we follow current convention and use 'DEF expansion' to refer to formation of ettringite, delayed because of heat curing, that leads to expansion of cement paste, mortar or concrete, in the absence of an external sulfate source. The environment of the cement paste plays a significant role in the likelihood of expansion following a heat cure (see, for example, the section on alkalis below), so the suggestion of the use of 'internal' is perhaps in some ways misleading. DEF described here only refers to internally generated ettringite.

4.4.2 Factors affecting severity of DEF

DEF is a fairly weakly expansive mechanism, and so is likely to be less severe in dense flaw-free pastes and concretes. This is clearly seen by the significant effect of the constraint present around cement paste on the onset and magnitude of expansion. Grattan-Bellew *et al.* (1998) showed that, for ASR-inactive quartz aggregate, the rate of expansion was inversely proportional to the mean aggregate size. Lawrence (1995) tested a range of mortars made from limestone and silica sands, observing that replacement of the coarse fraction of the siliceous sand with limestone was particularly effective in limiting expansion, presumably because the bond to limestone was much better. Lower expansions were also seen for cement pastes than for the corresponding concretes (Yang *et al.*, 1996). Indeed Diamond and Ong (1994) showed that the use of an ASR-active aggregate induced ASR damage around the aggregate, weakening the concrete and making it more susceptible to DEF expansion. Thermal cycling, which might also be expected to cause micro-cracking at interfaces, has also been shown to increase the rate of expansion, although not significantly changing the time of onset or the overall expansion amount (Fu *et al.*, 1997).

While much data have been obtained detailing the expansion of mortars and concrete, fewer data are available regarding strength development in systems suffering from DEF expansion. Lewis (1996) tested mortars made from a range of cements (w/c = 0.5 and sand/cement = 3) and measured compressive strength and weight gain on wet storage against expansive behaviour. Expansion data were measured on 16 mm by 16 mm by 160 mm bars, while the other properties were measured from 25 mm cubes, so there is some expected variation between

samples, particularly as different storage containers were also used, implying that samples may have experienced different alkali levels in the storage solutions (see below). At 20ºC, all mortars were non-expansive and reached compressive strengths of approximately 50 MPa with a weight gain at early age of approximately 1%. Some samples cured at 90ºC did not expand; these samples also gained approximately 1% mass and reached around 30–40 MPa. The weight gain was attributed to consumption of water by hydration, and the lower ultimate strength from heat curing to a coarser microstructure. Mortars made from some cements expanded at 90ºC and these gained weight and strength initially in a similar manner to the non-expansive mortars. However, drops in strength and significant additional weight gains took place coincident with expansion.

The timing and duration of heat curing is important. Very long (>24 h at 90ºC) heat curing leads to delayed or reduced expansion (Lawrence, 1995) presumably because the components needed for the delayed ettringite formation chemically react to form other products (for example hydrogarnets) and are no longer available. Similar results were found by Famy (1999). It is also found that delaying the heat curing process leads to much reduced expansion (Famy *et al.*, 2002b), and it is postulated that this is because the bulk of the C-S-H is then formed at 20ºC and only C-S-H formed at 90ºC can store sufficient aluminate and sulfate to promote subsequent DEF expansion.

It is not possible to predict the expected behaviour of a material solely from the composition of the cement used, although composition clearly is one important factor as demonstrated by Kelham (1996a). For example, high levels of alkali destabilise ettringite relative to AFm more than lower levels do. The ratio of aluminum to sulfur is important in determining the expected final phase assembly. However the silicate components of the cement are also very important since it appears that, prior to ettringite reformation, sulfur (and possibly aluminium) must be stored by adsorption on to the C-S-H gel component of the hydrates. DEF appears to be associated with reactive cements which give high early strength (Kelham 1996a,b), suggesting that substantial amounts of C-S-H gel must be formed during the heat curing in order to sorb sufficient sulfate to allow subsequent formation of sufficient quantities of ettringite within the outer product C-S-H gel to cause DEF expansion (Taylor *et al.*, 2001; Famy, 1999).

Some workers have suggested that slow release of sulfates from clinker sulfate phases may lead to late formation of ettringite and expansion. However, a study by the PCA of the solubility of sulfate in a range of North American cements (Klemm and Miller, 1996) showed that, in 33 cements tested, nearly all of the sulfate was released while the concrete remained plastic. Thus slow release of sulfate was unlikely to be a major cause of DEF. Indeed slow release of sulfate might also be expected to cause expansion at room temperature but results by many investigators (e.g., Kelham, 1996a,b; Yang *et al.*, 1996, 1999; Famy, 1999) do not show such expansion.

Another important factor in DEF is the storage environment. As in the case of ASR, very high relative humidities are needed for expansion to occur. Famy *et al.* (2001) showed that wet storage led to a more rapid expansion than storage above water. This is easily explained, since ettringite has a very high water content and is unstable at low relative humidities. Famy *et al.* (2001) also showed that the ionic strength of the storage solution was important. Storage of bars in solutions of high alkali content reduced or delayed expansion. They postulated that, if high alkali levels were maintained in the pore fluid, then ettringite was destabilised and its reformation delayed. An alternative explanation of this phenomenon can be envisaged if DEF involves an osmotic mechanism since a high external ionic strength would impede osmotically induced expansion.

This sensitivity of DEF to the storage environment is important practically since, in many studies of DEF, bars cast at various times and ages have been stored in a common water bath with the alkali concentration gradually increasing as pore fluid from the various bars leached into the water. Thus the storage conditions varied for bars cast at different times. Testing for expansion should always be carried out with care taken over the storage conditions. For example, all bars could be stored in their own containers, each with a fixed quantity of water. The sensitivity to alkali leaching might also explain why DEF has been a particular problem in environments such as railroad sleepers and abutment walls, where water flow and leaching can take place.

4.4.3 Microstructural features and proposed mechanisms of DEF expansion

Samples which have undergone DEF exhibit a characteristic microstructure after expansion, in which clear rims are seen around aggregate particles, largely filled with oriented ettringite. To some degree the thickness of the rims follows the size of the aggregate particles, although not all rims are continuous or filled and there are additional cracks through the cement paste. The diversity of microstructures seen is discussed by Taylor *et al.* (2001).

Materials subjected to heat curing have a significantly altered microstructure when compared with materials cured at ambient temperature. Heat curing causes a rapid production of hydrates at early age, and leads to the formation of dense rims around the larger cement particles. Smaller cement particles fully react, often leaving Hadley-grain-like (Barnes *et al.*, 1978) features behind. These features persist to late age, with samples having much coarser and more open microstructures compared to samples cured at room temperature. In many cases, the rims around large cement grains are found to consist of distinguishable concentric rims of hydrates, which have different densities, formed at different stages of the curing process. For example, Famy *et al.* (2002b) have shown the presence of two or even three toned rims. The material formed during heat

curing is brighter in backscattered electron images of polished sections in the scanning electron microscope due to its higher density (Famy *et al.*, 2002c), while hydrates formed subsequent to the heat cure are darker because they have a lower density. These differences in microstructure and density no doubt account for the observation that materials that have been heat cured attain lower ultimate strengths than companion samples cured at room temperature, even where DEF expansion and strength regression do not occur.

At both ambient and elevated temperature, ettringite ends up present in voids in the microstructure, so the presence of large deposits of ettringite is an insufficient indicator for the diagnosis of DEF. The characteristic pattern of rims around aggregate must also be present, along with evidence of the concrete having been heat cured.

Analyses in the SEM can be used to probe the microchemistry taking place in samples. Samples cured at room temperature are found to have ettringite and/or AFm deposits mixed in with the outer C-S-H from early age. In contrast, in heat cured samples, only admixture of AFm is seen, while the Al and S from ettringite that would have formed are sorbed on to the C-S-H. Work by Lewis (Lewis, 1996 summarised in Scrivener and Lewis, 1996) showed that expansive and non-expansive materials could be distinguished by the level of sulfate adsorbed on to the inner C-S-H (measured in the rims present around the largest cement grains).

More recently, Famy (1999) extended this work and showed that, for samples in which expansion took place, there were significant levels of AFm present in outer product C-S-H, along with high levels of sulfate sorbed on to inner and outer product C-S-H. She proposed that the expansion was caused by conversion of AFm present in small pores into ettringite. This led to expansion of the paste and the onset of damage. Subsequently ettringite migrated to the aggregate rims where large visible deposits were found. In order for damage to occur, there needed to be sufficient AFm present in outer product, along with sufficient sulfate adsorbed on to inner and outer product. Taylor *et al.* (2001) discussed the details of this mechanism in their review.

However, this is just one of a number of mechanisms that have been proposed. We will consider three here:

1. Paste expansion in which the cement paste expands, leaving rims around the aggregates which later infill with ettringite either when it forms or more likely by Ostwald ripening from much smaller ettringite crystals which formed earlier embedded in the paste. A number of causes can be postulated for expansion of the paste. If ettringite forms in small pores from AFm as suggested by Famy (1999), then it is possible to generate sufficient pressures to cause expansion. Expansion is possibly delayed after the ettringite formation, but this can be explained by a creep mechanism, or by an osmotic mechanism.

2. Formation of expansive ettringite rims has been proposed by a range of other authors. It has been suggested that this mechanism cannot generate sufficient pressures to cause expansion (Scherer, 1999), since the degree of supersaturation can only be low, and very high supersaturations would be needed to generate sufficiently large forces in such large rims. There is in addition some evidence that the width of the rims around aggregates is a function of aggregate size, which would be expected for a paste expansion mechanism, but not for a mechanism of crystal growth at aggregate surfaces. However, it is possible to imagine a mechanism in which diurnal temperature changes allow stepwise crystal growth and gradual levering apart of surfaces (as happens at the macro scale if expansion joints in concrete become gradually filled leading to damage to the surrounding slabs) so it may be premature to exclude this mechanism. Additionally DEF does often occur when the concrete is damaged by other degradation mechanisms such as ASR – in these cases only a weak expansive force may be needed.
3. The osmotic mechanism was proposed for expansive ettringite formation by Thorvaldson (1954). This mechanism is implicated in other forms of damage to concrete such as ASR and freeze thaw attack. The transformation of AFm to AFt in the paste leads to consumption of considerable water, which may produce an increase in the ionic strength of the surrounding liquid resulting in osmotic pumping of water into the paste. Interestingly this mechanism easily accounts for the delay in expansion since water transport must take place *following* the formation of ettringite.

This topic has been highly controversial partly because of a number of lawsuits trying to assign responsibility for problems between relevant parties. Now that legal activity is reduced, consensus seems to be shifting towards the paste expansion mechanism but it may be time for the contribution of osmotic forces (Thorvaldson, 1954) to be re-examined within the context of paste expansion, since there is some evidence that expansion does not immediately follow ettringite formation, despite the fact that most techniques to probe ettringite formation become more efficient with increasing crystallite size (i.e., with ongoing Ostwald ripening). It is also important not to exclude the possibility that the mechanism can vary with circumstances. For example, if a mortar bar suffers from DEF and is then subsequently re-heated and re-exposed to moisture (Famy, 1999, fig. 7.46, p. 207), a very rapid burst of additional expansion takes place. At this stage, there is little constraint, and so formation of ettringite in rims is much more likely to be able to generate expansion. In contrast the onset of initial expansion needs much higher forces, and it is harder to see how these could be generated by simple crystal growth. Recently, Scherer (2004) has suggested that sufficient forces are generated transiently in very small pores fracturing the concrete, and that the constraints on expansion are then much reduced so that subsequent expansion can take place due to smaller forces in larger pores.

In summary then, DEF is a complex process which is still not fully understood. It can be avoided most readily by limiting maximum curing temperatures. Aside from DEF, internal sulfate attack caused by the presence of excessive sulfate in concreting materials is generally avoidable by adhering to the compositional limits in standards for cements and aggregates.

4.5 Conclusions on sulfate attack

From the foregoing sections, it will be evident that guidance on measures to minimise the risks of premature degradation of concrete from the different forms of sulfate attack has had to become increasingly complex in recent years. While it must allow for the varied effects of different exposure environments, it must also take account of the complex chemistry of interaction between sulfates and the constituent phases and microstructure of the hydrating cement. This can make for rather unwieldy guidance documents that are difficult to apply, even when they are restricted to a particular location. Thus in the UK, where a series of Building Research Establishment Digests has long formed the main basis for advice in British standards on the requirements of concrete exposed to sulfate-bearing soil and groundwater, the guidance published in Building Research Station Digest 90 (1968) had a simple one-page table in which exposure sites were divided into five classes on the basis of sulfate level in either soil or groundwater. Progressively tighter limits on the types of cement suitable and on cement contents and water to cement ratios were imposed for increasing severity of sulfate class. An essentially similar approach was followed by successive documents in the series until BRE Digest 363 was revised in 1996 (BRE, 1996) to draw attention to the fact that the risks of TSA required explicit recognition.

In marked contrast to the above, however, the 3rd edition of BRE Special Digest 1 (2005) is divided into six parts and runs to no fewer than 62 pages. In dealing with the chemical aggressiveness of the ground, it sets out procedures for determining the Design Sulfate Class (DS Class) from the soluble sulfate (and magnesium) and the potential sulfate (in cases where sulfide-bearing minerals may oxidise); it then proposes the classification of natural and brownfield sites in terms of an Aggressive Chemical Environment for Concrete Class (ACEC Class), dependent on the DS Class together with the pH and mobility of groundwater. Its recommendations for the specification of an appropriate quality of concrete, the Design Chemical Class (DC Class), to be used in contact with the ground are formulated from consideration of the ACEC Class together with the hydraulic gradient of the groundwater, the type and thickness of the concrete element, and the intended working life (50 or 100 years). Additional protective measures (APMs) are recommended for dealing with certain highly aggressive conditions, whilst relaxation of the recommendations for deriving DC Class are proposed for surface carbonated precast concrete (for reasons explained in Section 4.3) and for specific precast concrete

products that are manufactured under conditions of rigorous quality control and considered to be of low permeability. Simple it is not. At the time of writing the present chapter, BS 8500 (2002) was being updated on the basis of guidance presented in BRE Special Digest 1, 3rd edition (2005).

A final comment that should be made here on the scope of BRE Special Digest 1 is that, while recognising that chloride ions are commonly found in soils and groundwaters in the UK, the document is restricted to dealing with situations where the levels of chloride concentration do not exceed those found in brackish water in brownfield sites (12000–17000 mg/l). In these cases, the chemical effects of chloride on concrete are considered to be innocuous. The effects of higher concentrations of chloride salts are obviously of relevance to the performance of concrete structures in marine environments and where de-icing salts are applied, but these situations are not dealt with in BRE Special Digest 1, which makes reference to BS 6349-1 (2000) for maritime structures and to BS 8500-1 (2002). It may be noted that, in such cases, the most important effects of chlorides are on the corrosion of reinforcing steel in concrete (considered in Ch. 5) and, in certain locations, the severity of freeze/thaw damage (considered in Ch. 7). With regard to the performance of coastal and offshore structures, however, it is of interest to record that, although seawater is of variable composition depending on location, it often contains around 3.5% by weight of salts with a pH in the region of 7.5–8.4 and, while its main ionic components are Na^+ and Cl^-, it also contains SO_4^{2-} at concentrations that would seemingly correspond to a DS-3 classification as well as significant levels of Mg^{2+} – see Table 4.2. The chemical action of seawater on concrete is therefore due to the influence of several reactions proceeding concurrently and, although the main concerns in this area have long been ascribed to the presence of $MgSO_4$ (Vicat, 1857), it has often been found that the effects of the SO_4^{2-} and Mg^{2+} in seawater are considerably milder than those that would be produced simply by exposure of concrete to solutions of pure $MgSO_4$ of similar concentrations (Lea, 1970; Taylor, 1997). As seawater varies considerably in composition and temperature from one location to another, and so does the severity of numerous related physical factors (wave action, abrasion, freezing, etc.), it is obvious that generalisations about its degradative effects on concrete are apt to prove misleading. The subject has been extensively researched in many parts of the world and further information is available from a number of sources, e.g. (ACI, 1980; RILEM Technical

Table 4.2 Typical concentrations (g/l) of ions in seawater

Ion	Na^+	K^+	Mg^{2+}	Ca^{2+}	Cl^-	SO_4^{2-}
Concentration	11.00	0.40	1.33	0.43	19.80	2.76

Data taken from Lea (1970).

Committee 32-RCA, 1985; Mehta, 1991; Hobbs and Matthews, 1998; Mehta, 1999; Thomas *et al.*, 1999). As the ancient marine structures that were referred to in Ch. 1 and others of more recent origin illustrate, the production of mortars and concretes that are capable of resisting the chemical effects of seawater over many years is quite possible if steps are taken to achieve appropriately low penetrability. The most important requirements are that the material should be made at suitably low water/cement ratio with adequate cement content, well compacted and properly cured; the use of pozzolanic or slag cements has also been found to provide enhanced durability in some situations (Massazza, 1998; Moranville-Regourd, 1998).

4.6 Degradative effects of water, acids and other aggressive chemicals

4.6.1 Background

In general, the rates of attack by aggressive chemicals on concrete may be affected by several factors, including the following:

- The concentrations of the reacting chemicals and their rates of replenishment in the aqueous medium surrounding the concrete.
- In the case of acids, the concentration of H^+ ions, determined by their strengths, i.e. their dissociation constants (K_a), and by the overall concentration of the acid concerned. (Note: mineral acids, such as H_2SO_4, are highly ionised and so, at the same overall concentration, attack concrete at a greater rate than do the partially ionised weak acids, such as carbonic acid.)
- The solubility products (K_{sp}) of the reaction products and their abilities to form insoluble protective films.

4.6.2 Leaching by water and acids

Pure water dissolves lime and, to some extent, alumina from the compounds in the cement matrix resulting in increased permeability and eventually an amorphous residue of hydrated silica, iron oxide and alumina (Lea, 1970). This process, known as leaching, involves several stages, in which initially portlandite (CH) is dissolved and then attack on C-S-H and calcium aluminate hydrates takes place (Taylor, 1997). However, this dissolution is very slow because of the limited solubilities of the reactants (K_{sp} for $Ca(OH)_2$ at 25ºC $= 5.5 \times 10^{-6}$) and so damage to concrete is usually negligible except when the concrete is highly permeable and water flows through it continuously. Flowing water prevents saturation being achieved and exposes further unreacted material. It also removes loosely attached insoluble material which may have formed a protective layer on the concrete after initial chemical attack. Thus dissolution continues and, in extreme cases, complete disintegration can occur.

An increased rate of fluid ingress will occur in structures subject to considerable hydrostatic pressure, such as dams, thin-walled concrete pipes and conduits, and the destructive effect can be severe (Lea, 1970; Harrison, 1987). Problems of leaching due to the solvent action of relatively pure water have been reported in certain Scandinavian dams which were made with porous concrete. Damage to pipes is more severe if they are laid in sand or sandy clay rather than in just clay because of greater percolation of water.

The presence of acids increases the rate of attack by reacting with and dissolving the basic constituents of hydrated cement (alkali hydroxides, calcium hydroxide, calcium silicate hydrates, calcium aluminate hydrates, monosulfate and ettringite) and certain aggregates, such as limestone. The quality of concrete is more important than the cement type in resisting acid attack. Well-cured and compacted concrete with low to moderate w/c is relatively dense with low permeability and therefore limits the rate of fluid ingress and, as a result, the extent of attack on the concrete, generally restricting it to surface erosion. Inclusion of ground granulated blast furnace slags or pozzolans in concrete may result in a slower rate of acid attack by lowering permeability and reducing calcium hydroxide content. However, the differences between Portland cement concretes and those containing some slag or pozzolanic cements are not thought to be of major significance in comparison with the differences between concretes of different quality (Hobbs and Matthews, 1998). Some improvement in resistance to certain organic acids (e.g., acetic, lactic) and mineral acids (HCl, H_2SO_4) has been shown for cements containing silica fume (Mehta, 1985). Enhanced resistance to acids (lactic and acetic) in silage effluent has also been reported for the addition of metakaolin to Portland cement concrete (De Belie *et al.*, 2000b).

Although limestone aggregate is more readily attacked than acid-resistant aggregates, this can sometimes be advantageous as it provides a reservoir of carbonate that prolongs the ability of the concrete to neutralise the acid and therefore can extend service-life. In addition, acid attack on the concrete occurs more evenly since both the cement and the aggregate are degraded. This is important in, for example, pipelines subject to acid attack because a relatively smooth and therefore hydraulically efficient surface is maintained, in contrast to the case of concrete made with gravel aggregate where acid attack produces an uneven surface leaving protruding aggregate and debris from detached aggregate (Lea, 1970).

The major sources of acids which affect concrete are derived from: (1) groundwater and acid soils (sulfuric, carbonic, humic, lactic), (2) agriculture, e.g. silos, manure stores, animal house floors (lactic, butyric, acetic), (3) acid rain (carbonic, sulfuric, nitric), (4) effluents and industrial processes (any), (5) sewers (sulfuric), (6) seawater (carbonic).

The only mineral acid commonly found in natural groundwater, generally in low moorland/marsh areas, is sulfuric acid. It is formed by the chemical (see

Section 4.2) and bacterial (see Section 4.7) oxidation of sulfide minerals such as pyrite and marcasite (FeS_2) present in the soil or rocks and also in fill materials (commonly shales) in construction sites. Any excess sulfuric acid not neutralised by minerals in the nearby rocks/soil can attack the concrete (Lea, 1970; Robins *et al.*, 1997). In addition, as was noted in Section 4.2.2, expansive reactions can occur between sulfuric acid and minerals in the soil, e.g. the formation of gypsum from calcite, resulting in ground heave and therefore damage to any adjacent concrete structures.

Sulfuric acid is also responsible for the corrosion of concrete in sewage systems where the conditions can become extremely acidic (pH < 1) (see Section 4.7). A further example of sulfuric acid attack on concrete (and also of other mineral acids) is in its use in industrial processes (where it can attack storage tanks and floors) and its spillage, leakage or dumping as chemical waste.

Under moist conditions, sulfuric acid and carbonic acid are formed from the waste gases, SO_2 and CO_2, produced in power station chimneys and railway tunnels and can result in attack on the concrete parts of the structures (Lea, 1970). More generally, polluted air contains a number of acidic gases, e.g. SO_2, NO_x and CO_2, which dissolve in moisture in the atmosphere to form acid rain, containing mainly sulfuric, nitric and carbonic acids (pH 3.5–4.5). Commonly, the effect of acid rain is to damage the surfaces of concrete structures and therefore mainly to affect appearance (Harrison, 1987). However, storage of specimens in CO_2-enriched atmospheres in the presence of salts such as sodium nitrite that can decompose to form NO_x has been shown to cause major alterations to the normal process of carbonation, resulting in the presence of significant concentrations of soluble calcium nitrate and nitrite in the pore solution phase of the material (Anstice *et al.*, 2005).

The main acids found in soft groundwaters in some mountain or high moorland regions are carbonic acid and humic acid. Carbonic acid is formed when CO_2 dissolves in water:

$$CO_2 + H_2O = H_2CO_3 \qquad 4.8$$

A small amount of CO_2 (0.03%) is present in unpolluted air but this gives rise to a very dilute solution of carbonic acid (of about pH 5.7). In, for example, peaty moorland areas, the water may dissolve more CO_2 from the decomposition of organic matter, though the pH is not significantly lowered unless other acids are present (Harrison, 1987). Larger amounts of carbonic acid, resulting in lower pHs (down to 3.8), can occasionally occur in water from deep underground owing to the increased solubility of CO_2 at high pressures, whereas levels of acidity due to CO_2 are generally insignificant in hard waters (containing dissolved calcium and magnesium salts).

CO_2 dissolved in soft water (without dissolved salts) is aggressive to concrete and reacts initially with calcium hydroxide to produce the relatively insoluble calcium carbonate:

$$Ca(OH)_2 + H_2CO_3 = CaCO_3 + H_2O \quad 4.9$$

This in turn reacts with more carbonic acid to form the more soluble calcium bicarbonate (also known as calcium hydrogen carbonate):

$$CaCO_3 + H_2CO_3 = Ca(HCO_3)_2 \quad 4.10$$

resulting in some dissolution of the concrete matrix.

The situation is more complex in the case of hard water containing dissolved salts. For example, carbonic acid in water passing over limestone reacts to form calcium bicarbonate (as in equation 4.10). The acidity is reduced and usually the amount of free carbon dioxide in the water is negligible. If, however, there is some free CO_2 present, part of this participates in the stabilisation of calcium bicarbonate (as in equations 4.8 and 4.10) and the rest, called 'aggressive CO_2', is capable of reacting with concrete. Generally, aggressive CO_2 is only present in significant quantities in relatively pure (soft) water. The amount of aggressive CO_2 is also affected by equilibria involving other salts, such as calcium and magnesium sulfates, often present in water.

The other common acidic constituents found in natural ground waters are collectively known as humic acid, which represents a complex mixture of weak acids, with molecular weights from around 1,000,000 down to around 500 (Chin and Gschwend, 1991), produced in soils by the decay of organic matter. Sometimes the term fulvic acid is applied to the lower molecular weight fraction, with humic acid being reserved for the higher molecular weight fraction. Water saturated with humic acid, despite its low solubility, has a pH of about 4 in the absence of neutralising rocks such as limestone (Lea, 1970). The actual acidity fluctuates with season and weather conditions. When humic acid reacts with concrete, it forms a mixture of calcium salts whose solubilities vary with the molecular weight of the individual acids.

Other acids which have a destructive action on concrete include water-soluble organic acids of relatively low molecular weight. Lactic acid has been found, for example, in swamp waters. Large amounts of lactic and acetic acids are produced from manure and feed supplies on floors of animal houses (De Belie *et al.*, 2000a) and can cause severe deterioration of concrete. (In the case of floors of animal houses, many other aggressive substances are also present, e.g. Cl^-, SO_4^{2-}, Mg^{2+}, NH_4^+.) The concrete walls and floors of silos can be attacked by the lactic, acetic and butyric acids formed in the production of silage. Lactic and butyric acids, produced in the souring of milk and butter, cause problems with tanks and concrete floors in dairies and cheese-making facilities. Similar problems are encountered due to acetic acid in the manufacture of vinegar and food pickling processes, and due to citric, malic, tartaric and oxalic acids in industries involving fruit-processing, with different severities of attack depending on the solubilities of the salts formed.

The strengths of many of the acids which react with concrete and the solubilities of their calcium salts are shown in Table 4.3.

Table 4.3 Strengths of some acids which react with concrete and the solubilities of their calcium salts

Acid		Strength (K_a)	Main reaction product with cement	
			Name	Solubility (g/100ml)
Mineral				
Sulfuric	1	V. high	Calcium sulfate	0.209
	2	1.20×10^{-2}		
Hydrochloric		V. high	Calcium chloride	74.5
Nitric		40	Calcium nitrate	121.2
Phosphoric	1	7.52×10^{-3}	Calcium phosphate	0.002
	2	6.23×10^{-8}		
	3	2.20×10^{-13}		
Carbonic	1	4.5×10^{-7}	Calcium hydrogen carbonate	16.6
	2	4.8×10^{-11}	Calcium carbonate	0.0014
Organic				
Lactic		1.37×10^{-4}	Calcium lactate	3.1
Acetic		1.76×10^{-5}	Calcium acetate	37.4 (34.7)
Butyric		1.54×10^{-5}	Calcium butyrate	soluble
Citric	1	7.45×10^{-4}	Calcium citrate	0.085
	2	1.73×10^{-5}		
	3	4.02×10^{-7}		
Malic	1	3.90×10^{-4}	Calcium l-malate	(Dihydrate)
	2	7.8×10^{-6}		0.812
Tartaric	1	1.04×10^{-3}	Calcium d-tartrate	(Tetrahydrate)
	2	4.55×10^{-5}		0.0266
Oxalic	1	5.90×10^{-2}	Calcium oxalate	0.00067
	2	6.40×10^{-5}		
Oleic			Calcium oleate	0.04
Stearic			Calcium stearate	0.004
Humic (a mixture)		Variable – low	Calcium humate	Variable

Strength in terms of $K_a = [H^+][A^-]/[HA]$ for the equilibrium $HA = H^+ + A^-$ in aqueous solution at 25C.
Solubility in terms of g/100 ml cold water (Weast, 1988)
Anhydrous salt unless otherwise stated.

4.6.3 Other chemicals which attack concrete

Many other chemicals, e.g. oils, fats, sugars, alkalis and salts, may attack concrete in particular circumstances. A wide range of such substances is described in *Chemistry of Cement and Concrete* by Lea (1970), *Concrete*

Corrosion Concrete Protection by Biczok (1972), and in reports by Kuenning (1966) and the Portland Cement Association (2001). Detailed discussion of their various effects is beyond the scope of this chapter and only brief mention will be made here of some of the more notable examples.

Vegetable and animal oils and fats (which are esters of fatty acids with glycerol), high molecular weight (insoluble) acids (C12–C24) found in oils and fats, e.g. oleic ($C_{17}H_{33}COOH$) and stearic ($C_{17}H_{35}COOH$) acids, and glycerol can all have a destructive action on concrete. Problems can arise, therefore, in the manufacture of soap, cooking oils and fats, certain processed foods, candles, lubricating oils, etc. Some free acids are found naturally in oils and fats especially in vegetable oils but more are produced on exposure to air. Thus, more rapid attack of concrete occurs when it is exposed to air than when immersed in water. Oils and fats also react with the alkalis in concrete, a process known as saponification, to form salts of fatty acids and glycerol. The viscosity of an oil determines its degree of penetration and therefore influences the extent to which it attacks concrete. Glycerol itself dissolves lime and a solution of 2% is very destructive of immature Portland cement concrete though has little effect on well-carbonated mature concrete (Lea, 1970). It should be noted that, although most non-mineral oils can attack concrete, certain oils, such as linseed and tung oil, can be protective if applied as a surface treatment and allowed to harden by drying (oxidation).

Sugars are produced in many industries, for example as pure sugars or constituents of fruit, confectionery and other foods, drinks and wood pulp. Reaction occurs between sugars and calcium ions in the cement products to form calcium salts and cause dissolution of calcium hydroxide, C-S-H and calcium aluminate hydrates (Lea, 1970; Taylor, 1997), thus resulting in loss of strength of hardened concrete.

Petroleum fractions, such as petrol, diesel, kerosene and fuel oil, do not attack mature concrete although they strongly affect the hardening of green concrete. This also applies to mineral lubricating oils but not to those containing vegetable oils. Creosotes, on the other hand, contain some acidic substances, such as phenols, and so may attack concrete (Lea, 1970).

Dilute solutions of alkalis have little effect on Portland cement concrete but concentrated solutions (e.g. 5M) of the alkali metal hydroxides (NaOH and KOH) attack concrete, probably by decomposing hydrated aluminate phases (Taylor, 1997). Such high alkali concentrations can be generated locally around steel cathodes in cementitious materials that are exposed to long-term electrochemical treatments at very high current densities ($> 1A/m^2$) (Bertolini *et al.*, 1996) and this may be related to softening of the cement matrix that has sometimes been reported to occur in the vicinity of embedded cathodes in concrete subjected to intense electrolysis (Rosa *et al.*, 1913).

Apart from sulfates, there are several other salts which can adversely affect concrete. These include salts of strong acids with weak bases which behave as

weak acids and so have a similar effect on concrete to these acids. In addition, ion exchange can occur between the cations in the salt and those in cement. Ammonium salts are generally more destructive than salts of other bases. NH_4^+ ions exchange with Ca^{2+} ions in cement paste, e.g. with calcium hydroxide:

$$2NH_4Cl + Ca(OH)_2 = CaCl_2 + 2NH_4OH \quad 4.11$$

$$NH_4OH = NH_3 + H_2O \quad 4.12$$

The ammonia produced may be gradually lost from solution so that the equilibrium shifts towards further dissolution of Ca^{2+} ions from the cement paste. Similarly, as was noted when dealing with the effects of sulfates, magnesium salts are more destructive than salts of alkali metals or calcium as Mg^{2+} ions exchange with Ca^{2+} ions in cement hydrate phases forming magnesium hydroxide (brucite) and silica gel. The latter two substances slowly react to form hydrated magnesium silicate which is associated with brittleness and loss of strength (Lea, 1970; Mehta, 1985). Highly concentrated solutions of chloride salts, such as magnesium chloride, can be destructive to concrete, reacting with calcium aluminate hydrates in Portland cement concrete to form chloroaluminate hydrates, and with CH to form expansive basic salts (Kurdowski, 2002, 2004).

4.6.4 Modelling chemical attack

Modelling the chemical degradation of concrete is complex because of the numerous chemical reactions and variety of conditions potentially involved. Models have been developed for leaching of Ca^{2+} ions by water (Bentz and Garboczi, 1992; Delagrave *et al.*, 1997), external sulfate attack/decalcification (Marchand *et al.*, 1999; Maltais *et al.*, 2004) or attack by one type of acid, e.g. carbonic acid (Grube and Rechenberg, 1989), but can only apply to a limited set of conditions. Development of realistic models is an ongoing problem (Beddoe and Dorner, 2005). Much work is being carried out to produce computer-based models of the behaviour of cement products used in stabilisation and solidification of hazardous wastes, in particular radioactive material. The lifetimes expected of these cement-based materials are much greater than those in other structures and so computer-modelling combined with carefully designed experimental work will be necessary for predicting performance (see, e.g., Adenot and Richet, 1997; Matte *et al.*, 2000, Yokozeki *et al.*, 2004).

4.6.5 Sources of guidance for attack on concrete by acid and other aggressive chemicals

Three exposure classes (XA1, XA2 and XA3) are described in BS EN 206-1 (2000) according to the aggressiveness of attack on concrete in natural soils and

groundwater (corresponding to slightly, moderately and highly aggressive respectively). The chemicals taken into account are sulfate, H^+ ions and also, in the case of groundwater, CO_2, Mg^{2+} and NH_4^+ ions. The Standard gives guidance on the maximum w/c ratios, minimum strength class and minimum cement contents for the different exposure classes.

More recently BRE Special Digest 1 (2005) has updated its guidance on the specification of concrete in aggressive ground. This includes attack on concrete by acids, as well as by sulfates, in natural ground and brownfield locations. The acids covered by the Digest are those most commonly found in natural groundwater, viz. sulfuric acid, humic acid and carbonic acid. As mentioned in Section 4.5 of this chapter, sites are classified according to the Aggressive Chemical Environment for Concrete (ACEC) which takes into account sulfate concentration, potential concentrations of sulfate based on pyrite/sulfide present, pH, magnesium ion concentration and mobility of groundwater. Additionally, HCl, HNO_3, and aggressive CO_2 can be incorporated into determining the ACEC Class. Based on this class and other factors (e.g., type of concrete element, intended working life, exposure to hydraulic gradient of groundwater), the BRE SD1 (2005) gives guidance on the Design Chemical (DC) Class, which defines the quality (maximum w/c ratios and minimum cement (or combination) contents) of concrete needed to resist chemical attack, and also on additional protective measures that can be applied. Concrete placed in ACEC Classes given the suffix 'z' needs to resist acid conditions. Since concrete quality is the main factor in determining acid resistance, no restrictions are placed on the use of any of the cement types listed in the BRE SD1 (2005). Recommendations are also given for the use of protective linings for the internal surfaces of precast concrete pipes, box culverts and segmental linings for tunnels and shafts under a range of aggressive conditions exacerbated by flowing water or effluents, such as relatively pure water with aggressive CO_2 at concentrations >15 mg/l, acidic solutions of pH < 5 and effluents, particularly sewage, containing sulfate at concentrations > 1400 mg/l.

Specialist advice is needed where concrete is exposed to other less frequently occurring chemicals. BS 5502-21 (1990) gives guidance on selection of concretes to be exposed to attack by milk, silage, slurry and other agricultural agents. A guide to the effect of many different substances on concrete and advice on selecting protective treatments is given by the Portland Cement Association (2001).

4.7 Microbiologically-induced corrosion of concrete

Microbial activity is now known to be involved in the corrosion of concrete in a variety of situations. These include sewage systems (Olmstead and Hamlin, 1900; Parker, 1951; Gu *et al.*, 2000), waste water and potable water treatment systems (Rigdon, 1984; Hall, 1989; Coleman and Gaudet, 1993), agricultural

structures (slurry and manure pits, silos) (De Belie *et al.*, 2000a), oil storage tanks (Mehta, 1991), cooling towers and other hydraulic facilities (Zherebyateva *et al.*, 1991; Allan, 1999), tunnels (Thornton, 1978; Mittelman and Danko, 1995; Robins *et al.*, 1997) and concrete foundations (Emami *et al.*, 1999: Moncarz *et al.*, 2002). Indirectly, concrete structures may be affected by ground heave as a result of microbial activity in pyritic soils (see Section 4.2). It is also likely that microbiologically-influenced degradation will affect the long-term stability of cement-based systems used in the solidification of low level radioactive waste (Rogers *et al.*, 1996; Idachaba *et al.*, 2001; Aviam *et al.*, 2004) and possibly also in the storage of high-level nuclear waste (Pedersen, 1999).

Various micro-organisms have been shown to participate in the corrosion of concrete. Commonly associated with this process are the aerobic sulfur-oxidising bacteria (SOBs), previously known as *Thiobacilli* (Parker, 1945a,b, 1947). These bacteria are autotrophic, that is they use CO_2 as their carbon source, and they derive their energy by oxidising reduced forms of sulfur present, for example, in soils containing sulfide minerals and in sewage. Initially, the pH of the concrete is too high to support growth of these bacteria but carbonation results in reduction of the pH to about 9 which allows growth of some species, such as *Thiobacillus thioparus*. Chemical oxidation of sulfides results in the formation of e.g. sulfur, thiosulfate and sulfite as well as a little sulfuric acid (Chen and Morris, 1972). A succession of different species of bacteria, active at different pHs, metabolise these different forms of sulfur to produce more sulfuric acid (Parker, 1947, 1951; Milde *et al.*, 1983; Diercks *et al.*, 1991; Islander *et al.*, 1991). The acidophilic species, *Acidithiobacillus* (previously *Thiobacillus*) *thiooxidans** and *Acidithiobacillus* (previously *Thiobacillus*) *ferrooxidans* (Kelly and Wood, 2000), continue to be active and produce sulfuric acid down to a pH of <1, where other bacteria fail to thrive. In addition, *Acidithiobacillus ferrooxidans* can oxidise any Fe^{2+} present, as in pyritic soil, to Fe^{3+}. The Fe^{3+} produced further oxidises sulfides, such as pyrite, to produce more sulfuric acid and highly acidic conditions arise. Initially, gypsum appears as a corrosion product on the surface of the concrete and ettringite forms beneath the surface where the pH is not as low (Mori *et al.*, 1991, 1992). These changes result in increased porosity and cracking. The actual mechanism of attack varies with different conditions. In sewers, for example, the sulfuric acid and the acidophilic SOBs penetrate into the concrete surface from the outside (Islander *et al.*, 1991; Davis *et al.*, 1998). The extreme acidity ($pH < 2$) and continual removal of the surface layer ultimately cause complete disintegration of the concrete (Parker, 1951).

Many other micro-organisms may be involved in the corrosion of concrete (Davis *et al.*, 1998; Nica *et al.*, 2000) and modern DNA-based technologies have led to the identification of large numbers of microbes which have previously not

* Also the same as *Thiobacillus concretivorus*.

been cultured (Amann *et al.*, 1995; Vincke *et al.*, 2001). Heterotrophic species of bacteria (those which obtain their energy by growing on organic carbon compounds) have commonly been found in association with the autotrophic SOBs (Harrison, 1984; Sand and Bock, 1984; Davis *et al.*, 1998; Nica *et al.*, 2000). It has been shown that the SOBs excrete organic acids which inhibit their own growth (Borichewski, 1967). The heterotrophs probably remove these acids using them as carbon sources and so allow further growth of SOBs (Harrison, 1984; Islander *et al.*, 1991). Thus the two types of organisms aid each other's survival. Other micro-organisms which have been identified as affecting the corrosion process directly include nitrifying bacteria, such as *Nitrosomonas* and *Nitrobacter* species, which produce nitric acid (Kaltwasser, 1976; Sand and Bock, 1991) and certain fungi, which may participate in the oxidation of sulfides (Cho and Mori, 1995) or penetrate the concrete and/or complex Ca^{2+} ions by producing organic acids (Gu *et al.*, 1998).

The most widespread occurrence of microbiologically induced corrosion (MIC) of concrete appears to be in sewage systems involving concrete pipes and manhole covers (see Fig. 4.4). As early as 1900, problems of corrosion of concrete and mortar in the outfall sewer in Los Angeles were described (Olmstead and Hamlin, 1900). Cases have since been reported all over the world (other cities of the USA, South Africa, Australia, India, the Middle East, Europe and Japan – see, e.g., Lea, 1970; Aldred and Eagles, 1982; Sand and Bock, 1984; Mori *et al.*, 1991). The problem arises above the sewage level in pipes which are not completely full, in particular at the crown of the sewer. Organic sulfur

4.4 Microbiologically-induced corrosion in a prefabricated sewer pipe (Case History 11.08.17.01 – reprinted with permission of Elsevier from *Corrosion Atlas,* 1997, compiled by Evert D.D. During).

compounds and sulfates, present in domestic sewage, industrial wastes and/or seawater, are acted on by bacteria which reside mainly in the sewage sludge and underwater slime deposits on the sewer walls. The sewage is rich in nutrients which act as carbon and nitrogen sources. Many bacteria exist which can release hydrogen sulfide anaerobically from organic sulfur compounds. Sulfate-reducing bacteria (SRBs), such as *Desulfovibrio desulfuricans*, also thrive under the anaerobic and near-neutral conditions in the sewage, converting sulfates to hydrogen sulfide. Greater quantities are produced with longer sewage retention times and higher temperatures (hence the problems in hot climates). Hydrogen sulfide does not generally have any significant effect on the submerged concrete. However, it is volatile and is released into the air space above the sewage, particularly under conditions of turbulent sewage flow. There the hydrogen sulfide dissolves in moisture condensed on the concrete surface and reacts with oxygen present in the air. The sulfur and other compounds thus produced are converted to sulfuric acid by a variety of sulfur-oxidising bacteria as described above. Corrosion therefore occurs above the waterline.

Although the factors affecting sulfide accumulation and corrosion of concrete are highly complex, empirical models for the rate of corrosion of concrete in sewers have been developed (see, e.g., Pomeroy, 1990). The process can be broken down into several stages:

- the rate of formation of sulfide in the sewage
- the flux of H_2S from the sewage into the air and thence from the air into the moisture on the exposed concrete surface
- the rate of conversion of H_2S to H_2SO_4 by SOBs in the moisture on the exposed concrete
- the rate at which acid reacts with the concrete.

Based on investigations in the Los Angeles County sanitation district, Pomeroy and co-workers developed what has become the most widely used model to forecast sulfide accumulation in partly filled sewage pipes (Pomeroy, 1990). They assumed that the sulfate concentration in the sewage was high and non-limiting, the oxygen concentration was low and the slime layer was fully active. It was then possible to make predictions about the flux of H_2S from the sewage, under ordinary flow conditions, into the air and thence into the moisture on the exposed concrete surface:

$$\text{Ø}_{SW} = 0.7(su)^{3/8} j[DS](b/P') \qquad 4.13$$

where Ø_{SW} = average flux of H_2S to the concrete ($g\,m^{-2}\,h^{-1}$), s = slope of sewer (m/100m), u = mean velocity in the sewer ($m\,s^{-1}$), j = proportion of undissociated H_2S (which is pH dependent), $[DS]$ = dissolved sulfide concentration ($mg\,l^{-1}$), b = surface width of sewage stream (m) and P' = perimeter of exposed concrete wall (m). Assuming that little H_2S escapes from the sewer and

that the H_2S which reaches the concrete surface is converted efficiently to H_2SO_4 by the SOBs in the moisture there, the rate at which the acid reacts with the concrete under steady state conditions is predicted as:

$$c = 11.5k\text{Ø}_{SW}(1/A) \qquad 4.14$$

where c = the average rate of corrosion of concrete (mm y^{-1}), k = the coefficient of efficiency for the acid reaction (varying from 1, when acid formation is slow, down to 0.3 for rapid acid production) and A = the alkalinity of the concrete (expressed as mass of equivalent $CaCO_3$ per mass of concrete). This is the model most commonly used for predicting corrosion rates but further work is needed to be able to make reasonable predictions of service life of concrete in sewers (see, e.g., Roberts *et al.*, 2002).

Various methods of controlling microbial corrosion of sewage systems have been suggested (Parker, 1951; Pomeroy, 1990; Boon, 1995; Fan *et al.*, 2001) and guidance is provided for concrete to be used in the construction of sewers (BS EN 752-3, 1997; BS EN 1610, 1998; ASTM, 2003; Building Research Establishment, 2005). A number of different coatings or linings have been used, e.g. PVC linings have been successful in long-term protection of concrete (Kienow and Kienow, 1991; Redner *et al.*, 1994). Reducing the sulfide content of sewage is the most important factor in preventing acid production and therefore corrosion. New sewers are designed to reduce turbulence, to limit retention times of the sewage and to have appropriate flow rates for aeration of the sewage in order to inactivate the SRBs and to reduce sludge deposition. Ventilation of sewers may help aerate the sewage but probably acts by reducing moisture on the concrete surface above the sewage. Attempts have been made to reduce the generation of H_2S from the sewage by dosing it with alkali or to neutralise the acid on the crown of the sewer and to deactivate the SOBs by spraying with $Mg(OH)_2$ (Sydney *et al.*, 1996). Removal of sulfides from sewage and/or prevention of their accumulation can be carried out by:

1. reducing the sulfur content of industrial effluents,
2. periodic flushing at high rates to remove sediments,
3. oxidation of sulfides and inhibition of SRBs by aerating with compressed air or pure oxygen or adding chemicals such as hydrogen peroxide or chlorine,
4. adding heavy metals to precipitate sulfides and inhibit SRB activity.

In fact, it is thought that a new wave of problems of corrosion of sewage systems that arose in the 1980s in the USA was due to limits that had been placed in the 1970s on the toxicity of wastes that could be discharged into the sewers (Mansfeld *et al.*, 1991; Morton *et al.*, 1991). These restrictions led to a significant reduction in the amount of heavy metals and cyanide entering the sewage system and therefore less inhibition of SRBs and a lower removal rate of sulfides.

A similar process of biocorrosion of concrete occurs in other systems which involve storage and/or transport of sludges, e.g. in slurry and manure pits (De Belie *et al.*, 2000a) and in waste water treatment facilities (Rigdon, 1984). In these cases, the H_2SO_4 produced causes deterioration of the concrete by acid dissolution of Ca^{2+} ions. This is thought also to be the case in concrete oil storage tanks in which the high temperatures of the oil stimulate bacterial and chemical attack (Mehta, 1991). A different mechanism is proposed for conditions where the pH of the concrete remains high, for example at certain hydraulic facilities (Zherebyateva *et al.*, 1991). Although the quantity of nutrients is much lower than that in sewage, bacteria exist which can break down the complex organic molecules that may be present as additives in the concrete; other bacteria can fix CO_2. Thus carbon sources are provided for SRBs which can reduce any sulfate present, under anaerobic conditions, to H_2S. In aerobic regions, the SOBs convert the H_2S to H_2SO_4. Nitric acid is produced by nitrifying bacteria and organic acids by a variety of bacteria.

Microbiological activity is also involved in the degradation of concrete structures in pyritic soil and/or rocks. Although sulfide minerals such as pyrite (FeS_2) are stable under anaerobic conditions, when pyritic soil is disturbed and therefore aerated, e.g. during construction activities, the pyrite undergoes slow chemical oxidation to ferrous sulfate and sulfuric acid as described in Section 4.2:

$$2FeS_2 + 2H_2O + 7O_2 = 2FeSO_4 + 2H_2SO_4 \qquad 4.15$$

In the presence of air, water and also sulfur-oxidising bacteria such as *Acidithiobacillus ferrooxidans*, pyrite is oxidised rapidly to sulfuric acid, ferrous and ferric sulfate:

$$4FeSO_4 + O_2 + 2H_2SO_4 = 2Fe_2(SO_4)_3 + 2H_2O \qquad 4.16$$

$$7Fe_2(SO_4)_3 + FeS_2 + 8H_2O = 15FeSO_4 + 8H_2SO_4 \qquad 4.17$$

Both the resultant acid and the sulfate can affect the ground itself and any concrete structures present (see Sections 4.2 and 4.6).

An interesting form of microbial corrosion of concrete was involved in the disintegration of concrete piles acting as foundations for an office block in the USA (Emami *et al.*, 1999: Moncarz *et al.*, 2002). The concrete deteriorated from the outside progressing inwards and only concrete in contact with certain anoxic marine sediments with a high organic content was found to have been affected; that in contact with seawater, sand or silt, low in organics, was apparently unaffected. The sediments had a low iron and a moderate sulfate concentration. They showed a high level of activity of the anaerobic sulfate-reducing bacteria, *Desulfovibrio* and *Clostridium*. Under such conditions it appears that SRBs may preferentially use Fe^{3+} as an oxidising agent (Coleman *et al.*, 1993). Since there was insufficient Fe^{3+} in the surrounding sediments, it was suggested that the

4.5 Collapsed concrete silo showing effects of acid attack (Queen's Printer for Ontario, 1990. Reproduced with permission).

bacteria may have removed Fe^{3+} from the hardened cement paste in the foundations causing increased susceptibility to sulfate attack. Thus the degradation of the concrete was proposed to be a result of microbiological removal of iron as well as sulfate attack.

Serious deterioration and collapse of concrete silos have occurred as a result of microbiological production of organic acids under anaerobic conditions (see Fig. 4.5). Silos are used in agriculture for the storage of grain or fermented moist food crops (silage). In particular, the formation of silage results in significant acid production. This process, called ensilage, takes place in several stages (Weinberg and Muck, 1996). After the crops are placed in the silo, there is an initial short phase in which various aerobic micro-organisms such as yeasts and enterobacteria use up the oxygen present. The ensiling process then enters the anaerobic phase which may be completed in several days or may take several weeks, after which relatively little change occurs. The predominant bacteria involved in the anaerobic stage are the lactic acid bacteria which ferment the water soluble carbohydrates in the silage to produce mainly lactic and, to a lesser extent, acetic acids. Butyric acid may also be produced by the action of *Clostridia* on lactic acid. Successful fermentation of silage causes a rapid drop in pH to about 3.8–5.0, largely as a consequence of lactic acid formation. Effluents from silos can have pHs as low as 3.5 (De Belie *et al.*, 2000a). Such low pHs, together with the solubility of the calcium salts formed in the reaction between concrete and the organic acids, can have quite a severe effect on the walls and floors of silos. Improved resistance to attack on the concrete by silage acids has been obtained by using appropriate water/cement ratios and including up to 30% pfa by weight of cement in the concrete mixes or by treating the hardened concrete with various coatings such as epoxy or polyurethane resin (De Belie *et al.*, 2000b).

Studies on the degradation of cementitious materials used in nuclear waste disposal are generally based on the assumption of purely physico-chemical processes because the realisation that microbial attack might be significant is fairly recent. However, micro-organisms known to attack concrete and com-

monly found in soils, such as at low-level nuclear waste disposal sites, include the SOBs, numerous heterotrophic bacteria and fungi. Accelerated tests to observe the effect of the acidophilic SOBs, such as *Acidithiobacillus thiooxidans*, on simulated cement-based radioactive waste forms have been carried out (Rogers *et al.*, 1996, Idachaba *et al.*, 2001). Biofilms developed on the surface and a lowering of the pH resulted in the dissolution of Ca^{2+} ions and the degradation of the cementitious material. Neutrophilic SOBs have also been shown to cause rapid degradation of hardened cement specimens containing Cs^{+} and Sr^{2+} ions with significant leaching of Ca^{2+} and Sr^{2+} ions and some loss of Si (Aviam *et al.*, 2004). The problem of microbial attack may also apply to cement-based materials used in the storage of high-level nuclear waste, since a considerable variety of micro-organisms has been found at depths >1 km (Pedersen, 1996, 1999). The development of models of the kinetics of microbial degradation of cement-based waste forms is still in its infancy (see, e.g., Idachaba *et al.*, 2003).

4.8 Conclusions

This chapter has presented a fairly brief overview of some of the main areas of concrete durability that depend on the ability of the hardened cement matrix to resist common forms of chemical and microbiologically induced degradation. Constraints on the length of the chapter meant that it was not possible, however, to include a number of interesting topics that would have merited further detailed discussion.

In particular this is so in the case of concrete made with calcium aluminate cements (also known as high alumina cements). These cements have had a chequered history since their introduction in France a century ago where they were originally produced in response to the need for cements with high resistance to sulfate attack. The problems later encountered as a consequence of the gradual phase transformations (known as 'conversion') of the hydrated cement that can degrade its mechanical properties led to an effective ban on structural applications in the UK in the mid-1970s (Neville, 1975). Since then there has been a substantial amount of research into to the nature and properties of these materials and a reassessment by the UK Concrete Society of their potential for applications in construction (Cather *et al.*, 1997). More recently, a number of reviews of calcium aluminate cements have been published (Scrivener and Capmas, 1998; Bensted, 2002d) and they were the topic of a fairly recent international conference (Mangabhai and Glasser, 2001).

4.9 References

ACI SP 65 (1980), *Special Publication* '*Performance of concrete in marine environments*', American Concrete Institute, Detroit.

Adenot F and Richet C (1997), 'Modelling of the Chemical Degradation of a Cement Paste', in Scrivener K L and Young J F (eds), *Mechanisms of Chemical Degradation of Cement-based Systems*, London, Spon, 341–349.

Aldred M I and Eagles B G (1982), 'Hydrogen sulphide corrosion of the Baghdad trunk sewerage system', *Water Pollution Control*, 81 (1), 80–96.

Allan M L (1999), *Evaluation of Coatings and Mortars for Protection of Concrete Cooling Tower Structures from Microbiologically Influenced Corrosion in Geothermal Power Plants*, Report on Contract No. DE-ACO2-98CH1O886, Washington, U.S. Department of Energy.

Amann R I, Ludwig W and Schleifer K-H (1995), 'Phylogenetic identification and in situ detection of individual microbial cells without cultivation', *Microbiological Reviews*, 59 (1), 143–169.

Anstice DJ, Page CL and Page MM (2005), 'The pore solution phase of carbonated cement pastes', *Cement and Concrete Research*, 35, 377–383.

ASTM (2003), 'Standard Specification for Concrete Sewer, Storm Drain, and Culvert Pipe', *Annual Book of ASTM Standards*, Section 4 Vol. 4.05 Designation C14M-99, West Conshohocken, PA, USA, ASTM International, 18–21.

Aviam O, Bar-Nes G, Zeiri Y and Sivan A (2004), 'Accelerated biodegradation of cement by sulfur-oxidising bacteria as a bioassay for evaluating immobilization of low-level radioactive waste', *Applied and Environmental Microbiology*, 70 (10), 6031–6036.

Barnes BD, Diamond S and Dolch WL (1978), 'Hollow shell hydration of cement particles in bulk cement paste', *Cement and Concrete Research*, 8 (3), 263–271.

Beddoe R E and Dorner H W (2005), 'Modelling acid attack on concrete: Part I. The essential mechanisms', *Cement and Concrete Research*, 35, 2333–2339.

Bensted J (1977a), 'Some problems of ettringite and of thaumasite in the gypsum plaster/cement contact area', in Murat M and Foucault M (eds), *Proceedings of the International RILEM Symposium on Calcium Sulfates and Derived Materials*, St-Rémy-Les-Chevreuse, France, 479–487.

Bensted J (1977b), 'Problemi che si verificano nell'identificazione della thaumasite/Problems arising in the identification of thaumasite', *Il Cemento*, 74 (3), 81–90.

Bensted J (1981a), 'Chemical considerations of sulphate attack', *World Cement Technology*, 12 (4), 178–179, 182–184.

Bensted J (1981b), 'Consideraciones químicas sobre el ataque por los sulfatos', *Materiales de Construcción*, No. 184, October–December, 97–99.

Bensted J (1983), 'Further aspects of the setting of Portland cement', *Silicates Industriels*, 48 (9), 167–170.

Bensted J (1988), 'Thaumasite – Un prodotto di deterioramento delle strutture, di cemento indurito/Thaumasite – A deterioration product of hardened cement structures', *Il Cemento*, 85 (1), 3–10.

Bensted J (1994), 'Applications of infrared spectroscopy to cement hydration', *Meeting on Techniques for Characterisation of Cement Hydration, Society of Chemical Industry, London, 21 April 1994*, London, SCI, 55pp.

Bensted J (1998), 'Scientific background to thaumasite formation in concrete', *World Cement Research*, 29 (11), 102–105.

Bensted J (1999), 'Laser Raman spectroscopy and cement hydration', *Colloquium on Techniques for Characterisation of Cement Hydration – New and Old Techniques, Society of Chemical Industry, London, 15 April 1999*, London, SCI, 19pp.

Bensted J (2000), 'Mechanism of thaumasite sulfate attack in cements, mortars and concretes', *Zement-Kalk-Gips International*, 53 (12), 704–709.

Bensted J (2001), 'Thaumasite sulfate attack – its scientific background and ramifications in construction', in Kurdowski W and Gawlicki M (eds), *Kurdowski Symposium – Science of Cement and Concrete*, Kraków, Wydawnictwo Naukowe 'Akapit', 189–198.

Bensted J (2002a), 'Gypsum in cements', in Bensted J and Barnes P (eds), *Structure and Performance of Cements*, 2nd edition, London and New York, Spon Press, 253–264.

Bensted J (2002b), 'A discussion of the review paper "Sulfate attack research – whither now?" by M. Santhanam, M.D. Cohen and J. Olek', *Cement and Concrete Research*, 32, 995–1000.

Bensted J (2002c), 'Hydration of Portland cement', in Ghosh S N (ed.), *Advances in Cement Technology*, 2nd edition, New Delhi, Tech Books International, 31–86.

Bensted J (2002d), 'Calcium aluminate cements' in Bensted J and Barnes P (eds), *Structure and Performance of Cements*, 2nd edition, London and New York, Spon Press, 114–139.

Bensted J (2003a), 'Thaumasite – direct, woodfordite and other possible formation routes', *Cement and Concrete Composites*, 25, 873–877.

Bensted J (2003b), 'Thaumasite – three-year review', *Concrete*, 37 (8), 7.

Bensted J and Barnes P (2002), *Structure and Performance of Cements*, 2nd edition. London and New York, Spon Press.

Bensted J and Varma S P (1973a), 'Studies of thaumasite – Part II.', *Silicates Industriels*, 39 (1), 11–19.

Bensted J and Varma S P (1973b), 'Silicaten met silicium in zes-coordinatie met zuurstof', *Klei en Keramiek*, 23 (4), 66–69.

Bentz D P and Garboczi E J (1992), 'Modelling the leaching of calcium hydroxide from cement paste: Effects on pore space percolation and diffusivity', *Materials and Structures*, 25, 523–533.

Bertolini L, Yu SW and Page C L (1996), 'Effects of electrochemical chloride extraction on chemical and mechanical properties of hydrated cement paste', *Advances in Cement Research*, 8(31), 93–100.

Biczók I (1972), *Concrete Corrosion Concrete Protection*, 8th edition, Budapest, Akadémiai Kiadó, 545pp.

Boon A G (1995), 'Septicity in sewers: causes, consequences and containment', *Water Science and Technology*, 31 (7), 237–253.

Borichewski R M (1967), 'Keto acids as growth-limiting factors in autotrophic growth of Thiobacillus thiooxidans', *Journal of Bacteriology*, 93 (2), 597–599.

British Cement Association (2001), *BCA Guide: Specifying concrete to BS EN 206-1/BS 8500: Concrete resistant to chemical attack*, Crowthorne, BCA.

British Cement Association (2005) 'The new chromium(VI) directive for cement: sheet 2: Cements, chromium, ferrous sulfate and other reducing agents', *Health & safety information sheet Document No. ST/IS/14b*, British Cement Association, Camberley, UK.

BS 4027 (1996), *Specification for sulfate-resisting Portland cement*, British Standards Institution, London.

BS 5328-1 (1997), *Concrete. Guide to specifying concrete*, British Standards Institution, London.

BS 5502-21 (1990), *Buildings and structures for agriculture. Part 21: Code of practice for selection and use of construction materials*, British Standards Institution, London.

BS 6349-1 (2000), *Maritime structures. Code of practice for general criteria*, British Standards Institution, London.

BS 8500-1 (2002), *Concrete. Complementary British Standard to BS EN 206-1. Method of specifying and guidance for the specifier*, British Standards Institution, London.

BS 8500-2 (2002), *Concrete. Complementary British Standard to BS EN 206-1. Specification for constituent materials and concrete*, British Standards Institution, London.

BS EN 197-1 (2000), *Cement. Composition, specifications and conformity criteria for common cements*, British Standards Institution, London.

BS EN 206-1 (2000), *Concrete. Specification, performance, production and conformity*, British Standards Institution, London.

BS EN 752-3 (1997), *Drain and sewer systems outside buildings*, British Standards Institution, London.

BS EN 1610 (1998), *Construction and testing of drains and sewers*, British Standards Institution, London.

Building Research Establishment (1996), *Sulphate and Acid Resistance of Concrete in the Ground, BRE Digest 363*, Watford, CRC Ltd (withdrawn).

Building Research Establishment (2001), *Concrete in Aggressive Ground*, *BRE Special Digest 1*, Watford, CRC Ltd. (Note: Revised 2003 and 2005.)

Building Research Establishment (2005), *Concrete in Aggressive Ground*, *BRE Special Digest 1*, 3rd edition, Watford, BRE Bookshop.

Building Research Station (1968), 'Concrete in sulphate-bearing soils and groundwater', *Building Research Station Digest 90*, HMSO, London (withdrawn).

Bye G C (1999), *Portland cement: composition, production and properties*, 2nd edition, Thomas Telford, London.

Cather R, Bensted J, Croft A, George C M, Hewlett P C, Majumdar A J, Nixon P J, Osborne G J and Walker MJ (1997), *Calcium Aluminate Cements in Construction – A Reassessment, Concrete Society Technical Report No. 46*, Slough, The Concrete Society.

Chen K Y and Morris J C (1972), 'Kinetics of oxidation of aqueous sulfide by O_2', *Environmental Science and Technology*, 6 (6), 529–537.

Chin Y-P and Gschwend P M (1991), 'The abundance, distribution, and configuration of porewater organic colloids in recent sediments', *Geochimica et Cosmochimica Acta*, 55, 1309–1317.

Cho K-S and Mori T (1995), 'A newly isolated fungus participates in the corrosion of concrete sewer pipes', *Water Science and Technology*, 31 (7), 263–271.

Coleman M L, Hedrick D B, Lovely D R, White D C and Pye K (1993), 'Reduction of Fe(III) in sediments by sulphate-reducing bacteria', *Nature*, 361, 436–438.

Coleman R N and Gaudet I D (1993), '*Thiobacillus neopolitanus* implicated in the degradation of concrete tanks used for potable water storage', *Water Research*, 27 (3), 413–418.

Collett G, Crammond N J, Swamy R N and Sharp J H (2004), 'The role of carbon dioxide in the formation of thaumasite', *Cement and Concrete Research*, 34 (9), 1599–1612.

Crammond N J (2003), 'The thaumasite form of sulfate attack in the UK', *Cement and Concrete Composites*, 25 (8), 809–818.

Cripps J C and Edwards R L (1997), 'Some Geotechnical Problems Associated with Pyrite Bearing Mudrocks', in Hawkins A B (eds), *Ground Chemistry Implications for Construction*, Rotterdam, Balkema, 77–87.

Davis J L, Nica D, Shields K and Roberts D J (1998), 'Analysis of concrete from corroded sewer pipe', *International Biodeterioration and Biodegradation*, 42, 75–84.

De Belie N, Richardson M, Braam C R, Svennerstedt B, Lenehan J J and Sonck B

(2000a), 'Durability of building materials and components in the agricultural environment: Part I, The agricultural environment and timber structures', *Journal of Agricultural Engineering Research*, 75, 225–241.

De Belie N, Lenehan J J, Braam C R, Svennerstedt B, Richardson M and Sonck B (2000b), 'Durability of building materials and components in the agricultural environment, Part III: Concrete structures', *Journal of Agricultural Engineering Research*, 76, 3–16.

De Ceukelaire L (1989), *Mineralogie van beton in verband met verweringsverschijnselen*, Doctoraatthesis, Rijksuniversiteit Gent, Ghent, Belgium.

De Ceukelaire L (1990), 'Ettringiet, thaumasiet en kweethetniet', *Cement (Amsterdam)*, 5, 30–33.

Delagrave A, Gérard B and Marchand J (1997), 'Modelling the Calcium Leaching Mechanisms in Hydrated Cement Pastes', in Scrivener K L and Young J F (eds), *Mechanisms of Chemical Degradation of Cement-based Systems*, London, Spon, 38–49.

Department of Environment, Transport and the Regions (1999), 'The thaumasite form of sulfate attack: Risks, diagnosis, remedial works and guidance on new construction', *Report of the Thaumasite Expert Group*, DETR.

Deutsche Ausschuß für Stahlbeton (1989), *Richtlinie zur Wärmebehandlung von Beton*, Berlin, Köln, Beuth-Verlag GmbH.

Diamond S (2003), 'Thaumasite in Orange County, California: an inquiry into the effect of low temperature', *Cement and Concrete Composites* 25 (8), 1161–1164.

Diamond S and Ong S (1994), 'Combined effects of alkali silica reaction and secondary ettringite deposition in steam cured mortars', in Gartner E M and Uchikawa H (eds), *Cement Technology*, [Ceramic Transactions Volume 40], American Ceramic Society, 79–90.

Diercks M, Sand W and Bock E (1991), 'Microbial corrosion of concrete', *Experientia*, 47, 514–516.

During E D D (1997), *Corrosion Atlas: a Collection of Illustrated Case Histories*, 3rd edition, Amsterdam, Elsevier, p. 661.

Edge R A and Taylor H F W (1969), 'Crystal structure of thaumasite, a mineral containing $[Si(OH)_6]^{2-}$ groups', *Nature* (London), 224, No. 5217, 363–364.

Edge R A and Taylor H F W (1971), 'Crystal structure of thaumasite $[Ca_3Si(OH)_6.12H_2O]$ $(SO_4)(CO_3)$', *Acta Crystallographica*, B 27, 594–601.

Eglinton M (1998), 'Resistance of concrete to destructive agencies' in Hewlett P C (ed.), *Lea's Chemistry of Cement and Concrete,* 4th edition, London, Arnold Publishers, 299–342.

Emami N K, Nicholson A, Wren J and Moncarz P D (1999), 'Micro-biological attack on concrete – a threat to concrete infrastructure', in Neale B S (ed.), *Forensic Engineers: a Professional Approach to Investigation*, London, Thomas Telford Publications, 101–108.

Erlin B and Stark D C (1965), 'Identification and occurrence of thaumasite in concrete', *Highway Research Record*, 113, 108–113.

Famy C (1999), *Expansion of heat cured mortars*, PhD Thesis, Imperial College, London.

Famy C, Brough A R, Scrivener K and Atkinson A (2001), 'Influence of the storage conditions on the dimensional changes of heat cured mortars', *Cement and Concrete Research*, 31 (5), 795–803.

Famy C, Scrivener K L and Taylor H F W (2002a), 'Delayed ettringite formation', in Bensted J and Barnes P (eds), *Structure and Performance of Cements,* 2nd edition, London and New York, Spon Press, 282–294.

Famy C, Brough A R, Scrivener K L and Atkinson A, (2002b), 'Effects of an early or a late heat treatment on the microstructure and composition of inner C-S-H products of Portland cements pastes', *Cement and Concrete Research*, 32 (2), 269–278.

Famy C, Scrivener K L and Crumbie A K (2002c) 'What causes differences of C-S-H gel grey levels in backscattered electron images?', *Cement and Concrete Research*, 32 (9), 1465–1471.

Fan C-Y, Field R, Pisano W C, Barsanti J, Joyce J J and Sorenson H (2001), 'Sewer and tank flushing for sediment, corrosion, and pollution control', *Journal of Water Resources Planning and Management*, 127 (3), 194–201.

Fleurence A, Levandowsky L, Loisel M and Pagano M (1972), 'Note sur le minéral thaumasite. Sa formation dans certains produits industriels', *Bulletin de la Société Française de Céramique*, 94 (1), 67–79.

Francis O J (1999), *Forms of sulfate-induced degradation of concrete*, MEng Project Report, Aston University (unpublished).

Fu Y, Ding J and Beaudoin J J (1997), 'Expansion of Portland cement mortar due to internal sulfate attack', *Cement and Concrete Research*, 27 (9), 1299–1306.

Grattan-Bellew P E, Beaudoin J J and Vallée V-G (1998), 'Effect of aggregate particle size distribution and composition on expansion of mortar bars due to delayed ettringite formation', *Cement and Concrete Research*, 28 (8), 1147–1156.

Grube H and Rechenberg W (1989), 'Durability of concrete structures in acidic water', *Cement and Concrete Research*, 19, 783–792.

Gu J-D, Ford T E, Berke N S and Mitchell R (1998), 'Biodeterioration of concrete by the fungus Fusarium', *International Biodeterioration and Biodegradation*, 41, 101–109.

Gu J-D, Ford T E and Mitchell R (2000), 'Microbiological Corrosion of Concrete', in Revie R W (ed.), *Uhlig's Corrosion Handbook*, 2nd edition, New York, John Wiley & Sons, 477–491.

Hall G R (1989), 'Control of microbiologically induced corrosion of concrete in waste-water collection and treatment systems', *Materials Performance*, 28 (10), 45–49.

Harrison A P (1984), 'The acidophilic thiobacilli and other acidophilic bacteria that share their habitat', *Annual Review of Microbiology*, 38, 265–292.

Harrison W H (1987), 'Durability of concrete in acidic soils and waters', *Concrete*, 21 (2), 18–24.

Hartshorn S, Sharp J and Swamy R N (1999), 'Thaumasite formation in Portland limestone cement pastes', *Cement and Concrete Research*, 29, 1331–1340.

Hawkins A B and Pinches G M (1997), 'Understanding Sulphate Generated Heave Resulting from Pyrite Degradation', in Hawkins A B (ed.), *Ground Chemistry Implications for Construction*, Rotterdam, Balkema, 51–75.

Hewlett P C (Ed.) (1998), *Lea's Chemistry of Cement and Concrete*, 4th edition. London, Arnold Publishers.

Hobbs D and Matthews J (1998), 'Minimum requirements for concrete to resist chemical attack', in Hobbs D W (ed.), *Minimum Requirements for Durable Concrete*, Crowthorne, British Cement Association, 131–162.

Idachaba M A, Nyavor K, Egiebor N O and Rogers R D (2001), 'A refinement of the biofilm formation method for waste forms stability evaluation', *Journal of Hazardous Materials*, B84, 95–106.

Idachaba M A, Nyavor K and Egiebor N O (2003), 'Kinetic analysis of data obtained from studies on microbial degradation of cement waste forms, using shrinking core models', *Journal of Hazardous Materials*, B99, 57–69.

Islander R L, Devinny J S, Mansfeld F, Postyn A and Shih H (1991), 'Microbial ecology

of crown corrosion in sewers', *Journal of Environmental Engineering*, 117 (6), 751–770.

Kaltwasser H (1976), 'Destruction of concrete by nitrification', *European Journal of Applied Microbiology*, 3, 185–192.

Kelham S (1996a), The effect of cement composition and fineness on expansion associated with delayed ettringite formation', *Cement and Concrete Composites*, 18 (3), 171–179.

Kelham S. (1996b), 'Effects of cement composition and hydration temperature on volume stability of mortar', 4iv060, 8pp in *Proceedings of the 10th International Congress on the Chemistry of Cement*, Amarkai AB and Congrex Göteborg, Göteborg.

Kelly D P and Wood A P (2000), 'Reclassification of some species of *Thiobacillus* to the newly designated genera *Acidithiobacillus gen. nov., Halothiobacillus gen. nov.* and *Thermithiobacillus gen. nov*.', *International Journal of Systematic and Evolutionary Microbiology*, 50, 511–516.

Kienow K K and Kienow K E (1991), 'Corrosion below: sewer structures', *Civil Engineering*, 61 (9), 57–59.

Klemm W A and Miller F M (1996), 'Plausibility of delayed ettringite formation as a distress mechanism – considerations at ambient and elevated temperatures', 4iv059, 10pp in *Proceedings of the 10th International Congress on the Chemistry of Cement*, Amarkai AB and Congrex Göteborg, Göteborg.

Kuenning W H (1966), 'Resistance of Portland Cement Mortar to Chemical Attack – A Progress Report', *Highway Research Record*, No. 113, Washington D C, Highway Research Board, 43–87.

Kurdowski W (2002), 'Chloride corrosion in cementitious systems', in Bensted J and Barnes P (eds), *Structure and Performance of Cements*, 2nd edition, London and New York, Spon Press, 295–309.

Kurdowski W (2004), 'The protective layer and decalcification of C-S-H in the mechanism of chloride corrosion of cement paste', *Cement and Concrete Research*, 34, 1555–1559.

Lafaille A and Protas J (1970), 'Nouvelles données sur la structure de la thaumasite', *Comptes Rendus Hebdomadaires des Séances de l'Académie des Sciences, Paris*, Série D 270, 2151–2154.

Lawrence C D (1995), 'Delayed Ettringite Formation: An Issue?' in Skalny J P and Mindess S (eds), *Materials Science of Concrete: IV*, 113–154, American Ceramic Society, Westerville, Ohio, USA.

Lea F M (1970), *Chemistry of Cement and Concrete*, 3rd edition, London, Arnold, 727pp.

Leifeld G, Munchberg W and Stegmaier W (1970), 'Ettringit und Thaumasit als Treibursache in Kalk-Gips-Putzen', *Zement-Kalk-Gips*, 23 (4), 174–177.

Lewis M C (1996), *Heat curing and delayed ettringite formation in concretes*, PhD Thesis, Imperial College, London.

Luke K (1998), personal communication.

Macphee D and Diamond S (Guest Eds.) (2003), 'Thaumasite in cementitious materials', *Cement and Concrete Composites, Special Issue*, 25 (8), 805-1202.

Malolepsy J and Mróz R (2006), 'Warunki powstowania thaumasytu'/Conditions of thaumasite formation, Cement – Wapno – Beton, No. 2, 93–101.

Maltais Y, Samson E and Marchand J (2004), 'Predicting the durability of Portland cement systems in aggressive environments – laboratory validation', *Cement and Concrete Research*, 34, 1579–1589.

Mangabhai R J and Glasser FP (2001), *Calcium Aluminates 2001*, London, IOM Communications.

Mansfeld F, Shih H, Postyn A, Devinny J, Islander R and Chen C L (1991), 'Corrosion monitoring and control in concrete sewer pipes', *Corrosion*, 47 (5), 369–376.

Marchand J and Skalny J P (eds) (1999), *Materials Science of Concrete – Special Volume: 'Sulfate Attack Mechanisms'*, American Ceramic Society, Westerville, OH, 371pp.

Marchand J, Samson E and Maltais Y (1999), 'Modelling microstructural alterations of concrete subjected to external sulfate attack', in: Marchand J and Skalny J P (eds) (1999), *Materials Science of Concrete – Special Volume: 'Sulfate Attack Mechanisms'*, American Ceramic Society, Westerville, OH, 211–257.

Massazza F (1998), 'Pozzolana and pozzolanic cements', in Hewlett P C (ed.), *Lea's Chemistry of Cement and Concrete*, 4th edition, London, Arnold Publishers, 471–631.

Matte V, Moranville M, Adenot F, Richet C and Torrenti J M (2000), 'Simulated microstructure and transport properties of ultra-high performance cement-based materials', *Cement and Concrete Research*, 30, 1947–1954.

Mehta P K (1985), 'Studies on chemical resistance of low water/cement ratio concretes', *Cement and Concrete Research*, 15, 969–978.

Mehta P K (1991), *Concrete in the Marine Environment*, London, Elsevier Applied Science, 217pp.

Mehta P K (1999), 'Sulfate attack in marine environment', in Marchand J and Skalny J P (eds), *Materials Science of Concrete – Special Volume: 'Sulfate Attack Mechanisms'*, American Ceramic Society, Westerville, OH, 295–299.

Milde K, Sand W, Wolff W and Bock E (1983), 'Thiobacilli of the corroded concrete walls of the Hamburg sewer system', *Journal of General Microbiology*, 129, 1327–1333.

Mindess S, Young J F and Darwin D (2002), *Concrete*, Englewood Cliffs, N.J. and London, Prentice Hall.

Mittelman M W and Danko J C (1995), 'Corrosion of a Concrete Dam Structure: Evidence of Microbially Influenced Corrosion Activity', in P. Angell (ed.), *Proceedings of the International Conference on Microbially Influenced Corrosion*, Houston, TX, NACE International, 15/1–15/7.

Moenke H (1964), 'Ein weiteres Mineral mit Silizium in 6er-Koordination', *Naturwissenschaften*, 51 (10), 239.

Moncarz P D, Emami N K and Wren J (2002), 'Micro-biological Attack on Deep Foundation Concrete', in *Proceedings of the 9th International Conference on Piling and Deep Foundations*, Nice, France, 111–116.

Moranville-Regourd M (1998), 'Cements made from blast-furnace slag', in Hewlett P C (ed.), *Lea's Chemistry of Cement and Concrete*, 4th edition, London, Arnold Publishers, 633–674.

Mori T, Koga M, Hikosaka Y, Nonaka T, Mishina F, Sakai Y and Koizumi J (1991), 'Microbial corrosion of concrete sewer pipes, H_2S production from sediments and determination of corrosion rate', *Water Science and Technology*, 23, 1275–1282.

Mori T, Nonaka T, Tazaki K, Koga M, Hikosaka Y and Noda S (1992), 'Interactions of nutrients, moisture and pH on microbial corrosion of concrete sewer pipes', *Water Research*, 26 (1), 29–37.

Morton R L, Yanko W A, Graham D W and Arnold R G (1991), 'Relationships between metal concentrations and crown corrosion in Los Angeles County sewers', *Research Journal of the Water Pollution Control Federation*, 63 (5), 789–798.

Neville A (2004), 'The confused world of sulfate attack on concrete', *Cement and Concrete Research*, 34, 1275–1296.

Neville A M (1975), *High Alumina Cement Concrete*, Lancaster, Construction Press.
Neville A M (1995), *Properties of Concrete*, 4th edition, Longman Group Limited, Harlow.
Nica D, Davis J L, Kirby L, Zuo G and Roberts D J (2000), 'Isolation and characterization of microorganisms involved in the biodeterioration of concrete in sewers', *International Biodeterioration and Biodegradation*, 46, 61–68.
Nixon P and Longworth I (2003), 'Thaumasite Expert Group Report: review after three years' experience', *Concrete*, 37, (4), 22–25.
Olmstead W M and Hamlin H (1900), 'Converting Portions of the Los Angeles Outfall Sewer into a Septic Tank', *Engineering News and American Railway Journal*, 44 (19), 317–318.
Parker C D (1945a), 'The Corrosion of Concrete. 1. The Isolation of a Species of Bacterium Associated with the Corrosion of Concrete Exposed to Atmospheres Containing Hydrogen Sulfide', *Aust J Exp Biol Med Sci*, 23, 81–90.
Parker C D (1945b), 'The Corrosion of Concrete. 2. The Function of *Thiobacillus concretivorus* (nov. spec.) in the Corrosion of Concrete Exposed to Atmospheres Containing Hydrogen Sulfide', *Aust J Exp Biol Med Sci*, 23, 91–98.
Parker C D (1947), 'Species of sulphur bacteria associated with the corrosion of concrete', *Nature*, 159 (4039), 439–440.
Parker C D (1951), 'Mechanics of corrosion of concrete sewers by hydrogen sulfide', *Sewage and Industrial Wastes*, 23 (12), 1477–1485.
Pedersen K (1996), 'Investigations of subterranean bacteria in deep crystalline bedrock and their importance for the disposal of nuclear waste', *Canadian Journal of Microbiology*, 42, 382–391.
Pedersen K (1999), 'Subterranean microorganisms and radioactive waste disposal in Sweden', *Engineering Geology*, 52, 163–176.
Pomeroy R D (1990), *The Problem of Hydrogen Sulfide in Sewers*, 2nd edition, London, Clay Pipe Development Association.
Portland Cement Association (2001), *Effects of Substances on Concrete and Guide to Protective Treatments*, IS001.10, Illinois, USA, Portland Cement Association, 36pp.
Ramdohr P and Strunz H (1967), *Klockmann's Lehrbuch der Mineralogie 15 Auflage*, Stuttgart, Ferdinand Enke-Verlag.
Redner J A, Hsi R P and Esfandi E J (1994), 'Evaluating coatings for concrete in wastewater facilities: an update', *Journal of Protective Coatings and Linings*, 11 (12) 50–61.
Rigdon J H (1984), 'Corrosion above the water surface in wastewater facilities', *Materials Performance*, 23 (2), 18–20.
RILEM Technical Committee 32-RCA: Resistance of Concrete to Chemical Attacks (1985), Subcommittee 'Long-time Studies', 'Seawater attack on concrete and precautionary measures', *Materials and Structures*, 18(105), 223–226.
Roberts D J, Nica D, Zuo G and Davis J L (2002), 'Quantifying microbially induced deterioration of concrete: initial studies', *International Biodeterioration and Biodegradation*, 49, 227–234.
Robins N S, Kinniburgh D G and Bird M J (1997), 'Generation of Acid Groundwater Beneath City Road, London', in Hawkins A B (ed.), *Ground Chemistry Implications for Construction*, Rotterdam, Balkema, 225–232.
Rogers R D, Hamilton M A, Veeh R H and McConnell J W (1996), 'Microbially Influenced Degradation of Cement-Solidified Low-Level Radioactive Waste Forms', in Gilliam T M and Wiles C C (eds), *Stabilization and Solidification of*

Hazardous, Radioactive and Mixed Wastes, Vol. 3, Philadelphia, ASTM Special Technical Publication 1240, 116–132.

Rosa E B, McCollum B and Peters O S (1913), 'Electrolysis of concrete', *National Bureau of Standards Technol. Papers*, No. 18.

Sand W and Bock E (1984), 'Concrete corrosion in the Hamburg sewer system', *Environmental Technology Letters*, 5, 517–528.

Sand W and Bock E (1991), 'Biodeterioration of mineral materials by microorganisms – biogenic sulfuric and nitric acid corrosion of concrete and natural stone', *Geomicrobiology Journal*, 9, 129–138.

Santhanam M, Cohen M D and Olek J (2001), 'Sulfate attack research – whither now?, *Cement and Concrete Research*, 31, 845–851.

Scherer GW (1999), 'Crystallisation in pores', *Cement and Concrete Research*, 29, 1347–1358.

Scherer GW (2004), 'Stress from crystallisation of salt', *Cement and Concrete Research*, 34, 1613–1624.

Scrivener K and Lewis M (1996), 'A microstructural and microanalytical study of heat cured mortars and delayed ettringite formation', 4iv061, 8pp. in *Proceedings of the 10th International Congress on the Chemistry of Cement*, Amarkai AB and Congrex Göteborg, Göteborg.

Scrivener K L and Capmas A (1998), 'Calcium aluminate cements' in Hewlett P C (ed.), *Lea's Chemistry of Cement and Concrete*, 4th edition, London, Arnold Publishers, 709–778.

Sims I and Huntley S A (2004), 'The thaumasite form of sulfate attack – breaking the rules', *Cement and Concrete Composites*, 26, 837–844.

Skalny J and Marchand J (2001), 'Sulfate attack on concrete revisited' in Kurdowski W and Gawlicki M (eds), *Kurdowski Symposium – Science of Cement and Concrete*, Kraków, Wydawnictwo Naukowe 'Akapit', pp. 171–187.

Skalny J, Marchand J and Odler I (2002), *Sulfate attack on concrete*, Modern Concrete Technology, 10, London and New York, Spon Press, 217pp.

Sydney R, Esfandi E J and Surapaneni S (1996), 'Control concrete sewer corrosion via the crown spray process', *Water Environment Research*, 68 (3), 338–347.

Taylor H F W (1997), *Cement Chemistry*, 2nd edition, London, Thomas Telford, 459pp.

Taylor H F W, Famy C and Scrivener K L (2001), 'Delayed ettringite formation', *Cement and Concrete Research*, 31 (5), 683–693.

Thomas MDA, Bleszynski RF and Scott CE (1999), 'Sulfate attack in a marine environment', in: Marchand J and Skalny J P (eds), *Materials Science of Concrete – Special Volume: 'Sulfate Attack Mechanisms'*, American Ceramic Society, Westerville, OH, 301–313.

Thornton H T (1978), 'Acid attack of concrete caused by sulfur bacteria action', *American Concrete Institute Journal*, 75 (11), 577–584.

Thorvaldson T (1954), 'Chemical aspects of the durability of concrete products', in *Proceedings of the 3rd International Symposium on the Chemistry of Cement* (1952), Cement and Concrete Association, London, 436–466.

Varma S P and Bensted J (1973), 'Studies of thaumasite', *Silicates Industriels*, 38 (2), 29–32.

Vicat L J (1857), *Recherches sur les causes physiques de la destruction des composés hydrauliques par l'eau de mer*, Paris.

Vincke E, Boon N and Verstraete W (2001), 'Analysis of the microbial communities on corroded concrete sewer pipes – a case study', *Applied Microbiology and Biotechnology*, 57, 776–785.

Weast R C (ed.) (1988), *Handbook of Chemistry and Physics*, 1st student edition, Boca Raton, CRC Press.

Weinberg Z G and Muck R E (1996), 'New trends and opportunities in the development and use of inoculants for silage', *FEMS Microbiology Reviews*, 19, 53–68.

Yang R, Lawrence C D and Sharp J H (1996) 'Delayed ettringite formation in 4-year-old cement pastes', *Cement and Concrete Research*, 26 (11) 1649–1659.

Yang R, Lawrence C D, Lynsdale C J and Sharp J H (1999), 'Delayed ettringite formation in heat cured portland cement mortars', *Cement and Concrete Research*, 29(1), 17–25.

Yokozeki K, Watanabe K, Sakata N and Otsuki N (2004), 'Modeling of leaching from cementitious materials used in underground environment', *Applied Clay Science*, 26, 293–308.

Zherebyateva T V, Lebedeva E V and Karavaiko G I (1991), 'Microbiological corrosion of concrete structures of hydraulic facilities', *Geomicrobiology Journal*, 9, 119–127.

Zhou Q, Hill J, Byars E A, Cripps J C, Lynsdale C J and Sharp J H (2006), 'The role of pH in thaumasite sulfate attack', *Cement and Concrete Research*, 36 (1), 160–170.

5

Corrosion and protection of reinforcing steel in concrete

C L PAGE, University of Birmingham, UK

5.1 Introduction

The use of embedded steel reinforcing bars to overcome the weakness of concrete in tension was first proposed about 150 years ago and, since the beginning of the 20th century, reinforced concrete has been employed as a structural material all over the world. Its applications have been extremely diverse and it has shown good durability in the vast majority of cases, despite the fact that plain carbon steel reinforcement is vulnerable to corrosion in the presence of water and oxygen. Since both of these substances are generally available within the pores of concrete, it is somewhat unexpected to find that the surfaces of steel reinforcing bars, exposed when concrete structures have been demolished after many years of service, typically exhibit the appearance of silvery-grey metal. The surface layer of rust, normally present at the time reinforcement is embedded in concrete, is no longer evident and the underlying metal has been effectively protected from corrosion by the surrounding concrete. But for this fortunate behaviour, the use of conventional steel reinforced concrete in many common applications would have been impractical.

Until the early 1970s, there appeared little reason for major concern about the corrosion of steel in concrete and the issue was largely ignored. Since then, however, widespread corrosion problems have emerged in many countries and engineers have often been confronted with the difficult task of dealing with corrosion-induced degradation of the sort shown in Figs 5.1 and 5.2. These examples demonstrate what can happen if reinforced concrete structures are exposed to aggressive conditions without due consideration of the requirements for protection of the reinforcement. The scale of the ensuing problems can be enormous, as indicated by recent estimates of between $6.43 billion and $10.15 billion for the annual direct cost of corrosion for US highway bridges, for which the indirect costs to users, attributable to traffic delays and lost productivity, are believed to be more than ten times the direct cost (Yunovich and Thompson, 2003).

5.1 Reinforced concrete building made with salt-contaminated concreting materials showing effects of reinforcing steel corrosion (Bahrain, circa 1980).

In this chapter, the nature of corrosion protection normally provided by concrete to embedded reinforcing steel will be examined and common mechanisms that can bring about its failure will be reviewed. The basis for design and construction of durable reinforced concrete structures will then be considered and an outline given of recent developments in some relevant codes and standards. Advances in the application of various forms of supplementary corrosion protection to new structures and techniques for appraisal and treatment of corrosion problems in existing structures will also be reviewed briefly.

5.2 Reinforced concrete bridge splashed with water containing deicing salt showing effects of reinforcing steel corrosion (USA, circa 1980).

5.2 Corrosion principles

5.2.1 Rusting of steel

Metallic corrosion processes in general, and the rusting of steel in particular, are by nature electrochemical. They therefore require an electrolyte, generally an aqueous solution that enables coupled anodic and cathodic reactions to occur, allowing the ions formed to migrate between the anodic and cathodic sites on the metal surface. This mechanism, which involves the transference of ions through the electrolyte in the form of 'corrosion currents', is illustrated in Fig. 5.3 for iron or steel corroding in an aqueous environment of near neutral pH value in the presence of dissolved oxygen. In this case, the primary dissolved products of the anodic and cathodic processes (Fe^{2+} and OH^- ions) undergo further reactions with oxygen and water to form the loosely adherent brown deposit of hydrated ferric oxide known as rust, which is of variable composition (approximating to FeOOH). Further information on the nature and theory of metallic corrosion processes in general may be found in many relevant textbooks, of which the following are good examples (Fontana, 1986; Jones, 1992).

Since rust occupies a much larger solid volume than the iron from which it was produced, its formation can generate tensile stresses of sufficient magnitude to cause cracking and spalling if the corrosion process occurs at a significant rate within the electrolyte phase contained in the pores of a dense, brittle material such as concrete. This can eventually lead to deterioration of the sort shown in Figs 5.1 and 5.2, which represent failures of the serviceability of the structures concerned. For reinforced concrete structures, visible evidence of corrosion (rust staining and/or cracking) is usually observable well before there is a significant risk of structural

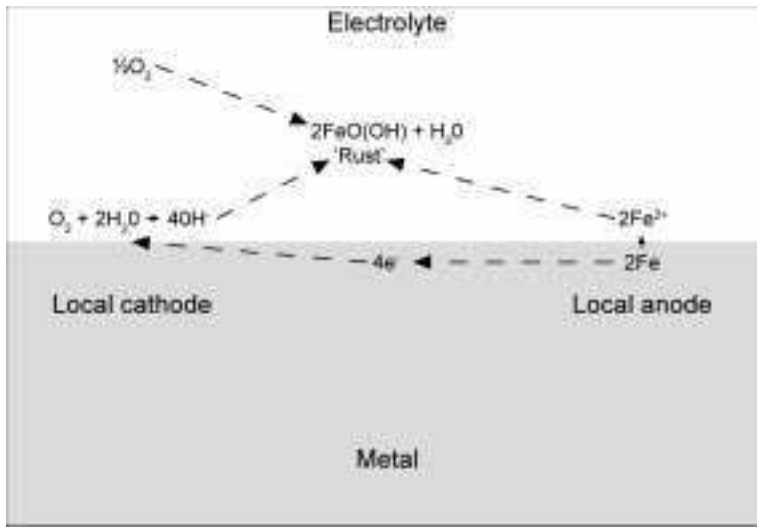

5.3 Electrochemical mechanism of rust formation.

collapse although the possibility of the latter should obviously not be ignored when condition appraisal is undertaken. For prestressed concrete structures, however, the risks of sudden collapse are of much greater concern and examples of this type of problem will be dealt with separately in Chapter 6 of this volume.

5.2.2 Passivity

The fact that appreciable corrosion of steel does not usually happen in dense concrete is primarily due to the alkalinity of the cement which, as discussed in Chapter 2, typically results in the pore liquid phase of hardened cement having a pH value in the range 13–14 owing to the presence of dissolved NaOH and KOH. When steel is exposed to alkaline aqueous solutions at pH > 11.5 in the presence of dissolved oxygen (or even at more mildly alkaline pH values if the solutions concerned are buffered), the metal forms a surface oxide layer, some nanometres thick, termed a passive film. This layer serves as a barrier to the anodic iron dissolution process and reduces the corrosion rate of the steel to an imperceptible level, corresponding to an average rate of reduction in metal thickness of less than 1 μm per year.

The effectiveness of the passive film in limiting the rate of anodic dissolution of steel may be illustrated by comparing experimentally observed relationships between applied potential and current density for steel anodes in typical neutral and alkaline solutions. These relationships, known as anodic polarisation curves (Page, 1988), indicate that, whereas in most aqueous solutions of pH 7 or lower, the rate of the anodic reaction:

$$Fe \rightarrow Fe^{2+} + 2e^{-}$$

increases exponentially as the potential of the steel anode is raised over a range of several hundred millivolts, this so-called 'active dissolution' phenomenon is not observed in aqueous solutions of pH > 11.5. Instead, the onset of formation of a passive film is marked by a sharp fall in the anodic current density when the potential is raised above a critical value (ca. −700 mV, SCE scale) at which a film-forming reaction is initiated:

$$2Fe + 3H_2O \rightarrow Fe_2O_3 + 6H^{+} + 6e^{-}.$$

Thereafter very little change in the anodic current density with further increase in the steel potential is observed as the passive film merely thickens very slowly until another critical potential is reached at which oxygen gas starts to be produced by electrolytic decomposition of water, behaviour that is illustrated in Fig. 5.4 for steel in saturated calcium hydroxide solution without chloride addition (pH ~ 12.5). This characteristic form of anodic polarisation curve, which signifies that passivity of the metal can be induced, has been shown experimentally to apply both to steel anodes in alkaline solutions and to those in hardened cement pastes, see, for example, Page and Treadaway (1982).

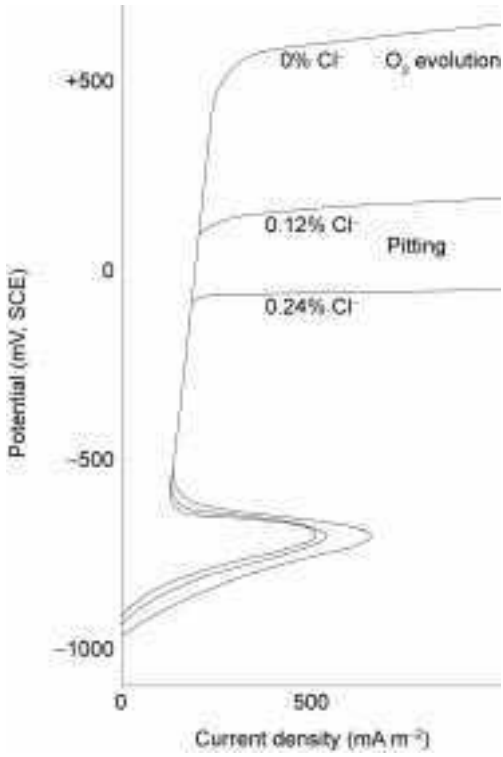

5.4 Typical potentiodynamic anodic polarisation curves for mild steel in saturated calcium hydroxide solution with various concentrations of added chloride – cf. data recorded by Page and Treadaway (1982).

5.2.3 Causes of the breakdown of passivity

Since passivity represents the principal mechanism by which steel is protected from corrosion in concrete, it is necessary to consider the various factors that might cause this protection to fail. A number of modifications to the chemical composition of the concrete may be involved, in particular the following:

- depletion of oxygen
- depletion of alkalinity due to carbonation
- introduction of chloride ions.

Depletion of oxygen

Concrete structures that are exposed to the atmosphere normally have an abundant supply of oxygen available, both to act as a cathodic reactant at the surface of embedded steel and to cause the transformation of the anodically formed Fe^{2+} ions to rust. Cases of general oxygen depletion are therefore

unlikely to occur except in circumstances where the material is fully immersed in water, buried in saturated soil or surrounded by similar waterlogged media. The effects of progressive reduction in the general availability of oxygen on the cathodic polarisation curves for the reaction:

$$O_2 + 2H_2O + 4e^- \rightarrow 4OH^-$$

are illustrated in Fig. 5.5. Also reproduced in this figure, known as an Evans diagram, is a portion of the anodic polarisation curve for steel in alkaline concrete (cf. that shown in Fig. 5.4). Assuming no external electrical power source is being used to supply current to a steel reinforcing bar (i.e. it is exhibiting natural corrosion behaviour), the corrosion currents passing through the anodes and cathodes on its surface must balance one another. Under these conditions, if the 'corrosion potential' of the metal (E_{corr}) is measured relative to a reference half-cell (a saturated calomel electrode, SCE, or similar), it will take values that become less noble (i.e. more negative) as the oxygen supply to the steel is progressively reduced, corresponding to the various points shown in Fig.

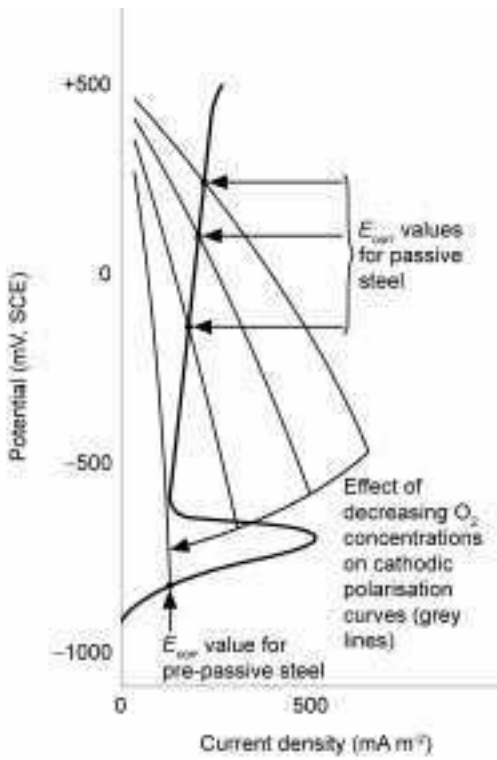

5.5 Evans diagrams showing how electrochemical behaviour of steel in concrete at various oxygen concentrations can change from a normal state of 'passivity' to one of 'cathodically restrained pre-passivity' at very low levels of oxygen.

5.5. This indicates that passivity can be sustained over a wide range of oxygen concentrations, but that eventually a stage is reached at which E_{corr} falls below a critical value, <-700 mV (SCE scale), necessary to maintain a passive film on steel, so the metal is no longer protected in the usual way. Because oxygen is now unavailable to sustain the cathodic reaction at a significant rate, however, the overall corrosion rate remains extremely small, a condition that has been variously termed 'active low-potential corrosion' (Arup, 1983; Page, 1988) or 'cathodically restrained pre-passivity' (Page, 1997). The latter usage avoids creating any misimpression about the practical significance of the condition, which can be readily converted to passivity in the event that the oxygen availability at the steel surface increases.

It should be emphasised that the relatively benign effects of *general oxygen depletion* described above must be distinguished from the more damaging consequences of *local oxygen depletion in corrosion macrocells*, which can give rise to a form of localised corrosion known as black or green rust. The environmental conditions under which this unusual type of corrosion may be produced are ones where well-separated anodic and cathodic zones develop over distinct sections of the reinforcement, the former being screened from direct oxygen access; the anodic zones tend to be located at positions where there is voided or badly jointed concrete, saturated with oxygen-denuded, saline water that leaches alkalis and enhances the solubility of Fe^{2+} ions. Under these circumstances, the normal formation of expansive brown hydrated ferric oxide is suppressed and the anodic dissolution of the metal can yield ferrous compounds, which are green initially but darken rapidly when exposed to air. This can cause substantial loss of metal cross section to occur without showing the usual signs of surface cracking and rust staining of the concrete. Particularly in structurally sensitive locations, it is therefore important to avoid creating inappropriate construction details that are likely to encourage localised ponding of oxygen-denuded saline water in contact with reinforcing bars. Examples of such undesirable details include badly designed and executed joints or failed waterproofing membranes.

Depletion of alkalinity due to carbonation

Depletion of alkalinity is normally the result of long-term exposure of concrete to the air in which variable proportions of carbon dioxide (and lesser quantities of other acidic gases) are present. This causes carbonation of the alkaline constituents of the cement, as illustrated below for portlandite, which reacts to form calcium carbonate, and C-S-H, which reacts to form calcium carbonate and hydrated silica gel:

$$Ca(OH)_2 + CO_2 \rightarrow CaCO_3 + H_2O$$

$$\text{C-S-H} + CO_2 \rightarrow CaCO_3 + SiO_2.x\,H_2O$$

Removal of a high proportion of the dissolved alkali metal hydroxides from the pore solution phase and incorporation of their cations into the hydrated silica gel reduces the pH within the affected surface region of the concrete to a value < 10 which is insufficient to stabilise the passive film on steel (Anstice *et al.*, 2005). Thus if the carbonated surface layer of the concrete penetrates to the level of the outermost embedded reinforcement, the normal mechanism of corrosion protection by passivation is no longer operative and, in certain circumstances, significant general corrosion of the affected steel may be initiated. Fortunately carbonation is usually a very slow process, at least in temperate climates, and its effects can be dealt with by means of straightforward preventative measures. Nevertheless, it can be an important cause of serviceability failures for aging structures so further details of the process, including factors affecting its rate and that of carbonation-induced corrosion, will be considered in Section 5.4.

Introduction of chloride ions

By far the most serious cause of corrosion problems affecting reinforcing steel is the introduction of chloride salts as contaminants of the concrete, which can occur either when the material is manufactured (e.g. Fig. 5.1) or during its subsequent exposure to a chloride-laden environment where it comes into contact with seawater or deicing salt (e.g. Fig. 5.2). In either case, the presence of a significant concentration of chloride ions in the alkaline electrolyte phase adjacent to the steel tends to cause localised breakdown of the passive film on the embedded metal, a phenomenon termed pitting, which can result in serious local loss in cross section of the affected regions of the bars with the surrounding regions being virtually unaffected, as shown in Fig. 5.6.

The effect that the presence of chloride ions has on the electrochemical behaviour of steel in alkaline electrolytes, such as saturated calcium hydroxide, is illustrated by the set of anodic polarisation curves shown in Fig. 5.4. These demonstrate that, as the concentration of chloride ions is progressively increased, the range of potentials over which the passive film remains intact

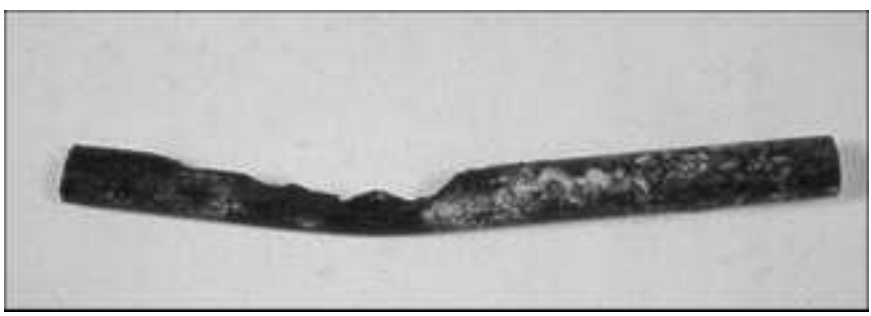

5.6 Effect of chloride-induced pitting on a reinforcing bar.

becomes smaller, the onset of pitting being denoted by a sharp increase in the anodic current density when the steel potential exceeds a critical value termed the 'pitting potential' (E_p), which is dependent on the chloride concentration and pH of the electrolyte. Conversely, once pitting has been initiated, the steel exhibits hysteresis in its anodic response and can be restored to a passive condition (repassivated) only if its potential is lowered from E_p to a level termed the 'repassivation potential' (E_r), which is also dependent on the chloride concentration and pH of the electrolyte. The electrochemical condition of passive steel at potentials $< E_r$ is referred to as one of 'perfect passivity', and at potentials in the range E_r to E_p as 'imperfect passivity' (Pourbaix, 1974).

More detailed consideration of the effects of chloride salts in relation to the corrosion of steel in concrete will be given in Sections 5.5 and 5.6.

5.3 The role of concrete cover

Traditionally in codes of practice for the structural use of concrete, it has been understood that the thickness and quality of concrete cover to reinforcing steel are important factors determining the level of protection provided to the embedded metal. As long ago as the mid-1970s, for example, the former British Standards Institution Code of Practice for the Structural Use of Concrete, CP110:1972 (as amended Feb 1976) stated: 'Cover to reinforcement should be determined by considerations of fire resistance and durability under the envisaged conditions of exposure.' It then went on to tabulate, for various conditions of exposure that were categorised as 'Mild', 'Moderate', 'Severe', 'Very Severe' or 'Subject to Salt Used for Deicing', nominal values of cover thickness in millimetres that were considered appropriate when different grades of concrete were used with characteristic strengths ranging from 20 to 50 MPa or greater. It also stated that the 'actual cover' was required to be 'not less than the required nominal cover minus 5 mm'. Such recommendations, however, were not based on explicit recognition of the mechanisms and rates of the processes liable to be involved in causing deterioration of the structures concerned or on their expected working lives and possible maintenance requirements. With the benefit of hindsight, it is also clear that the stated cover tolerance of only 5 mm was an over-optimistic assumption in many cases.

By the early 1980s, it had become evident that a more scientific basis for the design of reinforced concrete structures to meet expected levels of performance in corrosive environments of different severity was needed. This led to concerted efforts at modelling the deterioration of reinforced concrete in such environments, the most significant contribution being the simple model proposed by Tuutti (1982), which has formed the basis for most of the subsequent developments in this area. As shown in Fig. 5.7, the model represents the service-life of a structure exposed to the action of carbonation and/or chloride ingress, in the absence of remedial interventions, as being the sum of two components:

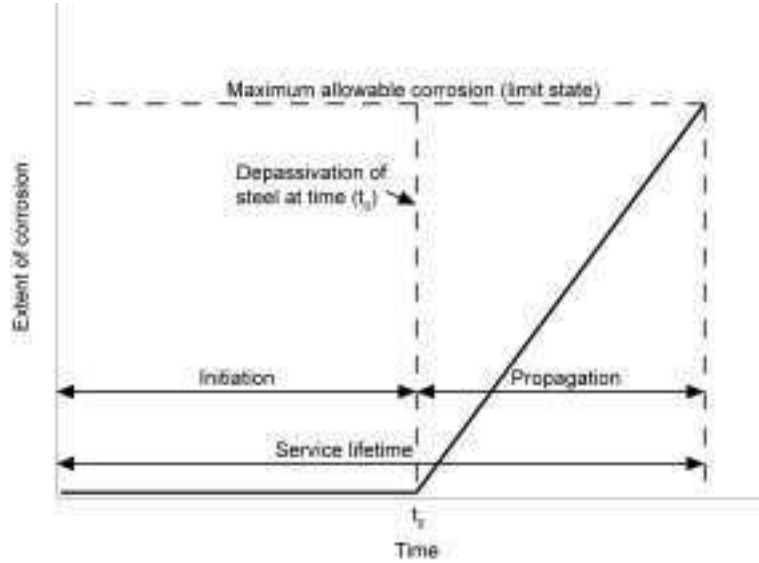

5.7 Service-life model for reinforced concrete exposed in a corrosive environment (Tuutti, 1982).

(a) an initiation time or 'safe-life' (t_0), during which the cover zone of the concrete is penetrated by the aggressive agents until they reach sufficient concentration at the surface of the outermost steel bars to cause depassivation;
(b) a propagation time or 'residual-life' (t_1), during which the depassivated steel corrodes at a rate that eventually results in a limit state being reached, usually identified by failure of serviceability associated with cracking or spalling of the concrete cover.

On the basis of this model, it has been generally understood that the recommendations in codes of practice regarding concrete cover thickness are intended to ensure that, except in cases where the exposure environment is so mild that the propagation time (t_1) can be assumed to be adequately long (e.g. in very dry internal atmospheres within buildings), the initiation time (t_0) should represent a substantial fraction of the intended service-life of the structure.

5.4 Carbonation and its effects

As noted previously, the reactions between atmospheric CO_2 and alkaline components of concrete produce a carbonated surface layer in which the pore solution pH value is depressed to near-neutral levels. A secondary effect of carbonation, also significant in terms of its influence on corrosion, is that it can cause the release of bound chloride ions into the pore solution phase of concrete that contains a modest level of chloride salt as a contaminant, thus exacerbating

the corrosive nature of the electrolyte (Tuutti, 1982). Carbonation depths may be measured by a number of methods, the simplest and most widely used of which involves the application of phenolphthalein indicator solution to a freshly exposed section of the concrete, the approximate boundary between carbonated and non-carbonated material being marked by an indicator colour change from colourless to pink, denoting a change in pH around a value of about 10 (RILEM TC CPC-18, 1985).

Assuming (i) that the rate of carbonation of concrete is controlled simply by diffusion of CO_2 across a carbonated layer of constant diffusion coefficient (D), (ii) that the quantity of CO_2 required to neutralise the alkaline components (a) within every unit volume of the concrete is constant and (iii) that the CO_2 concentration varies linearly between fixed boundary values of c_1 at the external surface and c_2 at the carbonation front, it may be shown (Kropp, 1995) that the depth of carbonation (x) in millimetres is related to the exposure time (t) in years by a parabolic relationship:

$$x = \left\{\frac{2D(c_1 - c_2)}{a}\right\}^{1/2} t^{1/2} = Kt^{1/2} \qquad 5.1$$

where the constant of proportionality K (mm/y$^{1/2}$) is a 'carbonation coefficient' for the particular system. Its magnitude reflects the influence of the various factors affecting the parameters D, a, and $(c_1 - c_2)$ which include the following:

D	dependent on: porosity, pore size distribution, pore continuity and tortuosity, degree of saturation, relative humidity and temperature
a	dependent on: cement content of concrete and CaO content of binder
$c_1 - c_2$	dependent on: atmospheric CO_2 concentration.

Although the assumptions involved in the above treatment are somewhat simplified, the parabolic expression has often been found to be reasonably accurate for describing the progress of carbonation in concrete which is sheltered from rain (Wierig, 1984). It is also useful in revealing several of the important factors related to concrete quality and environment that influence carbonation rates. For instance, variables that affect D include water/cement ratio, compaction and curing as they control the pore structure of concrete. Similarly the effects of environmental variables that affect the degree of saturation of the pores can be interpreted because, whilst carbonation requires some internal moisture to be present to allow the 'through-solution' conversion of portlandite to calcium carbonate and other reactions to take place, an increasing proportion of water-filled pores tends to impede gaseous diffusion of CO_2 and so retards carbonation. As shown in Fig. 5.8, the net result is that maximal rates of carbonation are observed when concrete is exposed to atmospheres in which the relative humidity is maintained at an intermediate level, typically in the range 50–75% RH (Richardson, 2002), which corresponds to values often encountered for internal air within buildings in temperate climates.

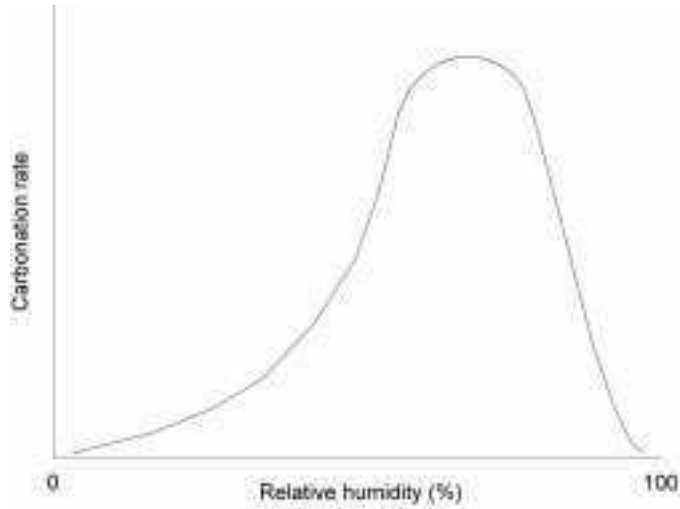

5.8 Typical effects of relative humidity on rate of carbonation of concrete.

Although the simple $x = Kt^{1/2}$ model outlined above gives a useful approximate method for predicting carbonation depths and has often been used practically in the assessment of structures (Menzies *et al.*, 1987), it has limitations, particularly when applied to concrete that is exposed to high relative humidities or to intermittent wetting for long periods. In these circumstances, it tends to predict higher long-term carbonation depths than those that are actually observed. Numerous empirical studies have been made of factors influencing the kinetics of carbonation in both laboratory and site concretes and it has commonly been found that, for a given type of concrete exposed in a given environment, the average depth of carbonation (x) as a function of time can be more closely approximated by relationships of the form:

$$x = A\ t^n \qquad 5.1a$$

where A and n are constants for the particular conditions and n is often < 1/2. In sheltered external UK exposure conditions, for instance, where average relative humidity values of ~80–85% may be expected, it has been suggested that the exponent $n \sim 0.4$ (Hobbs, 2001) and at higher relative humidities or in unsheltered locations where periodic wetting is experienced even lower values of n are found.

In considering the risk of carbonation-induced corrosion, it is important to distinguish between those conditions that favour high rates of carbonation and those that are conducive to rapid corrosion of steel in carbonated concrete, because fortunately the two sets of circumstances do not generally coincide. Whereas high rates of carbonation are associated with exposure to internal atmospheres in buildings and low rates of carbonation with damp, unsheltered

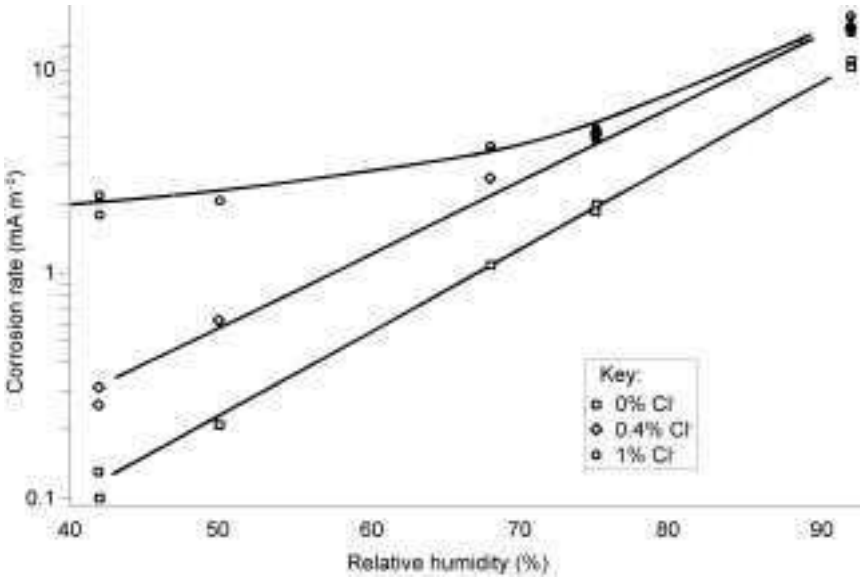

5.9 Effects of relative humidity on corrosion rate of embedded steel in carbonated mortars with various levels of chloride (Glass *et al.,* 1991).

outdoor exposures, the rates of corrosion of steel in carbonated concrete depend mainly on the electrolytic conductivity of the material, which increases as the proportion of the pores occupied by water (as opposed to air) increases (Alonso *et al.*, 1988). This gives rise to relationships between carbonation-induced corrosion rate and relative humidity of the type shown in Fig. 5.9 (Glass *et al.*, 1991). It indicates that the corrosion rates measured for steel bars that were constantly exposed to carbonated mortar without chloride contamination in atmospheres of RH < 70% were no greater than those typical of passive steel in non-carbonated concrete (< 1 mA/m^2). It also demonstrates that the presence of moderate levels of chloride contamination (0.4–1.0% by mass of cement) can have a significant influence on the rates of corrosion that may be induced in carbonated concrete. This illustrates the difficulty that arises when the presence of more than one corrosion-inducing agency contributes to the aggressiveness of the exposure conditions for a particular structure.

In the new European standard for concrete, the English language version of which has been published as BS EN 206-1 (2000), efforts have been made to categorise classes of exposure in such a way as to make explicit the different types of aggressive agency that are expected to cause corrosion or other forms of degradation. Thus for concrete with reinforcement or embedded metal that is kept permanently in a very dry environment, such as that inside buildings with air maintained at very low humidity, there is believed to be negligible risk and the exposure class is designated X0. For concrete containing reinforcement or other embedded metal that is exposed to air and moisture, however, the

environment is one where corrosion induced by carbonation must be considered and exposure classes designated XC1, XC2, XC3 or XC4 have been introduced according to the descriptions provided in Table 5.1(a). An informative annex in BS EN 206-1 gives indicative limits for maximum water/cement ratio, minimum cement content and minimum strength class for each of these exposure classes based on CEM1 (Portland cement) concrete with an intended working life of 50 years. It should be noted that these indicative limits are not of general applicability and specifiers are required to consult the corresponding advice on limiting values given in national annexes or complementary standards, such as BS 8500 (2002) in the UK.

In addition to concrete quality, nominal values of concrete cover thickness (expressed as minimum values plus an assumed tolerance to accommodate fixing precision) have also to be specified for the various exposure classes. As far as the UK is concerned, the complementary British Standard BS 8500 recommendations are intended to meet the minimum requirements of 50- and 100-year working lives whilst continuing the established UK practice of allowing a trade-off between concrete quality and cover thickness. The rationale for the British complementary standard recommendations in relation to exposure

Table 5.1 (a) Exposure classes related to corrosion induced by carbonation

Class designation	Description of environment
XC1	Dry or permanently wet
XC2	Wet, rarely dry
XC3	Moderate humidity
XC4	Cyclic wet and dry

(b) Exposure classes related to corrosion induced by chlorides other than from seawater

Class designation	Description of environment
XD1	Moderate humidity
XD2	Wet, rarely dry
XD3	Cyclic wet and dry

(c) Exposure classes related to corrosion induced by chlorides from seawater

Class designation	Description of environment
XS1	Exposed to airborne salt but not in direct contact with seawater
XS2	Permanently submerged
XS3	Tidal, spray and splash zones

From BS EN 206-1, 2000

classes XC1, XC2, XC3 and XC4 has been set out by Hobbs *et al.* (1998) who based their analysis on published data for well-compacted concretes made from CEM1 (Portland cement) and binders containing pulverised fuel ash, slag and silica fume.

In summary it may be noted that, for temperate climates such as those of the UK, there is normally no intrinsic difficulty in designing structures that should be expected to remain free from significant carbonation-induced corrosion problems for working lives of 50 or 100 years. Where problems have arisen, they have almost invariably been associated with inadequate control of concrete construction practices (compaction, curing, etc.) or with failure to achieve specified cover thickness. The latter is of particular concern because, assuming a simple parabolic relationship between carbonation depth and time, failure to achieve a specified minimum cover of say 25 mm by only 5 mm (i.e. 20%) will reduce the expected time taken for carbonation to reach the embedded steel by approximately 36%. As surveys of the accuracy of achievement of cover have shown (Clark *et al.*, 1997), specified negative tolerances of 5 mm applied to nominal cover have commonly not been achieved in reality. According to the BRE (2000a), while for good quality precast concrete, a range of ± 5 mm of the mean cover may just be attained, this is seldom the case for in-situ concrete where, with good practice, a range of ± 10 mm of the mean cover will generally be found; in cases where there is little supervision, however, the range may be ± 20 mm and specific biases in cover may also occur in, for example, the soffits of slabs and beams or columns with offset reinforcement cages.

Before concluding this section on carbonation and its effects, it should be noted that the desire to move away from prescriptive specifications for durability of concrete has stimulated numerous efforts to devise appropriate accelerated testing procedures to provide the data required in models of carbonation-induced corrosion that may be used as a basis for performance specifications. A summary of one such approach was presented recently by Schiessl and Lay (2005). The attendant difficulties for a process such as carbonation, that typically takes many years to penetrate through concrete cover subjected to natural exposure, are evident since major departures from normal conditions are necessary if the tests are to be completed in conveniently short times. Whether such tests can be assumed to have the desired effect of producing a constant degree of acceleration when applied to different types of concrete, incorporating different constituents, subjected to different curing regimes, etc., remains uncertain, as demonstrated in recent research on modelling the effects of natural and accelerated carbonation (Ishida *et al.*, 2004). Several of the practical difficulties associated with development of a standard test method for assessing the carbonation resistance of different types of concrete under different conditions have also been examined by Jones *et al.* (2000, 2001). Another approach to modelling carbonation-induced corrosion that depends, not on input data derived from accelerated carbonation testing, but on chemical analysis of the

cementitious components of the concrete has been advocated in a recent report of the Concrete Society (Bamforth, 2004). In this model, the concept of an 'equivalent buffering capacity' (i.e., an equivalent content of a benchmark Portland cement) is used in accounting for the effects of mineral additives, such as ground granulated blast furnace slag, pulverised fuel ash, silica fume and metakaolin, incorporated in blended and composite cements.

5.5 Effects of chloride contamination

As noted in Section 5.2.3, chloride ions may be introduced into concrete as either mix contaminants or from external sources such as seawater and deicing salts. If present at sufficient concentration, they can depassivate steel and cause pitting corrosion to occur even under the conditions of high bulk electrolyte pH characteristic of concrete pore solutions. The question as to what constitutes a 'threshold level' of chloride contamination that will cause pitting corrosion to occur under various circumstances, however, has proved to be one of the more elusive issues in the field of concrete durability research. It was a topic of debate as long as 30 years ago (Page, 1975) and has continued to attract significant interest in more recent times. This has some important ramifications, first because codes of practice must set limits on the levels of chloride allowed in concreting materials that are reasonably safe while not being unduly restrictive, and secondly because the corrosion initiation time or 'safe-life' of reinforced concrete exposed to a chloride-laden environment is the time taken for chloride penetration of the cover to reach the threshold level at the surface of the embedded steel.

In considering factors that may influence chloride threshold levels, it is useful to outline some of the main features of chloride-induced pitting of steel, both in alkaline environments generally and in concrete under various circumstances. The following points are believed to be significant.

- Pitting corrosion involves a localised process of passive film breakdown, which causes the composition of the electrolyte inside a developing pit to become progressively enriched with respect to chloride ions and denuded with respect to hydroxyl ions due to hydrolysis of the anodic products (Jones, 1992). These features are illustrated schematically in Fig. 5.10 (Page and Havdahl, 1985).
- Pitting is a stochastic process and, all other things being equal, the risk increases as the concentration of chloride ion is increased relative to that of hydroxyl ion in the bulk electrolyte phase in contact with the steel. Evidence for this was provided by early studies of the behaviour of steel in aqueous alkaline environments simulating concrete pore solutions (Hausmann, 1967; Gouda, 1970). It was confirmed by investigations of the behaviour of steel in laboratory specimens of concrete exposed to chloride ingress and pore

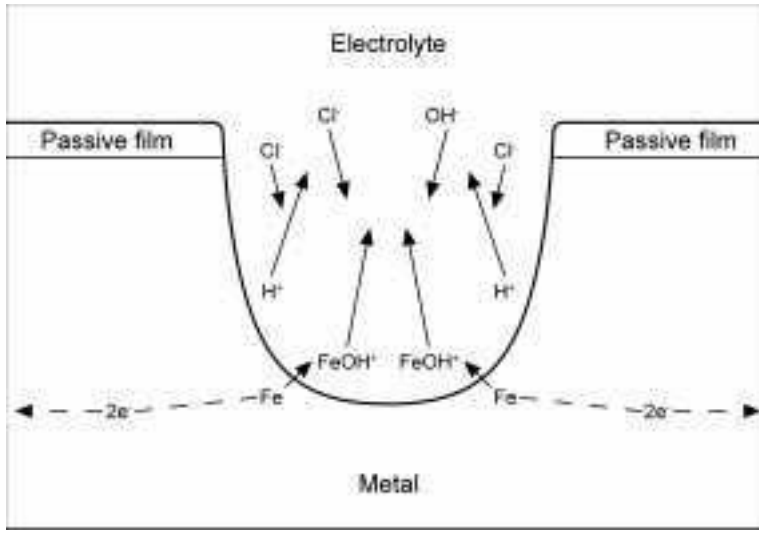

5.10 Changes in electrolyte composition within a developing pit.

solution analysis (Page *et al.*, 1991; Lambert *et al.*, 1991), as illustrated by the results shown in Fig. 5.11. Note, however, that the critical ratio of $[Cl^-]/[OH^-] \sim 3$, at which the probability of initiating corrosion in the laboratory specimens represented by the data in Fig. 5.11 started to become significant, was considerably higher than the corresponding critical ratios of < 1, based

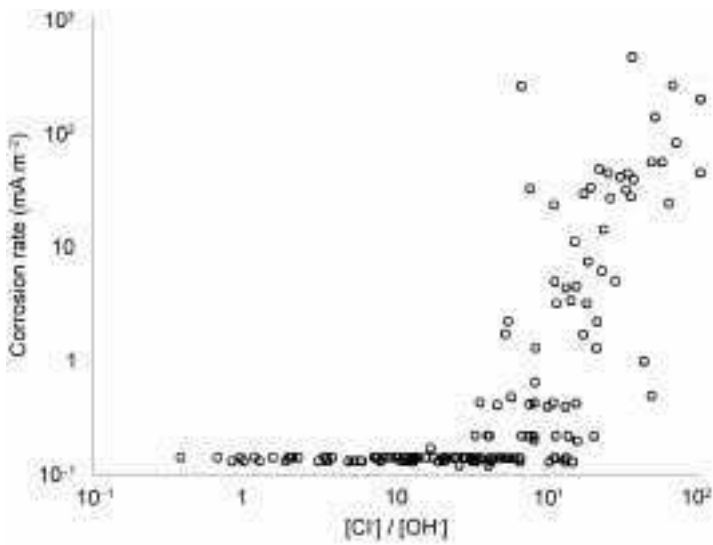

5.11 Relationship between corrosion rate of embedded steel bars and ratio of chloride:hydroxyl ion concentration of neighbouring pore liquid of concrete exposed to ingress of sodium chloride (Lambert *et al.,* 1991).

on studies involving aqueous alkaline environments intended to simulate concrete pore solutions (Hausmann, 1967; Yonezawa *et al.*, 1988; Goni and Andrade, 1990).

- For steel in concrete, the risk of pitting corrosion developing at a given chloride concentration in carefully produced laboratory specimens is often far lower than that observed for concrete in actual structures with the same level of chloride contamination. Thus the corrosion rates in Fig. 5.11, when plotted against the more readily measured total chloride content of the concrete (expressed by mass of cement), yielded a relationship suggesting that the risk of significant corrosion was negligible until a threshold chloride level of about 1.5% was exceeded (Lambert *et al.*, 1991). As illustrated in Table 5.2, however, earlier surveys of UK reinforced concrete highway bridges (Vassie, 1984) had indicated that chloride levels well below this (in the range 0.2–0.4% by weight of cement) could be associated with significant corrosion risk, and broadly similar conclusions had also been reached from surveys of UK buildings. It was suggested that the disparity in performance between real structures and laboratory specimens was due, at least partly, to differences in the integrity of the interfacial layer of cement hydration products formed in close proximity to the passive film on steel in concrete (Page and Treadaway, 1982; Lambert *et al.*, 1991); this interfacial layer, which is believed both to buffer the electrolyte in the vicinity of incipient anodic sites (thus inhibiting the local acidification required for sustainable pit growth to occur) and also to limit the migration of chloride ions towards the local anodes, is obviously more prone to disruption by macroscopic voids, cracks, etc. in site concrete than in carefully prepared laboratory specimens. Recent evidence in support of this hypothesis has been provided by measurements of the influence of deliberately introduced interfacial voids on the chloride threshold in laboratory specimens (Glass *et al.*, 2001) and by investigation of the effects of interfacial defects caused by bleeding in reinforced concrete columns (Soylev and François, 2003).
- The effect of steel potential on the risk of pitting, which was referred to in Section 5.2.3, gives rise to various possible domains of behaviour for steel in

Table 5.2 Relationship between chloride content and incidence of corrosion-induced cracking in UK reinforced concrete highway bridge (Vassie, 1984)

Chloride range (% by mass cement)	Proportion showing corrosion (%)
<0.2	2.0
0.2–0.4	22.5
0.4–1.0	32.4
1.0–1.5	64.4
>1.5	75.9

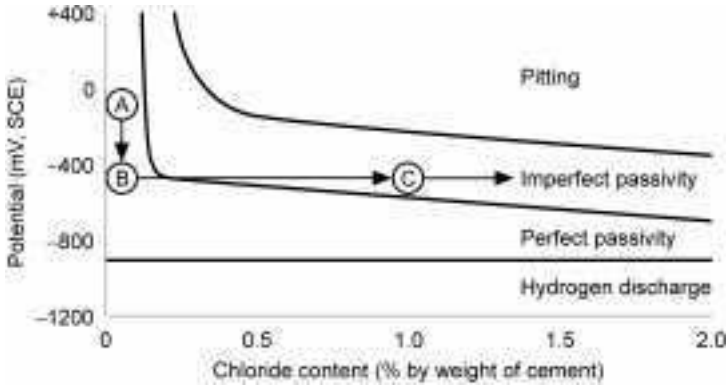

5.12 Approximate domains of electrochemical behaviour of steel in concrete with different levels of chloride contamination. Modest depression of the steel potential due to limitation of oxygen availability or application of cathodic prevention (A to B), before significant chloride penetration of the concrete cover occurs (B to C) induces 'imperfect passivity' and causes suppression of pitting (Pedeferri, 1996).

concrete as illustrated schematically in Fig. 5.12, adapted from Pedeferri (1996). Under water-saturated conditions of natural exposure that are associated with restricted oxygen access, the potential of the metal is liable to be depressed to values that are often more negative than about −500 mV (SCE scale) and normally below E_p; if this occurs then the initiation of pitting will be suppressed although the oxygen-denuded concrete may subsequently become contaminated with chloride at relatively high concentrations, an electrochemical condition referred to as 'imperfect passivity', as explained in Section 5.2.3; if the steel potential becomes further depressed below E_r, the even more stably protected state known as 'perfect passivity' may eventually be attained in which the repassivation of pre-existing pits is also induced.

5.5.1 Chloride limits in concrete mix materials

It follows from the above considerations that there is no unique threshold proportion of chloride contamination that applies generally and, in view of the wide disparity between the behaviour often recorded for laboratory-made and site-produced concrete, chloride limits for use in specification of concrete mix materials have had to be based on engineering judgement, taking account of knowledge of the condition of existing structures. This retrospective approach of course suffers from the drawback that it cannot be applied directly to deal with new construction incorporating innovative materials because the relevant long-term service records are simply not available. There is therefore pressure to devise rapid methods of determining chloride thresholds applicable to concrete made with different cements, admixtures, etc. Research in this area has not yet

produced a general consensus, however, and the cautionary tale of calcium chloride, which was widely used over several decades as a cheap and effective accelerating admixture, should serve as a warning to those of a cavalier disposition with regard to chloride limits.

In the UK until the mid-1970s, the former British Standards Institution Code of Practice for the Structural Use of Concrete (CP110:1972) permitted calcium chloride to be used as an admixture in reinforced concrete at levels of up to 1.5% $CaCl_2$ by weight of cement (equivalent to 0.96% Cl^- by weight of cement). Similar limits on the levels of chloride allowed in concreting materials were also imposed at that time in several other countries (Ramachandran, 1976). Owing to the widespread problems of chloride-induced corrosion encountered in practice, an amendment to CP110 was introduced in May 1977 requiring much tighter controls on the total levels of chloride arising from admixtures, aggregates or other internal sources. This effectively stopped the deliberate introduction of calcium chloride admixtures to concrete containing steel reinforcement, prestressing steel or other embedded metal.

The new European Standard BS EN 206-1 (2000) has maintained the proscription on deliberate use of chloride-based admixtures and introduced various classes of maximum chloride content from all sources (corresponding to 0.1, 0.2 and 0.4% Cl^- by mass of cement) applicable to concrete containing steel reinforcement or other embedded metal (apart from corrosion-resistant lifting devices). They are used in accordance with the provisions of complementary national standards such as BS 8500-1:2002, that are intended to apply to situations of different perceived risk, the most obvious case for special concern being prestressed concrete, for which a maximum of 0.1% chloride is allowed. Similarly in BS 8500-1:2002, a limit of 0.2% chloride is specified for reinforced concrete made from Sulfate Resisting Portland Cement, which is required to contain no more than 3.5% C_3A. The C_3A component of Portland cement has long been known to play a significant role in binding chloride ions in the form of sparingly soluble chloro-aluminate hydrates (Roberts, 1962; Richartz, 1969) so reducing the proportion remaining in the pore solution phase. The level of C_3A is therefore believed to be one of the influences accounting for the ability of different Portland cements to sustain different rates of corrosion at constant modest levels of chloride addition (Page *et al.*, 1986; Masslehuddin *et al.*, 1996). There are, however, several factors besides C_3A content that affect chloride binding by different cements under different conditions (Larsen, 1998; Wowra and Setzer, 2000) and we do not yet have a clear understanding of the ways in which these influence the supply of free chloride ions to incipient anodic sites on steel in concrete.

In summing up this section, it is fair to say that, while many attempts have been made to quantify the various risk factors that determine the wide scatter of corrosion initiation probabilities represented at a given total chloride level (BRE, 2000b), there has been limited progress in this area. This is clearly illustrated in a recent review of chloride thresholds (Glass and Buenfeld, 1997)

and reflects the fact that the threshold chloride content is not dominated by any one parameter, which could provide a simple 'index' for comparing different types of concrete. It is actually a function of interacting variables that include, but are not limited to, factors that affect the potential of the steel and those that influence the composition and microstructure of the interfacial zone of the concrete in the immediate vicinity of the embedded metal. This implies that there is often no straightforward answer to questions as to whether, for instance, particular formulations of blended or composite cement, used in conjunction with specific admixtures, will produce chloride threshold values significantly different from those found for other more traditional types of reinforced concrete. Exposure tests of reasonably long duration, performed under conditions that are as realistic as possible, are required to decide these issues and electrochemical corrosion monitoring techniques of the sorts to be considered in Section 5.8 can be helpful if used appropriately in conjunction with such tests.

5.6 Chloride penetration

As far as new reinforced concrete structures are concerned, most modern codes of practice have adopted strict limits on maximum levels of chloride permitted in concreting materials, so future corrosion problems arising purely from this source should be rare as long as carbonation does not penetrate through the cover concrete. Avoidance of excessive carbonation is of course necessary because even relatively low levels of chloride in carbonated concrete have been found to exacerbate the corrosion rate of embedded steel significantly (Glass *et al.*, 1991). In cases where carbonation is unlikely to pose any real threat, however, there remains a problem of how to avoid chloride-induced corrosion for structures exposed to external chlorides derived from seawater or deicing salts. Research into factors that determine the rates of penetration of chloride ions into concrete has therefore been a topic of worldwide activity and, in recent years, a series of international workshops on this subject has been held (RILEM, 1997, 2000, 2005).

As was noted in Chapter 2, the means by which ions penetrate into concrete (and/or may be removed from it) are often complex and dependent to a large extent on the moisture condition of the material at the time of exposure. To describe the various processes involved in reasonable detail, even assuming idealised initial and boundary conditions apply, would require consideration of several different types of transport mechanism (diffusion, convection/capillary suction and migration) coupled with the effects of ion/ion and ion/pore surface interactions. Such a treatment is beyond the scope of the present chapter and the primary focus here will be on more immediately pragmatic issues. Essentially we need to consider how adequately, or otherwise, current knowledge enables us to model chloride ingress into concrete with a view to predicting corrosion initiation times in reinforced concrete with reasonable accuracy.

In a recent review, Buenfeld (2004) has classified models for predicting deterioration of concrete under three headings, viz. empirical, semi-empirical and mechanistic. Mechanistic models are categorised as those which mathematically represent individual transport processes and chemical reactions, based on measurable coefficients, and combine their effects to make an overall prediction. Semi-empirical models are described as those which relate deterioration to what are loosely referred to as 'quasi-transport' coefficients, largely dependent on concrete properties (but representing the combined effects of transport processes, chemical reactions, exposure time, etc.). Empirical models are those that base their predictions purely on previously observed behaviour without consideration of the processes involved in bringing about deterioration.

With the widespread availability of low-cost computing, there has been growing interest in developing mechanistic approaches to modelling of the transport of chloride (and other ions) in hardened concrete exposed under various conditions, see for example (Truc, 2000; Marchand, 2001; Johannesson, 2003; Wang *et al.*, 2005). These usually make use of modified forms of the Nernst-Planck equation, which is a general expression for the mass transfer of ions in very dilute electrolytes (Bard and Faulkner, 1980), to represent the fluxes (J_i) of the various ionic species present in the concrete pore electrolyte in terms of their individual diffusion coefficients (D_i), concentrations (C_i), and charge numbers (z_i). The approach was originally applied by Yu (1990) in an attempt to simulate the results of some earlier experimental investigations of diffusion of several ions (Na^+, Cl^-, OH^-) in hardened cement paste specimens, which had been exposed to a salt solution and subjected to detailed pore solution analyses at various positions along the diffusion path (Sergi, 1986).

The provision of adequate experimental data to validate such 'multi-species' models, however, is generally problematic and some of the 'measurable' coefficients they incorporate are very difficult to estimate with reasonable confidence. These include, the activity coefficients of individual species in mixed electrolytes of high ionic strength and coefficients involved in 'binding isotherm' relationships between free and bound ionic concentrations, etc. To date, empirical or semi-empirical, models have therefore been more commonly employed and the most widely (but not always appropriately) used service-life model of any type has been based on a standard analytical solution of Fick's second law of diffusion, a partial differential equation relating the temporal and spatial variations in concentration (C) of the diffusing substance via a 'diffusion coefficient' (D)[1] (Crank, 1975). The solution concerned is commonly known as the 'error function' equation and the form in which it has often been applied for the prediction of unidirectional chloride penetration into concrete, is expressed

1. For uni-directional transport of a substance of constant 'D' along the x-axis: $\frac{\partial C}{\partial t} = D\frac{\partial^2 C}{\partial x^2}$.

as follows:

$$C(x,t) = C_i + (C_s - C_i)erfc\left[\frac{x}{\sqrt{4D_{app}t}}\right] \qquad 5.2$$

where:

$C(x,t)$ is the chloride content of the concrete at depth x after time t
C_i is the uniform initial chloride content of the concrete
C_s is the surface chloride content of the concrete
D_{app} is the 'apparent diffusion coefficient' of chloride ion in the concrete.
erfc is the error function complement ($1 - erf$).

The prefix 'apparent', as used here and previously elsewhere (Sergi *et al.*, 1991) in the term 'apparent diffusion coefficient' (D_{app}), should be noted because its meaning (i.e., seeming, as distinct from real) is important. It reflects the fact that D_{app} is neither a basic material property, nor even purely a measure of diffusion resistance for concrete in a specific environment. It is merely a regression parameter obtained by arbitrarily fitting measured chloride penetration profiles in concrete to equation 5.2, as illustrated in Fig. 5.13. It is worth emphasising this point because there has been confusion in the literature regarding the terminology employed in this context by different authors and some misunderstanding of the distinction between D_{app} and other transport coefficients, e.g. those obtained from steady-state chloride diffusion measurements, designated 'effective diffusion coefficients' (Page *et al.*, 1981). A discussion of relationships between various forms of 'diffusion coefficient' that

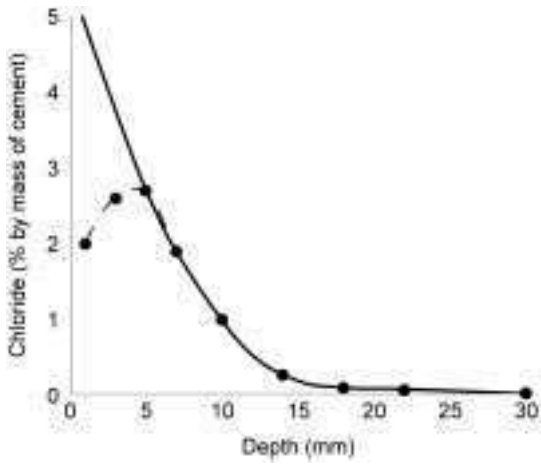

5.13 Typical chloride penetration profile after 1.5 years exposure, arbitrarily fitted to equation 5.2, ignoring two points nearest to surface ($D_{app} = 1.7 \times 10^{-13}$ m^2/s; $C_s = 5.45\%$ Cl^- by mass cement). Alternative methods of curve fitting yield different values of D_{app} and C_s (Nilsson, 2005).

have been used to characterise chloride transport in concrete is provided by Tang (1996) and a clear demonstration of the wide variations in calculated values of the regression parameters, D_{app} and C_s, that can arise when various arbitrarily chosen curve fitting procedures are applied to a given set of chloride ingress data, is presented by Nilsson (2005).

With regard to the use of 'apparent diffusion coefficients', it should also be recognised that the error function solution of Fick's second law was derived for unidirectional diffusion (under constant assumed initial and boundary conditions) of an uncharged substance into a semi-infinite slab of material for which the diffusion coefficient was assumed to be independent of both time and depth (Crank, 1975). Chloride penetration into concrete is never a simple process of this type because, even if the material is fully saturated from the outset (not often the case in reality) and its properties are assumed not to vary significantly with time or depth (highly improbable in practice), chloride ions are negatively charged particles, so their movement is always coupled to the transport of other ions; also some of the chloride ions that enter the concrete interact with, and become bound chemically and/or physically by, solid hydration products of the cement. Thus the 'apparent diffusion coefficient' may be regarded as a 'quasi-transport' coefficient, which is dependent not only on what Diamond in Chapter 2 calls the 'permeation capacity' of concrete but also on its 'chloride binding capacity'. As far as ionic diffusion is concerned, the 'permeation capacity' depends largely on the continuity and tortuosity of the coarser pores within the material and, from simple analysis of steady state chloride diffusion data, it would appear that chloride ions are not transported at significant rates through hydrated cement pastes unless pores wider than about 30 nm are present (Ngala and Page, 1997).

In spite of the fundamental objections that can be raised to using 'quasi-transport' coefficients such as D_{app} to describe chloride penetration into concrete, they have now been employed in this context by many authors for several decades. This follows from early research on the penetration of deicing salts into cement pastes and concrete (Collepardi *et al.*, 1972) and even earlier investigations of the diffusion of several radioactively labelled anions and cations into hydrated cements (Spinks *et al.*, 1952), where the error function solution to Fick's second law was applied. They have commonly been used in service-life prediction models, often incorporating empirical corrections that are intended to rectify some of the obvious discrepancies that appear when measured chloride penetration profiles are interpolated to equation 5.2. Thus, for instance, deviations from the error function relationship that are often observed near the externally exposed surface of concrete (see Fig. 5.13) have been dealt with either by ignoring data from this region and extrapolating the best-fit curve to the remaining points to yield values for D_{app} and an 'apparent' surface chloride content (c_s) or by other arbitrary methods. Similarly, the fact that measured values of D_{app} are not constant for a given type of concrete, but show marked

time-dependency (particularly so for concretes made from blended and composite cementitious binders that develop increasing diffusion resistance over very long periods in moist environments), has been dealt with by introducing an empirical 'time-dependent apparent diffusion coefficient' ($D_{app(t)}$) into equation 5.2; this is usually expressed by a relationship of the following form (Mangat and Molloy, 1994; Bamforth, 2004):

$$D_{app(t)} = D_{app(0)} \left[\frac{t}{t_0}\right]^n \qquad 5.3$$

where:

$D_{app(0)}$ is the apparent diffusion coefficient measured at reference age (t_0)
n is an empirically determined 'age factor' for the particular concrete.

While this would appear to provide a straightforward method of accounting for differences in the rates of microstructure development and evolution of chloride penetration resistance for different types of concrete, detailed methods of determining values of n are not yet well established. As demonstrated in a recent investigation that examined three such current methods, this can lead to major variability in service-life predictions that are based on the various measured n values (Nokken *et al.*, 2006). The requirement for long-term data to be available to provide credible information about 'age factors' is therefore obvious. It is also relevant to note that such data need to have been acquired under reasonably realistic conditions of moisture history as different types of concrete are liable to show different sensitivity to this variable, something that may be reflected in their long-term resistance to chloride penetration. The nature and properties of the C-S-H phases in different cementitious binder systems vary substantially (Taylor, 1997) and there is concern that the enhanced susceptibility to early-age cracking of some types of very low water/cement ratio concrete incorporating certain types of blended or composite cement may adversely affect their durability (Shah and Weiss, 2000). This is one of the main areas where further research is needed as the poorly defined relationships that often exist between crack distribution, crack width, cover depth and severity of chloride-induced corrosion of embedded steel in concrete of different types has generated extensive debate but basic understanding has not proved easy to achieve (Darwin *et al.*, 1985; Schiessl and Raupach, 1997).

Another area of evident research need is related to the development of effective ways of reducing current uncertainty regarding chloride threshold levels for different types of concrete under different exposure conditions because of the sensitivity of predicted service lives to the assumed chloride threshold value (C_{crit}). Thus, if the error function solution of Fick's second law (equation 5.2) is used to estimate chloride penetration profiles for concrete with stipulated values of, say, $D_{app} = 10^{-12}$ m^2/s, $C_s = 2\%$ Cl^- by mass of cement, $C_i = 0\%$ Cl^- by mass of cement, the corrosion initiation time (t_0) varies as a function of the

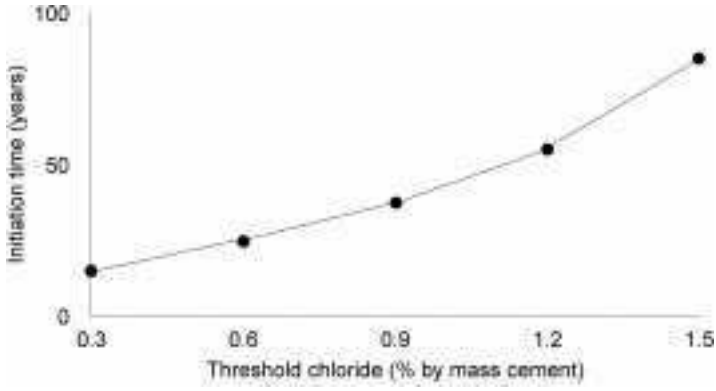

5.14 Relationship between estimated corrosion initiation times and chloride threshold values. (See text for modelling assumptions.)

assumed chloride threshold value (C_{crit}), as shown in Fig. 5.14. The relationship indicates that substantial improvements in t_0 are to be expected if fairly modest increases in C_{crit} can be reliably achieved in reinforced concrete structures (as distinct from laboratory specimens).

In concluding this section, it is suggested that there are good reasons for caution when applying current methodologies for prediction of the initiation time for corrosion of steel in concrete exposed to the most severe chloride environments (Andrade *et al.*, 2005). Partly this is due to lack of rigorous mechanistic models of chloride ingress validated by adequate data but, perhaps even more importantly, to current uncertainties regarding chloride threshold levels. Useful progress has been made, nevertheless, in developing improved guidance for specification of reinforced concrete suited for different chloride environments corresponding to the exposure classes described in the European standard BS EN 206 and complementary national standards such as BS 8500. These classes are as designated in Tables 5.1(b) and (c) and the rationale for corresponding limiting values of nominal cover, minimum cement content, and maximum water/cement ratio, applicable to reinforced concrete made with various cementitious binders, has been discussed by several authors (Hobbs and Matthews, 1998; Hobbs, 2001; Richardson, 2002; Thomas and Matthews, 2004). In BS 8500, the recommendations on limiting values for reinforced concrete exposed to a risk of chloride-induced corrosion (XD and XS exposures) are for an intended working life of at least 50 years. This standard gives no precise recommendations for an intended working life of at least 100 years in XD and XS exposures because, as it states, the spread of data from research and surveys of actual structures indicate that understanding of the processes involved is not yet adequate to produce such recommendations.

5.7 Supplementary corrosion avoidance and protection measures

While the conventional approaches for avoiding premature corrosion in reinforced concrete that depend primarily on the control of concrete quality are always recommended, supplementary corrosion avoidance measures can also be worthwhile in certain cases. In this section, some of the numerous available supplementary protection options will be considered. A comprehensive review of the topic is beyond the scope of this chapter, however, and interested readers may find useful sources of further information referred to in Section 5.10.

A general point that should be emphasised here is that effective design for corrosion control normally requires an intelligent combination of measures rather than a single 'all-or-nothing' application of a particular technique. Thus it is always good practice to examine opportunities for reducing the severity of the local environment to which vulnerable parts of a structure will be exposed. This can often be accomplished simply by means of appropriate detailing to avoid the formation of crevices or joints that will retain corrosive liquids and by making provision for free drainage; a number of illustrative examples of good and bad design details have been provided elsewhere (CEB, 1992; Bertolini *et al.*, 2004). Equally it should be borne in mind that if supplementary corrosion protection is to be specified in a form that will not be readily accessible for inspection and treatment in the event of failure, there is a need for convincing evidence of long-term performance relevant to the particular exposure conditions to be provided.

5.7.1 Anti-carbonation measures

As discussed previously, there is ample evidence that normally specified cover thicknesses and qualities of ordinary structural concrete that comply with the relevant guidance in codes of practice can provide adequate protection to embedded reinforcing steel for working lives of 50 or 100 years in temperate environments where carbonation-induced corrosion is the sole concern (Hobbs and Matthews, 1998). Only in special cases therefore (e.g., where cover depths have to be restricted) should supplementary protection be necessary and, in such circumstances, anti-carbonation coatings of various types are often applied to concrete surfaces to improve their resistance to CO_2 ingress (Robinson, 1987; Davies *et al.*, 2002). Effective anti-carbonation coatings may be expected to exhibit a number of properties that enable them to exclude CO_2 and water, adhere to the substrate, allow water vapour to escape and, in certain climates, resist thermal cycling, UV degradation, etc. A number of European Standards relevant to coatings for masonry and concrete have been undergoing development in recent years, two of the most significant with respect to anti-carbonation coatings being BS EN 1062-6 (2002) and BS EN 1504-2 (2004).

Several other supplementary measures against carbonation-induced corrosion are also sometimes advocated; for instance, zinc coatings, applied to reinforcing steel by hot dip galvanising, are considered effective for structures exposed to carbonation in the absence of significant chloride contamination (Treadaway *et al.*, 1989; Bautista and Gonzalez, 1996). It is important when using galvanised steel reinforcement, however, to ensure that adequate coating thicknesses are specified in relation to the required service life, bearing in mind that, in routine processing, hot dip galvanising is said generally to result in thicknesses of at least 100 μm (Yeomans, 2002). Measurements of the corrosion rates of galvanised coatings in carbonated mortars exposed to certain moist environments have shown values can sometimes significantly exceed 1 μm/year, particularly so when chlorides are present in the material (Gonzalez and Andrade, 1982), but it has been suggested that even 80 μm thick galvanised coatings would typically be expected to last over 100 years in carbonated concrete that is free from chloride (Bertolini *et al.*, 2004).

5.7.2 Supplementary protection against chlorides

The need for supplementary protection of reinforced concrete against the corrosive effects of chloride salts is far more common than that for carbonation-induced corrosion and several approaches have been employed which rely on: (a) surface treatment of the concrete to improve its resistance to chloride penetration, or (b) measures aimed at improving the tolerance of the reinforcement to levels of chloride in excess of normal 'threshold' values. In the former category, a wide range of different surface treatments has been used with a view to controlling chloride ingress and these belong to a number of generic groups, including membranes and barrier coatings (principally film-forming organic polymers and polymer-modified cementitious coatings), pore blocking impregnants (both organic and inorganic materials that penetrate the pores of concrete and block them), and pore lining impregnants (silicones, silanes, siloxanes and similar substances that penetrate into the pores and line them with a hydrophobic surface film to inhibit water ingress). The nature and properties of these materials have been reviewed elsewhere (Concrete Society, 1997; Basheer *et al.*, 1997; Bertolini *et al.*, 2004; Bamforth, 2004) and their performance has been found to vary substantially, both within and between generic types of material. A European standard, addressing issues on testing for effectiveness and durability of surface protection systems, has also been published recently (BS EN 1504-2, 2004) as one of a gradually evolving ten-part series of standards dealing with repair and protection of concrete being prepared under the auspices of CEN Technical Committee TC104. Further information may be obtained from the website of the Concrete Repair Association at www.cra.associationhouse.org.uk.

As regards measures aimed at improving the tolerance of the reinforcement to levels of chloride in excess of normal 'threshold' values, a long list of

techniques has been applied with varying degrees of success. This is unsurprising given the many factors that can affect chloride threshold values for plain carbon steel reinforcement. Salient features of the following approaches to improving chloride tolerance will be considered briefly here:

- corrosion resistant alloy steel reinforcement
- coated plain carbon steel reinforcement
- corrosion inhibitive admixtures
- cathodic prevention.

Corrosion resistant alloy steels

The case for judicious use of corrosion resistant alloy steels as reinforcement for concrete exposed to severe chloride contamination has been strengthened in recent years in spite of the relatively high initial cost of the more resistant alloys. This has happened partly as a result of independent long-term studies of the performance of different varieties of corrosion resisting steel, a notable example being the work reported by Treadaway *et al.* (1989), which demonstrated the excellent durability of certain types of stainless steel over a ten year exposure period in concrete containing high levels of chloride. It is important to note, however, that the term 'stainless steels' is used collectively to describe a large family of over 60 iron alloys with a very wide range of properties. The alloys concerned all contain a minimum of 12% chromium (with carefully controlled levels of several other significant alloying elements such as nickel, molybdenum, carbon, etc.) and their microstructures are categorised as ferritic, austenitic, martensitic or duplex (austenitic-ferritic). Compositional limits and microstructures are usually designated according to BS EN 10088-3 (1995) in Europe (or a similar AISI classification in the USA), typical compositions of the austenitic and duplex types most widely used for reinforcing bars being given in BS 6744 (2001) and in a guidance document entitled 'Stainless Reinforcing Steels' available from the website of UK CARES at www.ukcares.com. Stainless steels owe their corrosion resistance to the formation of stable passive films and their varying susceptibility to localised forms of corrosion, such as pitting, crevice attack and stress-corrosion cracking, is highly sensitive to features of alloy composition, heat treatment and environment.

Reviews of the nature and performance of stainless steels used in concrete have been published recently (European Federation of Corrosion, 1997; Nürnberger, 2005) and a feature of significant interest has been the observation that the alloys concerned tend to behave as relatively inefficient cathodes when galvanically coupled to carbon steel in concrete, providing they are free from oxide scale of the kind that may be formed during welding or heat treatment (Sørensen *et al.*, 1990; Bertolini *et al.*, 2004). This has led to proposals for stainless steel reinforcement to be used selectively in the most vulnerable parts

of concrete structures with plain carbon steel reinforcement used in other less severely exposed regions, as galvanic interactions between the two materials are believed to be of less concern than was once feared. It is of course possible to eliminate such galvanic interactions entirely by means of plastic sleeves or paints to prevent contact between the dissimilar metals but this would add to the cost of using stainless steel reinforcement (Bamforth, 2004).

Coated plain carbon steels

Many different metallic and non-metallic coatings have been applied to reinforcing steel with a view to improving its resistance to chlorides. The most widely used coating of the former type has been zinc, applied by hot dip galvanising, but there has been long-standing controversy over the effectiveness of this technique as a means of achieving required service lives for structures exposed to high levels of chloride contamination (Arup, 1979; Bautista and Gonzalez, 1996). Several factors are known to influence the performance of galvanized coatings in chloride-contaminated concrete, in particular the proportion of chloride, the alkalinity of the cement and the metallurgical structure of the coating (Gonzalez and Andrade, 1982; Page *et al.*, 1989). This can result in very high variability in the rates of consumption of galvanised coatings being observed under different circumstances and, while it is clear that galvanised coatings are capable of delaying the onset of significant corrosion of reinforcing steel, it can be difficult to translate this into reliable estimates of the number of additional years of maintenance-free service.

According to some authorities, it appears that only a slight increase in life will be obtained in severe chloride environments (ACI Committee 222, 1996). Others have proposed that a threshold level of 1% chloride by weight of cement may be adopted for design purposes when galvanised steel reinforcement is used (Bamforth, 2004). It has been suggested that the coating itself should not be used as the primary or sole means of corrosion protection, rather it should be used in conjunction with an adequate cover of dense impermeable concrete suited to the type of structure and exposure conditions (Yeomans, 2002). It is also advised that galvanised bars should not be used in metal-to-metal contact with uncoated steel to prevent the formation of galvanic couples (ACI, 1996). If galvanised bars are to be welded, it is to be expected that local loss of coating will occur and it is recommended that the affected area should be cleaned and treated with a suitable zinc-rich paint (Bertolini *et al.*, 2004).

Of numerous non-metallic coatings for steel reinforcement that have been proposed, the only type to be widely used has been fusion bonded epoxy (FBE), applied as powder to cleaned and heated bars to form a layer that is usually ~ 200 μm in thickness. FBE coated reinforcement has been used in North America since the mid 1970s in highway bridge decks and other structures exposed to deicing salt and, in the late 1970s, it was also used for the substructure elements

of marine bridges in the sub-tropical state of Florida. The coating is intended to isolate the steel from contact with moisture and chloride ions, but the chief difficulty in using FBE coated bars effectively has been preventing damage to the coating during transportation, handling, fixing, placing and compaction (ACI, 1996; Yeomans, 1994). Since extensive corrosion of FBE coated reinforcement in the substructures of marine bridges in Florida was reported (Sagues *et al.*, 1990; Sagues and Powers, 1997) there has been controversy over the effectiveness of the approach, a brief but informative history of which has been provided by Manning (1995). In consequence, further investigations were initiated in 1993 by the American Federal Highway Administration (FHWA), the various findings of which are summarised in a FHWA report (Virmani and Clemena, 1998).

European experience with FBE reinforcement has been more limited than that in North America and serious doubts have been expressed over the North American practice of using epoxy coated bars in the more severely exposed regions of structures (e.g., the top mat of a bridge deck) coupled to uncoated bars elsewhere. The reason for this concern is that the uncoated bars are expected to provide cathodes of large area in comparison with the anodes formed at breaks in the epoxy coating (Bamforth, 2004).

Corrosion inhibitive admixtures

Corrosion inhibitors are substances which, when added (in small quantities) to an aggressive environment, reduce the corrosion rate of a particular metal in that environment. They are sometimes regarded, in a sense, as 'retarding catalysts' (Fontana, 1986) or as substances that 'form a protective coating *in situ* by reaction of the solution with the corroding surface' (Jones, 1992). The term, as applied to steel in concrete, will be used throughout this chapter to describe 'chemical substances that prevent or retard corrosion by action at the steel/concrete interface' (European Federation of Corrosion, 2001), and this implies that adequate (preferably small) concentrations of inhibitor need to be available at the steel/concrete interface in order for corrosion inhibition to be induced. Substances that prevent or retard corrosion of steel in concrete in other ways, e.g. by modifying bulk transport properties of the concrete and thereby limiting the availability of aggressive agents at the steel, are not normally considered as corrosion inhibitors (Bertolini *et al.*, 2004; Büchler, 2005).

The classification of a substance as a 'corrosion inhibitor' does not define its mode of action precisely and different inhibitors can work in different ways, some of them retarding the anodic process (anodic inhibitors), others retarding the cathodic process (cathodic inhibitors) and some combining both of these functions (mixed inhibitors). Good examples of corrosion inhibitors (of the anodic type) for steel in aqueous media are alkalis, such as NaOH, KOH and $Ca(OH)_2$. As discussed in Section 5.2.2, these are the substances produced

during cement hydration that normally passivate steel, retarding its anodic dissolution and so reducing its corrosion rate to an imperceptible level in an environment such as uncontaminated, dense concrete.

Over the past 50 years, there have been many attempts to enhance the protective character of concrete pore electrolytes by introducing corrosion inhibitive admixtures at the time of manufacture of concrete. Clearly, however, any such chemical admixture for concrete has to fulfil a number of criteria in order that adverse effects on workability, cement hydration, development of mechanical properties or other characteristics of the material may be avoided and this effectively rules out several compounds that are often used as corrosion inhibitors for steel in other circumstances.

Of the corrosion inhibitors that have been employed as admixtures in fresh concrete, by far the most widely applied has been calcium nitrite. This has been used since the late 1970s in the USA and has also found applications in other countries for providing supplementary protection against chloride-induced corrosion (Berke and Weil, 1994). It is an anodic inhibitor, which is thought to reinforce the passive film on steel by oxidation of Fe^{2+} ions produced anodically at defects in the film (Gaidis and Rosenberg, 1979):

$$Fe^{2+} + 2OH^- + 2NO_2^- \rightarrow \gamma\text{-}Fe_2O_3 + 2NO + H_2O$$

In the presence of chloride ions, it has been suggested that the ratio of concentrations of $[NO_2^-]/[Cl^-]$ must exceed a critical value, ~0.5–1.0, for full passivity to be maintained (Gaidis and Rosenberg, 1987; El-Jazairi and Berke, 1990; Andrade *et al.*, 1986). In circumstances where inadequate dosages of nitrite are used or where its concentration is reduced locally, e.g. by leaching from cracked or permeable concrete, there may be a risk of intensified pitting in the presence of chloride ions. To guard against this, it is important that calcium nitrite-based admixtures should be used only in conjunction with appropriate quality control measures. This is to ensure that the initial concentration of inhibitor is adequate and that other measures aimed at promoting durability are in place, including adequate cover, low water/cement ratio concrete and controlled maximum surface crack widths (Berke and Weil, 1994).

Despite the relatively long record of performance of calcium nitrite-based admixtures, concerns regarding their long-term effectiveness, toxicity and environmental impact have tended to limit their fields of application (Bertolini *et al.*, 2004; Büchler, 2005). Efforts to identify alternative corrosion inhibitive admixtures have continued and, during the 1990s, several new types have been introduced, including a number of proprietary formulations based on amines, alkanolamines and their salts with various acids (Maeder, 1994; Elsener *et al.*, 1999) or emulsified mixtures of esters, alcohols and amines (Nmai *et al.*, 1992). Limited information about the detailed compositions of these organic inhibitors has been published and none has yet established a record of long-term performance comparable with that of calcium nitrite. A state-of-the-art review on

corrosion inhibitors for steel in concrete has been published for the European Federation of Corrosion (2001).

Cathodic prevention

The term 'cathodic prevention' was proposed by Pedeferri to describe the application of the well known technique of cathodic protection as a preventative (rather than as a curative) measure to reinforced or prestressed concrete structures prior to the onset of chloride-induced corrosion (Pedeferri, 1996). Cathodic protection, in its more usual applications as a remedial measure for existing structures that have already suffered corrosion, will be considered in Section 5.9. Whether used on new or old structures, however, the main features of the technique are similar and simply involve applying a direct current between the reinforcing bars (acting as the cathode of a cell) and an external anode of an appropriate type, the magnitude of the current density being adjusted to a level needed to induce passivation rather than pitting. For cathodic prevention, the required current density is generally very small, $< 2\,mA/m^2$, as it is necessary only to shift the potential by a small amount to achieve a condition of 'imperfect passivity' in which the initiation of pitting is suppressed even though high levels of chloride may eventually penetrate through the concrete cover (see Fig. 5.12).

There are several practical advantages to designing and installing cathodic protection systems for new structures rather than applying them as retrofit measures to existing ones after corrosion has been initiated, although this clearly raises the initial cost and must be evaluated bearing in mind the prospect that new and improved anode systems might become available during the early years of a new structure's working life. For these and other reasons, the deliberate application of cathodic prevention to new reinforced concrete structures in highly aggressive chloride-laden environments has been limited to date, although it has been used on major structures in several countries (Broomfield, 1997). It is interesting, however, to observe that the reinforcement in many offshore structures is connected to cathodic protection systems that are ostensibly being used to protect the exposed steelwork on the structures, so the reinforcement concerned actually receives unintended cathodic prevention current densities, estimated to be in the range $0.5–1.0\,mA/m^2$ (ACI, 1996).

5.8 Assessment and monitoring of corrosion in reinforced concrete

The investigation of reinforced concrete structures that are suspected to be suffering from corrosion is commonly undertaken by specialist materials engineers working in conjunction with structural engineers. Before starting inspection and testing, it is necessary to make a general assessment of the state of the

structure concerned in order to confirm that it is reasonably safe to proceed with the proposed activity. It is also necessary to consider possible structural implications that may be associated with the various forms of corrosion (and/or other types of degradation) that may be identified. These aspects are within the province of the structural engineer and will not be discussed further in this contribution. Accurate diagnosis and location of the material degradation phenomena that have precipitated the investigation, and identification of their causative factors, however, are necessary precursors to any successful, cost-effective remedial treatment of the condition. Several useful accounts have been provided of the methodological steps and investigative techniques that are normally employed in carrying out such investigations (Pullar-Strecker, 1987; Broomfield, 1997; BRE, 2000b; Bertolini *et al.*, 2004) and only a brief discussion of corrosion-related aspects will be given here.

The initial requirements are usually to establish whether:

(a) characteristic symptoms of cracking and staining of the concrete, that might be attributable to corrosion, are present at the surface – investigated by means of visual inspection and photography;
(b) there is evidence of sub-surface delamination, that might be attributable to corrosion – usually investigated by means of a simple hammer/chain drag survey or, in some cases where large areas have to be surveyed, with the aid of instrumental methods, e.g. sub-surface radar or infra-red thermography;
(c) the distribution and cover depth of the reinforcing bars indicates that corrosion is likely to have been responsible for the above damage – investigated by means of an electromagnetic cover-meter survey;
(d) there is evidence of electrochemical corrosion activity, particularly in regions of the structure that have not already exhibited signs of cracking or delamination – investigated by means of half-cell potential mapping (see Fig. 5.15), which is the subject of a recent draft RILEM Recommendation (RILEM TC 154-EMC, 2003).

Assuming the above indicators point to a corrosion problem, then the causative factors will need to be identified by measurements of the depths of carbonation and chloride analysis at representative locations. The phenolphthalein test, which is employed for measuring carbonation depths (RILEM TC CPC-18, 1985), is generally regarded as straightforward and reasonably reliable, though other methods are considered preferable in certain cases, e.g. when testing high alumina cement (HAC) concrete (BRE, 2000b). Chloride analyses, however, have sometimes proved problematic and large scatter in the results from round robin tests has been reported in various regions; these issues have been addressed by RILEM Technical Committee 178-TMC in recent reports and recommendations (Castellote and Andrade, 2001a,b). The question as to how data regarding carbonation depths and chloride profiles may be used to estimate corrosion initiation times was considered briefly in Sections 5.4–5.6 and, as

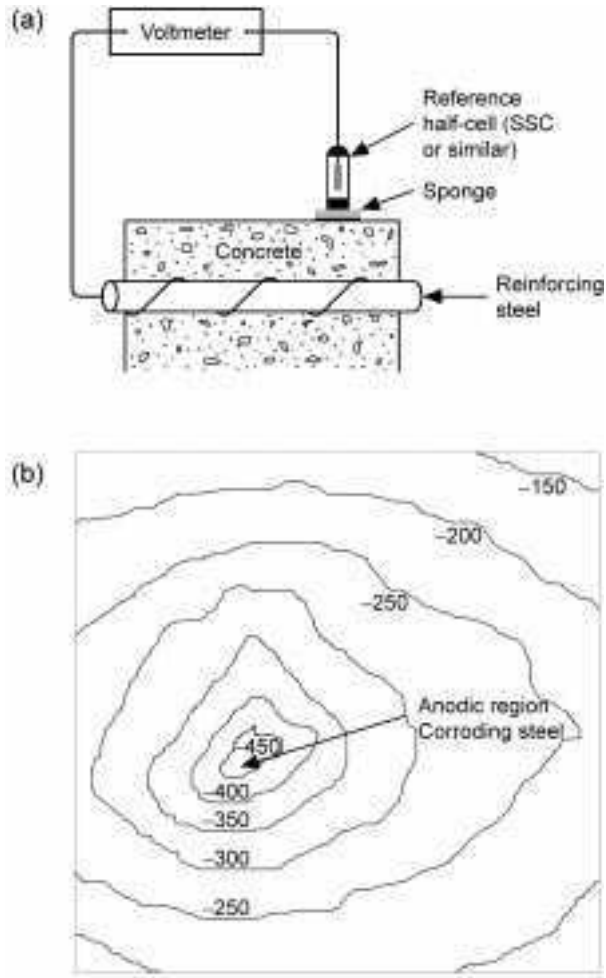

5.15 (a) Circuit for measurement of potential of reinforcing steel relative to a reference half-cell (e.g. SSC – a silver/silver chloride electrode in 1 M KCl). (b) Typical iso-potential contours (mV, SSC scale) recorded for reinforcement in a concrete slab with a single corroding region surrounded by passive steel.

already noted, particularly as far as chloride profiles are concerned, there are still a number of current uncertainties that remain to be resolved.

In cases where corrosion initiation is found already to have occurred and the causes have been identified, the issue of how to manage the problem for the remainder of the intended working life of the structure concerned raises questions of how rapidly the corrosion may be expected to propagate to a limit state at various locations. While potential mapping can provide a valuable guide to the distribution and scale of the anodic areas at a given time, it does not yield information about corrosion rates directly. Concrete resistivity measurements,

which can be made non-destructively on site (Polder *et al.*, 2000), may be correlated empirically with observed corrosion rates of steel after depassivation has occurred in concrete of particular composition but the relationship is not of universal applicability (Bertolini *et al.*, 2004).

Attempts to estimate the instantaneous corrosion rates (i_{corr}) of steel reinforcement in concrete directly may be made by various electrochemical techniques (Andrade and Alonso, 1996; Gowers and Millard, 1999), the most widely used of which involves adaptation of the well-known method of polarisation resistance (R_p) measurement (also known as linear polarisation) devised by Stern and coworkers (Stern and Geary, 1957, Stern and Weisert, 1958). The application of this method to measure the corrosion rate of steel in concrete was originally proposed and subsequently developed for on-site use by Andrade and co-workers (Andrade and Gonzalez, 1978; Feliu *et al.*, 1989) and it has recently become the basis of a RILEM Recommendation (RILEM, 2004).

Although linear polarisation has been extensively applied to provide useful data about rates of corrosion of steel in concrete, it is recognised that there are inherent sources of error that limit the accuracy of the measurements, when compared with gravimetric estimates of corrosion (Andrade and Martinez, 2005). Particular problems arise from: (i) uncertainty in the magnitude of the proportionality constant (B) in the Stern-Geary equation, $R_p = B/i_{corr}$, (relating R_p to the reciprocal of the instantaneous corrosion rate, i_{corr}) which varies for different systems, and (ii) errors in confining the areas of reinforcing steel undergoing polarisation when the technique is applied to a large reinforced concrete structure, as distinct from a small laboratory specimen. It is also important to note that instantaneous corrosion rates can vary substantially with time and ambient conditions, and so may not provide a representative guide to cumulative corrosion losses unless measurements are made repeatedly over an extended period at a given location.

For the above reasons, the use of i_{corr} data in structural models aimed at providing quantitative predictions of the time for corrosion propagation to cause a limit state to be reached is subject to fairly large uncertainties. Commonly it is therefore assumed that, since a value of $i_{corr} = 1\ \mu\text{A cm}^{-2}$ corresponds to a rate of loss of steel section of just over 10 μm/year whilst somewhere between 10 and 100 μm of steel section loss normally generates sufficient expansive corrosion product to crack concrete cover (Broomfield, 1997), the broad criteria shown in Table 5.3 may be applied in the interpretation of i_{corr} data for reinforced concrete.

While the various techniques described above can provide a means of assessing the corrosion state of an existing structure at a given time, it is becoming increasingly common for major structures in aggressive environments to have installed in them corrosion monitoring devices (sensors) that may be used to provide early warning of the development of corrosion. These may be based on a number of methods for non-destructive detection of changes that are

Table 5.3 Broad relationship between observed levels of corrosion activity in reinforced concrete and instantaneous corrosion rates from polarisation resistance measurements (Broomfield, 1997)

i_{corr} (μA cm^{-2})	Corrosion level
$<$0.1	Negligible
0.1–0.5	Low to moderate
0.5–1.0	Moderate to high
$>$1.0	High

associated with the onset of corrosive conditions. Examples include linear polarisation probes (Broomfield *et al.*, 2002), galvanic sensors (Short *et al.*, 1991, 1994), macrocell probes (Raupach and Schiessl, 1997), chloride ion specific electrodes and resistivity sensors (Zimmermann *et al.*, 1997).

5.9 Remedial treatment of corrosion in reinforced concrete

The remedial treatment of corrosion problems in reinforced concrete has become a field of major activity in recent years and there are often a great many options to be considered by engineers, when faced with the question of how to maintain a particular structure cost effectively for the remainder of its intended service life. This has led to the development of draft recommendations on repair strategies for structures damaged by corrosion, such as those formulated by a RILEM Technical Committee over a decade ago (RILEM TC 124-SRC, 1994) as a precursor to the gradual introduction of a series of new European standards on concrete repair in general (BS EN 1504, in ten parts when completed). These new standards are intended to aid those responsible for the selection of repair strategies, for specifying methods and for implementing them. A review of their applicability to structures subject to corrosion damage has been given in a BRE publication (BRE, 2000c) and a useful summary of their purposes, from the viewpoint of a consulting engineer involved in infrastructure management, has been contributed by Robery (2004). As mentioned previously, further information about the expected timetable for introduction of the new standards is also available from the website of the Concrete Repair Association (www.cra.associationhouse.org.uk).

Some of the more interesting developments in remedial methods for treating corrosion problems in reinforced concrete in recent years have involved the introduction of innovative electrochemical techniques and these will be the main focus of discussion in the remainder of this section. Before considering these techniques, however, it is worth noting that there are conventional methods of dealing effectively with carbonation-induced corrosion to produce long-lasting repairs but, when chloride-induced corrosion is involved, the situation can be far

more uncertain, particularly if the structure concerned is extensively salt-contaminated. The term conventional repair is used here, as elsewhere (Bertolini *et al.*, 2004), to indicate a process involving physical removal and replacement of non-protective concrete (i.e. carbonated or chloride-contaminated material) by a suitable cementitious material with the aim of restoring a passivating alkaline environment around the reinforcement. Other important steps, such as cleaning the exposed reinforcement after removal of the non-protective concrete, measures to ensure adequate bond and compatibility of the repaired and non-repaired materials, application of appropriate surface treatments to the structure to improve its appearance and resistance to further ingress of corrosive agents, etc., are also required and good workmanship is always necessary.

When structures are extensively contaminated with chloride salts, it may be difficult or uneconomic to treat reinforcement corrosion effectively by the conventional approach outlined above. To do so, not only is physical removal of the already cracked and delaminated regions of the concrete a requirement, it may also prove necessary to remove substantial amounts of physically sound but chloride-contaminated material. If this is not done thoroughly, the prognosis for a durable repair will be very poor because elimination of the most intensely anodic regions of the steel (from the patched zones of the structure) simply causes new anodic regions to form in the chloride-contaminated areas that surround them (Vassie, 1984). These so-called incipient anodes, that are coupled to passive steel cathodes situated in the freshly repaired zones, are now polarised to potentials in the range where pitting can be initiated whereas they had previously been protected against pitting by the cathodic current supplied to them by the corroding steel to which they had been coupled prior to repair.

An electrochemical solution to the incipient anode problem was found when impressed current cathodic protection systems were developed for application to reinforced concrete structures suffering from chloride-induced corrosion. This approach was pioneered by Stratfull in the US (1974) and has undergone numerous adaptations over the past 30 years. Its major advantage is that it can be applied to structures with substantial levels of chloride remaining in them after repair of the cracked and delaminated regions has been undertaken. However, it requires a direct current power supply to be available, as well as an appropriate form of anode to distribute the current through the concrete to the embedded steel reinforcement and a monitoring system to enable the performance to be checked at intervals. The aim is to polarise the steel to a potential at which new pitting is suppressed and existing pit growth is at least substantially retarded or preferably arrested (see Fig. 5.16). This can generally be accomplished by applying cathodic current densities in the range $< 20\,mA/m^2$ (i.e., up to one order of magnitude higher than those needed for cathodic prevention) and adjusting them as necessary throughout the remaining service life of the structure.

A number of reviews of cathodic protection of reinforced concrete have been published in recent years (Pedeferri, 1996; Bertolini *et al.*, 1998; Page and Sergi,

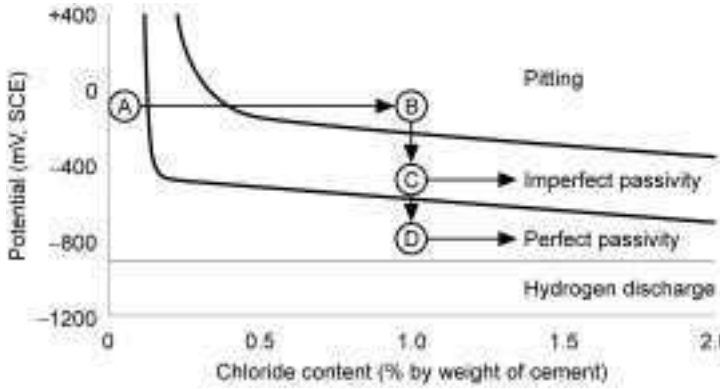

5.16 Approximate domains of electrochemical behaviour of steel in concrete with different levels of chloride contamination. Depression of the steel potential due to application of cathodic protection after significant chloride penetration of the concrete cover has induced pitting (A to B) may produce a state of 'imperfect passivity' (B to C) in which formation of new pits is suppressed and existing pit growth retarded, or 'perfect passivity' (B to D) in which pitting is entirely arrested (Pedeferri, 1996).

2000) and standards are available in Europe and North America (BS EN 12696, 2000; NACE RP 0290, 2000). Important areas of development have been concerned with impressed current anode systems (Wyatt, 1993), of which there are now several types suited to different applications (exemplified in Fig. 5.17). There has also been growing interest in the use of sacrificial anodes in situations where the provision of a power supply and monitoring system may be difficult, e.g. to protect the splash and tidal zones of certain marine structures (Kessler *et al.*, 1995; Broomfield, 2000) and also to provide local control of corrosion (by cathodic prevention) in the vicinity of patch repairs (Sergi and Page, 2000; Jordan and Page, 2003).

Other electrochemical remediation techniques that are related to cathodic protection, in that they involve the application of direct current between an external anode placed (in suitable electrolytes) on the surface of the concrete and embedded reinforcing steel acting as a cathode, are known as electrochemical realkalisation (ER) and electrochemical chloride extraction (ECE) – see Fig. 5.18. The former is aimed at restoring the alkalinity (and hence the passivating nature) of carbonated cover concrete while the latter is aimed at removing chloride ions from the cover zone of salt-contaminated concrete. An important distinction between these methods and cathodic protection is that they both involve much larger current densities (~1–2 A/m^2), which are applied only temporarily, typically over about 1–2 weeks for ER and 6–10 weeks for ECE. This implies that there is no requirement for monitoring to be maintained throughout the remaining service lives of the structures concerned, but establishing acceptable criteria for the end-points for the treatments has been

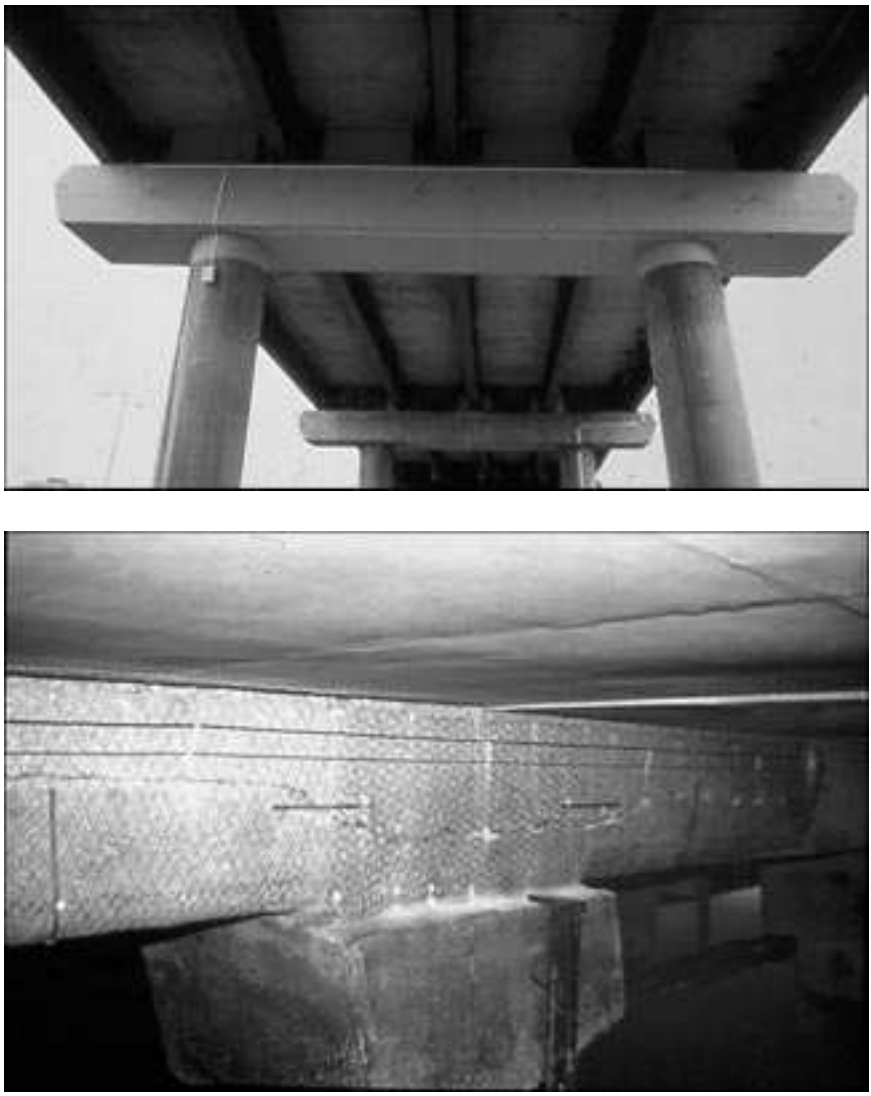

5.17 (a) Conductive paint extended anode for applying cathodic protection to a reinforced concrete structure. (b) Activated titanium mesh anode (shown prior to being coated with a concrete overlay) for applying cathodic protection to a reinforced concrete structure.

a matter of considerable debate. Also, particularly for ECE, the passage of high current densities over fairly long periods induces compositional changes within the cover concrete that increase progressively with the duration and magnitude of the applied current density, effects that have been studied experimentally (Bertolini *et al.*, 1996) and by modelling (Castellote *et al.*, 2000; Li and Page, 2000). As a consequence, the possibility of inducing adverse side-effects such as

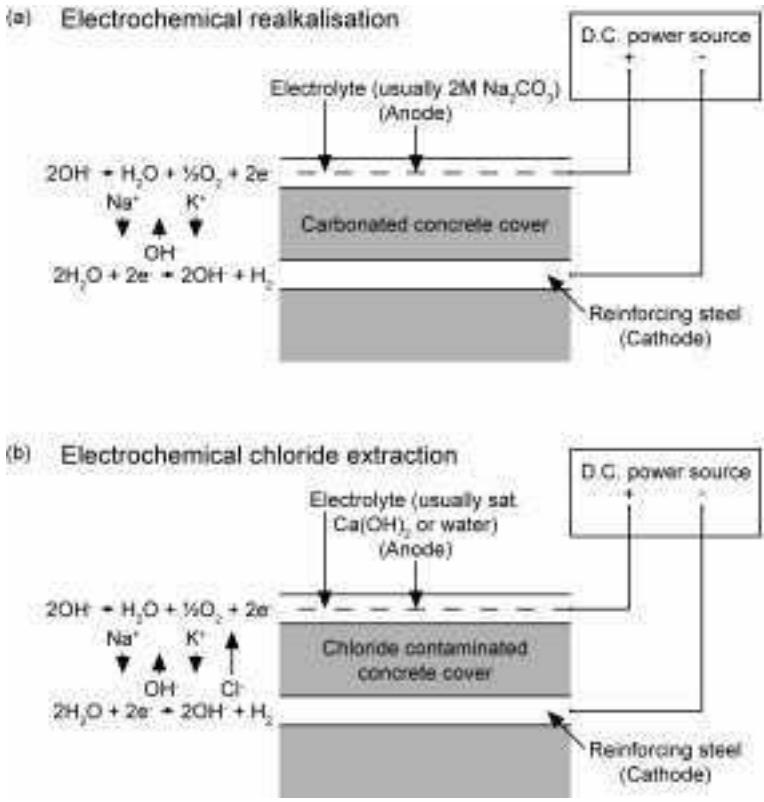

5.18 Essential features of (a) electrochemical realkalisation and (b) electrochemical chloride extraction applied to reinforced concrete.

alkali-silica reaction (Page and Yu, 1995) and degradation of the steel/concrete bond (Vennesland *et al.*, 1996; Buenfeld and Broomfield, 2000) should be considered when ECE is proposed for treatment of particular structures. A number of reviews encompassing ER and ECE have been published during the past decade (European Federation of Corrosion, 1998; Page, 2002; Bertolini *et al.*, 2004; Polder, 2005) to which readers requiring further detailed information are directed.

During the past 10–15 years, various attempts have been made to devise alternative, cost-effective remedial measures for dealing with corrosion in reinforced concrete structures, which involve using corrosion inhibitors in treatments applied via the external surfaces of structures in which corrosion has already been initiated. This is a different matter from the use of inhibitors as concrete admixtures where their intended role is primarily to delay the onset of corrosion (as discussed in Section 5.7.2). It raises a number of questions about: (a) the ability of the inhibitors concerned to retard pre-initiated corrosion in carbonated and/or chloride contaminated concrete, (b) their ability to be trans-

ported (both inwards and outwards) through concrete cover of varied quality and thickness, (c) the concentrations that need to be achieved and sustained in the vicinity of the embedded steel reinforcement to provide effective corrosion inhibition without adverse side-effects. These matters have been discussed in various reviews (Page *et al.*, 2000; European Federation of Corrosion, 2001; Büchler, 2005; Bertolini *et al.*, 2004) and laboratory research has attempted to clarify some of the issues raised for particular inhibitors (for examples, Elsener *et al.*, 2000; Ngala *et al.*, 2002, 2003, 2004; Tritthart, 2003; Page *et al.*, 2002, 2005; Fedrizzi *et al.*, 2005). In the cases of certain organic base corrosion inhibitors, efforts have also been made to develop electrochemical methods of injecting them rapidly into hardened concrete (see for example Asaro *et al.*, 1990; Phanasgaonkar *et al.*, 2000; Sawada *et al.*, 2005). Such laboratory-based studies, however, have recognised limitations and there is a clear need for carefully designed and monitored site trials to be undertaken if the advantages and limitations of various corrosion inhibitors in these and other applications in the field of concrete repair are to become better understood. This could provide a useful focus for future research efforts.

5.10 Sources of further information and advice

Further information on the subject matter of this chapter may be found in various books that deal specifically with corrosion of steel in concrete (for examples, RILEM TC 60-CRC, 1988; Bentur *et al.*, 1997; Broomfield, 1997; Bertolini *et al.*, 2004; Böhni, 2005). A number of major conferences, several of which have already been cited, have also been devoted to the subject and a notable recent addition to the research literature has been the Final Report of the European Concerted Action COST 521 Corrosion of Steel in Reinforced Concrete Structures (European Commission, 2003).

A related topic, not considered within the scope of this chapter, is the use of fibre reinforced composites, particularly glass fibre reinforced polymers, as alternatives to steel bars for concrete reinforcement. These have undergone development during the last two decades but unresolved durability issues, particularly under severe environmental conditions, are recognised as a major obstacle to their broader acceptance in civil engineering. Interested readers will find further information in a recent review article (Nkurunziza *et al.*, 2005).

5.11 References

ACI Committee 222 (1996), *Corrosion of Metals in Concrete*, American Concrete Institute.

Alonso C, Andrade C, Gonzalez J A (1988), 'Relation between resistivity and corrosion rate of reinforcements in carbonated mortar made with several cement types', *Cement and Concrete Research*, **18**, 687–698.

Andrade C, Alonso C (1996), 'Corrosion rate monitoring in the laboratory and on site', *Construction and Building Materials*, **10**, 315–328.

Andrade C, Gonzalez J A (1978), 'Quantitative measurements of corrosion rate of reinforcing steels embedded in concrete using polarisation resistance measurements', *Werkstoffe und Korrosion*, **29**, 515–519.

Andrade C, Martinez I (2005), 'Calibration by gravimetric losses of electrochemical corrosion rate measurement using modulated confinement of the current', *Materials and Structures*, **38**, 833–841.

Andrade C, Alonso C, Gonzalez J A (1986), 'Some laboratory experiments on the inhibitor effect of sodium nitrite on reinforcement corrosion', *Cement, Concrete and Aggregates*, **8**(2), 110–116.

Andrade C, Castellote M, Page C L (2005), 'Are service-life models appropriate for use in design of reinforced concrete structures for exposure to chloride salts?', *Proc. 3rd International RILEM Workshop on Testing and Modelling the Chloride Ingress into Concrete (RILEM PRO 38)*, Madrid, 2002, Andrade C, Kropp J (eds), RILEM Publications, Cachan, 93–104.

Anstice D J, Page C L, Page M M (2005), 'The pore solution phase of carbonated cement pastes, *Cement and Concrete Research*, **35**, 377–383.

Arup H (1979), 'Galvanised steel in concrete', *Materials Performance*, **18**(4), 41–44.

Arup H (1983), 'The mechanisms of the protection of steel by concrete', *Corrosion of Reinforcement in Concrete Construction*, Crane A P (ed.), Ellis Horwood, Chichester, 151–157.

Asaro M F, Gaynor A T, Hettiarachchi S (1990), 'Electrochemical chloride removal and protection of concrete bridge components', Strategic Highway Research Program Report, *SHRP-S/FR-90-002*, National Research Council, Washington, DC.

BRE (2000a), Digest 444: Part 1, *Corrosion of Steel in Concrete – Durability of reinforced concrete structures.*

BRE (2000b), Digest 444: Part 2, *Corrosion of Steel in Concrete – Investigation and assessment.*

BRE (2000c), Digest 444: Part 3, *Corrosion of Steel in Concrete – Protection and remediation*.

BS 6744 (2001), *Stainless steel bars for the reinforcement of and use in concrete – Requirements and test methods*, British Standards Institution, London.

BS 8500-1 (2002), *Concrete – Complementary British Standard to BS EN 206-1 – Part 1: Method of specifying and guidance to the specifier*, British Standards Institution, London.

BS 8500-2 (2002), *Concrete – Complementary British Standard to BS EN 206-1 – Part 2: Specification for constituent materials and concrete*, British Standards Institution, London.

BS CP 110 (1972), *Part 1: Design, materials and workmanship*, British Standards Institution, London (withdrawn).

BS EN 206-1 (2000), *Concrete – Part 1: Specification, performance and conformity*, British Standards Institution, London.

BS EN 1062-6 (2002), *Paints and varnishes – Coating materials and coating systems for exterior masonry and concrete – Part 6 Determination of carbon dioxide permeability*, British Standards Institution, London.

BS EN 1504-2 (2004), *Products and systems for the protection and repair of concrete structures – Definitions, requirements, quality control and evaluation of conformity – Part 2: Surface protection systems for concrete*, British Standards Institution, London.

BS EN 10088-3 (1995), *Stainless steels – Part 3: Technical delivery conditions for semi-finished products bars, rods and sections for general purposes*, British Standards Institution, London.

BS EN 12696 (2000), *Cathodic protection of steel in concrete*, British Standards Institution, London.

Bamforth P B (2004), *Enhancing Reinforced Concrete Durability*, Technical Report No. 61, The Concrete Society, Camberley.

Bard A J, Faulkner L R (1980), *Electrochemical Methods*, Wiley, New York.

Basheer P A M, Basheer L, Cleland D J, Long A E (1997), 'Surface treatments for concrete: assessment methods and reported performance', *Construction and Building Materials*, **11**, 413–429.

Bautista A, Gonzalez J A (1996), 'Analysis of the protective efficiency of galvanizing against corrosion of reinforcements embedded in chloride contaminated concrete', *Cement and Concrete Research*, **26**, 215–224.

Bentur A, Diamond S, Berke N S (1997), *Steel Corrosion in Concrete*, Spon, London.

Berke N S, Weil T G (1994), 'World wide review of corrosion inhibitors in concrete', *Advances in Concrete Technology*, Malhotra V M (ed.), CANMET, Ottawa, 899–1022.

Bertolini L, Yu S W, Page C L (1996), 'Effects of electrochemical chloride extraction on chemical and mechanical properties of hydrated cement paste', *Advances in Cement Research*, **8**, 93–100.

Bertolini L, Bolzoni F, Lazzari T, Pastore P, Pedeferri P (1998), 'Cathodic protection and cathodic prevention in concrete: Principles and applications', *Journal of Applied Electrochemistry*, **28**, 1321–1331.

Bertolini L, Elsener B, Pedeferri P, Polder R (2004), *Corrosion of Steel in Concrete*, Wiley-VCH Verlag GmbH & Co. KgaA, Weinheim.

Böhni H, ed. (2005), *Corrosion in Reinforced Concrete Structures*, Woodhead, Cambridge/CRC Press, Boca Raton, FL.

Broomfield J P (1997), *Corrosion of Steel in Concrete*, Spon, London.

Broomfield J P (2000), 'Corrosion of steel in concrete', *Uhlig's Corrosion Handbook*, 2nd edition, Revie R W (ed.), Wiley, New York, 581–600.

Broomfield J P, Davies K, Hladky K (2002), 'The use of permanent corrosion monitoring in new and existing reinforced concrete structures, *Cement and Concrete Composites*, **24**, 27–34.

Buenfeld N R (2004), 'Advances in predicting the deterioration of reinforced concrete', *Institute of Concrete Technology Yearbook: 2004–2005*, 23–38.

Buenfeld N R, Broomfield J P (2000), 'Influence of electrochemical chloride extraction on the bond between steel and concrete', *Magazine of Concrete Research*, **52**, 79–91.

Büchler M (2005), 'Corrosion inhibitors for reinforced concrete', Böhni H (ed.), *Corrosion in Reinforced Concrete Structures*, Woodhead, Cambridge/CRC Press, Boca Raton, FL, 190–214.

Castellote M, Andrade C (2001a), 'Round-Robin test on chloride analysis in concrete – Part 1: Analysis of total chloride content', *Materials and Structures*, **34**(243), 532–556.

Castellote M, Andrade C (2001b), 'Round-Robin test on chloride analysis in concrete – Part 2: Analysis of water soluble chloride content', *Materials and Structures*, **34**(244), 589–598.

Castellote M, Andrade C, Alonso C (2000), 'Electrochemical removal of chlorides: modelling of extraction resulting profiles and determination of the efficient time of treatment', *Cement and Concrete Research*, **30**, 615–621.

CEB (1992), *Durable Concrete Structures*, Bulletin d'Information, No. 183, Comité Euro-International du Béton, Lausanne.

Clark L A, Shammas-Toma M G K, Seymour D E, Pallet P F, Marsh B K (1997), 'How can we get the cover we need?', *The Structural Engineer*, **75**(17), 289–296.

Collepardi M, Marcialis A, Turriziani R (1972), 'Penetration of chloride ions into cement pastes and concretes', *Journal of the American Ceramic Society*, **55**(10), 534–535.

Concrete Society (1997), *Guide to Surface Treatments for Protection and Enhancement of Concrete*, Technical Report No. 50, Concrete Society, Camberley.

Crank J (1975), *The Mathematics of Diffusion*, 2nd edition, Oxford University Press, Oxford.

Davies H, Bassi R, Yates A P J (2002), 'Anti-carbonation coatings', *Handbook of Coatings for Concrete*, Bassi R, Roy S K (eds), Whittles, Latheronwheel, 128–136.

Darwin D, Manning D G, Hognestad, Beeby AW, Rice P F, Ghowral A Q (1985), 'Debate: Crack width, cover and corrosion', *Concrete International*, May, 20–35.

El-Jaizairi B, Berke N S (1990), 'The use of calcium nitrite as a corrosion inhibiting admixture to steel reinforcement in concrete', *Corrosion of Reinforcement in Concrete*, Page C L, Treadaway K W J, Bamforth P B (eds), Society of Chemical Industry/Elsevier Applied Science, London, 571–585.

Elsener B, Büchler M, Stalder F, Böhni H (1999), 'Migrating corrosion inhibitor blend for reinforced concrete: Part 1 – Prevention of corrosion', *Corrosion*, **55**(12), 1155–1163.

Elsener B, Büchler M, Stalder F, Böhni H (2000), 'Migrating corrosion inhibitor blend for reinforced concrete: Part 2 – Inhibitor as repair strategy', *Corrosion*, **56**(7), 727–732.

European Commission (2003), EUR 20599 – COST Action 521 – Corrosion of Steel in Reinforced Concrete Structures – Final Report, Cigna R., Andrade C, Nürnberger U, Polder R, Weydert R, Seitz E (eds), Office for Official Publications of the European Communities, Luxembourg.

European Federation of Corrosion (1997), Publication No 18, *Stainless Steel in Concrete – State of the art report*, Nürnberger U (ed.), Institute of Materials, London.

European Federation of Corrosion (1998), Publication No 24, *Electrochemical Rehabilitation Methods for Reinforced Concrete Structures – State of the art report*, Mietz J (ed.), Institute of Materials, London.

European Federation of Corrosion (2001), Publication No 35, *Corrosion Inhibitors for Steel in Concrete – State of the art report*, Elsener B (ed.), Institute of Materials, Maney, London.

Fedrizzi L, Azzolini F, Bonora P L (2005), 'The use of migrating corrosion inhibitors to repair motorways' concrete structures contaminated by chlorides', *Cement and Concrete Research*, **35**, 551–561.

Feliu S, Gonzalez J A, Andrade C, Feliu V (1989), 'Determining the polarization resistance in reinforced concrete slabs', *Corrosion Science*, **29**, 105–113.

Fontana M (1986), *Corrosion Engineering*, 3rd edition, McGraw-Hill, New York.

Gaidis J M, Rosenberg A M (1979), 'The mechanism of nitrite inhibition of chloride attack on reinforcing steel in alkaline aqueous environments', *Materials Performance*, **18**(11), 45–48.

Gaidis J M, Rosenberg A M (1987), 'The inhibition of chloride-induced corrosion in reinforced concrete by calcium nitrite', *Cement, Concrete and Aggregates*, **9**(1), 30–33.

Glass G K, Buenfeld N R (1997), 'The presentation of the chloride threshold level for corrosion of steel in concrete', *Corrosion Science*, **39**, 1001–1013.

Glass G K, Page C L, Short N R (1991), 'Factors affecting the corrosion rate of steel in carbonated mortars', *Corrosion Science*, **32**, 1283–1294.

Glass G K, Reddy B, Buenfeld N R, Viles R F (2001), 'Process for the protection of reinforcement in reinforced concrete', PCT Patent Application WO 01/55056 A1.

Goni S, Andrade C (1990), 'Synthetic concrete pore solution chemistry and rebar corrosion rate in the presence of chlorides', *Cement and Concrete Research*, **20**, 525–539.

Gonzalez J A, Andrade C (1982), 'Effect of carbonation, chlorides and relative ambient humidity on corrosion of galvanized rebars embedded in concrete', *British Corrosion Journal*, **17**, 21–28.

Gouda V K (1970), 'Corrosion and inhibition of reinforcing steel: 1. Immersed in alkaline solution', *British Corrosion Journal*, **5**, 198–203.

Gowers K R, Millard S G (1999), 'Electrochemical techniques for corrosion assessment of reinforced concrete structures', *Proc. Inst. Civ. Engrs. Structures and Buildings*, **134**, 129–137.

Hausmann D A (1967), 'Steel corrosion in concrete', *Materials Protection*, **6**(11), 19–23.

Hobbs D W (2001), 'Concrete deterioration: causes, diagnosis and minimising risk', *International Materials Reviews*, **46**(3), 117–144.

Hobbs D W, Matthews J D (1998), 'Minimum requirements for concrete to resist deterioration due to chloride-induced corrosion, *Minimum Requirements for Durable Concrete*, Hobbs D W (ed.), British Cement Association, Crowthorne, 43–89.

Hobbs D W, Marsh B K, Matthews J D, Petit S (1998), 'Minimum requirements for concrete to resist carbonation-induced corrosion of reinforcement', *Minimum Requirements for Durable Concrete*, Hobbs D W (ed.), British Cement Association, Crowthorne, 11–42.

Ishida T, Maekawa K, Soltani M (2004), 'Theoretically identified strong coupling of carbonation rates and thermodynamic moisture states in micropores of concrete', *Journal of Advanced Concrete Technology*, **2**(2), 213–222.

Johannesson B F (2003), 'A theoretical model describing diffusion of a mixture of different types of ions in pore solution of concrete coupled to moisture transport', *Cement and Concrete Research*, **33**, 481–488.

Jones D A (1992), *Principles and Prevention of Corrosion*, Macmillan, New York.

Jones M R, Dhir R K, Newlands M D, Abbas A M O (2000), 'A study of the CEN test method for measurement of the carbonation depth of hardened concrete', *Materials and Structures*, **33**, 135–142.

Jones M R, Newlands M D, Abbas A M O, Dhir R K (2001), 'Comparison of 2 year carbonation depths of common cement concretes using the modified draft CEN test', *Materials and Structures*, **34**, 396–403.

Jordan L C, Page C L (2003), 'Mortars for encapsulating sacrificial anodes in reinforced concrete', *Materials and Corrosion*, **54**, 387–393.

Kessler R J, Powers R G, Lasa I R (1995), 'Update on sacrificial anode cathodic protection on steel reinforced concrete structures in seawater', *Corrosion 95*, NACE International, Houston, TX, Paper 516.

Kropp J (1995), 'Relations between transport characteristics and durability', *RILEM Report 12: Performance Criteria for Concrete Durability*, Kropp J and Hilsdorf H K (eds), 97–137.

Lambert P, Page C L, Vassie P R W (1991), 'Investigations of reinforcement corrosion: 2. Electrochemical monitoring of steel in chloride-contaminated concrete', *Materials and Structures*, **24**(143), 351–358.

Larsen, C K (1998), 'Chloride binding in concrete', *D Ing Thesis*, Norwegian University of Science and Technology, Trondheim.

Li LY, Page C L (2000), 'Finite element modelling of chloride removal from concrete by an electrochemical method', *Corrosion Science*, **42**, 2145–2165.

Maeder U (1994), 'A new class of corrosion inhibitors', *Proc. Corrosion and Corrosion Protection of Steel in Concrete*, Swamy R N (ed.), Sheffield Academic Press, Sheffield, 851–864.

Mangat P S, Molloy B T (1994), 'Prediction of long-term chloride concentration in concrete', *Materials and Structures*, **27**, 338–346.

Manning D G (1995), 'Corrosion performance of epoxy-coated reinforcing steel: North American experience', *Construction and Building Materials*, **10**(5), 349–365.

Marchand J (2001), 'Modelling the behaviour of unsaturated cement systems exposed to aggressive chemical environments', *Materials and Structures*, **34**, 195–200.

Masslehuddin M, Page C L, Rasheeduzzafar, Al-Mana A I (1996), 'Effect of temperature on pore solution chemistry and reinforcement corrosion in contaminated concrete', *Corrosion of Reinforcement in Concrete Construction*, Page C L, Bamforth P B, Figg J W (eds), Society of Chemical Industry/Royal Society of Chemistry, Cambridge, 67–75.

Menzies J, Moore J, Currie R (1987), 'The durability of structural concrete in modern buildings in the United Kingdom', *ACI SP-100 Concrete Durability*, Scanlon J M (ed.), American Concrete Institute, Detroit, 143–168.

NACE Standard RP0290 (2000), Standard Recommended Practice, *Impressed current cathodic protection of reinforcing steel in atmospherically exposed concrete structures*, NACE International, Houston, TX.

Ngala V T, Page C L (1997), 'Effects of carbonation on pore structure and diffusional properties of hydrated cement pastes', *Cement and Concrete Research*, **27**, 995–1007.

Ngala V T, Page C L, Page M M (2002), 'Corrosion inhibitor systems for remedial treatment of reinforced concrete: Part 1 – Calcium nitrite', *Corrosion Science*, **44**, 2073–2087.

Ngala V T, Page C L, Page M M (2003), 'Corrosion inhibitor systems for remedial treatment of reinforced concrete: Part 2 – Sodium monofluorophosphate', *Corrosion Science*, **45**, 1523–1537.

Ngala V T, Page C L, Page M M (2004), 'Investigations of an ethanolamine-based corrosion inhibitor system for surface treatment of reinforced concrete', *Materials and Corrosion*, **55**, 511–519.

Nilsson L-O (2005), 'Concepts in chloride ingress modelling', *Proc. 3rd International RILEM Workshop on Testing and Modelling the Chloride Ingress into Concrete (RILEM PRO 38)*, Madrid, 2002, Andrade C, Kropp J (eds), RILEM Publications, Cachan, 29–48.

Nkurunziza G, Debaiky A, Cousin P, Benmokrane B (2005), 'Durability of GFRP bars: A critical review of the literature', *Progress in Structural Engineering and Materials*, **7**(4), 194–209.

Nmai C K, Farrington S A, Bobrowski G S (1992), 'Organic-based corrosion inhibiting admixture for reinforced concrete', *Concrete International*, **14**(4), 45–51.

Nokken M, Boddy A, Hooton R D, Thomas M D A (2006), 'Time-dependent diffusion in concrete – three laboratory studies, *Cement and Concrete Research*, **36**, 200–207.

Nürnberger U (2005), 'Stainless steel in concrete structures', *Corrosion in Reinforced Concrete Structures*, Böhni H (ed.), Woodhead, Cambridge/CRC Press, Boca Raton, FL, pp. 134–162.

Page C L (1975), 'Mechanism of corrosion protection in reinforced concrete marine structures', *Nature*, **258**, 514–515.

Page C L (1988), 'Basic principles of corrosion', *Corrosion of Steel in Concrete*, RILEM TC 60-CSC Report, Schiessl P (ed.), Chapman and Hall, London, pp. 3–21.

Page C L (1997), 'Corrosion and its control in reinforced concrete', *Institute of Concrete Technology Yearbook: 1998–1999*, 37–52.

Page C L (2002), 'Application of electrochemical techniques for maintenance of corroding reinforced concrete structures', *Proc. 1st fib Congress 'Concrete Structures in the 21st Century'*, Osaka, Session 12, 147–158.

Page C L, Havdahl, J (1985), 'Electrochemical monitoring of corrosion of steel in microsilica cement pastes', *Materials and Structures*, **18**(103), 41–47.

Page C L, Sergi G (2000), 'Developments in cathodic protection applied to reinforced concrete', *Journal of Materials in Civil Engineering*, **12**, 8–15.

Page C L, Treadaway K W J (1982), 'Aspects of the electrochemistry of steel in concrete', *Nature*, **297**, 109–115.

Page C L, Yu S W (1995), 'Potential effects of electrochemical desalination of concrete on alkali-silica reaction', *Magazine of Concrete Research*, **47**, 23–31.

Page C L, Short N R, El Tarras A (1981), 'Diffusion of chloride ions in hardened cement pastes', *Cement and Concrete Research*, **11**, 395–406.

Page C L, Short N R, Holden W R (1986), 'The influence of different cements on chloride-induced corrosion of reinforcing steel', *Cement and Concrete Research*, **16**, 79–86.

Page C L, Sergi G, Short N R (1989), 'Corrosion behaviour of zinc coated steel in silica fume concrete', *ACI SP-114, Fly ash, Silica fume, Slag, and Natural Pozzolans in Concrete, Proc 3rd International Conference*, Trondheim, Malhotra V M (ed.), American Concrete Institute, Detroit, pp. 887–896.

Page C L, Lambert P, Vassie P R W (1991), 'Investigations of reinforcement corrosion: 1. The pore electrolyte phase in chloride-contaminated concrete', *Materials and Structures*, **24**(142), 243–252.

Page C L, Ngala V T, Page M M (2000), 'Corrosion inhibitors in concrete repair systems', *Magazine of Concrete Research*, **52**, 25–37.

Page M M, Page C L, Ngala V T, Anstice D (2002), 'Ion chromatographic analysis of corrosion inhibitors in concrete', *Construction and Building Materials*, **16**, 73–81.

Page M M, Page C L, Shaw S J, Sawada S (2005), 'Ion chromatographic analysis of amines, alkanolamines and associated anions in concrete', *Journal of Separation Science*, **28**, 471–476.

Pedeferri P (1996), 'Cathodic protection and cathodic prevention', *Construction and Building Materials*, **10**(5), 391–402.

Phanasgaonkar A, Cherry B, Forsyth M (2000), 'Protection of reinforcement in concrete by combining surface applied migratory corrosion inhibitors with an electric field', *Proc. Corrosion and Prevention 2000*, Auckland, NZ, Paper no. 24.

Polder R B (2005), 'Electrochemical techniques for corrosion protection and maintenance', *Corrosion in Reinforced Concrete Structures*, Böhni H (ed.), Woodhead, Cambridge/CRC Press, Boca Raton, FL, pp. 215–241.

Polder R, Andrade C, Elsener B, Vennesland Ø, Gulikers J, Weydert R, Raupach M (2000), 'Test methods for on site measurement of concrete resistivity', *Materials and Structures*, **33**, 603–611.

Pourbaix M (1974), 'Applications of electrochemistry in corrosion science and in practice', *Corrosion Science*, **14**(1), 25–82.

Pullar-Strecker P (1987), *Corrosion Damaged Concrete: Assessment and Repair*,

Butterworths, London.
Ramachandran V S (1976), *Calcium Chloride in Concrete*, Applied Science, London.
Raupach M, Schiessl P (1997), 'Monitoring system for the penetration of chlorides, carbonation and the corrosion risk for the reinforcement', *Construction and Building Materials*, **11**, 207–214.
Richardson M G (2002), *Fundamentals of Durable Reinforced Concrete*, Chapter 5, 'Carbonation', Spon, London.
Richartz W (1969), 'Die Bindung von Chlorid bei der Zemmenterhärtung', *Zement-Kalk-Gips*, **22**, 447–456.
RILEM TC CPC-18 (1985), 'Measurement of hardened concrete carbonation depth', *Materials and Structures*, **18**, 435–440.
RILEM TC 60-CSC (1988), *Corrosion of Steel in Concrete*, Schiessl P (Ed.), Chapman & Hall, London.
RILEM TC 124-SRC (1994), 'Repair strategies for concrete structures damaged by corrosion', *Materials and Structures*, **27**, 415–436.
RILEM (1997), *Proc. International RILEM Workshop on Chloride Penetration into Concrete (RILEM PRO 2)*, St. Rémy-lès-Chevreuse, 1995, Nilsson L-O, Ollivier J P (eds), RILEM Publications, Cachan.
RILEM (2000), *Proc. 2nd International RILEM Workshop on Testing and Modelling Chloride Ingress into Concrete (RILEM PRO 19)*, Paris, 2000, Andrade C, Kropp J (eds), RILEM Publications, Cachan.
RILEM TC 154-EMC (2003), 'Half-cell potential measurements – Potential mapping on reinforced concrete structures', *Materials and Structures*, **36**, 461–471.
RILEM TC 154-EMC (2004), 'Test methods for on-site corrosion rate measurement of steel reinforcement in concrete by means of the polarization resistance method', *Materials and Structures*, **37**, 623–643.
RILEM (2005), *Proc. 3rd International RILEM Workshop on Testing and Modelling the Chloride Ingress into Concrete (RILEM PRO 38)*, Madrid, 2002, Andrade C, Kropp J (eds), RILEM Publications, Cachan.
Roberts M (1962), 'Effect of calcium chloride on the durability of pre-tensioned wire in prestressed concrete', *Magazine of Concrete Research*, **14**(42), 143–154.
Robery P (2004), 'A consulting engineer's view of repairs', *Institute of Concrete Technology Yearbook: 2004–2005*, 93–100.
Robinson H L (1987), 'Evaluation of coatings as carbonation barriers', *Construction Repair*, February, 12–18.
Sagues A, Powers R G (1997), 'Corrosion and corrosion control of concrete structures in Florida – What can be learned?' *Repair of Concrete Structures*, Svolvær, Norway, Blankvoll A (ed.), Norwegian Road Research Laboratory, Oslo, 49–58.
Sagues A, Powers R, Zayed A (1990), 'Marine environment corrosion of epoxy-coated reinforcing steel, *Corrosion of Reinforcement in Concrete*, Page C L, Treadaway K W J, Bamforth P B (eds), Society of Chemical Industry/Elsevier Applied Science, London, 539–549.
Sawada S, Page C L, Page M M (2005), 'Electrochemical injection of organic corrosion inhibitors into concrete', *Corrosion Science*, **47**, 2063–2078.
Schiessl P, Lay S (2005), 'Influence of cement composition', *Corrosion in Reinforced Concrete Structures*, Böhni H (ed.), Woodhead, Cambridge/CRC Press, Boca Raton, FL, pp. 91–134.
Schiessl P, Raupach M (1997), 'Laboratory studies and calculations on the influence of crack width on chloride-induced corrosion of steel in concrete', *ACI Materials Journal,* **94**(1), 56–62.

Sergi G (1986), 'Corrosion of steel in concrete: cement matrix variables', PhD Thesis, Aston University.

Sergi G, Page C L (2000), 'Sacrificial anodes for cathodic prevention of reinforcing steel around patch repairs applied to chloride-contaminated concrete', European Federation of Corrosion, Publication No 31, *Corrosion of Reinforcement in Concrete – Corrosion Mechanisms and Corrosion Protection*, Mietz J, Polder R, Elsener B (eds), IOM Communications, London, 93–100.

Sergi G, Yu S W, Page C L (1991), 'Diffusion of chloride and hydroxyl ions in cementitious materials exposed to a saline environment', *Magazine of Concrete Research*, **44**, 63–69.

Shah S P, Weiss W J (2000), 'High performance concrete: strength, permeability and shrinkage cracking', *Proc. PCI/FHWA International Symposium on High Performance Concrete,* Orlando, Florida, 331–340.

Short N R, Page C L, Glass G K (1991), 'A galvanic sensor for monitoring corrosion of steel in carbonated concrete', *Magazine of Concrete Research*, **43**, 149–154.

Short N R, Page C L, Glass G K (1994), 'Design and operation of a galvanic sensor for in-service monitoring of the corrosion of steel in concrete', *Proc. 2nd European Conference on Smart Structures and Materials*, McDonach A, Gardiner P T, McEwen R S, Culshaw B (eds), SPIE, Washington, Proceedings Vol. 2361, 172–175.

Soylev T A, François R (2003), 'Quality of steel-concrete interface and corrosion of reinforcing steel', *Cement and Concrete Research*, **33**, 1407–1415.

Sørensen B, Jensen P B, Maahn E (1990), 'The corrosion properties of stainless steel reinforcement', *Corrosion of Reinforcement in Concrete*, Page C L, Treadaway K W J, Bamforth P B (eds), Society of Chemical Industry/Elsevier Applied Science, London, pp. 601–610.

Spinks J W T, Baldwin H W, Thorvaldson T (1952), 'Tracer studies of diffusion in set Portland cement', *Canadian Journal of Technology*, **30**, 20–28.

Stern M, Geary A L (1957), 'Electrochemical polarization: 1. A theoretical analysis of the shape of polarization curves', *Journal of the Electrochemical Society*, **104**, 56–63.

Stern M, Weisert E D (1958), 'Experimental observations on the relations between polarization resistance and corrosion rate', *Proc. American Society for Testing and Materials*, **59**, 1280–1291.

Stratfull R F (1974), 'Experimental cathodic protection of a bridge deck', *Transportation Research Record*, **500**, 1–15.

Tang L (1996), 'Chloride transport in concrete – measurement and prediction', PhD Thesis, Chalmers University, Gothenburg.

Taylor H F W (1997), *'Cement Chemistry'*, 2nd edition, Thomas Telford, London.

Thomas M D A, Matthews J D (2004), 'Performance of pfa concrete in a marine environment', *Cement and Concrete Composites*, **26**, 5–20.

Treadaway K W J, Cox R N, Brown B L (1989), 'Durability of corrosion resisting steels in concrete', *Proc. Inst. Civ. Engnrs.*, Part 1, **86**, 305–331.

Tritthart J (2003), 'Transport of a surface-applied corrosion inhibitor in cement paste and concrete', *Cement and Concrete Research*, **33**, 829–834.

Truc O (2000), 'Prediction of chloride penetration into concrete – Multi-species approach', PhD Thesis, Chalmers University, Gothenburg.

Tuutti K (1982), *Corrosion of Steel in Concrete*, Report Fo 482, Swedish Cement and Concrete Institute, Stockholm.

Vassie P R W (1984), 'Reinforcement corrosion and the durability of concrete bridges', *Proc. Institution of Civil Engineers, Part 1,* **76**, 713–723.

Vennesland Ø, Humstad E P (1996), 'Electrochemical removal of chlorides from concrete: Effect on bond strength and removal efficiency', *Corrosion of Reinforcement in Concrete Construction*, Page C L, Bamforth P B, Figg J W (eds), Society of Chemical Industry/Royal Society of Chemistry, Cambridge, 448–455.

Virmani P, Clemena G G (1998), *Corrosion Protection: Concrete Bridges*, Report No. FHWA-RD-98-088, US Department of Transportation, Federal Highway Administration, McLean, VA (http://www.tfhrc.gov./structur/corros/corros.htm).

Wang Y, Li L Y, Page C L (2005), 'Modelling of chloride ingress into concrete from a saline environment', *Building and Environment*, **40**, 1573–1582.

Wierig H-J (1984), 'Longtime studies on the carbonation of concrete under normal outdoor exposure', *Proc. RILEM Seminar on Durability of Concrete Structures under Normal Outdoor Exposure*, Hannover, 239–249.

Wowra O, Setzer M J (2000), 'About the interaction of chloride and hardened cement paste', *Proc. 2nd International RILEM Workshop on Testing and Modelling the Chloride Ingress into Concrete*, Andrade C, Kropp J (eds), RILEM Publications, Cachan, 3–12.

Wyatt B S (1993), 'Anode systems for cathodic protection of reinforced concrete', *Cathodic Protection: Theory and Practice*, Ashworth V, Googan C (eds), Ellis Horwood, Chichester, 293–311.

Yeomans S R (1994), 'Performance of black, galvanized, and epoxy-coated reinforcing steels in chloride-contaminated concrete', *Corrosion*, **50**(1), 72–81.

Yeomans S R (2002), 'Galvanized reinforcing steel', *Corrosion Management*, **11**(2), 3–6.

Yonezawa T, Ashworth V, Proctor R P M (1988), 'Pore solution composition and chloride effects on the corrosion of steel in concrete', *Corrosion*, **44**(7), 489–499.

Yu S W (1990), 'Ionic and molecular diffusion in cementitious materials', PhD Thesis, Aston University.

Yunovich M, Thompson N G (2003), 'Corrosion of highway bridges: economic impact and control methodologies', *Concrete International*, **25**(1), 52–57.

Zimmermann L, Schiegg Y, Elsener B, Böhni H (1997), 'Electrochemical techniques for monitoring the conditions of concrete bridge structures', *Repair of Concrete Structures*, Svolvær, Norway, Blankvoll A (ed.), Norwegian Road Research Laboratory, Oslo, 213–222.

6

Degradation of prestressed concrete

U NÜRNBERGER and G SAWADE, University of Stuttgart, Germany and B ISECKE, Federal Institute for Materials Research and Testing, Germany

6.1 Introduction

Most of the prestressed concrete structures built during the last 50 years, where design and construction have adhered to best practice, have proved to be highly durable.[1,2] Analysing the incidence of occasional problems has confirmed that serious failures are rare in proportion to the volume of prestressing steels used worldwide. During the past 40 years, there have been isolated examples of serious failure in post-tensioned and pre-tensioned components (Fig. 6.1).[1,3–7] These failures happened either before tension members were grouted (during construction), or during later use, and have been attributed to corrosion – more precisely to stress corrosion cracking in high-strength prestressing steel. In recent years, several serious corrosion-related failures have occurred[5–9] and problems relating to the durability of prestressed concrete structures have become the subject of renewed discussion among all involved in the construction process.

The major factors that reduce durability are inadequate design (poor construction), incorrect execution of the planned design (poor workmanship), unsuitable mineral-based building materials, and the use of unsuitable post-tensioning system components, including inappropriate types of prestressing steel. Inadequate design and poor workmanship mean that corrosion control will not be effective. Components will deteriorate rapidly due to environmental influences such as carbonation or chloride ingress, and the anticipated lifetime will be shortened. Unsuitable building materials will also promote corrosion and/or stress corrosion cracking. Sensitive prestressing steels cannot withstand even normal building-site conditions without the risk of failure during use.

Most corrosion defects are caused by water, which seeps through zones of porous concrete or into vulnerable areas such as leaking seals, joints, anchorages or cracks. The water then flows through the network of ducts, depending on the quality of grouting. The major threat is corrosion due to chlorides, which originate from either de-icing salts or seawater.

6.1 Collapse of southern outer roof of Berlin Congress Hall.

Fractures in prestressing steel and failures of prestressed concrete structures can, as a rule, be attributed to corrosion-induced cracking. The mechanism of these failures is often not well understood, so it is difficult to establish the necessary recommendations for design, building materials and prestressing systems that would prevent future problems.

This chapter presents a survey of degradation of prestressed concrete, highlighting the following features:

- development of pre- and post-tensioned forms of construction
- types and metallurgical characteristics of prestressing tendons
- forms and mechanisms of corrosion-assisted failure in prestressing steels
- reasons for failure in prestressing steel and severe failure cases in structures, with a particular emphasis on post-tensioning tendons
- advances in corrosion control measures for prestressed steel and
- structural health monitoring techniques.

6.2 Forms of prestressed concrete constructions

6.2.1 General

Two different methods exist for assembling and prestressing steel tendons:[10] (i) pre-tensioning, where the prestressed tendons are surrounded directly by concrete, and (ii) post-tensioning, where the prestressing steels run along ducts which are then filled by injection with mortar. A third method, unbonded tendons in greased ducts, is a new technique that has several advantages over traditional post-tensioning with bonding.

Post-tensioned construction has been a very important technique for many years, especially in the construction of bridges and storage tanks, due to its decisive technical and economic advantages. The most important advantages offered by post-tensioning are:

- slimmer designs which provide a considerable saving in concrete and steel compared with reinforced concrete

- smaller deflections than with steel and reinforced concrete
- good crack behaviour, which tends to protect the steel against corrosion
- almost unchanged serviceability even after considerable overload, since temporary cracks close again after the overload has disappeared and
- high fatigue strength, since the amplitude of the stress changes in the prestressing steel under alternating loads are quite small.

For the above reasons, post-tensioning is used in many aspects of building construction. In addition to the general features of post-tensioned construction, post-tensioned slabs have several advantages over reinforced concrete slabs, including:

- structures are more economical due to the use of prestressing steels with a very high tensile strength instead of normal reinforcing steels
- larger spans and greater slenderness; the latter results in reduced dead load, which also has a beneficial effect on the columns and foundations, reducing the overall height of buildings or enabling additional floors to be incorporated in buildings of a given height
- very good behaviour under permanent load in terms of deflections and cracking
- higher punching shear strength with appropriate layout of tendons and
- considerable reduction in construction time due to use of pre-formed elements.

6.2.2 Historical review

Although some early post-tensioned slab structures were constructed in Europe, the first real development of this method took place in the USA and Australia. The first post-tensioned slabs were erected in the USA in 1955, using unbonded post-tensioning. In succeeding years, numerous post-tensioned slabs were designed and constructed for use in the lift slab method of construction. Post-tensioning enabled the lifting weight to be reduced and deflection and cracking performance to be improved. Theoretical studies and experiments on post-tensioned plates were undertaken, and the joint efforts of researchers, design engineers and prestressing firms resulted in the introduction of standards and recommendations which helped to promote the widespread use of this form of construction in the USA and Australia. To date, more than 50 million m^2 of slabs have been post-tensioned in the USA alone.

In Europe, the early 1970s saw a renewed interest in this form of construction, with some structures completed in Great Britain, the Netherlands and Switzerland. Intensive research work, especially in Switzerland, the Netherlands and Denmark and more recently in the Federal Republic of Germany, has expanded our knowledge of the behaviour of such structures. These studies form the basis for standards now in existence or in preparation in

several countries. The method is now fully recognised in Europe and has already found considerable application, especially in the Netherlands, Great Britain, Switzerland and Germany.

6.2.3 Post-tensioning with or without bonding of tendons

Bonded post-tensioning

In this method, the prestressing steel is placed in ducts and, after stressing, is bonded to the surrounding concrete by grouting with cement suspension. Round corrugated ducts are normally used. For the relatively thin floor slabs of buildings, however, round ducts would reduce possible eccentricity of the prestressing steel too much, particularly at cross-over points, so flat ducts are better. They normally contain tendons comprising four strands of a nominal 13 mm diameter, a design which has proved effective in most construction applications.

Unbonded post-tensioning

In the early stages of development of post-tensioned concrete in Europe, post-tensioning without bonding was also used in a few structures (for example, in 1936/37 in a bridge constructed in Aue/Saxony in Germany according to a design by Dischinger, and in 1948 for the Meuse Bridge at Sclayn in Belgium, designed by Magnel). After a period without any substantial applications, unbonded post-tensioning has once again been used for some important structures in recent years.

In the first applications in building work in the USA, prestressing steel was greased and wrapped in paper, to facilitate its longitudinal movement during stressing. More recently, the following method for sheathing the steel has generally become common. The strand is first given a continuous film of permanent corrosion-preventing grease in a continuous operation, either at the manufacturer's works or at the prestressing firm. A plastic tube of polyethylene or polypropylene of at least 1 mm thickness is then extruded over this. The plastic tube forms the primary and the grease the secondary form of corrosion protection. Strands sheathed in this manner are known as monostrands. The nominal diameter of the strands is 13 mm or 15 mm, the latter becoming more common in recent years.

Bonded or unbonded tendons

The question of whether bonded or unbonded tendons are preferable was and still is debated frequently. The subject will not be discussed in detail here, but the most important arguments for and against will be listed. Arguments in favour of post-tensioning *without* bonding include the following:

- Maximum possible tendon eccentricities, since tendon diameters are minimal; of special importance in thin slabs.
- Prestressing steel protected against corrosion as soon as it leaves the factory.
- Simple and rapid placing of tendons. Very low losses of prestressing force due to friction.
- Grouting operation is eliminated.
- In general more economical.

Arguments for post-tensioning *with* bonding include the fact that local failure of a tendon (due to fire, explosion, earthquakes, etc.) has only limited effects on the overall performance of the slab.

In the USA, post-tensioning without bonding is used almost exclusively, whereas post-tensioning with bonding is employed more widely in Australia and Europe. Among the arguments for bonded post-tensioning, the better performance of the slabs in failure conditions is frequently emphasised. It has, however, been demonstrated that equally good structures can be achieved with unbonded post-tensioning by suitable design and construction techniques. Local circumstances (such as prevailing national standards) may become the decisive factor in the choice of one type of post-tensioning over the other.

6.3 Types and metallurgical characteristics of prestressing steel

6.3.1 Requirements and properties

Prestressing steels[10] are used in prestressed concrete elements which are under tensile stresses due to their dead weight and service loads.[11] The prestressing applied should prevent or permit only to a limited extent (partial prestressing) tensile stresses occurring within the concrete. Prestressing steels are subjected to static stresses on which dynamic components are sometimes superimposed. The steels should have a high elastic limit (0.01% proof stress) so that the stressing loss (related to the initial prestressing) due to relaxation and shrinkage remains low. This related stressing loss is lower the higher the elastic elongation of the steel during prestressing, which depends on the absolute value of the elastic limit of the prestressing steel.

Very high yield stresses, or 0.2% proof stresses, and tensile strengths are necessary to ensure that sufficiently high steel straining and thus compression stresses in the concrete are conserved after the contraction processes in the concrete are complete. During long-term static tensile loading, inelastic straining can occur even at stresses lower than those in short-term loading. The extent of this straining depends on several factors – apart from the steel type – including the applied stress value, temperature and time. This long-term behaviour leads to a reduction of the initial stressing level, and this is compounded by contraction of the concrete due to shrinkage and creep. The long-term behaviour of steel can

be described either by creep (length change at constant stress) or relaxation (stress reduction at constant gauge length). Therefore, for prestressing steels, certain conditions concerning creep behaviour and relaxation must be met.

Loads from traffic may lead to tensile fatigue in the prestressing steels in prestressed concrete structures, which will be superimposed on the prestressing loads. As a result, certain requirements must be fulfilled with respect to fatigue strength. It has to be assumed that for all prestressing methods, the measures necessary for anchorage, for example bending, bulging and keying, will significantly reduce the fatigue strength of the prestressing steels used. The behaviour of prestressing steels in corrosive conditions is also of the utmost importance as all prestressing steels are prone to hydrogen-induced stress corrosion cracking, depending on the environmental conditions. All steels of this type should therefore be adequately resistant towards the initiation of hydrogen-induced cracks under site conditions and during service.

6.3.2 Production, dimensions and types of delivery

The yield strength (0.2% proof stress) of prestressing steels should be high to make their use effective and economical. Depending on the product type, different treatments can be used to increase the strength. Prestressing steels of up to 16 mm diameter are produced in wire rolling mills, wound into coils and used as wires or stranded wires. Diameters between 16 and 36 mm are also rolled and used as bars. For wires, there are two different methods for obtaining high yield strength values: quenching and tempering of low-alloyed steels, and cold straining by drawing unalloyed steel.

For the first method, the desired strength is reached by quenching and tempering wires hot-rolled into smooth or ribbed products. Continuous welded coils made of smooth or ribbed wires are austenitised, and subsequently quenched and tempered to achieve a fine-grained microstructure with finely dispersed precipitates. In the cold-straining method, steel wires hot-rolled in a smooth groove and with a ferritic–pearlitic microstructure are drawn through a die plate at ambient temperature. The reduction in cross-section leads to an increase of the dislocation density, which results in an increase of tensile and yield strength (or 0.2% proof stress), respectively. Some of the wires are subsequently cold-shaped. Finally, all cold-drawn wires are heated to moderate temperatures (annealed wires), some under tensile stress (stabilised wires).

Stranded wires are made from cold-drawn smooth wires using stranding machines with specified lengths of twist. The necessary heating (annealing) takes place after stranding, partly under tensile stress (stabilised stranded wires). Using offset welding of single wires, stranded wires can be produced in nearly unlimited length without reducing the load capacity.

The high yield strength of bars (usually >16 mm diameter) is achieved by a combination of two measures related to chemical composition and cold

straining. The chemical composition of these steels leads to a pearlitic microstructure after cooling from the rolling temperature; adding vanadium results in strengthening precipitations which lead to increasing yield strength values. Cold-straining by drawing and subsequent heating to temperatures of 250 to 350ºC, results in further improvements in the elastic limit and yield strength when compared to the as-rolled condition.

In addition to the methods for achieving high yield strength values, all cold deformed prestressing steels are annealed to moderate temperatures in order to improve long-term behaviour under fatigue loading conditions. For drawn wires and stranded wires, this process is mostly done under tensile stresses to modify unfavourable relaxation behaviour.

To achieve sufficient fatigue strength in ribbed and shaped bars, the geometry of the ribs is also significant, and there are special requirements, depending on the dimensions of the bars, in particular for maintaining minimum radii at the transition of the cross-sections to avoid significant stress concentrations in these areas. Table 6.1 gives an overview of standard approved prestressing steels while Table 6.2 shows examples of the chemical composition of standard prestressing steels.

6.4 Mechanisms of corrosion-assisted brittle fracture[12,13]

The type and manner of corrosion are essential influencing factors affecting the behaviour of prestressing steels under unforeseen or inappropriate service conditions. Simply determining that corrosion was involved does not analyse a failure sufficiently, nor will it help in future damage prevention. Depending on the prevailing corrosion situation and the load conditions, as well as the prestressing steel properties, the following kinds of fracture can be distinguished:

- Brittle fracture due to exceeding the residual load capacity. Brittle fracture is particularly promoted by:
  - local corrosion attack (pitting), and
  - hydrogen embrittlement.
- Fracture as a result of stress corrosion cracking, where we distinguish between:
  - anodic stress corrosion cracking, and
  - hydrogen-induced stress corrosion cracking.
- Fracture as a result of fatigue and corrosion influences, distinguishing between:
  - corrosion fatigue cracking, and
  - fretting corrosion/fretting fatigue.

In the following sections, these types will be described in more detail with regard to prestressed concrete construction.

Table 6.1 Prestressing steels and their mechanical properties

Product			Steel grade		Nominal values for the mechanical properties			
Type	Surface	Dia. (mm)	Short name[a]	Condition of treatment	Elastic limit[b] (N/mm^2)	0.2%, proof stress (N/mm^2)	Tensile strength (N/mm^2)	Elongation after fracture A_{10} (%)
Bar steel, round	Smooth or ribbed[c]	26–36	St 835/1031	Hot-rolled, strained and tempered	735	835	1030	7
		15	St 885/1080		735	885	1080	7
		26–36	St 1080/1230		950	1080	1230	6
Wire, round	Ribbed	16	St 1325/1470	Quenched and tempered	1175	1325	1470	6
	Smooth or ribbed	6–14	St 1420/1570		1220	1421	1570	6
	Smooth	8–12.2	St 1375/1570	″	1130	1375	1570	6
	Smooth or shaped	5.5–7.5	St 1470/1670	Cold-drawn	1225	1471	1670	6
	Smooth or shaped	5.0–5.5	St 1570/1770	″	1325	1570	1770	6
Wire, flat	Shaped	4.5×10 to 7.9×15.5	St 1420/1570	Quenched and tempered	1220	1420	1570	6
Strand	7-wires	9.3–18.3	St 1570/1770	Cold-drawn	1150	1570	1770	6

[a] the two numbers represent the nominal values for 0.2% proof stress and tensile strength in N/mm^2
[b] 0.01% limit of elongation
[c] thread ribs

Table 6.2 Chemical composition of the prestressing steels in use

Type of prestressing steel	Reference data for the chemical composition[a]				
	% C	% Si	% Mn	% Cr	% V
Wire, quenched and tempered	0.5	1.6	0.6	0.4	–
Wire and stranded wire, cold-drawn	0.8	0.2	0.7	–	–
Bar steel	0.7	0.7	1.5	–	0.3[b]

[a] according to ladle analysis
[b] only for St 1080/1230

6.4.1 Brittle fracture

Brittle fracture may occur in high-strength steels, particularly under the influence of rapidly applied tensile stress. This is the case in prestressing steels when there is a fracture under loads below those corresponding to the permissible prestrain, due to:

- stress concentration in local notches (e.g., corrosion pits)
- high stressing speed and low temperature and/or
- embrittlement of the steel structure after hydrogen absorption (hydrogen embrittlement).

Influence of corrosion

Uniform corrosion (e.g., after prolonged weathering on a building site) generally does not have any major impact on load-bearing capacity unless the cross-section is substantially reduced. Reduction in cross-section may happen if prestressing steels in ungrouted tendon ducts are exposed over a long period of time to water and oxygen via non-airtight anchorages or construction joints. If, however, the prestressing steel suffers local corrosion attack in the form of pitting corrosion, the load-bearing capacity may fail at an early stage due to brittle fracture (Fig. 6.2). The following effects are capable of triggering such attacks in prestressing steel:

- The presence of contaminated water in the yet-to-be injected ducts of post-tensioning tendons, which results from bleeding of the concrete during construction. The steel may suffer from severe pitting corrosion in the ungrouted and non-prestressed condition, and the load-bearing capacity can be reduced considerably. Bleeding is the separation of fresh concrete, when the solid content sinks down and displaced water rises or penetrates the inner hollows. The separated water may contain significantly high amounts of sulfates and chlorides (Table 6.3) due to leaching of the construction materials, cement,

6.2 Brittle fracture as a result of chloride-assisted corrosion attack.

aggregates and water. The high sulfate concentration results from the gypsum in the cement. The watery phase of fresh concrete penetrates into the ducts through the anchorages, couplings and defects in the steel sheet of the duct and accumulates at the deepest points. The alkaline water carbonates quickly in the presence of air. The steel can therefore suffer from intense pitting even before being prestressed and grouted, which can lead to pitting depths of up to 1 mm within a few weeks.

- Ingress of water containing chloride in a non-grouted tendon duct, e.g. above non-airtight anchorages or joints, may lead to damaging local corrosion in the prestressing steel throughout its lifetime (Fig. 6.2). Comparable attacks must be expected where the concrete cover is too thin or too permeable and so permits chloride salts to penetrate to the tendon.

The performance characteristics of corroded prestressing steels can be determined in tensile, fatigue and stress corrosion tests[14] (Fig. 6.3). Tests to establish the residual load-bearing capacity are carried out on damaged prestressing steel samples, for instance as part of the inspection of older buildings, and help provide the information necessary for effective repair. High strength prestressing steels are far more sensitive to corrosion attack than reinforcing steels. This sensitivity

Table 6.3 Analysis of bleeding water[25]

sulfate	1.90–5.20	g/l
chloride	0.13–0.18	g/l
calcium	0.06–0.09	g/l
sodium	0.18–0.37	g/l
potassium	3.60–7.30	g/l
thiocyanate	0.13–0.50*	g/l
pH-value	10–13	

* thiocyanate was found only in a special case (see Section 6.5.1, unsuitable mineral building materials).

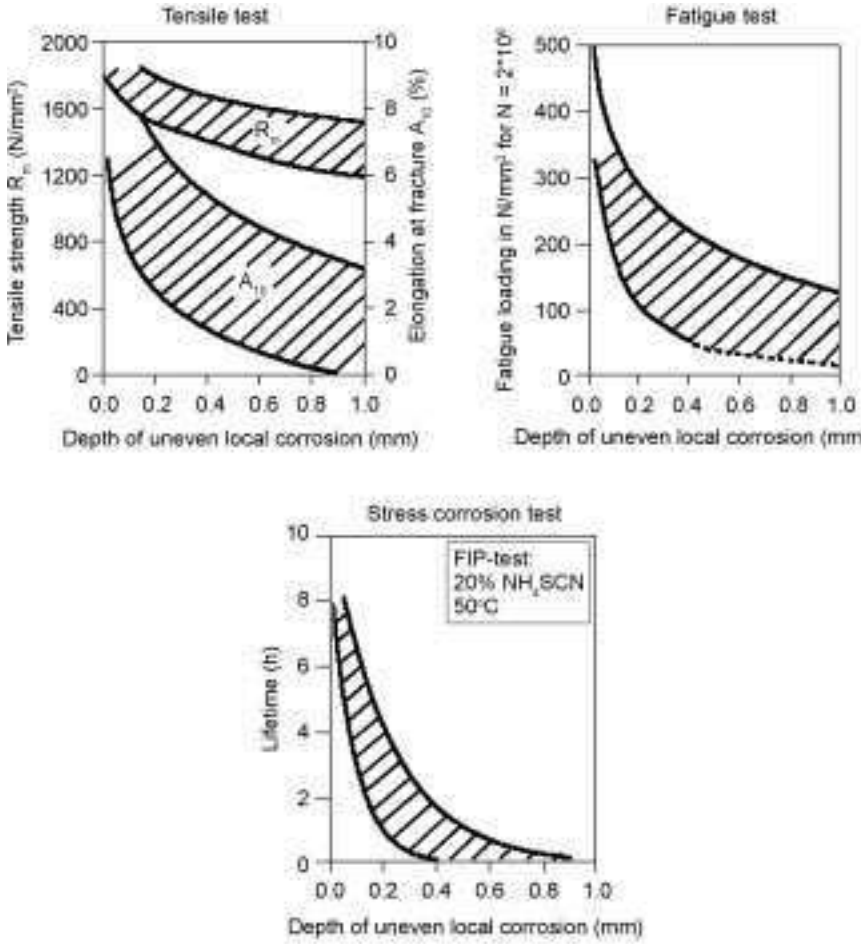

6.3 Properties of cold-deformed prestressing steel wires (tensile strength 1770 N/mm^2), $dS = 5$ mm, in relation to depth of uneven local corrosion[14] (scattering of 90% of the test results).

is revealed by testing with tensile testing being less effective than fatigue tests which, in turn, are less sensitive than stress corrosion tests. In the case of uneven local corrosion, a corrosion depth of 0.6 mm may be enough to cause breakage in a cold-deformed wire under tension at 70% of the specified tendon strength of about 1800 N/mm^2 (Fig. 6.3, tensile test). At pitting depths greater than 0.2 mm, cold-drawn wires may show fatigue limits (fatigue limits for stress cycles of $N = 2 \cdot 10^6$) of 100 N/mm^2 or less (Fig. 6.3, fatigue test). As-new smooth surfaced steels normally show a fatigue limit of more than 400 N/mm^2.

Of all the performance characteristics of prestressing steels, local corrosion has the most detrimental effect on the susceptibility to hydrogen-induced corrosion cracking. In a test developed by FIP (see Section 6.6), the prestressing steel

is immersed under tension in an ammonium thiocyanate solution and a minimum and average time of exposure before failure is specified. For cold-drawn wire and strands, these values are of the order of 1.5 and 5 hours respectively. In the example shown in Fig. 6.3 (stress corrosion test), these lifetimes are not achieved at corrosion depths of > 0.2 mm.

Effect of hydrogen (hydrogen embrittlement)

In a specific corrosion situation, prestressing steel corrosion may cause atomic hydrogen to be cathodically discharged. These hydrogen atoms are then absorbed by the prestressing steel, which, if prestressed at the same time, may suffer hydrogen-induced stress corrosion cracking (Section 6.4.2). If the prestressing steel is free of any tensile stresses (not prestressed), hydrogen can be absorbed if corrosion has occurred. The steel will not crack but, depending on the quantity of hydrogen absorbed and the specific hydrogen sensitivity of the alloy concerned, the prestressing steel may become brittle. This adverse effect on the mechanical characteristics[15] is more serious in its influence on the deformation properties than on the tensile strength (Fig. 6.4).

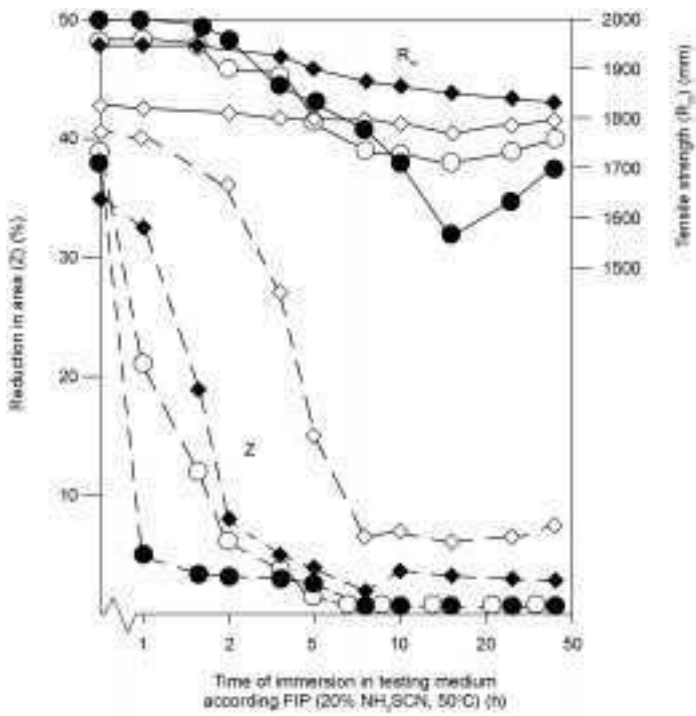

6.4 Tensile strength (R_m) and reduction in area (Z) of cold deformed prestressing steel wires (4 steel melts) after charging with hydrogen.[15]

Fractures in prestressing steel resulting from corrosion-induced hydrogen embrittlement may occur, for instance, when prestressing to a high stress level, or shortly after the prestressing, when the steel has spent some time in unfavourable corrosion conditions and has therefore absorbed high quantities of hydrogen. If steel tendons are properly and swiftly processed, however, such damage should not occur.

6.4.2 Fractures due to stress corrosion cracking

The term ‘stress corrosion’ stands for the process of crack initiation and crack propagation under the influence of a specific corrosive environment and static tensile stresses. It is characterised by cracking without deformation, often without apparent steel degradation and without visible corrosion products. The residual internal stresses already present contribute to the tensile stresses necessary for cracking. Contrary to other types of corrosion, the failure of construction elements due to cracking is not necessarily connected to any noticeable earlier damage. The brittle stress corrosion fracture initiates at one or more points on the steel surface perpendicular to the applied normal stress (Fig. 6.5). An ellipsoidal initial fracture zone is distinguished, which represents the region of crack initiation, together with a zone of crack propagation over the remainder of the fracture surface.

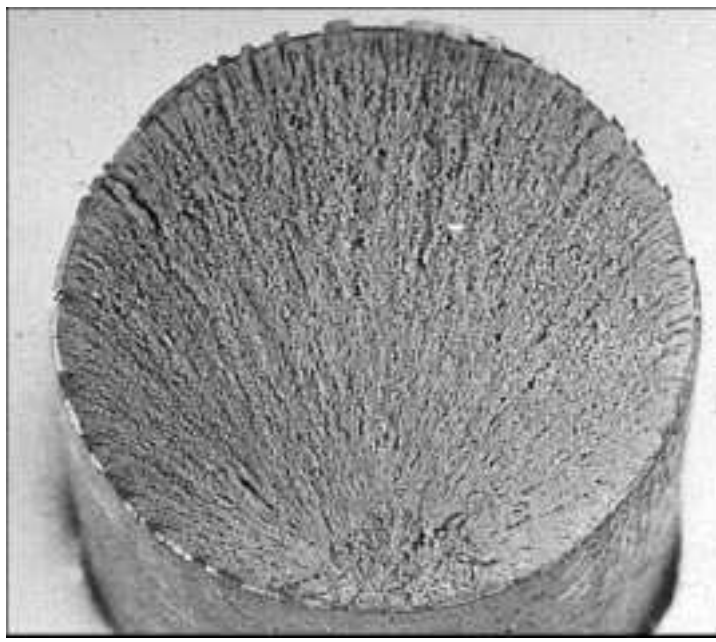

6.5 Fracture of a high strength steel bar because of stress corrosion cracking.

Anodic stress corrosion cracking

In the presence of nitrate-containing, non-alkaline electrolytes (pH-value < 9) unalloyed and low-alloy steels may suffer from anodic stress corrosion cracking. Crack formation and crack propagation are due to selective metal dissolution (e.g., along grain boundaries of the steel structure) with simultaneous high tensile stresses.[6] In certain uses of prestressed concrete, e.g. fertiliser storage and stable buildings, the environmental conditions causing this kind of cracking can be anticipated. For brickwork in stables, saltpetre $Ca(NO_3)_2$ may be formed by urea. In the presence of moisture, the nitrates may diffuse into the concrete and may cause stress corrosion cracking in pretensioned concrete components, affecting the tension wires if the concrete cover is carbonated, which occurs in poor quality concrete.[16,17] Nitrate sensitivity is a pre-condition for anodic stress corrosion cracking in prestressing steels. Low-carbon steels are very susceptible to nitrate-induced stress corrosion cracking. The prestressing steels currently in use, however, are highly resistant to this type of corrosion.[18]

Hydrogen-induced stress corrosion cracking[6,7,19–22]

Mechanism

Fractures in prestressing steel that are referred to as hydrogen-induced stress corrosion cracking (H-SCC) may occur during the erection of the construction or during later use. The following conditions are necessary:

- a sensitive material or appropriate environmental conditions
- a sufficient tensile load and
- at least a partial corrosion attack.

The risk of fracture due to H-SCC therefore results from a combination of the properties of the prestressing steel and environmental parameters. No special agent is needed for crack initiation: water or condensation water may suffice.[20,23] What is required for H-SCC is the presence of adsorbed atomic hydrogen, which is present under certain corrosion conditions in neutral and, particularly, acidic aqueous media through the cathodic partial reaction within corrosion cells.

During the corrosion process, hydrogen atoms are released from the water and then absorbed by the steel. In prestressing steels, hydrogen under mechanical stresses can create precracks in critical structural areas such as grain boundaries. These cracks may grow and result in fracture (Fig. 6.6). Atomic hydrogen released on the steel surface can be absorbed and enriched by diffusion in multiaxially stretched plastic zones, crack tips, corrosion pits and precipitates in the steel structure. Reduction in the cohesive strength of the metal lattice permits sufficient concentrations of hydrogen to dissolve in critical regions of the steel, which can cause the development of very fine cracks, resulting in ‘sub-critical’

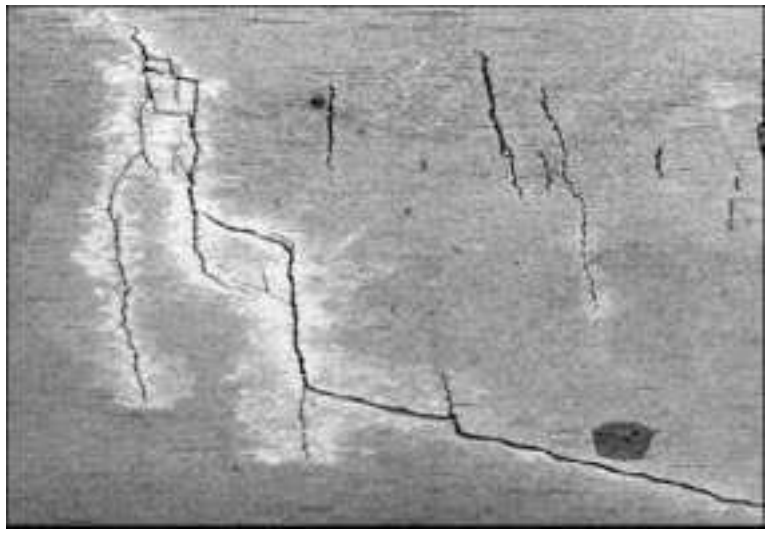

6.6 Hydrogen-induced cracking of cold deformed wire.

crack growth. In the case of prestressing steel, the development of this type of damage is influenced by the susceptibility of the alloy. Stress corrosion tests performed in solutions containing thiocyanate (SCN^-) determine the relative susceptibility of prestressing steels (Section 6.6). One can assume that the more sensitive a prestressing steel is to H-SCC, the lower the critical content of hydrogen that will lead to crack propagation. Increasing the hydrogen content of the steel and increasing tension will promote hydrogen-assisted cracking, but there are steels that do not inevitably fail under the influence of high hydrogen content.

Special conditions have to exist to activate the formation of absorbable hydrogen. To understand the correlations between procedures on site and development of damage, the chemical reactions of corrosion should be considered (Table 6.4). Harmful hydrogen can arise only:

- if the steel surface is in an active state or depassivated (this is expressed by reaction 1 in Table 6.4)
- if the cathodic reaction of corrosion is discharging hydrogen ions (this is described by reaction 3 in Table 6.4) or water decomposition (this is described by reaction 4 in Table 6.4) and
- if the adsorbed atomic hydrogen is not changed into the molecular state (see reaction 5 in Table 6.4).

A reduction in available oxygen may encourage formation of adsorbed atomic hydrogen (which hinders reaction 6 in Table 6.4). At the surface of corroding steel, the amount of absorbable hydrogen atoms rises:

Table 6.4 Chemical reactions of corrosion

Anodic iron dissolution	
$Fe \rightarrow Fe^{2+} + 2e^-$	reaction 1
Cathodic reactions	
if pH > 7	
$½\ O_2 + H_2O + 2e^- \rightarrow 2OH^-$	reaction 2
if pH < 7	
$H^+ + e^- \rightarrow H_{ad}$ (hydrogen discharge)	reaction 3
if potential is low	
$H_2O + e^- \rightarrow H_{ad} + OH^-$ (water decomposition)	reaction 4
Rivalry reaction with regard to → and ↓	
$2\ H_{ad} \rightarrow H_2$ (recombination)	reaction 5
is prevented in the presence of promoters	
$2\ H_{ad} + ½\ O_2 \rightarrow H_2O$	reaction 6
if oxygen is present	

- with increasing hydrogen concentration (reaction 3 or 4 is accelerated)
- in the presence of so-called promoters (reaction 5 is hindered)
- in an electrolyte with low oxygen concentration (reaction 6 is hindered).

From a practical point of view, hydrogen-assisted damage is favoured:

- in acid media (reaction 3 is accelerated) or if the steel surface is polarised to low potentials, e.g. if the prestressing steel has contact with zinc or galvanised steel (reaction 4 is possible)
- in the presence of promoters such as sulfides, thiocyanates or compounds of arsenic or selenium (reaction 5 is hindered) or
- in crevices, because the electrolyte in the crevice will have a low oxygen concentration (reaction 6 is hindered).

In concrete structures, the attacking medium is mostly alkaline, and acids are rare. The promoters mentioned above are significant factors, however, as they prevent the recombination of hydrogen atoms to form molecular hydrogen. For prestressing steels, sulfides and thiocyanates are particularly important.[3,20,24–26] Contaminants or active ingredients in building materials which act as promoters for hydrogen absorption can accelerate crack initiation in sensitive steels considerably, even at very low concentrations.[25,27,28] Such substances dissolved in water are used to test how susceptible prestressing steels are to hydrogen-induced cracking.

In natural environments pitting-induced H-SCC can occur (Fig. 6.7). Pitting-induced H-SCC is when a crack initiates in a corrosion pit on the steel surface. Corrosion pits often form under drops of water and where alkaline salt-enriched media are found in concrete constructions (e.g., partly carbonated bleeding

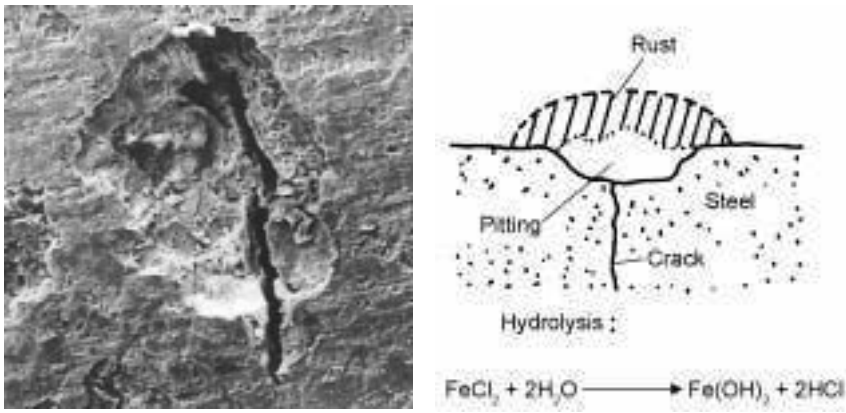

6.7 Pitting induced stress corrosion cracking.

water), (Table 6.3). In the corrosion pits, the pH falls because the Fe^{2+}-ions are hydrolysed.

$$FeCl_2 + H_2O \rightarrow Fe(OH)_2 + 2HCl \qquad 6.1$$

Pitting or spots of local corrosion can be explained by differential aeration or concentration cells. Condensation water and salt-enriched aqueous solution (bleed water, Section 6.4.1) that occur when erecting constructions are the most significant threat.

In prestressed construction, local corrosion attacks are due to carbonation of concrete and mortar, or chloride contamination. In the case of sensitive prestressing steel, all but minimal concentrations of hydrogen can lead to irreversible damage, and a local corrosion attack too small to produce visible corrosion products on the steel surface may lead to fracture. All types of uneven local corrosion should be prevented to exclude failures due to hydrogen-assisted cracking. The occurrence of pulsating low frequency loads or service-related strain changes in the steels, including those at low strain rates, will also raise the risk of failure because these conditions favour the absorption of atomic hydrogen and thus H-SCC.[29]

Figure 6.8 compares the behaviour of a quenched and tempered prestressing steel sensitive to hydrogen in a stress corrosion cracking test with and without low amplitude (30–80 N/mm^2) fatigue loading.[30] The aqueous test solution contained 5 g/l SO_4^{2-} and 0.5 g/l Cl^- with and without 1 g/l SCN^- as a promoter for hydrogen absorption. The stress corrosion cracking test under static stress was carried out at 80% of the tensile strength. This stress corresponds to the constant maximum stress in the tensile fatigue test. Figure 6.8 represents the stress cycle number as a function of the amplitude, calculated at frequency $f = 5\,s^{-1}$, against lifetime in hours. The hydrogen-insensitive steel in the promoter-containing solution failed within a test period of 5000 hours in the static test, but did not fail in the promoter-free solution. In a low-amplitude

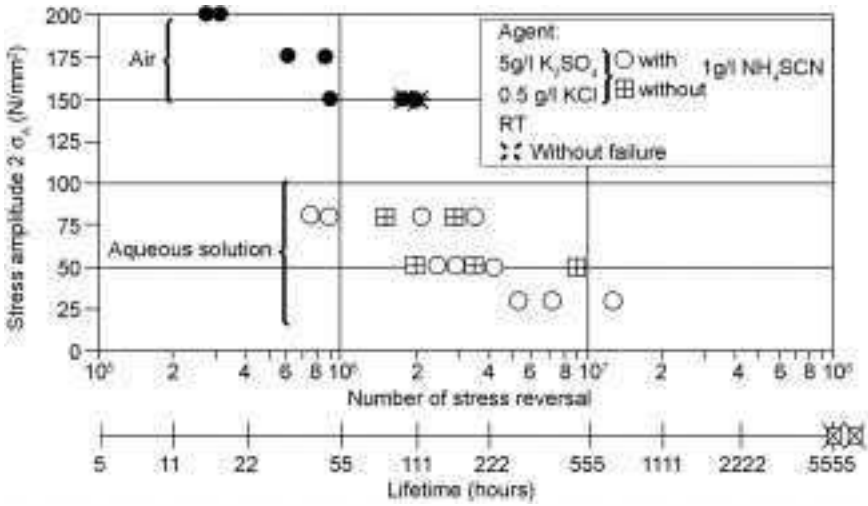

6.8 Stress corrosion-behaviour of prestressing quenched and tempered steel (strength 1420 N/mm^2), ∅12.2 mm without and with dynamic stress of low amplitude.[30]

fatigue test, the lifetime in the promoter-containing solution decreased progressively with rising amplitude. In the case of alternating stress, it is striking that fractures also occurred in steels in the promoter-free solution. These tests led to the conclusion that fatigue loadings at low amplitude or elongations tend to significantly increase the susceptibility of prestressing steels to stress corrosion cracking.

Susceptibility of prestressing steel

In the case of sensitive prestressing steel, the presence of very small amounts of hydrogen can lead to irreversible damage. Therefore the susceptibility of the steel to hydrogen is of enormous importance and prestressing steels are investigated using special stress corrosion tests (Section 6.6). The susceptibility of prestressing steels to hydrogen embrittlement depends on the chemical composition of the steel, the production process and subsequent treatment (e.g., thermal treatment). All types of prestressing steels mentioned in Section 6.3 (hot-rolled, quenched and tempered, cold-deformed steel) can be used without fear of corrosion problems if optimal characteristics are achieved. On the other hand, problems can occur with all types of steel if individual patches show production-induced deviations from optimal characteristics.

Some differences in susceptibility to hydrogen embrittlement between different steel types can be attributed to differences in their microstructures.[6,19] Hydrogen in the steel tends to diffuse to sites where the microstructure allows the largest degree of disturbance, i.e. to lattice imperfections and especially to

the grain boundaries. Hydrogen-induced cracks frequently run along the grain boundaries of the steel and, at the micro-level, are intergranular. Steel types where the majority of the grain boundaries are perpendicular to the applied forces are most at risk. This group includes hot-rolled and quenched and tempered steels. In the latter case, the austenite grain boundaries are of concern. In the case of cold-formed wires and strands, the deformed grain boundaries run predominantly in the direction of the applied force, hence the weakest points in the structure are not predominantly subjected to the most unfavourable effects of stress. This explains why, in the presence of high hydrogen supply, cold-drawn wires and strands manufactured from these types of wires perform better than hot-rolled and quenched and tempered steel.[31]

Substantial variability in susceptibility to H-SCC can be observed in different types of steel, depending on composition and/or thermal treatment. Sensitivity of steel structures to hydrogen embrittlement increases in the following order: pearlitic grades, quenched and tempered, bainitic steels formed by continuous cooling, and finally martensitic structures.[6] Because of the high sensitivity of martensitic steel, it is not used where there is any risk of hydrogen-induced stress corrosion cracking. Prestressing steels with bainitic structures have resulted in numerous structural failures (see Section 6.5) and the use of this steel in construction is no longer permitted.

With quenched and tempered steel, the martensite content can increase susceptibility to cracking due to internal stresses. The hardening and tempering process (thermal treatment) has a substantial influence on sensitivity to hydrogen.[23] In order to reduce this sensitivity, newer types of quenched and tempered prestressing steel have lower carbon content and added chromium. These modifications improve the through-hardening and tempering properties, and result in traces of residual martensite being practically excluded. In the new type of quenched and tempered prestressing steel, manganese content was decreased and silicon content was increased. As a consequence absorption, solubility and diffusivity of hydrogen was considerably diminished.[32,33]

Hydrogen sensitivity in prestressing steel is frequently related to the influence of segregating elements, and in particular their elimination from the grain boundaries or from their vicinity.[19] In particular this sensitivity is increased due to an interaction between hydrogen and the segregation products of phosphorus (P), antimony (Sb), tin (Sn), sulfur as sulfides (S) and arsenic (As).[34] The sulfur and arsenic compounds work as promoters for hydrogen absorption in the steel. In order to minimise harmful non-metallic inclusions and segregation at grain boundaries, substantial modifications of the production technology for prestressing steels have been made over the last 35 years to reduce the content of residual and trace elements. Today, sulfur and phosphorus are usually well below 0.015% and the arsenic content is below 0.005%.

The hardness or strength of steel is a major variable characteristic in pre-stressing steels that influences the susceptibility to hydrogen-induced stress

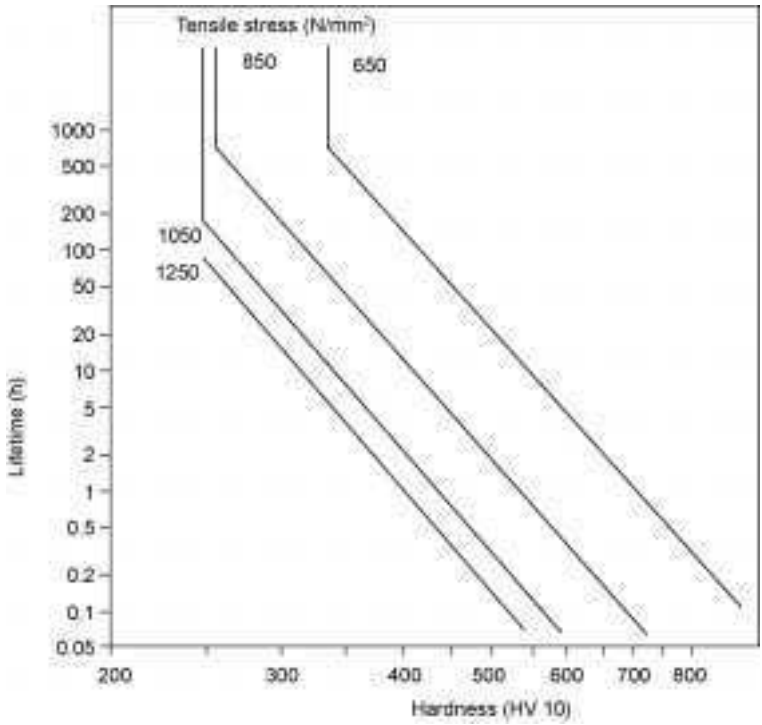

6.9 Influence of hardness and tensile stress on the lifetime of unalloyed steel in saturated H_2S-solution; the hardness is adjusted by C-content, cold-deforming or quenching and tempering (after Carius in ref. 6).

corrosion. Figure 6.9 shows the results of stress corrosion tests on high strength unalloyed steel in relation to hardness and tensile stress. Prestressing steels are situated in the Vickers hardness range of approximately HV 350 to HV 600. With decreasing tensile stress and decreasing hardness, service life increases. At constant stress, service life decreases in relation to hardness approximately as follows:

$$\text{HV } 250 : \text{HV } 350 : \text{HV } 450 : \text{HV } 550 = 1265 : 60 : 6 : 1$$

For prestressing steels in a certain steel grade (hot-rolled, quenched and tempered, cold-formed), the influence of hydrogen on crack formation increases with increasing strength[6,7,19,22,23] (Fig. 6.10). According to the relationship:[35,36]

$$L = \frac{C}{\sigma^3 \cdot {R_m}^9} \qquad 6.2$$

the lifetime L decreases with the 3rd power of the stress σ and the 9th power of the strength R_m (the factor C is a characteristic value for the material stability in the medium concerned). It has been shown, using the example of a hot-rolled prestressing steel and a required prestress of 800 N/mm^2, using greater amounts

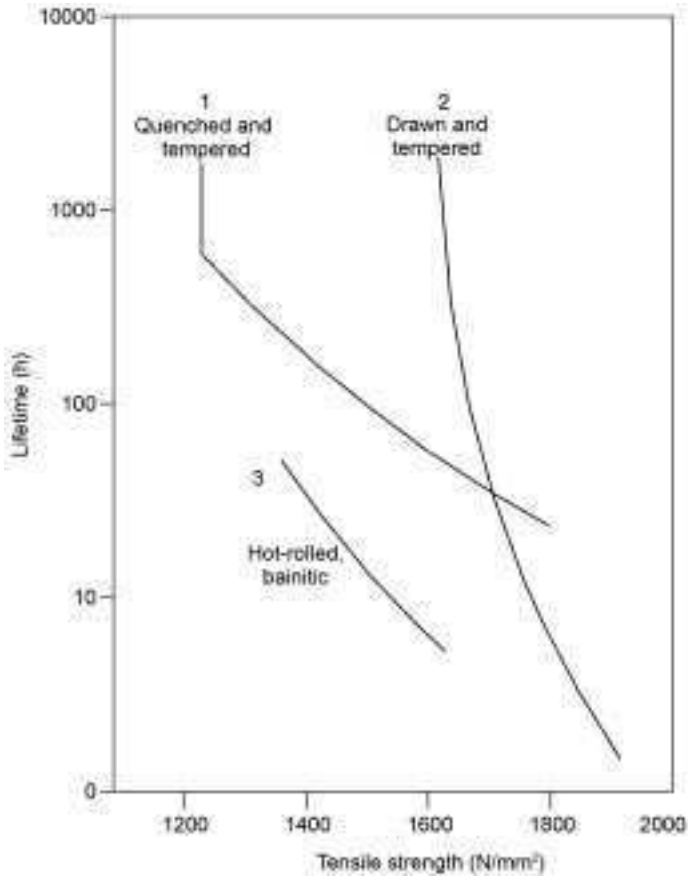

6.10 Influence of strength of prestressing steel on lifetime in stress corrosion test ($\sigma_0 = 0.8\ R_m$).[6]
1 – saturated H_2S-water
2, 3 – 20% NH_4SCN-solution (FIP-test).

of a low strength steel offers higher security against hydrogen-induced corrosion cracking than using smaller amounts of a high-strength steel.[37] Steel St 835/1030 had a 6.5 times longer service life at a higher stress level (0.75 R_m) than steel St 1080/1230 at a lower stress level (0.60 R_m).

These results suggest that increasing strength goes with an increased tendency towards hydrogen-induced stress corrosion in the presence of corrosion-promoting influences (water, carbonated concrete, chloride). Our own assessment of numerous stress corrosion tests conducted in accordance with the FIP-standard (see Section 6.6.2) showed that increasing the strength of cold-deformed steel from 1700 to 2000 N/mm^2 leads to a drop in the service life by a factor of 100. Based on these results, suggested maximum strengths for different steel types are:[6]

- hot-rolled ~ 1400 N/mm^2
- quenched and tempered ~ 1700 N/mm^2
- cold-drawn ~ 1950 N/mm^2

As a result of this, the maximum strength of prestressing steels is limited in Germany, and since about 1980 high strength steel rods St 1080/1320 (St 110/135) have been taken out of the prestressing steel market for the above reasons. The German objection to the new European standard for prestressing steels EN 10138 is for the same reasons.[38] In particular, German authorities object to the strength increase of cold-formed wires and strands produced particularly by some West European manufacturers of prestressing steel. It is recognised that this remains a controversial area which requires further investigation through such projects as the European COST Action 534 'New Materials and Systems for Prestressed Concrete Structures'.

6.4.3 Fractures due to fatigue and corrosion

Prestressing steels can only be subjected to a noticeable stress in dynamically strained reinforced concrete structures if the concrete is cracked.[39] The stress amplitudes of prestressing steel under high dynamic loads (e.g., high traffic load on a bridge) may then amount to >200 N/mm^2 in the crack region. In the non-cracked state, the steels will show stress ranges below 100 N/mm^2. Cracks may occur in partially prestressed concrete structures. Since such cracks tend to open and to close under the influence of a superimposed fatigue stress, a number of factors must be considered and these are discussed below.

Corrosion fatigue cracking

If corrosion-promoting aqueous media penetrate through a crack in the concrete to a dynamically stressed tendon, corrosion fatigue cracking is possible, although this type of corrosion has not been observed in prestressing steel construction so far. Corrosion fatigue cracking[6] occurs because a metallic material under dynamic stress in a corrosive medium (e.g., water or salt solution) will show much more unfavourable fatigue behaviour than a similar material under fatigue loading in air. Whereas steels exhibit a 'fatigue limit' when tested in dry air (i.e., a critical stress amplitude below which failure does not occur even after very large numbers of cycles are applied), this is not maintained in corrosive environments. A decrease in fatigue limit caused by corrosion is more distinct the higher the strength of the steel and the more aggressive the attacking medium. Hence high strength prestressing steels, when simultaneously attacked by, for instance, an aqueous chloride-containing medium, may show very unfavourable fatigue behaviour.

In traffic-carrying bridge structures, it is only the low-frequency stresses that lead to high stress amplitudes, an additional contributor to corrosion fatigue

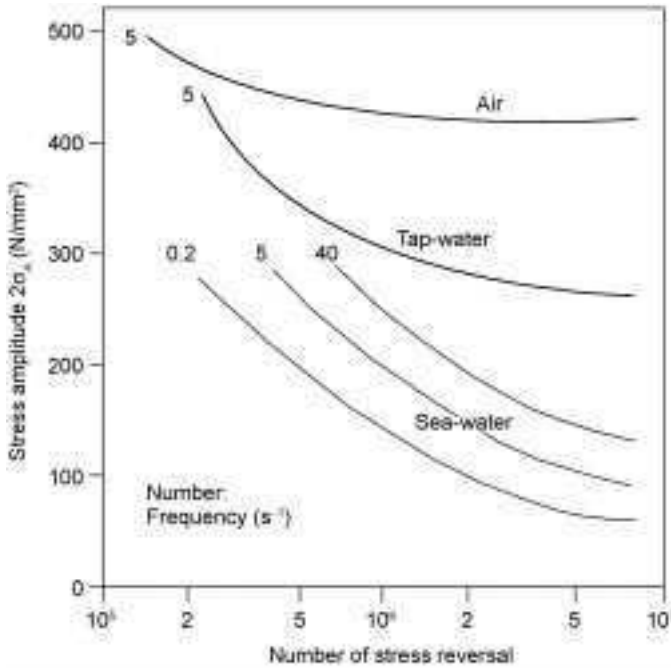

6.11 Fatigue behaviour under pulsating tensile stresses of cold-drawn prestressing steel wires ($R_m \approx 1750\,\mathrm{N/mm^2}$) in air and corrosion-promoting aqueous solutions.[6,29]

cracking. At lower frequencies, the influence of corrosion will increase and the fatigue limit will consequently drop. Figure 6.11 shows the decrease in corrosion fatigue limit for a cold-drawn prestressing steel wire in an air-water-chloride solution. For frequencies of $0.5\,\mathrm{s^{-1}}$ the fatigue limit for stress cycles of 10^7 is below $100\,\mathrm{N/mm^2}$. The problem of corrosion fatigue cracking in cracked components can be remedied by sufficient concrete cover and limiting the crack width. This keeps pollutants away from the prestressing steel surface.

Fretting corrosion/fretting fatigue

Cracks can occur in concrete due to fatigue loading displacements between the tendon and the injection mortar or the steel duct. In bent tendons, a high radial pressure acts simultaneously on the fretting prestressing steel surface. If air or oxygen reaches the fretting location through the concrete crack, fretting corrosion can occur.[6] Fretting corrosion is described as damage to a metal surface in a manner similar to wear due to oscillating friction under radial pressure with another surface. In the presence of oxygen, oxidation will occur at the reactive surface.

In fatigue-loaded steels subject to simultaneous fretting corrosion stress, fretting fatigue makes fatigue behaviour much worse.[40,41] This is attributable to

the occurrence of additional tensile stresses in the fretting area. In concrete embedded tendons, subjected to a relative movement and a radial pressure in the concrete crack between prestressing steel and duct or injection mortar respectively, tolerable fatigue limits of about 150 N/mm^2 for cycles to fracture of 2×10^6 were found.

In prestressed concrete constructions, the anchorages of the tendons also show a reduced fatigue limit as a result of fretting corrosion.[42] Under dynamic stress, the fatigue limit of the anchored tendon, depending on the type of anchorage, is reduced to between 80 and 150 N/mm^2. For this reason, anchorages are always positioned in areas of least stress changes. In fatigue experiments, the prestressing steels always fracture in the force transmitting area, i.e., at the beginning of the anchorage. Here, the fatigue limit is reduced due to relative movements between the prestressing steel and the anchor body under simultaneous high radial pressures. In prestressed concrete bridges, the coupling joints are particularly problematic. If such joints crack as a result of imposed stresses (e.g., due to non-uniform solar heating and insufficient reinforcement crossing the coupling joint), the tendon couplings will suffer major stress fatigue cycles from traffic loads, which can also lead to fractures in the prestressing steel due to the stress-sensitive couplings.

6.5 Case histories of structural collapses[2,3,5,12]

6.5.1 Reasons for failure of prestressing steel

Premature failure of prestressing steel in prestressed concrete structures is usually induced by corrosion. The most obvious type of failure occurs when high-strength steel fails because, in areas of corrosion pitting, its notched bar tensile strength is exceeded. In such a case, the failure is brittle in character (Section 6.4.1). The effect of local corrosion on the strength and deformation characteristics of a component is related to the type of prestressing steel used. Drawn steel is stronger than hot rolled steel which in turn is stronger than quenched and tempered steel.[14] In practice, pure brittle failures in prestressed concrete are rare,[3] and are not involved in the cases of spectacular failure discussed in Section 6.5.2. Pitting depths of at least 1 mm are required for notched-bar tensile strength to be lower than the actual stress applied to the steel.

The failure of prestressing steel in structures is predominantly attributable to hydrogen-induced stress corrosion cracking (pages 200–208). Stress corrosion in steel susceptible to hydrogen is promoted by conditions that enable the formation of atomic hydrogen on the steel surface. These conditions include:

- Activation or depassivation of certain regions of the steel surface.
- Conditions that promote pitting corrosion and the formation of shallow pits (e.g., sulfate and chloride attack).

- Presence of certain substances (so-called promoters), which prevent the harmful atomic hydrogen recombining to form harmless molecular hydrogen. Substances such as sulfur, arsenic, thiocyanate and selenium compounds, which are occasionally found in concrete constructions, are particularly active as promoters.

In the case of prestressed structures, such conditions can occur before the injection of concrete or mortar. It is most important to take suitable preventative measures against corrosion before the tendons are grouted. Conditions that favour corrosion may also appear later, and hence corrosion protection must be permanently maintained for the structure's lifetime.

Failure during service, appearing after several years or decades of use, is typically a consequence of inadequate protection. Insufficient alkaline protection due to carbonation and/or de-passivation after chloride attack are the major causes of eventual deterioration and even of steel failure.[1–3,5–7,43] In the following discussion, the reasons for corrosion of post-tensioning tendons in internally grouted ducts in particular will be reviewed.

As noted in Section 6.1, major issues which strongly influence the level of durability achieved are:[1–3,5,7,44]

- inadequate design (poor construction)
- incorrect execution of planned design (poor workmanship)
- unsuitable mineral composition of building materials
- unsuitable post-tensioning system components, including prestressing steel.

Inadequate design (and poor construction)

Planning errors include mistakes made during design as well as an insufficient assessment of the behaviour of the structure. The following are some examples of faults occurring during the building phase:

- inefficient drainage systems
- missing or inefficient waterproofing systems
- poor construction and joints
- cracking in the concrete.

The drainage system in structures such as bridges or multi-storey car parks must remove water efficiently not only from the surface, but also the water that has passed through the surfacing down to the deck waterproofing system. The design of the drainage path should be such that, if there is a leak or a blockage, water does not find access to the prestressing system. The use of waterproofing systems, e.g. on concrete bridge decks, provides a protective barrier against ingress of salt-containing water, in particular from the bridge surface. In the past, there were often no systems available that could provide a complete seal or which could be guaranteed to remain waterproof throughout the lifetime of the

construction. As a consequence, construction joints leaked. Modern high-quality liquid-applied membranes are more effective than earlier systems.

Poorly made construction joints may leak. It is therefore advisable to keep anchorages, e.g. in the deck slabs of bridges, away from construction joints, and to prevent any access for leaks from joints into these sensitive systems. Where the prestressing anchorages are inevitably located at construction joints, care should be taken in design. A high proportion of expansion joints leak and their effectiveness and life span are very dependent on the quality of installation and maintenance. Appropriate drainage paths for leakages should be provided to prevent leaks accessing the prestress anchorages or the bearings and to ensure that the water cannot collect at these points.

Cracking in concrete occurs for a number of reasons. Cracks occur mainly in regions with higher stresses due to loading and higher deformations. Wide cracks significantly increase the risk of corrosion. Crack widths should be limited in accordance with normal design practice. Special care is required to minimise the risk of cracking, particularly in the vicinity of anchorages.

Incorrect execution of planned design

Major mistakes in work execution continue to be:

- failure to inject mortar adequately into ducts around tendons in post-tensioned concrete
- manufacture of an insufficiently protective concrete cover.

Fundamental mistakes made by the construction workforce cannot be excluded completely in any type of construction, but the most effective way to avoid these mistakes is to employ better trained personnel. Poorly executed grouting of post-tensioned members, which can also be associated with the use of unstable cement grouts, is a major reason for corrosion damage where the prestressing steel is exposed to water polluted by chlorides from de-icing salt or at a coastal location. Ungrouted tendons in dry structures located in regions with a dry continental climate have been found with no corrosion at all.[3,5]

However, poor workmanship can cause wider problems, ranging from poor compaction of concrete and high permeability to cases where the specified level of covering of steel members has not been achieved. Experience has shown that neither the steel sheath nor even a well-compacted grout can form a sufficiently tight barrier, if aggressive water percolates through porous concrete or if the concrete cover is too small and loses its passivating effect due to chloride ingress or carbonation. Although defective grouting of the ducts is a primary condition for the development of corrosion, it is not enough on its own to generate damaging corrosion.

Unsuitable mineral building materials

The systematic use of unsuitable building materials, resulting in significant component failures, has damaged the image of prestressed concrete construction considerably. Particular problems have been caused by high alumina cement and chloride-containing curing accelerators, which, for economic reasons, were used for the manufacture of ceiling cross-sections and pretensioned prefabricated girders.[24,26] In the case of high alumina cement, damp heat in building such as stables can lead to increased porosity and carbonation, as well as strong decay of the concrete due to conversion of the cement matrix. The sulfide contained in some high alumina cements used in Germany in the 1950s also functions as a promoter for hydrogen uptake in prestressing steels, leading to hydrogen-induced stress corrosion cracking. A series of ceiling collapses due to corrosion decay (pitting corrosion) and stress corrosion cracking in prestressing steels led to the removal of all components in stable ceilings and above other wet rooms that had been manufactured with high alumina cement or with chloride-containing curing accelerators. In 1958 and 1962 respectively, chloride-containing curing accelerators and high alumina cement were banned from use in reinforced concrete in Germany.

Another problem arose when thiocyanate was added in low concentrations to plasticisers used as additives for concrete.[25] Thiocyanate acts similarly to sulfide in encouraging hydrogen-induced stress corrosion cracking. In a typical damage assessment for prestressing steel failures with post-tensioning tendons not yet injected, Table 6.3 shows the presence of chloride, sulfate and thiocyanate found in the concrete where failures in prestressed steel components had occurred. Sulfates and thiocyanates in particular are capable of collecting in water from bleeding concrete. Dissolved in water, they penetrate non-injected ducts, favouring pitting corrosion (sulfate) or hydrogen adsorption (thiocyanate) respectively in prestressing steels.

Unsuitable (sensitive) prestressing steels

The susceptibility of prestressing steels to corrosion attack is of great significance for the durability of prestressed concrete structures. All types of corrosion (e.g., pitting corrosion, hydrogen embrittlement, stress corrosion cracking, corrosion fatigue, fretting corrosion) must be taken into account. A prestressing steel is considered to be susceptible to hydrogen-induced stress corrosion cracking (pages 200–208) where minimal hydrogen quantities stemming from corrosion are sufficient to cause irreversible damage to the prestressing steel. It took years to recognise that some steels were unsuitable due to, among other things, the absence of suitable test procedures to recognise susceptibility to hydrogen-induced stress corrosion cracking at an early stage. The most notorious examples of steels that are not sufficiently resistant to hydrogen are

hot-rolled bars with bainitic structure and the old type of quenched and tempered wires[3,5,23] (Section 6.5.2).

6.5.2 Examples of serious structural failure[3,5]

Serious examples of corrosion-related damage in prestressed concrete structures seldom occur. The following are examples of serious failures which are briefly described and evaluated below.

Damage due to errors in planning and execution

Congress Hall in Berlin/Germany[4,45]

One of the most spectacular prestressed concrete structure failures occurred in 1980. The southern outer roof of the Berlin Congress Hall collapsed 23 years after its construction. The shape of the outer roof was characterised by an external hollow reinforced concrete arch, clamped at two counter bearings on the east and west sides. The arch was connected to the inner auditorium roof using 7 cm thick plates, separated by joints. Each of the outer roof slabs contained two to four tendons, which were housed in ducts. The tendons contained seven to ten prestressing wires made of a traditional type of quenched and tempered prestressing steel. These tendons back-anchored the external reinforced concrete arch to the internal circulating ring beam and held the arch in a stable position.

On 21 May 1980, there was a partial collapse of the outer roof (southern part). The failure investigation concluded that, when the design calculation was performed, the actual loading of the prestressing bands for the back-anchorage of the arches had not been estimated with sufficient accuracy. Cracks had formed in the concrete in a narrow boundary zone along the arch and the ring, as well as inside the joint concrete. The accompanying large curvatures of the concrete plate in the cracked zones led to high bending stresses in the tendons, and, due to the movements of the arches, these stresses alternated.

To these design-related problems were added serious faults during construction, aggravating the effects of the design errors:

- Water could penetrate the roof (e.g., by leaking through the roof membrane) and could reach the tendons in the severely cracked boundary zones.
- The joint concrete was very porous and became strongly carbonated with a high chloride content. Chloride was transported in the water and penetrated into the injection grout around the tendons.
- In an area of the outer roof, some tendons were not placed centrally inside the reinforced concrete slabs, but were placed almost without concrete covering on the ring beam (Fig. 6.12). Due to their own weight and the external loads of the roof, these tendons were curved sharply downward. At the same time, the corrosion protection of the bottom surfaces was almost completely lost.

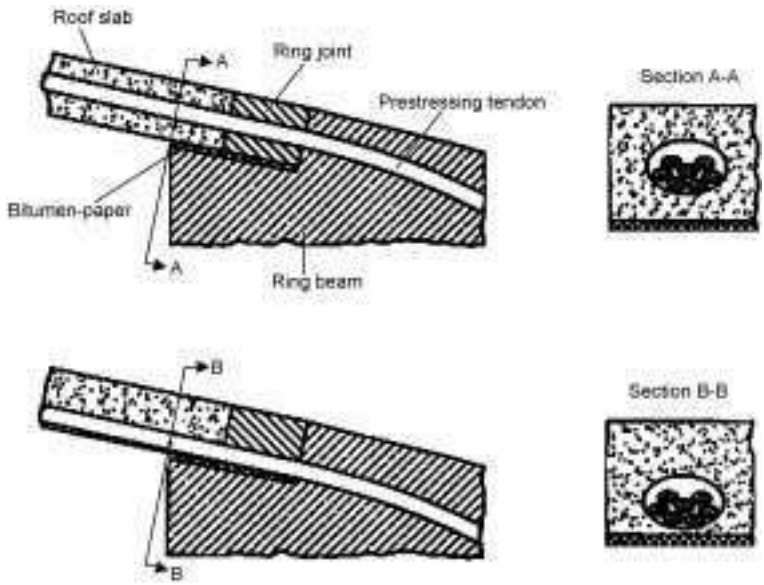

6.12 Details of the roof of Berlin Congress Hall. Top: prestressing tendon with sufficient concrete cover (planning). Bottom: prestressing tendon with too small concrete cover (execution).

Hence, in the case of these tendons, high corrosion exposure and high bending loads were superimposed. Moreover, some tendons were either not grouted or only partially grouted.

- Sealing plugs made from cork had been used as spacers for the prestressing wires in many of the anchorage bodies for the tendons. These created particularly unfavourable corrosion conditions because the cork absorbed water and so, where the steel and cork were in contact, there was no alkaline protection, leading to hydrogen formation.

The tendons corroded particularly around the connections between roof beams and ring beams, as well as in the vicinity of the cork spacers in the anchorages. The tendons then fractured in these two areas due to hydrogen-induced stress corrosion cracking. The use of old-type quenched and tempered prestressing steel (which was particularly sensitive to hydrogen ingress), and the alternating bending loading of the prestressing reinforcement, caused by inevitable movements of the arch due to changes of temperature and wind, greatly increased the rate and the extent of the structural component damage.

Bridge over Muckbachtal on Würzburg–Heilbronn motorway, Germany[5]

A bridge was built over the Muckbachtal river as part of the motorway connecting Würzburg and Heilbronn in 1970–71. It was a box girder bridge

consisting of two decks, each prestressed with eight longitudinal tendons running in webs. Each tendon comprised 12 wires of 12 mm diameter made from quenched and tempered steel. The tendon profiles were modified to the bending moment axis.

In the longitudinal direction, the bridge was slightly tub-shaped, with the centre situated near the lowest point. Because of the small longitudinal slope, the drainage points were arranged with a short distance between them (approximately 5 m in most cases). Across the bridge, surface water was transported by 100 mm diameter pipes (Fig. 6.13). These cast iron pipes had several sleeved couplings along their length. Over time, the sealing of the sleeves became faulty (as the sealing compounds became embrittled) and in many cases, water could drip onto the inclined inner surfaces of the outer webs of the box girders. The surface of the motorway was treated with de-icing salt during the winter months, and for approximately 25 years, chloride-contaminated water reached the concrete surface of the webs and the adjacent bottom slab via the leaking drains

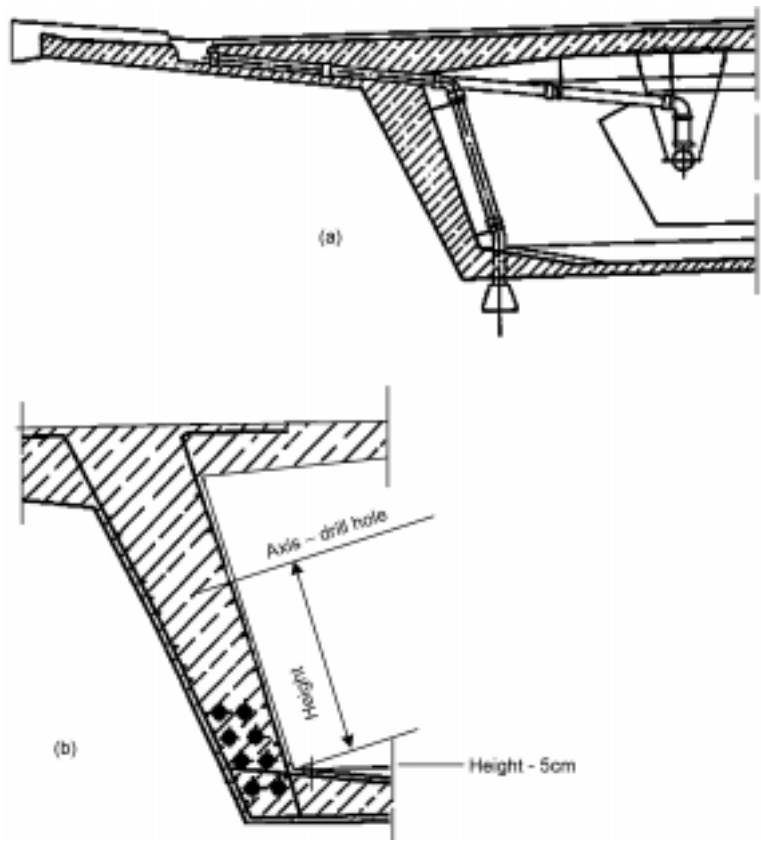

6.13 Position of the drainage pipe in box girder (a) and of the prestressing tendon in web (b) (schematic).

every winter. The relatively short wet winter periods were then followed by longer dry periods, so very high concentrations of chloride developed in the concrete coverings of both reinforcing and prestressing steels. The chlorides were able to penetrate deep inside the concrete at these places, and corrosion was exacerbated because low-quality concrete containing porous aggregates had been used in construction. Chloride concentrations of several per cent were traced to a depth of approximately 5 cm below the points where water could get in.

During a bridge inspection, hollow-sounding areas were found in the concrete inside the box girders below the leaking drains. The reinforcing bars located underneath the leaks were rusty and their cross-section had been reduced by up to 50%. The prestressing tendons were also found to be severely damaged. This non-uniform chloride-induced corrosion attacked the sheath and then corroded the prestressing steels, and also led to fractures of the wires. In one case, 12 wires were broken in four tendons exposed on the inside of the web. The other wires were so damaged by corrosion that future fractures were inevitable.

The extent and the intensity of the damage to the reinforcing steel and prestressing tendons depended on their positioning and the thickness of the concrete cover. The normal concrete cover was 5 cm. The most severe chloride corrosion damage to tendons situated inside in the web and fractures of wires were found below a large number of defective drains where the reinforcing steel meshes had a low concrete cover (1 to 2.5 cm). From this it was concluded that, from a construction point of view, the damage was due to having too thin a concrete cover for the reinforcements located in chloride-contaminated regions. The first stage was corrosion-induced detachment, where the concrete peeled away from the severely corroded reinforcing steel, leaving a cavity in which water containing chloride could collect and concentrate. In the second stage, the chlorides initiated the destruction of the tendons.

These failures, which are representative for others of this type, are attributed to serious construction errors. The defective drains, which led to intensive and unexpected chloride contamination of the concrete, resulted from poor design and execution, which were combined with insufficiently expert bridge inspection. The thickness of the concrete cover inside the webs of the box girders (which was only a problem in wet conditions) was identified as a common design fault and eliminated in the mid-1970s when ‘The Additional Technical Regulations for Structures’ (ZTV-K 76) were introduced by the German Federal Ministry of Transport. Today, surface water drains get special attention when constructing new bridges of this type, and are examined in detail during regular routine bridge inspections. The Muckbachtal bridge was repaired by placing an external tendon that ran through all the sections of the bridge, and by adding tendons in the most severely damaged areas. The chloride-contaminated concrete was removed and re-profiled before making repairs below all the drain points on the inside of the inclined webs and on the top side of the bottom plates.

Failures due to unsuitable construction materials

Concrete, injection grout

Typical examples of the effect on stress corrosion resistance of particular mineral construction materials include the use of high alumina cements containing sulfides (susceptible to damage in or above humid spaces) and hardening accelerators containing $CaCl_2$, especially in the case of (prefabricated) pretensioned concrete elements. The use of these materials was forbidden after numerous failures.[25] The use of high alumina cement in reinforced concrete was banned in Germany in 1962. Since 1958, only cements with a limited chloride content (0.1 mass-%) may be used in prestressed concrete, and the use of chloride-containing hardening accelerators in reinforced concrete structures has been forbidden.[37]

The introduction of concrete additives as part of modern concrete technology caused corrosion problems because active substances and other materials, which may modify corrosion resistance even in very small concentrations, could get into the concrete. A particularly significant example is the use of thiocyanate as an active substance in a plasticiser when making concrete for reinforced structures. Such plasticisers mistakenly got into fresh concrete used for manufacturing prestressed concrete elements and caused damage. Thiocyanate has been forbidden as an active substance in concrete plasticisers, because it promotes hydrogen absorption by the prestressing steel.

Railway overpass in Berghausen (Karlsruhe/Germany)[3,25]

In 1979, numerous fractures occurred in the prestressing steel at the lowest points in the central area of a railway overpass deck with a beam cross-section. These fractures occurred between a few hours after and several days after prestressing, but before grouting. The prestressing steel consisted of a single 36 mm diameter prestressing steel bar with pearlitic structure (strength 1230 N/mm^2). Water (approximately 250 ml to 1 litre) was found in the ducts where the prestressing steel had fractured in each sheath.

Investigations revealed initial rusting of the prestressing steels, resulting in shallow corrosion pits up to 0.5 mm deep that induced the fractures. The pronounced uneven local corrosion occurred within 2 to 3 weeks after concreting, and was due to penetration of water into the prestressing ducts. Salt-enriched water of neutral pH is extraordinarily corrosive locally because the sulfates and chlorides concentrate due to leaching of the fresh concentrate as it hardens. The main constituents of this corrosive medium are the potassium salts K_2SO_4 and KCl (Table 6.3). In this case, up to 5 g sulfate (SO_4) per litre and 0.25 g chloride (Cl) per litre was measured in the water around the tendons. In addition, up to 0.5 g/l of thiocyanate reached the prestressing steel in the ducts via the water from leaching of the concrete. As has been noted, thiocyanate, acts as a promoter

for hydrogen absorption, causing pitting-induced stress corrosion cracking, which leads to premature fracture failures. The thiocyanate had originally entered the concrete as a constituent of the plasticiser, which was itself not certified for use with prestressed concrete. This plasticiser contained 4 mass-% SCN^- as the effective substance. In the hardened concrete, however, only traces of thiocyanate were found (0.006 mass-%).

Thiocyanate is known to work as a promoter that favours the absorption of hydrogen by prestressing steel. After considering the damage found and the results of subsequent laboratory tests, the use of thiocyanate as an active substance for concrete plasticisers was forbidden. In order to prevent corrosion-promoting substances being transmitted to the concrete when using concrete additives or bonding agents, it is now mandatory to check using a special electro-chemical method[36] before any new materials may be used in Germany.

The localised pitting corrosion attacks were primarily attributed to salt-containing water from the concrete. Current recommendations are to remove settling water a short time after concreting by blowing out and, if possible, by additional washing out. Nowadays the harmful effects of concrete settling water are also reduced naturally by adopting the limited periods between concreting and injecting set out in the German standard DIN 1045.

Prestressing steel

Damage caused by stress-corrosion cracking in prestressing steel presupposes the use of steel with sufficient susceptibility to corrosion-induced failure under particular conditions. Appropriate environmental conditions are also necessary, either to favour active corrosion or to interrupt or terminate passivation. Substantial problems have occurred with certain grades of steel where no serious errors appear to have been committed either in the planning or building construction stages. In these cases, the rules concerning corrosion protection were obeyed in all important points during transportation, storage and processing of the steel, and no unsuitable building materials were used. Following detailed investigations, these particular grades of steel were classified as highly sensitive to hydrogen and unsuitable for normal building works, and have been prohibited for use in prestressing applications in Germany. The steel characteristics have been modified to try and develop practical grades of steel resistant to hydrogen attack.

Structures manufactured using bainitic hot-rolled prestressing steel[3]

Using ferritic-pearlitic steel grade St 55/85 as an example (with tensile strength measured in kp/mm^2 units), the strength of hot-rolled prestressing steels has gradually been increased by alloying and processing measures. From early 1974, a new prestressing steel grade St 110/135, a low-alloy hot-rolled steel with a

bainitic structure, was used for single rods in prestressed concrete. Within a few years of use, several structures using this grade of prestressing steel failed. This was very surprising because investigation of notched-bar tensile properties and fracture-mechanics suggested that this grade of prestressing steel possessed improved (less brittle) failure characteristics in comparison to the previously used prestressing steel St 85/105.[37] However, failure in practice demonstrated that behaviour determined during brittle failure investigations in the laboratory cannot be extrapolated to actual applications in every case. Under construction site conditions, the low alloy silicon-manganese-chromium steel St 110/135 proved to be substantially more susceptible to hydrogen-induced stress corrosion cracking than the hot-rolled prestressing pearlitic steel St 85/105, manufactured out of silicon-manganese-carbon steel.

In the numerous structures made with steel grade St 110/135, corrosion-induced fractures occurred during the construction stages, either before grouting the tendons or a few hours afterwards. In total, 65 fractures were found in 27 separate projects on wires with diameters of 26, 32 and 36 mm in the four years this steel was used (1974 to 1978). These projects ranged from bridges to building components and water tanks. With some fractures, internal steel defects (cavities, core segregations) and other surface defects (hardening cracks, laminations) were also present. Fractures occurred from 0.7 hours to 1200 days after prestressing. In the case of the later fractures, the tendons had not been grouted. Rods which had broken within a few days of prestressing and before grouting were generally free from any corrosion visible to the naked eye. In most cases, there were no unusual quantities of aggressive constituents at the fracture initiation sites or on the steel surfaces. The broken prestressing bars were, however, often wet and in the presence of concrete bleed water.

The actual tensile strength of the broken steel lay between 1350 and 1880 N/mm^2. In many cases, the strength was high within the grade and sometimes well above the prescribed tensile strength. On average, the higher the strength, the sooner the steel cracked. Therefore, increasing the rods' tensile strength also increased the tendency to hydrogen-induced stress corrosion cracking. Corrosion-induced damage in prestressed concrete structures made using the prestressing steel grade St 110/135, which occurred both during the construction phase and on older constructions, was attributed to the high structure-conditioned susceptibility of this steel to stress corrosion under usual construction site conditions. It was found to be difficult to create uniform strength levels under alloying and production conditions, and so many over-strength casts, with an unusually high tendency to crack and fracture, came on the market. It was not possible to separate out these over-strength casts using normal, self-regulated controls. The corrosion problems associated with stronger types of prestressing steel could have had an adverse effect on the general reputation of all prestressed concrete structures, and so the further use of this steel grade for prestressed structures was forbidden.

Structures manufactured using quenched and tempered prestressing steel of older type (Laboratory building in Mannheim/Germany)[1,7,8]

Quenched and tempered prestressing steels were used in the form of round wires (smooth or ribbed) or ribbed oval wires from the early 1950s, especially in Germany. The ribbed oval wires were prestressed in innumerable pretensioned precast concrete members of many different types to provide large numbers of post-tensioned prestressed bridges and high-rise structures. The development of quenched and tempered steels was driven by a combination of economics and the characteristics of the steel, including high strength with good toughness, very good bond characteristics, and low relaxation.

The behaviour of the early types of carbon-alloyed quenched and tempered steel was not always satisfactory with respect to stress corrosion during processing, and fractures occurred during or shortly after prestressing. Signs of inadequate stability under unfavourable site conditions[3] and susceptibility to some testing laboratory testing solutions, led to the development of steel with reduced carbon content and about 0.5 mass-% chromium, giving increased resistance to hydrogen-induced stress corrosion cracking.[46] However, numerous structures still exist which were constructed using the old type of steel (manufactured until 1965). In addition, old-style quenched and tempered prestressing steel continued to be used until 1990, particularly in pre-tensioned members, in the former East Germany.

From 1989 onwards, examples of collapse and near-collapse have occurred with structural members made using this steel type, even where evidently unfavourable environmental conditions were not present:

- After 28 years of service, beams in a laboratory building collapsed, breaking almost in the centre (Fig. 6.14).
- After 30 years of service, an open crack in the concrete of a beam in a factory was found – again at the mid-span.
- During the demolition of the 25-year-old roof of another factory, the beams broke while being dismantled.
- After 33 years of service, numerous pre-cracks and fractures of wires were found on a bridge from Henningsdorf prestressed with quenched and tempered steel.[9,47]

These events were primarily caused by accumulated fractures of the wires in the tendons, and the results of the investigations were practically identical in each case. As an example, the first failure mentioned above will be examined in more detail. The two tendons in the beams, made of 16 ribbed oval wires, were covered with a sufficiently thick and dense (impermeable) concrete cover. The ducts were free from any external corrosion, since their concrete cover was neither carbonated nor contained chloride. After opening the tendons, older fractures were found covered with rust and/or grouting mortar. These fractures probably originated from when the beam was manufactured. The fractures were

(a)

(b)

6.14 Broken beam as a result of stress corrosion cracking. Top: survey. Bottom: broken tendon.

randomly distributed over several metres at the lowest point of the tendons. There were also well-preserved recent fractures in the ruptured cross-section of the beam. The tendons were correctly grouted. The injection mortar was damp, although it contained neither carbonated material nor chloride. In the case of the broken wires, there was no corrosion visible to the naked eye, but small corrosion pits and outgoing cracks could be seen under the microscope. A large number of cracks had occurred but were not related to any heavily pitted eroded areas. The steel ducts showed initial rusting on the inside and lime-like deposits with some concentration of potassium sulfate along a former water level. This old type of quenched and tempered prestressing steel had a tensile strength of 1750 N/mm^2; i.e. the actual strength was clearly above the required nominal minimum of 1570 N/mm^2, which heightened its sensitivity to hydrogen.

It was concluded that, during the production of the concrete beams, either concrete setting water penetrated into the ungrouted tendons and caused the wire to pre-crack and fracture, or condensation water had already damaged the highly sensitive steel in a similar way. It was shown that the steel grades used were highly sensitive to hydrogen-induced cracking when in contact with condensation water.[23] While embedded in a permanently wet injection mortar, the existing pre-cracks in the steel could grow and eventually lead to the final failure. A large number of wire fractures in a cross-section finally caused the fracture of the beam. In lab tests,[8] it was shown that wires with pre-cracked sensitive prestressing steel can fracture when placed in an alkaline environment (e.g. Table 6.5). In a stress corrosion test using a saturated solution of $Ca(OH)_2$, retarded fractures of steel occurred after 330 hours, with the stress level set at 40% of the tensile strength. Under crevice corrosion conditions, usually found in the case of bundles, the service-life of pre-cracked samples was shortened to 40 hours. Samples without pre-cracks were still not broken after 5000 hours.

Studies of serious damage that occurred after several decades of service in structures prestressed with the old quenched and tempered steel showed that the unusually high susceptibility to hydrogen was primarily or exclusively responsible for the delayed failures. This type of steel has not been in production for 40 years. Damage analysis and the results of research demonstrate that, before grouting, corrosion pitting, pre-cracks and fractures had already occurred. Due to the high stress-corrosion susceptibility of these types of steel, the damage could develop up to complete failure of the members even in correctly grouted sheaths and without any other environmental conditions that favoured cracking. The early damage in the form of pre-cracks and single fractures is explained by the instability of these wires in the moist climate of the ungrouted ducts,[23] or on contact with concrete setting water.[7] Both these circumstances are part of everyday practice at construction sites. Because of these correlations and because structures post-tensioned with the sensitive steel are still in use, investigations aimed at controlling the potential risks in existing structures were instigated. Non-destructive magnetic leakage flux measurements and destructive checks with single wire sampling are presently in use.

Table 6.5 Results of stress corrosion cracking tests of statically loaded quenched and tempered prestressing wires without and with pre-cracks in saturated solution of $Ca(OH)_2$ at 30°C, $\sigma = 0.4R_m$[8]

Pre-crack	Crevice corrosion conditions	Lifetime in hours (mean value of 3 tests)
no	no	>5000
no	yes	>5000
yes	no	330
yes	yes	40

6.6 Corrosion testing of prestressing steel

6.6.1 Historical development

The technological development of prestressing steels was accompanied by research to establish parameters and test methods for susceptibility to H-SCC. Early prestressed concrete structures mostly used hot rolled steel rods with a yield stress around 600 N/mm^2 and a tensile strength of 900 N/mm^2. This steel quality, St 600/900, does not differ much from St 835/1030 used today, except that the yield strength is increased by straining to 835 N/mm^2. This type of prestressing steel shows high resistance to the formation and growth of hydrogen-induced cracks under corrosive loads.[1,3,6,20,43]

When high strength quenched and tempered and cold drawn prestressing steels with a tensile strength up to 1800 N/mm^2 [48-52] were introduced, damage caused by cracking was reported for the first time. The original case was of delayed fractures that could be attributed to SCC, which occurred within a few days after prestressing. This and the many other cases of damage in structures made of aluminous cement[3,53,54] led to investigations that would provide more information about the mechanism of hydrogen-induced SCC and help metallurgical development and design of prestressing steel.

Cases of damage had been reported prior to this experience, for example at the 1955 Federation International de la Precontrainte Congress.[55] Engineers observed wires broken due to corrosion on the reel in three projects (see e.g. ref. 3). As a result, quenched and tempered steel was effectively no longer used in the Netherlands after about 1952.

The initial tests used well-known test solutions that had been proven for unalloyed steels used for other purposes. This was not only because of a lack of information about the mechanism of hydrogen-induced stress corrosion, but also because the composition of the electrolytes that would occur during construction was unknown. Thus highly concentrated solutions of calcium and ammonium nitrate, developed for testing boiler steels for caustic embrittlement,[56] were used. With better knowledge of the mechanism of crack formation in prestressing steels, and especially the influence of hydrogen generated by corrosion, test solutions with high hydrogen activity were introduced, such as saturated aqueous H_2S solution, well known from tests of oil pipelines, or NH_4SCN solutions. Specimen design was limited to bend specimens because they were easier and more cost-effective to produce than tensile specimens.

At the beginning of 1974, a new prestressing steel, type St 1080/1320 (St 110/135) (smooth and ribbed), was introduced for prestressing steel rods in prestressed concrete structures. However, within the first year of use, damage occurred in a number of structures where this steel was used, and the number of failures increased to 60 within a short period of time.[3] This was unexpected since it had been assumed from the results of notched-bar tensile and fracture

mechanics tests that this steel had much better brittle fracture properties than the steel St 835/1030 (St 85/105) previously in use.

This experience showed that the behaviour demonstrated in brittle fracture tests in the laboratory was not always transferable to actual conditions in a way which is valid for all prestressing steel qualities. It was found that, under construction conditions, St 110/135 is essentially more susceptible to delayed cracking than St 85/105. The two steel qualities differ mainly in their chemical composition and their microstructure, rather than in their manufacturing processes. As a result of these failures, it was decided to develop a test method that would enable definitive statements to be made about the suitability of prestressing steels under construction conditions. DIBt (formerly IfBt) and EU initiated an extensive cooperative research programme (using the research facilities of FMPA Stuttgart, BAM Berlin, MPI Düsseldorf, Krupp AG Rheinhausen) which resulted in the development of a test method[45] that would be capable of distinguishing between susceptible and non-susceptible prestressing steel qualities and therefore identifying those that could be used safely under construction conditions. Details of this test method and a parallel development, the FIP test, are described in the following sections.

6.6.2 Test method with electrolyte solution not representative of actual service – FIP test[57]

The demand for a test to assess the susceptibility of prestressing steels to stress corrosion cracking dates back to when prestressing steels were introduced. Federation International de la Precontrainte published the first reports,[58,59] which described the evaluation of SCC for various prestressing steels. The data were obtained from research and round-robin tests with different electrolyte solutions that did not necessarily reproduce actual conditions, with and without electrochemical control (polarisation) and at prestressing levels between 0.5 and 0.95 R_m.

The following electrolyte solutions were evaluated:

- boiling $Ca(NO_3)_2$ solution
- saturated aqueous H_2S solution with and without electrochemical control
- 20% NH_4SCN solution with and without electrochemical control
- 5M H_2SO_4 with cathodic polarisation
- distilled water with cathodic polarisation and
- saturated $Ca(OH)_2$ solution with anodic and cathodic polarisation.

As expected, the corrosion behaviour differed considerably. The uncertainty in hydrogen activity during the test contributed to a large scatter of time-to-failure values, so the stress corrosion cracking behaviour could not be assessed accurately

or ranked. Evaluating the different methods, it was concluded that only the tests in the concentrated ammonium thiocyanate solution were promising. This method, known as the FIP test,[36] used the following test conditions:

Corrosive medium: 200 g NH_4SCN in 800 g H_2O temperature: 50ºC ± 1ºC, preferably ± 0.2ºC

- Test cell: controlled heating, no circulation of the corrosive medium, plastic materials recommended
- Specimen: specimen is to be cleaned only with acetone (in view of health and safety concerns, trichlorethylene is presumably no longer permitted)
- Loading: constant load of 80% of the actual ultimate tensile strength, obtained on a reference, kept constant during the experiment
- Result: time to fracture of the specimen will be determined under these test conditions. Because of the relatively large spread of the results (which is normal with corrosion tests), it is recommended that 3 to 12 specimens are tested to obtain a representative value, evaluated by Gaussian distribution on a logarithmic time scale. A test is stopped if the specimen does not break within 500 hours.

More details can be obtained from the literature.[36] The test conditions, under which specimens are at open circuit potential, demonstrate that a variety of parameters can overlap in an uncontrolled manner during the test. Values for the time to failure were therefore spread widely and the only classification possible was into prestressing steel classes. In fact, no results relevant to construction and service conditions could be achieved. Tables 6.6 and 6.7[36] show the effect of specimen characteristics and test conditions on the time to failure, but a quantitative correlation of parameters influencing time to failure is not possible. Lifetimes relevant to construction and service cannot be estimated from these results. The type of electrolyte does not allow these results to be extrapolated to behaviour in practice.

Thresholds for the time to failure can only be defined for single classes of prestressing steels. They depend on diameter, microstructure and type of delivery. The FIP test provides insufficient information to distinguish the particular susceptibilities of different types of prestressing steel. Nevertheless, for all types within one category (hot-rolled, quenched and tempered or cold-drawn) the susceptibility increases with increasing strength and higher prestressing level.[22] To date, no reliable values have been proposed. In the draft for EN-standardisation of this test (prEN 10138-3 Prestressing steels – Part 3: strand), the proposed time to failure is so short that almost any material would pass the test.

Nürnberger[6] has used the FIP test to evaluate susceptibility to hydrogen-induced SCC, and determined that prestressing steels can be classified as extremely susceptible if time-to-failure remains below the following values:

Table 6.6 Influence of experimental conditions on time to failure, L, during NH_4SCN test

Influence	Degree of influence		Remaining deviation	Remark
	Qualitative	Quantitative		
Corrosive medium				
Temperature	Very strong	50°C → 45°C → LX2	50°C ± 1°C → L ± 15%	To keep as constant as possible
Concentration of SCN-	Strong	20% → 7.25% → LX2	20% ± 1% → L ± 3.5%	
Purity of NH_4SCN	Little	–		
pH-value of the solution	Strong	–		Self-adjusting in the test
Anodic or cathodic polarisation	Very strong	–		In the FIP-test not provided
Circulation of the solution	Very strong	–	Without and with circulation →L∼X2 to 3	
Test cell				
Diameter of test cell	Strong			All these influences are constant in one laboratory
Material	Can be strong			
Length of the test cell	Little			
Open or closed test cell	Little			
Position horizontal/vertical	Little			
Tensile stress				
Stress level	Very strong	0.8 → 0.5 R_m →L∼X4	0.8 ± 0.01 R_m →L ± 3.5%	

The disadvantages of this test are as follows: the use of a non-practical electrolyte with high hydrogen activity and low initial pH value ($4 < pH < 4.4$) leads to a high hydrogen loading of the steels and to fractures of all prestressing steels within short testing times ($1\,h < t < 500\,h$).

Table 6.7 Effect of specimen characteristics on time to failure, L, during NH_4SCN test (C1 and C2 are constants)

Specimen characteristics	Effect		Remark
	Qualitative	Quantitative	
Diameter of the sample	Strong	$L \sim C_2 \cdot D^2$	The dependence includes the influence of R_m
Tensile strength (R_m)	Very strong	$L \sim C_1 \cdot D^2$	Deviation of R_m within one heat can be between $\pm 2\% \rightarrow L \pm 27\%$
Chemical composition	Little to very strong		Dependent on the steel type – very different effects of the elements, i.e. Cr
Structure of the steel	Very strong		
Surface smooth/shaped	Strong		Shaped L is higher than with smooth surface
Surface roughness	Strong		If more than 40 μm
Stabilising stress relieving	Strong		
Stresses in the surface	Very strong		
Notches	Strong		
Surface defects	Strong		Can reduce L to 1/10 compared with no surface defect

- cold-drawn wire 2–3 h
- quenched and tempered wire 10–45 h
- hot-rolled bar 30–50 h.

Again it must be emphasised that FIP tests are not suitable for comparing different types of prestressing steel (hot-rolled, cold-drawn, quenched and tempered). Therefore, results must not be used as a ranking scale for susceptibility.

More recent experiments[59] show that the ranking achieved with FIP tests can also be obtained if hydrogen and mechanical loads are not applied at the outset. Susceptibility of steel can obviously be determined more easily from deformation values (elongation after fracture, reduction of area after fracture) under slow-strain rate tests directly after hydrogen charging.

6.6.3 Test method with electrolyte solution representative of actual service – DIBt test

Various failures of prestressed concrete structures caused by hydrogen-induced stress corrosion cracking at the beginning of the 1980s led to the development of a constant load test based on laboratory as well as on-site investigations.[20,60] In

this test, the prestressing steel specimens as delivered were stressed in a stressing frame under constant strain to $0.8\,R_m$, at 50ºC. Based on the results from chemical analyses of on-site samples of water taken from prestressing ducts, the electrolyte solution for the test contained 0.014 mol/l chloride, 0.052 mol/l sulfate and 0.017 mol/l thiocyanate (pH = 7.0). The SCN^- ions promote hydrogen uptake and therefore made conditions more severe than under normal conditions. As noted previously, thiocyanate ions have been found in some cases where damage had occurred,[6] and were shown to have originated from concrete admixtures (in which SCN^- is no longer permitted).

During a test period of 2000 h, a measurable amount of hydrogen was absorbed by the specimens and led to embrittlement. Specimens made of susceptible materials failed before 2000 h was reached. Compared to tests in concentrated thiocyanate or nitrate solutions, this test has the advantage that the decisive criterion is the occurrence or non-occurrence of a fracture within a certain time period, rather than within a relatively short failure time. Further advantages arise from the fact that the test solution closely simulates corrosion conditions around the prestressing steels within the ducts under construction conditions, and that the results obtained with this test for different prestressing steels are reproducible and correspond to practical experience.

In comparison with the FIP test, slightly higher initial and then nearly constant low hydrogen activity at the prestressing steel surface is required to ensure reproducible results. This has been proved by permeation measurements.[20,60,61] The higher the pH of the solution, the lower the general corrosion rate. The more favourable conditions for surface layer formation result in a longer testing time. However, with this test the results can be better extrapolated to the behaviour of prestressing steels in practice. Experiments using what is now known as the DIBt test have been carried out successfully for a wide range of steels.[20,61–64]

This method has been described by Grimme *et al.*[20] It was found (Fig. 6.15) that all approved prestressing steels on the market passed the time limit of 2000 h without fracture, while steels known to be susceptible to SCC, from cases of reported damage or known not to be suitable for construction practice (St 1080/1320, bainitic microstructure[3]), failed within 2000 h due to hydrogen-induced SCC. A criterion based on time to failure could thus be defined that appeared valid for all types of prestressing steels tested.

Applying the DIBt test to prestressing steels that had failed due to SCC after long-term use in actual structures, showed that this test would have classified them as susceptible and hence not approved, supporting the suitability of this method. Results[23,64] showed that annealed prestressing steels of the ‘old type’ (i.e. without Cr-alloying and manufactured prior to 1965) and also comparable steels from the former GDR do not pass the test and should be classified as ‘not approvable’ according to today’s standards.

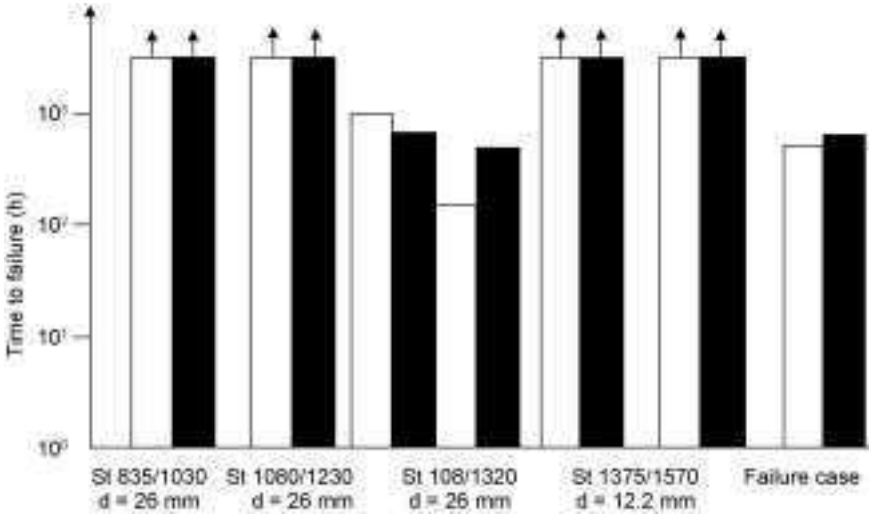

6.15 Time to failure of various prestressing steels in practice related DIBt-test solution.[20]

6.7 Monitoring techniques for prestressed concrete constructions

6.7.1 General remarks

The main difficulty in assessing the condition of prestressed concrete structures is that failure of the prestressed members may occur as a sudden collapse without any visible warning signs. An example is the Ynys y Gwas bridge in Great Britain. It collapsed in 1985 after 32 years in service as a result of tendon corrosion, a short time after a regular visual inspection in which no evidence for any damage was discovered.[65] There are further examples of similar collapses in other countries.[6] Visual examination of prestressed concrete members, which includes the detection of moisture, cracking and spalling on the concrete surface, is therefore not sufficient and so non-destructive testing methods are necessary for the following purposes:

- detecting areas with corrosion
- locating tendons and ducts
- detecting voids and grouting defects
- detecting cracks in tendons.

There is not enough space in a brief section like this to provide a comprehensive review of the wide range of non-destructive testing methods used internationally. The following methods are briefly reviewed:

- potential mapping

- pulse techniques
- geo-radar/ground penetrating radar
- radiography
- ultrasonic methods
- impact-echo method
- magnetic flux leakage (MFL) measurement.

Other methods, such as acoustic emission, are not discussed here, but are covered elsewhere.[66,67]

6.7.2 Detection of corrosion

Areas of corrosion in prestressing tendons pose a considerable risk for prestressed concrete members. Flaws in the ducts also expose the steel tendons to hydrogen-induced stress corrosion.

The half-cell potential mapping method can be used for the detection of corrosion of tendons in pre-tensioned concrete.[6] It is not, however, appropriate for the detection of corrosion in tendons in post-tensioned concrete, since it cannot monitor what is happening to the tendons within the metal or plastic ducts within which they are housed. In this method, the differences in potential between the tendon and a suitable reference electrode placed at various points on the concrete surface are measured (Fig. 6.16). The concrete surface is moistened to provide sufficient electrical conductivity. In general, corrosion is greatest at positions of high negative potential with large potential gradients around them. However, reliable conclusions about possible corrosion cannot be drawn from individual potential values. The cumulative percentage curve, which shows the percentages of readings as a function of potential, provides a useful analysis method in practice.[68] An inflection point in this curve indicates the existence of active corrosion.

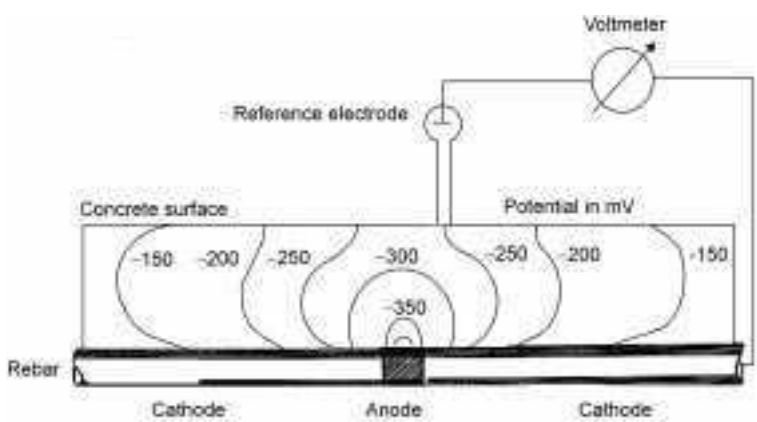

6.16 Principle of the potential measurement method.[69]

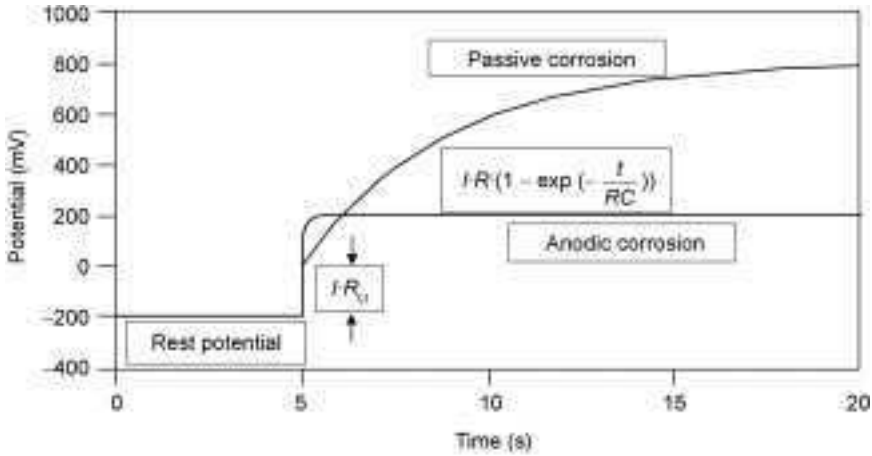

6.17 Transient response to galvanostatic pulse.[71]

Additional information on the electrochemical condition of tendons may be obtained by means of linear polarisation or by pulse techniques, as described elsewhere.[70,71] An example of the latter is the galvanostatic pulse technique, in which a small constant electrical current is applied to the tendon via a counter electrode on the concrete surface and the steel potential is monitored as a function of time (Fig. 6.17). The analysis of the transient response of the measured potential from the starting time to the steady state with the potential V_{max} leads to the following simplified relation between the resistance (R_Ω) of the concrete, the charge transfer resistance of the steel/concrete interface (R) and the capacitance (C) of the double layer[71]:

$$V(t) = IR_\Omega + IR \cdot \left(1 - \exp\left(\frac{-t}{RC}\right)\right) \qquad 6.3$$

The parameters R_Ω, R and C can be determined from equation 6.3. Small values of R indicate the existence of active corrosion. This method has been claimed to work substantially better than the usual measurement of the rest potential, especially in the case of wet concrete.[72] Electrochemical monitoring methods of the kind described above are well established. However, the measurement and interpretation of the results must be carried out by trained and experienced staff.

6.7.3 Locating tendons and ducts

Knowing the position of tendons or the ducts within which they are housed is a necessary precondition for investigating prestressed concrete members. The position of tendons or ducts often does not correspond to the original plans, particularly in older buildings, or the plans are no longer available.

Since tendons are situated within plastic or metal ducts in post-tensioned concrete, devices that work on the basis of magnetic induction, or which use the eddy current method, are unable to detect the tendons themselves. A technique such as geo-radar (ground penetrating radar) is suitable for locating the ducts within which the tendons are housed. It cannot detect tendons in steel ducts since steel fully reflects radar waves.[73–75] In this method, electromagnetic waves (frequency approx. 1 GHz) are sent from the concrete surface to the ducts by means of an antenna. These waves are backscattered by objects with a different electrical conductivity or permittivity compared to concrete. The reflected waves are registered as a function of time, as so-called A-scans (time spectrum of the wave amplitude at a single measuring point). The run-time t of the backscattered signal displays the spacing, z, between the receiving antenna and the reflector as:

$$t = \frac{2\sqrt{\epsilon}}{c} z \qquad 6.4$$

with c = velocity of light, ϵ = relative permittivity of concrete (see Fig. 6.18).

These measurements are carried out along a line or profile. By applying the A-scan along the profile at given points (e.g., position C), the B-scan is obtained (Fig. 6.18). The x-axis is the position of the antenna on the profile, the z-axis contains the grey or coloured code of the received A-scan at this point of the profile. Reflectors (e.g., tendon ducts) positioned perpendicular to the profile create a typical hyperbola in the B-scan:

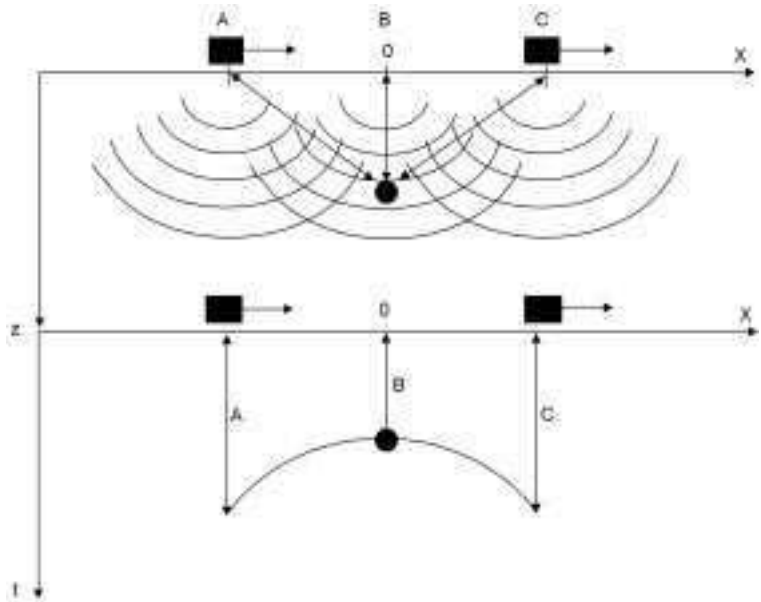

6.18 Backscatter hyperbola of a diffuser (schematic illustration).[74]

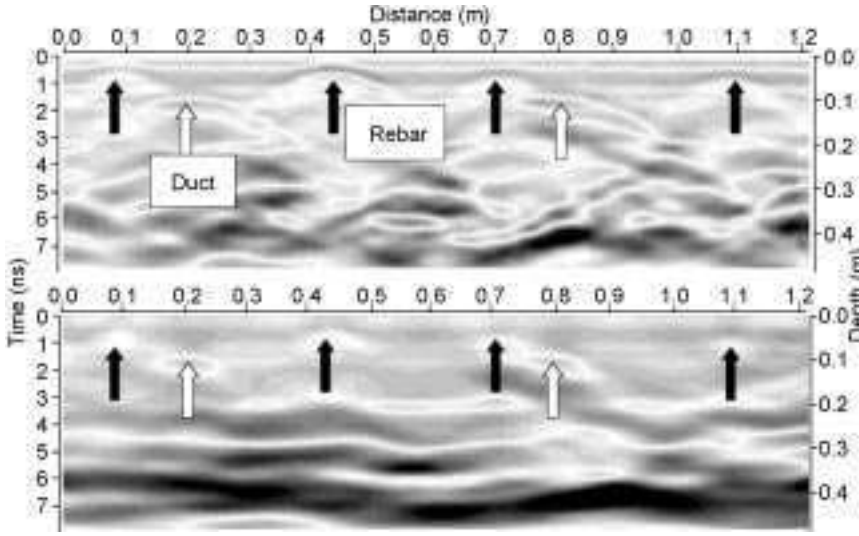

6.19 Localisation of tendons behind the rebars (B-scan) and SAFT-reconstruction.

$$t = \frac{2\sqrt{\epsilon}}{c}\sqrt{x^2 + z^2} \qquad 6.5$$

As the radar antenna approaches the reflector, the run-time gets shorter.

The location of the ducts within which the tendons are housed is shown in Fig. 6.19. The lower image is enhanced to give a better representation of the reflectors. The position of the reflector can be computed using the B-scan by means of the SAFT algorithm[76,77] (see also Section 6.7.4). Every point inside the area under consideration can be assumed to be a possible reflector. The amplitudes along the associated backscatter hyperbola are added with respect to the phase. A large signal in the reconstructed SAFT image denotes a possible reflector. The measurements are influenced by moisture and salt in the concrete. The wave propagation speed reduces and the reflected waves are considerably attenuated, which makes locating the ducts more difficult. There are suitable antenna systems (monostatic antennas which are oriented parallel to the tendons) commercially available for this radar method. The position of the antenna is measured with a position recorder. Execution and evaluation of the radar measurements must be carried out by trained staff.

6.7.4 Detection of grouting defects

Grouting defects in ducts reduce the corrosion protection around the tendons. Hence, it is important to be able to detect grouting defects using non-destructive methods. The following methods are suitable in principle:

- radiography (X-ray method)
- ultrasonic methods (reflection or transmission)
- impact echo method (elastic waves).

These methods are discussed in the following sections.

Radiography

Radiography is the only method for detecting grouting defects in ducts that is currently widely used in practice. For this purpose, an imaging beam (gamma or X-rays) is directed at the concrete surface and is received on a detector which is arranged on the posterior side of the concrete member (Fig. 6.20). Flaws such as cavities (e.g., grouting defects) as well as the position of ducts can be detected from the intensity of rays received. Newer equipment permits concrete members to be screened up to a thickness of about 1.5 m.[79] The dimensions of the images are *ca.* 0.3 × 0.5 m. The necessary exposure times vary depending on the concrete cover, from 10 min up to 1–2 hours. Images of an incompletely and a completely grouted duct are shown in Fig. 6.21. On the left side, the incomplete grouting at the top of the duct is shown by the blackened area. If steel ducts are used, it is more difficult to analyse grouting defects since the radiation penetrating through the duct is reduced. The advantage of the radiographic method is its ability to provide information about the internal area of the duct. However, the disadvantages are the need to conform to the laws for radiation protection, the considerable weight of the equipment and the long exposure time required. In addition, radiography works as

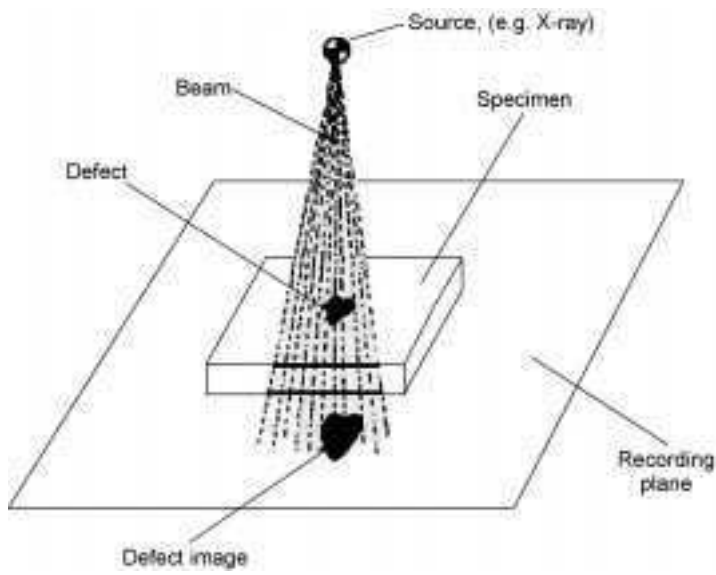

6.20 Principle of radiographic method.[78]

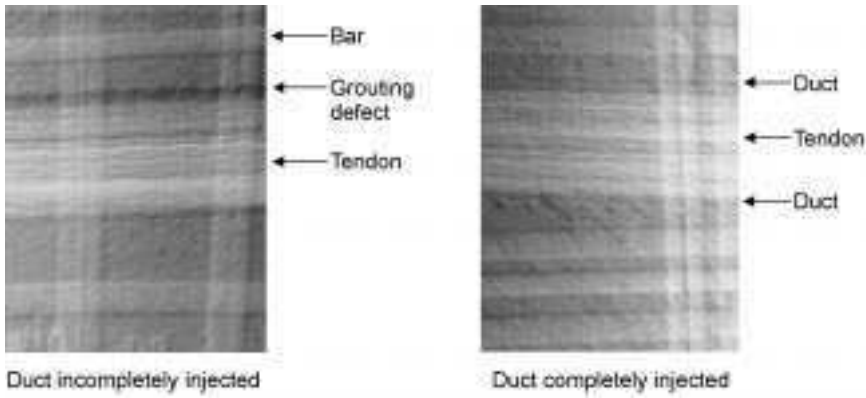

6.21 Tendon with non-grouted area.[79]

a 'point-wise method' which does not allow a quick scan of members, so radiography is only used in exceptional circumstances.

Ultrasonic and impact echo methods

With the ultrasonic and impact echo methods, elastic waves are generated on the concrete surface. In the impact-echo method, waves are scattered and reflected by faults (see Fig. 6.22) and so allow predictions concerning possible defects to be made. Flaws can be identified by means of deviations from the normal wave velocity. In contrast to the ultrasonic method, signals are evaluated in the

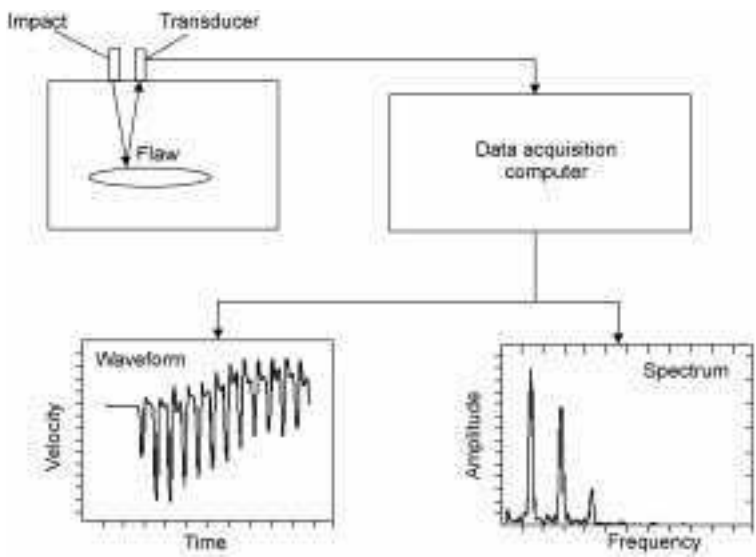

6.22 Principle of impact-echo-method.[80]

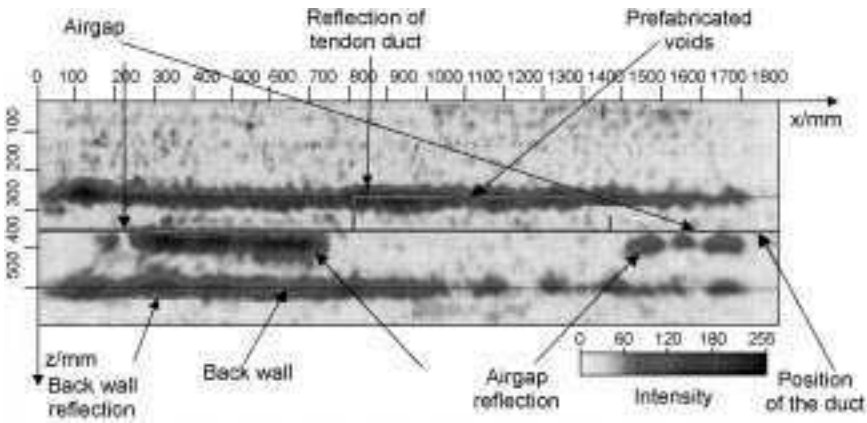

6.23 Image of grouted and ungrouted areas of a duct.[81]

frequency domain. It is difficult to apply the ultrasonic method to concrete because of the strong attenuation of the ultrasonic waves due to scattering and absorption caused by pores and grains in the concrete. To overcome this, ultrasonic waves in the range of 10–200 kHz are used. The associated wavelengths range from 0.3 to 0.015 m. Ultrasonic measurements can detect voids but are not always effective in detecting grouting defects in field conditions.[82]

Large-aperture procedures for scanning the members are necessary. The Synthetic-Aperture-Focusing Technique (SAFT) is effective and has been applied for some time now. The probe transmits waves into the concrete, and the reflected waves (e.g., reflected from tendons) received by the transducers are recorded by a computer. Every image-point, which represents a possible reflector or diffuser, must be considered. The image-point records the amplitude according to the time the wave takes to travel. High values denote the existence of a reflector at a point. In laboratory conditions, it is possible to detect grouting defects using SAFT. Figure 6.23 shows a reconstructed SAFT image using ultrasonic shear-waves with a polarisation parallel to the tendon. Between 800 and 1400 mm, the grouting defect becomes visible due to the absence of the echo from the tendon.

The detection of grouting defects and locating tendons should be possible using the scanning impact-echo method (SIEM).[80] However, reliable and consistent results have not yet been achieved.[83] At present, it is not possible to use the ultrasonic and impact-echo methods to detect grouting defects in prestressed members on site, but research based on SAFT aimed at improving these methods is in progress.

6.7.5 Detection of ruptures in pre-stressing steel

Radiography, time domain reflectometry (TDR) and magnetic methods are in principle suitable for detecting corrosion of steel tendons. In practice,

radiography is normally too expensive and requires access to both sides of the prestressed member. The TDR method also fails to detect some tendons because their proximity means they are connected electrically with one another,[84] but it works very well with electrically isolated tendons.[85]

Amongst magnetic techniques, only the magnetic flux leakage measurement method (MFL) is appropriate for detecting ruptures in steel tendons in typical prestressed concrete members. The MFL method was first used to investigate prestressed concrete members by Kusenberger.[86] Later, the MFL method was enhanced to allow its use in field conditions.[87–93] Steel ropes have also been evaluated using this method for some time.[94] The MFL method is based on magnetostatics. In contrast to radar and ultrasonic methods, the concrete has no influence on the measurements.

The MFL method works as follows. The tendon under consideration is magnetised by an exciting magnetic field $H_0(p, x - x_0)$, which is generally generated by a moveable yoke-magnet. $x_0(t)$ denotes the actual position of the yoke-magnet, p describes the amount of the exciting field. The exciting field generates a magnetisation $M(x, x_0)$ in the tendon. The magnetic leakage field H_S is caused by the magnetisation M of the tendon:

$$H_S = -\frac{1}{4\pi}\int_V \frac{div\, M}{r}\, dV \tag{6.6}$$

where r denotes the distance between the measurement point (position of the magnetic field sensor) and the position of the tendon. V denotes the volume of the whole tendon.

The material behaviour (the relation between the magnetic field $H = H_0 + H_S$ and the magnetisation M) can be assumed as:

$$\frac{dM}{dH} = \alpha \cdot sign\left(\frac{dH}{dt}\right) \cdot (M_S \tanh(\xi H) - M) + \frac{\xi \cdot M_S}{\cosh^2(\xi H)} \cdot (1 - \gamma) - \gamma \tag{6.7}$$

where *sign* denotes the algebraic sign of the rate of change of the magnetic field H.

Figure 6.24 shows a typical hysteresis curve of a ferromagnetic material similar to prestressing steel with the parameters: $M_S = 15000$ A/cm; $\alpha = 0.06$; $\xi = 0.06$ cm/A; $\gamma = 1$.

Local disturbances of the magnetisation due to ruptures or reduction of the cross-section cause typical magnetic leakage signals. The magnetic flux leakage measurements can be performed during magnetisation (active field measurement) or as a residual field measurement after defined sequences of magnetisations.

To conduct the magnetic measurements, a probe containing the magnetisation device (electrically controlled yoke-magnet) and the magnet sensors (Fig. 6.25), is moved along the path of the prestressed tendons. Figure 6.26 shows signals typical of a rupture or crack in a tendon for measurements in the active field (AF) and the residual field (RFM) after magnetisation. In Fig. 6.26 the probe was moved from 0 to 300 cm. At this position, the exciting field was switched

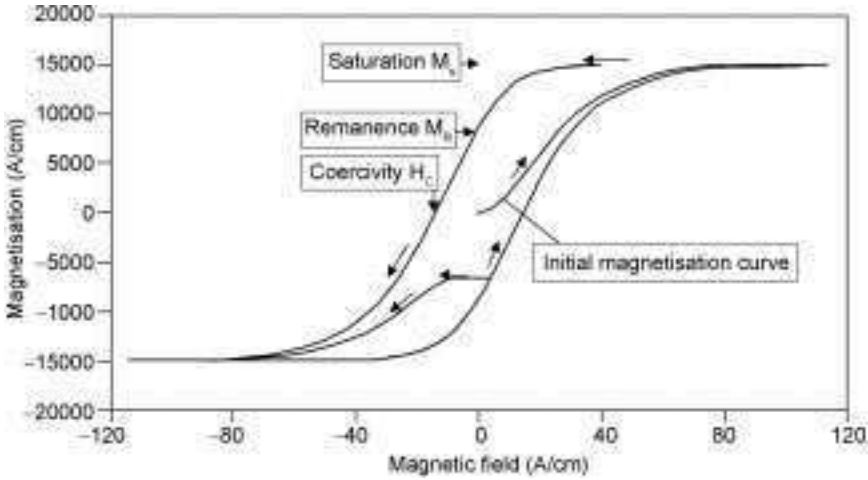

6.24 Typical hysteretical curve (M_S – saturation, M_R – residual magnetisation).

off. It can be seen that the length of the yoke-magnet affects the shape of the magnetic signals.

The MFL signals are affected not only by possible cracks in the tendons but also by the ducts and especially the stirrups, which have a smaller distance to the probe than the tendons. To suppress these unwanted signals, several techniques for measurement and analysis have been developed.[90] After a suitable sequence

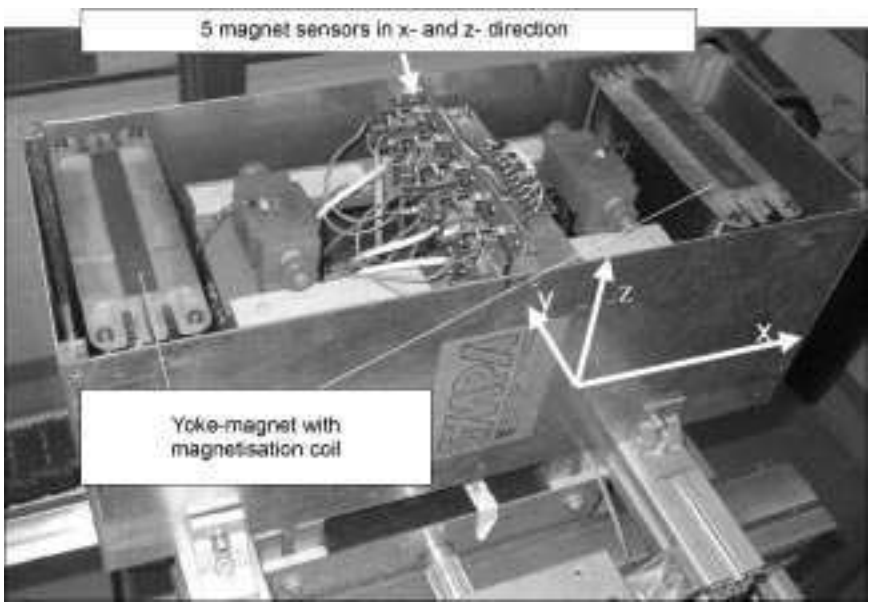

6.25 Probe for magnetic flux leakage measurement.

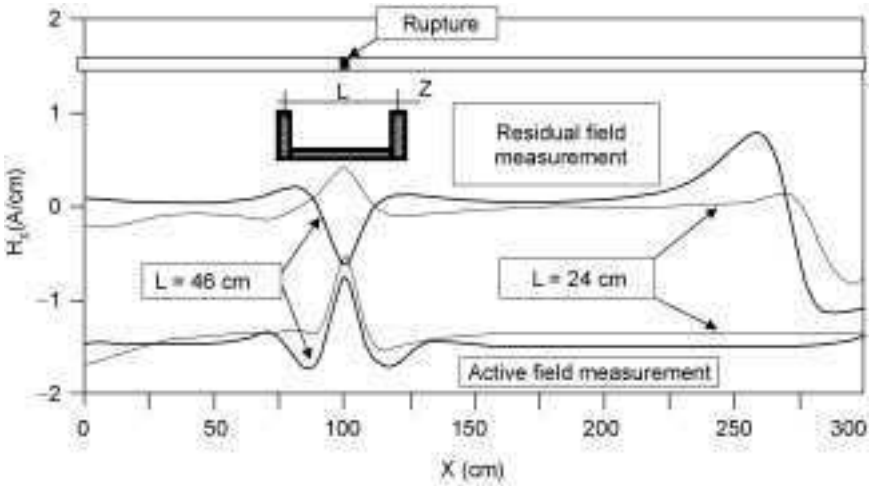

6.26 Typical signal of a rupture (axial-component) at a distance $z = 10$ cm.

of magnetisations, the relationship between signals caused by cracks or corrosion in tendons and the signals caused by ducts and stirrups can be improved.

The signals caused by stirrups can be filtered out more easily in the case of residual field measurements than in the case of measurements in the active field.[91] Measurements in the active field show more details than the residual field measurements, but the signal analysis is more difficult. In Fig. 6.27 the signals from the ducts or tendons under investigation show a typical saw-tooth shape (residual field signal) caused by the stirrups. The sum of both signals after filtering (removing of the signal portion of the stirrups) is shown at the top of Fig. 6.27. This remaining signal is evaluated by means of a correlation with a typical signal caused by a crack as shown in the lower part of Fig. 6.27. At the positions $x = 200$ and $x = 250$ cm, a good agreement with typical signals caused by cracking can be seen. By comparison with laboratory tests, it can be concluded that the tendon (concrete cover about 10 cm) has about 2–3 broken wires out of a total of 16 wires.

Investigating a prestressed member using MFL may be conducted as follows:

1. Location of the tendon, attaching the probe as near as possible to the tendon.
2. Application of a useful schedule of magnetisations to the member, i.e. a sequence of several passes for magnetisation and measuring.
3. Signal analysis (filtering signals caused by stirrups, correlation of remaining signals with signals typical for cracks, evaluation of the signals).

In Fig. 6.28, measuring equipment is shown at the site of a bridge investigation. Because of the magnetisation necessary, the probe is rather heavy, weighing approximately 50 kg. For this reason, using this method on site has to be carefully planned with regard to the necessary support constructions.

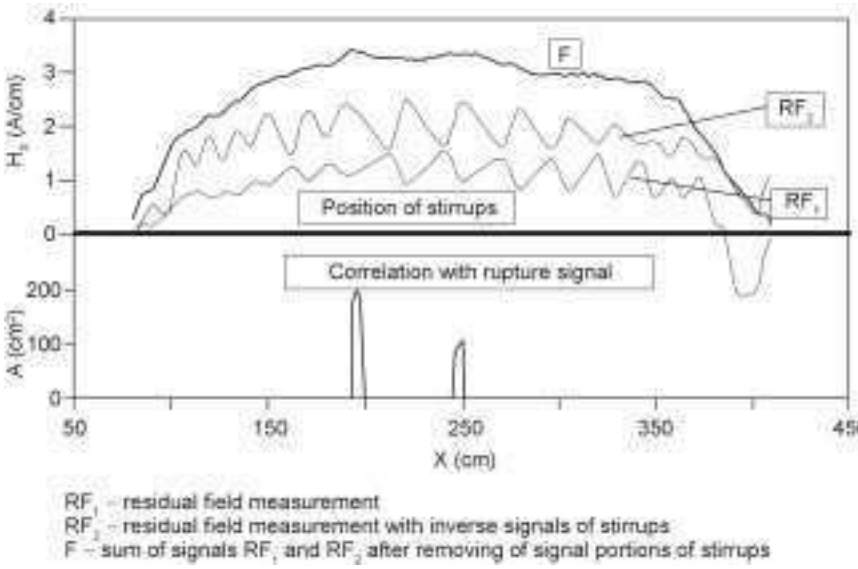

6.27 Signal analysis – filtering out of signal portions of stirrups and rupture analysis.

Experience in the field has shown that in post-tensioned members areas with heavy damage (i.e. considerable loss of the cross-section as a result of ruptures in several wires), as well as ruptures of single tendons in a duct, can be clearly recognised. However, ruptures of single wires or incipient cracks in a post-tensioned tendon cannot be detected, especially in cases where there are magnetic signals originating from any other embedded mild steel reinforcement

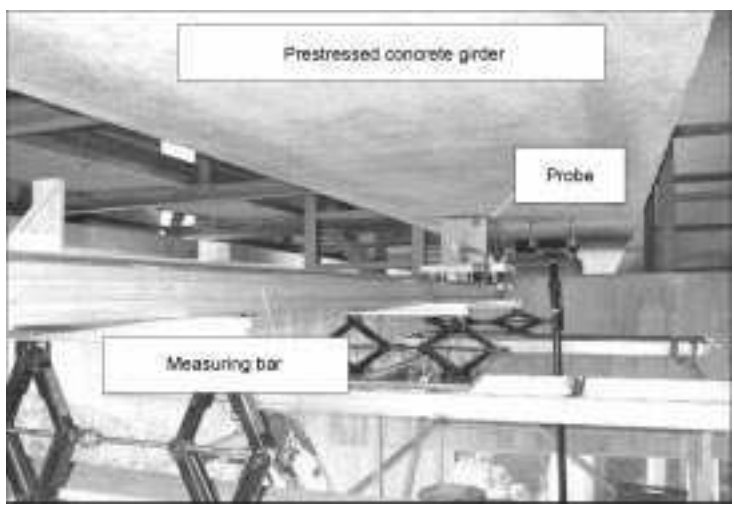

6.28 MFL equipment on site.

elements such as anchorage points. The MFL method permits a relatively quick non-destructive scan of prestressed members. Visual inspection after uncovering the steel should, however, be performed to confirm these findings.

6.8 Conclusions

All over the world serious damage in post- and prestressed components has occurred due to stress corrosion cracking of prestressed steel during the past 40 years. Because the associated design, execution and building materials used were not unusual this problem has caused great concern. An important factor is that prestressed steel is unable to withstand the combined effects of variable quality of construction and corrosion within the construction itself. As a result, some important measures and changes have been introduced to reduce the occurrence of damage related to stress corrosion cracking. They include improved standards and recommendations[2,95,96] for planning and execution of new constructions and for strengthening older structures. Research has been done to develop non-destructive measuring techniques to investigate older prestressed constructions. Building materials which cannot guarantee durable protection of the embedded steel have been forbidden, and more effective control (e. g. testing the resistance of prestressing steel against stress corrosion cracking) can now prevent unsuitable materials coming on the market.

6.9 References

1 Mietz J, Nürnberger U, Beul W, *Untersuchungen an Verkehrsbauten aus Spannbeton zur Abschätzung des Gefährdungspotentials infolge Spannungsrißkorrosion der Spannstähle*, Berlin Stuttgart, BAM FMPA 1994.
2 *fib* Bulletin 15, *Durability of post-tensioning tendons*, Federation de la Precontrainte, Lausanne, 2001, 284pp.
3 Nürnberger U, 'Analyse und Auswertung von Schadensfällen bei Spannstählen', *Forschung, Straßenbau und Straßenverkehrstechnik*, 1980 **308** 1–195.
4 Isecke B, 'Besondere Probleme des Korrosionsschutzes im Spannbetonbau', in *Korrosionsschutz im Massivbau*, Ehningen, Expert-Verlag GmbH, 1990.
5 Nürnberger U, *Influence of material and processing on stress corrosion cracking of prestressing steel case studies*, fib technical report, bulletin 26, Lausanne, 2003.
6 Nürnberger U, *Korrosion und Korrosionsschutz im Bauwesen*, Wiesbaden, Bauverlag, 1995.
7 Nürnberger U, 'Einflüsse von Werkstoff und Verarbeitung auf die Spannungsrißkorrosion von Spannstählen', *Werkstoffe und Korrosion*, 1997 **48** 602–612.
8 Isecke B, Menzel K, Mietz J, Nürnberger U, 'Gefährdung älterer Spannbetonbauwerke durch Spannungsrißkorrosion', *Beton- und Stahlbetonbau*, 1995 **90** 120–123.
9 Mietz J, Fischer J, Isecke B, 'Spannungsrißkorrosion an Spannstählen', *Materials and Corrosion*, 1999 **50** 535–540.
10 Weise H, Krämer W, Bartels W and Brand W-D, 'Bewehrungsstähle für den Stahlbeton- und Spannbetonbau', in *Werkstoffkunde Stahl*, Bd. 2, Springer Verlag, Berlin, Heidelberg and Verlag Stahleisen, Düsseldorf 1985.

11 Leonhardt F, *Spannbeton für die Praxis*, Berlin, München, Düsseldorf, Wilhelm Ernst & Sohn, 1973.
12 Nürnberger U, 'Corrosion induced failure mechanisms of prestressing steel', *Materials and Corrosion*, 2002 **53** 591–601.
13 Nürnberger U, *Corrosion induced failures of prestressed concrete structures*, The first fib congress, Osaka, Japan, 2002.
14 Neubert B, Nürnberger U, *Erkennen von Spannverfahrensschädigung – Untersuchung der statischen und dynamischen Kenngrößen in Abhängigkeit von Rostgrad*, Stuttgart, FMPA Otto-Graf-Institut, 1983.
15 Nürnberger U, Beul W, *Entwicklung einfacher und reproduzierbarer Prüfverfahren für die Empfindlichkeit von Spannstählen gegenüber Spannungsrißkorrosion*, Stuttgart, FMPA Baden-Württemberg, Otto-Graf-Institut, 1996.
16 Nürnberger U, 'Corrosion induced cracking of reinforcing steel', in: Mietz J, Elsener B, Polder R, *Corrosion of Reinforcement in Concrete*, *ECF Publication,* 1997.
17 Nürnberger U, 'Zum Einfluß werkstoffunabhängiger Größen auf die Spannungsrißkorrosion unlegierter, kohlenstoffarmer Stähle in Kalziumnitratlösungen', *Werkstoffe und Korrosion*, 1977 **28** 312–321.
18 Rehm G, Nürnberger U, 'Spannungsrißkorrosion hochfester Stähle' *Cement (niederländisch) XXIV,* 1972 106–115.
19 Isecke B, *Kritische Beurteilung neuer Spannstahlentwicklungen*, Berlin, Forschungsbericht i. A. des Deutschen Betonvereins e. V., 1993.
20 Grimme D, Isecke B, Nürnberger U, Riecke E M, Uhlig G, *Spannungsrißkorrosion in Spannbetonbauwerken,* Düsseldorf, Verlag Stahleisen mbH, 1983.
21 Rehm G, Nürnberger U, Frey R, 'Zur Korrosion und Rißkorrosion bei Spannstählen', *Werkstoffe und Korrosion*, 1981 **32** 211–221.
22 Nürnberger U, 'Mehr Sicherheit im Spannbetonbau; Chloridgehalte und Feuchte beachten; Korrosion behindern'. *Maschinenmarkt,* 1989 **95** 30–40, 68–72 and 128–134.
23 Mietz J, Pasewald K, Isecke B, 'Untersuchungen zum wasserstoffinduzierten Sprödbruch vergüteter Spannstähle', *Vortragsbeiträge 33. DAfStb-Forschungskolloquium*, Berlin, BAM, 1996.
24 Rehm G, 'Schäden an Spannbetonbauteilen, die mit Tonerdeschmelzzement hergestellt wurden', *Betonsteinzeitung*, 1963 **29** 651–661.
25 Rehm G, Nürnberger U, Frey R, 'Zur Korrosion und Spannungsrißkorrosion von Spannstählen bei Bauwerken mit nachträglichem Verbund', *Bauingenieur*, 1981 **56** 275–281.
26 Rauen A, 'Der Sonderfall Tonerdeschmelzzement', in *Korrosionsschutz im Ingenieurbau*, VDI-Berichte 1988.
27 Rehm G, Nürnberger U, 'Neue Methoden zur Beurteilung des Spannungsrißkorrosionsverhaltens von Spannstählen', *Betonwerk + Fertigteil-Technik*, 1992 **48** 287–294.
28 Plähn J: *Untersuchungen über den Einfluß des Sulfidgehaltes und des pH-Wertes der Umgebung von Spannstählen auf ihr Sprödbruchverhalten*, Hannover, Bericht des Lehrstuhls und Instituts für Baustoffkunde und Materialprüfung der Technischen Universität Hannover, 1978.
29 Wiume D, Nürnberger U, 'Schwingfestigkeitsverhalten hochfester Seildrähte in korrosiven Medien,' *Werkstoffe und Korrosion*, 1986 **37** 485–493.
30 Nürnberger U, Beul W, 'Wasserstoffinduzierte Spannungsrißkorrosion von zugschwellbeanspruchten Spannstählen' in*: Bewehrte Betonbauteile unter Betriebsbedingungen* Verlag Wiley-VCH, 2000.

31 Riecke E, 'Über den wasserstoffinduzierten Sprödbruch hochfester Stähle', *Archiv Eisenhüttenwesen*, 1973 **44** 647–656.
32 Schneider K, 'Einfluß des Silizium- und Mangangehaltes im ölschlußvergüteten Spannstahl St 140/160 auf die Beständigkeit gegenüber Wasserstoffrißkorrosion', *Neue Hütte*, 1971 **16** 529–535.
33 Shiraga T, Ishikawa N, Ishiguro M, Yamashita E, Mizoguchi S, 'Effects of Ni, Si and Cu on the properties of steel bars for prestressed concrete', *NKK Technical Review*, 1996 **75** 11–18.
34 Bernabai U, Brombara G, Borruto A, 'Metals Technology', 1983 **10** 20.
35 Stolte E, 'Über die Spannungsrißkorrosion an Spannstählen', *Beton- und Stahlbetonbau*, 1968 **63** 116–118.
36 Hampejs G, 'Spannungsrißkorrosion von Spannstählen – Prüfung im Ammoniumrhodanidversuch', *Betonwerk + Fertigteil-Technik*, 1986 **52** 303–307.
37 Nürnberger U, Neubert B, 'Entwicklung und Bewertung des Regelwerkes im Spannbetonbau aus korrosionstechnischer Sicht', in *Fortschritte im Konstruktiven Ingenieurbau*, Berlin, Verlag Ernst & Sohn, 1984.
38 DIN EN 10138, Prestressing Steels, 2000.
39 Nürnberger U, 'Dauerschwingverhalten von Spannstählen', *Bauingenieur*, 1981 **56** 311–319.
40 Patzak M: *Die Bedeutung der Reibkorrosion für nichtruhende Verankerungen und Verbindungen metallischer Bauteile des konstruktiven Ingenieurbaus*, Stuttgart Dissertation Universität Stuttgart, 1979.
41 Cordes H, 'Dauerhaftigkeit von Spanngliedern unter zyklischen Beanspruchungen', *Schriftenreihe Deutscher Ausschuß für Stahlbeton*, 1986 **370**.
42 Rehm G, Nürnberger U, Patzak M, 'Keil- und Klemmverankerungen für dynamisch beanspruchte Zugglieder aus hochfesten Stählen', *Bauingenieur*, 1977 **52** 287–298.
43 Erdmann J, Kordina K, Neisecke J, *Baustoffuntersuchungen an Spannbetonbauwerken zur Ermittlung des Langzeitverhaltens von Spannstählen*, Institut für Baustoffe, Massivbau und Brandschutz der TU Braunschweig, 1982.
44 König G, Maurer R, *Sicherheit von Spannbetonbrücken,* Forschung, Straßenbau und Straßenverkehrstechnik, 1990 **590**.
45 Isecke B, 'Neuartige Korrosionsprobleme an Bündelspanngliedern mit nachträglichem Verbund', *Bautechnik*, 1983 **60** 1–7.
46 Fried. Krupp Hüttenwerke AG, Werk Rheinhausen, *Beiträge zum FIP-Symposium 'Spannstähle'*, Madrid, 1968.
47 Mietz J, Fischer J, Isecke B, 'Spannstahlschäden an einem Brückenbauwerk infolge von Spannungsrißkorrosion', *Beton- und Stahlbetonbau*, 1998 **93** 195.
48 Matthaes K, Z. *Metallkunde*, 1956 **47** (1) 37–42.
49 Jänicke W, Stolte E and Litzke H, *Materialprüfung*, 1965 **7** (12) 449.
50 Brechbühl W, *Draht-Welt*, 1962 **48** (4) 138.
51 Jänicke W, *Werkstoffhandbuch Stahl und Eisen VDEh*, Düsseldorf: 4. Auflage Bl. N3, 1965.
52 Lehnert W, *Neue Hütte*, 1968, **12**, 716.
53 Naumann F K and Bäumel A, *Arch. Eisenhüttenwes*., 1961 **32** (2) 89.
54 Rehm G, *Betonstein – Ztg.*, 1963 **29** (12) 651–656.
55 Bruggeling A S G, General Report, 'Erfahrung und Schwierigkeiten bei der Herstellung und Verwendung von Spannstählen', *Proc. 2nd Congr. of FIP*, Amsterdam, 1955, 164–177.
56 Houdremont E, Bennek H and Wentrap H, 'Über die interkristalline Korrosion des Flugeisens, ihre Erforschung und Bekämpfung', *Tech. Mitt. Krupp*, 1940 **3** 111.

57 Report on Prestressing Steel – 5. Stress corrosion cracking resistance test for prestressing tendons, *Federation Internationale de la Precontrainte (FIP),* 1980.
58 FIP – Commission on Prestressing Steels in Proc. *3rd Symp. on Stress Corrosion of Prestressing*, 1981.
59 Nürnberger U and Beul W, *Entwicklung einfacher und reproduzierbarer Prüfverfahren für die Empfindlichkeit von Spannstählen gegenüber Spannungsrißkorrosion*, Abschlußbericht DafStb, 1996.
60 'Bestimmungen für die Durchführung von Spannungsrißkorrosionversuchen', DIBt – Berlin 1992.
61 Schiesst C and Moersch J, *Einfluß einer erhöhten Beanspruchung auf die Festigkeitsgrenze von gezogenen Spannstählen*, Abschlußbericht zum Forschungsvorhaben DIBt – F422, 1997.
62 Mietz J, Isecke B and Pasewald K, *Zulässige Krümmungsradien von Spannstählen (Stäbe) bei erhöhter Vorspannung*, Abschlußbericht zum DafStb – Forschungsvorhaben V341, 1995.
63 R. Krumbach R, Meichsner H and Schubert L, *Beton- und Stahlbetonbau,* 1997 **92** 325.
64 Mietz J, 'Investigations on hydrogen-induced embrittlement of quenched and tempered prestressing steels', *Mater. Comos*., 2000 **51** 80.
65 Podolny W Jr, 'Corrosion of prestressing steels and its mitigation,' *Journal PCI*, 1992 **37** (5) 34–55.
66 Cullington D W, MacNeill D, Paulson P and Elliot J, 'Continuous acoustic monitoring of grouted post-tensioned concrete bridges', *Nondestructive Testing and Evaluation International*, 2001 **34**(2) 95–105.
67 Bungey J H, Millard S G and Grantham M G, *Testing of Concrete in Structures*, 4th edn, Taylor and Francis, 2006.
68 Elsener B, Böhni H, 'Lokalisierung von Korrosion im Stahlbetonbau – Möglichkeiten und Grenzen', *Schweizer Ingenieur und Architekt,* 1987 **19** 528–533.
69 Menzel K, Preusker H, 'Potentialmessung – Eine Methode zur zerstörungsfreien Feststellung von Korrosion an der Bewehrung', *Bauingenieur,* 1988 **64** 181–186.
70 DGZfP, *Merkblatt B3: Merkblatt für elektrochemische Potentialmessungen zur Ermittlung von Bewehrungsstahlkorrosion in Stahlbetonbauwerken*, 1990.
71 Millard S N, Bungey, Gowers, 'Rapid assesment of corrosion of in-situ reinforcement concrete by analysis of transient response to galvanostatic pulse', Int. Symposium *Nondestructive Testing in Civil Engineering (NDT-CE)*, Berlin 1995 121–134.
72 Wojtas H, 'Elektrochemisache, zerstörungsfreie Prüfmethoden für Zustandsanalysen und Qualitätssicherung bei Instandsetzung von Stahlbetonbauten', *Int. Zeitschrift für Bauinstandsetzen*, 1997 **3** 581, 602.
73 Maierhofer C, Leipolt S, Wöstmann J, 'Strukturuntersuchungen in Beton mit dem Impulsradar', In: Bauwerksdiagnose, *DGZfP-Berichtsband*, 1999 **66** CD 47–57.
74 Krause H-J, *Supplementary sheet: Detection of Tendons using ground-penetration-radar*, FZ Jülich 2002.
75 Bungey J H, 'Subsurface radar testing of concrete – a review', *Construction and Building Materials*, 2004 **18**(1) 1–8.
76 Langenberg K J, 'Applied inverse problems for acoustic, electromagnetic and elastic wave scattering', *Basic methods of tomography and inverse problems*, *Malvern Physic Series*, 1987 127–469.
77 Tschartke D, 'Fehlerdiagnose in der Ultraschallprüfung durch iterative Modellierung', *Diss.* 2002 TU Berlin.

78 Bray D E, Stanley R K, *Nondestructive Evaluation*, New York, McGraw-Hill, 1989.
79 Brown K, Leger J, 'Use of the Megascan^{TM} imaging process in inspection systems for post-tensioned bridges an other major structures', *Int. Symposion Non-Destructive Testing in Civil Engineering (NDT-CE 2003)*, Berlin, 2003, contr. v 203.
80 Sansalone M J, Street W B, *Nondestructive Evaluation of Concrete and Masonry*, Bullbrier Press, 1994.
81 Krause M; Mielentz F, Milmann B, Streicher D, Müller W, 'Ultrasonic imaging of concrete elements state of the artusing 2D synthetic aperture', *Int. Symposion Non-Destructive Testing in Civil Engineering (NDT-CE 2003)*, Berlin, 2003, contr. v 051.
82 Wiggenhauser H, 'Duct inspection using impact-echo', *Symposion Non-Destructive Testing in Civil Engineering (NDT-CE 2003)*, Berlin, 2003, contr. v 101.
83 Tinkey Y, Olson L D, Bednon R, Lieberle C, 'Impact echo scanning technology for internal grout condition evaluation in post-tensioned bridge-ducts', *Symposion Non-Destructive Testing in Civil Engineering (NDT-CE 2003)*, Berlin, 2003, contr. v 041.
84 Elsener B, Böhni H, Bräunlich R, Markees A, *Zerstörungsfreie Spannkabelprüfung mit reflektometrischer Impulsmessung*, Forschungsbericht, Eidgenössisches Verkehrs- und Energiewirtschaftsdepartement, Bundesamt für Strassenbau, Arbeitsgruppe für Brückenunterhaltung, 1997, 81/93.
85 Wichmann H-J, Holst A, Hariri K, Budelmann H, 'Detection and localisation of fractures in tendons by means of electromagnetic resonance measurement', *Int. Symposion Non-Destructive Testing in Civil Engineering (NDT-CE 2003)*, Berlin, 2003, contr. v 104.
86 Kusenberger F N, Barton J R, *Detection of flaws in reinforcement steels in prestressed concrete bridges*, Washington DC, Final ReportFH-WA/RD-81/087, Feral Highway Administration 1981.
87 Sawade G, Menzel K, 'Zerstörungsfreie Feststellung von Spannstahlrissen in vorgespannten Deckenträgern', *Werkstoff und Korrosion*, 1989 **40** 456.
88 Hillemeyer B, Flohrer C, Schaab A, 'Zerstörungsfreie Ortung von Spannstahl-brüchen in Spannbeton-Deckenträgern', *Beton- und Stahlbau,* 1989 **84**, 168–270.
89 Sawade G, Straub J, Krause H-J, Bousack H, Neudert G, Ehrlich R, 'Signal analysis methods for remote magnetic examination of prestressed elements', *Proc. Intl. Sympos. on NDT in Civil Engineering (NDT-CE)*, Berlin, Vol.II, DGZfP, 1077–1084, 1995.
90 Scheel H, *Spannstahlbruchortung an Spannbetonbauteilen mit nachträglichem Verbund unter Ausnutzung des Remanenzmagnetismus*, Berlin, Ph.D. Thesis, D 83, Technical University Berlin, 1997.
91 Sawade G, *Mobiles SQUID-Meßsystem zur Bauwerksinspektion, Teilvorhaben Magnetisierungsvorrichtung und Signalverarbeitung*, Forschungsbericht 13 N 7249/3, Bundesministerium für Bildung Wissenschaft, Forschung und Technologie, 2001.
92 Krause H-J, Glaas W, Zimmermann E, Faley M I, Sawade G, Mattheus R, Neudert G, Gampe U, Krieger J, 'SQUID array for magnetic inspection of prestressed concrete bridges', *Physica C*, 2002 **368**(1–4) 91–95.
93 Ghorbanpoor A, 'Magnetic-based NDE of steel in prestressed and post-tensioned concrete bridges', *Proc. Structural Materials Technology III*, San Antonio, Texas, 1998 343–349.
94 Nussbaum J-M, *Zur Erkennbarkeit von Drahtbrüchen in Drahtseilen durch Analyse des magnetischen Störstellenfeldes*, Diss. Universität Stuttgart, 1999.
95 fib, 2001, Factory applied corrosion protection of prestressing steel, p. 20.
96 fib, 2002, Grouting of tendons in prestressed concrete, guidlines, bulletin 20, p. 52.

7

Concrete aggregates and the durability of concrete

M D A THOMAS, University of New Brunswick, Canada and
K J FOLLIARD, University of Texas at Austin, USA

7.1 Introduction

Aggregates are the major constituents of concrete and typically occupy between 60% and 80% of the concrete volume. Properties of both fresh and hardened concrete are influenced by the quality of aggregates and yet their role is often overlooked. This chapter provides a brief review of the general requirements of concrete aggregates; the main focus concerns how aggregates can affect concrete durability. Although most aggregates are strong, hard, volumetrically stable, free of harmful impurities and chemically inert, some aggregates can behave in an undesirable manner and lead to premature failure of the concrete. Frost-susceptible aggregates can result in cracking (commonly called durability cracking, D-cracking or D-line cracking) and deterioration of concrete exposed to cycles of freezing and thawing in service; this phenomenon is discussed in the third section of the chapter (see also Chapter 9). The fourth section deals with harmful constituents of aggregates including organic matter, clay/silt content, coal/lignite materials, soft particles and salts. Sections 7.5 to 7.8 cover alkali-aggregate reactions (AAR) due to reaction between the alkali hydroxides from cement (and other sources) with either unstable siliceous (alkali-silica reaction, ASR) or carbonate (alkali-carbonate reaction, ACR) constituents of certain aggregates. AAR can result in expansion and cracking of concrete. In addition to a description of the reaction mechanisms, information is provided on testing to identify potentially reactive aggregates, measures for preventing deleterious expansion when reactive aggregates are used in new concrete and techniques for mitigating or suppressing expansion in existing structures affected by AAR. The final section discusses future trends in aggregate production including the use of manufactured fines and the use of recycled concrete and other waste materials as aggregates.

7.2 General requirements of aggregates for use in concrete

In most cases, aggregates perform very well in Portland cement concrete. Aggregates, because they occupy about 60 to 80% of the total volume of

concrete, affect many key fresh and hardened concrete properties and also contribute to the long-term performance of the concrete structure, including its long-term durability and resistance to cracking. Aggregates also allow for the overall cost of concrete to remain lower, thereby making concrete an economically competitive product. Given the importance of aggregates in concrete, it is essential to understand the general aggregate properties needed to ensure quality concrete and to also be aware of potential durability-related issues. Because the emphasis of this chapter and book is durability, only a brief coverage of general requirements is provided. For a more detailed discussion of general aggregate properties, various references are available (Mehta and Monteiro, 1993; Neville, 1996; Kosmatka *et al.*, 2002). This section will briefly discuss general requirements for aggregates, with an emphasis on how these aggregate properties may impact long-term durability.

Aggregates affect the fresh, hardened, and durability characteristics of concrete. Their impact is quite direct, even at early ages, in some cases (e.g., thermal conductivity, elastic modulus) and less direct or more long-term for other cases (e.g., AAR).

Physical characteristics of aggregates, such as gradation, absorption, and specific gravity are important properties for mixture proportioning and general quality control and assurance. They can also be important to durability in several ways. For example, for some aggregate types, absorption and specific gravity values can serve as useful indices for frost susceptibility (as discussed in detail in Section 7.3). Aggregate grading, shape, and texture have significant effects on water demand for fresh concrete, and any water added to the concrete to offset workability issues will increase the permeability of the concrete and exacerbate frost-related damage. The presence of microfines (or aggregate particles passing the #200 sieve) will particularly influence the water demand of concrete, especially if the microfines contain clay. Aggregates have a direct impact on the thermal properties of concrete, especially thermal conductivity, specific heat, and coefficient of thermal expansion (CTE). The thermal conductivity and specific heat values of aggregates play a key role in early-age mass concrete elements as these values will affect directly the heat transfer process. The CTE affects both the early-age behavior and also the long-term thermal stability of concrete (in terms of effects on daily thermal strains, curling, warping, etc.). Although aggregates mainly affect concrete shrinkage and creep indirectly by providing internal restraint to these causes of volume change, some fine-grained aggregates can, themselves, undergo shrinkage upon drying (Meininger, 1998).

The mechanical properties of aggregates, such as strength, elastic modulus, abrasion (and wet attrition) resistance, and resistance to polishing can all have some impact on durability. The strength of aggregates can have a somewhat minor effect on concrete of relatively low strength (say 20 MPa or less) because the bond strength is typically weak, with failure around aggregates. For denser, stronger concrete mixtures (e.g., over 50 MPa), the aggregate strength may

become more important as the interfacial transition zone (ITZ) is so high in strength and low in porosity that failure can occur through the coarse aggregates. The elastic modulus of aggregates plays a significant role in early-age properties, especially with regard to cracking potential, and in long-term properties, such as deflections. Because coarse aggregates play such a key role in concrete stiffness, measuring the elastic modulus of concrete containing a subject aggregate is a good surrogate for aggregate stiffness determination. The resistance of aggregates to abrasion becomes important when heavy abrasion to the concrete surface is anticipated (e.g. floors of industrial warehouses or surfaces exposed to studded tires, etc.). Abrasion resistance may also be a factor in the breakdown of aggregates during handling, mixing, and placing concrete. Dry abrasion tests, like the Los Angeles (LA) abrasion test (AASHTO T 96), involve rotating aggregates in a test vessel with steel balls as charges. The trend in recent years has been towards wet attrition tests, such as the Micro-Deval test (CSA A23.2-23A, AASHTO T 327), which tend to better represent the type of distress observed in field concrete. The resistance of an aggregate to polishing is important, especially for pavements and other types of flatwork. Typically, the top layer of concrete is mortar-rich, where the polish resistance of the fine aggregate tends to govern behavior. Although methods exist to measure polishing of aggregates or concrete containing the subject aggregates, they are not commonly available in many locations. Tests that indirectly assess polish resistance, such as the acid insoluble test (ASTM D 3042), focus on the composition of the aggregate and its inherent link to polish resistance. The acid insoluble test estimates the amount of non-carbonate (usually siliceous) material in the aggregate sample; this information can be useful because, generally, the higher the acid insoluble fraction, the higher the polish resistance, and hence, the better the skid resistance on pavements (Meininger, 1998). Generally, limestone sands tend to result in more polishing in the cover concrete than siliceous sands, and some agencies and owners limit the amount of carbonates in sands.

The chemical or mineralogical properties of aggregates can significantly affect concrete performance and long-term durability. The effects of mineralogy, aggregate composition, and pore structure are especially related to alkali-aggregate reactivity (Sections 7.5–7.8) and frost susceptibility (Section 7.3), and the presence of impurities and harmful constituents and their effect on durability are discussed in Section 7.4.

7.3 Frost resistance of aggregates

Although most issues related to frost resistance of concrete are associated with damage emanating from the paste (e.g., due to internal disruption or surface scaling), there are cases where the aggregates, themselves, either exhibit distress or cause distress of the surrounding paste. This section discusses the basic mechanisms responsible for this aggregate-related distress and describes the

manifestations of such distress in field concrete, such as pop-outs and durability cracking (D-cracking). Particular emphasis is placed on discussing the aggregate characteristics, such as pore size distribution, total porosity, and size, that have most impact on frost resistance. Some information is also provided on how to identify those aggregates that may lead to poor frost resistance.

7.3.1 Factors affecting frost resistance of aggregates

Air-entrainment is an accepted method of ensuring durability of concrete in a cold environment, with regard to both internal distress and external damage from salt scaling (see also Chapter 9). However, even when concrete is properly air-entrained, certain types of coarse aggregates can cause distress. The mechanisms responsible for this distress are discussed next.

Frost damage in hydrated cement paste has been attributed to several potential mechanisms, including hydraulic pressure, osmotic pressure, ice lens formation, and others. When the source of the distress is from within the aggregates, the most likely mechanism is related to hydraulic pressure, where water undergoes approximately a 9% increase in volume as it freezes to form ice (Powers, 1955). Hydraulic pressure is more likely to be the main culprit within aggregates because of their coarser pore structure, compared to that of hydrated cement paste (Pigeon and Pleau, 1995).

The tendency for an aggregate to generate internal stresses upon freezing is primarily a function of its internal pore structure. The ability for a given aggregate to withstand the resultant stress is a function of its strength (and stiffness), permeability (to water as it is forced out under pressure), and size (due to effects on distance for water to reach the escape boundary). In addition, the structure of the surrounding hydrated cement paste (or more accurately, mortar) has an important impact as it will influence the flow of water as it is being expelled by the aggregate upon freezing. Both the aggregate and hydrated cement paste phases are influenced by the degree of saturation (Fagerlund, 1976). The following is a discussion on what properties of aggregates most influence frost resistance; this is followed by discussion on the role of the surrounding mortar.

Perhaps the single most important feature of an aggregate that affects frost resistance is the pore size distribution, a fact highlighted by several researchers (Kaneuji *et al.*, 1980; Hudec, 1989). Aggregates with a significant number of pores smaller than 5 μm tend to remain nearly saturated, even at moderate humidity levels, and aggregates with smaller pore sizes tend to exhibit lower permeability, thereby generating higher hydraulic pressures (Pigeon and Pleau, 1995). Also, as discussed later in this chapter, one of the most common manifestations of aggregate-related frost damage is D-cracking of pavements or other jointed flatwork, and aggregates that tend to contribute to D-cracking are those with pores in the range of 0.1 to 5 μm. Pores larger than 5 μm typically do not remain completely filled with water (at modest relative humidities) and so

do not result in frost damage, while the water in pores finer than 0.1 μm tends not to freeze readily because of freezing point depression (ACI, 1996).

In addition to the importance of pore size distribution on frost resistance of aggregates, the total porosity of aggregates plays a role. In a comprehensive study involving a range of aggregates with different pore size distributions and porosities, Kaneuji *et al.* (1980) showed that, for aggregates with similar pore size ranges, the aggregate with higher total porosity was the less frost resistant. In the same study, the impact of total porosity was further recognized by the fact that, regardless of pore size distribution, if the total porosity of a given aggregate was low enough (e.g., aggregates with absorption capacities less than 1.5%), durability was not a problem.

Thus, for aggregates, both the pore size distribution and total porosity affect frost resistance. However, for convenience, it is possible to group aggregates into three categories, based solely on total porosity (Pigeon and Pleau, 1995) – low porosity, intermediate porosity, and high porosity. Aggregates with low porosity are generally durable because the amount of freezable water is so low. Aggregates with intermediate porosity are the least durable because, upon full saturation, they contain appreciable freezable water, and the pore structure is restrictive enough to impede the expulsion of water upon freezing. Aggregates with high porosity are generally durable because they tend to have a coarse pore system, which is easily drained as the relative humidity drops below 100% and, when water does freeze within the aggregate, the porous structure (and inherent high permeability) allows for the freezing water to be expelled without causing significant hydraulic pressure (Pigeon and Pleau, 1995).

Because hydraulic pressure is the prevalent mechanism governing aggregate-related distress, it is logical that the size of aggregates affects the development (and release) of pressure within aggregates as water is expelled upon freezing. According to Powers (1955), the extent of the hydraulic pressure is a function of several parameters, including permeability, tensile strength, freezing rate, and distance to escape boundary. When the source of distress is from within an aggregate, the distance to an escape boundary is directly related to the aggregate size. For a given aggregate, there exists a critical size above which frost damage may occur because the distance to an escape boundary is too large for flow of water to relieve the internal stress generated around the freezing sites (Verbeck and Landgren, 1960). For fine-grained aggregates with low permeability, such as chert, the critical particle size may be within the range of normal aggregate sizes (Kosmatka *et al.*, 2002). In fact, many non-durable coarse aggregates can be rendered durable by crushing them, thereby reducing the aggregate dimension below the critical size. This is discussed in more detail later in this chapter with regard to D-cracking. The critical particle size for coarse-grained aggregates or those with pore systems interrupted by numerous macropores (voids too large to hold moisture by capillary action) may be sufficiently high to be of no consequence for typical coarse aggregates used in construction (Kosmatka *et al.*, 2002).

In the previous paragraph, the concept of critical size of aggregate was introduced, with the explanation that the aggregate size relates to the distance to an escape boundary, as per the hydraulic pressure theory. This was somewhat of a simplification in that the exterior surface of an aggregate does not actually constitute an escape boundary; rather, it represents an interface between the coarse aggregate and the surrounding mortar. Thus, the properties of the surrounding mortar will also have a significant impact on the ability of a given aggregate to expel water without damage to the aggregate or surrounding area. The structure of the interfacial transition zone (ITZ) and the hydrated cement paste will both influence this behavior. The ITZ is typically more porous than the surrounding bulk cement paste and tends to have more calcium hydroxide (with a preferred crystal orientation) (Mehta and Monteiro, 1993). In particular, the permeability, availability of entrained air bubbles, and presence of cracking within the ITZ and/or hydrated cement paste will determine whether some or all of the expelled water from aggregates can be accommodated without generating excessive hydraulic pressure. The quality of the hydrated cement paste, especially as influenced by w/c_m and presence of supplementary cementing materials (SCMs), will impact on the frost resistance of aggregates significantly. Lower w/c_m concrete containing SCMs tends to reduce the ingress of external water, thereby reducing the degree of saturation of aggregates.

Although it is not possible to accurately predict which aggregates will exhibit or cause damage due to freezing and thawing based solely on mineralogy, there are some relevant trends in behavior that can be identified. Most non-durable aggregates are sedimentary, can be calcareous or siliceous, and can be gravel or crushed rock (Neville, 1996). Some examples of susceptible aggregates include sandstones, shales, limestones, and especially cherts (Cordon, 1966). Of the above susceptible aggregates, chert is considered the most damaging and prone to D-cracking and pop-outs (Larson and Cady, 1969). Typically, igneous or metamorphic rocks are not frost susceptible due to their inherent low porosity; examples of durable aggregates include granites and basalts (Pigeon and Pleau, 1995).

Just as is the case with frost action on hydrated cement paste, the importance of degree of saturation should not be overlooked when considering aggregate-related frost damage. For an aggregate to be damaged internally or to exude freezing water to damage the surrounding paste, sufficient water must be present within the aggregate. As per the hydraulic pressure theory, aggregates must have at least 91.7% internal moisture content to generate appreciable pressure (Fagerlund, 1976). The ability of an aggregate to reach this degree of saturation is, of course, a function of the exposure condition that the subject concrete encounters, the permeability of the concrete, and the pore structure of the aggregate. As discussed earlier, the porosity and pore size distribution of a given aggregate will influence the rate of water ingress into the aggregate, and the size of the pores will influence the freezing point of the water within the aggregate. It

is important to note that the presence of deicing salts will tend to increase the degree of saturation within the concrete (as well as within the aggregates near the exposed surface), and this can exacerbate damage caused by frost-susceptible aggregates. The penetration of deicing salts (or other sources of dissolved salts) can also lead to osmotic pressures within the concrete, and the extent to which this plays a role within aggregates depends on the porosity or permeability of aggregate particles and their proximity to the salt front.

7.3.2 Manifestations of aggregate-related damage in field concrete

The extent of damage caused by frost-susceptible aggregates in field concretes is dependent on the exposure conditions of the concrete, the proximity of such aggregates to the exposed surface, and the quality (especially permeability) of the mortar layer above and surrounding the aggregates. Although the distress can be throughout the concrete in extreme cases, many instances of aggregate-related problems are manifested in surface deterioration, such as D-cracking or pop-outs, as described next.

D-cracking, also referred to as durability cracking or D-line cracking, appears as a series of closely spaced, crescent-shaped cracks that occur along joints or pre-existing cracks in concrete flatwork, such as pavements or sidewalks. The cracking and staining often appear in an hourglass shape on the pavement surface at affected joints and cracks (see Fig. 7.1). Cracking tends to initiate near joints or cracks due to the ingress of water, thereby increasing the degree of saturation of the concrete, as well as the amount of freezable water.

D-cracking is caused when water in susceptible aggregates freezes, leading to expansion and cracking of the aggregate and/or surrounding mortar. The rapid expulsion of water from the aggregates may also contribute to dissolution of soluble paste components (Van Dam *et al.*, 2002). D-cracking generally takes 10

7.1 D-cracking in concrete pavement.

to 20 years (or more) to develop, with deterioration often beginning at the bottom of the slab where free moisture is available. The length of time necessary for D-cracking to occur is a function of the aggregate type and pore structure, climatic factors, availability of moisture, and concrete quality, especially its permeability.

The coarse aggregate type clearly plays a role in the development of D-cracking. Most D-cracking-susceptible aggregates are of sedimentary origin and are most commonly composed of limestone, dolomite, or chert (Stark, 1976). Key aggregate properties related to D-cracking susceptibility are mineralogy, pore structure, absorption, and size. In addition, the potential for D-cracking is also exacerbated in the presence of deicing salts, especially so for certain carbonate aggregates (Dubberke and Marks, 1985).

When D-cracking-susceptible aggregates must be used in cold weather applications, the options for ensuring durability are somewhat limited. Crushing certain aggregates below their critical size can help to minimize the risk of D-cracking by reducing the escape distance for freezing water, thereby reducing hydraulic pressure and subsequent damage. However, not all aggregates, when crushed to relatively small sizes, are immune to D-cracking; some carbonate aggregates still show poor durability when their particle size is reduced. Another method reported to improve the frost resistance of concrete containing certain aggregates prone to D-cracking is to increase the entrained air content of the mixture, which helps to alleviate hydraulic pressure developed near aggregate particles (Schlorholtz, 2000). Although decreasing aggregate particle size or increasing the entrained air content of concrete have been identified as potential methods of mitigating D-cracking, the most common practical approach is to identify non-durable aggregates and preclude their use in key applications.

Another common manifestation of frost-susceptible aggregates in field concrete (especially pavements, bridge decks, etc.) is pop-outs. Pop-outs occur at the surface of concrete, where near-surface aggregates either fail or cause the mortar above the aggregates to fail. It should be noted that there are other causes for pop-outs in concrete (e.g., alkali-silica reaction or presence of soft aggregates like shale), which are discussed elsewhere in this chapter.

Pop-outs typically range in diameter from 25 mm to 100 mm and depth from 13 mm to 50 mm, leaving behind a conical depression at the top surface of concrete (Miller and Bellinger, 2003). Aggregates with high porosities tend to be the most prone to pop-outs (due to the large amount of water that can be expelled), and larger aggregate particles are worse than smaller aggregates (due to the increased water stored in larger aggregates and the longer escape path for freezing water) (Pigeon and Pleau, 1995). The tendency for pop-outs is influenced not only by the aggregate pore structure, but also by the characteristics of the ITZ and mortar layer above the aggregate. As in the general case for frost resistance of aggregates, pop-outs are exacerbated by the presence of deicing salts, which tend to increase the degree of saturation in this critical near-surface

region of concrete. Air-entrained concrete mixtures with lower w/c_m ratios and SCMs, when properly designed, placed, and cured, can be helpful in reducing pop-outs, mainly by reducing the ingress of water and deicing salts into the upper portions of slabs. Aggregates that tend to cause pop-outs in concrete often also cause D-cracking, but the opposite is not necessarily typical (Pigeon and Pleau, 1995).

7.3.3 Identification of frost-susceptible aggregates

A key step in designing durable concrete in cold weather applications is to identify whether an aggregate of interest may be susceptible to frost damage, which may manifest itself as internal distress within concrete or surface damage, such as D-cracking (especially for pavements) and pop-outs. The process of identifying salt-susceptible aggregates may involve a review of past field performance or, more likely, of relevant laboratory data.

Past field performance of a given aggregate source may provide very useful information, but one must exercise caution in relying too heavily on past field performance to predict future performance of aggregates from the same source used in new construction. When reviewing past field performance of a given aggregate source, one must ensure that the materials, mixture proportions, environmental conditions and exposure (especially deicing salts) and other relevant parameters are similar for the existing structure (or pavement) from which field performance information is available and the new structure planned for construction. Even if the parameters highlighted above for the existing and new projects are similar enough to warrant a valid comparison, one must still consider the following issue. Owing to inherent changes in aggregate mineralogy and properties from one portion of a quarry or pit to another, it is not uncommon for the frost-resistance aspects of aggregates from a specific production facility to vary considerably with time. Thus, information obtained on aggregates from any single quarry must be used with some caution. However, general trends in behavior can often be gleaned from quarry- or pit-specific data, especially when historic performance has been either excellent or poor. For aggregate sources with mixed or marginal performance histories, laboratory evaluations are essential for determining frost susceptibility.

There are a variety of laboratory tests for evaluating the frost resistance of aggregates, ranging from those that test solely the aggregate to those that test concrete containing the subject aggregate. There does not appear to exist a single test that can be used to clearly delineate a frost-resistant aggregate from a frost-susceptible aggregate, especially given the complexities of the underlying mechanisms of frost damage and the variety of manifestations of damage in field concrete, such as D-cracking and pop-outs. This difficulty in predicting aggregate performance from a single laboratory test is compounded by the fact that the specific exposure conditions to which concrete is subjected play a major role

in determining the frost resistance of a given aggregate. Factors such as element type (pavement, slab, etc.), design and construction details (joint spacing, width, etc.), and degree of environmental severity (number of freeze-thaw cycles, presence of deicing salts, availability of moisture, etc.) vary significantly from one application to another. Despite these complexities, there are still several laboratory tests that can provide excellent insight into the physical, mineralogical, and chemical characteristics that govern a given aggregate's frost resistance. Some of these approaches are described briefly next; a more detailed discussion of these methods is available in National Cooperative Highway Research Program Research Results Digest 281 (NCHRP, 2003).

Tests performed solely on aggregate samples are discussed first, leading to discussions on testing aggregates in concrete. Some of the direct aggregate tests do not actually evaluate frost resistance, but rather they measure other relevant aggregate properties that affect frost resistance, such as absorption or porosity.

Aggregate absorption often has an important impact on frost resistance of aggregates and its manifestation in field-damaged concrete. For certain aggregate types, there is a good correlation between absorption capacity and frost resistance, but for others, the correlation is quite weak (mainly because some high porosity aggregates show good frost resistance). Pigeon and Pleau (1995) have suggested that a maximum absorption capacity of 2% be imposed on aggregates to prevent aggregate-related damage from freezing and thawing cycles. Various agencies and highway departments have imposed absorption capacity limits (e.g., 1.7% maximum imposed by Minnesota Department of Transportation). Aggregates of higher porosities and absorption capacities may suffer damage upon freezing since water is expelled from the aggregate. Although certain aggregates exhibiting higher absorption may be prone to D-cracking or pop-outs, absorption should not be considered an absolute index of frost resistance because many aggregates with relatively high absorptions are quite durable. Thus, local experience and familiarity with a given aggregate type or source should be used to determine if absorption is related to the durability of that aggregate (NCHRP, 2003). Standard aggregate absorption tests (e.g., ASTM C 127 and 128) are typically used in specifications. More advanced tests, such as nitrogen absorption or mercury intrusion porosimetry, can be used to obtain information on internal porosity, pore structure, and absorption capacity, but these are not as commonly available or economically viable for most commercial and highway department laboratories. Other general aggregate tests that may ascertain information about frost resistance are specific gravity (because it tends to relate to absorption) and gradation. As noted previously, the size of an aggregate tends to affect its frost resistance and certain non-durable aggregates can be rendered durable by reducing the size below its critical value.

Besides measuring basic aggregate properties (e.g., absorption, specific gravity, grading), more specific aggregate testing that aims at triggering distress (and typically measuring mass loss) is also widely used. Unconfined aggregate

tests, that is, aggregates tested by themselves, are fairly common measures for assessing frost resistance. These tests are quicker than testing of concrete and can be used more economically to track aggregate quality and performance. There are a variety of different unconfined aggregate tests. Most involve freeze-thaw cycles of aggregates in water or salt solutions, but there are dozens of permutations on how the test can be performed. Some tests, AASHTO T 103-91 (Procedure B), for example, use immersion of the aggregates in alcohol-water solution to increase the penetration of water during the soaking period. The use of a salt solution has been reported to improve the correlation between laboratory freezing and thawing results and D-cracking in concrete pavements (Rogers *et al.*, 1989), especially because deicing salts tend to exacerbate damage due to D-cracking. The Canadian Standards Association test (*CSA A23.2-24A – Test Method for the Resistance of Unconfined Coarse Aggregate to Freezing and Thawing)* is one version of this test and involves soaking aggregates in 3% sodium chloride solution for 24 hours prior to the start of the test, with five cycles to follow in that same salt solution. The CSA specifies a maximum mass loss in this test of 6% for severe exposure conditions and 10% for less severe conditions. The CSA version of this test was found by Senior and Rogers (1991) to have good precision and correlation with freezing and thawing damage in pavements.

Sulfate soundness tests (e.g., ASTM C 88) are fairly common methods used in routine quality control of aggregates. They involve subjecting aggregate samples to repeated soaking in either magnesium or sodium sulfate solution, followed by oven drying, and recording of the mass loss after various test cycles; rather than inducing freeze-thaw cycles within the aggregates, these tests trigger crystallization and/or hydration pressures in the pores of aggregates, which can lead to significant damage. They are not regarded as reliable indicators of frost resistance but can provide a rapid means of acquiring comparative data for a given aggregate source.

The wet attrition of fine and coarse aggregates has gained in popularity in recent years, with the Micro-Deval test emerging as the most common method (NCHRP, 2003). Rogers *et al.* (1991) found a good correlation between mass loss in the Micro-Deval test and magnesium sulfate soundness testing, but better reproducibility for the Micro-Deval test (mainly due to lower sensitivity to aggregate grading). CSA specifications limit the loss for fine aggregates to 20% and the loss for coarse aggregates to between 14 and 17% (CSA, 2000).

In addition to the laboratory methods just described, two tests have been developed specifically to address D-cracking potential of aggregates. These methods, the Iowa Pore Index Test (IPIT) and the Washington Hydraulic Fracture Test (WHFT), are discussed next.

The IPIT was developed in an attempt at quantifying the volume of micropores in aggregates, which has been found to correlate with the potential for D-cracking (Dubberke and Marks, 1992). The test involves placing a dried

aggregate sample in a pressure meter, filling the vessel with water, and subjecting it to a pressure of 241 kPa. The volume of water forced into the aggregates in the first minute, referred to as 'primary load', is aimed at defining the macropores in aggregates. The volume of water injected into the sample between one and 15 minutes, known as 'secondary load', is intended to generate quantitative data on the micropores. Some researchers and practitioners have specified values for the IPT that correlate well (either by themselves or in combination with other tests) with field performance of aggregates in their localities. For example, the Iowa Department of Transportation specifies a maximum secondary load value of 27 ml, and field performance in Iowa has shown that aggregates that exceed this load value may be prone to D-cracking (NCHRP, 2003). Winslow (1987) reported that the IPIT was a good indicator of D-cracking in Illinois for crushed carbonate aggregates, but not for carbonate gravels, most likely due to the rapid early absorption exhibited by gravels under the test conditions. Rogers and Senior (1994) reported that aggregates with greater than 2% absorption (measured in water after 24 hours) and with IPIT secondary loads greater than 27 ml generally exhibited poor field performance.

The Washington Hydraulic Fracture Test (WHFT) was developed by Jannsen and Snyder (1994) and later modified (Embacher and Snyder, 2001) to assess aggregate frost resistance. Aggregates are put under pressure but, rather than measuring the volume of penetrating water, the degradation of the aggregate sample is measured as the pressure is removed from the saturated aggregate, dispelling the internal water and causing hydraulic pressures. The damage to the aggregate sample is estimated by the change in gradation of the aggregates as larger particles are fractured to form smaller ones. More work is needed to determine whether this method accurately predicts frost damage of aggregates, but it is promising in that the test actually triggers water expulsion and causes aggregate fracture. The shortcoming of this test, and any other test that involves solely aggregates, is that it does not actually involve a cementitious matrix, thereby making it impossible to assess the effects of materials and mixture proportions on external penetration of water or solution or on the resistance to stresses from water expelled from aggregates.

Performing freezing and thawing tests on concrete containing an aggregate of interest is a common method of assessing the frost resistance of aggregates. Accelerated freezing and thawing tests, such as ASTM C 666, involve subjecting concrete specimens to rapid thermal cycles (e.g., 0 to 40ºC), while tracking damage by measuring mass loss, length change, or changes in dynamic modulus (using resonant frequency or pulse velocity, etc.). To assess the D-cracking potential for a given aggregate in concrete, researchers have used different testing regimes, with variations of the freezing and thawing cycle time and exposure conditions of the beams (in water or air, in rigid containers or cloth wrap, etc.). Koubaa and Snyder (1996) proposed soaking carbonate aggregates

in chloride solution before casting the concrete and test concrete to highlight the salt susceptibility of aggregates.

Stark (1976) found that length change was a better indicator of D-cracking susceptibility than other common test outputs (e.g., resonant frequency). Stark's recommendation was to use a 0.035% expansion limit after 350 cycles of ASTM C 666 (modified to reduce the number of freeze-thaw cycles to two per day).

When an aggregate has been identified as being frost susceptible (through field and/or laboratory performance), it should either be avoided in certain applications or used prudently to ensure durability. When local sources are the only options, and these sources are non-durable, efforts should be made to improve the frost resistance of the aggregates in the concrete of concern as much as is possible. Options include reducing the aggregate size (below the threshold size), optimizing the concrete mixture (with reduced permeability and tight air void structure), ensuring good drainage and good structural detailing, or blending the poor aggregate with a more durable one. How a given aggregate responds to these attempts at mitigation dictates how suitable it will be for the intended application. Unfortunately, in some cases, frost-susceptible aggregates are difficult to control and will result in field distress, regardless of the quality of the surrounding concrete. In these cases, just as in the case for alkali-carbonate reactive rocks, selective quarrying is needed to identify the poor-performing aggregate and avoid its use in aggressive, cold-weather applications.

7.4 Harmful constituents and impurities in aggregates

The presence of even small amounts of harmful constituents and impurities in aggregates can have a major impact on concrete performance and thus it is important to be able to identify the type and amount of these undesired materials. Table 7.1 provides a broad overview of the various harmful constituents of concern and their potential effects on concrete (Kosmatka *et al.*, 2002). The material found in the minus #200 fractions or 'microfines' is particularly of interest, as impurities and clays are often found in this range. It is good practice to routinely measure the amount of microfines, and when concerned about the nature of the microfines, additional testing may be warranted. Simple tests like the sand equivalent test (AASHTO T 176) and methylene blue test (AASHTO TP 57) are useful in assessing the relative amount of 'clay-like' materials and trying to identify smectite clays in aggregates, respectively. Some clays can adversely affect concrete workability and can interact with some polycarboxylate-based superplasticizers (lowering the efficiency of their water-reducing action). The presence of mica, which can be quantified petrographically by point count, is important because excessive mica contents (> 10% in specific size fraction) may lead to increased water demand, segregation, and bleeding (Rogers, 2002).

Table 7.1 Harmful constituents in aggregates (after Kosmatka *et al.*, 2002)

Harmful constituent	Potential effect(s) on concrete
Organic impurities	Affect setting and hardening, may cause deterioration
Materials finer than the #200 sieve (i.e.. microfines)	Affect bond, increases water requirement
Coal, lignite, or other lightweight materials	Affect durability, may cause stains and pop-outs
Soft particles	Affect durability
Clay lumps and friable particles	Affect workability and durability, may cause pop-outs
Chert of less than 2.40 specific gravity	Affects durability, may cause pop-outs
Alkali-reactive aggregates*	Abnormal expansion, map cracking, pop-outs

* Discussed in Sections 7.5 through 7.8.

Most of the potentially harmful constituents described above have an indirect impact on concrete durability. That is, most tend to affect early-age properties such as setting time, workability and water demand, which can in some cases have an adverse impact on the quality of the hardened concrete. If water is added at the job site to compensate for increased water demand, for example, the added water would reduce strength, increase permeability, and decrease long-term durability. Similarly, if the adverse effects led to cracking of concrete (due, for instance, to impurities strongly retarding hydration of a concrete slab that then suffers from plastic shrinkage), the long-term performance of concrete can be reduced.

Other types of impurities and undesirable materials in aggregates can have a more direct impact on concrete performance. For example, cherts, AAR-susceptible aggregates, clay lumps, friable products, and coal can all lead to surface pop-outs (Kosmatka *et al.*, 2002). In addition to those contaminants referred to in Table 7.1, it should be noted that alkalis can be released from some aggregates, exacerbating the tendency for AAR, as discussed in Section 7.7. Also the presence in aggregates of significant amounts of deleterious salts, particularly chlorides and sulfates, will contribute to the risks of corrosion of reinforcing steel (see Chapter 5) and chemical degradation of the cement matrix (see Chapter 4).

7.5 Alkali-aggregate reaction (AAR)

7.5.1 Introduction

Alkali-aggregate reaction (AAR) is a reaction between the alkali hydroxides present in the pore solution of concrete and certain constituents of some aggre-

gates; under certain conditions the reaction may produce deleterious expansion and cracking of the concrete. There are two distinct types of alkali-aggregate reaction in concrete; these are (i) alkali-silica reaction (ASR), which involves the reaction of certain silica minerals within the aggregate, and (ii) alkali-carbonate reaction (ACR), which involves the reaction of carbonate minerals.

Problems due to ASR were first identified in the State of California in the 1930s and reported by Thomas Stanton of the California State Division of Highways in 1940 (Stanton, 1940). Since this time ASR has been identified in many countries throughout the world and the problem is one of the major causes of premature concrete deterioration. There has been much research in this area and there are now established procedures for identifying potentially reactive aggregates and preventing deleterious expansion when such aggregates are used. There are also a number of techniques for managing ASR-affected structures. These issues together with the mechanisms of the reaction are discussed in this chapter.

Alkali carbonate reaction (ACR) was first discovered by Swenson (1957) as the cause of concrete deterioration in Canada and was subsequently implicated in cases of degradation of concrete structures in the USA (Hadley, 1961). Unlike ASR, problems with ACR are restricted to a few isolated locations worldwide. Consequently, there has been comparatively little research conducted on this topic. Although there are established protocols for identifying alkali-carbonate reactive aggregates there are no recognized measures for controlling the reaction beyond avoiding the use of the reactive material in concrete. Discussion of ACR in this chapter will be restricted to a summary of the reaction mechanisms.

7.5.2 Alkalis in Portland cement

The predominant source of alkalis in concrete is the Portland cement. As noted in Chapter 2, Portland cement contains relatively minor amounts of both sodium (Na) and potassium (K) and these are usually expressed as oxides, Na_2O and K_2O, in a typical chemical analysis. Since these alkalis tend to behave fairly similarly in Portland cement concrete, it is common practice to convert the potassium oxide component of a cement to an equivalent amount of sodium oxide and report the total equivalent sodium oxide content, which is calculated as follows:

$$Na_2Oe = Na_2O + 0.658 \times K_2O \qquad 7.1$$

where Na_2Oe is the equivalent sodium content, Na_2O is the sodium oxide content, K_2O is the potassium oxide content and the 0.658 is a conversion factor based on the relative molecular weights of the oxides (Na_2O/K_2O). A typical chemical analysis for a Portland cement is shown in Table 7.2. The equivalent alkali content of this particular cement is 0.63% Na_2Oe (= 0.15% + 0.658 × 0.73%) and the equivalent alkali content of Portland cements generally ranges from about 0.20 to 1.20% Na_2Oe.

Table 7.2 Typical chemical analysis for Portland cement

Oxide	SiO_2	Al_2O_3	Fe_2O_3	CaO	MgO	Na_2O	K_2O	SO_3	LOI
%	20.55	5.07	3.10	64.51	1.53	0.15	0.73	2.53	1.58

Although the alkalis represent a small component of Portland cement, they dominate the pore solution chemistry of concrete and, as discussed in detail in Chapter 2, after the first day of hydration at normal temperatures, the pore solution has become essentially a mixed solution of NaOH and KOH with low levels of other dissolved ionic species. The concentration of alkali metal hydroxides in solution depends on a number of factors, particularly the alkali content of the cement, the water/cement ratio (w/c) and the degree of hydration, and typically ranges from about 0.15 to 0.85 mol/l, corresponding to pH values ranging from approximately 13.2 to 13.9.

Helmuth *et al.* (1993) developed an empirical equation for predicting the hydroxyl ion concentration of the pore solution of mature Portland cement pastes as follows:

$$[OH^-] = 0.339(Na_2Oe)/(w/c) + 0.022 \pm 0.06\,\text{mol/l} \qquad 7.2$$

For example, equation 7.2 predicts a hydroxyl ion concentration of 0.43 mol/l in the pore solution of a hydrated cement paste produced with a cement with an alkali content of 0.60% Na_2Oe and w/c = 0.50.

Alkalis may be contributed from other concrete-making materials (e.g., supplementary cementing materials, aggregates or admixtures) or external sources (e.g., deicing salts or seawater) and this is discussed in Section 7.7.2.

7.5.3 Alkali-silica reaction (ASR)

Briefly, alkali-silica reaction is a reaction between the alkali hydroxides in the pore solution of concrete and thermodynamically unstable silica in certain aggregates. The reaction product is an alkali-silica gel (of varying composition) which has the tendency to imbibe water and swell. The swelling pressures can be sufficient to induce expansion and cracking of the concrete. Figure 7.2 shows a photomicrograph of a thin section prepared from ASR-affected concrete. The bottom left-hand corner of the image shows a sand-size particle of reactive flint. The particle has reacted with the alkalis, expanded and cracked, and the crack extends out from the aggregate into the surrounding hydrated cement matrix to the right of the particle. The crack is partially filled with alkali-silica gel. Figure 7.3 shows how this reaction manifests itself in an unreinforced concrete wall. The internal expansion results in randomly distributed cracks at the exposed surface; this phenomenon is often termed pattern cracking or map cracking.

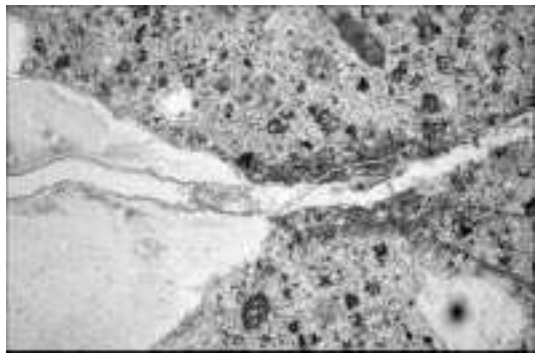

7.2 Thin section of ASR-affected concrete showing reactive flint particle (left) with gel-filled crack emanating into surrounding cement paste (right) – width of view is approximately 2 mm.

Despite its name, the alkali-silica reaction is actually a reaction between the hydroxyl ions (OH^-) in the pore solution and certain siliceous components of the aggregate; the reactive silica is not directly attacked by the alkali metal cations (Na^+ and K^+). When poorly crystalline hydrous silica is exposed to a strong alkaline solution, there is an acid-base reaction between the hydroxyl ions in solution and the acidic silanol (Si-OH) groups (Dent Glasser and Kataoka, 1981) as follows:

$$\equiv\text{Si-OH} + OH^- \rightarrow \equiv\text{Si-O}^- + H_2O \qquad 7.3$$

As further hydroxyl ions penetrate the structure, some of the siloxane linkages (Si-O-Si) are also attacked:

$$\equiv\text{Si-O-Si}\equiv + OH^- \rightarrow 2\ \equiv\text{Si-O}^- + H_2O \qquad 7.4$$

The negative charges on the terminal oxygen atoms are balanced by alkali cations (Na^+ and K^+) that simultaneously diffuse into the structure. The disruption of siloxane bridges weakens the structure and, provided sufficient

7.3 Map-cracking of concrete wall affected by ASR.

reserves of alkali hydroxide are available, the process continues to produce an alkaline silicate solution.

Despite general acceptance of the chemical reactions involved, a number of different mechanisms of expansion have been proposed. Hansen's (1944) osmotic theory regards the cement paste surrounding reactive grains as a semi-permeable membrane through which water (or pore solution) may pass but not the larger complex silicate ions. The water is drawn into the reacting grain where its chemical potential is lowest. An osmotic pressure cell is formed and increasing hydrostatic pressure is exerted on the cement paste, inevitably leading to cracking of the surrounding mortar.

Hansen's laboratory experiments confirmed that osmotic pressures were generated by sodium silicate solutions when separated from water by a cement paste membrane. Indeed, this is the principle behind the osmotic cell test for assessing aggregate reactivity (Stark, 1983) In this test, adjacent cells, filled with sodium hydroxide solution, are separated by a cement paste membrane; a sample of aggregate is introduced into one cell and the rate of osmotic flow (into the cell containing the aggregate) provides a measure of aggregate reactivity.

McGowan and Vivian (1952) disputed the classical osmotic theory on the basis that cracking of the surrounding cement paste 'membrane' due to ASR would relieve hydraulic pressure and prevent further expansion. Their work showed that expansion was accompanied by the formation and widening of cracks due to mechanical (absorption) rather than hydraulic forces. They proposed an alternative mechanism based on the physical absorption of water by the alkali silica-gel and subsequent swelling of the gel. Tang (1981) concurred with the water imbibition and swelling theory; his observations of polished sections suggested that expansion occurs before the reaction product becomes fluid. Thus, the presence and composition of a semi-permeable membrane is insignificant.

Powers and Steinour (1955a, 1955b) proposed a compromise, suggesting that both osmotic and imbibition pressures may be generated depending on whether the alkali-silicate complex is fluid or solid. In their hypothesis, the reaction product itself may act as a semi-permeable membrane depending on its composition. Regardless of the mechanism, the fundamental cause of swelling is thermodynamically the same, i.e. the entry of water into a region where the effect of a solute or of adsorption reduces its free energy.

7.5.4 Sources of reactive silica

Silica, SiO_2, is a component of many rocks; however, not all forms of silica react significantly with the pore solution of concrete. For example, quartz is a very stable silica mineral owing to the fact that it has a well-ordered crystalline structure. Opal, on the other hand, has a more disordered (amorphous) structure, despite having the same chemical composition as quartz (i.e. SiO_2). Alkali-silica

reaction does not occur in concrete produced with pure quartz sand; indeed, quartz sand is used as the standard aggregate in mortar tests conducted on cement. ASR will occur rapidly in concrete produced with an aggregate containing opaline silica, provided there is sufficient alkali present, and this reaction can, under certain circumstances result in expansion and cracking of the concrete.

The following silica minerals have been shown to react deleteriously in concrete: opal, tridymite, cristobalite, volcanic glass, chert, cryptocrystalline (or microcrystalline) quartz and strained quartz. These minerals may be found in the following rock types: shale, sandstone, silicified carbonate rocks, chert, flint, quartzite, quartz-arenite, gneiss, argillite, granite, greywacke, siltstone, arenite, arkose and hornfels. However, this does not mean that all sources of such rocks will produce deleterious reaction when used in concrete. For example, granitic aggregate is widely used in concrete and only certain sources produce damaging ASR. The reactivity of a rock depends on the type and quantity of reactive minerals present, if any. The presence of reactive minerals can usually be detected by a trained petrographer. However, appropriate performance testing of specific aggregate sources is recommended to confirm alkali-silica reactivity. Test methods are discussed in Section 7.6.

7.5.5 Alkali-carbonate reaction (ACR)

The alkali-carbonate reaction occurs between alkali hydroxides and certain argillaceous dolomitic limestones; these dolomites are characterized by a matrix of fine calcite and clay minerals with scattered dolomite rhombohedra. The reaction is manifested by the rapid expansion and extensive cracking of concrete, and structures affected by ACR usually show cracking within five years or less.

Although there is a lack of consensus regarding the precise mechanisms involved, it is generally agreed that the reaction is accompanied by the dedolomitization process, as follows:

$$\underset{\text{'Dolomite'}}{Ca.Mg(CO_3)_2} + 2ROH \rightarrow \underset{\text{'Calcite'}}{CaCO_3} + \underset{\text{'Brucite'}}{Mg(OH)_2} + R_2CO_3 \qquad 7.5$$

where R represents K or Na. However, since this reaction results in a reduction in solid volume, the expansion must be attributed to an alternative mechanism. Several theories have been proposed for the expansion mechanism (Swenson and Gillott 1964; Tang *et al.*, 1987; Fournier and Berube, 2000) and include:

- hydraulic pressures caused by the migration of water molecules and alkali ions into the restricted spaces of the calcite/clay matrix around the dolomite rhombs

- adsorption of alkali ions and water molecules on the surfaces of the 'active' clay minerals scattered around the dolomite grains and
- growth and rearrangement of the products of dedolomitization (i.e., brucite and calcite).

The alkali carbonate produced in the dedolomitization reaction may react with lime in the cement paste as follows:

$$R_2CO_3 + Ca(OH)_2 \rightarrow CaCO_3 + 2ROH \qquad 7.6$$

thereby 'regenerating' alkalis for further reaction. Thus, provided sufficient alkali is available to initiate the reaction, the process may continue independently of the amount of alkalis available in the concrete. This could explain why low-alkali cements are not effective in controlling damaging reaction in some cases.

7.6 Test methods for identifying aggregate reactivity

The first step in assessing the potential of an aggregate for AAR expansion and cracking is the performance of a petrographic analysis by a trained petrographer, the methodology being as recommended by a RILEM technical committee (Sims and Nixon, 2003). However, a petrographic analysis may not identify certain reactive materials (some may not be readily identified by optical microscopy), and the results of the analysis should not be used summarily to reject or accept an aggregate for use in concrete. Nevertheless, valuable insight into potential AAR reactivity can be gained through a petrographic analysis of a given aggregate, and information can also be obtained through petrography on physical, chemical, and mineralogical properties of aggregates that may affect other concrete properties.

Although there are various rapid chemical test methods available for evaluating the potential for either the alkali-silica reactivity or the alkali-carbonate reactivity of an aggregate source, in the authors' opinion, the most reliable means of assessment is to test the potential for expansion in concrete.

Concrete expansion tests for identifying aggregate reactivity have been standardized in many countries and, although the tests may differ in details, they typically involve the fabrication of concrete prisms using the aggregate under test and specific concrete mixture proportions. In most cases, either the cement content of the mixture or the alkali content of the cement, or both, are increased above normal values to increase the rate of reaction. The prisms are stored in conditions of high humidity (e.g. over water in sealed containers) and, usually, at elevated temperature (e.g. 38ºC/100ºF is widely used) to further accelerate the rate of reaction. The length change of the prisms is monitored during storage and the expansion is used to determine the reactivity of the aggregate. Figure 7.4 shows typical expansion curves for concrete prisms manufactured using a non-

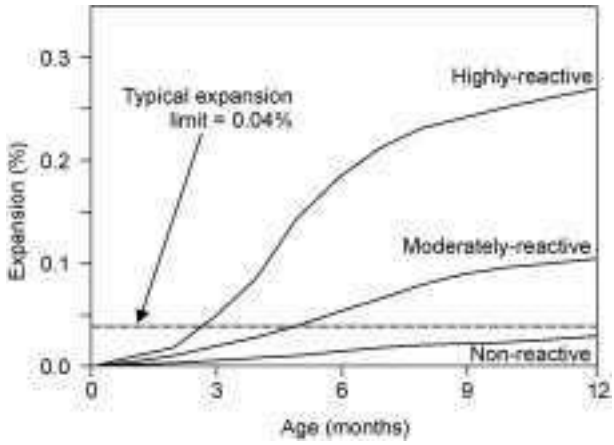

7.4 Typical expansion curves for concrete prisms with aggregates of different reactivity (prisms stored over water at 38ºC).

reactive, moderately-reactive and highly-reactive aggregate. Although expansion limits and test durations vary between different guidelines and specifications, a widely-used limit for identifying reactive aggregates is 0.04% after 12 months storage at 38ºC. In other words, aggregates that produce concrete expansion less than this value are considered innocuous (non-reactive) and those that produce expansion above this value are considered to be potentially reactive. Concrete prism tests are generally considered to be suitable for evaluating both alkali-silica and alkali-carbonate reactivity. Potentially reactive aggregates should either be avoided or only used in concrete with appropriate preventive measures (see Section 7.7).

Various mortar bar tests have been developed to evaluate the potential for alkali-silica reaction (ASR). Such tests usually employ one or more methods for accelerating expansion including: augmentation of cement alkalis, addition of alkali to the mortar mix, immersion of mortar bars in alkaline solution, elevated temperature and even autoclaving. At this time the most commonly used mortar bar test, often referred to as the accelerated (in North America) or ultra accelerated (in Europe) mortar bar test, involves the immersion of mortar bars in a solution of 1 M NaOH at 80ºC. Length change is monitored during immersion and the test is capable of identifying most reactive aggregates after just 14 days immersion in the hot alkaline solution. The test conditions are very aggressive and there are many aggregates with satisfactory performance in the field or in concrete prism tests that fail the accelerated mortar bar test. Consequently, this test should not be used to reject aggregates and the potential reactivity of aggregates that fail this test should be confirmed by more reliable concrete prism testing. The (ultra) accelerated mortar bar test is not suitable for evaluating some alkali-carbonate reactive rocks and an additional test method has been proposed recently by a RILEM technical committee for use in such cases (Sommer *et al.*,

2005). Further consideration is beyond the scope of this chapter and readers interested in the ongoing international efforts aimed at developing improved screening procedures for AAR-susceptible aggregates are directed to the work of RILEM Technical Committee 191-ARP. A review of the work of this committee's activities and those of the earlier RILEM Technical Committee 106-AAR was presented at the 12th International Conference on Alkali-Aggregate Reaction in Concrete (Sims *et al.*, 2004).

7.7 Preventive measures for ASR

There are various methods available for minimizing the risk of ASR-induced expansion in concrete, including:

- use of non-reactive aggregate (or exploitation of the 'pessimum' effect)
- limiting the alkali content of the concrete
- use of supplementary cementing materials (SCMs) and
- use of lithium compounds.

Limiting the alkalis in concrete or using either SCMs or lithium compounds has not been found to be effective for controlling expansion due to alkali-carbonate reaction (ACR) and, consequently, the use of alkali-carbonate reactive rocks in concrete should be avoided.

7.7.1 Use of non-reactive aggregate (or exploitation of the 'pessimum' effect)

Although the use of aggregates that are not susceptible to ASR would be the most obvious option for avoiding the problem, non-reactive aggregates are unavailable in many locations, and importing non-reactive material may not be economically viable. Furthermore, ASR has occurred in a number of cases where prior testing of the aggregate indicated the aggregates were not deleteriously reactive. Methods of testing aggregates for reactivity have increased in severity, and acceptance criteria have become more stringent with the passage of time to reflect the increasing number of aggregates implicated in field cases of ASR. Adoption of existing testing practices, however, does not guarantee that aggregates will give satisfactory performance in every situation. Consequently, even if aggregates are found not to be deleteriously reactive, further precautions are frequently taken if circumstances demand.

However, because siliceous aggregates that are potentially susceptible to ASR often exhibit a well-characterized 'pessimum' proportion (i.e., maximal expansion at a particular ratio of reactive SiO_2: Na_2Oe), it is sometimes possible to avoid deleterious expansive effects of ASR simply by using a high enough proportion of the reactive aggregate in concrete to ensure that the mix composition is maintained well beyond its 'pessimum' range (Hobbs, 1988).

7.7.2 Limiting the alkali content of the concrete

Stanton's (1940) formative work on ASR indicated that expansive reaction is unlikely to occur when the alkali content of the cement is below 0.60% Na_2Oe. This value has become the accepted maximum limit for cement to be used with reactive aggregates in the United States, and appears in ASTM C 150 Standard Specification for Portland cement as an optional limit when concrete contains deleteriously reactive aggregate. However, this criterion takes no account of the cement content of the concrete which, together with the cement alkali content, governs the total alkali content of concrete, and is considered to be a more accurate index of the risk of expansion when a reactive aggregate is used in concrete. Some national specifications take cognizance of this fact by specifying a maximum alkali level in the concrete; this limit is reported (Nixon and Sims, 1992) to range from 2.5 to 4.5 kg/m^3 Na_2Oe in the UK. In some countries (e.g., Canada), the limit may vary, depending on the reactivity of the aggregate.

There is currently no test method available that is suitable for determining the 'safe level' of alkali for a particular aggregate. Most test methods require an artificially high alkali content to accelerate the rate of reaction and conducting the test with low-alkali cement may fail to produce expansion in the laboratory even though the same combination of materials could result in long-term expansion under field conditions. In addition, small laboratory specimens are more prone to leaching of the alkalis during test and higher levels of alkali are required under laboratory conditions (e.g., concrete prism tests) to compensate for this phenomenon.

Aggregates that normally are not reactive when used in concrete with low-alkali cement may be deleteriously reactive in concrete of higher alkali content. This may occur through alkali concentration caused by drying gradients, alkali release from aggregates, or the ingress of alkalis from external sources, such as deicing salts or seawater. Stark (1978) reported increases in soluble alkali from 1.1 to 3.6 kg/m^3 Na_2O_e close to the surface of some highway structures. Migration of alkalis due to moisture, temperature, and electrical gradients has also been demonstrated by laboratory studies.

A number of workers have demonstrated that many aggregates contain alkalis that may be leached out into the concrete pore solution, thereby increasing the risk of alkali-aggregate reaction. Stark and Bhatty (1986) reported that, in extreme circumstances, some aggregates release alkalis equivalent to 10% of the Portland cement content.

Supplementary cementing materials (SCM), such as fly ash, silica fume, slag and natural pozzolans may also contain significant quantities of alkali, and this is discussed in the next section.

Alkalis may penetrate concrete from external sources such as brackish water, sulfate-bearing groundwater, seawater, or deicing salts. Nixon *et al.* (1987) showed that seawater (or NaCl solutions) present in the mixing water elevates

the hydroxyl-ion concentration and increases the amount of expansion of concrete. Several researchers have also shown that exposure of concrete to saline environments, from which NaCl (and other alkali metal salts) penetrate into the material, can enhance expansion and cracking due to ASR (Chatterji *et al.*, 1987; Oberholster, 1992; Kawamura *et al.*, 1996; Sibbick and Page, 1998). Deicing salts, such as potassium acetate or sodium formate, typically used on airfield pavements as less corrosive alternatives to NaCl, may also be expected to exacerbate ASR, although there is little or no information about this in the literature.

7.7.3 Use of supplementary cementing materials (SCMs)

Supplementary cementing materials (SCMs) are materials that contribute to the properties of concrete through either pozzolanic reaction (e.g., low-calcium fly ash, silica fume, or calcined clay), or hydraulic reaction (e.g., ground granulated blastfurnace slag, hereinafter called slag), or both (high-calcium fly ash). These materials are generally used to partially replace the Portland cement component, the level of replacement varying widely from less than 10% to more than 50% depending on the nature of the SCM.

There is a substantial body of published literature dealing with the effect of SCMs on ASR, but there is still conflicting evidence regarding the conditions under which SCMs are effective and how much is required to suppress deleterious expansion in concrete. A general statement that can be made is that nearly all SCMs can be used to prevent expansion provided they are used in sufficient quantity; the amount required varies widely depending on, among other things, the following:

- the nature of the SCM (especially mineralogical and chemical composition)
- the nature of the reactive aggregate (generally, the more reactive the aggregate, the higher the level of SCM required)
- the availability of alkali within the concrete (i.e., from the Portland cement and other sources)
- the exposure conditions of the concrete (i.e., concrete exposed to external sources of alkali may require higher levels of SCM).

For example, the amount of SCM required to control expansion in a concrete with a highly reactive aggregate and high-alkali cement might vary as shown in Table 7.3.

Generally the amount of SCM required decreases as the reactive silica content of the SCM increases or as the calcium or alkali content of the SCM decreases (Fig. 7.5). In other words, an SCM with high silica and low amounts of calcium and alkali, such as silica fume, tends to be effective at low levels of replacement (Thomas and Bleszynski, 2001). Slag, on the other hand, is much less efficient due to its lower silica and higher calcium contents, and has to be

Table 7.3 Range of minimum replacement levels required for different supplementary cementing materials to control expansion due to ASR

Type of SCM	Level required (%)
Low-calcium fly ash (< 8% CaO)	20 to 30
Moderate-calcium fly ash (8–20% CaO)	25 to 35
High-calcium fly ash (> 20% CaO)	40 to 60
Silica fume	8 to 12
Slag	35 to 65
Metakaolin (calcined kaolin clay)	10 to 20

used at much higher levels of replacement to control expansion (Thomas and Innis, 1998).

SCMs control expansion due to ASR by reducing the availability and, to a lesser extent, the mobility of alkalis in the concrete (Shehata *et al.*, 1999). The alkalis, sodium and potassium, in concrete are partitioned between the solid phases (i.e., bound by the hydrates) and the liquid phases (i.e., pore solution) of the concrete. Only the alkali hydroxides in the pore solution can attack the reactive components of the concrete. The binding capacity of the hydrates is to a large extent a function of the calcium-silica ratio of the C-S-H that forms. C-S-H with a lower Ca/Si ratio has an increased alkali-binding capacity (Bhatty and Greening, 1978) since the surface charge becomes less positive as the calcium content decreases and this attracts more positive cations (Na^+ and K^+) from the surrounding pore solution (Glasser and Marr, 1985).

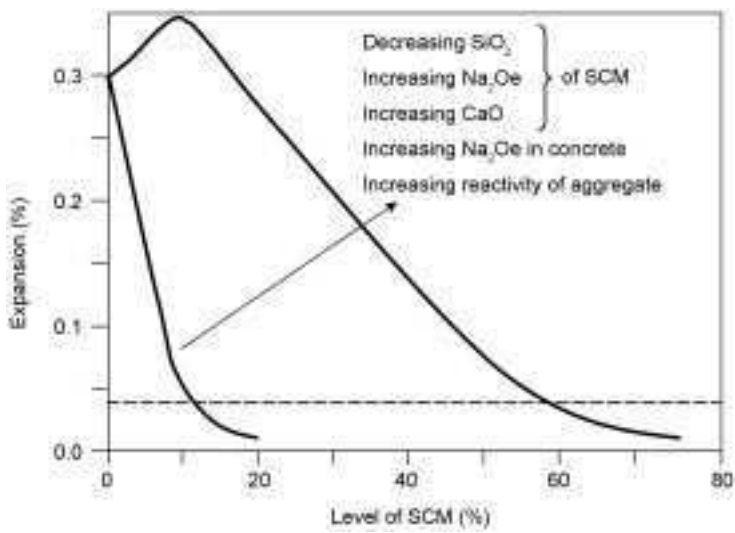

7.5 Relationship between expansion and level of SCM showing how the level of SCM required to minimize expansion increases as the composition of the SCM changes or the reactivity of the aggregate increases.

The effect of SCMs on the pore solution composition will depend on the amount of alkali (Na_2Oe) they contribute, and the degree to which the presence of the material changes the Ca/Si ratio of the hydrates that form. Thus SCMs with low levels of Na_2Oe and CaO, and high levels of reactive SiO_2, will contribute little alkali to the system, but significantly increase the alkali-binding capacity of the hydrates (by reducing the Ca/Si ratio). Figure 7.6 shows the hydroxyl ion content of the pore solution extracted from 2-year-old hydrated cement paste samples that were produced with $w/c_m = 0.50$ and 79 different combinations of cementing materials including Portland cements of different alkali level, binary blends of Portland cement with a range of different fly ashes, slag, silica fume and natural pozzolans, and ternary blends of Portland cement with either silica fume plus fly ash or silica fume plus slag (Thomas and Shehata, 2004). It is evident that the hydroxyl (and alkali) ion concentration is a function of the alkali, calcium and silica content of the blended cement.

Concrete prism tests can be used to evaluate the efficacy of different SCMs and to determine the level of SCM required to control expansion with a specific reactive aggregate. It is generally considered necessary to extend the duration of the concrete prism test from one year (used to evaluate aggregate reactivity) to two years when evaluating SCM to ensure that expansion is prevented and not merely retarded. Concrete prism tests are generally not suitable for assessing the combination of low-alkali cement plus SCM for the reasons discussed in Section 7.7.2. Additional alkalis are required in the concrete prism test to accelerate the reaction and compensate for the loss of alkalis due to leaching during testing.

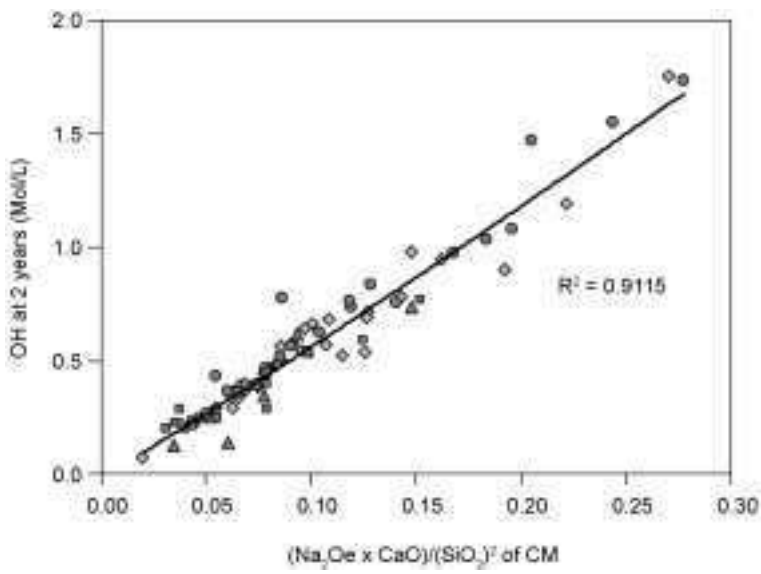

7.6 Relationship between the chemical composition of blended cements and the alkalinity of the pore solution in 2-year-old paste samples ($w/c_m = 0.50$).

The (ultra) accelerated mortar bar test has also been used to evaluate SCM/reactive aggregate combinations and to determine the amount of SCM required to control expansion with a particular reactive aggregate. Generally, combinations of reactive aggregate and SCM that expand less than 0.10% after 14 days immersion in 1 M NaOH solution at 80ºC are considered to have a low risk of expansion when used in concrete under normal field conditions (Thomas and Innis, 1999).

7.7.4 Use of lithium-based compounds

The ability of lithium-based compounds to suppress deleterious expansion due to alkali-silica reaction (ASR) in mortar and concrete was first demonstrated by McCoy and Caldwell (1951) over 50 years ago. They showed that, out of more than 100 chemical compounds tested, various salts of lithium (e.g. LiCl, Li_2CO_3, LiF, Li_2SiO_3, $LiNO_3$, and Li_2SO_4) were the most promising and could virtually eliminate the expansion of mortar containing Pyrex glass provided they were used in sufficient quantity. Since then, there have been numerous studies, most conducted in the last decade or so, which corroborate this earlier discovery. Although most lithium compounds have a beneficial effect, recent work has indicated that lithium nitrate ($LiNO_3$) is the most efficient form for suppressing ASR as its incorporation in concrete does not result in a significant augmentation of the pore solution hydroxyl concentration (Stokes *et al.*, 1997). Lithium nitrate solution is now marketed by a number of companies in North America as an 'ASR-suppressing admixture'. In all cases, the product is sold as a 30% solution of $LiNO_3$.

It is somewhat paradoxical that lithium compounds are effective suppressants of ASR as lithium is an alkali metal like sodium and potassium. The precise mechanism by which lithium controls ASR is not known, although many theories have been put forward (Feng *et al.*, 2005). The simplest and most commonly used explanation is that lithium salts will interact with reactive silica in a similar way to sodium and potassium salts, but the reaction product is an insoluble lithium-silicate with little propensity to imbibe water and swell.

The initial work of McCoy and Caldwell (1951) showed that the amount of lithium required to control expansion was a function of the availability of other alkalis (Na + K) in the system and they concluded that the expansion of mortar bars containing reactive Pyrex glass could be effectively suppressed provided that the lithium-to-sodium-plus-potassium molar ratio was greater that 0.74, i.e. [Li]/[Na+K] > 0.74. Since then numerous workers have demonstrated a similar relationship between the amount of lithium required and the amount of alkali available, but the minimum value of [Li]/[Na+K] has been shown to vary depending on a number of issues such as the form of lithium, nature of reactive aggregate and, perhaps, the method of test used (Feng *et al.*, 2005).

Recent research (Tremblay *et al.*, 2004) has highlighted the influence of aggregate type on the amount of lithium required to suppress expansion due to

ASR. In this study, which included 12 reactive aggregates from sources in Canada, the [Li]/[Na+K] ratio required to prevent the expansion of concrete prisms exceeding 0.04% after 2 years storage at 38ºC was between 0.56 to 0.74 for 6 of the 12 aggregates and 0.93 to 1.11 for 3 aggregates. The ratio of [Li]/[Na+K] = 1.11 was not sufficient for the remaining 3 aggregates.

Currently, concrete expansion tests are considered to be the most reliable laboratory test methods for evaluating lithium-based compounds and determining the amount of lithium required with a specific aggregate. Although, a number of modifications have been proposed to the (ultra) accelerated mortar bar test to render it suitable for use with lithium compounds, there are few data available to assess the reliability of the modified tests.

Guidelines on the use of lithium compounds for preventing ASR in new construction or retarding expansion in existing ASR-affected structures have been published by the Federal Highways Administration in the USA (Folliard *et al.*, 2003).

7.8 Management of ASR-affected structures

If a structure is suspected to suffer from alkali-silica reaction, the following actions may be necessary:

- Conduct a forensic evaluation to determine whether ASR has contributed to the observed distress and whether any other deterioration mechanisms are operating – i.e. diagnose the cause(s) of distress.
- Evaluate the condition of the structure to confirm whether the structural integrity or serviceability have been negatively affected by ASR.
- Conduct a prognosis to determine the potential for further reaction and expansion.
- Evaluate strategies for repairing the concrete and preventing or retarding further reaction and expansion.

Guidelines on the evaluation and management of structures affected by ASR have been published by the Canadian Standards Association (2000) and CANMET (Fournier *et al.*, 2004).

If it has been determined that ASR is a major contributor to the deterioration of the concrete and that there is significant potential for further reaction and expansion, few options may be considered to mitigate the reaction. However, the existence of other deterioration processes needs to be determined and, if present, should be dealt with by the repair strategy. If the condition of the structure has deteriorated to the extent that it is no longer structurally safe or it does not adequately perform its required function, these shortcomings have to be addressed. For example, if the concrete is severely cracked and embedded steel reinforcement has begun to corrode, the repair strategy should include methods

for preventing further corrosion and crack sealing to protect the steel, in addition to methods for retarding reaction and expansion due to ASR.

Methods for mitigating the effects of ASR can be divided into two categories: (i) dealing with the symptoms of distress and (ii) dealing with the cause of distress.

Methods for mitigating the symptoms include filling cracks, cutting joints to allow further expansion to take place, thereby relieving internal stresses within the concrete or pressures on adjacent members or structures, and providing restraint to further expansion.

Caulking cracks with an epoxy grout (or similar compound) can help protect embedded reinforcement and reinstate the integrity of the cracked concrete. However, it will not retard the rate of reaction and expansion, and new cracks will inevitably form with time if the reaction is allowed to proceed.

Cutting joints to allow for expansion to take place has been used in a number of hydraulic structures, with the principal aim in these cases being to relieve stresses on embedded mechanical equipment such as sluice gates or turbines. Joints can also be cut to isolate expanding structures from adjacent structures or to relieve internal stresses in pavements. Providing space for expansion does not deal with the reaction, and it is likely that the expansion and cracking will increase because of the reduction in restraint. Providing restraint in the form of rock anchors or post-tensioned tendons has also been used in hydraulic structures to prevent unwanted expansion and distortion of the structure. Fibre-reinforced plastics have been used to wrap elements such as columns.

The only two practical means for addressing the cause of damage (i.e., to retard or prevent further reaction) are either to dry the concrete to eliminate the moisture required to sustain ASR or to change the nature of the reaction by introducing lithium compounds.

Silane sealers have been used successfully to reduce the relative humidity in ASR-affected concrete piers, railway sleepers (Oberholster, 1992) and median barriers (Berube *et al.*, 2002). Silanes applied to concrete render the surface of the concrete hydrophobic and prevent the ingress of liquid water into the concrete. However, water vapor can still pass through the layer, reducing the moisture content and hence reducing the relative humidity with time. Figure 7.7 shows a photograph of treated and untreated sections of a barrier wall in Quebec.

Lithium compounds have been used to treat existing structures suffering from ASR, although the efficacy of such treatments has yet to be corroborated. A detailed review of lithium treatment for ASR control was recently published by the US Federal Highway Administration (Folliard *et al.*, 2003). A number of pavements have been treated by applying a solution of lithium hydroxide or lithium nitrate topically to the pavement surface; testing has demonstrated that the penetration of lithium from a topical treatment is limited to the upper 25 to 50 mm of the pavement (Thomas and Stokes, 2004). However, it can be argued that the extent of deterioration is often more severe in the surface layer and that

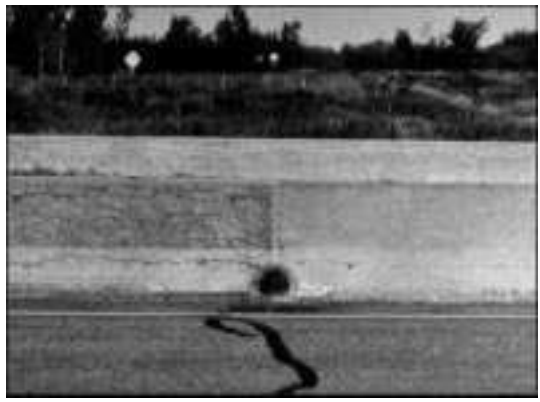

7.7 Photograph of ASR-affected barrier wall comparing untreated section (left) with silane-treated section (right).

retarding the reaction in that area will still extend the service life of the pavement. Alkali concentrations can occur in the surface layer due to the migration and evaporation of water, and the application of deicing salts.

Techniques have been developed to increase the rate and depth of lithium penetration; these include electrochemical migration and vacuum impregnation (Folliard *et al.*, 2003; Thomas and Stokes, 2004). These techniques have been applied to a few structures in the field, but there is a need for information on their effectiveness in promoting lithium penetration and suppressing expansion due to ASR.

7.9 Conclusions

For the most part, aggregates serve their intended purposes in concrete, both from an economic and technical perspective, allowing for a cost-effective end product with satisfactory long-term durability. However, there are certain cases where the inherent durability of aggregates is not adequate, or where the aggregate reacts chemically within the concrete.

This chapter summarizes some of the causes of aggregate-related distress or instability in concrete, with particular emphasis on frost resistance and alkali-aggregate reactivity. For the major causes of aggregate-related distress (AAR and frost attack), as well as the less common or damaging causes, substantial information exists to identify potentially non-durable aggregates. In many cases, measures can be taken to improve the durability of concrete containing these problematic aggregates, for instance, by using fly ash to suppress ASR. In other cases, however, adequate measures do not currently exist to eliminate concrete durability problems associated with particular aggregates (e.g., those prone to ACR and some frost-susceptible aggregates).

As natural resources become more depleted and high quality aggregates

become less widely available, the need to evaluate new aggregate sources and types efficiently and accurately will become more critical. The increased use of marginal aggregates (ones that were historically avoided), manufactured sands (with low inherent resistance to polishing), and recycled products (e.g., recycled concrete as coarse aggregates) will all bring the potential issues of durability to the forefront. The key to making the most durable concrete from these aggregates is to understand the underlying causes of aggregate-related distress and to apply this knowledge to the design, construction, and maintenance of new concrete structures.

7.10 References

American Concrete Institute (ACI), 1996. 'Guide for Use of Normal Weight Aggregate in Concrete,' *ACI Report 221R*.

AASHTO TP 57, 2004. American Association of State Highway Transportation Officials, *Standard Test Method for Methylene Blue Value of Clays, Mineral Fillers and Fines*.

AASHTO T 96, 2002. American Association of State Highway Transportation Officials *Resistance to Degradation of Small-Size Coarse Aggregate by Abrasion and Impact in the Los Angeles Machine*.

AASHTO T103-91, 2000. American Association of State Highway Transportation Officials, *Standard Method of Test for Soundness of Aggregates by Freezing and Thawing*.

AASHTO T 176, 2002. American Association of State Highway Transportation Officials *Plastic Fines in Graded Aggregates and Soils by the Use of the Sand Equivalent Test*.

AASHTO T 327, 2005. American Association of State Highway Transportation Officials, *Standard Method of Test for Resistance of Coarse Aggregate to Degradation by Abrasion in the Micro-Deval Apparatus-ASTM Designation*.

ASTM C127-04, 2006. 'Standard Test Method for Density, Relative Density (Specific Gravity), and Absorption of Coarse Aggregate', ASTM International, Book of Standards, Volume 04-02, West Conshohocken, PA.

ASTM C128-04a, 2006. 'Standard Test Method for Density, Relative Density (Specific Gravity), and Absorption of Fine Aggregate', ASTM International, Book of Standards, Volume 04-02, West Conshohocken, PA.

ASTM C88-05, 2006. 'Standard Test Method for Soundness of Aggregates by Use of Sodium Sulfate or Magnesium Sulfate', ASTM International, Book of Standards, Volume 04-02, West Conshohocken, PA.

ASTM C150-05, 2006. 'Standard Specification for Portland Cement', ASTM International, Book of Standards, Volume 04-01, West Conshohocken, PA.

ASTM C666/C666M-03, 2006. 'Standard Test Method for Resistance of Concrete to Rapid Freezing and Thawing', ASTM International, Book of Standards, Volume 04-02, West Conshohocken, PA.

ASTM D 3042, 2003. American Society for Testing and Materials, *Test for Acid Insoluble Residue in Carbonate Aggregates*.

Berube, M-A., Chouinard, D., Pigeon, M., Frenette, J., Rivest, M. and Vezina, D. 2002. 'Effectiveness of sealers in counteracting alkali-silica reaction in highway median barriers exposed to wetting and drying, freezing and thawing, and deicing salt.'

Canadian Journal of Civil Engineering, 29, 2, pp. 329–337.

Bhatty, M.S.Y. and Greening, N.R. 1978. 'Interaction of alkalis with hydrating and hydrated calcium silicates.' Proceedings of the Fourth International Conference on the Effects of Alkalis in Cement and Concrete, Purdue, pp 87–112.

Canadian Standards Association, 2000. 'Guide to the Evaluation and Management of Structures Affected by Alkali-Aggregate Reaction.' CSA A864-00, Canadian Standards Association, Mississauga, Canada, 449p.

CSA A23.2-23A, 2000. *Canadian Standards Association, Resistance of Fine Aggregate to Degradation by Abrasion in the Micro-Deval Apparatus*.

Chatterji, S., Thaulow, N., and Jensen, A.D. 1987. 'Studies of the Alkali-Silica Reaction Part IV: Effect of Different Alkali Salt Solutions on Expansion', *Cement and Concrete Research*, 17: 777–783.

Cordon, W.A. 1966. 'Freezing and Thawing of Concrete: Mechanisms and Control,' Monograph No. 3, American Concrete Institute, Detroit, Michigan, USA.

Dent Glasser, L.S. and Kataoka, N. 1981. 'The chemistry of alkali-aggregate reactions.' Proceedings of the 5th International Conference on Alkali-Aggregate Reaction, Cape Town, S252/23.

Dubberke, W. and Marks, V.J. 1985. 'The Effect of Salt on Aggregate Durability.' *Transportation Research Record 1031*, Transportation Research Board, National Research Council, pp. 27–34.

Dubberke, W. and Marks, V.J. 1992. 'Thermogravimetric analysis of carbonate aggregates.' *Transportation Research Record 1362*, Transportation Research Board, National Research Council, pp. 38–43.

Embacher, R.A. and Snyder, M.B. 2001. 'Refinement and Validation of The Hydraulic Fracture Test,' Draft Final Report, Minnesota Department of Transportation.

Fagerlund, G. 1976. The Critical Degree of Saturation Method – a General Method of Estimating the Frost Resistance of Materials and Structures. Report 12:76. The Cement and Concrete Research Institute. Stockholm. Sweden.

Feng, X., Thomas, M.D.A., Bremner, T.W., Balcom, B.J., and Folliard, K.J. 2005. 'Studies on lithium salts to mitigate ASR-induced expansion in new concrete: a critical review', *Cement and Concrete Research*, 35, 1789–1796.

Folliard, K.J., Thomas, M.D.A. and Kurtis, K.E. 2003. 'Guidelines for the use of lithium to mitigate or prevent ASR.' FHWA-RD-03-047, Federal Highway Administration, Washington, D.C.

Fournier, B., and Berube, M.A. 2000. 'Alkali-aggregate reaction in concrete: a review of basic concepts and engineering implications', *Canadian Journal of Civil Engineering*, 27, 167–191.

Fournier, B., Berube, M-A., Thomas, M.D.A., Smaoui, N. and Folliard, K.J. 2004. 'Evaluation and management of concrete structures affected by alkali-silica reaction – a review.' MTL 2004-11 (OP), CANMET, Ottawa, 60pp.

Glasser, F.P. and Marr, J. 1985 'The alkali binding potential of OPC and blended cements', *Il Cemento*, 82, 85–94.

Hadley, D.W. 1961. 'Alkali reactivity of carbonate rocks – expansion and dedolomitization', *Proceedings of the Highway Research Board*, 40, 462–474.

Hansen, W.C. 1944. 'Studies relating to the mechanism by which the alkali-aggregate reaction proceeds in concrete', *Journal of the American Concrete Institute*, 15, 3, 213–27.

Helmuth, R., Stark, D., Diamond, S., Moranville-Regourd, M. 1993. 'Alkali-Silica Reactivity: An Overview of Research', SHRP-C-342, Strategic Highway Research Program, National Research Council, Washington, DC.

Hobbs, D.W. 1988. Alkali-silica reaction in concrete. Thomas Telford, London, 183pp.

Hudec, P. 1989. 'Deterioration of rocks as a function of grain size, pore size, and rate of capillary absorption of water', *Journal of Materials in Civil Engineering*, 1(1), 3–9.

Janssen, D. J., and Snyder, M. B. 1994. 'Resistance of Concrete to Freezing and Thawing', *SHRP-C-391*, Strategic Highway Research Program, National Research Council.

Kaneuji, M., Winslow, D.N., and Dolch, W.L. 1990. 'The relationship between aggregate pore size distribution and its freeze-thaw durability in concrete', *Cement and Concrete Research*, 10(3), 433–441.

Kawamura, M. Takeuchi, K. and Sugiyama, A. 1996, 'Mechanisms of the influence of externally supplied NaCl on the expansion of mortars containing reactive aggregates', *Magazine of Concrete Research*, 48, 176, 237–248.

Kosmatka, S.H., Kerkhoff, B., and Panarese, W.C. 2002. *Design and Control of Concrete Mixtures, EB001*, Portland Cement Association, 372pp.

Koubaa, A. and Snyder, M.B. 1996. 'Evaluation of Frost Resistance Tests for Carbonate Aggregates', *Transportation Research Record 1547*, Transportation Research Board, National Research Council, pp. 35–45.

Larson, T.D. and Cady, P.D. 1969. 'Identification of frost-susceptible particles in concrete aggregates', National Cooperative Highway Research Program, Report No. 66, Washington, DC, USA.

McCoy, W.J. and Caldwell, A.G. 1951. 'New approach to inhibiting alkali-aggregate expansion', *Journal of the American Concrete Institute*, 22(9), 693–706.

McGowan, J.K. and Vivian, H.E. 1952. 'Studies in cement-aggregate reaction: correlation between crack development and expansion of mortars', *Australian Journal of Applied Science*, 3, 228–232.

Mehta, P.K. and Monteiro P.J.M. 1993. *Concrete: Structure, Properties, and Materials*, 2nd edition, Prentice Hall, Englewood Cliffs, NJ.

Meininger, R.C. 1998. 'Aggregate Tests Related to Performance of Portland Cement Concrete Pavement', Final Report, NCHRP Project 4-20A.

Miller, J.S. and Bellinger, W.Y. 2003. 'Distress Identification Manual for the Long-term Pavement Performance Program (Fourth Revised Edition),' Federal Highway Adminstration, FHWA-RD-03-031.

National Cooperative Highway Research Program (NCHRP), 2003. 'Aggregate Tests for Portland Cement Concrete Pavements: Review and Recommendations', Research Results Digest 281 (from NCHRP 4-20C Final Report by Folliard, K.J. and Smith, K.).

Neville, A. 1996. *Properties of Concrete*, John Wiley & Sons, New York.

Nixon, P.J., and Sims, I. 1992. 'Alkali Aggregate Reaction – Accelerated Tests Interim Report and Summary of National Specifications', Proceedings of the 9th International Conference on Alkali-Aggregate Reaction in Concrete, Vol.2 Published by The Concrete Society, Slough, pp. 731–738.

Nixon, P.J., Canham, I., and Page, C.L. 1987. 'Aspects of the Pore Solution Chemistry of Blended Cements Related to the Control of Alkali-Silica Reaction', *Cement and Concrete Research*, 17(5), 839–844.

Oberholseter, R.E. 1992. 'The Effect of Different Outdoor Exposure Conditions on the Expansion Due to Alkali-Silica Reaction', Proceedings of the 9th International Conference on Alkali-Aggregate Reaction in Concrete, Vol. 2, The Concrete Society, Slough, pp. 623–628.

Pigeon, M. and Pleau, R. 1995. *Durability of Concrete in Cold Climates*, E & FN Spon, 244 pp.

Powers, T.C. 1955. Basic Considerations Pertaining to Freezing and Thawing Tests, Research Department Bulletin RX058, Portland Cement Association.

Powers, T.C. and Steinour, H.H. 1955a. 'An investigation of some published researches on alkali-aggregate reaction. I. The chemical reactions and mechanism of expansion', *Journal of the American Concrete Institute*, 26(6), 497–516.

Powers, T.C. and Steinour, H.H. 1955b. 'An interpretation of some published researches on the alkali-aggregate reaction. Part 2: a hypothesis concerning safe and unsafe reactions with reactive silica in concrete'. *Journal of the American Concrete Institute*, 26(8), 785–811.

Rogers, C.A. 2002. Personal communications.

Rogers, C.A. and Senior, S.A. 1994. 'Recent Developments in Physical Testing of Aggregates to Ensure Durable Concrete,' *Advances in Cement and Concrete*, Proceedings of Engineering Foundation Conference, American Society of Civil Engineers.

Rogers, C.A., Senior, S.A. and Boothe, D. 1989. 'Development of an Unconfined Freeze-Thaw Test for Aggregates', *Engineering Materials Report EM-87*, Ontario Ministry of Transportation.

Rogers, C.A., Bailey, M. and Price, B. 1991. 'Micro-deval for evaluating the quality of fine aggregate for concrete and asphalt.' *Transportation Research Record 1301*, Transportation Research Board, National Research Council.

Senior, S.A. and Rogers, C.A. 1991. 'Laboratory Tests for Predicting Coarse Aggregate Performance in Ontario', *Transportation Research Record 1301*, Transportation Research Board, National Research Council, pp. 97–106.

Schlorholtz, S. 2000. 'Determine Initial Cause for Current Premature Portland Cement Concrete Deterioration', Iowa Department of Transportation Project TR-406, pp. 95–103.

Shehata, M.H., Thomas, M.D.A and Bleszynski, R.F. 1999 'The effect of fly ash composition on the chemistry of pore solution', *Cement and Concrete Research*, 29, 1915–1920.

Sibbick, R.G. and Page, C.L. 1998. 'Mechanisms affecting the development of alkali-silica reaction in hardened concretes exposed to saline environments', *Magazine of Concrete Research*, 50(2), 147–159.

Sims, I. and Nixon, P.J. 2003. 'RILEM Recommended Test Method AAR-1: Detection of Potential Alkali-Reactivity of Aggregates', *Materials and Structures*, 36(261), 480–496.

Sims, I., Nixon, P.J. and Marion, A.-M. 2004. 'International collaboration to control alkali-aggregate reaction: the successful progress of RILEM TCs 106-AAR and 191-ARP'. Tang, M. and Ding, M. (eds), Proc. 12th Int. Conf. on Alkali Aggregate Reaction in Concrete, Beijing, Oct. 2004, Vol. 1, pp. 41–50.

Sommer, H., Nixon, P.J. and Sims, I. 2005. 'AAR-5: Rapid preliminary screening test for carbonate aggregates', *Materials and Structures*, 38(282), 787–792.

Stanton, T.E. 1940. 'Expansion of concrete through reaction between cement and aggregate', *Proceedings of the American Society of Civil Engineers*, 66(10), 1781–1811.

Stark, D. 1976. 'Characteristics and utilization of coarse aggregates associated with D-cracking', Bulletin RD047.01p, Portland Cement Association, Skokie, IL.

Stark, D. 1978. 'Alkali-silica Reactivity in the Rocky Mountain Region', Proceedings of the 4th International Conference on Effects of Alkalis in Cement and Concrete, Publication No. CE-MAT-1-78, Purdue University, W. Lafayette, Indiana, pp. 235–243.

Stark, D. 1983. 'Osmotic cell test to identify potential for alkali-aggregate reactivity', Proc. 6th Int. Conf. On Alkalis in Concrete, (Ed. G.M. Idorn and S. Rostam), Danish Concrete Association, Copenhagen, pp. 351–357.

Stark, D. and Bhatty, M.S.Y. 1986. 'Alkali-silica Reactivity: Effect of Alkali in Aggregate on Expansion', In *Alkalis in Concrete*, ASTM STP 930, American Society for Testing and Materials, Philadelphia, pp. 16–30.

Stokes, D.B., Wang, H.H. and Diamond, S. 1997. 'A lithium-based admixture for ASR control that does not increase the pore solution pH', Proc. 5th CANMET/ACI Int. Conf. on Superplasticizers and Other Chemical Admixtures in Concrete, (Ed. V.M. Malhotra), ACI SP-173, American Concrete Institute, Detroit, pp. 855–867.

Swenson, E.G. 1957. 'A reactive aggregate undetected by ASTM tests', *Proceedings of American Society for Testing and Materials*, 57, pp. 48–51.

Swenson, E.G. and Gillott, J.E. 1964. 'Alkali-carbonate rock reaction', *Highway Research Record*, 45, 21–40.

Tang, M. 1981. 'Some remarks about alkali-silica reactions', *Cement and Concrete Research*, 11, 477–478.

Tang, M., Liu, Z. and Han, S. 1987. 'Mechanism of alkali-carbonate reaction', Proceedings of the 7th International Conference on Concrete Alkali-Aggregate Reactions, (Ed. P.E. Grattan-Bellew), Noyes Publications, New Jersey, pp. 275–279.

Thomas, M.D.A. and Bleszynski, R.F. 2001. 'The use of silica fume to control expansion due to alkali-aggregate reactivity in concrete – a review.' *Materials Science of Concrete VI*, (Ed. S. Mindess and J. Skalny), American Ceramics Society, Westerville, OH, pp. 377–434.

Thomas, M.D.A. and Innis, F.A. 1998. 'Effect of slag on expansion due to alkali-aggregate reaction in concrete', *ACI Materials Journal*, 95(6).

Thomas, M.D.A. and Innis, F.A. 1999. 'Use of the accelerated mortar bar test for evaluating the efficacy of mineral admixtures for controlling expansion due to alkali-silica reaction', *Cement, Concrete, and Aggregates*, 21(2), 157–164.

Thomas, M. and Shehata, M. 2004. 'Use of blended cements to control expansion of concrete due to alkali-silica reaction', Proc. 8th CANMET/ACI Int. Conf. on Fly Ash, Silica Fume, Slag and Natural Pozzolans in Concrete, Supplementary Papers, Las Vegas, pp. 591–607.

Thomas, M.D.A. and Stokes, D.B. 2004. 'Lithium impregnation of ASR-affected concrete: preliminary studies', Proceedings of the 12th International Conference on Alkali-Aggregate Reaction in Concrete, Beijing World Publishing Corporation, Beijing, October, Vol. 1, pp. 659–667.

Tremblay, C., Berube, M.A., Fournier, B., Thomas, M.D.A. and Stokes, D.B. 2004. 'Performance of lithium-based products against ASR: application to Canadian reactive aggregates, reaction mechanisms and testing', Proceedings of the 12th International Conference on Alkali-Aggregate Reaction in Concrete, Beijing World Publishing Corporation, Beijing, October, Vol. 1, pp. 668–677.

Van Dam, T. J., Sutter, L. L., Smith, K. D., Wade, M. J., and Peterson, K. R. 2002. 'Guidelines for Detection, Analysis, and Treatment of Materials-Related Distress in Concrete Pavements, Volume 1: Final Report,' *FHWA-RD-01-163*, Federal Highway Administration, Washington, DC.

Verbeck, G. and Landgren, R. 1960. 'Influence of physical characteristics of aggregates on frost resistance of concrete', *Proceedings of the American Society of Testing and Materials*, 60, 1063–1079.

Winslow, D. N. 1987. 'The rate of absorption of aggregates', *Cement, Concrete, and Aggregates*, Vol. 19, No. 2, pp. 154–158.

8

Degradation of concrete in cold weather conditions

M RICHARDSON, University College Dublin, Ireland

8.1 Introduction

8.1.1 Overview

Concrete and cement composites are forgiving materials and the expectation of a long service life at an extreme ambient temperature is not unreasonable. Extreme temperatures in hot and cold climates do not in themselves present a threat because dry concrete has an acceptably low coefficient of thermal expansion and moderate movements can be taken into consideration in design. A durability threat does, however, exist when moist concrete in cold climates is exposed to repeated temperature cycles that cause freezing and thawing of pore water. The number of cycles is more significant than the absolute lowest temperature. Expansion of wet concrete can be considerable and stresses induced within the concrete may be unacceptable.

This chapter explores the fundamental issues involved in producing freeze-thaw resistant concrete. The phenomenon is reviewed, factors of influence are examined and the particular effects of deicing agents are considered. Air entrainment has a role to play and this is considered in detail. Test methods and related specification issues, current and future, are examined. The prospect of moving to performance-based specifications and design for durability is also addressed.

8.1.2 Fundamental issues

Freezing of water is accompanied by expansion. A closed container with at least 91.7% of its volume full of water will experience pressure on the walls during freezing. The figure can be thought of as an approximation to the ‘critical saturation level’, beyond which freezing might be expected to induce damage in a porous brittle material. This simple theory does not adequately explain all aspects of what happens when concrete freezes (see, e.g., Pigeon and Pleau, 1995) but it nevertheless introduces the concept that freezing of a proportion of the pore water in the cementitious matrix, or the moisture in absorbent

aggregates, may cause deleterious expansion. Expansion that can be accommodated is not a problem but restraint of movement will give rise to tensile stresses. The induced stresses may exceed the material's tensile capacity leading to cracking. The deleterious effect is cumulative. A vicious cycle may develop whereby the cracked concrete admits more water to the pore structure during thaw and the volume of ice increases during freeze, leading to greater stresses and cracking.

Vulnerable elements typically include canopies, kerbs, parapets, copings, ledges, and corbels. Vulnerable infrastructure includes pavements, reservoirs, dams, tanks and other hydraulic structures. Special circumstances may also arise in structures such as freezer stores and storage facilities for very low temperature liquids. It is noteworthy that parts of a structure are immune from the problem even in countries where the annual number of freeze-thaw cycles is significant. Protection from rain and prevention of water exposure will keep the water volume below critical levels. Foundations are normally adequately protected by depth of covering. Elements of structure that are most at risk are those that are saturated at time of freezing.

The problems associated with freeze-thaw generally occur in the cementitious matrix of concrete but some porous aggregates are also significant contributory factors, as discussed in Chapter 7. The influence of porous aggregate can, however, be beneficial if it is strong enough to withstand the expansive pressures, while at the same time providing much-needed space to accommodate the ice and redistributed pore water.

8.1.3 Deleterious freeze-thaw effects

Failure to adequately specify concrete subject to repeated freezing and thawing may lead to various types of internal or near-surface damage but the distinctions between these phenomena are often somewhat arbitrary (Harrison *et al.*, 2001); common manifestations include (i) cracking adjacent to joints (known as D- or D-line cracking), (ii) delamination with general surface scaling or (iii) localised pop-outs.

D-line cracking

D-line cracking may be observed in pavement slabs. These pattern cracks occur in the zone adjacent to free edges and joints. They are orientated approximately parallel to joints, both longitudinal and transverse. The cracks initially appear near to the joint or pavement edge. Later freeze-thaw cycles may cause additional cracking, which manifests itself on the surface progressively further from the joint. This may lead to the pattern illustrated schematically in Fig. 8.1 (and in the photograph shown as Fig. 7.1). The phenomenon is caused by expansion of coarse aggregate particles at depth and is a function of maximum

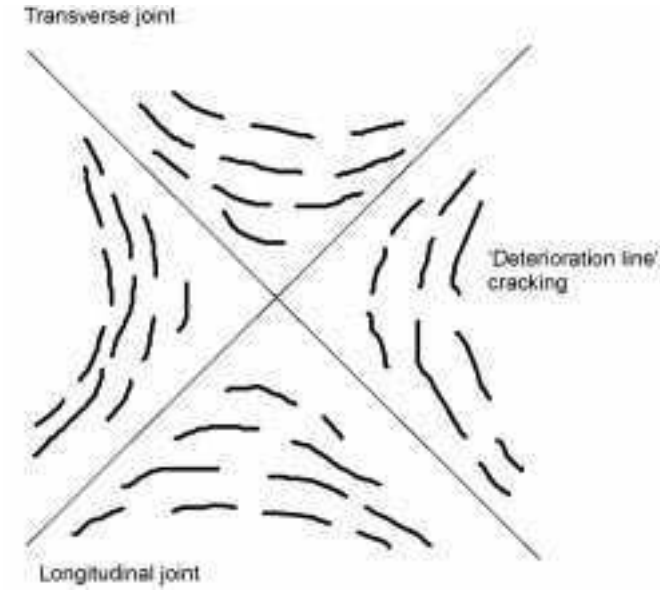

8.1 Freeze-thaw damage – D-line cracking.

aggregate particle size (D_{max}). The larger the aggregate the greater is the potential deleterious effect (see Chapter 7).

Delamination and scaling

Delamination of a surface manifests itself as surface scaling and is either caused by the differential behaviour of layers above and below the frozen zone or the formation of ice lenses. Wet upper layers of concrete may freeze with progressive frozen layers parallel to the surface. In the case of concrete pavements, a wick effect may then draw water from soil under the pavement and feed the freezing process. Expansion of the frozen layers may lead to delamination, a similar phenomenon to that of frost heave in soils (Henry, 2000). Another scenario conducive to delamination occurs in pavements subject to prolonged periods of low temperature. The lower layers may remain frozen for days at a time even though the surface layers thaw during the day. Nocturnal subzero temperatures may lead to the development of an ice front at the surface that moves towards the lower frozen layers. The water lens trapped between the two frozen zones may freeze, expand and cause stresses that delaminate a surface layer as illustrated in Fig. 8.2.

A problem with scaling may also arise locally over aggregate particles near the surface. The weak thin layer of cover concrete over coarse aggregate particles is vulnerable to delamination, as illustrated in Fig. 8.3, if ice forms from the water expelled from the freezing aggregate.

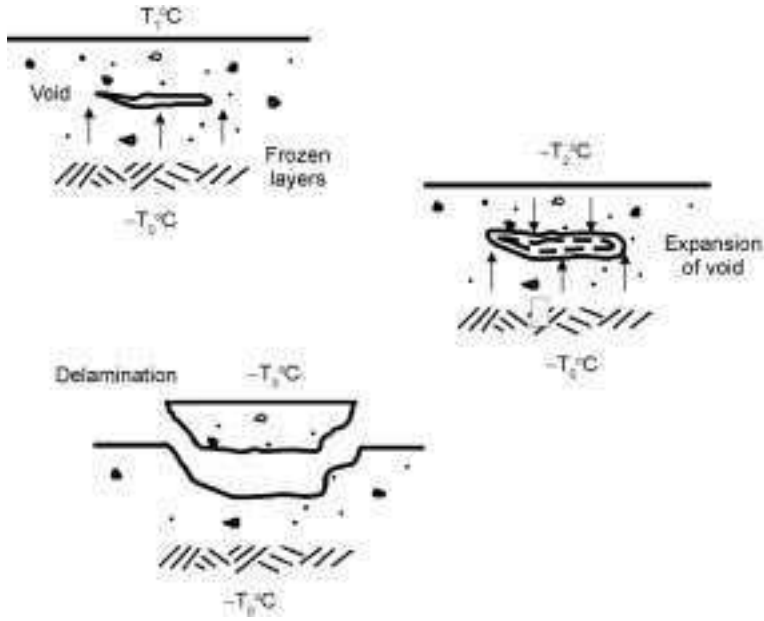

8.2 Process of delamination as air temperature drops from T_1°C through $-T_2$°C to $-T_3$°C while interior is below freezing point at temperature $-T_0$°C.

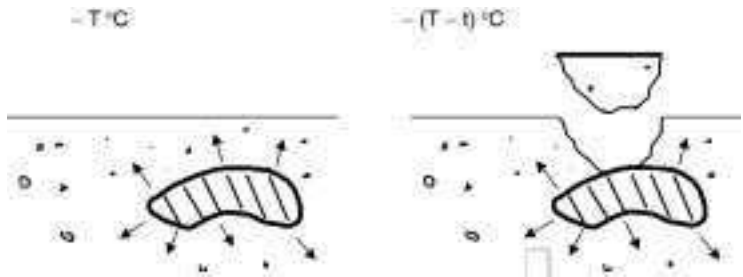

8.3 Surface scaling as air temperature drops by t°C from an initial freezing level of T°C.

'Pop-outs'

The term 'pop-out' is used to describe the detachment of small conical shaped pieces of concrete from the surface. This may occur where freeze-thaw susceptible coarse aggregate is used. Highly absorbent aggregate particles near the surface may become saturated and fracture on freezing. The stresses may crack the cover concrete over the particle. Conical shaped pieces of concrete then detach from the surface, exposing fractured aggregate at the base of the pop-out, as illustrated in Fig. 8.4.

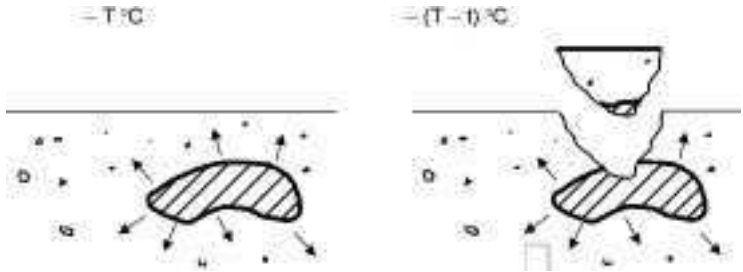

8.4 Localised damage – 'pop-out' – as air temperature drops by t°C from an initial freezing level of T°C.

8.1.4 Minimising the risk of failure

Appropriate measures can be taken to minimise the risk of durability failure due to freezing and thawing. All immature concrete must be protected if freezing temperatures are likely in the period after casting. It is inadvisable to cast concrete when temperatures drop below 2ºC on a falling thermometer unless specific precautions are taken for cold weather concreting (Pink, 1978; Murdock *et al.*, 1991). Production of hardened concrete with adequate durability in freeze-thaw exposure conditions involves control of one significant parameter or a combination of control measures. Significant issues are the amount of water in the concrete, the ability of the pore network to accommodate expansion and the characteristics of the aggregates, especially their water absorption. This chapter reviews the freezing process in porous materials, factors of influence, the exacerbation of damage by deicing agents, use of air entrainment, test methods and specification issues.

Production of durable concrete in cold climates is readily achievable but it requires knowledge of the phenomenon and appropriate control measures where warranted.

8.2 Freezing processes in porous materials

8.2.1 Primary phenomena

Freezing processes in porous media such as concrete are multifaceted. Since the seminal work of T C Powers and co-workers was published, starting well over 50 years ago (Powers, 1945, 1949, 1975; Powers and Helmuth, 1953) many different theories have been advanced to account for various features of the observed phenomena. These include important contributions by a number of researchers, for example Litvan (1972, 1973, 1980), Fagerlund (1992), Marchand *et al.* (1994), and Setzer (1976, 1997). The origins of freeze-thaw damage in any one incidence of concrete degradation may be based on a combination of actions described in the various theories. An appreciation of the

freeze-thaw durability issue involves consideration of a number of phenomena of which the following are believed to be the most important:

- the effect of temperature on volume
- the influence of freezing on redistribution of solute concentrations
- the influence of pore size on the freezing temperature of pore liquids
- the relationship between flow and pressure.

8.2.2 Volume and temperature

The relationship between volume and temperature in a given state is significant in materials with a high coefficient of thermal expansion. The volume change during a change of state is of even greater interest in the case of water in concrete. The change of water density in a temperature range from $+30$ºC to -30ºC leads to a situation whereby water on freezing to ice has a volume approximately nine per cent greater than that from which it was formed (Neville, 1995).

The freezing process begins within the capillary pore structure. The volume increase of the pore water is of immediate concern in saturated concrete but freeze-thaw damage is exacerbated by additional factors. One such factor is water supply to growing ice crystals induced by osmotic pressure. This is related to concentration gradients caused by redistribution of solutes (Powers, 1975).

8.2.3 Redistribution of solute concentration

The capillary pore water contains solutes, in particular alkalis and salts. The ice crystals that grow as the temperature drops below freezing point are formed from pure water. This drives the solutes into surrounding unfrozen pore water. This water contains both existing solutes and those driven from the now frozen pure water. There is an increase in solute level leading to a concentration gradient.

Further growth of ice crystals in a capillary pore has a dual effect. Firstly, as the volume of ice increases, it expels water from the capillary to the gel pore network. Secondly, it leads to a continual increase in the concentration gradient. The resultant osmotic pressure eventually becomes a significant driving force and unfrozen water, including gel pore water, diffuses towards the developing ice body. The phenomenon is outlined in Fig. 8.5. Thus even concrete that is not fully saturated is at risk. The self-feeding growth of the ice body as temperatures fall may result in dilation of the pore cavity and development of potentially deleterious expansive pressures (Helmuth, 1960).

8.2.4 Freezing point of pore liquids

The freezing point of a liquid is a function of temperature and pressure. The pore structure of concrete includes a wide range of diameters (see Chapter 2) and this influences the freezing phenomenon. Ice formation begins in the coarsest

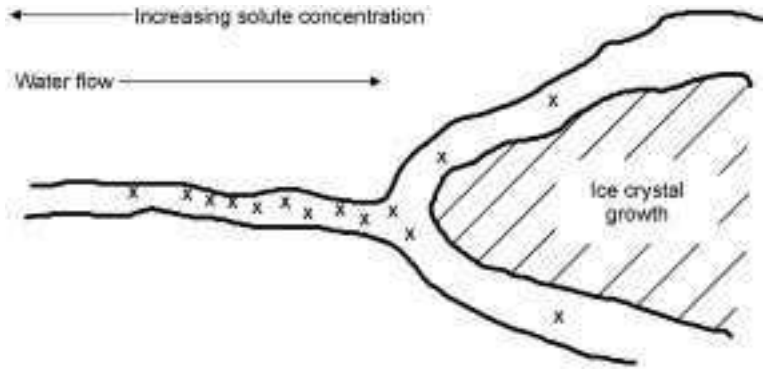

8.5 Water movement during growth of an ice body.

capillary pores while water in the adjacent gel pores within C-S-H initially remains unfrozen. There is a thermodynamic relationship between freezing point and pore radius because the surface energy of the pore walls leads to adsorption of water molecules and so to a depression in the freezing point through a reduction of the pore water's chemical potential. A thin film of adsorbed water at the pore surface remains unfrozen even after ice is formed in the pore and, the greater the specific surface of the pores, the more the freezing point is depressed. Pores with a radius of 5 nm or less could remain unfrozen in temperatures above −20ºC and only two-thirds of the pore water may be frozen by −60ºC (see for example Sellevold and Bager, 1980; Pigeon and Pleau, 1995; Comité Euro-International du Beton, 1989).

Given the extensive nature of the C-S-H component of hydrated cement and its ultra-fine pore structure (see Chapter 2 and Powers, 1958) it is consequently possible that temperatures could fall to −30ºC and less than half of the pore water in a typical example of concrete might be frozen. Issues of significance are the degree of saturation, the ability of the concrete to facilitate enforced movement of unfrozen water and accommodate the growth of ice bodies. Growth of an ice body requires a seed ice crystal. Water may become supercooled if a seed crystal does not exist. Thus there are many factors to account for the variability in the phenomenon of conversion of water to ice in concrete at subzero temperatures. Indeed Stark and Ludwig (1997) have demonstrated that water quality has a considerable influence on the frost resistance of concrete.

8.2.5 Flow and pressure

The fact that ice has a volume approximately nine per cent greater than the water from which it was formed leads to a forced flow of water when ice crystals begin to form in concrete. An ice body forms locally in a cavity from pure water until

the cavity is filled. The excess unfrozen water and air is pushed out into the surrounding network. The ice forms a moving front and pushes water ahead of it. The flow may be modelled by Darcy's law for transport of fluids through a porous medium. Flow occurs under a pressure head and resistance to flow is proportional to the length of the flow path. Thus, conditions may arise where the flow is impeded due to insufficient pore volume. Resistance to the flow develops a hydraulic pressure. These expansive pressures may reach a level at which the tensile strength of the concrete is exceeded and cracks develop. In addition, the water movement during freeze thaw cycles may result in capillary water moving into microcracks. In subsequent freezing cycles this water may cause propagation of these cracks leading to significant cumulative damage over time (Pigeon and Pleau, 1995).

8.3 Freeze-thaw in concrete – factors of influence

8.3.1 Key factors

Four key factors of influence on deleterious freeze-thaw behaviour are the porosity/permeability, aggregate characteristics, moisture state and climatic conditions. In the case of highway structures, deicing agents will also be significant and this is discussed in the next section. The maturity of concrete when it first freezes is, of course, also an issue.

In addition to the key factors discussed further in this section, it must also be noted that good curing is a given requirement for good concrete. The initial curing of concrete is vital to durability from many viewpoints. In the context of freeze-thaw performance it is important that the surface layers are well hydrated. This requires careful curing to limit the excessive loss of water from these layers. Furthermore immature concrete is vulnerable to frost damage due to its relatively high capillary pore water content and its very low tensile strength. Protection of immature concrete from any freezing cycles that occur in the days after pour is essential. Pink (1978) gives advice on protective measures until the concrete has attained a cube strength of 2 N/mm^2, at which stage it is assumed to be strong enough to withstand freezing.

8.3.2 Porosity and permeability

Porosity and permeability are not proportionately linked. Although highly permeable concrete is generally frowned upon, it is interesting that high porosity concrete has the advantage of providing safety valves for ice to expand into, assuming that the concrete is not saturated. This is the basis of air entrainment as a control measure. However, low permeability concrete, derived from low water/cement ratio mixes, is traditionally associated with durable concrete and so it is in the case of freeze-thaw exposure. Such low permeability concretes are

beneficial in two respects. The impermeability of the concrete reduces the amount of free water that can enter the pore structure of the hardened concrete from external sources. Additionally the hydrated concrete contains minimal amounts of water that is freezable at normally encountered temperature ranges or available as free water to feed ice formation.

It has already been stated that pore diameter influences the temperature at which water will freeze. The water in the largest pores is the first to form ice at a given temperature. Further drops in temperature cause the water in the capillary network to freeze but the gel pore water remains unfrozen. The volume and proximity of spaces into which the expelled water may escape greatly influences the degree of resistance to damage. Thus a balance is required between high porosity and low permeability.

8.3.3 Aggregate characteristics

Consideration of the factors influencing freeze-thaw behaviour involves considerable attention to the pore structure of the hardened cementitious matrix. However, the pore structure of the aggregate must also be taken into account for reasons that have been discussed in some detail in Chapter 7.

8.3.4 Moisture state

The volume expansion occurring on conversion of water to ice and associated water movement cannot be accommodated in fully saturated concrete. The drier the concrete, the more capacity it has to absorb the pressures associated with ice formation and water flow under hydraulic and osmotic influences. Thus minimising the degree of saturation of the pore structure is an important controlling parameter.

Concrete structures at greatest risk of saturation are those permanently exposed to water and those occasionally exposed to water under pressure. Deicing agents also encourage saturation because the critical relative humidity below which drying is induced for a pore of given radius increases as the solute concentration of the pore liquid increases (Harrison *et al.*, 2001). Free water in the concrete is not only influenced by the environment but also by the detailing of the elements of the structure. Drainage features that minimise the contact time between water and concrete are particularly beneficial.

8.3.5 Climatic conditions

Exposure conditions that represent the greatest threat to concrete in cold climates are those that combine a number of parameters. These include the frequency of freeze-thaw cycles, the absolute lowest temperature reached, the period of freezing, and the rate of cooling. The lower the temperature and the

longer the freezing period the more extensive the effect on the volume of pores exposed to potentially damaging conditions. Concrete has a low rate of heat transfer and therefore significant penetration of the ice front requires very low temperatures, long periods of freezing, or a combination of both. The rate of cooling can be a factor. The slower the rate of cooling, the greater is the opportunity for dissipation of the pressures from expansion and expulsion of water from the capillaries. This may prevent the cumulative build up of tensile stresses beyond the capacity of the concrete.

The cumulative effect of freeze-thaw cycling makes the frequency of cycle more significant than the period spent at low temperature.

8.4 Deicing agents

Severe scaling of concrete surfaces has been associated in many instances with the application of deicing agents. These agents are spread on snow and ice to form a solution with a lower freezing point than water so that melting occurs earlier. Deicing agents may be chloride based. These deicing salts are notorious for their deleterious effect on the passivity of embedded reinforcement (see Chapter 5) but equally they may cause surface scaling. This is because deicing agents can increase the degree of saturation of the concrete they are in contact with, may encourage differential response of layers to freezing, may subject concrete surface layers to thermal shock and may exacerbate osmotic pressure. These factors are discussed further in this section.

The degree of saturation of concrete is dependent on the rate of water take-up and the rate of evaporation. The degree of saturation at a given temperature and external relative humidity is higher in salt-contaminated pore water than in concrete free from the influence of deicing salts. Thus for typical drying conditions a greater proportion of the pore structure retains water and has a high degree of saturation.

The differential response of layers to freezing temperatures in concrete regularly exposed to deicing agents is due to the ingress of melt water from previous cycles. Even in well drained pavements and decks, the melt water which contains deicing agent will penetrate the surface and make its way into the layers just below the surface. The impregnated layers will have a depressed freezing point in comparison with water-soaked layers. Over time rainwater washes deicing agent from the uppermost surface layers, which may then contain purer water than those below at time of next freeze. Differential behaviour of these surface layers may occur leading to the expansive outer layer breaking free with consequent scaling.

Thermal shock is an inevitable consequence of the action of deicing agent in fulfilling its role. The melting of ice or snow on a pavement surface through the application of salt requires energy. This energy is drawn from the concrete and this leads to a rapid temperature drop in the layers of concrete near the surface.

The situation is temporary but the consequent thermal shock may cause stresses in the concrete thus leading to cracking and scaling.

The distribution of deicing agent in concrete is not even because its entry is via the external surface. This uneven distribution becomes more pronounced during freezing cycles because the ice formation will be accompanied by rejection of deicing chemicals leading to higher concentration differences. This increases osmotic pressure. The contribution of osmotic pressure to ice crystal growth, referred to in Section 8.2, will clearly be exacerbated if deicing salt application increases the solute concentration gradient in the pore water (Neville, 1995).

8.5 Air entrainment

8.5.1 Concept

Traditionally, enhanced durability of concrete is associated with reducing the water/cement ratio. This has some benefit in the case of freezing and thawing by reducing the free water content, which reduces the amount of water available for ice formation. However, the improved microstructure, consequent on lowering the water/cement ratio, may restrict the movement of water and cause stress build-up. Air entrainment provides a controlled method of accommodating the water movement caused during ice formation. Entrained air bubbles protect the surrounding spheres of concrete (Powers, 1949).

The concept of protection is illustrated in Fig. 8.6. During the freezing phase water has space to move without causing undue pressure and, on thawing, the water in the entrained voids is drawn back out into the narrower pore network by capillary forces. Controlled entrainment of air is achieved by adding an admixture to the concrete that is capable of distributing discrete air bubbles.

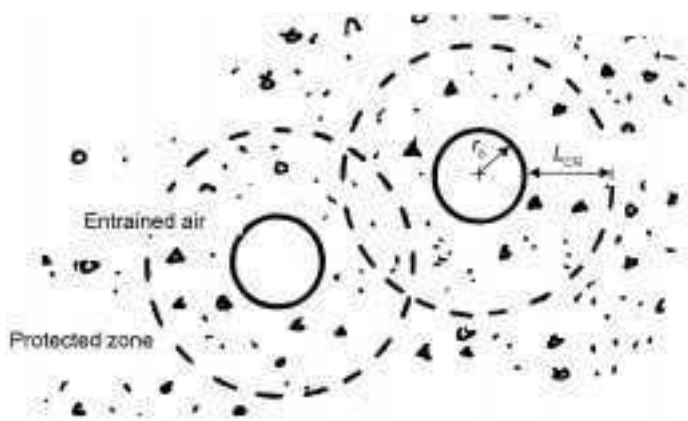

8.6 Significance of path length in air-entrained concrete.

Enhanced freeze-thaw durability by air entrainment involves provision of a sufficient content of entrained air for a given threat combined with a satisfactory distribution of air bubbles. This not only provides millions of safety valves per cubic metre of concrete but, as a beneficial side effect, it may also enhance the surface layers of slabs and pavements. Air entraining admixtures increase the workability and cohesiveness of mixes. This reduces bleed water and laitance thus making surface layers more robust and less likely to fail.

8.5.2 Effective use

Parameters of relevance in the production of serviceable concrete are: air content, spacing, specific surface, allowance for strength loss and interaction with cementitious materials. Before discussing these aspects in more detail, it must be noted that air entrainment does not enhance the performance of concrete made with aggregates susceptible to significant deterioration in freeze-thaw conditions (American Concrete Institute, 1994).

Air content

The air content required in a particular situation depends on the volume of frozen water to be accommodated and this is a function of the exposure conditions. Target mean air content was used in specifications in the past. Advice in former standards (e.g., British Standard BS5328) was based on the required mean air content being approximately nine per cent of the cement paste volume, equated as 5.5 per cent of the concrete volume in the case of concrete with a maximum aggregate size of 20 mm, rising to 7.5 per cent for 10 mm aggregate and 4.5 per cent for 40 mm aggregate. Europe has more recently adopted a move to standardise specifications on minimum air content (Comité Européen de Normalisation, 2000b). The mean entrainment level is typically of the order of four to six per cent but it is contingent on degree of exposure. The upper limit on air content is the specified minimum value plus four per cent.

Spacing

A key aspect of successful air entrainment is spacing. Resistance to flow is proportional to flow path and therefore the path length to an air bubble needs to be short enough to dissipate hydraulic pressure. Osmotic pressure also dissipates if the path length is adequately short. The concept is illustrated in Fig. 8.6, which introduces modelling parameters from Powers (1949), later developed by Fagerlund (1997). It may be noted that each air bubble, of radius r_b, protects a spherical zone around it of wall thickness L_{cr}. The critical spacing is double this value. Powers noted that the critical spacing is proportional to tensile strength and permeability, while inversely proportional to the degree of saturation and freezing rate.

Specific surface

A large number of small air voids is an effective control measure in freeze-thaw environments whereas an equivalent air volume in the form of a small number of large voids is not. It follows that spacing is an issue but it also indicates that the radius r_b has a bearing. This is best expressed through specific surface. Specific surface is the surface area to volume ratio. The higher the specific surface the smaller are the air bubbles. Entrained air bubbles have typical diameters of 50 μm and specific surface is of the order of 25 mm^{-1} (Neville, 1995).

Allowance for strength loss

Air entrainment leads to a loss of concrete strength. Typically the direct strength loss is about 5.5% per percentage of air entrainment though this effect can be somewhat offset by the improved workability (reduced water demand) of air entrained concrete (Wright, 1953). These factors need to be taken into account by specifiers when framing specifications that include requirements both in respect of air content while targeting a certain minimum strength for structural purposes. Richer mixes need more air entraining admixture than leaner ones. An optimum figure must be determined when considering durability enhancement without loss of required structural capacity.

Interaction with cementitious materials

The suitability of a particular air entraining admixture with cementitious materials must be considered by the producer and specifiers. Most admixtures were developed at a time when CEM I type concretes were the norm. Research is required on the interaction of air entraining admixtures with supplementary cementitious materials. The admixtures used are typically based on animal and vegetable fats, oil or natural wood resins. The key requirement is a surfactant, which stabilises the air bubbles formed during mixing and distributes them uniformly through repellent forces.

There is some evidence of interaction between an air entraining admixture and pulverised fuel ash (pfa). It was noted in a study by Dhir *et al.* (1999) that pfa concretes with vinsol resin admixtures performed satisfactorily in freeze-thaw trials but the admixture demand was higher than for comparable CEM I concretes. The demand increased by a factor of two for air contents of up to 4.5 per cent and a further increase in demand occurred with higher air contents. It was further demonstrated that demand increased for ashes with high loss on ignition.

8.6 Test methods

8.6.1 Overview

There are several established test methods for determining the properties of air entrainment or the resistance of concrete to cumulative freeze-thaw cycling.

These latter tests are particularly interesting in that freeze-thaw testing may serve as an introduction for many specifiers to performance-related design of durable concrete. The durability design method involves consideration of freeze-thaw deterioration mechanisms in a quantitative way and appropriate material parameters may then be determined.

Ultimately it is hoped that our understanding of rate-determining parameters will be adequate to allow full consideration, when framing specifications, of the required service life and an acceptable probability of failure from freeze-thaw. In the interim the introduction of specifications based on relative performance may be a significant step forward from purely prescriptive specifications. The approaches available for determining appropriate parameters are based on past records of satisfactory experience, performance test methods and predictive models.

Performance test methods for freeze-thaw resistant concrete have been referred to in the recently published European specification standard EN206-1. The reference occurs in an annex which briefly mentions possible future developments in durability-related performance specifications in respect of freeze-thaw resistance. Although the references to developments in this area are necessarily somewhat tentative in view of the present uncertain state of knowledge, they do, nevertheless, signal the drafters' hope of significant progress in these areas by the time the next major update of the standard is undertaken.

Performance test methods for freeze-thaw resistant concrete involve empirical benchmarking of levels of performance in standard test methods. The adequacy of a proposed mix may then be determined by reference to a relevant approval test on the assumption that the latter provides a suitable index of freeze-thaw resistance in service. The test demonstrates the potential success or failure of a particular mix in meeting the performance level defined by the specification. It is envisaged that some performance testing would be conducted specifically for a particular contract. Alternatively, a proposed concrete mix might be deemed to meet the specification where adequate performance has been established by previous tests on similar concretes or weaker mixes than that proposed. The process is still in development and Siebel (1999) noted that the measured scaling in proposed European standardised methods has not yet been calibrated with behaviour in service and so only comparative testing is possible.

Much research is underway on the mathematical modelling of deterioration mechanisms involved in freeze-thaw of concrete. These models, once validated, may be very beneficial in aiding the full implementation of performance-based specifications. The models are aimed at relating the rate of concrete deterioration to key measurable parameters of the concrete, the mix constituents and/or exposure conditions. This would allow optimisation studies to be carried out in the course of mix design or selection.

A simple benchmark level of performance in a standard test method is the mass loss due to scaling in harsh freeze-thaw conditions. The criterion for acceptance of an unknown concrete is the loss of mass equal to or less than that

of a reference concrete produced to a mix design and with constituents that have an established reputation in the region of providing freeze-thaw resisting concrete. Reference concrete for non-air entrained mixes would also conform to specified values of minimum cube strength, maximum water/cement ratio and minimum cement content. Air entrained concrete mixes would also have to conform to specified values of water/cement ratio, cement content and air content.

Several test methods are available in both the case of fresh concrete and hardened concrete. The first group of tests is concerned with the testing of fresh concrete prior to use on site to verify that the specified level of air entrainment has been achieved. The second group of tests on hardened concrete, aimed at assessing its anticipated performance in service, involves using concrete prisms, cylinders, cubes, 50 mm thick slabs cut from cubes or 70 mm thick specimens cast in cube moulds. Test methods include national standards that are widely used internationally, draft methods under development as international standards, tests related to specific aspects of the deterioration process and draft methods specifically targeted at the future need for performance tests allied to performance-based specifications.

It was noted in Section 8.2 that the deterioration process is a multifaceted issue with effects combining to cause failure. This complicates the test process. For example, it may be shown that there is a good correlation between deterioration in freeze-thaw tests and the water absorption of non-air entrained concrete. This reflects one particular parameter – the degree of saturation. Other tests exploit study of the relative effect on other parameters.

8.6.2 Testing of fresh concrete

The most commonly employed tests on fresh air entrained concrete measure the total air content. The pressure method, described in ASTM C231, is widely used and is based on Boyle's Law. It is assumed that solid constituents in fresh concrete and water are incompressible so that volume change under pressure is due to the contraction of air voids. Volume change and difference in pressure are directly related to air content in two air meter designs, described as 'Type A' and 'Type B' respectively. Another approach, the volumetric method, such as that described in ASTM C173, uses an apparatus that allows water to replace air voids in agitated concrete while monitoring the displaced air volume. A third technique, the gravimetric method, described in ASTM C138, compares the difference between actual and theoretical unit weights to estimate the volume represented by air.

Specifications typically define a target mean volume of air to be entrained as a percentage of the concrete and these test methods are therefore adequate. However, the requirement in service is for a certain volume of air as a percentage of the cement paste, properly distributed through a myriad of bubbles

conforming to limitations on diameter and spacing. Thus the air content test is useful as a quality control check but it does not provide any indication of the distribution of the air content.

The need for a test method better related to the performance requirements of entrained air led to the development of an alternative method that can measure air content, spacing factor and specific surface in a short period of time. The principle of the test is that the rate of rise of an air bubble in water is related to its size. The test method, reported by Price (1996), exploits the ability to monitor the change in buoyancy of a plate supported by a liquid and air bubbles. The test involves injecting a sample of fresh concrete into a viscous liquid at the base of a column of water. Entrained air bubbles are released and rise through the column where they strike a plate. The change in buoyancy of the plate with time is monitored. The buoyancy change can be related to air content, specific surface and spacing factor.

8.6.3 Testing of hardened concrete specimens

Reference to tests on hardened concrete specimens may become commonplace in future specifications. These tests are described in documents from standards organisations and currently, or in the recent past, comprise ASTM C666, ASTM C671, ASTM C672, ASTM C682 and CEN/TS 12390-9. The CEN technical specification (12390-9) is based on Swedish Standard SS 13 72 44, DAfStb Heft 422 (Bunke, 1991) and RILEM recommendation TC 117-FDC. The essential features of the methodologies employed in current tests are outlined.

Microcrack development, ASTM C666

The American standard method ASTM C666 involves checking internal damage associated with microcrack development by determining the dynamic elastic modulus during severe freeze-thaw cycles. The test specimens are exposed to a maximum of 300 freeze-thaw cycles in a temperature range of +4.4ºC to −17.8ºC. The cycles may be conducted in containers of water or the specimens may be frozen in air and thawed in water. The cycles are short with rapid freezing and cooling. The dynamic elastic modulus is monitored after various numbers of cycles to yield a ‘durability factor’ based on the initial dynamic modulus, the dynamic modulus after 300 cycles and the number of cycles required to reduce the relative dynamic modulus to 60%.

Surface scaling, ASTM C672

Surface scaling may be encouraged by ponding water or deicing solution on concrete slabs that are subjected to freeze-thaw cycles. American standard method ASTM C672 involves checking the visual appearance of the surface at

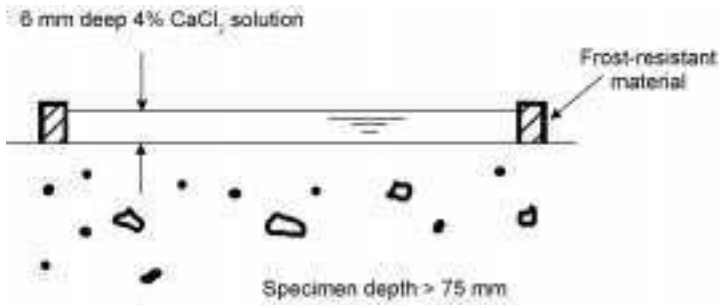

8.7 Test regime for surface scaling – ASTM C672 methodology.

intervals over a programme that extends to 50 cycles. Rectangular specimens with a minimum surface area of 72 square inches (approximately 46 500 mm^2) and minimum thickness of three inches (approximately 75 mm) are cast, cured and surmounted by a freeze-resistant dyke to form a pond. The test regime is illustrated in Fig. 8.7.

Scaling, CEN/TS 12390-9

The convergence of practice towards a common European test has focussed on tests for scaling resistance. A pre-normative standard was submitted to CEN members for enquiry in 2002 as prEN 12390-9, Part 9 of the test method series on hardened concrete. It was recommended that it be published as a European Technical Specification and not as a Euronorm. The specification provides three methods for testing of slabs and the reference method is based on a Swedish standard. The alternative methods are based on a German cube test and a RILEM test that uses specimens cast in standard cube moulds (two specimens per mould).

The reference method involves monitoring the amount of material scaled from the surface of sawn concrete specimens exposed to 56 cycles of freezing and thawing, while covered with water or salt solution. Four specimens are prepared per test as slabs, 50 mm thick, with 150 mm × 150 mm sawn surfaces derived from 21-day-old cubes. Rubber sheets are glued to the faces other than the sawn test face. The 25-day-old specimens are sealed into an insulated mould and covered, at an age of 28 days, by a freezing medium to a depth of three millimetres, creating the test set-up illustrated in Fig. 8.8. The freezing medium may be either demineralised water or a three per cent sodium chloride solution. The medium is covered by a polyethylene sheet to prevent evaporation. A daily freeze-thaw cycle is achieved by exposing the specimen to a temperature range of +20ºC (±4ºC) to −20ºC (±2ºC) in accordance with a specified time-temperature curve, illustrated in Fig. 8.9. The amount of scaled material is assessed after 7, 14, 28, 42 and 56 cycles. The cumulative value after 56 cycles is used for evaluating the scaling resistance.

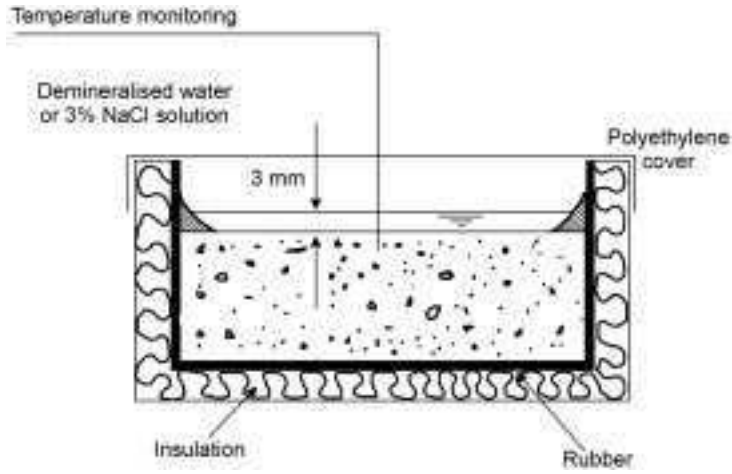

8.8 Test regime for surface scaling test – CEN/TS 12390-9 (Reference method).

The first of the two alternative methods, based on the German cube test, involves immersing two pairs of 100 × 100 × 100 mm cubes in a freezing medium of demineralised water or three per cent sodium chloride solution. Fifty-six daily freeze-thaw cycles are conducted in a temperature range of +20ºC (±2ºC) to −15ºC (±2ºC) to the time-temperature curve illustrated in Fig. 8.10. Each set of four cubes is stored in a pair of brass or stainless steel containers as illustrated in Fig. 8.11. Scaling is monitored at 7, 14, 28, 42 and 56 days. Scaling resistance is assessed by determining the mean and individual mass of scaled material after 56 cycles.

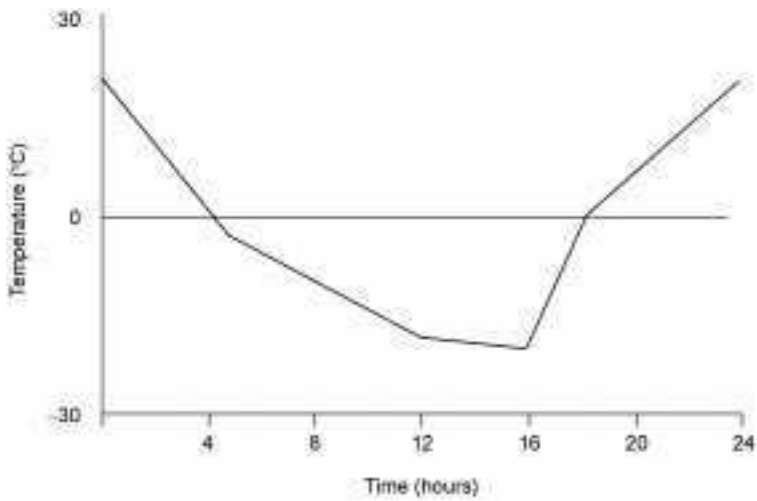

8.9 Time–temperature curve – CEN/TS 12390-9 (Reference method).

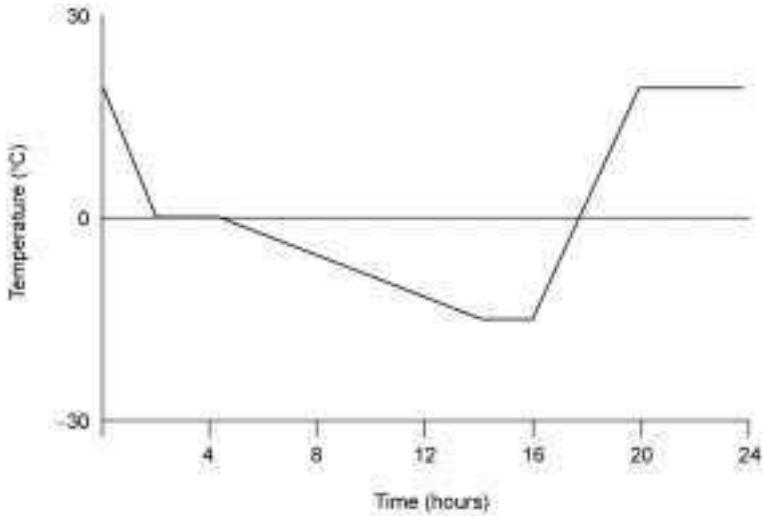

8.10 Time–temperature curve – CEN/TS 12390-9 (German cube test method).

The other alternative method is based on specimens derived from cubes that are partially immersed in a freezing medium. This encourages capillary suction. RILEM Technical Committee TC 117-FDC, which developed the test, designated two variations of the procedure as 'CF' and 'CDF', reflecting the freezing medium. The tests are based on demineralised water and three per cent sodium chloride solution, designated as 'CF' (Capillary suction and Freeze thaw test) and 'CDF' (Capillary suction of Deicing chemicals and Freeze thaw test) respectively. Specimens are prepared by casting concrete in a 150 mm cube mould with a PTFE plate inserted vertically at the midpoint of the sides. This yields two specimens of about 70 mm thickness. Five specimens are required per test. The test surface –

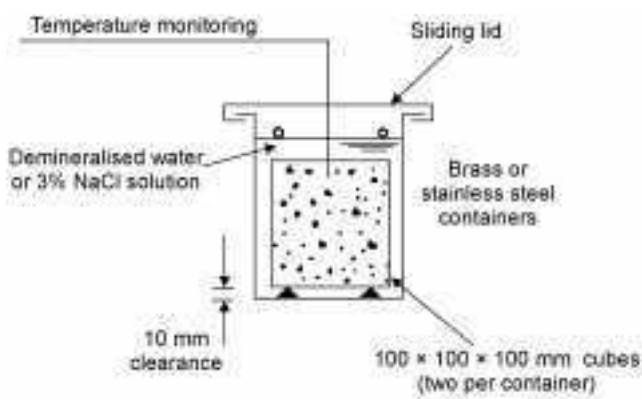

8.11 Test regime for surface scaling test – CEN/TS 12390-9 (German cube test method).

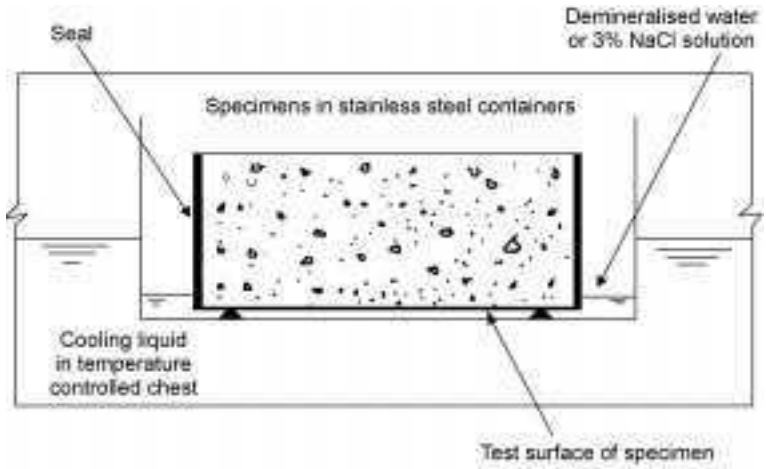

8.12 Test regime for surface scaling test – CEN/TS 12390-9 (RILEM CF/CDF method).

that cast against the PTFE – is untreated but all other sides are sealed by aluminium foil and butyl rubber or by epoxy resin. The 28-day-old specimens are partially immersed to a depth of approximately five millimetres in the freezing medium. The nature of the prepared specimen is such that capillary suction is encouraged through the test surface only. The specimens are subjected to two freeze-thaw cycles per day by cycling from +20ºC to −20ºC in each twelve-hour period. The test set-up and the time-temperature curve are illustrated in Figs 8.12 and 8.13, respectively. The test specimens are placed in containers which are put into a liquid cooling bath. The amount of scaled material is determined after 4, 6,

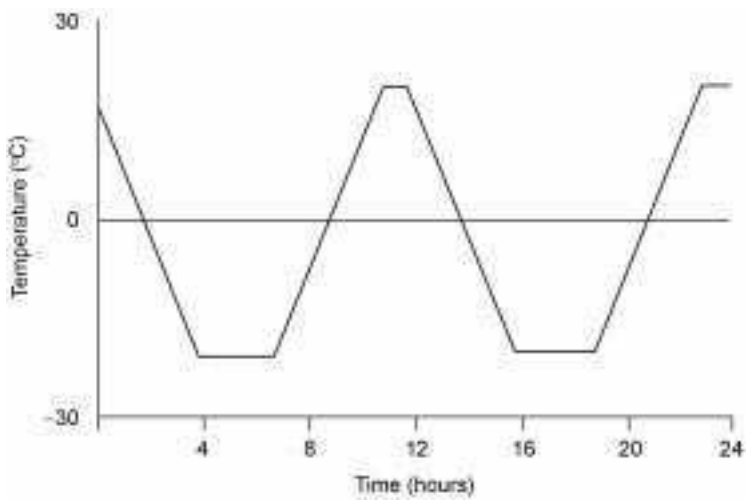

8.13 Time–temperature curve – CEN/TS 12390-9 (RILEM CF/CDF method).

14 and 28 freeze-thaw cycles in the case of sodium chloride immersion, and after 14, 28, 48 and 56 freeze-thaw cycles in the case of demineralised water immersion. The scaled material is detached from the specimens by placing the containers in an ultrasonic bath. The mass of scaled material in the solution is then analysed. Scaling resistance is evaluated by determination of the mean and individual values after 28 cycles (CDF) and 56 cycles (CF).

8.6.4 Testing of aggregate

As stated previously, the resistance of an aggregate to the effects of freezing and thawing is related to its strength and to its pore size and distribution. Different ways of identifying frost susceptible aggregates have been developed in different countries and a number of these have been discussed in detail in Chapter 7 (see Section 7.3.3). In view of recent developments in European practices, however, it is relevant to note here that the European standard on aggregates for concrete, EN12620, calls up a number of tests in respect of thermal and weathering properties of aggregates. Some of these methodologies have roots in long-established tests. The primary methodologies used internationally are encompassed in standard tests such as ASTM C88, EN 1367-1 and EN 1367-2, essential features of which are outlined in this section. Many of the reference tests are based on water as a freezing medium but it is recognised that the presence of seawater or deicing agents present a more severe threat to the integrity of the material.

Other tests include those for determination of frost heave, such as British Standard BS812:Part 124. Some indication of the potential durability of aggregates used in concrete in cold climates has also been derived from the Los Angeles test, as described for example in ASTM C131 or European Standard EN 1097-2.

Standard EN 12620 emphasises the significance of petrographic examination in the first instance. Examination in accordance with Standard EN 932-3 may identify potential vulnerabilities in the form of weak or highly absorptive particles that merit physical testing. The Standard flags aggregates derived from highly weathered rocks, some conglomerates and breccias as potential examples of susceptible material.

Soundness, ASTM C88 and EN 1367-2

As noted in Chapter 7, attempts to simulate the internal expansive forces in aggregate generated by freezing are often made by tests involving cyclical immersion in saturated sulfate solutions and oven drying. Although the reliability of such tests as predictors of frost resistance is questionable, they are simple to perform and yield comparative information on the soundness of aggregate, which is estimated by determining the mass of material lost from the aggregate during the test process. The ASTM C88 test permits use of sodium sulfate or magnesium

sulfate solutions, while the European test EN 1367-2 limits its scope to use of the harsher magnesium sulfate solution. The basic methodology, for example as set out in the European standard, involves sample preparation, complete immersion while contained in a basket, washing, drying and hand sieving.

The sample is typically derived from 10 mm to 14 mm aggregate. Sufficient material is sieved using 10 mm and 14 mm sieves to eliminate undersized and oversized pieces while yielding a mass of about 500 g per specimen. Two test specimens are required per test. Guidance is also provided for sample preparation in the case of smaller and larger aggregates. The aggregate is dried in an oven for 24 hours and cooled in a desiccator to room temperature. It is then sieved, washed free of dust using distilled water, oven-dried, cooled and resieved. The specimens are then transferred to mesh baskets. The mesh baskets are typically 120 mm diameter and 160 mm high, to accommodate the 420 to 430 g specimens with a mesh size that is coarse enough to allow free circulation of the solution but fine enough to trap the aggregate particles at the start of the test. Each period of immersion in sulfate solution is of 17 hours duration after which drainage, oven drying and cooling is conducted. Five cycles are required to complete the test to the European standard and a complete cycle requires a period of 48 hours. Problems can arise with the stability of the solutions and the standard provides for monitoring the density to ensure that it remains within specified limits during the test. The ASTM test provides for both a quantitative and qualitative examination. The European test calls for quantitative assessment with the results recorded as 'magnesium sulfate values' (MS) calculated as the percentage mass loss. The aggregates are categorised in accordance with the limits indicated in Table 8.1.

The use of these categories in specification is discussed in Section 8.7.

Resistance to freezing and thawing, EN 1367-1

The potential behaviour in service of aggregate subjected to cyclical freezing and thawing may also be assessed by means of a test set out in European standard EN 1367-1. The test may be performed on single size aggregate specimens in the range 4 mm to 63 mm, with 8 mm to 16 mm being the preferred

Table 8.1 Categorisation of aggregate through EN 1367-2, a magnesium sulfate soundness test

'MS' category	Percentage mass loss in test
MS_{18}	≤ 18
MS_{25}	≤ 25
MS_{35}	≤ 35
$MS_{Declared}$	> 35

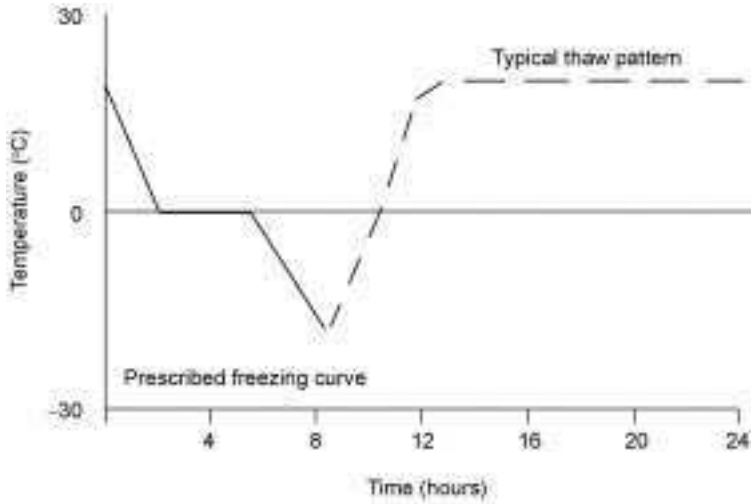

8.14 Time–temperature curve – 'F' (freeze-thaw value) test.

size fraction. Three test specimens are required. The test specimens are washed, dried and cooled to ambient temperature before their mass is established at the beginning of the test. The aggregates are then soaked in distilled or demineralised water for 24 hours using metal cans of approximate dimensions 130 mm diameter and 200 mm height. The aggregates in the cans are then subjected to ten freeze-thaw cycles in a temperature range of +20ºC (±3ºC) to −17.5ºC (±2.5ºC) to the minimum requirements of the time-temperature curve illustrated in Fig. 8.14, such that each freeze-thaw cycle can be completed within 24 hours. The mass loss is determined at the end of the cycles by wet sieving the contents of each can on a sieve that is half the lowest sieve size used in specimen preparation. The retained mass is determined after oven-drying and cooling. The mean value of mass loss of the three specimens is used to determine the 'freeze-thaw value' (F). The aggregates are categorised in accordance with the limits indicated in Table 8.2 based on the reference test method described above, using distilled or demineralised water. The use of these categories in specification is discussed in Section 8.7.

Table 8.2 Categorisation of aggregate through EN 1367-1, freezing and thawing test

'F' category	Percentage mass loss in test
F_1	≤ 1
F_2	≤ 2
F_4	≤ 4
$F_{Declared}$	> 4

Work is in progress to establish a harsher method of test for the use of aggregates in very severe freeze-thaw exposure conditions. This would involve a similar methodology to that described in EN 1367-1 but would use a one per cent sodium chloride solution or a saturated solution of urea.

8.7 Specification and production of durable concrete in freeze-thaw environments

8.7.1 Concrete and aggregate specifications

Specification of freeze-thaw resistant concrete is exemplified by European practice outlined in the primary specification documents for concrete and aggregates for concrete, EN206-1 and EN 12620 respectively. The former sets out a comprehensive framework for integrating specific concerns in a prescriptive approach to durability. These concerns include provision for freeze-thaw resistance, where applicable. The latter provides guidance to specifiers where specific provision is to be included in specifications for frost resistant aggregates.

8.7.2 Specification issues in Standard EN 206-1

The prescriptive approach to durability in EN 206-1 maintains the durability grade principle of Deacon and Dewar (1982) that underpins the advice in concrete design standards such as those published in the UK since the 1980s. This approach is based on the principle that a clear relationship exists between durability expectation and minimum concrete grade, minimum binder content and maximum water/binder ratio. Exposure classifications based on a range of deterioration mechanisms are used and these are further sub-divided to take account of varying degrees of severity in each major class. The subclasses relevant to freeze/thaw attack are presented in Table 8.3. The recommended limiting values of concrete composition and properties are presented in Table

Table 8.3 Classification of freeze/thaw exposure classes and subclasses in EN 206-1

Class	Degradation mechanism	Subclass	Environment
XF	Freeze/thaw attack	XF1	Moderate water saturation, no deicing agent
		XF2	Moderate water saturation, with deicing agent
		XF3	High water saturation, no deicing agent
		XF4	High water saturation, with deicing agent or sea water

F.1 of the Standard, which is generally adapted in locally determined national annexes.

The recommended limiting values are based on the following assumptions:

- an intended working life of 50 years
- concrete made with cement type CEM I
- maximum nominal upper size of aggregate in the range of 20 to 32 mm
- cover to reinforcement in compliance with the minimum requirements of European design standard EN 1992-1-1:2004 (Eurocode 2).

Research on deterioration rates is being conducted in many institutes to better inform requirements for service lives in excess of 50 years. However, in the case of freeze-thaw resistance, Hobbs *et al.* (1998) argue that the limiting values for a 100-year life should be the same as for 50 years. This is due to the event-dependence of the process and the fact that concrete capable of resisting freeze-thaw events on an on-going basis should be durable, irrespective of age.

Section 4 of Eurocode 2 is concerned with durability and cover to reinforcement. It is harmonised with EN206-1 in respect of exposure classes. Although a clear trade-off table between cover and strength, a feature of earlier codes, does not appear the concept survives in the form of different values for different 'structural classes'. The recommended structural class (design working life of 50 years) is 'Structural Class S4' but this aspect is not very significant in the case of freeze-thaw, since it is the quality of the pore structure of the concrete that determines durability in cold climates.

The set of four exposure subclasses differentiated in respect of freeze-thaw attack, designated XF1, XF2, XF3, and XF4, is based on a matrix of two degrees of saturation ('moderate' and 'high') and the absence or presence of deicing agent or seawater. Harrison (2000) explained that CEN intended the terms 'moderate saturation' and 'high saturation' to imply a moderate and high risk of damage, respectively. However, Hobbs *et al.* (1998) noted that the differentiation is not entirely clear and could be on the basis of a lower number of freeze-thaw cycles per annum or a lower likelihood of freeze-thaw events whilst saturated, when distinguishing the exposure classes XF1 and XF2 from XF3 and XF4.

Control of the pore distribution and permeability of the concrete is approached in one of two ways. One approach involves keeping the free water content so low that the amount of expansion will not be deleterious. This is achieved by minimising the permeability and porosity of the concrete. The second approach involves increasing the porosity of the concrete in a controlled manner through air entrainment so that the pores can act as safety valves, providing space for the freezing water to expand without stressing the concrete. In either case the amount of free water in the concrete is minimised by specification of moderately low water/cement ratio concrete. This prevents inclusion of excessive amounts of mix water and limits ingress from external sources during service.

Table 8.4 Limitations on composition – informative example adapted from EN 206-1

	Freeze-thaw exposure class			
	XF1	XF2	XF3	XF4
Maximum w/c ratio	0.55	0.55	0.50	0.45
Minimum strength class	C30/37	C25/30	C30/37	C30/37
Minimum cement content (kg/m^3)	300	300	320	340
Minimum air content (%)	None	4.0% or test concrete performance	4.0% or test concrete performance	4.0% or test concrete performance
Other requirements	Aggregate to EN 12620 with sufficient freeze-thaw resistance			

Note: Specifiers must consult Table F.1 ('xxx') in national annexes to EN 206-1 where 'xxx' represents the national vehicle registration identity code for the place of use of the concrete.

The exposure classes in EN 206-1 take account of the degree of saturation and the presence, if any, of external sources of salt from deicing agents and seawater. As described in Section 8.4 the presence of salt increases the risk of damage due to the detrimental influence of solute concentration gradient.

The informative annex in EN 206-1 presents indicative limits for maximum water/cement ratio, minimum cement content, minimum strength class, minimum air content (except for class XF1) and a requirement for freeze-thaw resisting aggregates for each exposure condition, as presented in Table 8.4. It cannot be over-emphasised that these are informative values only, based on the mean of values representative of European practice; specifiers must consult the appropriate advice on limiting values in national annexes or complementary standards valid in the place of use of the concrete. For example, the informative annex to EN 206-1 shows a requirement for freeze-thaw resisting aggregates in accordance with the recommendations of the harmonised aggregate standard. Unanimity on this requirement is not apparent in national annexes and complementary standards in respect of exposure class XF1.

Exposure class XF1 covers the case of concrete exposed to significant attack by freeze-thaw cycles whilst wet and having 'moderate water saturation'. Examples include the vertical surfaces of members exposed to rain and freezing.

Exposure class XF2 covers concrete exposed to significant attack by freeze-thaw cycles whilst wet, having 'moderate water saturation' in the presence of deicing agent. Examples therefore include the vertical surfaces of road structures exposed to freezing and airborne deicing agents. The values for class XF2 in the informative table in Annex F of EN 206-1 indicate typical requirements that are the same as in class XF1 but with the inclusion of a minimum air content of four per cent and consequently the minimum strength class is lower. A higher minimum strength class is also implied as an alternative to an air-entrained

concrete, through performance testing. Experience in some countries indicates that the use of non-air-entrained mixes of minimum strength class C40/50 can provide adequate resistance.

Exposure class XF3 covers concrete exposed to significant attack by freeze-thaw cycles whilst wet and described as having 'high water saturation'. Examples of concrete in this context include horizontal surfaces of members exposed to rain and freezing.

Exposure class XF4 covers the case of concrete exposed to significant attack by freeze-thaw cycles whilst wet and having 'high water saturation' in the presence of deicing agent or seawater. Examples of concrete covered by class XF4 include bridge decks, surfaces exposed to spray containing deicing agents, and surfaces in the splash zone of marine structures. Some initial difficulty may arise in categorising the exposure of an element in a highway structures as either class XF2 or XF4. If the consequences of failure are significant, in terms of access for repair or threat to passing traffic, it may be prudent to opt for XF4, the severest class.

8.7.3 Specification issues in Standard EN 12620

Satisfactory history of use of an aggregate in conditions similar to those proposed can often be used to deem an aggregate acceptable. Where this is not possible Standard EN 12620 includes an informative annex containing guidance on verifying the freeze-thaw resistance of an aggregate. It also identifies potential examples of susceptible material, including the following: altered porous basalt, chalk, marl, mica schist, phyllite, porous flint, schist, and particles loosely cemented by clay minerals. Petrographic examination can highlight cases requiring further investigation by physical tests.

Some guidance is given on the value of water absorption as an indicator of freeze-thaw resistance. It is noted that aggregates with water absorptions of less than one per cent, determined in accordance with Standard EN 1097-6, are generally considered resistant. It is recognised in the Standard that some materials with higher absorption values are also resistant.

The likely durability of an aggregate against freeze-thaw can be indicated by the producer by declaring the magnesium sulfate or freeze-thaw value 'MS' or 'F'. Informative guidance on selecting an aggregate is provided in Standard EN 12620 for a particular climate and end use through the advice presented in Table 8.5.

8.8 Future trends

8.8.1 Developments in durability modelling

The future achievement of durable concrete may increasingly be based on the use of durability design models and performance-based specifications. These

Table 8.5 Guidance on degree of freeze-thaw resistance of aggregate for use in particular climates and end uses, adapted from EN 12620

Environment	Climate		
	Mediterranean	Atlantic	Continental
Partial saturation, no salt	Not required	F_4 or MS_{35}	F_2 or MS_{25}
Saturated, no salt	Not required	F_2 or MS_{25}	F_1 or MS_{18}
Salt (seawater or road surfaces)	F_4 or MS_{35}	F_2 or MS_{25}	F_1 or MS_{18}
Airfield pavements	F_2 or MS_{25}	F_1 or MS_{18}	F_1 or MS_{18}

models relate the resistance of the structure, $R(t)$, to the deterioration mechanism 'load', $S(t)$, on the structure. The design constraints may be framed in a number of ways such as the 'Lifetime Safety Factor Method', 'Intended Service Period Design', and the 'Lifetime Design Method'. For example the problem could be framed in the following probabilistic form:

$$P\{R(t) - S(t) < 0\}_T \leq P_{f\,max} \qquad T = t_{mean} \tag{8.1}$$

and this leads to a target service life (t_g) which is the time at which the acceptable probability of failure ($P_{f\,max}$) occurs. The material properties required to achieve this duration of satisfactory performance would be based on the anticipated mean service life (t_{mean}), which becomes the design service life (t_d). This introduces the concept of a 'lifetime safety factor', which is described by the relationship:

$$t_d = \gamma_t \; t_g \tag{8.2}$$

where γ_t is a safety factor.

The mathematical solutions to the problem of design for durability are not straightforward because allowance must be made for the multitude of variables involved and their statistical distributions. Mathematical modelling of freeze-thaw behaviour is as yet not fully developed. Thus durability design for freeze-thaw resistant concrete through the use of mathematical models in service life prediction is not currently possible. Nevertheless the three comparative tests for freeze-thaw performance, outlined in CEN/TS 12390-9, are paving the way for the introduction of performance-related design methods with respect to durability.

Formulation of valid mathematical models of the freeze-thaw phenomenon is complicated by the unpredictable pattern of damaging cycles and the difficulty of verifying the apparent influence of mix parameters in laboratory tests with service life experience of structures in service. Freeze-thaw durability failure is event-driven, as illustrated in Fig. 8.15, and does not follow a predictable time-related pattern. The level of damage per cycle can vary greatly, the rate of damage will vary from year to year depending on climatic conditions and the

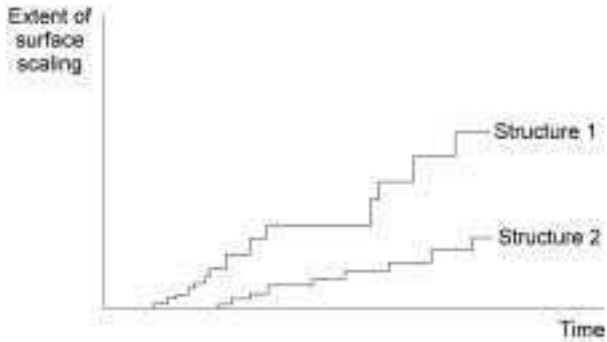

8.15 Example of potential service histories of concrete in a cold climate.

dwell period between series of cycles could vary greatly. Laboratory test methods are generally conducted with daily cycles in a range from +20ºC to −20ºC but performance in these trials cannot be readily translated to field experience due to the influence of temperature and degree of saturation. Nevertheless Fagerlund (1997, 2004) has outlined possible approaches for durability design based on the degree of saturation. The basis of the models is that concrete fractures at a critical degree of saturation.

8.8.2 Model based on critical spacing factor

The critical degree of saturation is a function of the nature of the material and is a consequence of the distance between a freezing site and the nearest air-filled space. During freezing, the build-up of expansive pressures and potentially damaging stress in the concrete matrix increases with increasing distance between the freezing site and the nearest air-filled space. It may therefore be postulated that there exists a critical distance, denoted D_{CR}, in respect of freeze-thaw damage. In practical terms, it is equivalent to the thickest possible water saturated cement paste zone around an air-filled void, such as a sphere, that can exist prior to initiation of damaging micocracks. This leads to the concept of a critical spacing factor, denoted L_{CR}. These two parameters are related by the following equation (Fagerlund, 1997):

$$D_{CR} = 2L_{CR}\left[\frac{2\alpha L_{CR}}{9} + 1\right]^{0.5} \qquad 8.3$$

where α = specific area of the enclosed air void.

Powers (1949) examined this phenomenon and developed a relationship for the spacing factor (see also Fig. 8.6) by consideration of Darcy's law of water flow through porous bodies:

$$\frac{{L_{CR}}^3}{r_b} + \frac{3{L_{CR}}^3}{2} = \frac{KT}{UR} \qquad 8.4$$

where L_{CR} = thickness of critical zone around air void
r_b = radius of air void
K = permeability coefficient of cementitious matrix
T = tensile strength of cementitious paste
U = quantity of water that freezes per unit fall of temperature
R = rate of freezing.

The spacing factor, denoted L, of a system of spherical pores in a material matrix may be determined from the Powers equation (1949), expressed as:

$$L = \frac{3}{\alpha}\left[1.4\left(\frac{V_P}{a}+1\right)^{1/3}-1\right] \tag{8.5}$$

and therefore

$$a = \frac{V_P}{0.364\left[\frac{L\alpha}{3}+1\right]^3-1} \tag{8.6}$$

where α = specific area of the part of the air pore system of interest
a = volume of this part of the air pore system
V_P = material volume, excluding the pore volume.

The equation is modified to take account of the fact that the air pores are not going to be completely dry. Therefore the required air content (a_0) is as follows:

$$a_0 = a_w + a_{CR} + a_b \tag{8.7}$$

where a_w = water-filled air pore volume
a_{CR} = air pore volume needed to prevent the spacing L_{CR} being exceeded when a_w is reached
a_b = safety margin.

The minimum air content required is therefore:

$$(a_0)_{min} = a_w + a_{CR} \tag{8.8}$$

and the value may be determined from the following formulae:

$$a_w = S_a(a_0)_{min} \tag{8.9}$$

where S_a is the degree of water-filling of the air pore system and

$$a_{CR} = \frac{V_P}{0.364\left[\frac{L_{CR}\alpha_{CR}}{3}+1\right]^3-1} \tag{8.10}$$

The safety margin a_b may then be added at a level that reflects the required service life.

It has been determined experimentally that the mean critical thickness (D_{CR})

is 1.2 mm for freeze-thaw in pure water and 1.8 mm in a 3% NaCl solution (Fagerlund, 1997). These values yield critical spacing factors (L_{CR}) of 0.40 mm and 0.54 mm respectively, assuming a specific surface (α) of 15 mm^{-1}. The values are valid for water/cement ratios in excess of 0.45.

8.8.3 Model based on the critical level of saturation

An alternative approach to that described in the preceding subsection is to determine a potential service life based on a model of the capillary degree of saturation as a function of the suction time (Fagerlund, 1993). The service life is also a function of the wetness of the environment. The capillary water uptake and long-term water absorption of the air pore system are the significant issues and are modelled by a time relationship.

The potential service life (t_p) is defined by the critical level of saturation (S_{CR}) which itself is related to the capillary degree of saturation (S_{CAP}). Thus:

$$S_{CR} = S_{CAP}(t_p) \tag{8.11}$$

and

$$S_{CAP}(t) = \left[\frac{1}{\epsilon}\right][\epsilon_0 + C{\alpha_0}^D a_0(\delta t)^E] \tag{8.12}$$

where ϵ = total porosity
ϵ_0 = porosity exclusive of air pores
C, D, E = constants
α_0 = specific area of the air pore system
a_0 = total air content
δ = diffusivity of dissolved air.

These relationships could be used to examine the potential service life in particular situations and form the basis for robust models to be used in durability design and performance-based specifications. In time, other variables could be added to take account of interactions. Later, statistical data could be used to refine the models and contribute to our understanding of the implications of this durability phenomenon in a period of global climate change.

8.9 Sources of further information and advice

The durability of concrete in exposure conditions prone to freeze-thaw cycling is a multifaceted problem. Harsh climates are found in many parts of the globe and local practices and test methods are based on vast experience of the phenomenon. This durability issue continues to be actively researched and lessons from service life histories, good and bad, continue to be well documented. Research is needed on mathematical modelling of the phenomenon and on

materials issues, such as the interaction of air entraining admixtures and secondary cementitious materials. The practitioner is further referred to the work of Pigeon and Pleau (1995) *Durability of Concrete in Cold Climates*, and researchers may be further inspired in their efforts by the papers presented to RILEM Technical Committee TC117 compiled by Marchand *et al.* (1997).

8.10 References

American Concrete Institute (1994) *Manual of concrete practice, Part 1*, Detroit, American Concrete Institute.

American Society for Testing and Materials (1994a) *Test for critical dilation of concrete specimens subjected to freezing*, ASTM C671.

American Society for Testing and Materials (1994b) *Evaluation of frost resistance of coarse aggregates in air-entrained concrete by critical dilation procedures*, ASTM C682.

American Society for Testing and Materials (1999) *Standard test method for soundness of aggregates by use of sodium sulfate or magnesium sulfate*, ASTM C88.

American Society for Testing and Materials (2001a) *Standard test method for density (unit weight), yield, and air content (gravimetric) of concrete*, ASTM C138/C138M.

American Society for Testing and Materials (2001b) *Standard test method for air content of freshly mixed concrete by the volumetric method*, ASTM C173/C173M.

American Society for Testing and Materials (2003a) *Standard test method for resistance of concrete to rapid freezing and thawing*, ASTM C666/C666M.

American Society for Testing and Materials (2003b) *Standard test method for scaling resistance of concrete surfaces exposed to deicing chemicals,* ASTM C672/C672M.

American Society for Testing and Materials (2003c) *Standard test method for resistance to degradation of small-size coarse aggregate by abrasion and impact in the Los Angeles machine,* ASTM C131.

American Society for Testing and Materials (2004) *Standard test method for air content of freshly mixed concrete by the pressure method*, ASTM C231.

British Standards Institution (1989) *Testing aggregates. Method for determination of frost heave*, BS 812:Part 124.

British Standards Institution (1997) *Guide to specifying concrete: methods for specifying concrete mixes,* BS5328:Part 1 and 2.

Bunke, N. (1991) Examination of concrete – recommendations and references as a supplement to DIN 1048, *Deutscher Ausschuss für Stahlbeton*, 422.

Comité Européen de Normalisation (1997) *Tests for general properties of aggregates – Part 3: Procedure and terminology for simplified petrographic description,* EN 932-3.

Comité Européen de Normalisation (1998a) *Tests for mechanical and physical properties of aggregates – Part 2: Methods for the determination of resistance to fragmentation*, EN 1097-2.

Comité Européen de Normalisation (1998b) *Tests for thermal and weathering properties of aggregates – Part 2: Magnesium sulfate test*, EN 1367-2.

Comité Européen de Normalisation (1999) *Tests for thermal and weathering properties of aggregates – Part 1: Determination of resistance to freezing and thawing*, EN 1367-1.

Comité Européen de Normalisation (2000a) *Tests for mechanical and physical properties of aggregates – Part 6: Determination of particle density and water absorption*, EN 1097-6.

Comité Européen de Normalisation (2000b) *Concrete – Part 1: Specification, performance, production and conformity*, EN 206-1.

Comité Européen de Normalisation (2002) *Aggregates for concrete*, EN 12620.

Comité Européen de Normalisation (2004) *Eurocode 2: Design of concrete structures, general rules for buildings*, EN 1992-1-1.

Comité Européen de Normalisation (2006) *Testing hardened concrete – Part 9: Freeze-thaw resistance – Scaling*, Technical Specification CEN/TS 12390-9.

Comité Euro-International du Beton (1989) *Durable Concrete Structures Design Guide*, Thomas Telford.

Deacon, C. and Dewar, J. (1982) Concrete durability – specifying more simply and surely by strength, *Concrete*, 16, 2: 19–21.

Dhir, R., McCarthy, M., Limbachiya, M., Sayad, H., and Zhang, D. (1999) Pulverised fuel ash concrete: air entrainment and freeze/thaw durability, *Magazine of Concrete Research*, 51, 1: 53–64.

Fagerlund, G. (1992) Effect of freezing rate on the frost resistance of concrete, *Nordic Concrete Research,* Oslo, 11: 20–36.

Fagerlund, G. (1993) *The long time water absorption in the air-pore structure of concrete*, Report TVBM-3051, Lund Institute of Technology, Division of Building Materials, Lund, Sweden.

Fagerlund, G. (1997) On the service life of concrete exposed to frost action, in Marchand, J., Pigeon, M., Setzer, M., *Freeze/thaw Durability of Concrete*, London, E & FN Spon, 23–41.

Fagerlund, G. (2004) *A service life model for internal frost damage in concrete*, Report TVBM-3119, Lund Institute of Technology, Division of Building Materials, Lund, Sweden.

Harrison, T. (2000) Resisting freeze/thaw attack, *Concrete*, 34, 6: 46–47.

Harrison, T. A., Dewar, J. D. and Brown, B. V. (2001) *Freeze-thaw resisting concrete – its achievement in the UK*, Report C559, CIRIA, London.

Helmuth, R.A. (1960) Capillary size restrictions on ice formation in hardened portland cement pastes, Proceedings Fourth International Symposium on the Chemistry of Cement, Washington, 855–869.

Henry, K. (2000) *A review of the thermodynamics of frost heave*, Technical Report ERDC/CRREL TR-00-16, US Army Corps of Engineers, Cold Regions Research & Engineering Laboratory, NTIS, Springfield VA, 25pp.

Hobbs, D., Marsh, B. and Matthews, J. (1998) Minimum requirements for concrete to resist freeze/thaw attack, in Hobbs, D.W., *Minimum Requirements for Durable Concrete*, Crowthorne, British Cement Association, 91–129.

Litvan, G.G. (1972) Phase transitions of adsorbates IV – Mechanism of frost action in hardened cement paste, *Journal of the American Ceramic Society*, 55 (1), 38–42.

Litvan, G.G. (1973) Frost action in cement paste, *Materials and Structures, Research and Testing*, RILEM, Paris, 6 (34): 293–298.

Litvan, G.G. (1980) Freeze/thaw durability of porous building materials, in Sereda and Litvan (editors) *Durability of Building Materials and Components,* ASTM, Special Publication STP691, 455–463.

Marchand, J., Pigeon, M. and Setzer, M., eds, (1997) *Freeze/thaw Durability of Concrete*, London, E&FN Spon.

Marchand, J., Sellevold, E.J. and Pigeon, M, (1994) The de-icer salt scaling deterioration

of concrete – an overview, Third International Conference, Durability of Concrete, (Malhotra, V.M., editor), American Concrete Institute Special Publication SP-145, 1–46.

Murdock, L.J., Brook, K.M., and Dewar, J.D. (1991) *Concrete Material and Practice*, London, Edward Arnold, 219.

Neville, A.M. (1995), *Properties of Concrete*, Harlow, Addison Wesley Longman.

Pigeon, M. and Pleau, R. (1995) *Durability of Concrete in Cold Climates*, London, E&FN Spon.

Pink, A. (1978), *Winter Concreting*, Crowthorne, British Cement Association, 10.

Powers, T. C. (1945) A working hypothesis for further studies of frost resistance of concrete, *Journal of the American Concrete Institute*, 16(4): 245–272.

Powers, T. C. (1949) The air requirement of frost-resistant concrete, *Proc. Highway Research Board*, 29: 184–211.

Powers, T. (1958) Structure and physical properties of hardened Portland cement paste, *Journal of the American Ceramic Society*, 41, 1: 1–6.

Powers, T. C. (1975) Freezing effects in concrete, ACI Special Publication SP-47, American Concrete Institute, Detroit, 1–11.

Powers, T. C. and Helmuth, R. A. (1953) Theory of volume changes in hardened Portland cement pastes during freezing, *Proc. Highway Research Board*, 32: 285–297.

Price, W. (1996) Measuring air voids in fresh concrete, *Concrete*, 30, 4: 29–31.

RILEM Technical Committee TC 117-FDC (1997) Freeze-thaw and deicing resistance of concrete, *Materials and Structures, Research and Testing*, RILEM, Paris, 30 (196), S3–S6.

Sellevold, E. J. and Bager, D. H. (1980) Low temperature calorimetry as a pore structure probe, Proc. 7th Int. Cong. on Chemistry of Cement, Paris, 4, 394–399.

Setzer, M. J. (1976) A new approach to describe frost action in hardened cement paste and concrete, Proceedings, Conference on Hydraulic Cement Pastes, their Structure and Properties, Cement & Concrete Association, Slough, 312–325.

Setzer, M. J. (1997) Action of frost and deicing chemicals – basic phenomena and testing, in Marchand, J., Pigeon, M., Setzer, M., *Freeze/thaw Durability of Concrete*, London, E & FN Spon, 3–22.

Siebel, E. (1999) Performance Testing 'Freeze-Thaw Resistance', *CEN TC104/DuraNet Workshop, Design of Durability of Concrete*, Berlin, 46–48.

Stark, J. and Ludwig, H.M. (1997) Influence of water quality on the frost resistance of concrete, in Marchand, J., Pigeon, M., Setzer, M., *Freeze/thaw Durability of Concrete*, London, E & FN Spon, 163.

Swedish Standards Institution (1995) Concrete testing – hardened concrete – frost resistance, Swedish Standard SS 13 72 44, Stockholm.

Wright, P.J.F. (1953), Entrained air in concrete, Proceedings, Institution of Civil Engineers, Part 1, 2(3), 337–358.

9

Degradation of fibre-reinforced cement composites

P PURNELL, University of Warwick, UK

9.1 Introduction

The durability of fibre-reinforced cements and concrete (frc) has been the subject of academic debate and commercial intrigue for around 40 years, which continues apace even as you read this. The level of interest is sustained by the considerable chemical and microstructural complexity of even the simplest frc. The time-dependent behaviour of the cementitious matrices is still not fully understood. This is particularly true of frc matrices, which are often of 'ordinary' Portland cement modified with various materials, or even of non-Portland cements. Residues of unhydrated cement continue to hydrate slowly for many years, and since many of the products of both this and primary hydration can be considered meta-stable, the hydrated phase assemblage will almost always be changing, albeit gradually, as time passes. Into this complexity we introduce fibres of various materials, compositions, morphologies and quality. The interactions between these fibres and the hydrating matrix are time-dependent over scales of months or years and occur on the microstructural level at the fibre-cement interface. The net result is that the engineering properties of some types of frc (in particular tensile/bending strength, toughness and strain to failure) can vary considerably with time; frequently, one or more will decline, giving rise to durability concerns.

Most fibres (with the exception of steel) are introduced as bundles of fibres rather than individual filaments and derive their reinforcing action from remaining as such. Initially, the matrix does not penetrate these bundles or completely surround the filaments (but may increasingly do so with time). In frc, the fibres tend to be more ductile than the matrix; frc is classed as a brittle matrix composite and the fibres are intended to imbue the composite with toughness. Analytical techniques derived for composites such as fibre-reinforced polymers (frp) – where typically fibres are intended to act as individual filaments, are more brittle than the matrix and intended to provide stiffness and/or strength – are, therefore, not appropriate for use with frc. Furthermore, frp is generally used in high specific value applications such as aerospace and sport, where a short-life/high-

maintenance paradigm applies to durability studies. Frc is used in buildings and infrastructure where the exact opposite – long-life/low-maintenance – ethos applies. Thus we can see the investigation and modelling of frc durability must be unique and cannot be inferred from studies on other composite materials. Indeed, although the causes of degradation in all frc fall into a small number of broad categories, the details of how the properties of a given class of frc change with time are different for each fibre-matrix combination considered. As previously exotic fibres such as carbon become economically viable for use in concrete, and the variety of cementitious matrices for use therewith expands, one thing becomes increasingly true; frc durability is a law unto itself.

The remainder of this introduction will define some of the terminology used in frc studies, give some background on fibre types, configurations and production methods, and provide a primer on the mechanical behaviour of brittle matrix composites. The following section will discuss the time-dependent behaviour of frc, in particular how changes in properties are related to changes in the microstructure of the various composites. It also assesses how the behaviour can be modelled and predicted, in particular by using accelerated ageing techniques. Finally, future trends in frc, such as the use of textile reinforcement and the potential for load-bearing frc components will be briefly debated and sources of further information advanced. Overall, this chapter will attempt to review as much of the literature as possible and synthesise concise conclusions concerning the current state of frc durability paradigms.

9.1.1 Terminology

A number of subject specific terms are useful in order to discuss concisely frc structure and behaviour. The term frc itself can refer to either fibre-reinforced cement or fibre-reinforced concrete. There are a number of distinctions between the two. The first normally refers to thin-sheet material produced with high cement content (often 1:1 by weight with fine aggregate but occasionally just cement) and no coarse aggregate. The fibre content is relatively high (up to 5% by volume) and the fibres are intended to provide primary reinforcement, i.e. to provide increased bending strength, tensile strength and/or toughness. It will be referred to as primary frc. The second refers to concrete with cement plus fine and coarse aggregate, to which relatively small amounts of fibre (<1% by volume) are added as secondary reinforcement to help control shrinkage cracking or provide post-failure integrity for safety reasons (i.e., to prevent spalling after accidental overload). It will be referred to as secondary frc. There is some overlap between the two classes. Many authors use the two 'frc' terms interchangeably and in many contexts, the difference is unimportant, but where it is relevant it has been explicitly made clear.

As mentioned above, the unit reinforcement element in most frc other than steel-frc is a bundled group of filaments with space between them, which may or

may not be filled with hydration product depending on the age of the composite and the nature of the matrix. Such a group of filaments is referred to as a 'strand'. A group of strands is referred to as a 'tow' or a 'roving'. A strand may be natural, as in sisal or coir-frc where the strand is a naturally occurring bundle of cellulose fibres containing both inter-filamental space and lumen pores, or artificial as in glass fibres, where strands of up to 200 filaments are grouped together during fibre manufacturing and held together by a soluble or partially soluble coating known as a 'size' (often derived from organics such as polyhydroxy-phenol). This size may also have an effect on the hydration at the interface and is normally designed to improve durability. Occasionally, frc is made with more than one type of fibre, e.g. glass and polypropylene. Such frc is referred to as hybrid-frc.

The amount of fibre in a given frc is normally expressed as fibre volume fraction V_f, defined as the volume of fibres divided by the volume of composite, and varies between about 0.1% and 10%. The limiting factor on V_f is generally its adverse effect on fresh concrete workability and/or compaction. Some analyses also require reference to matrix volume fraction V_m, which is $1 - V_f$.

As with ordinary concrete, most frc is made with matrices based on Portland cement (PC), i.e. that based on $3CaO.SiO_2$ (alite) and $2CaO.SiO_2$ (belite) as the main hydrating compounds. However, the use of pozzolanic additives and non-Portland cements is widespread, especially as the use of such matrices may confer durability benefits. A matrix made from PC with additions of additives such as metakaolin, condensed silica fume, pfa or ggbs is referred to as a modified matrix. A matrix based on a different chemistry, such as high-alumina cement or calcium sulpho-aluminate cement is referred to as a non-Portland (nP) matrix. There is some overlap between the modified and nP matrices, particularly in the addition of calcium sulpho-aluminates such as synthetic ye'elemite ($4CaO.3Al_2O_3.SO_3$) to PC. Although an additive such as this would normally suggest that the matrix be referred to as modified, the additive radically alters the hydration behaviour and hydrated phase assemblage such that it should really be considered as nP.

9.1.2 Reinforcement: layouts and fibres

A variety of different fibres are used to reinforce concrete and the nature of their distribution throughout the concrete – the layout – has implications for the effectiveness of their reinforcing action. Fibres may be continuous (or 'long') or more commonly discontinuous (or 'short'). They may also be aligned or randomly distributed in 2-D or 3-D (Fig. 9.1). Mixed fibre layouts are possible; in corrugated thin sheets, short randomly oriented 2-D fibres, distributed throughout the matrix, may be supplemented by continuous aligned fibres in the ridges and troughs to provide directional stiffness. The use of textiles or woven mats of fibres is also being investigated by many organisations. The effect of layout on behaviour is explained in more detail in Section 9.1.3.

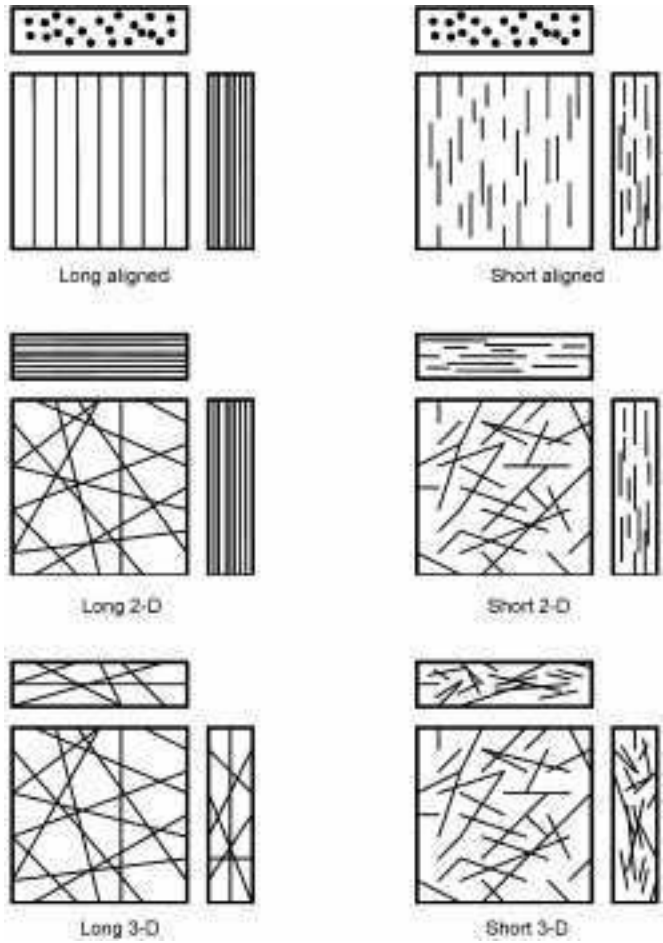

9.1 Reinforcement layouts.

Almost every imaginable type of fibre has been investigated as reinforcement for concrete at some time. A brief summary of the commercially important or promising types in use is given below, derived partly from a number of excellent general-purpose frc references (Bentur and Mindess, 1990, Majumdar and Laws, 1991, Majumdar, 1992, Johnston, 2001, Zheng and Feldman, 1995) in which further details can be found.

Glass fibres

Glass fibres are used mainly in thin-sheet frc. E-glass fibres, as used for reinforcement of polymers, corrode very quickly in cement matrices so the fibres are normally made from an alkali-resistant glass based on SiO_2–Na_2O–

Al_2O_3–ZrO_2 chemistry. They are supplied in rovings of up to 64 strands. Each strand normally has ~200 filaments of ~14 μm diameter. Nowadays the size used to hold the strands together also actively modifies hydration at the fibre-cement interface, imparting greater durability; this is known as 'second-generation' fibre (as opposed to older 'first-generation' fibres where the size was not active vis-à-vis durability). The roving may be supplied in continuous or pre-chopped form to suit different frc manufacturing routes. Glass-fibre mats or weaves are increasingly popular. Glass fibres are used mainly to provide primary reinforcement at V_f ~ 5% but can also be used for crack control at lower volume fractions. Typical properties include a strand strength of 1500 MPa, modulus of 70 GPa and a strain to failure of ~2%.

Polymer fibres

Most common polymers have a modulus of elasticity rather lower than that of a cementitious matrix and thus their use in frc is normally limited to providing 'post-peak' (see Section 9.1.4) toughness, strength or impact resistance. However, since these are all very useful properties, wide use is made of various polymer fibres. Most common is polypropylene (PP), usually in the form of a fibrillated film made from splitting and stretching PP sheets or extruded tapes. The film is 15–100 μm thick, split into fibrils 100–600 μm wide. Thus the individual 'filaments' are tape-like rather than cylindrical. The modulus and strength of such fibres can vary widely, from 1–18 GPa and 300–700 MPa respectively depending on the manufacturing method. Since the PP is hydrophobic, it is usually surface treated to improve bond with, and dispersion throughout, the cementitious matrix. Typical V_f is about 5%.

Polyethylene (PE), acrylics, polyvinyl alcohol (PVA) and nylon fibres have all also been investigated for use in frc but of these, only PVA has been developed commercially specifically for frc. Polyester fibres are not suitable for frc.

Some recent research interest has been shown in using aramid fibres (e.g., Kevlar®, Twaron®) in frc. These have much higher moduli and strengths than ordinary polymers (up to 125 GPa and 3000 MPa respectively) and thus would provide more efficient primary reinforcement. The price of such fibres at present restricts their commercial development in frc but this may change.

Natural fibres

A huge variety of natural fibres – i.e. those derived from plants (or rarely, animal pelts) – have been used to reinforce brittle matrices over the millennia. The motivation is normally use of a local, cheap and sustainable resource, as from a technical point of view, such fibres and their derivatives are inferior to, e.g. glass, steel or PP. They are generally divided into two classes. Unprocessed fibres are naturally fibrous materials subject to minimal processing before use, e.g. jute (a

plant stem), sisal (derived from a leaf) or coir (coconut husk fibres). Processed fibres are cellulose fibres extracted from, e.g. wood chips or bamboo; this class may include fibres derived from a waste stream, e.g. sugar cane fibres or nut husk fibres. They all have features in common; each individual fibre is in effect a strand, containing in the order of 100 cells, each <50 μm across and 1–2 mm long. Each cell has a central pore or 'lumen' and walls made of a composite of crystalline cellulose fibres in a matrix of lignin and hemi-cellulose. The cells have a tendency to absorb water and the fibre properties are strongly dependent on the water content. Increased processing aims to reduce the lignin and hemi-cellulose content and thus concentrate the cellulose fibres, increasing strength, stiffness, water resistance and integrity. Properties are highly variable; strength ranges from 200–800 MPa, and modulus from 10–30 GPa.

Carbon and other ceramic fibres

Carbon fibre is the darling of the high-performance product industry and known to expert and layman alike; thus it was inevitable that it would be investigated eventually for use in frc. It remains expensive but as the price of fibres falls it may one day become a viable ingredient for commercial frc, and the amount of research work reported on it requires that it be mentioned. Carbon fibres come in two types; PAN-based and pitch-based, which refers to the starting materials used. The former have superior properties to the latter and are correspondingly more expensive, and so pitch-based fibres are normally considered for frc. Each fibre is a tow, made up of ~10 000 filaments each up to 15 μm in diameter. The filaments consist of stacked layers of graphite. The properties of the fibre increase as the regularity of this stacking increases, i.e. a greater proportion of the layers are aligned parallel to the fibre axis. For pitch-type fibre, the modulus and strength is about 30 GPa and 600 MPa respectively. PAN-type fibres are about 10 times stiffer and 4 times stronger than this. Matrices for carbon-frc have to be specially designed in order to ensure that the fibres are properly dispersed.

Other ceramic fibres have occasionally been used in frc, e.g. alumina, alumino-silicate or wollastonite but with little commercial success.

Asbestos fibre

Asbestos-frc has been, historically, the most prolific and successful frc variant, used the world over for roofing, cladding, fire-proofing, etc. The term asbestos covers a range of naturally occurring crystalline silicate fibrous materials. The individual fibres are less than 0.1 μm across and form bundles, which in the natural state may contain millions of fibres, but are broken down to strands of 10–100 fibres during processing. Their properties make them ideal for reinforcing cement; they are very stiff and strong (170 GPa and up to 4500 MPa),

bond exceptionally well to the cement matrix and are not prone to degradation during processing or because of the harsh cement matrix conditions. Unfortunately, accidental ingestion of these very fine silicate fibres by production and installation/demolition workers is known to cause a variety of respiratory diseases, including bronchial, lung and stomach cancers (Health and Safety Commission, 1979). The use of asbestos-frc is now banned in most developed countries and the commercial need to find replacements is the motivation behind much relatively recent frc research.

Steel fibres

By tonnage, steel-frc is probably the most successful of all. Steel fibres are rather different from any of those described above. They are generally of larger cross-section, with an 'equivalent diameter' of 0.5–1 mm and lengths varying between 20 and 60 mm. They may have a shaped cross-section, often varying along the length to form hooked, barbed or crimped fibres, intended to increase the anchorage between the fibre and the matrix. Carbon steels are normally used; where a greater degree of corrosion resistance is required (e.g., in marine applications), alloy steels, stainless steels or galvanised steels may be substituted. The modulus of steel fibres is ~200 GPa, and strengths vary between 350 and 1000 MPa. Steel fibres cannot be added in sufficient quantity to provide any primary reinforcement (V_f normally <2% for workability reasons), thus they are intended to provide crack control and post-peak toughness. Steel-frc is often used as a matrix for high-performance steel-bar reinforced concrete (RC) as the steel fibres reduce crack width in cracked sections and thus slow down corrosion of the rebars.

9.1.3 Production methods for frc

Production methods for frc fall into three main categories: pre-mix, spray-up and automated processes. Pre-mix simply uses normal concrete mixing technology, with pre-chopped fibres added to the mix in the same way as any other constituent. This method tends to be used where only low fibre volumes are required, i.e. for fibre reinforced concrete. As V_f exceeds about 1–2% depending on the fibre type, balling of fibre in the mixture results in poor distribution of fibres; the mix also tends to become unworkable and difficult to compact.

For higher fibre contents (and thus enhanced properties), spray-up techniques are used. These tend to use systems where the concrete or mortar matrix and fibres are sprayed separately, either from dual or concentric nozzles. The fibre and matrix are mixed as they impinge on the mould or substrate surface and are often compacted by hand or automated rollers following the spray head. Varying the rate at which fibres are delivered controls the volume fraction. The fibre may be delivered as a continuous roving and chopped at the spray head (as in glass-

frc), or sprayed pre-chopped (as in steel-frc 'shotcrete'). Some additional hand lay-up may take place simultaneously, e.g. to add extra textile to reinforce corners or rebates. The spraying process may be partly automated.

Automated processes tend to produce continuous sheets of frc. Most are developed from the Hatschek process. Water-rich slurries of fibre and matrix are de-watered to form thin layers, which are laminated to achieve the required thickness. The sheets are formed (e.g., corrugated, curved) on mandrels while still green. The process depends for its success on the ability of the fibre to flocculate in such a way as to prevent cement particles from being washed away. The process was developed from paper-making technology for manufacture of asbestos-frc, which is ideally suited to this method. Some efforts are being made to adapt the process for other fibre systems.

Recently, woven textiles of various or combined fibres have been developed for use as reinforcement for cementitious products (e.g., Curbach, 2003). This has opened the way for a variety of composite production methods to be used for frc, e.g. pultrusion (Peled and Mobasher, 2005). The state-of-the-art report in textile reinforced concrete was reported in early 2006 by RILEM Technical Committee TRC-201 (RILEM, 2006).

9.1.4 Aspects of the mechanical behaviour of brittle matrix composites

In order to discuss the time-dependent changes in the behaviour of frc, it is necessary to introduce in broad terms the concepts used to describe the mechanical behaviour of such composites in general. This is because degradation often does not just involve simply a change in the value of a single property, e.g. strength, but often involves a change in the mode of failure.

Composite materials approach

Figure 9.2a shows an idealised stress-strain curve for a typical frc. Four important regions can be identified. In region I – the pre-cracking region – the matrix and fibre act together in the normal composite manner. The composite modulus, E_c, can be predicted from the moduli of the matrix, E_m, and the fibres, E_f, using the rule of mixtures, i.e.:

$$E_c = E_m V_m + \eta_l E_f V_f \qquad 9.1$$

The factor η_l is a combined efficiency factor ($0 < \eta_l < 1$) to account for the fact that in most frc, the fibres are rarely aligned with the direction of stress but distributed in a random 2-D or 3-D alignment depending on the application. The value of η_l varies depending on the modelling assumptions made but is typically about 0.375 and 0.2 for 2-D and 3-D fibre layouts respectively (Bentur and Mindess, 1990). In any case, it can be seen by inserting typical values into

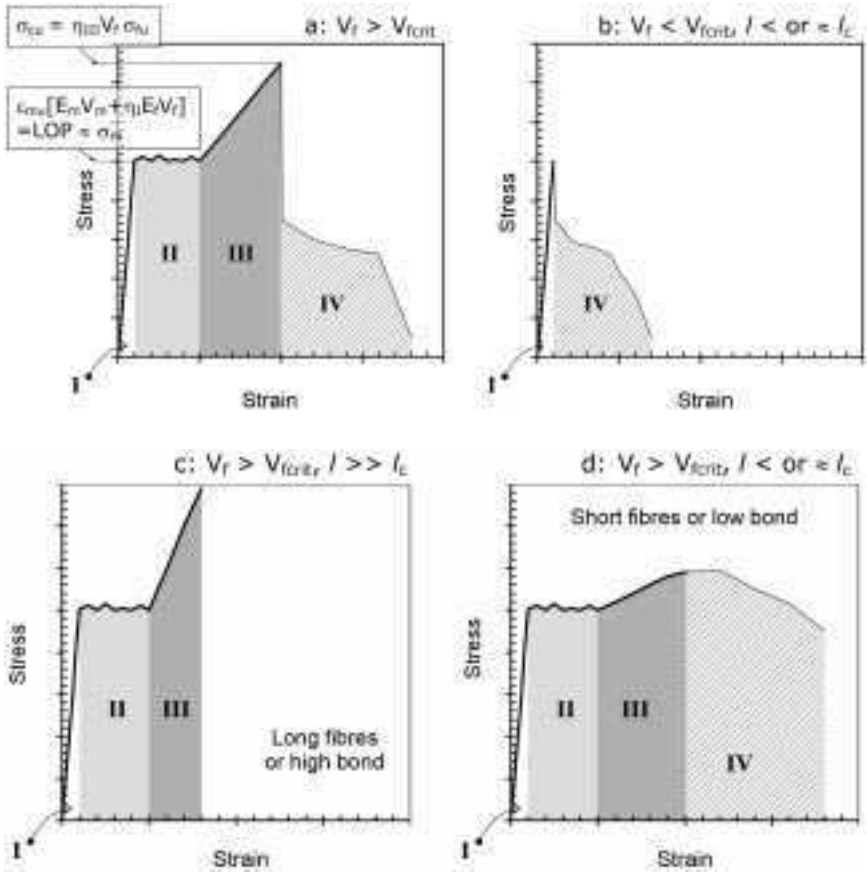

9.2 Schematic stress-strain curves for frc. a) General curve. b) Low fibre content, short fibres. c) High fibre content, long fibres. d) High fibre content, short fibres.

equation 9.1 that the improvement in pre-cracking properties imparted to the matrix by the fibres is minimal.

When the failure strain of the matrix ϵ_{mu} is reached, the first crack occurs and region II – the multiple cracking region – begins. The stress at which this happens, variously referred to in frc literature as the loss of proportionality (LOP), 'bend-over point' (BOP) or 'first crack strength', can be calculated from equation 9.1 by assuming that the strain at first crack is the failure strain of the matrix and assuming strain compatibility between fibre and matrix, but is rarely much different to the matrix strength σ_{mu}. In this region, stress is progressively transferred from the matrix to the fibre as the matrix develops a network of increasingly closely spaced cracks. This is the beginning of the 'useful' action of the reinforcement in frc – imparting strain capacity and toughness far in excess of that of the matrix alone. Toughness is related to the area under the stress-

strain curve; it can be seen that compared to that imparted by even modest fibre action, the toughness of the matrix alone is essentially zero. The existence of region II was predicted by Aveston *et al*. (1971) ('ACK theory') and has been confirmed by most subsequent investigators. This region can only be properly mobilised if there are sufficient fibres to carry sustained, increasing load when the matrix breaks; thus there is a critical volume fraction of fibres V_{fcrit} that can be approximated to (Purnell, 1998):

$$V_{fcrit} = \frac{\sigma_{mu}}{\eta_I \sigma_{fu}} \qquad 9.2$$

where σ_{fu} is the ultimate tensile strength of the fibre.

In region III – the post-cracking region – the fibres alone carry the load and the modulus can be predicted from equation 9.1 by assuming $E_m = 0$ (since it is fully cracked) and substituting a post-cracking efficiency factor η_{III} for η_I. The post-cracking efficiency factor depends on the orientation and the length l of the fibres relative to the 'critical length', l_c. The critical length of a fibre is the minimum fibre length required of a fibre embedded in a matrix such that, on failure of the composite, the full failure stress is developed in the fibre, i.e. it breaks rather than pulls out of the matrix (Fig. 9.3). Thus l_c depends on the strength of the fibre and the strength of the bond between the fibre and the matrix; good bond and/or low fibre strength give low values of l_c and vice-versa. Values of η_{III} for practical frc range from about 0.05 for a 3-D $l < l_c$ layout, to 0.33 for a 2-D $l \gg l_c$ layout (Bentur and Mindess, 1990); in general, η_{III} increases with l/l_c. Region III ends when the fibres reach their ultimate tensile strength and the ultimate tensile strength of the composite σ_{cu} is thus reached. It can be approximated as:

$$\sigma_{cu} = \eta_{III} V_f \sigma_{fu} \qquad 9.3$$

Region IV – the post-peak region – is when the maximum stress capacity of the composite has been exceeded. Many investigators consider that it is mode IV

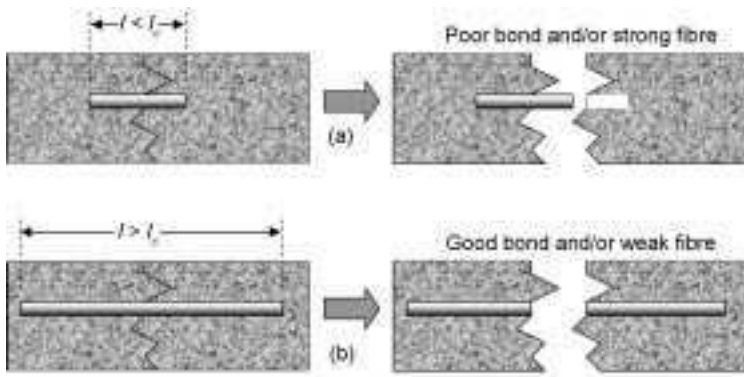

9.3 Critical length and fibre pullout.

behaviour that expends the greatest energy during composite failure and thus imbues the composite with the greatest toughness. This is especially true in frc made such that V_f is less than or comparable to V_{fcrit}, a common occurrence, e.g. when using relatively weak natural fibres or when adding more fibres would cause workability problems (e.g., steel-frc). In such cases, regions II and/or region III may be greatly reduced or even absent from the stress-strain curve and all the toughness over and above that of the matrix is derived from post-peak pullout, region IV behaviour (Fig. 9.2b). For frc where $l \gg l_c$ (i.e., bond is very strong or fibres are very long) this region is very small or non-existent, as there is sufficient stress transfer between the fibre and matrix for the fibres to fracture and the composite will simply break in two upon reaching peak stress (Fig. 9.2c). Where the fibre length is comparable to or less than l_c (i.e., bond is weak or fibres are short) many of the fibres will not have had their full stress capacity mobilised at peak composite stress and they will begin to pull-out of the matrix; although initial ultimate strength may be lower, the toughness will be increased (Fig. 9.2d). In most cases, there will be some overlap between regions III and IV.

However, the manifestation of this type of behaviour is frequently unpredictable and critically dependent on the testing regime used. In a load controlled stress-strain test (i.e., where load is uniformly incremented with time), region IV is never seen; it can only be seen in a stroke-controlled test (i.e., where displacement is uniformly incremented with time) and even then is highly sensitive to the stroke rate used. While it is not disputed that region IV behaviour is important, it is imperative that attempts to quantify it and discuss its nature employ standard tests (e.g. ASTM C1018) and not the ad-hoc procedures so common in the literature.

Fracture mechanics approach

Fracture mechanics principles are often invoked to describe the reinforcing effect of fibres, especially at low fibre volume fractions typical of steel-frc. The detail of the modelling is outside the scope of this chapter but it is reviewed by Bentur and Mindess (1990). In broad terms, two concepts are important with regard to durability of frc. First, in cracked frc, fibres are known to span the cracks and help hold them together. This helps to suppress further propagation of cracks (i.e., it requires that more energy input is required for cracks to grow than in unreinforced materials) and thus increases the toughness of the composite. Secondly, since the fibre-matrix interface tends to be weaker than the bulk matrix (analogously to the transition zone in ordinary concrete), cracks travelling through the matrix will tend to divert along this interface. Geometrical considerations and studies of the strain energy release rate for debonding vs normal cracking suggest that further propagation will require more energy input than in unreinforced matrix and thus again, an increase in toughness is predicted.

9.2 Time-dependent behaviour

Figure 9.4 shows the decrease in bending strength (expressed as a fraction of the 28-day strength, i.e. the initial strength after curing, at the start of service) for five types of PC based matrix frc, reinforced with either first or second generation alkali-resistant (AR) glass fibre, two types of natural fibre, sisal or coconut (coir), and polypropylene fibre, exposed outside in UK weather. The fibres in each case were intended to provide primary reinforcement. It can be seen that there are appreciable losses in strength with time, but that the magnitude of the loss is different for each frc, even within similar classes (i.e., glass or natural fibres). Thus it is difficult to make generalisations concerning the 'durability' of frc systems and each frc should be evaluated carefully. In general though, it appears from the available evidence that the durability of common primary frc proceeds polypropylene > 2nd generation AR glass >> 1st generation AR glass >> unprocessed natural fibres.

Although strength is the most frequently monitored property during ageing, other properties are often of more interest. As the action or efficiency of the fibres is degraded, by whatever mechanism, composite strength will decrease until the fibres confer no strength benefit, but the matrix strength will be retained

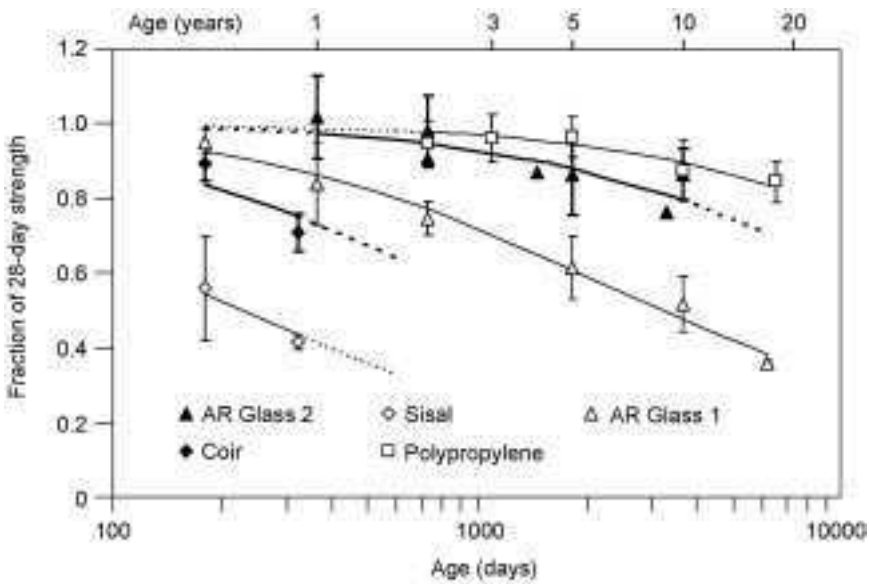

9.4 Strength vs. time for selected frc formulations subjected to natural exposure. Key: AR Glass 2, second-generation AR glass/OPC frc (Majumdar and Laws, 1991, Cole, 1990); AR Glass 1, first-generation AR glass/OPC frc (Majumdar and Laws, 1991); Polypropylene: polypropylene/OPC/pfa frc (Hannant, 1998); Sisal, Coir, OPC frc (Tolêdo *et al.*, 2000). Curves: best fit of Purnell *et al.* (2001a) and Purnell and Beddows (2005) type relationship ($S = [1 + kt]^{-0.5}$). Error bars: ±1 standard deviation where available.

since this tends to remain constant or increase with time. Thus strength in primary frc will only degrade until it is equal to the matrix strength, at which point it will remain more or less constant. In primary frc the matrix strength is typically around 20–50% of the original composite strength but in secondary frc, where the fibre content is close to or below the critical volume fraction and fibres are mainly intended to provide post-peak toughness (e.g., Fig. 9.2b), the original composite strength will be practically the same as the matrix strength. In such cases, it is more appropriate to monitor a toughness index (normally derived from the area under the stress-strain curve up to some specified strain) or strain-to-failure. Since both these properties of the matrix are negligible compared to that of the original composite, they will effectively degrade to zero. Such properties are, however, rather more difficult to measure than strength and often display very large scatter and hence strength remains the most popular metric. For example, processed natural fibre, i.e. cellulose-frc, is normally manufactured such that the fibre volume fraction is lower than or comparable to V_{fcrit} and it is thus not appropriate to monitor strength as a degradation metric; indeed, it increases by about half over five years outdoor exposure owing to continued hydration of the matrix and increased bond (hence increased l_c and fibre efficiency factors). However, strain to failure is reduced from about 3% to that of the matrix (i.e., <0.1%) within this period (Akers and Studinka, 1989), indicating that the benefits of fibre reinforcement have been largely lost after such time even though strength has increased.

Polymers other than polypropylene have also been used to reinforce concrete (Zheng and Feldman, 1995, Akers *et al.*, 1989, Majumdar, 1992). Most either do not bond well to cement or are not stiff/strong enough to confer significant benefits and thus no weathering data exists. Akers and co-workers (1989) studied ageing of PVA-frc up to seven years. No strength loss was reported but it is not clear that the original fibre volume fraction was significantly above V_{fcrit} and thus this is not a conclusive result. Majumdar (1992) reported that strength was retained in PVA-frc after five years weathering but again the fibre volume fraction was very low, as evidenced by there being very little difference between the first-cracking and ultimate strength. Aramid-frc displayed no loss in properties after two years weathering (Walton and Majumdar, 1978) but more recent commentators express concern over the longer-term compatibility of aramid fibres with cement (Johnston, 2001, pp. 189–190). Polyester fibres are not suitable for concrete reinforcement as they degrade quickly in cement (Zheng and Feldman, 1995).

Carbon fibres have been generally assumed to be unaffected by the corrosive alkaline environment in cement composites and thus immune to the associated deterioration mechanisms (Majumdar, 1992, Ohama, 1989); recent investigators agree (Chung, 2000) although little if any long-term weathering data exists in the literature. Katz and Bentur (1995) and Katz (1996) have noted that the strength and toughness of carbon-frc reaches an optimum at ~30 days, after

which a slight drop in properties may be observed owing to matrix densification; presumably these properties then stay constant. The magnitude of the effect was dependent on the matrix formulation, i.e. the proportion of silica-fume (see Section 9.2.3) added.

The durability of steel-frc has received comparatively little attention and tends to be approached in a different context in that it is compared with that of traditional reinforced concrete (RC), i.e. studies report the observation or otherwise of surface spalling and any compromise to structural integrity rather than decline in material properties. Bentur and Mindess (1990) and Johnston (2001) summarise steel-frc durability studies up to about the end of the century. Even under several months of severe accelerated corrosion conditions such as wetting/drying cycles in hot salt solutions, $V_f = 2\%$ steel-frc can retain at least 70% of its strength and 40% of its toughness (Kosa and Naaman, 1990). Granju and Balouch (2005) showed that fibre corrosion was not correlated with flexural strength or toughness loss after one year in a simulated marine environment even for pre-cracked specimens. Under normal conditions, no degradation other than superficial corrosion of surface fibres seems to have been reported. In a review, Hoff (1987) concluded that steel-frc will only degrade if it is cracked, even in marine environments.

9.2.1 Mechanisms

The causes of the time-dependence of properties fall into two broad categories, regardless of the type of fibre involved. First is fibre corrosion. The nature of most hydraulic cements is alkaline. During manufacture, the alkali metal compounds present as impurities in the clays or shales used as raw materials are converted by the high clinkering temperatures into alkali oxides and/or sulphates, which are incorporated into the structure of the cement clinker. On gauging with water during concrete mixing, these highly soluble alkalis are released into the mixing water, raising the pH significantly. As the cement hardens, the mixing water is used up and the alkalis are thus concentrated in the remaining free water, contained within the capillary porosity of the cement paste, known as the pore solution. Cement pore solution can reach a pH of up to 13.7, or 700 mmol/l (OH^-), the OH^- content being associated mainly with K^+ ions but also with Na^+ ions; the pore solution is buffered by the $Ca(OH)_2$ (portlandite) produced by the hydrating cement, but contrary to popular belief the Ca^{2+} content of the pore solution is generally very low (i.e., <40 mmol/l) owing to the common ion effect (see e.g., Taylor, 1997 for more details on cement chemistry). The integrity of many fibres is compromised at these very high alkalinities and thus fibre corrosion, leading to a loss of strength of the reinforcement, is always a composite degradation mechanism that must be considered. This holds even for fibres which are supposedly immune to alkali attack, since the timescales which must be considered – i.e. the service lifetimes

of typical frc components, often decades – are much longer than most exposure experiments. As well as reducing the strength of primary reinforcement, weakening of the fibre may also lead to a change of failure mode. As the fibre strength is reduced, l_c is also reduced and thus the mode may change from fibre pull-out to fibre fracture, i.e. region IV behaviour (Fig. 9.2) may be reduced or lost. For steel fibres, the alkaline environment passivates the steel and protects it from corrosion, as in ordinary RC described elsewhere in this book.

There is also evidence that some fibres, particularly glass, may be susceptible to physicochemical attack by direct contact with calcium hydroxide in the matrix to a level over and above that caused by alkalinity alone (Proctor and Yale, 1980).

In certain applications, the ingress of external agents deleterious to certain fibres, such as chlorides or acidic organics, must also be considered. Although of primary importance for steel-frc (for example, chlorides disrupt the passivation of steel fibres as with the steel in RC) this may occasionally be of concern for other frc. Frc made with natural fibres, the properties of which vary with moisture content, may be degraded by water ingress.

A variety of effects caused by the continued hydration of the cementitious matrix also have the potential to cause composite degradation. Given the continued availability of water, residual anhydrous cement in the matrix (of which there is always a small amount) will continue to hydrate, producing more hydration products and increasing the strength of the matrix. The hydrated phase assemblage itself will also tend to slowly evolve since it is essentially composed of meta-stable phases. Although this continued hydration and evolution might only involve a very small fraction of the cement paste, the resultant effects on the fibre-matrix interactions can be profound.

We can see from equation 9.2 that V_{fcrit} is dependent on the matrix strength; as the matrix becomes stronger, a greater proportion of fibres are required to take up the load thrown onto them as the matrix begins to crack and thus transfer stress to the fibres. Thus for composites designed with a fibre content very close to V_{fcrit}, continued strengthening of the matrix may change the composite behaviour at first crack from ductile to brittle, as regions II and III of the stress-strain curve (Fig. 9.2) cannot be realised. If $l \gg l_c$ then region IV may also be absent. Careful design of the composite should avoid this.

Continued hydration also tends to 'densify' the interface between the fibres and matrix. When frc is first made, the interface is relatively porous, with little intimate contact between the fibre and matrix. The interfacial zone is thus relatively weak, which is often beneficial for the composite for several reasons. At young ages, cracks travelling through the matrix tend to be diverted through this weaker zone. As the matrix ages, hydration products (particularly portlandite) fill the spaces in the interfacial zone, reducing the porosity and increasing the hardness and strength; it becomes energetically, and thus statistically, more likely that a crack will travel through the fibre rather than around it. This reduces

the toughness of the material. Also, fibres bridging cracks tend to become bent, owing to crack paths being tortuous and fibres generally not being aligned with the stress axis. They will have to bend through tighter radii of curvature as the matrix hardens, since the matrix immediately adjacent to the point where the fibre emerges from the crack face is less compliant. This induces greater stress in the fibres and increases the likelihood of them breaking. The bond between a fibre or strand will also increase as the interfacial zone densifies. As the bond strength increases, l_c reduces. It becomes more likely that fibre failure, rather than pullout will occur, region IV behaviour (Fig. 9.2) is not developed and the toughness will be reduced (even though the tensile/bending strength may well increase appreciably, since l/l_c and hence η is increased).

A related phenomenon is 'bundle filling'. In young frc reinforced with strands or tows, there is normally space between the individual filaments into which the matrix has not penetrated. The reinforcement can thus act in a rope-like manner, with filaments moving over each other, adding significantly to the post-peak toughness of the composite. As the composite ages, continued hydration and migration of species within the cement matrix leads to precipitation of hydration products, especially portlandite, between the filaments and this may eventually fill all the available space. The rope-like behaviour is lost and the toughness of the composite may be compromised.

The relative importance of each of these degradation mechanisms is dependent on the particular fibre-matrix combination. Some combinations are particularly prone to specific mechanisms, while in others the dominant mechanism is still the subject of research and debate. The mechanisms are examined in more detail in Sections 9.2.4 and 9.2.5 in the context of the changing microstructure of frc and modelling of degradation.

9.2.2 Accelerated ageing

Before strategies for improving the durability of frc can be discussed, it is necessary to outline the methods by which much of the relevant data has been obtained. As frc is a relatively young material, a body of 'real-time' weathering data did not exist at the time efforts were made to improve frc durability; there is still a lack of long-term natural weathering data. As new formulations designed for durability were advanced, accelerated ageing procedures were used to attempt to validate the purported improvements and these procedures are still in widespread use today. Two technical types of test can be identified; continuous ageing and cyclic ageing. The former aims to accelerate the degradation either by immersing samples of the composite in water at elevated temperature (typically $\geq$ 50ºC) and thus thermally accelerating the fibre-matrix reaction, or in aggressive solutions (i.e., solutions of de-icing salts or sea-water) where the diffusion of ions into the composite is accelerated by increasing the concentration gradient. Hot aggressive solutions are sometimes used for extreme tests.

Hot water is used for two reasons: it provides thermal inertia and also many frcs do not appear to suffer degradation owing to 'dry' elevated temperature alone; indoor stored grc seems to suffer no degradation. The degradation mechanism appears to involve water in some way, chemical or physical. Aggressive solutions, generally of chloride ions, are usually only used in studies of steel-frc; hot water is used for glass-frc and others. Cyclic tests attempt to replicate the cycles of temperature and/or moisture frc components are likely to be exposed to during service. These cyclic tests normally involve alternate and repeated exposure to hot/wet/cold/dry environments or freeze/thaw cycles. For steel-frc, 'splash' exposure to salts to simulate, e.g. tidal zone marine exposure, is also used.

It should be noted that these tests are not interchangeable; certain tests are more appropriate for certain frc formulations, e.g. hot water for glass-frc, and cyclic wet-dry for natural frc; for ageing of cellulose fibre-reinforced concrete, it is also considered important that at least one of the steps should promote carbonation of the matrix (Bentur and Mindess, 1990, pp. 161–163); ageing of steel-frc almost always involves salts.

Tests can also be divided into two other categories: 'deemed-to-satisfy' (DS) tests and predictive tests. DS tests are intended as a quality control measure; if, for example, a coupon of composite is tested after a fixed ageing period or number of cycles and is found to have properties that exceed some pre-determined value or percentage of the unaged properties, then it is deemed to have 'passed' and the material is fit for purpose. No prediction of the long-term behaviour of the composite in service is advanced or inferred, only that it is in some way 'durable' since it has passed the test. Predictive testing, on the other hand, attempts to correlate periods or numbers of cycles of accelerated ageing with longer periods of in-service weathering and thus goes some way towards quantifying the lifetime that can be expected from the material. Although in theory either cyclic or hot water testing can fall into either category, in practice continuous ageing, especially hot water ageing tends to be used for predictive testing and cyclic ageing for DS testing with few exceptions.

Investigators have also frequently subjected fibres (as opposed to composites) to accelerated ageing regimes and thus inferred their likely behaviour in a cement matrix. These tests generally involve immersion of samples of fibre in hot alkaline solutions, often of analogous composition to cement pore solution, for various lengths of time and measurement of resultant reduction in strength. Such tests, although useful for helping to assess new fibres, should be treated with caution with respect to their use in predicting durability, since the action of the cement matrix on the fibre is not just controlled by its alkalinity. Sisal and coconut fibres were shown to completely lose their strength after 300 days in $Ca(OH)_2$ solution of pH 12 (Tolêdo Filho *et al.*, 2000). Aramid (Twaron) fibres have been subjected to immersion in concentrated NaOH for 24 hours in both stressed and unstressed conditions, with no ill effect (Vilkner, 2003) but no

longer term data is evident. Such tests have long been used with prospective glass compositions and results are reviewed by Majumdar and Laws (1991, pp. 15–25) but new glass or ceramic formulations now tend to be tested in actual frc samples (e.g., Cheng *et al.*, 2003, Ma *et al.*, 2005) although some fundamental work continues to use just fibres (Gao *et al.*, 2003, Orlowsky *et al.*, 2005).

The best known (and most frequently abused) accelerated ageing rationale for frc is probably that derived for OPC matrix AR-glass grc by Proctor and co-workers in the late 1970s (Litherland *et al.*, 1981, Proctor *et al.*, 1982). A combination of tests on composites aged by hot water immersion and composites exposed at various locations around the world were combined with data from a specially developed durability test for fibre strands known as the 'strand-in-cement' (SIC) test. The SIC test involves a specimen comprising a strand of fibres (for grc, typically about 200 filaments, each of about 14 μm diameter) being partially encased in a small cylinder of cementitious matrix. The specimen is aged by immersion in hot water for a specified time and the strand subsequently tested in tension with the small cylinder of matrix still in place (Fig. 9.5). They concluded that a single degradation mechanism with an activation energy of about 90 kJ/mol controlled strength loss in all these cases and the data was pooled into an Arrhenius-type relationship correlating the accelerated ageing tests with longer periods of in-service weathering. This allowed 'acceleration factors' to be advanced, e.g. that 1 day of hot water immersion ageing at 50, 60 and 80ºC induced the same strength loss as 101, 272 and 506 days of weathering in a UK climate respectively. This predictive rationale lead to hot water ageing being accepted as the *de facto* standard method for validating new grc formulations with respect to durability, which it remains (e.g. Orlowsky and Raupach, 2003, Hempel et *al.*, 2003, Brockmann and Raupach, 2002). However, the method was only derived with OPC composites in mind. Concern over its application by other investigators to non-standard grc (and even frp) with evidently different ageing characteristics and mechanisms, together with shortcomings of the model regarding service life prediction and the lack of a micromechanical model, lead to the rationale being updated by Purnell and co-workers (Purnell *et al.*, 2001a). The basis and implications of their model is discussed in more detail in Section 9.2.5, but it is clear that a unique set of

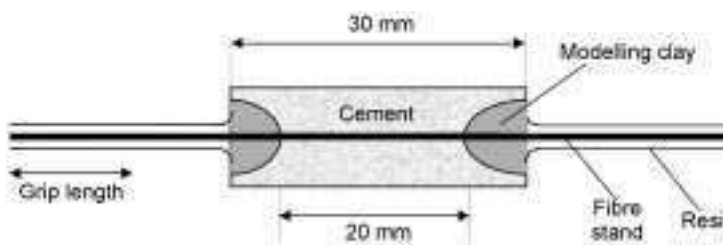

9.5 SIC test specimen schematic (adapted from Litherland *et al.*, 1981).

acceleration factors applies to each matrix formulation used with AR glass (Beddows and Purnell, 2003, Purnell and Beddows, 2005); by implication, acceleration factors derived for grc should not automatically be applied to other types of frc.

Another accepted accelerated ageing test method for grc is codified in European standard DD EN 1170-8:1997 *Precast concrete products. Test method for glass-fibre reinforced cement. Cyclic weathering type test*. This involves cyclic ageing, where each cycle involves 24 hours immersion in water at 20ºC, 30 minutes of forced drying in air at 70ºC and 1 m s^{-1} airflow, 23 hours in air at 70ºC and 30 minutes of forced cooling in air at 20ºC and 1 m s^{-1} airflow, with samples tested in bending after 10, 25 and 50 cycles. The test is notoriously difficult to apply as it requires specialist equipment and contains no predictive component, only serving as a comparison. As such, it is unpopular with researchers but has some adherents in industry (e.g., Cian and Della Bella, 2001).

Some attention has been paid to the accelerated ageing of cellulose and/or natural fibre based-frc. In early work, the hot water ageing rationales developed by Proctor and co-workers (Litherland *et al.*, 1981, Proctor *et al.*, 1982) for glass-frc were used for sisal-frc (Bergström and Gram, 1984) but found to be inappropriate. Bentur and Akers subsequently established methods for accelerated ageing of cellulose-frc in a series of papers (Bentur and Akers, 1989a,b; Akers and Studinka, 1989). Two 24 hour/cycle cyclic regimes were proposed; ambient/elevated temperature (AE) and CO_2 rich/elevated temperature (CE), both followed by three-point bend testing based on ISO 39611 – 1980 E. The AE cycle was 9 h in water at 20ºC; 3 h in air at 20ºC; 9 h infra-red radiation 80ºC in air; and 3 h cooling to 20ºC in air. The CE cycle was 8 h in water at 20ºC; 1 h in oven at 80ºC; 5 h in oven at 20ºC in an atmosphere saturated with CO_2; 9h in oven at 80ºC; and 1 h cooling to 20ºC. Cycling was continued for 3 months. The CE cycle was found to most closely approximate a 5-year period of natural weathering and was thus considered the most appropriate method. This regime continues to be used to age cellulose frc (Kim *et al.*, 1999) although other investigators have used slightly modified carbonation tests in addition to freeze-thaw methods (MacVicar *et al.*, 1999). All investigators lean towards the same conclusions: the strength and modulus of the material increases by about 20–50% (as a result of the carbonation of the matrix increasing matrix strength and possibly bonding) but the strain to failure is reduced to values similar to that of the unreinforced matrix i.e. <0.1%. The same regime has been used for PVA-frc (Akers *et al.*, 1989) but again at very low V_f. Some application-specific tests are also used. Cellulose-frc is used for sewer pipes (an application previously filled by asbestos-frc) and as such is exposed to external deleterious agents that can cause acidic and/or biological attack on the fibres and/or matrix. Fisher *et al*. (2001) exposed cellulose-frc samples to sewage in aerobic and anaerobic treatment plants, and also immersed samples in sulphuric acid (pH ~5). It was concluded that there might be advantages in using

cellulose-frc over steel-frc in these applications. For frc with natural fibres, simple wetting and drying cycles (e.g. 1 day immersion at room temperature followed by 6 days drying in ambient lab conditions) seems to be considered appropriate, although since such composites suffer degradation of properties in relatively short time under normal weathering, it is debatable whether accelerated ageing is necessary (Tolêdo Filho *et al.*, 2000, 2003).

Since ingress of aggressive salts rather than fibre-matrix interactions are the controlling factor, tests used for steel-frc tend to have a different focus compared with other frc types and performance is often compared to RC. Durability in the splash zone of marine structures seems to have attracted the most attention, since this is deemed the most severe possible environment, and testing attempts to simulate this. Wetting and drying cycles using 3.5% NaCl solution at 20, 50 and 80ºC for up to 10 months with or without enhanced carbonation induces significant degradation in steel-frc. Strength and toughness are reduced by 20 and 60% respectively for samples carbonated prior to exposure; only toughness is reduced significantly in uncarbonated samples, by about 35% (Kosa and Naaman, 1990). Mangat and Gurusamy (1988) compared a laboratory marine spray chamber with natural tidal exposure and showed that, with respect to chloride ingress into the concrete, the chamber was about 10 times more 'aggressive' than natural exposure owing to the increased salt content. Recent investigators have used a year of 2-week cycles, each of 1 week of 3.5 g/l NaCl salted fog and 1 week 'dryness' (Granju and Balouch, 2005) or up to 1500 freeze-thaw cycles in fresh water or 3.5 g/l NaCl saline solution in accordance with ASTM C666A (Mu *et al.*, 2002).

Accelerated ageing of other frc types does not appear to have been afforded the same degree of investigation, with a variety of different *ad hoc* methods extant in the literature. Polypropylene-frc has been assessed using 50 wet/dry cycles followed by impact testing, and 50 freeze/thaw cycles followed by flexural/compressive testing (Puertas *et al.*, 2003), which caused some decrease in flexural strength but left compressive strength unchanged. Recently, Al_2O_3-based ceramic fibre reinforced concrete has been immersion aged at 70ºC (Ma *et al.*, 2005). Carbon-frc has been subjected to freeze-thaw ageing (based on ASTM C666) for between 30 cycles (Chen and Chung, 1996) and 300 cycles (reported in Ohama, 1989) and water immersion at 75ºC for five months (reported in Ohama, 1989) with little if any effect on strength. Bentur and Mindess (1990, p. 355) discuss how carbon-frc does not show any long-term response to hot water or cyclic accelerated ageing and conclude that it is unlikely to suffer any durability problems.

9.2.3 Enhancements in durability through fibre and matrix modification

Choosing fibre and matrix combinations that reduce or eliminate deleterious interactions or interact in a benign manner can enhance the durability of frc. The

normal approach, however, concentrates either on improving the resistance of the fibres to attack by varying their chemical composition or surface treatment, or on using modified or non-Portland cementitious matrices that are less hostile to fibres, either owing to lower pore solution alkalinity, reduced propensity to precipitate hydration products at the fibre-matrix interface, or reduced permeability to restrict the ingress of deleterious agents.

Glass-fibre development is relatively mature. It was clear from the first incarnations of glass-frc that E-glass fibre (as used by the frp industry) would be chemically unstable in the highly alkaline cement matrix. Alkali-resistant (AR) glass was developed in the 1970s by Pilkingtons, based on soda-lime-silica glass with the addition of about 16% zirconia, and marketed as Cem-FIL. Glass-frc made from AR fibres was not immune to degradation, however, and further developments were made to the soluble coating or 'size' applied to the fibre (originally applied for manufacturing purposes). Incorporation of polyhydroxy-phenols in the size modifies the hydration behaviour of the cement matrix at the interface and significantly improves durability of AR glass-frc (Majumdar and Laws, 1991, p. 13). AR-glass fibres with such coatings are known as 'second-generation' fibres and are now the industry standard. The development of these sizings is ongoing. From time to time, other glass systems are proposed, e.g. based on strontium (Karasu and Cable, 2000) or barium (Cheng *et al.*, 2003) but these have yet to come to commercial significance. Steel fibres, although stable in the alkaline cement matrix, are susceptible to corrosion if this alkalinity is disturbed by, e.g. carbonation or chloride ions, as with RC. Thus in extreme environments such as marine applications, steel fibres may be galvanised (coated with zinc). Steel alloyed with small amounts of chromium or nickel, but not 'fully stainless', will provide significant resistance to rusting (Johnston, 2001, p. 229) but normal stainless steel (i.e., ~15% Cr) may also be used (Mangat and Gurusamy, 1988). Both galvanised and stainless fibres show significantly greater resistance to rusting during ageing compared with low carbon steel fibres (Mangat and Gurusamy, 1988). Other fibres tend to be of fixed composition (e.g., carbon, polypropylene, cellulose) and are thus not amenable to having their alkali resistance intrinsically increased.

An experimental method of increasing durability is to pre-impregnate the fibre strands with material intended either to block precipitation of hydration products between the filaments or modify the nature of hydration such that less deleterious hydration products result. Glass-fibre strands have been impregnated with microsilica or acrylic polymers (Bartos and Zhu, 1996); natural fibres have also been treated with microsilica (Tolêdo Filho *et al.*, 2003). In both cases, resistance to accelerated ageing and/or weathering was improved markedly. This approach has yet to be commercially adopted but would appear to be attractive.

By far the most common approach involves modifying the cement matrix, in order to improve its compatibility with fibres, either by using additives to Portland cement or using non-Portland cement matrices. A great deal of

literature exists on this topic, especially concerning glass-frc; pre-1988 literature is summarised in the books by Majumdar and Laws (1991), and Bentur and Mindess (1990). Additives are generally intended to reduce the pore solution alkalinity of the matrix and/or react with the calcium hydroxide produced during hydration; thus pozzolanic materials, as used to enhance ordinary concrete, are common additives. Condensed silica fume/microsilica (csf), metakaolin, ground granulated blast furnace slag (ggbs) and pulverised fuel ash (pfa) have all been investigated for use with most fibre types. For steel-frc, the same additives are frequently used, but the intention, as with RC, is to reduce the permeability of the matrix and thus ingress of chloride ions, carbonation and water (de Gutiérrez *et al.*, 2005). However, few if any studies directly assess the improvements in steel-frc durability, in terms of mechanical property degradation, afforded by matrix modification.

Csf is a by-product of the ferro-silicon industry and consists of extremely fine particles (<1 μm) of essentially pure silica, which react rapidly with $Ca(OH)_2$. It is used as a matrix enhancer for natural/cellulose-frc (Tolêdo Filho *et al.*, 2003, MacVicar *et al.*, 1999), ceramic-frc (Ma *et al.*, 2005), carbon-frc (Chen and Chung, 1996, Katz and Bentur, 1995, Katz 1996) (where its primary function is to aid fibre dispersion and compaction) and glass-frc (Bartos and Zhu, 1996, Marikunte *et al.*, 1997, Zhu and Bartos, 1997). It is effective in increasing the durability of natural fibre composites exposed to weathering and cyclic wet/dry ageing, but has limited or variable effect on that of glass-frc subjected to hot-water ageing (see also Bentur and Mindess, 1990, pp. 264, 410; Majumdar and Laws, 1991, pp. 105–107). Addition levels vary between 10% and 40% replacement of cement, but at higher levels of replacement it has a profoundly negative effect on workability and thus requires higher water/cement (w/c) ratios for manufacture, which is undesirable. In steel-frc, 15% cement replacement by csf is reported to reduce chloride ingress and chloride diffusion coefficient by a factor of 3 (de Gutiérrez *et al.*, 2005); 8.5% cement replacement by csf had an uncertain effect on de-icer salt scaling resistance (Cantin and Pigeon, 1996). Yan *et al.* (1999) reported that 25% cement replacement by csf doubled the fatigue resistance of steel-frc.

Metakaolin is a calcined china clay which reacts readily with $Ca(OH)_2$ in the matrix and reduces the alkalinity of the pore solution (Purnell *et al.*, 1999). It has been extensively investigated as an additive for glass-frc to improve durability (e.g. Marikunte *et al.*, 1997, Purnell *et al.*, 1999, Zhu and Bartos, 1997, Soukatchoff and Ridd, 1991, Ball, 2003, Beddows and Purnell, 2003). Normally added at 20–25% cement replacement, almost all investigators agree that it significantly improves the durability performance of glass-frc both under accelerated (i.e., hot water) and natural weathering. The degree of improvement depends on how accelerated ageing results are interpreted (see pages 349–52 and Purnell and Beddows, 2005) but it is sufficiently well established for commercial formulations to be used; the metakaolin is also believed to improve surface

finish and resistance to loss of appearance via surface dusting or efflorescence (e.g., Gilbert and Ridd, 2001). It does not appear to have been used to improve durability in conjunction with other fibre types except as reported by de Gutiérrez *et al.* (2005) who did not monitor changes in mechanical properties with time but were concerned with chloride diffusion. Use of metakaolin as 15% cement replacement in steel-frc was reported to reduce chloride diffusion by a similar factor to csf.

Ggbs has been used with natural-frc (Tolêdo Filho *et al.*, 2003) and glass-frc (Majumdar and Laws, 1991, p. 102) with limited success. It was reported to have a beneficial effect on glass-frc at very high cement replacement levels (70%) but this does not seem to have spurred commercial interest, although some Japanese (Takeuchi *et al.*, 1999) formulations use blastfurnace slag cement in conjunction with other admixtures. The DuraPact matrix (Pachow, 2001), glass-frc made with which purports to have a guaranteed 50-year lifespan, is based on blastfurnace slag cement combined with microsilica (Purnell, 1998). Ggbs does not appear to be as effective in reducing chloride diffusion in steel-frc as csf or metakaolin (de Gutiérrez *et al.*, 2005) even at 70% cement replacement. Pfa has been used in polypropylene-frc (Hannant, 1998) and glass-frc (Majumdar and Laws, 1991, pp. 94–102, Cyr *et al.*, 2001). Polypropylene-frc with pfa was the material examined in the long term study by Hannant (1998) (see also Fig. 9.1). Such composites appear to retain most of their strength after 18 years of weathering but no comparison with an unmodified OPC matrix was performed. The addition of pfa to glass-frc appears to have some benefit with regard to durability (Majumdar and Laws, 1991, pp. 94–102). The durability improvements reported by Cyr *et al.* (2001) are from a hybrid system including both pfa and silica fume and thus cannot be attributed to pfa alone.

For both pfa and ggbs, it should be noted that slower setting and hardening, and thus lower matrix strengths at early ages, will result from their addition to the matrix.

Another approach pioneered in glass-frc is the use of polymer modification of the matrix. Majumdar and Laws (1991, pp. 112 *et seq.*) dedicate a whole chapter to the topic. A wide variety of polymers have been tried but attention has most recently focused on an acrylic polymer dispersion ('Forton'). Originally designed as a curing aid for thin concrete sections to prevent water loss by evaporation leading to shrinkage cracking, it is added to glass-frc to improve workability in the fresh state and improve mouldability. It is also widely believed to improve durability and the '5/5' formula, comprising OPC-glass-frc with the addition of 5% Forton polymer solids by volume and 5% AR-glass fibres by weight, is ubiquitous in the glass-frc literature, so much so that it is often referred to implicitly as a 'base' to which modifiers such as metakaolin are then added (e.g., Glinicki *et al.*, 1993). The mechanism by which it enhances durability is different to the pozzolans in that it does not reduce alkalinity of $Ca(OH)_2$ formation, but is thought to either coat the fibres with an inhibitive layer or modify hydration at the

interface by occupying space that might otherwise fill with $Ca(OH)_2$. There has been some debate as to whether polymer-modification of the matrix can actually lead to improved durability as accelerated ageing procedures often yield conflicting results (e.g., Zhu and Bartos, 1997, Qian *et al.*, 2003). The most recent research unequivocally demonstrates that hot-water ageing is unsuitable for polymer modified glass-frc (Purnell and Beddows, 2005) and also that the addition of polymer to both plain OPC and modified matrices confers very significant durability benefits (Ball, 2003); over 19 years of natural weathering, reduction in modulus of rupture (MOR) was negligible and compared to plain OPC matrix glass-frc the degradation of strain-to-failure was reduced by 75%. Polymer modification of the matrix is uncommon with other fibre types but a summary is given by Bentur and Mindess (1990, pp. 421 *et seq.*). Polymer modified concrete is occasionally used as a matrix for steel-frc but the polymer is generally included to help with workability, not durability, although some authors claim it may help in that regard (Corinaldesi and Moriconi, 2004).

Other, non-Portland (nP) common cementitious systems have also been investigated for use with frc. Again, this practice is better developed for glass-frc than for other systems. The use of nP systems for glass-frc is summarised by Majumdar and Laws (1991, pp. 112 *et seq.*). High-alumina cement (HAC) and super-sulphated cement are both less alkaline than OPC and thus candidates for glass-frc. Worries over the integrity of the HAC matrix at moderately elevated temperatures (the 'conversion' reaction), which led to the banning of HAC for structural use in the UK, have caused glass-frc producers to be cautious over its use despite its superior durability characteristics. Super-sulphated cement also showed improved resistance to ageing but is not a common choice for glass-frc as it is susceptible to weakening on carbonation, which is enhanced for the thin sections typical of frc.

The last ten years has seen an increase in interest in nP matrices based on calcium sulpho-aluminates. These cements, with $4CaO.3Al_2O_3.SO_4$ (ye'elemite or Klein's compound) as the major active ingredient, hydrate in the presence of a source of lime to form mainly ettringite, with little or no calcium hydroxide remaining in the hydrated phase assemblage and a lower pore solution alkalinity than OPC. Development of such cements has been led by China (Qi and Tianyou, 2003) and Japan (Takeuchi *et al.*, 1999) but analogues are available in the UK (Gartshore *et al.*, 1991) and the US (e.g., Molloy *et al.*, 1995). Little data exists on the long-term properties of glass-frc made with such cements but it shows extraordinary resistance to hot-water accelerated ageing (e.g., Jiangjin *et al.*, 2001); however, caution is required in interpreting such results (see Section 9.2.5 and Purnell and Beddows, 2005). Development of these matrices is continuing and they appear to offer the best option for completely durable glass-frc. The use of nP matrices with other fibres has received little coverage in the literature. Puertas *et al.* (2003) have investigated alkali-activated blast-furnace slags and pfas reinforced with polypropylene fibres, subjected to cyclic ageing.

Results were unclear and did not show any significant benefit compared with OPC. Frantzis and Baggot (2000) reported a 'durability' testing procedure for the bond between steel-fibres and magnesium phosphate or calcium aluminate cements but did not suggest that such matrices conferred any durability benefits cf. Portland cement.

Combination of approaches is common. Most obvious is the combination of polymer with a pozzolanic additive, since they act via different mechanisms and thus might be expected to have a synergistic effect. The recent comprehensive paper on long-term weathering of polymer modified glass-frc by Ball (2003) reports on samples combining polymer with metakaolin and csf tested at intervals up to 13 years. Neither the combined or solely polymer-modified samples degraded significantly over this period thus no firm conclusion can be reached. Many of the formulations mentioned above involve combination of, e.g. sulpho-aluminate and metakaolin (Calcrete) (Gartshore *et al.*, 1991), blast-furnace slag cement and sulpho-aluminates (Nashrin) (Takeuchi *et al.*, 1999) or blast-furnace slag cement and microsilica (Durapact) (Pachow, 2001). Since each of the components purports to improve the durability by effectively the same mechanism, any synergy is minimal and one component tends to dominate, but since it is unlikely that combinations would reduce durability cf. unmodified matrices, the detail is only of academic interest.

The cementitious matrix in frc is susceptible to reaction with the carbon dioxide in the atmosphere, a phenomenon known as carbonation. During this reaction, portlandite in the matrix is converted to $Ca(CO)_3$ and thus the buffering capacity of the pore solution is lost, alkalis are either converted to carbonates or absorbed in the C-S-H phase (which also carbonates, becoming decalcified) and the alkalinity of the matrix drops sharply. Its strength also increases. Thus in theory, a carbonated matrix is more compatible with most fibres (except steel). Natural carbonation can take years for frc components, but attempts have been made to apply accelerated carbonation to improve their durability. Accelerated ageing tests for natural fibre or cellulose-frc include a carbonation component since these materials tend to carbonate readily when exposed to weathering. There seems to be some confusion in the literature regarding the difference between carbonation as a treatment or an ageing process but the recent consensus seems to be that early curing of such composites in a CO_2-rich environment improves their durability (Tolêdo Filho *et al.*, 2003, MacVicar *et al.*, 1999). Purnell *et al.* (2001b, 2003) used super-critical CO_2 to effect carbonation of OPC matrix glass-frc components within hours. The treatment significantly increased the resistance of such composites to accelerated ageing, improved mechanical properties in general and improved their dimensional stability under wetting and drying (Seneviratne *et al.*, 2002). In steel-frc, carbonation is undesirable and thus not used as a treatment.

9.2.4 Microstructural aspects related to frc durability

The properties of all frc are controlled to some degree by the interface between the fibres and the matrix, and the microstructural characteristics of this region have a significant impact on durability. Many investigators have studied this region using scanning electron and optical microscopy and their findings are summarised in the major reference sources (Majumdar and Laws, 1991, pp. 143–163, Bentur and Mindess, 1990, pp. 317–319, 412–413). This section will focus on key points relating to mechanisms of ageing. It is convenient to discuss frc with monofilament reinforcement in the form of single fibres (i.e., steel-frc) separately from frc with multifilament reinforcement in the form of strands or tows (i.e., glass, carbon, polypropylene and natural-frc) since there are a number of microstructural issues that only affect the latter category.

Multifilament frc

Figures 9.6 and 9.7 show the unaged interfacial microstructure for typical OPC matrix frc materials with multi-filament reinforcement, glass and coir respectively. The interface between the reinforcement unit and matrix is porous and spaces within the unit (interfilamental spaces in glass, and cell lumen in coir-frc) remain largely free from hydration product. Figures 9.8 and 9.9 show the microstructure of the same frcs after ageing such that significant degradation of mechanical properties has taken place. In both materials, a significant proportion of the interfacial and interfilamental/lumen space has been filled with hydration product, identified as $Ca(OH)_2$ in the glass-frc and assumed to be the same in the coir-frc. This phenomenon is variously known as mineralisation, petrification and 'bundle filling'. It is generally assumed to be associated with an increase in bond between the fibres and the matrix. In cases where the unit

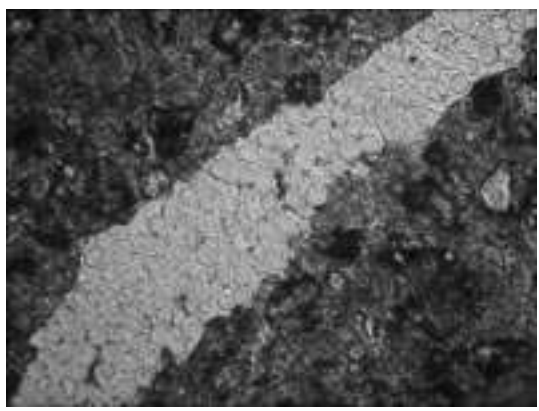

9.6 Unaged interfacial microstructure of PC matrix glass-frc, optical thin section, darkfield polarised light horizontal field of view (HFOV) 380 microns.

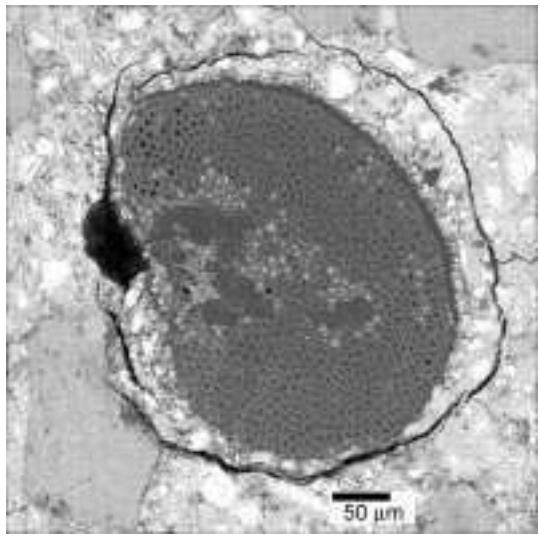

9.7 Unaged interfacial microstructure of PC matrix coir-frc, backscattered electron micrograph. Reprinted from (Tolêdo *et al.*, 2000) by permission of Elsevier.

reinforcing element is a strand, e.g. glass- and carbon-frc, an increase in fibre-fibre bond is assumed as well. This can change the mode at failure from fibre pull-out to fibre fracture (i.e., loss of region IV behaviour, Fig. 9.2) if the critical value of bond is surpassed; matrix densification effects will also begin to occur (see Section 9.2.1). The transition from pullout to fracture has been observed in various types of glass-frc by Bartos and Zhu (1996), who also first identified an intermediate 'telescopic' pull-out mode (see Fig. 9.11 on page

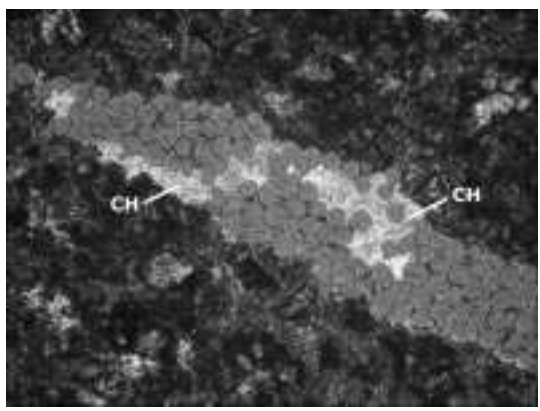

9.8 Aged interfacial microstructure of PC matrix glass-frc aged for 56 days in water at 65°C, optical thin section petrography, polars crossed at 77°, CH = calcium hydroxide crystals.

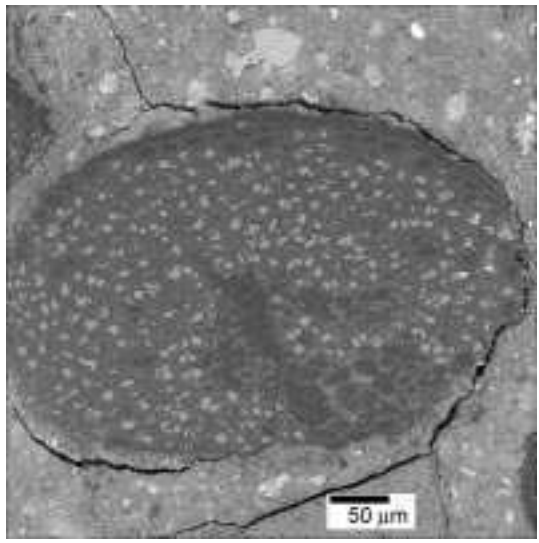

9.9 Aged interfacial microstructure of PC matrix coir-frc aged for 25 cycles of wetting and drying, backscattered electron micrograph. Reprinted from (Tolêdo *et al.,* 2000) by permission of Elsevier.

345), and natural/cellulose-frc (Mohr *et al.*, 2005, Bentur and Akers, 1989b). Enhanced fibre-fibre bond with ageing in glass-frc has been directly measured by Zhu and Bartos (1997) using novel micro-indentation apparatus. Purnell *et al.* (1999) showed that bond in glass-frc increased during the first few weeks of ageing and then stabilised about 2–3 times its initial value. Kim *et al.* (1993) suggest that the fracture toughness of the glass-frc interface increases by three orders of magnitude during curing.

Examination of fibre surfaces exposed in aged or weathered frc rarely shows any significant fibre corrosion, i.e. loss of section or gross pitting, regardless of the fibre type or the extent to which properties have been degraded (e.g., Purnell *et al.*, 2000, Tolêdo Filho *et al.*, 2000, Katz and Bentur, 1995, Ball, 2003). In the short term at least, in frc where the fibres are known to be immune to alkali attack, i.e. carbon-frc, loss of strength and toughness may still be observed with ageing (Katz and Bentur, 1995, Katz 1996). For some time most investigators, therefore, have attributed loss of properties in all frc to matrix densification, bond enhancement and bundle filling/mineralisation effects (e.g. Bentur, 1985, Cohen and Constantiner, 1985, Diamond, 1985). For many frc composites this is true, but fibre corrosion should not be thus discounted. First, bundle filling and/or bond increase is not always associated with degradation. In glass-frc composites made with sulpho-aluminate based matrices, the interfilamental space is completely filled with hydration products even in unaged samples with no detriment to strength (Fig. 9.10); in OPC/2nd generation AR glass-frc, degradation can occur without complete bundle filling being observed (see below) and

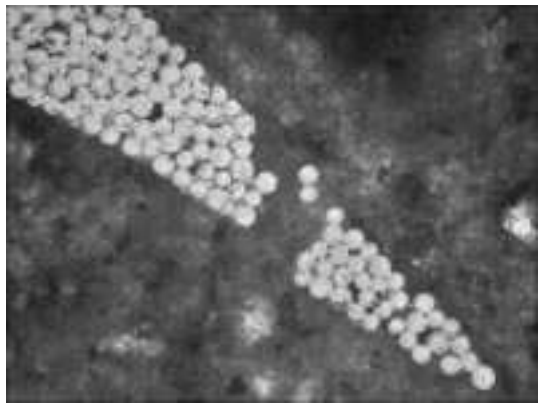

9.10 Microstructure of sulpho-aluminate modified glass-frc, unaged sample, thin section petrography polars crossed at 75°.

bond can reach a maximum without detriment to mechanical properties (Purnell *et al.*, 1999). Secondly, a transition in failure mode from pull-out to fracture does not necessarily require an increase in bond; a decrease in fibre strength will also trigger such a transition. In natural fibre composites, pull-out may be observed as the dominant failure mode even after mechanical properties have been significantly degraded (Mohr *et al.*, 2005) and the mode may change from pull-out to fracture without mineralisation of the fibre (Bentur and Akers, 1989a). Thirdly, for glass and carbon, a brief examination of the fracture mechanics of fibres suggests that their strength is governed by the size and population distribution of surface flaws. The surface manifestation of critical flaws is likely to be so small (~10 nm) as to be very difficult to detect on in-situ fibres using an SEM; nucleation and growth of such flaws could thus cause strength loss without readily detectable fibre surface damage (Purnell and Beddows, 2005). Recent work using Weibull analysis and atomic force microscopy on AR-glass fibres subjected to various ageing treatments has established that the maximum surface defect size (as opposed to manifestation) is ~50 nm and confirmed that flaw size and population density of surface flaws control the strength of the fibres (Gao *et al.*, 2003).

The microstructure of frc modified for enhanced durability is varied. The size applied to second generation AR-glass fibres reduces the precipitation of portlandite at the fibre-matrix interface and within the fibre bundle. The ubiquitous monolithic portlandite deposits completely surrounding fibres in first generation OPC matrix glass-frc after ageing (e.g,. Majumdar and Laws, 1991, p. 149) are not seen in modern glass-frc (e.g., Purnell *et al.*, 2000). Reports on frc modified with csf are variable. Katz and Bentur (1995) did not observe a significant difference between the interfacial microstructure of OPC and OPC-csf matrix carbon-frc using SEM but mercury intrusion porosimetry (MIP) indicated that the csf induced a significant reduction in porosity after accelerated

ageing. Bartos and Zhu (1996) reported that csf modification (10% cement replacement) to the matrix of glass-frc did not significantly change the development of interfacial and interfilamental microstrength with ageing (measured using a micro-indentation technique to 'push out' individual filaments). However, matrix modification by metakaolin (25%) was effective in preventing development of microstrength and this was correlated with reduced degradation compared with OPC matrix glass-frc (Zhu and Bartos, 1997). Purnell *et al.* (2000) used thin section petrography to observe a change in the nature of interfilamental deposits in metakaolin modified glass-frc; portlandite was not deposited between the filaments but an amorphous reaction product of metakaolin was. This was again correlated with reduced degradation during ageing. The microstructure of glass-frc made with sulpho-aluminate modified cements is quite different. In contrast to normal glass-frc, the matrix completely penetrates the fibre bundles and surrounds all the filaments even in the unaged condition, without detriment to mechanical properties, and the microstructure does not change with ageing; fibre pullout is still observed even after ageing (see Fig. 9.11). However, the matrix contains no portlandite. Thus it would appear that bundle filling is only detrimental if the precipitated material contains portlandite. SEM examination of the interface in polymer-modified glass-frc shows a film of polymer partially covering the fibre surface at young ages (Bentur and Mindess, 1990, p. 262) but this film is not apparent in micrographs of naturally weathered samples (Ball, 2003) and the microstrength of the interfacial and interfilamental bond is not affected by polymer modification of the matrix (Zhu and Bartos, 1997). Given the fragility of the film coating the fibres, it is likely that polymer modification confers durability by impeding water and thus potential precipitate migration within the matrix in general with some temporary and/or minor enhancement at the interface. The microstructure of frc modified

9.11 Microstructure of sulpho-aluminate modified glass-frc, SEM of aged (28 days at 65°C) fracture surface showing pseudo-ductile 'telescopic pullout'.

with pfa and ggbs has not received significant recent study and Majumdar and Laws (1991, p. 154–155) noted that under the SEM, the microstructure of glass-frc so modified was not markedly different from normal glass-frc.

Carbonation, either as a treatment or an ageing process, also induces microstructural changes. In natural fibre reinforced concretes, carbonation changes the interface from being open and porous to very dense and homogenous (MacVicar *et al.*, 1999) and also encourages the mineralisation of the porous fibre (Bentur and Akers, 1989b), correlating with increases in composite strength and decreases in toughness. Treatment of glass-frc with supercritical carbon dioxide also homogenised the matrix but did not promote interfilamental precipitation analogous to mineralisation, but in fact impeded subsequent precipitation during ageing. It did however fill void space at the interface with crypto-crystalline calcium carbonate and reduce the porosity of the matrix as measured using MIP (Purnell *et al.*, 2003).

Monofilament frc

The microstructure of monofilament frc – i.e., steel-frc – has not received the extensive attention afforded to multifilament frc, probably because it is relatively simple. The dominant feature of the steel-cement interface is a monolithic layer of calcium hydroxide around 10 μm thick surrounding the fibre, itself surrounded by an outer transition zone of relatively porous material 10–20 μm thick (Bentur *et al.*, 1985, Page, 1982). However, very few studies have explicitly related observations of changes at the fibre-concrete interface to time-dependent behaviour, mainly because it is assumed to correlate with rusting of the steel fibres. Bentur (Bentur and Mindess, 1990) showed that there was a correlation between a reduction in fibre diameter and loss of both strength and toughness. A 30% reduction in fibre diameter correlated to a ~10% reduction in frc strength and a 50% reduction in frc toughness. The same degree of reduction was achieved in frc made with corroded fibres and accelerated aged frc samples, suggesting that the effect was almost solely due to fibre corrosion. Where significant toughness was lost, a change in failure mode from pull-out to fracture was observed. Some studies suggest that the steel fibre-cement bond decreases with time (Fu and Chung, 1997, Kim *et al.*, 1993), in contrast to multifilament frc. In short, it seems that durability of steel-frc is controlled by simple fibre corrosion, which is only significant in extreme chloride-bearing environments and composites can be easily designed to account for this.

9.2.5 Models of the degradation process

There are many models of the mechanical behaviour of frc, within some (but certainly not all) of which one can find some explanation for time dependent behaviour. A full description of all such models would require its own chapter

and so this discussion is restricted to those models which explicitly address degradation. Models range from empirical descriptions of the strength loss process under natural and accelerated ageing, to complex analytical treatments based on consideration of micro-mechanical changes at the fibre-matrix interface. Some models have attempted to combine the two. The models tend to reflect the debate surrounding the degradation mechanisms described above in that each of the current models is based on an assumption concerning the main mechanism in action, i.e. that degradation is caused either by matrix/interface densification, or fibre strength loss.

The earliest model in which a durability issue can be recognised is the 'ACK' model describing the behaviour of brittle matrix composites (Aveston *et al.*, 1971). Examination of equation 9.2 shows that increases in matrix strength and/or decreases in fibre strength, both of which can be observed in some frc with time, may reduce the effective value of V_f to below the critical value and thus change the failure mode from multiple cracking to single fracture. This can be easily avoided by careful design of the composite. Assuming that there is sufficient fibre to avoid single fracture, then after the first matrix crack (i.e., regions II-IV, Fig. 9.2) it is a combination of fibre strength and 'bond strength' (i.e., matrix densification) that controls behaviour; most models can be classified as assuming that one or the other of these parameters is dominant.

Matrix densification models

The model of Katz and Bentur (1996) was developed for carbon-frc but has general application. It is based on the principle that 'physical densening of the matrix' is the cause of strength and toughness loss with time. Two concurrent processes were modelled; the increase in fibre-matrix bond with time, and the reduction in 'support length' l_s of an inclined fibre forced to bend while bridging a matrix crack. The latter of these processes was first proposed as contributing to the degradation of frc (specifically glass-frc) and modelled by Stucke and Majumdar (1976), who also provided many supporting electron micrographs showing the process in action. As the matrix hardens, the support zone (Fig. 9.12) becomes smaller, i.e. less of the matrix crumbles under the fibre. The radius of curvature R and the support length l_s decreases and the bending stress in the fibre σ_B, given by

$$\sigma_B = \frac{2E_f r \sin\theta/2}{l_s + 2r\sin\theta/2} \qquad 9.4$$

is increased. The Katz and Bentur model also takes into account additional factors such as the non-uniform fibre lengths caused by breakage during mixing. Bond and support length were assumed to vary with time at a similar rate to the compressive strength of the matrix. The bond processes alone were shown to cause a monotonic increase in strength efficiency of the fibres, while toughness

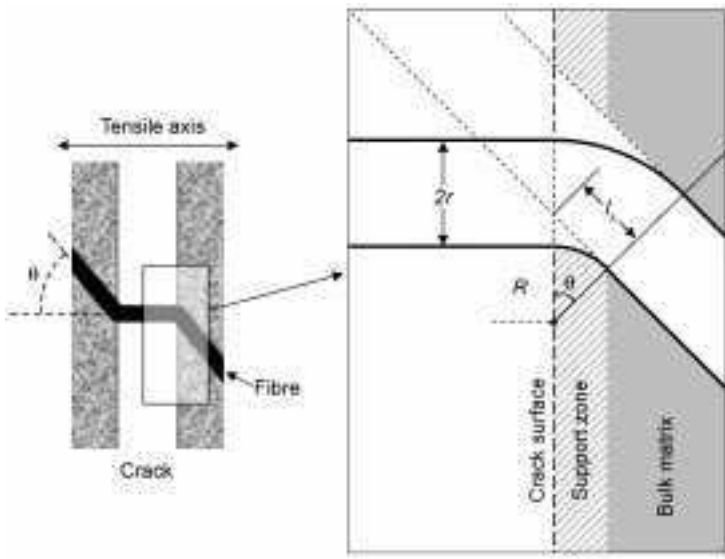

9.12 Model to describe the bending of an inclined fibre crossing a crack (adapted from Stucke and Majumdar, 1976).

efficiency peaked after ~10 days; both parameters then settled to a constant value within 40 days. The support reduction process alone caused the 'active fibre fraction' to continuously decrease with time although it is not clear whether this is asymptotic beyond 60 days. This led to short-term peaks in both strength and toughness efficiencies, which tailed off up to 90 days; again, whether this is asymptotic is not clear. Combining the two effects produced curves that closely matched the behaviour of real carbon-frc composites under accelerated ageing for up to 200 days at 60ºC (Fig. 9.13). The model was later extended (Katz, 1996) to account for the effect of variations in fibre modulus and showed that the matrix densification degradation mechanism increases in severity as fibre modulus or radius increases, and does not apply for 'ductile' fibres. This was confirmed by experiments on frc made with a range of carbon and polymer fibres.

The model of Kim *et al.* (1999), developed for cellulose-frc, also assumes that degradation is caused by increases in bond with time. Modelling is based around the concept of the fracture toughness of the material being equal to the sum of the stress intensity factor (sif) caused by loading and the negative sif caused by closing traction of fibres across a crack. This is an extension of the concept first presented by Naaman and Shah (1979). The model requires 14 separate input parameters including the interfacial chemical debond energy and the fibre snubbing coefficient, some of which are awkward to measure, and is solved numerically. It does predict broad trends in ageing of cellulose-frc but rests on a 'one crack failure' assumption which is invalid for most frc with

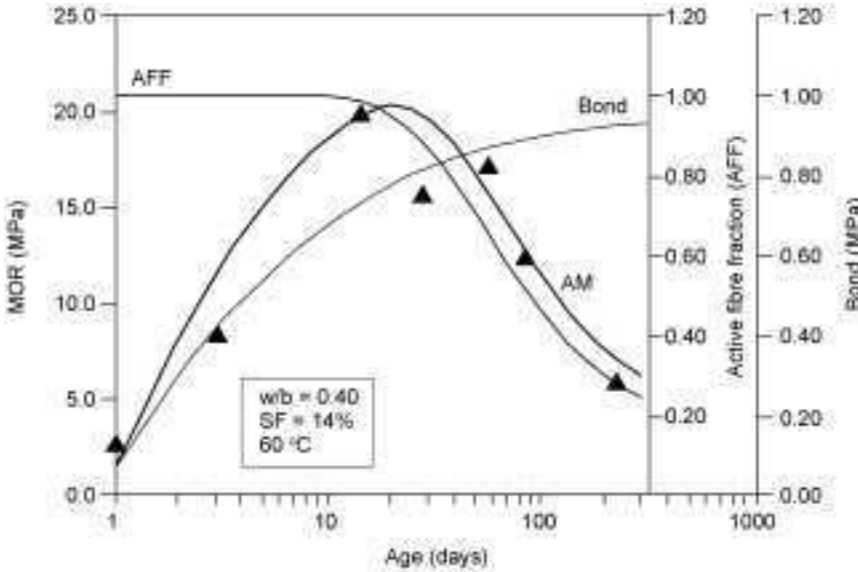

9.13 Combination of effects of bond and bending (AFF) to strength vs. time behaviour in carbon-FRC. Reprinted from (Katz and Bentur, 1996) by permission of Elsevier.

$V_f > V_{fc}$. Also derived from the Naaman and Shah concept is the model advanced by Mobasher and Li (1995), based on a fracture mechanics/finite element treatment of the change in pull-out behaviour with interfacial stiffness. The model is designed around steel-frc. They calculated increases in interfacial stiffness, and adhesional and frictional bond of roughly 4 and 2 respectively after 3 days of accelerated ageing.

Fibre strength loss models

Purnell and co-workers (Purnell *et al.*, 2001a; Purnell and Beddows, 2005) have taken a different approach in a model designed around glass-frc but with wider application. They modelled strength loss in fibres (and thus composites) as being caused by the slow, subcritical growth of surface flaws on the fibre. A stress corrosion process known as 'static fatigue' is assumed to drive this process, which in alkaline environments can be triggered by very small stresses (e.g., shrinkage or thermal mismatch stresses) and may be aggravated by the growth of portlandite crystals at the interface. By combining relations describing the fracture mechanics of fibres, the growth of flaws and 'rule of mixtures' theory, they derived a relatively simple relationship between normalised strength S (= strength ÷ original strength) and time t controlled by a single parameter k which is a function of temperature T in an Arrhenius relationship (equations 9.5 and 9.6).

$$S = \frac{1}{\sqrt{1 + kt}} \tag{9.5}$$

$$k = k_0 \exp\left(\frac{-\Delta G}{RT}\right) \tag{9.6}$$

This allows the hot-water accelerated ageing process to be rationalised and used to predict strength-time curves for various glass-frc formulations. The model was fitted to a very large data set of over 1100 samples which comprised new data, literature data and commercial data (Fig. 9.14). This essentially updated the work of Proctor and co-workers (Proctor *et al.*, 1982, Litherland *et al.*, 1981) and showed that the acceleration factors derived by them cannot be applied to modified matrix glass-frc as the activation energy ΔG of the strength loss process is different compared with OPC glass-frc (57–59 kJ/mol cf. 94 kJ/mol); this implies that a different degradation process is at work, which they conclude is connected to the lack of $Ca(OH)_2$ availability in modified matrices. In fact, using Proctor and co-workers factors to validate modified matrix glass-frc can overestimate durability by almost an order of magnitude at 60ºC (Table 9.1). The model can also be used to predict 'mean ductile life', i.e. the time between manufacture and the fibre strength being depleted to the point where all region II and III behaviour (Fig. 9.2) is lost. The ductile life is dependent on the ratio of the first crack strength to the initial strength, which in term depends on the fibre content and the service temperature, but for typical modern grc was predicted as ~60 years for OPC-glass-frc and ~80 years for metakaolin and/or sulpho-aluminate modified matrix glass-frc (Purnell and Beddows, 2005).

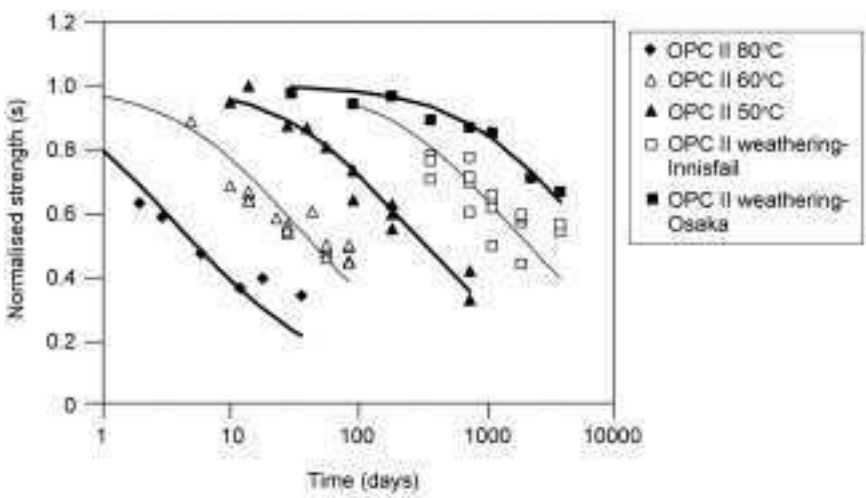

9.14 Example fit of Purnell model ($S = [1 + kt]^{-0.5}$) to OPC matrix glass-frc S vs. time data from various sources.

Table 9.1 Acceleration factors for glass-frc with respect to UK weather for various ageing temperature/matrix combinations (Purnell and Beddows, 2005), compared with those advanced by Proctor and co-workers (Proctor *et al.*, 1982, Litherland *et al.*, 1981). For example, 1 day ageing at 50°C for OPC-glass-frc is equivalent to 120 days of UK weathering according to Purnell *et al.*, or 101 days according to Proctor *et al.*

	Ageing temperature	
Matrix	50°C	60°C
OPC	120	340
Sulpho-aluminate	20	39
OPC + metakaolin	18	35
Proctor *et al.*	101	272

The model of Orlowsky and co-workers (Orlowsky *et al.*, 2005, Orlowsky and Raupach, 2005, Orlowsky, 2005) is partly based on the Purnell model in that FRC strength loss is assumed to be controlled by the growth of flaws, unavoidably introduced during roving manufacture and fibre processing, leading to fibre weakening. When AR-glass filaments were aged in simulated pore solutions at different temperatures and tensile strength monitored, strength loss was observed even in the absence of apparent driving forces for static fatigue (Fig. 9.15, square

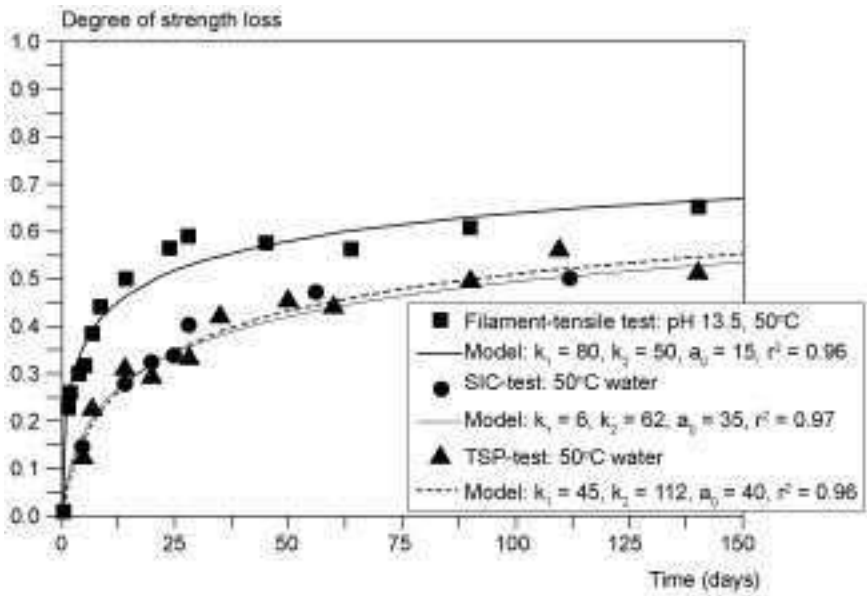

9.15 Comparison of TSP-, SIC- and Filament-tensile test results and application of the corrosion model (Orlowsky, 2005). Degree of strength loss = 1−(strength ÷ original strength). Figure reproduced by kind permission of Dr.-Ing. J. Orlowsky, ibac, University of Aachen, Germany.

dots). Thus it was concluded that degradation was caused by the growth of flaws driven by chemical attack alone and there was no driving stress. A 3-parameter model of time-dependent strength loss $\Delta f_{l,t}$(= 1 − (strength ÷ original strength), i.e. $1 - S$, see equation 9.5) was advanced. Parameters required are the initial flaw depth a_0, flaw extension X and the coefficients k_1 and k_2, which relate to the solution and diffusion controlled part of the corrosion reactions respectively:

$$\Delta f_{l,t} = 1 - \sqrt{\frac{a_0}{a_0 + X}} \tag{9.7}$$

$$\left(\frac{X}{k_1} + \frac{X^2}{2k_2}\right) - t = 0 \tag{9.8}$$

Note that equation 9.7 is an alternative form of equation 9.5 with $kt = X/a_0$: both are based on a fracture mechanics approach that relates surface flaw growth to fibre strength loss. Figure 9.15 shows the model fitted to data from SIC and composite (TSP) specimens aged in water, and filaments aged in alkaline solution respectively at 50ºC. The modelling suggested that the rate of attack slows with time, owing to diffusion of OH^- ions being slowed by the formation of a stable zirconium-rich inner layer and/or recondensation of silanol groups as an outer layer inhibiting further flaw growth (Orlowsky *et al.*, 2005). This is consistent with previous work investigating the surface composition of AR-glass aged in alkaline solutions (Chakraborty *et al.*, 1979). They also showed that there is a critical humidity (Orlowsky, 2005) – in environments which exceed this, strength loss is related to temperature – and developed a miniature-moisture-sensor to determine the moisture at the surface of the AR-glass inside concrete (Orlowsky *et al.*, 2005, Orlowsky, 2005). Combining measurements from this equipment and the modelling approach above allows arbitrarily complex weathering (i.e., involving wet and dry periods) to be fully modelled. This is a promising approach.

Which of the models is 'correct' is a common topic for debate. In fact, it is more appropriate to discuss which model is most useful for a given frc type. Fibre corrosion models are less appropriate if $V_f \approx V_{fcrit}$, i.e. the composite is designed primarily to exhibit region IV toughness (Fig. 9.2), since time-dependence of such behaviour is dominated by bond effects. Matrix densification or bond models are less appropriate if the fibre length is much longer than the critical length since little pullout will be evident regardless of age (although fibre bridging effects will still come into play). Ductile fibres are not prone to weakening via flaw growth, nor do they have problems with inclined bridging of cracks, and so neither model may be appropriate; consideration of ACK theory may be sufficient. It is almost certain that fibre weakening and matrix densification proceed in tandem and thus the target for future research is a model that incorporates both effects.

9.2.6 Volume stability and cracking

Many of the long-term performance problems of fibre-reinforced cement composites are not the result of changes in the composites' properties, but are induced by volume changes in the material caused by temperature and humidity changes. The shrinkage potential of fibre-reinforced cement thin sheets may exceed considerably the shrinkage of concrete. Typical shrinkage strains for the latter are usually less than 0.05%, whereas for the thin sheet composites swelling values in the range from 0.10% to almost 2% have been measured (Baum and Bentur, 1994). It should be noted that this is the situation in thin sheet frc but not in fibre-reinforced concrete where shrinkage is equal to or smaller than that of the unreinforced concrete. The higher swelling in the thin sheet composites is a result of a variety of influences, including higher cement content than in a typical concrete mix (i.e., less aggregates) as well as the presence of fibres that are moisture-sensitive, such as cellulose or natural fibres. In addition, the thin geometry of many of the thin sheet fibre-reinforced cements leads to higher drying rates.

Volume changes induced during natural exposure by wetting and drying may cause internal damage due to microcracking. This has been demonstrated for wood particle-reinforced cement (Becker and Laks, 1985) in which ageing in water did not lead to strength loss, whereas drying/wetting cycles resulted in loss in strength, with the magnitude of loss becoming greater for the more extreme drying cycles. Degradation was the result of internal damage due to volume changes. Damage of this kind might be expected to be greater for testing under restrained conditions where internal stresses of greater magnitude are expected to occur as the result of the restrained volume changes. Thus, reduction in properties and cracking might be observed even for composites where the volume changes are smaller than in wood particle-reinforced cement (Becker and Laks, 1985).

Dimensional changes can cause problems not connected with loss of material properties. In some applications of thin sheet frc such as cladding, dimensional changes may lead to bowing, micro- and macro-cracking of panels. The extent of the damage will depend on both the material degradation and the nature of the joints, fixings and underlying structure; this type of long-term performance problem can be more critical than the changes in the properties of the material with time (Fordyce and Wodehouse, 1983, Hansen *et al.*, 1990, Williamson, 1985). Unfortunately, this problem has not received adequate attention in the open literature, which usually highlights durability issues related to the properties of the material itself. The required approach is either to study the restrained shrinkage performance of the material itself (Becker and Laks, 1985), or to test full-scale panels, including their connections to the structure, as recommended in ISO 8336. Restrained shrinkage of frc has been studied more intensively in recent years to examine the extent to which the presence of a small content of

fibre reinforcement can reduce shrinkage and related cracking in concrete (Banthia *et al.*, 1993, Sarigapbuti *et al.*, 1993, Kovler *et al.*, 1993). These studies, although not directly intended for the evaluation of long-term performance of thin sheet fibre-reinforced cement, provide a basis for methodology and scientific background needed to address such issues. Standardisation of such tests is currently underway, using configurations similar to those reported by See *et al.* (2003).

9.2.7 Hybrid composites

Many researchers have attempted to use mixed fibres to produce a synergy of mechanical properties, processing properties and/or cost, often driven by the desire to move to automated production. Popular hybrids include glass/carbon, steel/polypropylene and glass/polypropylene. However, few have explicitly addressed any durability issues that might be raised by using hybrids. Xu *et al.* (1998) reported the results of 6-year weathering on polypropylene/glass-frc sheets but no significant degradation in mechanical properties was observed. Banthia and Nandakumar (2003) have discussed the durability potential of polypropylene/steel-frc but did not present any long-term results. It seems that there are no durability synergies that can be obtained from hybrid fibre reinforcement. The durability of hybrid-frc is therefore controlled by the time-dependent behaviour of the least durable fibre and durability analysis of such composites must focus on the extent to which any mechanical synergy can be retained as the least durable reinforcement degrades.

9.3 Future trends

Virtually all current commercial applications for frc – cladding, facades, etc., have one fundamental aspect in common; none of them involve the carrying of sustained live load. Design specifications are generally conservative in that they ensure that service stresses remain below the first crack stress, i.e. within region I on Fig. 9.2. The fibres are, to all intents and purposes, acting as a 'safety net' – to provide some reserve toughness in the case of accidental overload. In order to extract full financial and technical efficiency from the (generally expensive) fibres, it will be necessary to design frc components where the fibres are carrying significant stresses in services, i.e. live loads. This brings durability concerns. First is that such components will be operating in a cracked condition, which would increase the permeability of the matrix with respect to ingress of external deleterious agents such as de-icing salts. However, providing the crack widths are small then this can be tolerated, as it is for normal RC. Secondly, if strength losses in frc – particularly glass-frc – are caused by static fatigue, then one might expect stressed fibres to degrade faster than unstressed ones. Continuing work at Aachen University (Orlowsky *et al.*, 2003) suggests that

components of glass-frc loaded to 80% of their failure stress whilst ageing do not necessarily degrade any faster than unstressed ones (although the results were somewhat scattered, as noted by the authors of the paper). This concurs with fundamental work on glass corrosion which suggests that the stress corrosion effect in alkaline environments is activated by very small stresses (e.g., those induced at the microstructural level by shrinkage, mismatch in thermal coefficient of expansion, crystal growth) (Sglavo and Green, 1999; Gehrke *et al.* as cited in Gy, 2003) and thus a relationship with 'bulk' stress might not be expected. Thus for glass-frc, and that with fibre types that do not appear to suffer fibre corrosion and are capable of primary reinforcement (carbon, polypropylene), there should be no durability-based reason why frc components may not support live structural loads. It is deficiencies in the modelling of the mechanical behaviour of regions II and III (Fig. 9.2) that should be of more concern.

Realisation of structural frc will also require more efficient placing of fibres, moving from 2-D or 3-D random arrangements to those where fibres are carefully placed to correspond with the locations and directions of the principal stresses. Thus a move from casting of premix, spraying or hand lay-up towards automated production will be necessary, and the key to this is the use of engineered textiles, rather than chopped fibres, as reinforcement. Modern textiles have an almost infinite variety of weaves, including 3-D layouts and can incorporate several types of fibre to maximise performance of the textile form. Use of such textiles requires matrices that have rheological characteristics that allow the textile form to be fully infiltrated with no voids, and so textile reinforced concrete (trc) research is concerned both with matrix and fibre development. There is a great deal of research currently underway on this topic; by the time this book is published, the RILEM state-of-the-art report on Textile Reinforced Concrete (trc) should be available (see page 323). As yet, no durability concerns specific to trc have been identified.

Use of modified or nP matrices is likely to increase as the undoubted durability benefits conferred thereby become more commonly known. Transfer of this matrix technology from glass-frc to other types also needs to occur, particularly the use of polymer modified matrices. Synergies can be expected by using polymer modification in combination with pozzolanic type additives or nP matrices since each technique confers enhanced durability by a different mechanism.

From an academic point of view, it is necessary that the two competing durability models – those that model fibre strength loss and those that consider matrix densification/bond enhancement – are in some way unified. It must be true that both mechanisms contribute to the degradation of frc, thus models should reflect this. This will probably require that toughness, rather than strength, be used as a universal metric of material integrity, since this can be meaningfully tracked in all frc regardless of fibre content relative to V_{fcrit}. This

in turn will require all investigators to accept one testing regime, which allows reproducible post-peak behaviour (region IV, Fig. 9.2) to be developed and can be performed on standard equipment.

9.4 Conclusions

The processes which cause time-dependent changes in the mechanical properties of frc have been extensively studied for many years. As a result, in comparison to other fibre composites, frc is extremely well characterised with respect to its durability.

It is clear that two main mechanisms are involved, related to fibre corrosion and matrix densification. Fibre corrosion weakens the reinforcement and causes loss of strength in primary frc. It may also trigger a change of failure mode from pseudo-ductile to brittle. Matrix densification is caused by continued hydration and evolution of the matrix, in particular the precipitation of calcium hydroxide at the fibre-matrix interface or, in multifilament frc, within fibre bundles. This may increase bond, decrease matrix compliance and reduce fibre flexibility, all of which can also trigger a change of failure mode. The relative importance of each mechanism depends on the type of reinforcing fibre used and the intended nature of the reinforcing action, which is in turn related to the fibre content relative to the critical value. For primary frc where the volume of fibres is well above the critical value, fibre corrosion effects are normally dominant. For secondary frc where the volume of fibres is lower, densification is normally of greater concern. In steel-frc, which has a monofilament rather than multi-filament nature, fibre corrosion caused or triggered by external agents has the greatest effect on durability, as with RC. The two mechanisms of strength loss are interlinked to some degree; for example, there is evidence that precipitation of calcium hydroxide not only fills bundles but also actively weakens fibres. In many frc components, the signatures of both processes can be observed.

There are two main model types to describe the time-dependent behaviour of frc; those based on fibre corrosion and those based on matrix densification. The choice of the most appropriate model also depends on which mechanism is deemed to be prevalent for the particular frc in question. None of the models enjoy universal acceptance but can be useful; they are particularly well developed for glass-frc. Future research must attempt to derive a model that combines the mechanisms and thus gains wider acceptance. For this to happen, a universal degradation metric based on some measurement of toughness needs to be derived.

Significant improvements in the durability of frc have been realised by developments in the chemistry of matrices, fibres and fibre coatings. Use of pozzolanic materials can potentially reduce the formation of calcium hydroxide during primary hydration and its subsequent migration and re-precipitation around the fibres. They may also provide useful reductions in the alkalinity of the matrix, thus impeding both major degradation mechanisms. Polymer modifi-

cation of the matrix may also confer durability, especially in glass-frc, and combinations of modified matrices and polymers hold the potential for extremely durable frc. In any case, ductile lifetimes in excess of 50 years can now be confidently expected from many modern frc formulations. Attention should be now be paid to the durability of components and systems, rather than that of the material itself, in order that these improvements can be fully exploited and load-bearing frc components produced.

9.5 Sources of further information and advice

The primary reference textbooks were mentioned early in the text (Bentur and Mindess 1990, Majumdar and Laws 1991, Johnston 2001) and are the best source of information about frc in general. In 2006 RILEM (www.rilem.org) published the state-of-the-art report of Technical Committee TRC-201 'Textile Reinforced Concrete' which includes sections on new fibre forms, production methods, modelling and applications. The Glass Fibre Reinforced Concrete Association International (GRCA, www.grca.org.uk) produces a number of publications, aimed mainly at architects and producers, including examples of glass-frc use and a specification for production of glass-frc. Most pre-mixed concrete suppliers have data sheets and guides on the use of fibre-reinforced concrete (e.g., Readymix, www.readymix.co.uk/pages/fibreReinforcedConcrete.asp). The UK Concrete Society (www.concrete.org.uk) publishes 'Steel fibre reinforced concrete industrial ground floors' (Concrete Society, UK, 1999, 24 pp) which covers mix design, construction and testing of steel fibre-reinforced concrete. The journal *Cement and Concrete Composites* (ISSN 0958-9465, www.sciencedirect.com/science/journal/09589465) has frequent articles on frc. The American Concrete Institute (www.aci-int.org/general/home.asp) has many publications on frc which can be browsed and purchased from its website; the ACI also offers an e-learning course in frc, suited to professional development requirements.

There are many research groups working on frc durability around the world, and a small selection of them are given below:

- Advanced Civil Engineering Materials Research Laborartory (ACE-MRL), University of Michigan: ace-mrl.engine.umich.edu
- National Building Research Institute, Israel Institute of Technology (Technion): www.technion.ac.il/~nbri/
- Civil Engineering Materials Group, University of British Columbia: www.civil.ubc.ca/home/mat
- Institute of Building Materials (ibac), Aachen University: www.ibac.rwth-aachen.de
  - collaboration with Textile Institute and others on Textile Reinforced Concrete: sfb532.rwth-aachen.de
  - collaboration with Dresden University: sfb528.tu-dresden.de

- Centre for Advanced Cement Based Materials, Northwestern University: acbm.northwestern.edu

At the time of writing, Google (www.google.com) searches for both spellings of frc will return a combined 33 000 documents.

9.6 Acknowledgements

The author is extremely grateful to Prof. Arnon Bentur of Technion (Israel) for his substantial contribution to the section 'Volume stability and cracking' and to Dr J. Hill for her helpful comments on the manuscript.

9.7 References

Akers S.A.S., Studinka J.B. (1989), Ageing behaviour of cellulose fibre cement composites in natural weathering and accelerated test, *Int J Cem Compos Lightweight Concr*, 11, 93–97.

Akers S.A.S, Studinka J.B., Meier P., Dobb M.G., Johnson D.J, Hikasa J. (1989), Long-term durability of PVA reinforcing fibres in a cement matrix, *Int J Cem Compos Lightweight Concr* 11, 79–91.

Aveston J., Cooper G.A., Kelly A. (1971), Single and multiple fracture, in *The Properties of Fibre Composites: Proceedings of the NPL Conference* Nov. 1971. UK, IPC Science & Technology Press, 15–26.

Ball H. (2003), Durability of naturally aged gfrc mixes containing forton polymer and SEM analysis of the fracture interface, in *Proceedings of the 13th Congress of the Glass Fibre Reinforced Concrete Association, October 2003, Barcelona, Spain* eds. J.N. Clarke, R. Ferry. UK, Concrete Society, paper 17, 30pp.

Banthia N., Nandakumar N. (2003), Crack growth resistance of hybrid fiber reinforced cement composites, *Cem Concr Compos* 25, 3–9.

Banthia N., Azzabi M., Piegon M. (1993), Restrained shrinkage cracking in fiber reinforced cementitious composites, *Mater Struct* 26, 405–413.

Bartos P.J.M., Zhu W. (1996), Effect of microsilica and acrylic polymer treatment on the ageing of grc, *Cem Concr Compos*, 18, 31–39.

Baum H., Bentur A. (1994), *Fiber Reinforced Cementitious Materials for Lightweight Construction: Development of Criteria and Evaluation of Their Long Term Performance*, research report. National Building Research Institute, Technion, Israel Institute of Technology, Haifa, Israel, 1994.

Becker R., Laks J. (1985), Cracking resistance of asbestos cement panels subjected to drying, *Durability of Building Materials* 3, 35–49.

Beddows J., Purnell P. (2003), Durability of new matrix glassfibre reinforced concrete, in *Proceedings of the 13th Congress of the International Glassfibre Reinforced Concrete Association, Barcelona, Spain October 2003*. Eds N. Clarke, R. Ferry. UK, Concrete Society, 2003 paper 16.

Bentur A. (1985), Mechanisms of potential embrittlement and strength loss of glass fiber reinforced cement composites, in *Proc. PCI Symp. Durability of Glass fibre Reinforced Concrete, Illinois, USA* edited by S. Diamond, USA, PCI, 108–123.

Bentur A., Akers S.A.S. (1989a), The microstructure and ageing of cellulose fibre reinforced autoclaved cement composites, *Int J Cem Compos Lightweight Concr*,

11, 111–115.
Bentur A., Akers S.A.S. (1989b), The microstructure and ageing of cellulose fibre reinforced cement composites cured in a normal environment, *Int J Cem Compos Lightweight Concr* 11, 99–109.
Bentur A., Mindess S. (1990), *Fibre Reinforced Cementitious Composites*, UK, Barking, Elsevier Science Publishers Ltd.
Bentur A., Diamond S., Mindess S. (1985), The microstructure of the steel fibre-cement interface, *J Mater Sci*, 20, 3610–3620.
Bergström S.G., Gram H-E. (1984), Durability of alkali-sensitive fibres in concrete, *Int J Cem Compos Lightweight Concr*, 6, 75–80.
Brockmann J., Raupach M. (2002), Durability investigations on textile reinforced concrete, in *9th International Conference on Durability of Building Materials and Component*, Brisbane Australia March 2002. Australia, CSIRO.
Cantin R., Pigeon M. (1996), Deicer salt scaling resistance of steel-fiber-reinforced concrete, *Cem Concr Res*, 26 (11), 1639–1648.
Chakraborty M., Das D., Basu S., Paul A. (1979), Corrosion behaviour of a ZrO_2-containing glass in aqueous acid and alkaline media and in a hydrating cement paste. *Int J Cem Compos*, 1 (3), 103–109.
Chen P-W., Chung D.D.L. (1996), Low-drying-shrinkage concrete containing carbon fibres, *Composites: Part B*, 27B, 268–274.
Cheng J., Liang W., Hu Y., Chen Q., Frischat G.H. (2003), Development of a new alkali resistant coating, *J Sol-Gel Sci Tech*, 27, 309–313.
Chung D.D.L. (2000), Cement reinforced with short carbon fibers: a multifunctional material, *Composites Part B: Engineering*, 31, 511–526.
Cian D., Della Bella B. (2001), Structural applications of grc for precast floors, in *Proceedings of the 12th International Glassfibre Reinforced Concrete Congress*, May 2001, Dublin, Eire, eds. N. Clarke and R. Ferry. UK, Concrete Society, 41–52.
Cohen M.D., Constantiner D. (1985), Morphological developments of high and low alkali cement paste at the glass fiber-cement interface, in *Proceedings of the PCI Symposium of Glassfiber Reinforced Concrete*, Illinois, USA, ed. S. Diamond, PCI, Illinois, USA, 158–173.
Cole B.J.B. (1990), *Properties of CemFIL 2 composites after 10 years weathering – 6th series April 1990*. CemFIL Technology, Research Support Technology Group, Lathom, UK.
Corinaldesi V., Moriconi G. (2004), Durable fiber reinforced self-compacting concrete, *Cem Concr Res*, 34 (2), 249–254.
Curbach M. (ed.) (2003), *Textile Reinforced Structures: Proceedings of the 2nd Collloquium on Textile Reinforced Structures*, Dresden, Germany 9-10/2003. Germany, Technische Universität Dresden.
Cyr M.F., Peled A., Shah S.P. (2001), Improving performance of glass-fiber-reinforced extruded composites, in *Proceedings of the 12th International Glassfibre Reinforced Concrete Congress, May 2001, Dublin, Eire*, eds. N. Clarke and R. Ferry. UK, Concrete Society, 163–172.
de Gutiérrez R.M., Díaz L.N., Delvasto S. (2005), Effect of pozzolans on the performance of fiber-reinforced mortars, *Cem Concr Compos* 27, 593–598.
Diamond S. (1985), The GFRC durability problem: Nature, characteristics, and test methods, in *Proc. PCI Symp. Durability of Glass fibre Reinforced Concrete, Illinois, USA* ed. S. Diamond, USA, PCI, 199–209.
Fisher A.K., Bullen F., Beal D. (2001), The durability of cellulose fibre reinforced concrete pipes in sewage applications, *Cem Concr Res* 31, 543–553.

Fordyce M.W., Wodehouse R.G. (1983), *GRC and Building.* UK, Seven Oaks, Butterworths.

Frantzis P., Baggot R. (2000), Bond between reinforcing steel fibres and magnesium phosphate/calcium aluminate binders. *Cem Concr Compos* 22, 187–192.

Fu X.L., Chung D.D.L. (1997), Bond strength and contact electrical resistivity between cement and stainless steel fiber: Their correlation and dependence on fiber surface treatment, *ACI Mater J* 94 (3), 203–208.

Gao S.L., Mäder E., Abdaker A., Offerman P. (2003), Environmental resistance and mechanical performance of alkali-resistant fibers with surface sizings, *J Non-Crystalline Sol* 325, 230–241.

Gartshore G.C., Kempster E., Tallentire A.G. (1991), A new high durability cement for GRC products, in *Proceedings of the 8th Biennial Congress of the Glass-fibre Reinforced Cement Association*, Maastrict, Netherlands 1991. UK, GRCA, 3–12.

Gilbert G.T., Ridd P.J. (2001), Continuing premix spray developments in the USA, in *Proceedings of the 12th International Glassfibre Reinforced Concrete Congress, May 2001, Dublin, Eire*, eds. N. Clarke and R. Ferry. UK, Concrete Society 189–196.

Glinicki M.A., Vautrin A., Soukatchoff P., Francois-Brazier J. (1993), Impact performance of glass fibre reinforced cement plates subjected to accelerated ageing, in *Proceedings of the 9th International Congress of the Glassfibre Reinforced Cement Association*, Copenhagen, Denmark. UK, GRCA pp. 1/1/I–1/1/X.

Granju J-L., Balouch S.U. (2005), Corrosion of steel fibre reinforced concrete from the cracks, *Cem Concr Res* 35, 572–577.

Gy R. (2003), Stress corrosion of silicate glass: A review. *J Non-Cryst Solids*, 316, 1–11.

Hannant D.J. (1998), Durability of polypropylene cement composites: 18 years of data, *Cem Concr Res* 28, 1809–1817.

Hansen N.W., Roller J.J., Daniels, J.I., Weinman T.L. (1990), Manufacture and installation of gfrc facades, in *Thin Section Fiber Reinforced Concrete and Ferrocement, ACI SP-124* ed. J.I. Daniels and S.P. Shah. American Concrete Institute, Detroit, MI, pp. 182–213.

Health and Safety Commission UK (1979), *Report of the Advisory Committee on Asbestos.* London, HMSO.

Hempel R., Schorn H., Schiekel M., Butler M. (2003), Durability of textile reinforced concrete, *in Proceedings of the 13th Congress of the Glass Fibre Reinforced Concrete Association*, October 2003, Barcelona, Spain eds. J.N. Clarke and R. Ferry. UK, Concrete Society, paper 24.

Hoff G. (1987), Durability of fiber reinforced concrete in a severe marine environment. In: Scanlon, J. (Ed.), *Concrete Durability*. USA, ACI SP 100, pp. 997–1041.

Jiangjin D., Mingfang C., Dongyou Q., Yunbei L., Shujiang Y. (2001), Low-alkalinity sulfoaluminate cement and its application in grc products in China, in *Proceedings of the 12th International Glassfibre Reinforced Concrete Congress, May, Dublin, Eire*, eds. N. Clarke and R. Ferry. UK, Concrete Society, 345–354.

Johnston C.D. (2001), *Fiber-reinforced Cements and Concretes* (Advances in Concrete Technology Volume 3). Netherlands, Overseas Publishers Association/Gordon and Breach Science Publishers.

Karasu B., Cable M. (2000), The chemical durability of SrO–MgO–ZrO_2–SiO_2 glasses in strongly alkaline environments, *J Eur Ceram Soc* 20, 2499–2508.

Katz A. (1996), Effect of fiber modulus of elasticity on the long term properties of micro-fiber reinforced cementitious composites, *Cem Concr Compos* 18, 389–399.

Katz A., Bentur A. (1995), Effect of matrix composition on the aging of CFRC, *Cem Concr Compos* 17, 87–97.

Katz A., Bentur A. (1996), Mechanisms and processes leading to changes in time in the properties of CFRC, *Adv Cem Based Mater* 3, 1–13.

Kim J.K., Zhou L.M., Mai Y.W. (1993), Interfacial debonding and fibre pull-out stresses. Part III: Interfacial properties of cement matrix composites. *J Mater Sci* 28 (14), 3923–3930.

Kim P.J., Wu H.C., Lin Z., Li V.C., deLhoneuk, B., Akers S.A.S. (1999), Micromechanics-based study of cellulose cement in flexure, *Cem Concr Res* 29, 201–208.

Kosa K., Naaman A.E. (1990), Corrosion of steel fiber-reinforced concrete, *ACI Mater J* 87 (1) 27–37.

Kovler K., Sikuler J., Bentur A. (1993), Restrained shrinkage tests of fibre reinforced concrete ring specimens: effect of core thermal expansion, *Mater Struc* 26, 231–237.

Litherland K.L., Oakley D.R., Proctor B.A. (1981), The use of accelerated ageing procedures to predict the long-term strength of grc composites, *Cem Concr Res* 11, 455–466.

Ma Y., Zhu B., Tan M. (2005), Properties of ceramic fiber reinforced cement composites, *Cem Concr Res* 35, 296–300.

MacVicar R., Matuana L.M., Balatinecz J.J. (1999), Aging mechanisms in cellulose fiber reinforced cement composites, *Cem Concr Compos* 21, 189–196.

Majumdar A.J. (1992), Fibre reinforced cement – thin sheets, in *Proceedings of the 9th International Congress on the Chemistry of Cement*, New Delhi, India, ed. National Council for Cement & Building Materials. New Delhi, NCB, 737–774.

Majumdar A.J., Laws V. (1991), *Glass Fibre Reinforced Cement*. BSP Professional Books, Oxford.

Mangat P.S., Gurusamy K. (1988), Corrosion resistance of steel fibres in concrete under marine exposure, *Cem Concr Res* 18, 44–54.

Marikunte S., Aldea C., Shah S.P. (1997), Durability of glass fiber reinforced composites: effect of silica fume and metakaolin, *Adv Cem Based Mater* 5, 100–108.

Mobasher B., Li C.Y. (1995), Modeling of stiffness degradation of the interfacial zone during debonding, *Compos Engng* 5, 1349–1365.

Mohr B.J., Nanko H.,. Kurtis K.E (2005), Durability of kraft pulp fiber-cement composites to wet/dry cycling, *Cem Concr Compos* 27, 435–448.

Molloy H., Harmon T., Jones J., Sone H. (1995), Thin concrete panels produced with AR glass chopped strand and scrim, in *Proceedings of the Glassfibre Reinforced Cement Association 10th Biennial Congress*, October 1995, Strasbourg, France. UK, GRCA, paper 1/7 pp. I–X.

Mu R., Miao C., Luo X., Sun W. (2002), Interaction between loading, freeze-thaw cycles, and chloride salt attack of concrete with and without steel fiber reinforcement, *Cem Concr Res* 32, 1061–1066.

Naaman A.E., Shah S.P. (1979), Fracture and multiple cracking of cementitious composites, in *Proceedings of the Twelfth ASTM National Symposium on Fracture Mechanics*, ed. S.W. Frieman. USA, Pa., ASTM Special Technical Publication 678, 183–201.

Ohama Y. (1989), Carbon-cement composites, *Carbon* 27, 729–737.

Orlowsky J., Antons U., Raupach M. (2003), Behaviour of glass-filament-yarns in concrete as a function of time and environmental conditions, In: *Proceedings of the 7th International Symposium on Brittle Matrix Composites*, Warsaw, 13–15

October 2003, (Brandt, A.M.; Li, V.C.; Marshall, I.H. (Eds)). Cambridge, Woodhead Publishing Limited, pp. 233–241.

Orlowsky, J. (2005), *Zur Dauerhaftigkeit von AR-Glasbewehrung in Textilbeton*. (in German) Ausschusses für Stahlbeton, PhD Thesis, Berlin: Beuth.

Orlowsky J., Raupach M. (2003), Long-term behaviour of textile reinforced concrete, in *Proceedings of the 13th Congress of the International Glassfibre Reinforced Concrete Association*, Barcelona, Spain October 2003. Eds N. Clarke, R. Ferry. UK, Concrete Society, 2003 paper 15.

Orlowsky, J., Raupach, M. (2005), Modeling the Loss of Component Strength of Textile Reinforced Concrete. Lisse: A.A. Balkema. In: *Composites in Constructions, Proceedings of the International Conference, CCC2005*, Lyon, France, 11–13 July 2005.

Orlowsky, J., Raupach, M., Cuypers, H., Wastiels, J. (2005), Durability modelling of glass fibre reinforcement in cementitious environment, *Mater Struc* 38 (276), 155–162.

Pachow U. (2001), New manufacturing technologies for grc, in *Proceedings of the 12th International Glassfibre Reinforced Concrete Congress, May 2001, Dublin, Eire*, eds. N. Clarke and R. Ferry. UK, Concrete Society, 197–202.

Page C.L. (1982), Microstructural features of interfaces in fibre cement composites, *Composites* (April), 140–144.

Peled, A., and Mobasher, B. (2005), Pultruded Fabric-Cement Composites, *ACI Materials J*., 102 (1), 15–23.

Proctor B.A., Yale B. (1980), Glass fibres for cement reinforcement, *Phil Trans Roy Soc* A294, 427–436.

Proctor B.A., Oakley D.R., Litherland K.L. (1982), Developments in the assessment and performance of grc over 10 years, *Composites* 13, 173.

Puertas F., Amat T., Fernández-Jimenez A., Vásquez T. (2003), Mechanical and durable behaviour of alkaline cement mortars reinforced with polypropylene fibres, *Cem Concr Res* 33, 2031–2036.

Purnell P. (1998), *The Durability of Glass Fibre Reinforced Cement made with New Cementitious Matrices*, PhD Thesis, Aston University, UK.

Purnell P., Beddows J. (2005), Durability and simulated ageing of new matrix glass fibre reinforced concrete, *Cem Concr Compos* 27, 875–884.

Purnell P., Short N.R., Page C.L., Majumdar A.J., Walton P.L. (1999), Accelerated ageing characteristics of glass-fibre reinforced cement made with new cementitious matrices, *Composites: Part A* 30, 1073–1080.

Purnell P., Short N.R., Page C.L., Majumdar A.J. (2000), Microstructural observations in new matrix glass fibre reinforced cement, *Cem Concr Res* 30, 1747–1753.

Purnell P., Short N.R., Page C.L. (2001a), A static fatigue model for the durability of glass-fibre reinforced cement, *J Mater Sci* 36, 5385–5390.

Purnell P., Short N.R., Page C.L. (2001b), Supercritical carbonation of glass-fibre reinforced cement Part I: Mechanical testing and chemical analysis, *Composites A* 32, 1777–1787.

Purnell P., Seneviratne A.M.G., Short N.R., Page C.L. (2003), Supercritical carbonation of glass-fibre reinforced cement Part II: Microstructural observations, *Composites A* 34, 1105–1112.

Qi C., Tianyou B. (2003), A review of the development of the grc industry in China, in *Proceedings of the 13th Congress of the Glass Fibre Reinforced Concrete Association*, October 2003, Barcelona, Spain eds. J.N. Clarke & R. Ferry. UK, Concrete Society, paper 37.

Qian X., Shen B., Mu B., Li Z. (2003), Enhancement of aging resistance of glass fiber reinforced cement, *Mater Struc* 36, 323–329.

RILEM (2006), 'Textile reinforced concrete', RILEM Technical Committee TRC-201, ISBN 2-912143-99-3.

Sarigapbuti M., Shah S.P., Vinson K.D. (1993), Shrinkage cracking and durability characteristics of cellulose fiber reinforced concrete, *ACI Mater J* 90, 309–318.

See T.H., Attiogbe E.K., Miltenberger M.A. (2003), Shrinkage cracking of concrete using ring specimens, *ACI Mater J* 100, 239–245.

Seneviratne A.M.G., Short N.R., Purnell P., Page C.L. (2002), Dimensional stability of super-critically carbonated glass-fibre reinforced concrete, *Cement & Concrete Research* 32, 1639–1644.

Sglavo V.M., Green D.J. (1999), Indentation determination of fatigue limits in silicate glasses. *Phys Chem Glasses* 82, 1269–1274.

Soukatchoff P., Ridd P.J. (1991), High durability glass fibre reinforced modified cementitious matrix, in *Proceedings of the 8th Biennial Congress of the Glass-fibre Reinforced Cement Association*, Maastrict, Netherlands 1991 UK, GRCA, 37–44.

Stucke M.S., Majumdar A.J. (1976), Microstructure of glass fibre-reinforced cement composites, *J Mater Sci* 11, 1019–1030.

Takeuchi Y., Hayashi, M. Tamaki T., Tanaka H. (1999), Glass fibre reinforced concrete using super low contractile admixture, in *Proceedings of the 2nd Asia-Pacific Special Conference on Fiber-Reinforced Concrete, Singapore, August 1999* eds. T.S. Lok, K. Tseng.

Taylor H.F.W. (1997), *Cement Chemistry* 2nd edn. London, Thomas Telford.

Tolêdo Filho R.D., Scrivener K., England G.L., Ghavami K. (2000), Durability of alkali-sensitive sisal and coconut fibres in cement mortar composites, *Cem Concr Compos* 22, 127–143.

Tolêdo Filho R.D., Ghavami K., England G.L., Scrivener K. (2003), Development of vegetable fibre-mortar composites of improved durability, *Cem Concr Compos* 25, 185–196.

Vilkner G. (2003), *Glass Concrete Thin Sheets Reinforced with Prestressed Aramid Fabrics*, Ph.D. Dissertation, Columbia University, New York.

Walton P.L, Majumdar A.J. (1978), Properties of cement composites reinforced with Kevlar fibres, *J Mater Sci* 13, 1075–1083.

Williamson G.R. (1985), Evaluation of glass fiber reinforced concrete panels for use in military construction, in *Proc. PCI Symp. Durability of Glass fibre Reinforced Concrete, Illinois, USA 1985* ed. S. Diamond, USA, PCI, 54–63.

Xu G., Magnani S., Hannant D.J. (1998), Durability of hybrid polypropylene-glass fibre cement corrugated sheets, *Cem Concr Compos* 20, 79–84.

Yan H., Sun W., Chen H. (1999), The effect of silica fume and steel fiber on the dynamic mechanical performance of high-strength concrete. *Cem Concr Res* 29, 423–426.

Zheng Z., Feldman D. (1995), Synthetic fibre-reinforced concrete, *Progress in Polymer Science* 20, 185-210.

Zhu W., Bartos P.J.M. (1997), Assessment of interfacial microstructure and bond properties in aged grc using a novel micro-indentation method, *Cem Concr Res* 27, 1701–1711.

10

Degradation of polymer-cement composites

N R SHORT, Aston University, UK

10.1 Introduction

Cementitious systems incorporating polymers have received considerable international attention, especially over the last 30 years or so. This interest is reflected in ten international congresses, numerous symposia, workshops and journal publications that are the source of a considerable amount of information, see for example, compilations of the literature (CIRIA, 2000; Ohama, 1997). The reason for this interest can be attributed to the improved engineering properties when compared to the unmodified materials, e.g. tensile/flexural strength, toughness and durability, the latter including resistance to carbonation, chloride penetration, and frost damage. Additionally, these systems may be used as repair materials where a good bond with the existing concrete or steel is required. Many polymer-concrete combinations are available and there are various ways in which to classify them. They will be considered here under the following headings although some systems would fit into more than one category.

- *Polymer-modified cement mortar and concrete (PMC)*: polymer particles in the form of a latex or redispersible powder are added to a fresh cementitious mix which is then cured.
- *Polymer concrete (PC)*: aggregate is mixed with a reactive resin, placed, and then cured.
- *Polymer impregnated concrete (PIC)*: a reactive monomer deeply penetrates a hardened concrete and is then cured.
- *Polymer coatings*: may include surface impregnation, paint systems and overlays where the polymer-concrete interface is of particular importance.

Excluded from this chapter are: (a) minor additions of polymer (e.g., admixtures) which are used solely to alter the rheological behaviour of the mix; (b) polymer fibre, grids and bars for reinforced concrete; (c) polymer incorporated as aggregate.

Unknowns in product formulations, their application methods, variable environmental conditions, a lack of long-term monitoring of property changes

and a reluctance to disclose failures, result in the use of case histories being of limited value. Additionally, in view of the large amount of literature available, an overview of the topic is considered appropriate here and this draws heavily on the work of the author and his research students.

10.2 Polymer-modified cement, mortar and concrete

10.2.1 Nature of systems

Widespread international use is made of these materials, e.g. as grouts and mortar patches for finish and repair work and concretes for bridge deck overlays. Basically, unreactive polymer latex is added to the water of a fairly conventional cementitious mix, which is then cured. The cement begins to hydrate, whilst the polymer particles from the latex coalesce to give a film which then binds the hydrated cement phases and aggregate. There are numerous proprietary polymer emulsions and redispersible powders available. Polymer type and composition vary widely and all dispersions include other constituents. The manufacturers of these systems are often reluctant to disclose their complete make-up and characteristics for commercial reasons. Specific properties of the hardened material depend very much on the formulation of the polymer dispersion, mortar mix design, and curing regime used. Unfortunately, in much of the considerable published information, the exact nature of the systems and the mixing and curing procedures used are not very well documented, making an understanding of their behaviour and a comparison between different systems difficult.

The most commonly used latexes are aqueous suspensions of styrene-butadiene-rubber (SBR) and various acrylics (Ac) containing 45–50% polymer solids. In SBR, the ratio of styrene to butadiene governs the properties of the polymer, with 60–65% styrene giving a good balance. Higher styrene contents would improve compressive and tensile strengths but reduce adhesion and raise the minimum film-forming temperature (MFT). Usually ~1% carboxylic acid is chemically bound onto the polymer particle surface. These groups ionise in the high pH environment of the fresh cement, Fig. 10.1(a) (Chandra, 1987) and this generally results in improved stability of the latex and adhesion of the PMC to existing substrates (Dennis, 1985). Similarly there are a wide variety of co- and ter-acrylic polymers with some of them being available in redispersible powder form. Ethylene-vinyl acetate (EVA) was one of first redispersible powders on the market. Powders which can be pre-bagged with the cement and aggregate are preferable from a practical and environmental view, compared to latexes which are supplied in plastic containers and require batching to be carried out on site.

In addition to the polymer, a sufficiency of surfactant is added which is then adsorbed onto the surfaces of the polymer particles and helps maintain their dispersion. This dispersion should be preserved during mixing and transfer operations in the high pH environment of the cement and over a practical range

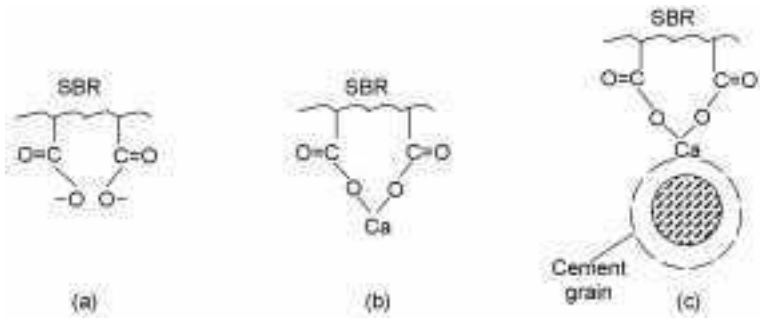

10.1 (a) Ionisation of carboxyl group; (b) interaction with calcium ions in solution; (c) binding to a cement grain.

of temperatures. They may be anionic, cationic or non-ionic and can affect latex-latex or latex-cement interactions. Any free surfactant in the mix water tends to stabilise air bubbles and so a de-foaming agent may be added to counter this. Other additions may also be present, e.g. anti-oxidants and bactericides.

Little detailed information is available on mix procedures although a typical mix design consists of a sand:cement ratio in the range of 3:1 to 2:1 with a polymer solids: cement ratio (p/c) of 0.10–0.20 by weight of cement and a w/c of about 0.3 compared to around 0.5 for the unmodified mortar (Dennis, 1985).

Whilst there is a wide range of latex systems available, they all tend to influence behaviour in the same manner in that: (a) when added to the fresh mix, the polymer particles improve workability to such an extent that, for a given workability, the w/c can be significantly reduced, which in turn reduces porosity and leads to improvements in compressive strength and durability, and (b) after curing, the polymer must be in the form of a film which leads to improved flexural strength, toughness and adhesion.

10.2.2 Influence on rheological behaviour

The presence of the suspended polymer particles in the fresh cementitious mix generally results in a much enhanced workability, allowing the use of lower w/c when compared with the unmodified systems. However, little guidance on the optimum w/c is available and an often stated aim in suppliers' literature is simply 'to use the minimum w/c ratio for the required workability', thus essentially leaving the decision to the operator in the field. Relative performance of the wide range of modified mortar systems is thus difficult to assess and will depend on the actual procedures used (Dennis, 1985, 1988). Usually this involves comparison at the same percentage of dry polymer by weight of cement and using either the same w/c ratio, or sufficient water to give the same workability, the latter being generally preferred. Since workability is a primary factor in governing the ultimate performance of these materials, it is important that the underlying principles are understood.

It is now generally accepted that most mortars conform to the Bingham plastic model of behaviour as given by equation 10.1 relating shear stress, τ to shear rate, $\dot{\gamma}$.

$$\tau = \tau_0 + \mu\dot{\gamma} \qquad 10.1$$

Two parameters, the yield value τ_0, and the plastic viscosity, μ are then needed to characterise such materials. The yield value is a measure of the inter-particle forces which have to be broken before flow can take place, whilst the plastic viscosity represents the internal friction between particles, once flow has commenced (Banfill, 1987).

Influence of mix variables on workability and comparisons of different properties at constant workability, using empirical tests such as slump, flow tray and flow table have been made (ACI, 1991; Ohama, 1985; Øye, 1989). However, whilst these tests are quick to perform and little skill is required, they take measurements under only a single set of experimental conditions and therefore cannot be used to determine the two independent constants given in equation 10.1. Recently it has been shown (Banfill, 1990, 1991) that, by using various types of viscometer, it is possible to overcome this problem for cement pastes, mortars and concretes.

Using a Haake Rotovisco, Salbin (1996) compared how various latex systems influenced the rheological behaviour of Portland cement pastes of mix design shown in Table 10.1. Values of τ_0 and μ are shown in Tables 10.2 and 10.3 respectively. Looking at this data, a number of observations may be made:

- Unmodified pastes containing low w/c do conform to the Bingham type of behaviour.

Table 10.1 Latex systems

Code	Type	Form
SBR 1	Styrene-Butadiene-Rubber 1% carboxylic acid	Emulsion
SBR 2	Styrene-Butadiene-Rubber 5% carboxylic acid	Emulsion
Aq	Aqueous component of SBR only	Solution
Ac 1	Acrylic copolymer	Emulsion
Ac 2	Acrylic copolymer	Emulsion
Ac 3	Acrylic copolymer	Powder
Ac 4	Acrylic terpolymer	Powder
VaVeAc	Vinyl Acetate-Versatate-Acrylic	Powder
VaVe	Vinyl Acetate-Versatate	Powder
EVA 1	Ethylene-Vinyl-Acetate	Emulsion
EVA 2	Ethylene-Vinyl-Acetate	Powder
EVA 3	Ethylene-Vinyl-Acetate	Powder

Table 10.2 Shear stress, τ_0 (Pa) for a number of polymer modified cements

P/C	W/C	OPC	SBR 1	SBR 2	Aq*	Ac 1	Ac 3	EVA 1	EVA 2
0.1	0.30	84.0	51.0			43.5		135.0	
0.1	0.35	37.0	15.0	325.0	45.0	17.5	40.0	53.0	45.7
0.1	0.40	20.0	5.8			9.0		20.0	25.1
0.1	0.45	16.0						16.0	
0.2	0.30	84.0	13.6			15.5		120.0	
0.2	0.35	37.0	4.6			8.5	55.0	57.0	26.4
0.2	0.40	20.0	1.7	125.0	27.5	4.8		32.6	18.9
0.2	0.45	16.0						20.5	

* Aqueous component of SBR 1

- The flow behaviour of the polymer modified fresh paste is similar in character to that of the unmodified paste. However, for SBR 1 and Ac 1, increasing p/c ratio resulted in a significant reduction of yield and plastic viscosity values to such an extent that, at w/c > 0.4, their behaviour becomes almost Newtonian (i.e $\tau_0 = 0$).
- EVA 1 and 2 had a very similar effect on workability, demonstrating that there is little difference in adding the polymer as an emulsion or redispersible powder. However, overall they showed a decrease in workability, particularly at higher concentrations. It is thought that this was the result of water being absorbed initially by the stabilising system used to coat the polymer particles.
- The behaviour of Ac 3 was quite different from that of Ac 1 showing no improvement in workability at additions of 10% and becoming significantly worse at greater additions. From the information provided by the suppliers it was impossible to determine the reasons for this behaviour.
- Increasing the degree of carboxylation of the SBR was shown to have a very significant effect on rheological properties. Pastes made with SBR 2 showed

Table 10.3 Coefficient of plastic viscosity, μ (Nsm^{-2}) for the same systems as in Table 10.2

P/C	W/C	OPC	SBR 1	SBR 2	Aqua*	Ac 1	Ac 3	EVA 1	EVA 2
0.1	0.30	0.68	0.54			0.41		1.74	
0.1	0.35	0.38	0.23	nm	0.45	0.23	0.64	0.26	0.55
0.1	0.40	0.23	0.12			0.13		0.20	0.25
0.1	0.45	0.14						0.18	
0.2	0.30	0.68	0.41			0.35		1.68	
0.2	0.35	0.38	0.19			0.18	1.9	1.90	1.20
0.2	0.40	0.23	0.10	nm	0.29	0.10		0.70	0.58
0.2	0.45	0.14						0.40	

* Aqueous component of SBR 1; nm = not measurable

much higher values of τ_0 and the shapes of the curves were such that μ could not be measured. This behaviour demonstrates the importance of ionisable groups at the surface of the polymer particles which are capable of interacting with other constituents of the mix.

In the case of transient flow behaviour, as demonstrated by changes in τ_0 with time, Fig. 10.2 showed that, for both OPC and SBR 1 modified OPC, the times to accelerated stiffening as measured by a rapid increase in τ_0 of the pastes are 50 and 300 minutes respectively, which is also co-incident with the acceleratory stage of cement hydration (see Kinetics in Section 10.2.3). This clearly demonstrates the retardation effect of SBR 1. In contrast, accelerated stiffening of the SBR 2 modified OPC occurs much earlier than the acceleratory period for cement hydration. This latter effect is related to the much larger interaction forces between polymer and cement particles as a result of increased carboxylation, Fig. 10.1(b) and (c) (Chandra, 1987).

In addition to the above, Salbin (1996) used a ViscoCorder to determine the influence of a similar range of polymers on the workability of a mortar with an aggregate: cement ratio of 2.5:1.0. Figures 10.3 and 10.4 show the influence of w/c on τ_0 and μ. The main points to note here include:

- Unmodified and modified mortars both conform to the Bingham model of behaviour.
- For a given mortar and polymer solids concentration, it was found that workability of an unmodified mortar was improved in the following order: Ac1 > SBR 1 and 2 > EVA.

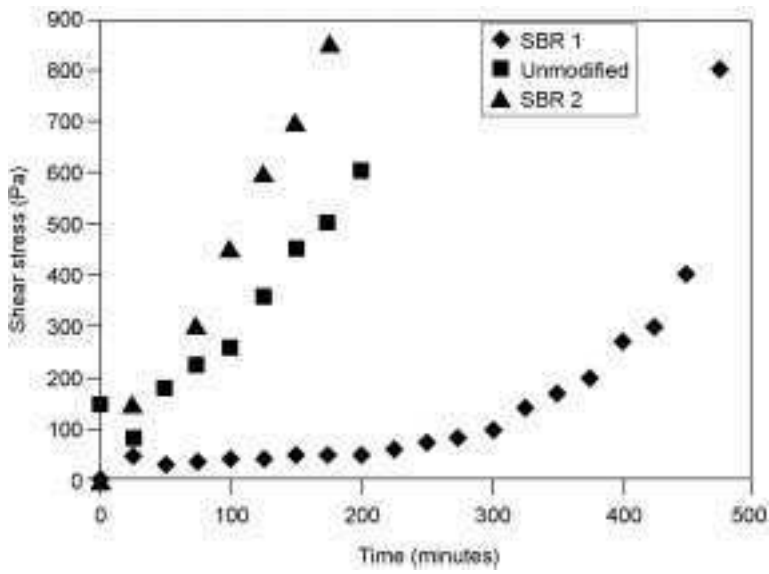

10.2 Transient behaviour of pastes.

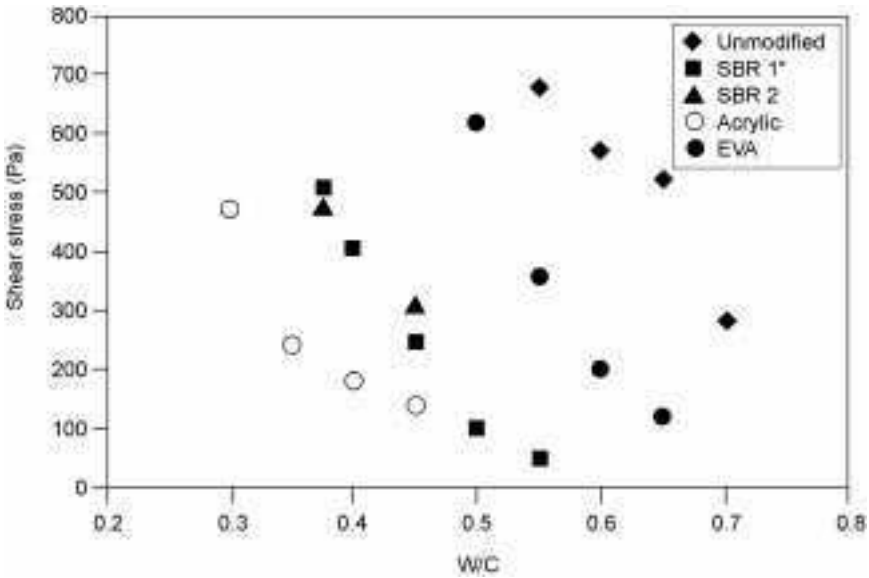

10.3 Shear Stress, τ_0 (Pa) for mortar modified with 20% of various polymers.

- No difference in the behaviour of SBR 1 and SBR 2 was found. Thus it may be concluded that carboxylation had little effect on the workability of the mortar mix compared to that of the cement pastes. This difference was attributed to the presence of aggregate particles which increase polymer-

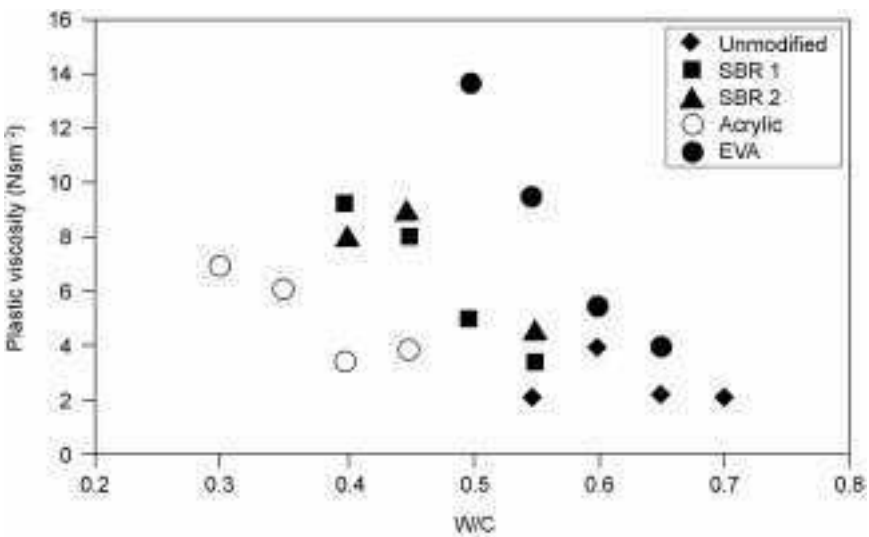

10.4 Coefficient of plastic viscosity, μ (Nsm^{-2}) for the same mortar systems shown in Fig. 10.3.

cement inter-particle separation distances and result in breakdown of the interaction forces. However, this does not mean that interactions are not important in other respects.

From these results it should be clear that many factors influence workability and subsequently porosity and durability. Thus, providing that the systems used are well characterised, the two-point workability techniques should be very useful for determining the influence of parameters, such as sand grading, aggregate/cement ratio and type of cement, on the workability of polymer modified mortars since the full information is not obtained by the empirical tests. These procedures should form the basis for determining rheological behaviour when comparing properties such as shrinkage, permeability and diffusion resistance, etc., of mortars modified with different polymer systems at constant workability.

10.2.3 Microstructure development

Mechanisms

The development of microstructure is considered to proceed by a basic three-step process (Isenburg, 1974; Ohama, 1987). Immediately after mixing, the system consists of well dispersed un-hydrated cement particles, aggregate, and polymer particles. After the dormant period, cement hydration starts to accelerate and, as water is consumed, the inter-particle separation distances decrease. As a result of this, the latex becomes unstable causing the polymer particles to flocculate and deposit on the C-S-H and aggregate surfaces. With further removal of water, the polymer particles coalesce to give a continuous three-dimensional film or membrane. This membrane binds the cement hydrates and aggregate and also improves the bond between the polymer modified cement and existing concrete or steel substrates. It has also been suggested that any ionised carboxyl groups will bond to cement grains via calcium ions forming ‘chemical anchors’, see Fig. 10.1(c), (Chandra, 1987; Ohama, 1998).

To achieve this type of microstructure, a conflicting set of curing conditions is required. Cement hydration needs water to give the necessary hydration products and the development of compressive strength. In contrast, the polymer phase requires dehydration so that the particles coalesce to form a continuous film, which is essential for improvements in flexural strength and toughness. Thus a two-stage curing regime is often recommended consisting typically of 24 or 48 hours ‘wet’ followed by 28 days ‘dry’.

The evidence for this mechanism stems from a publication based on work carried out many years ago (Isenburg, 1974) where a distinct polymer film bridging a crack was observed by scanning electron microscopy (SEM). In practice it is very difficult to elucidate the true nature of the polymer films, although modern instruments have facilitated observations on the micrometer

scale for a wide range of polymer systems (Su, 1996; Ollitrault-Fichet, 1998; Jenni, 2002). Sample preparation is important and observations may be made of fracture surfaces or cross-sections, with or without etching of the cement phases (Zeng, 1996a). In some areas the film is present on a very fine scale and exists as a discontinuous mesh or in a fibrous form which is intertwined with cement hydration products. In other areas the film is more distinct bridging pores and micro-cracks. The films formed when the polymer is added as a redispersible powder have been compared to those formed when the polymer is added as latex (Afridi, 2003). It was found that the former have an inferior quality compared to the latter, which was attributed to a less uniform polymer distribution in the mix and poor coalescence of the polymer particles during curing.

Kinetics

It is considered that the addition of polymer latexes will generally retard the hydration of cements. Isothermal conduction calorimetry has been used (Zeng, 1996b) to study the hydration kinetics of SBR latex modified cement. The effect of increasing amounts of SBR on heat evolution is shown in Fig. 10.5. It is clear in this case that the SBR acted as a retarder of cement hydration in that it increased the induction period and time to maximum heat output whilst reducing the total heat outputs. Low concentrations of SBR (<10%) had a significant effect during the acceleration period, reducing the rate of alite reaction and degree of hydration by about a half. Higher concentrations (>10%) suppressed the nucleation of cement hydration products and thus increased the induction period, with only small further reductions in the rate of alite reaction and degree of hydration.

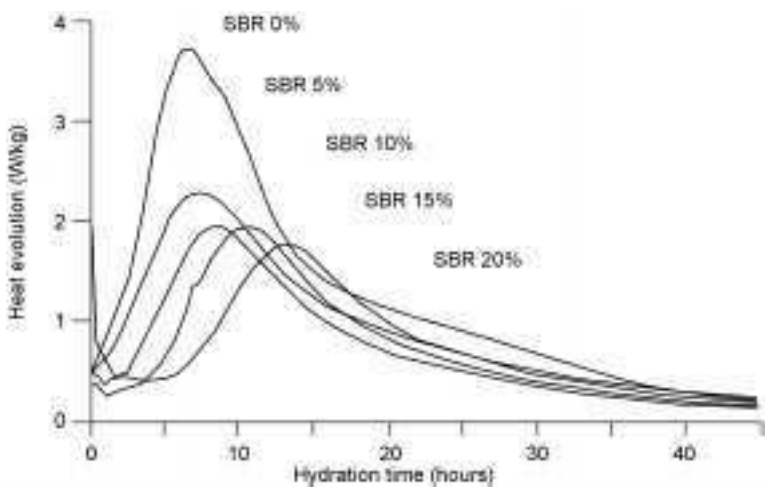

10.5 Conduction calorimetric curves of SBR modified OPC; w/c 0.3, 22°C.

Calculated activation energies for the hydration of unmodified and modified cements containing up to 10% polymer were very similar and suggest that the rate controlling step, diffusion of ions through a reacted layer, was unaltered in the presence of polymer particles. That the actual rate is reduced suggests that polymer particles are occupying some of the sites (see Fig. 10.1(c)) available for calcium dissolution and subsequent hydration. This has been confirmed by SEM observations (Su, 1996). In the case of the modified cements containing 20% polymer, the activation energy was much lower than that for the unmodified cement. This suggests that a different mechanism is now controlling the rate of hydration, which may involve restricted movement of water to hydration sites. That the actual rate is low may be because the configuration of polymer particles is such that they provide a more tortuous path for water diffusion, e.g. through a sheath formed by the polymer around the cement particles.

Whilst the constituents of the aqueous component of the latex had little influence on kinetics, an increased concentration of carboxyl groups in the polymer significantly increased retardation. It is thought that this was a result of increased binding between the carboxyl groups and hydration sites on the surface of the cement grains.

It is evident from this work that polymer-cement interactions are important since they have the ability to influence hydration kinetics and thus in turn influence porosity and polymer film development, both of which have a long-term effect on durability.

Porosity

The influence of polymer modification on the total porosity and pore size distribution of cement pastes has been studied by mercury intrusion porosimetry (Zeng, 1996a). Whilst there are clear reservations in using this technique (partly for the reasons indicated in Chapter 2 and also because of the compressibility of the polymers) results were checked by comparing values of total porosity with those obtained by solvent exchange, water absorption and helium pycnometry. This showed that the different techniques resulted in different absolute total porosity values, but trends with, e.g. curing time, curing condition and polymer type and content were essentially the same (Zeng, 1996a).

Wet curing of a PMC tends to result in an increase in total porosity and give a coarser pore structure compared with similar unmodified cement, at constant w/c. This may be attributed to the retarding effect of the polymer although the effect is reduced over time so that, with longer curing, e.g. 90 days, little difference is found. Real reductions in porosity come from the ability to use lower w/c, whilst at the same time maintaining the workability.

Whilst the wet-dry curing regimes result in improved mechanical properties, such a regime is contrary to that which would be expected for a low porosity surface layer (Cather, 1994) e.g. desirable, for good resistance to chloride

ingress. In other than water-saturated curing, it is thought that the water loss will be most rapid at the outer surface and lowest at some point remote from the surface. However, it has also been suggested that the rate of evaporation from polymer modified cements is lower compared with that from unmodified cements (as determined by mass loss for the total sample) and that this decreases with an increase in latex content (Ohama, 1982). Pore size distribution curves for wet-dry cured unmodified and 10% and 20% SBR modified cement paste at w/c 0.35 are shown in Fig. 10.6 (Salbin, 1996; Short, 1997). Samples were taken from the first 2 mm of surface and at depths of 15 and 30 mm from a prism with one exposed surface, which had been subjected to a curing regime of one day wet and 27 days dry. In the case of the unmodified cement, there is no distinct difference between the pore size distributions at 15 and 30 mm depths, total porosity and initial pore entry diameter being about 0.11 cc/g and 0.20 μm respectively. These values are consistent with those obtained for specimens cured for 28 days wet. However, the surface layer has a coarser pore structure with a total porosity of 0.14 cc/g and initial pore entry diameter of 1.90 μm. This difference is presumably a result of insufficient hydration through evaporation of water from the surface layer. Thus a curing affected zone (CAZ) exists although it does not extend to 15 mm from the surface. In cement modified with 10% SBR, the surface layers are much coarser than the middle and bottom layers and furthermore the layers are much coarser than in the case of those taken from unmodified cement. It would appear that, for this SBR, the wet-dry curing regime had an adverse effect on pore structure. Increasing the polymer content to 20% SBR results in slightly less coarse pore structures compared with specimens containing 10% polymer. They are, however, still coarser than those of the unmodified cement specimens. It may be that greater polymer contents reduce evaporation of water to some extent, but with this particular polymer the effect is not very significant.

In the case of Acrylic and Ethylene Vinyl Acetate modified cements, changes in pore structure as a result of the wet-dry curing regime were not as severe as in the case of SBR, although a CAZ still exists. The reasons for this difference are not clear and this emphasises the need to appreciate that different commercial systems may behave in different ways. Investigations should concentrate on moisture movement at the surface of specimens and not in the bulk of the specimens as a whole.

10.2.4 Polymer-cement interactions

The simple model of microstructure development outlined in Section 10.2.3 suggests a mechanism whereby the cement and polymer particles cure independently of each other producing a physical binding of the cement hydrates and aggregates by a distinct polymer film. In practice the situation is much more complex as discussed in the section on hydration kinetics and microstructure.

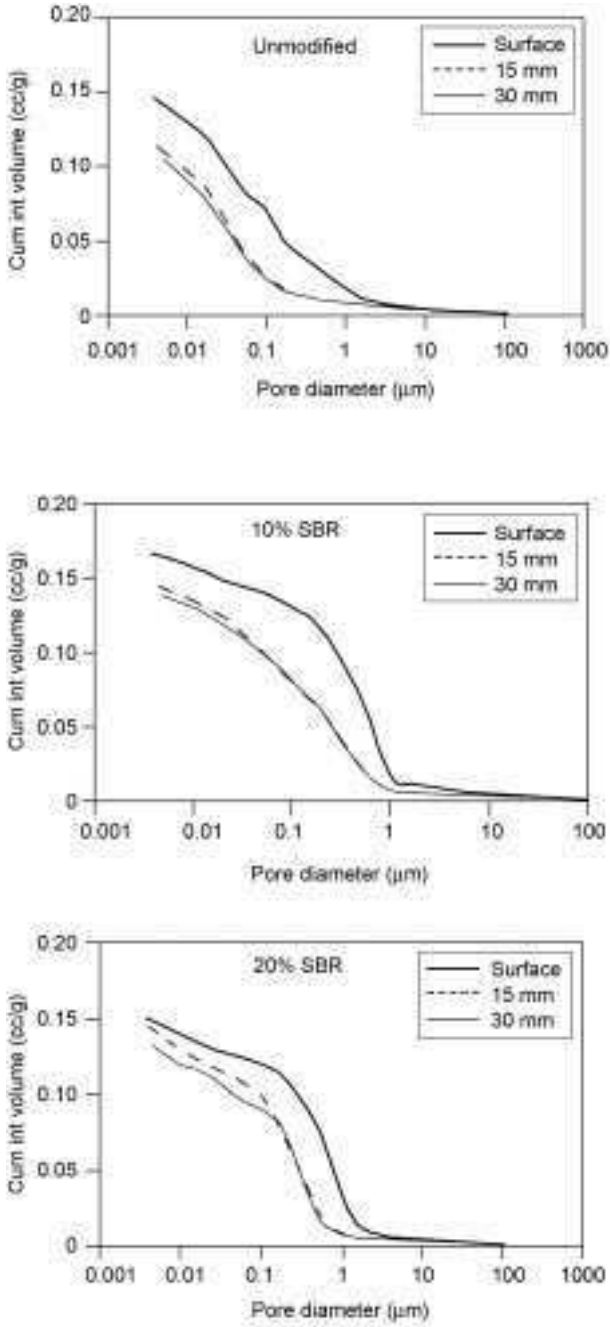

10.6 Pore size distribution curves for wet-dry cured unmodified, 10% and 20% SBR modified cement paste at w/c 0.35. Samples taken from the surface and depths of 15 and 30 mm.

Polyvinyl acetate (PVA) offers very poor water resistance in that, when the PMC is immersed in water, it swells and undergoes partial alkaline hydrolysis (equation 10.2) to give a water soluble polyvinyl alcohol and acetic acid or calcium acetate.

$$–(CH_2.CH.COOCH_3)– + \tfrac{1}{2}Ca(OH)_2 \rightarrow –(CH_2.CH.OH)– + \tfrac{1}{2}Ca(COOCH_3)_2 \quad 10.2$$

Such reactions can lead to significant loss in strength after only a year in natural weathering situations. In an effort to overcome this problem, PVA has been copolymerised with ethylene to give EVA. Even then it has been found (Silva, 2002) that the acetate groups of EVA are capable of undergoing alkaline hydrolysis, interacting with calcium ions from the paste to form an organic salt, calcium acetate. SEM investigation of EVA modified, compared to unmodified, pastes showed that the calcium hydroxide content was decreased, ettringite crystals appeared to be well formed and many Hadley's grains were observed. These observations are consistent with retardation of the hydration process. In addition a calcium-rich porous phase similar to calcium hydroxide in structure was observed, the porosity being attributed to attack by the acetic acid generated during hydrolysis.

During the 1970s chlorinated polymers such as polyvinyl di-chloride (PVdC) were popular because of their very good mechanical properties. However, it quickly became apparent that they could cause accelerated corrosion of reinforcing steel. Pore solution extraction and analysis showed, (Larbi, 1990) that, over time, an increase in the ratio of $[Cl^-]$:$[OH^-]$ ions occurred. An ion-exchange reaction occurs between hydroxyl ions in the pore solution and the chloride bound to the polymer (equation 10.3) giving a hydroxylated polymer and chloride ions in the pore solution.

$$–(CH_2.CCl_2)– + 2OH^- \; –(CH_2.COH.OH)– + 2Cl^- \quad 10.3$$

More recently ter-polymers consisting of n-butyl acrylate, methyl acrylate and a 'functional monomer' have become available. The nature of this functional monomer is not clear but comparison with similar dental cements suggests that it may be based on an acrylic (or similar) acid which should be capable of bonding strongly (chemical anchors) to cement particles (Shaw, 1989).

10.2.5 Mechanical properties

Stiffness

It is generally considered (Ohama, 1998) that the addition of polymer will reduce the stiffness of the PMC and will do so in proportion to the amount of polymer added. There is, however, very little data available to confirm this, and it has been suggested (Bureau, 2001) that the reduction is really only noticeable

in the case of SBR modified mortars at p/c > 12.5%. No data is available on long-term behaviour.

Strength

A model describing the relationship between porosity, microstructure and strength of cement paste has been proposed by Kendal *et al.* (1983). The model differentiates between micro-cracks or elongated pores, which are long enough to initiate crack propagation but probably represent < 0.1 of the pore volume fraction, and the remaining pores which have a high volume fraction ~0.9 but are too small to initiate failure. This approach suggests that the tensile stress, σ, required for crack propagation in cement paste is given by equation 10.4:

$$\sigma = [E_0 R_0 (1-p)^3 \exp(-kp)/\pi a]^{1/2} \qquad 10.4$$

where E_0 and R_0 are the Young's modulus and fracture energy at zero porosity respectively, p is the porosity volume fraction, a is the crack length and k is a constant. Measurement on a range of samples, including ones made with a water soluble polymer, showed that the tensile and flexural strength of cement paste is largely governed by the length of the largest (crack-like) pores, but there is also an influence of the volume of porosity through reducing the elastic modulus and fracture energy.

Whilst this equation has not been applied to polymer modified mortars it represents one way of explaining available strength data and determining the way forward for improvements.

Typical polymer modified mortars of aggregate : cement ratio 2 : 1, 15% polymer and w/c 0.38–0.45 have compressive and flexural strengths in the region of 30 MPa and 8 MPa respectively, compared with values of around 20 MPa and 3 MPa for the unmodified mortar (Ohama, 1998). The improvement in compressive strength can be attributed to the use of a lower w/c (for the same workability) thus reducing p in equation 10.4. This has been confirmed by (Barluenga, 2004; Wang, 2005) who showed that, at constant water cement ratio, the compressive strength of polymer modified mortars tends to decline with increase in p/c, this being attributed to increased porosity

The improvement in flexural strength is considered practically advantageous and is one of the main reasons for modification. It is probable that the presence of a polymer film effectively reduces the value of a in equation 10.4. The mechanism may involve polymer bridging of cracks, a process that would be facilitated by the presence of the chemical anchors discussed in Section 10.2.3. When failure occurs, the fracture surface shows fibrils of polymer (Bureau, 2001).

Whilst the strength values can be improved by, e.g. changing the type of cement or aggregate size, etc., changes in latex have little effect, although redispersible powder always seem to be somewhat inferior. This suggests that the presence of the polymer film cannot overcome the effect of flaws below

some critical length, a_{crit}. There may thus be little point in empirical attempts to enhance strengths of PMC by means of polymer development until the nature of a_{crit} is more clearly understood.

Adhesion

An important aspect of PMC is their improved adhesion to substrates such as existing concrete, steel and many other materials. There are a number of test configurations used for assessing adhesion with the tensile (pull-off), flexural and slant-shear variations being the most popular. Values depend on factors such as test method, nature of substrate, e.g. porosity and environment, and often show considerable scatter. Wet curing does not provide a very good bond and failures tend to be adhesive (i.e., at the interface). Wet-dry curing gives a much improved bond which increases as p/c increases and bond strengths three times those of the unmodified materials can be obtained. Failure is mainly cohesive in nature. Subsequent prolonged re-wetting can reduce this improved bond with a return to adhesive type of failure. The reason for this is unclear but one possibility may be that hydration products, formed during further hydration, disrupt the interfacial polymer film rather than consolidating it. This could be compounded by water absorption-induced swelling of the polymer phase (Salbin, 1996).

10.2.6 Durability

Water absorption

When comparing PMC of given type produced at constant workability, it is found that the water absorption and permeability are reduced as the p/c is increased and this may be attributed to reduced porosity. However, there is some loss in strength, especially flexural, although this is not usually considered to be of practical significance as strengths are still greater than for unmodified mortar. In keeping with these observations, the frost resistance of PMC is much improved. Thus, whereas an unmodified mortar may suffer damage in fewer than 100 cycles of freezing and thawing, e.g. -18 to $+4$ºC, there is no change with the PMC even after 300 cycles (Ohama, 1998).

Carbonation

With regard to carbonation, a trial showed that, for an SBR modified mortar, carbonation depths were 2–3 mm compared to 10–20 mm, depending on exposure conditions, for the conventional material, (Ohama, 1998).

Acid attack

Most PMCs are attacked by inorganic and organic acids and sulfates since these agencies attack the cement phase. They are also attacked by organic solvents

which dissolve the polymer films. However since porosity is lower than is the case for unmodified mortars then rates will also be lower (Ohama, 1998).

Chloride diffusion

Values of the effective diffusion coefficients (D_{eff}) of chloride ions in a variety of polymer modified cements, using a well established steady-state diffusion technique (Page, 1981), have been determined (Zeng, 1996a) and are given in Table 10.4. Samples were compared at constant w/c and were all well cured. A number of interesting points were noted from the results obtained which may be summarised as follows:

- In the case of the unmodified cement reducing w/c led to reduced values of D_{eff}, as might be expected and results are comparable with those reported in other work.
- At a given w/c, the addition of 10% SBR 1 reduced D_{eff} by about a half. Increasing the addition to 20% had little further effect. However, comparison at constant w/c underestimates the real benefit of adding the latex. With the ability to reduce w/c whilst maintaining workability (see Section 10.2.2), a comparison should be made between say 0.4 w/c for the unmodified and 0.3

Table 10.4 Effective diffusivity coefficients for diffusion of chloride ions in PMC @ 25°C

System	Chloride effective diffusivity coefficient D ($\times 10^8$ cm^2 s^{-1})		
W/C	0.3	0.35	0.4
OPC	2.19	3.59	10.10
+ 10% SBR 1	1.23		4.28
+ 20% SBR 1	1.26		3.92
+ 10% SBR 2			6.81
+ 20% SBR 2			4.35
+ 10% Ac 1	2.08		7.12
+ 20% Ac 1	1.56		6.52
+ 10% Ac 2	14.8		
+ 10% Ac 3			5.26
+ 10% Ac 4	2.80		
+ 10% VaVeAc			7.61
+ 10% VaVe	2.88		
+ 10% EVA 1	2.77	3.85	
+ 10% EVA 2		3.45	
+ 10% EVA 3		2.70	

w/c for the modified pastes. In this case the reduction in D_{eff} is then nearly an order of magnitude.

- Most of the other types of latexes were also effective in reducing D_{eff} but none were quite as good as the SBR. Note, however, that Ac 2 is an exception to this general observation. This polymer had a considerable retarding effect on cement hydration and consequently produced a very open pore structure which in turn resulted in a value of D_{eff} much higher than that for the unmodified paste. Thus it should not be assumed that all latexes will be beneficial.
- Whether the polymer was added as a redispersible powder or latex made little difference to the values of D_{eff} recorded.

Claims that PMCs of the types studied may have improved resistance to chloride ion penetration due to the large pores being filled with polymer or sealed with a continuous polymer film are unlikely to be correct since, if anything, the polymers tended to increase porosity and the polymer films, when tested separately, were not effective chloride diffusion barriers in themselves. The values of D_{eff} through polymer films produced by drying in a Petri dish were found to be 8.65 and $11.35 \times 10^{-8}\,cm^2\,s^{-1}$ for SBR 1 and AC 1 respectively (Zeng, 1996a).

As discussed earlier, the wet-dry curing regime is not one that would normally be considered appropriate for good durability and the existence of a CAZ has been shown. Slices taken from such a sample do indeed show a larger value of D_{eff} in the CAZ, Table 10.5 (Salbin, 1996). It should be noted, however, that this value of D_{eff} decreases over time as further hydration of the cement occurs due to wetting in the diffusion cell. This finding may account for anecdotal observations of higher chloride concentrations found at the surface of some PMC structures but with little penetration of chloride in depth due to the rapidly reducing porosity away from the evaporation surface.

From a practical point of view, these results show that when comparing different systems it is very important to clearly state the basis on which the comparison is made, i.e. constant w/c or constant workability. In addition the fabrication and curing procedures used in preparing samples for the diffusion

Table 10.5 Effective diffusivity coefficients for diffusion of chloride ions in PMC @ 25°C Samples containing 20% SBR 1, w/c 0.35 and cured for 48 hours wet then 28 days dry.

Layer	Chloride effective diffusion coefficient D ($\times 10^8\,cm^2\,s^{-1}$)
Top section early stages of diffusion	9.47
Top section later stages of diffusion	5.49
Bottom section	2.41

test should be clearly stated and compared with the recommended procedures when the material is used in practice.

Thermal/fire

The thermal resistance and incombustibility of PMC are not as good as those of unmodified material. Mechanical properties deteriorate rapidly with increased temperature, their resistance being governed by the nature of the polymer used especially glass transition temperature and the p/c. Incombustibility depends on the nature of the products formed during thermal decomposition. These factors tend to restrict the use of PMC to below 100–150ºC (Ohama, 1998).

10.3 Reactive polymer matrix composites

10.3.1 Introduction

These materials are quite different from polymer-modified mortars in that they do not contain any hydraulic cement. They consist of a synthetic resin binder incorporating a hardener and filler such as well-graded powder, sand or coarse aggregate. These are mixed on site, placed and then allowed to cure giving a material with generally good mechanical properties (in terms of compressive, tensile, flexural strengths), adhesive bond strength, and chemical and abrasion resistance. Applications of these materials include repair mortars and crack injection formulations, adhesives, grouts for mechanical fixings, floor finishes such as sealers and toppings, and pre-cast drainage channels and pipes. Several recent and detailed reviews are available (CIRIA, 2000).

The most widely used resins include those of the following generic types: epoxies, unsaturated polyesters, methacrylates, polyurethanes, vinyl esters and furans. Their chemical nature allows the formulation of a wide variety of products ranging from low viscosity solvent systems for void impregnation and crack injection to heavily filled products much like conventional mortars.

Thermosetting resins are used so that, when combined with curing agents or catalysts at ambient temperatures, they undergo further polymerisation (cross-linking) to give a three dimensional structure. The correct degree of cross-linking is very important in that it determines the glass transition temperature of the polymer and other long-term properties.

The amount of curing agent or catalyst governs the rate of reaction at a given temperature so that, if the material were applied on site at low ambient temperatures of say ~10ºC, more is required, whilst at higher ambient temperatures of say ~35ºC the converse is true. In addition, the reactions are influenced by the exothermic nature of polymerisation, the thickness of the coating and variations in ambient temperature. Most reactions do not proceed to completion but, if reactive polymer matrix composites are formulated appropriately, a sufficient

degree of cross-linking is attained at ambient temperatures to give the required service properties.

10.3.2 Application

Since there is a very wide range of systems available, it is very important that the right one is chosen for the specific application in mind. Assuming that the correct choice is made, it is then very important that the correct procedures are used on site and in the case of pre-cast factory products.

Correct proportioning and thorough mixing of resin and activator or catalyst is required in order to achieve the correct curing rate and this must also be consistent throughout the product. Application should also be within the specified temperature range and sufficient time allowed for the desired properties to be achieved. For example, incorrect mixing can result in some areas being hard whilst other parts remain soft or rubbery.

On-site use invariably requires a good bond to an existing concrete or steel substrate and this can only be achieved if the surfaces are clean and any loose material or corrosion products are removed. Good interfacial contact is required which can usually be achieved by the use of primers. In addition, whilst some systems are formulated for application to damp surfaces, the majority require that the surface moisture content be reduced to <5% during application and cure. Capillary movement of moisture from deeper within the substrate may occur later and lead to reduction of bond or blistering in the case of floorings and coatings. Little is known about the factors driving this process but they probably involve the pore size distribution of concrete, presence of interfacial soluble compounds and the source of moisture. Osmotic blistering may occur on steel and concrete substrates through water ingress as a result of salts on the steel surface (poor cleaning) or, in the case of concrete, the use of incorrect primers containing water-soluble compounds, (Dively, 1994; FeRFA, 1990). In addition to the above, long-term adhesion depends on factors such as level of applied stress, fatigue, exposure to moisture, and temperature fluctuations.

10.3.3 Water absorption

Reactive polymer matrix composite materials generally have a high resistance to water transmission, although the extent depends very much on their formulation. Over the long-term, slow diffusion may lead to reversible equilibrium moisture contents of up to 10%. Eventually this can lead to the creation of pathways for ingress of deleterious species such as chloride ions, reduction in modulus and strength by acting as a plasticiser and degradation of the resin by hydrolysis. These effects are increased by air entrainment, due to poor mixing or compaction, and as temperatures are increased. Moisture ingress via the polymer, a porous substrate or exposed edges can lead to degradation of the adhesive bond.

The mechanism is not fully understood but probably involves plasticising and swelling of the polymer in the interfacial region and alkaline hydrolysis of the resin.

10.3.4 Creep

These materials are visco-elastic in nature and thus, over time, may undergo creep and stress relaxation even at ambient temperatures. For many applications, service stresses are low compared to ultimate values and the effects are limited. However, for applications involving adhesive bonding and other load bearing applications, the consequences may have to be considered. Thus, it may be necessary to determine the limiting stress level below which creep rupture does not occur for applications such as anchoring. In complex loading systems such as shrinkage or differential thermal expansion and contraction, stress relaxation may alleviate stress concentrations. The extent of these effects is governed by factors such as degree of cross-linking in the resin and the type/level of filler, see for example (Mays, 1992).

10.3.5 Thermal properties

In general the coefficients of thermal expansion for unfilled (lower modulus) and filled (higher modulus) products are ~40–100 and 20–40 $\times$ 10^{-6} ºC^{-1} respectively. This compares with ~10 $\times$ 10^{-6} ºC^{-1} for typical substrate materials and can lead to the development of significant thermal stresses. Thus for high modulus systems which undergo little stress relaxation, temperature changes ~30ºC can lead to stresses which, over time, can lead to shear failure in a concrete surface, loss of adhesive bonding from a steel substrate or cracking of the resin. Closer matching can be obtained by careful attention to filler type and loading, and obtaining the best balance between thermal expansion coefficient, modulus and stress relaxation.

The fire performance of these resin-based materials is inferior to steel or concrete and must be taken into account when considering potential applications. Whilst this factor would preclude their use in a few situations, there are many where it is of little consequence.

10.4 Polymer impregnated concrete

A polymer impregnated concrete is produced via a process whereby an existing hardened concrete (structure or factory component) is dried at around 150ºC and then impregnated with a low viscosity monomer, usually methyl methacrylate, which is subsequently cured in situ. Impregnation is often achieved by soaking at atmospheric pressure although the process may be facilitated by evacuation and/or higher pressures. Polymerisation is accomplished by a thermal catalytic

or promoted catalytic process or is radiation induced. The resulting polymer fills, or lines the surface, of the pores of the concrete modifying the properties of the hardened mortar. Extensive reviews of early work (Swamy, 1979; Shaw, 1989) showed that increases in modulus of elasticity, strength (compressive, flexural and tensile) and improvements in durability could be effected, although the extent of these improvements does depend on the depth of impregnation achieved and porosity of the original concrete. The process shows the most marked improvements when starting with high porosity, low compressive strength concretes. Since these reviews were written, there has been only a little additional investigative work reported (Ohama, 1997; Fowler, 1999). More recent work (Chen, 2005) has compared soaking time and polymerisation temperature on the mechanical properties of PIC in a systematic way and confirmed the possible improvements. Decreases in surface absorption compared with normal concrete are attributed to significant decreases in total porosity with maximum pore diameters of <50 nm. Despite the much improved properties and early application of PIC for remedial treatment of road bridge decks in the US, their high processing costs has generally precluded further use apart from limited precast operations in Japan, (Ohama, 1997).

However, one developing area where polymer impregnation may prove beneficial is the wear resistance of concrete used in floor construction. Treatments have been found to significantly increase the abrasion resistance of all types of concrete (Sadegzadeh, 1988), although improvements are greatest with low compressive strength concrete (Sebok, 2004).

10.5 Characteristics of paints and polymeric surface treatments for concrete

A wide range of products and systems are available and may be classified as pore liners, pore blockers and coatings according to their function, the materials used and method of application. Whilst these systems are generally regarded as beneficial, lack of characterisation of the materials application procedures used makes quantitative comparison between the different products difficult. Similarly, there is little detailed understanding of the mechanisms of how they work or how they may be optimised.

Pore liners

The concrete surface is saturated with organo-silicon compounds such as silanes and siloxanes. In the presence of moisture, these react with the hydrated cement matrix forming a discontinuous film on the surfaces of the pores and capillaries within the concrete, maintaining an open and ‘breathable’ pore structure. The hydrophobic nature of this chemically modified surface layer reduces moisture ingress and provides good protection against, e.g. chloride ion penetration

(Basheer, 1998). Depth of penetration achieved in a given time depends on such factors as pore size distribution of the mortar matrix, water content and the composition and reactivity of the compound being impregnated (Sosoro, 1998; Basheer, 1998). Whilst formulations of silanes/siloxanes are popular, there is some concern regarding their toxicity and this has instigated investigations into more environmentally friendly alternatives (Chamberlain, 2005). One such solution is water-based and after application is said to precipitate hydrophobic crystals that adhere to the pore walls of the concrete. Although details of the material used are vague the treatment is said to conform to Highways Agency Standard (BD 43/03, 2003).

Pore blockers

These materials essentially harden the surface of the concrete and reduce its porosity by partially or totally filling the pores and capillaries of the cement matrix. Silicates and silicofluorides, which react with any free lime, are available for this purpose although the polymers used for polymer impregnation described in Section 10.4 may be used. Compared to pore liners, there is little penetration of the concrete surface, (Basheer, 1997).

Coatings

The aim here is to produce a continuous protective layer on the surface with a typical thickness of 0.1–5.0 mm depending on the application. Coatings function by sealing the surface of the concrete against water absorption, whilst allowing transmission of water vapour (Dietricht, 1998) and ingress of carbon dioxide and chloride ions. They should also be effective in crack bridging. A range of systems are available with epoxy and polyurethane performing better than acrylic, chlorinated rubber and polymer emulsion coatings (Almussallam, 2003) although noticeable variations in performance of the same type but from different sources was found. Some results (Ibrahim, 1999) suggest that a combination of silane treatment plus an acrylic top coat was very effective in reducing carbonation and chloride ion ingress. Presumably in this case the silane acts a coupling agent between the polymer and concrete.

Guidance on the use of these systems is given in two Standards (BS EN 1504-1: 1998 and BS EN 1062-1: 1997) with the approach being described by Hurley (2004).

10.6 Interfacial characteristics

Although a large amount of data have been obtained for a range of polymer-cement composite properties, relatively little is known, apart from that discussed

in Section 10.2.4, about the nature of polymer-cement interfaces and interactions that may take place between the two components. In the field of composites generally, it is widely accepted that interfaces between different components are important in determining properties such as strength and durability. It is reasonable to assume that this will also be true in the case of polymer-cement composites.

Studying the interface between the cement and polymer phases in a composite involves a number of practical difficulties. As the cement phase is porous, it is quite probable that polymer will penetrate surface pores resulting in a complex and diffuse interfacial layer. The actual interfacial region itself is hard to reveal and if interaction products have been formed, amounts may be very small and difficult to extract and analyse separately from the cement or polymer phases.

Different specimen geometries may be mechanically loaded with the aim of achieving at least some interfacial failure thus permitting subsequent surface examination of the interfacial region. This is, however, difficult to achieve in practice even with carefully notched samples with the locus of failure often passing through bulk material. An alternative method is the selective dissolution of either the polymer or cement phase, in theory leaving the interfacial region available for surface analysis. In addition, the amounts of interaction products may be magnified by increasing the surface area, e.g. using a powdered cement rather than trying to cast against a flat surface.

A number of systems have been investigated (Short, 1999; Shaw, 1989) with these points in mind, concentrating on the case when the monomer, methyl methacrylate (MMA), comes into contact with hydrated cements and is subsequently cured to give poly(methyl methacrylate) (PMMA).

It was found that the monomeric MMA reacted with the cement to form primarily calcium methacrylate. This reaction proceeds in two stages:

(a) Hydrolysis of MMA in the highly alkaline environment to give methacrylic acid and methanol:

$$H_2C{=}C(CH_3)C{=}OOCH_3 + H_2O \rightarrow H_2C{=}C(CH_3)C{=}OOH + CH_3OH \quad 10.5$$

(b) Subsequent reaction of the methacrylic acid occurs with basic cement minerals, particularly calcium hydroxide, to give calcium methacrylate:

$$2\{H_2C{=}C(CH_3)C{=}OOH\} + Ca(OH)_2 \rightarrow \{H_2C{=}C(CH_3)C{=}OO\}_2\,Ca + 2H_2O \quad 10.6$$

Since the calcium methacrylate formed is highly water soluble, a reaction such as this would be generally detrimental to the properties of a polymer–cement composite. Water is a limiting reagent in these reactions and the amount of methacrylate formed is proportional to the initial amount of water present in the cement. In practice, if the highly water-soluble methacrylate were leached

from the polymer–cement interface over time then the properties of the composite would be modified. This confirms the need for thorough drying of the cement or aggregate prior to contact with the monomer if adhesion is to be maximised.

10.7 Future trends

Interest in polymer-cement composites has increased considerably in recent years with systems finding widespread use in the concrete repair and maintenance sector and speciality applications such as bridge deck overlays. In these cases, improved properties such as flexural strength, bond to existing material and durability are paramount. Some sectors which currently have a small market should grow and these include areas such as factory-produced pre-cast units, materials that incorporate general wastes or encapsulate hazardous wastes, and materials that, by saving resources, result in a more sustainable environment. High cost tends to preclude their use for more general, high volume applications and the inability to maintain their properties at high temperatures adds a further restriction. Since odour and toxicity of the polymer systems can be a problem, albeit short-term, it would seem prudent to anticipate more stringent restrictions through enhanced environmental legislation.

Relatively small incremental improvements in properties have been made over the years and there is much knowledge and experience available with regard to the various systems and their applications. However, even in established markets, further improvements in properties and reliability are desirable and, for new markets, the improvements would probably have to be substantial to justify cost and environmental considerations. Some questions that come to mind include the following:

- Can we find ways to improve the performance of polymer latexes in both liquid and powder forms (and especially the latter which is more desirable from environmental and quality control points of view)?
- How do the various monomer and polymer systems interact with the cement phases to influence rheology, hydration kinetics and microstructure development under various curing regimes?
- What determines, especially long-term, the bond between polymer modified cement, silanes and polymer coatings to existing (porous) concrete and aggregate substrates?
- How can we identify the true polymer-cement interface in these complex systems?

The answers to these, and other, questions will only be achieved by research, in particular research that utilises the latest techniques in polymer and cement chemistry and sophisticated instrumental methods of analysis. Procedures in the concrete laboratory should become more scientifically based. Even then this will

probably only work if there is good collaboration between the researchers and those supplying the various components of the systems, applying the materials in the field and monitoring their life. A start has been made on standards but more needs to be done so that the properties of materials, as defined in the laboratory, are achieved by recognised application procedures in the field.

10.8 Sources of further information and advice

American Concrete Institute (2003), 'Polymer modified concrete', Report of ACI committee 548, Report number ACI 548.3R-03. www.aci-int.org

ACI, BRE, Concrete Society, ICRI (2003), *Concrete repair manual*, Volumes 1 and 2, 2nd edition.

Bassi R and Roy S K, eds. (2002), *Handbook of Coatings for Concrete*, Whittles, Latheronwheel.

CIRIA (2000), 'The use of epoxy, polyester and similar reactive polymers in construction', Vol.1 The materials and their practical applications, Vol. 2 Specification and use of the materials, Vol. 3 Materials technology, CIRIA, London. www.ciria.org.uk

Concrete Repair Association www.concreterepair.org.uk

Concrete Society (1994), Polymers in Concrete, Technical Report 39, The Concrete Society. Windsor. www.concrete.org.uk

Fowler D W (1999), 'Polymers in concrete: a vision for the 21st century', *Cem and Conc Comps,* 21, 449–452.

Miller M (2005), *Polymers in Cementitious Materials*, Rapra Technology. www.rapra.net/

Ohama Y (1997), 'Recent progress in concrete-polymer composites', *Advn Cem Bas Mat*, 5, 31–40.

Ohama Y (1998), 'Polymer-based admixtures', *Cem and Conc Comps*, 20, 189–212.

The Resin Flooring Association, FeRFA. www.ferfa.org.uk

10.9 References

ACI (1991), *State-of-the-art Report on Polymer-modified Concrete*. Report No. ACI 548.3R.91, Detroit, American Concrete Institute.

Afridi M U K, Ohama Y, Demura K and Iqbal M Z (2003), 'Development of polymer films by the coalescence of polymer particles in powdered and aqueous polymer-modified mortars', *Cem Conc Res*, 33, 1715–1721.

Almusallam A A, Khan F M, Dulaijan S U and Al-Amoudi O S B (2003), 'Effectiveness of surface coatings in improving concrete durability', *Cem Conc Comps*, 25, 473–481.

Banfill P F G (1987), 'Feasibility study of coaxial cylinders viscometer for mortar', *Cem Conc Res*, 17, 329–339.

Banfill P F G (1990), 'Use of the ViscoCorder to study the rheology of fresh mortar', *Magazine of Concrete Research*, 42 (153), 213–221.

Banfill P F G (1991), 'The rheology of fresh mortar', *Mag Conc Res*, 43 (154), 13–21.

Barluenga G and Hernandez-Olivares F (2004), 'SBR latex modified mortar rheology and mechanical behaviour', *Cem Conc Res,* 34, 527–535.

Basheer P A M and Long A E (1997), 'Protective qualities of surface treatments for concrete', *Proc Instn Civ Engrs Structs & Bldgs*, 122, 339–346.

Basheer L, Cleland D J and Long A E (1998), 'Protection provided by surface treatments against chloride induced corrosion', *Mat and Struct*, 31 (211), 459–464.

BD 43/03 (2003), 'Design Manuel for roads and Bridges', 2 (4), The Highways Agency, HMSO.

BS EN 1062-1:1997 Paints and varnishes – Coating materials and coating systems for exterior masonry and concrete. Part 1: Classification.

BS EN 1504-1:1998 Products and systems for the protection and repair of concrete structures – Definitions, requirements, quality control and evaluation of conformity – Part 1: (Series of ten standards with surface protection covered in prEN 1504-2).

Bureau L, Alliche A, Pilvin Ph, and Pascal S (2001), 'Mechanical characterisation of a styrene-butadiene modified mortar', *Mat Sci Eng,* A308, 233–240.

Cather R (1994), 'Curing: The True Story', *Mag Conc Res*, 46, 57–161.

Chamberlain D (2005), 'An approved alternative to silane', *Concrete*, 39 (2), 36–37.

Chandra S and Flodin P (1987), 'Interactions of polymers and organic admixtures on Portland cement hydration', *Cem Conc Res,* 7, 875–890.

Chen C H, Huang R, Wu J K and Chen C H (2005), 'Effect of rebar coating on corrosion resistance and bond strength of reinforced concrete', *Const Build Mats*, 19, 404–412.

CIRIA (2000), 'The use of epoxy, polyester and similar reactive polymers in construction', Vol.1 The materials and their practical applications, Vol. 2 Specification and use of the materials, Vol. 3 Materials technology, CIRIA, London. *www.ciria.org.uk*

Dennis R (1985) 'Latex in the Construction Industry', *Chem Ind*, (15), 5 August, 505–511.

Dennis R (1988), 'Polymer dispersion of latexes' in Hewlett P C, *Cement Admixtures: Uses and Application,* 2nd edn, Harlow, Longman, 130–143.

Dietricht M (1998), 'Surface treatments and corrosion inhibitors for the protection of reinforced concrete structures', *Chimia*, 52 (5), 212–217.

Dively R W (1994), 'Osmotic blistering of coatings and linings applied to concrete surfaces', *Mat Perf*, 33 (5) 42–44.

FeRFA (1990), *Osmosis in flooring*, FeRFA, Aldershot.

Fowler D W (1999), 'Polymers in concrete: a vision for the 21st century', *Cem and Conc Comps,* 21, 449–452.

Hurley S (2004), 'Coatings for concrete: new European Standards', *Concrete*, 38 (7), 24–26.

Ibrahim M, Al-Gahtani A S, Maslehuddin M and Dakhil F H (1999), 'Use of surface treatment materials to improve concrete durability', *J Mat Civ Eng*, 11 (1), 36–40.

Isenburg J E and Vanderhoff (1974), 'Hypothesis for reinforcement of polymer cement by polymer latexes', *J Am Ceram Soc*, 57, 242–245.

Jenni A, Herwegh M, Zurbriggen R, Aberle T and Holzer L (2002), 'Quantitative microstructure analysis of polymer-modified mortars', *J Microscopy*, 212, 2, 186–196.

Kendal K, Howard A J and Birchall J D (1983), 'The relation between porosity, microstructure and strength, and the approach to advanced cement-based materials', *Phil Trans R Soc Lond,* A 310, 139–153.

Larbi J A and Bijen J M (1990), 'Interaction of polymers with Portland cement during hydration: A study of the chemistry of the pore solution of polymer modified cement systems', *Cem and Conc Res*, 20, 139–147.

Mays G C and Hutchinson A R (1992), *Adhesives in Civil Engineering*, Cambridge University Press, Cambridge.

Ohama Y (1985), Polymer-Modified Mortars and Concretes, in Ramachandran V S, *Concrete Admixture Handbook, Properties, Science and Technology*, Park Ridge, USA, Noyes Publications, 337–429.

Ohama Y (1987), 'Principle of latex modification and some typical properties of latex-modified mortars and concretes', *ACI Mat J*, Nov–Dec, 511–518.

Ohama Y (1997), 'Recent progress in concrete-polymer composites', *Advn Cem Bas Mat*, 5, 31–40.

Ohama Y (1998), 'Polymer-based admixtures', *Cem and Conc Comps*, 20, 189–212.

Ohama Y and Kan S (1982), 'Effects of Specimen Size on Strength and Drying Shrinkage of Polymer-Modified Concrete', *Int J Cem Comp & Ltwt Conc*, 4, 229–233.

Ollitrault-Fichet R, Gauthier C, Clamen G and Boch P (1998), 'Microstructural aspects in a polymer-modified cement', *Cem Conc Res*, 28, 1687–1693.

Øye B A (1989) *Repair Systems for Concrete – Polymer Cement Mortars, An evaluation of some polymer systems,* PhD Thesis, Inst Uorganisk Kjemi, Norges Tekniske Hogskole, Universitetet I Trondheim.

Page C L, Short N R and El Tarras (1981), 'Diffusion of chloride ions in hardened cement pastes', *Cem and Conc Res,* 11, 395–406.

Sadegzadeh M and Kettle R J (1988), 'Abrasion resistance of surface treated concrete', *Cem, Conc and Aggs*, 10, 20–28.

Salbin M, (1996), 'The nature of the bond between polymer modified mortars and concrete', PhD Thesis, Aston University.

Sebok T and Stranel O (2004) 'Wear resistance pf polymer-impregnated mortars and concrete', *Cem Conc Res*, 34, 1853–1858.

Shaw I M (1989) 'Interactions between organic polymers and cement hydration products', PhD Thesis, Aston University, Birmingham, UK.

Short N R and Salbin M K (1997), 'The influence of curing conditions on the surface porosity of polymer modified cements', Proc 4th CANMET/ACI int conf *Durability of Concrete*, SP-170, 2, 1009–1028, Sydney Australia, American Concrete Institute.

Short N R and Shaw I M (1999), 'Polymer-concrete interactions', In: Dhir R K and Hewlett P C Eds., *Role of Interfaces in Concrete*, Proc Int Sem, 39–50, Dundee, Thomas Telford.

Silva D A, Roman H R and Gleize P J P (2002), 'Evidence of chemical interaction between EVA and hydrating Portland cement', *Cem Conc Res,* 32, 1383–1390.

Sosoro M (1998), 'Transport of organic fluids through concrete', *Mat Struct,* 31, 162–169.

Su Z, Sujata K, Bijen J M J M, Jennings H M and Fraaij A L A (1996), 'The evolution of microstructure in styrene acrylate polymer-modified cement pastes at the early stage of cement hydration', *Advn Cem Bas Mat*, 3, 87–93.

Swamy R N (1979), 'Polymer reinforcement in cement systems', *J. Mat Sci,* 14, 1521–1553.

Wang R, Wang P-M and Li X-G (2005), 'Physical and mechanical properties of styrene-butadiene rubber emulsion modified cement mortars', *Cem Conc Res,* 35, 900–906.

Zeng S (1996a), 'Polymer Modified Cement: Hydration, Microstructure and Diffusion Properties', PhD Thesis, University of Aston, Birmingham, UK.

Zeng S, Short N R and Page C L (1996b), 'Early age hydration kinetics of polymer modified cement, *Advn in Cem Res*, 8, 1–9.

Index